CORA Cork Open Research Archive
Cartlann Taighde Oscailte Chorcaí

Title	Design, synthesis and development of novel indolocarbazole derivatives as potential anti-cancer agents
Authors	Pierce, Laurence Thomas
Publication date	2011-04
Original Citation	Pierce, L.T. 2011. Design, synthesis and development of novel indolocarbazole derivatives as potential anti-cancer agents. PhD Thesis, University College Cork.
Type of publication	Doctoral thesis
Link to publisher's version	http://library.ucc.ie/record=b2027884~S0
Rights	© 2011, Laurence T. Pierce - http://creativecommons.org/licenses/by-nc-nd/3.0/
Download date	2026-11-07 13:07:07
Item downloaded from	https://hdl.handle.net/10468/382



UCC
University College Cork, Ireland
Coláiste na hOllscoile Corcaigh

Design, Synthesis and Development of Novel Indolocarbazole Derivatives as Potential Anti-Cancer Agents



ucc

Coláiste na hOllscoile Corcaigh, Éire
University College Cork, Ireland

Larry Pierce, B.Sc.

101371321

Thesis presented for the degree
of Doctor of Philosophy to

NATIONAL UNIVERSITY OF IRELAND
University College Cork

Department of Chemistry and Analytical & Biological Chemistry
Research Facility

Supervisor: Dr. Florence McCarthy

Head of Department: Prof. John Sodeau

April 2011

Acknowledgments

At the outset, I would like to acknowledge the contribution of Dr. Florence McCarthy for encouraging me to commence postgraduate study and explore my research interests within his research group. I have been privileged to achieve success in this regard, but none of this would have been possible without your guiding belief and insightful direction.

It is also fitting to pay tribute to the fellow members of our research group and my profound recognition of their contribution to what was always an extremely enjoyable and stimulating work environment. I would like to thank Dr. Fiona Deane for her patient advice during my first formative year in the lab, and I am indebted to Michael Cahill, Charlotte Miller, Kieran Greaney, Hannah Winfield, Elaine O'Sullivan and Dr. Niamh O'Connell for all their support and co-operation over the course of this project. Research colleagues from various groups in the Cavanagh and Kane Buildings are too numerous to mention, but have all contributed to my enjoyable experiences both inside and outside the lab, by being great friends and sources of inspiration to me. To Chris and Garry, and the 46 College Road reprobates, who taught me the merits of housekeeping and spur of the moment barbeques. To Denis, Sinead, Tina, Donncha, Angela, Kevin, Andrea, Brian and the Synthos F.C franchise, I wish a very special thank you for all you've done over the last few years. I would like to profoundly thank Carla for her support and counselling, and for making my life so special each and every day.

Provision of technical services within UCC was also critical to the success of this work. I would like to thank Dr. Dan McCarthy and Dr. Lorraine Bateman for providing assistance with NMR spectroscopy, Dr. Florence McCarthy and Mick O'Shea who provided mass spectrometry services, Dr. Simon Lawrence and Kevin Eccles for X-ray structure analysis, Dr. Ken Devine for agarose gel electrophoresis, Derry Kearney for glass-blowing, as well as Chrissie Flaherty in chemical stores, Noel Browne for solvent delivery and Dr. Matthias Jauch for IT support. I would also like to thank Prof. Anita Maguire for her initial assistance in supporting my Ph.D. application, as well as academics in UCC from whom I have learned much in my research. I also wish to thank the NCI for biological evaluation of my novel compounds. Financial assistance from the IRCSET Embark initiative was also appreciated.

Finally, I would like to thank my family for supporting my decision to commit to this study. For Mam, Dad and John M. in beautiful Ballyheigue, beside the Atlantic Ocean, I dedicate this work and look forward to the future, and to the beginning of new shared voyages of discovery...

I hereby confirm that the body of work described within this book, for the degree of Doctor of Philosophy, is the result of research carried out by me, within University College Cork, under the supervision of Dr. Florence McCarthy, and that this thesis has not been previously reproduced elsewhere, to the best knowledge of the author, in whole or in part, prior to presentation for this degree.

_____ Date: _____

Abstract

This thesis describes work carried out on the design of new routes to a range of bisindolylmaleimide and indolo[2,3-*a*]carbazole analogs, and investigation of their potential as successful anti-cancer agents.

Following initial investigation of classical routes to indolo[2,3-*a*]pyrrolo[3,4-*c*]carbazole aglycons, a new strategy employing base-mediated condensation of thiourea and guanidine with a bisindolyl β-ketoester intermediate afforded novel 5,6-bisindolylpyrimidin-4(3*H*)-ones in moderate yields. Chemical diversity within this H-bonding scaffold was then studied by substitution with a panel of biologically relevant electrophiles, and by reductive desulfurisation. Optimisation of difficult heterogeneous literature conditions for oxidative desulfurisation of thiouracils was also accomplished, enabling a mild route to a novel 5,6-bisindolyluracil pharmacophore to be developed within this work.

The oxidative cyclisation of selected acyclic bisindolyl systems to form a new planar class of indolo[2,3-*a*]pyrimido[5,4-*c*]carbazoles was also investigated. Successful conditions for this transformation, as well as the limitations currently prevailing for this approach are discussed. Synthesis of 3,4-bisindolyl-5-aminopyrazole as a potential isostere of bisindolylmaleimide agents was encountered, along with a comprehensive derivatisation study, in order to probe the chemical space for potential protein backbone H-bonding interactions. Synthesis of a related 3,4-arylindolyl-5-aminopyrazole series was also undertaken, based on identification of potent kinase inhibition within a closely related heterocyclic template.

Following synthesis of approximately 50 novel compounds with a diversity of H-bonding enzyme-interacting potential within these classes, biological studies confirmed that significant topo II inhibition was present for 9 lead compounds, in previously unseen pyrazolo[1,5-*a*]pyrimidine, indolo[2,3-*c*]carbazole and branched *S*,*N*-disubstituted thiouracil derivative series. NCI-60 cancer cell line growth inhibition data for 6 representative compounds also revealed interesting selectivity differences between each compound class, while a new pyrimido[5,4-*c*]carbazole agent strongly inhibited cancer cell division at 10 μM, with appreciable cytotoxic activity observed across several tumour types.

Abbreviations/ Definitions

ABCG2	ATP-binding cassette G2 protein
Abl	proto-oncogene protein kinase kinase ABL1
AGC	PKA, PKG and PKC
ALK	anaplastic lymphoma kinase
AML	acute myeloid leukemia
BIM	bisindolylmaleimide
Boc	*tert*-butoxycarbonyl group
Boc_2O	*t*-butoxycarbonic anhydride
BOM	benzyloxymethyl
Brk	breast tumour kinase
n-BuLi	*n*-butyllithium
CAMK	calcium/ calmodulin-dependent protein kinases
CAN	ceric ammonium nitrate
CDK1	cyclin-dependent kinase 1 (or cdc2)
ChAT	Cas/Hef1-associated signal transducer protein
ChK1	checkpoint kinase 1
CK	casein kinase
c-KIT	mast/ stem cell growth factor receptor
c-Met	hepatocyte growth factor receptor
CMGC	CDK, MAPK, GSK3 and CLK kinases
CML	chronic myelogenous leukemia
m-CPBA	*m*-chloroperoxybenzoic acid
CPT	camptothecin
CSK	c-src tyrosine kinase
DBU	1,8-diazabicyclo[5.4.0]undec-7-ene
DCC	dicyclohexylcarbodiimide
DCE	1,2-dichloroethane
DCM	dichloromethane
DDQ	2,3-dichloro-5,6-dicyano-1,4-benzoquinone
DMAD	dimethylacetylene dicarboxylate
DMAP	*N*,*N*-dimethylaminopyridine
DMB	3,4-dimethoxybenzyl
DMDO	dimethyldioxirane
DMF	*N*,*N*-dimethylformamide
DMSO	dimethylsulfoxide
EGFR	epidermal growth factor receptor
EPT	ellipticine
ErbB	erythroblastic leukemia viral oncogene
FGFR	fibroblast growth factor receptor
Flt3	fms-like tyrosine kinase receptor-3
GPCR	G-protein coupled receptor
GSK	glycogen synthase kinase
HER2	human epidermal growth factor receptor 2
HGF/SF	hepatocyte growth factor/ scatter factor
HMPA	hexamethylphosphoramide
HNSCC	head and neck squamous cell carcinoma
IAA	indole-3-acetic acid
ICZ	indolocarbazole
IIQ	indenoisoquinoline

IL-8	interleukin-8
JAK	Janus kinase
JNK	c-Jun N-terminal kinase
KRAS	Kirsten rat sarcoma viral oncogene homolog
LDA	lithium diisopropylamide
LiHMDS	lithium hexamethyldisilazide
MLK	multiple lineage kinase
MOM	methoxymethyl
NBS	*N*-bromosuccinimide
NCI	National Cancer Institute
NRTK	non-receptor tyrosine kinase
NSCLC	non-small cell lung cancer
PDB	Protein Databank
PDGFR	platelet-derived growth factor receptor
PDK	phosphoinositide-dependent kinase
PIFA	phenyliodine bis(trifluoroacetate)
PI3K	phosphoinositide-3-kinase
PKB	Protein kinase B (or Akt)
PKC	Protein kinase C
PMB	*p*-methoxybenzyl
$POCl_3$	phosphorus oxychloride
PPSE	polyphosphoric acid trimethylsilyl ester
$pp60^{v\text{-}rsc}$	proto-oncogene protein 60 (Rous sarcoma virus)
RACK	receptor for activated C-kinase
REB	rebeccamycin
rt	room temperature
SAR	structure-activity relationship
SEM	[2-(trimethylsilyl)ethoxy]methyl
STA	staurosporine
STE	homologs of yeast Sterile 7, 11 and 20 kinases
TBAB	tetrabutylammonium bromide
TBAF	tetrabutylammonium fluoride
TBDMS	*tert*-butyldimethylsilyl
Teoc	2-(trimethylsilyl)ethoxycarbonyl
TFA	trifluoroacetic acid
THF	tetrahydrofuran
THP	tetrahydropyran
TIPS	triisopropylsilyl
TK	tyrosine kinases
TKL	tyrosine kinase-like kinases
T.M	transition metal
TMS	trimethylsilyl
Ts	*p*-toluenesulfonyl group
p-TSA	*p*-toluenesulfonic acid
U.V	ultra-violet
VEGFR	vascular endothelial growth factor receptor
ZAP-70	zeta-chain-associated protein kinase 70
Δ	heat
hυ	electromagnetic radiation
μW	microwave

"A man is as great as the thoughts he thinks,
as the worth he has attained;
As the fountains at which his spirit drinks,
and the insight he has gained"

- *C.E. Flynn*

For Mam and Dad, with all my love

Table of Chapters

Acknowledgments *ii*

Abstract *iv*

Abbreviations/Definitions *v*

1.0 Biological Introduction **1**

2.0 Chemical Introduction **67**

3.0 Aims and Objectives **129**

4.0 Chemical Results and Discussion **134**

5.0 Experimental **206**

6.0 Biological Results and Discussion **276**

7.0 Current Perspectives **301**

Appendices

Chapter 1

Biological Introduction

Contents

1.0 Biological Introduction 2
1.1 Cancer 2
1.2 Importance of indolocarbazole alkaloids 3
1.2.1 Staurosporine – a promiscuous lead for new inhibitor development 5
1.3 Mechanisms of action of indolocarbazoles at the molecular level 6
1.3.1 Protein kinase inhibition: From clinical challenges to selective candidates 7
1.3.1.1 Classification of protein kinases: a target for signal transduction therapy 7
1.3.1.2 Structural basis of ATP-competitive protein kinase inhibition 9
1.3.1.3 Structural features of staurosporine: an ICZ kinase inhibitor template 12
1.3.1.4 Selectivity profile of staurosporine 13
1.3.1.5 Non-STA indolocarbazole TK inhibitors 15
1.3.1.6 Indolocarbazole derivatives as modulators of aberrant cell cycle activity 18
1.3.1.7 PKC inhibition: a new anti-tumour strategy 21
1.3.1.8 Indolocarbazoles as GSK-3β inhibitors 24
1.3.1.9 Conclusion 25
1.3.2 Topoisomerase I inhibition and putative intercalative effects 26
1.3.2.1 Topo I 'poisons' at the DNA-enzyme interface: a potent anti-cancer lead 29
1.3.2.2 Indenoisoquinolines – polycyclic non-CPT intercalatory topo I inhibitors 30
1.3.2.2 DNA binding and topo I poisoning activities of rebeccamycin-type ICZs 31
1.3.2.3 Overview of SAR in ICZ topo I inhibition 34
1.3.2.4 Conclusion 37
1.4 Significant milestones in ICZ research 39
1.4.1 Introduction to the structure-bioactivity paradigm within ICZs 40
1.4.1.1 Bioactivity of ICZs lacking an F-ring 40
1.4.1.2 F-ring variants of ICZs with bridged ribofuranose linkages 42
1.4.1.3 STA analogues containing modified pyranose moieties 43
1.4.1.4 Heterocyclic ring modifications in ICZs 45
1.4.2 Conclusion 48
1.5 Current development of indolocarbazoles as clinical therapeutic agents 49
1.5.1 Bisindolylmaleimides 49
1.5.2 Staurosporine derivatives 50
1.5.3 K-252a derivatives 52
1.5.4 Rebeccamycin derivatives 53
1.6 Final perspective on future indolocarbazole development 55
1.7 References 58

1.0 Biological Introduction

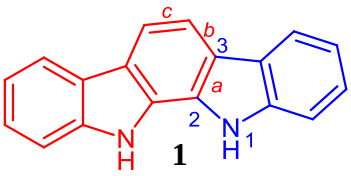
1.1 Cancer

Cancer is a pernicious affliction which affects up to 1 in 3 people at some stage in life. It will also have an increasingly negative impact on global public health based on current trends of higher average life expectancy and elevated incidence of age-related diseases. According to a study by the NCRI, the number of new cases of invasive cancer in Ireland increased from 17,148 in 1994 to 22,775 in 2005, an annual increase of 2.7%; the age-adjusted incidence rate (cases per 100,000 of population) increased by 1.1% annually for women and 0.9% for men over the same period. The largest increases in rate were in prostate cancer (7.1% annual increase), melanoma (3.3%) and breast cancer (2.4%), while increased mortality was also observed in melanoma (4.2%) and colorectal cancer (1.7%).[1] Based on recent projections, the number of new cancer cases in Ireland will double between 2000 and 2020.

The term cancer is applied specifically to a malignant neoplasm. Cells are deemed neoplastic when they fail to respond normally to the usual regulatory signals dictating cell growth.[2,3] This loss of cell control tends to result in excessive, unregulated cell proliferation - forming a lump or tissue mass in solid tumours called a neoplasm. Two types of neoplasm exist: benign and malignant, with the latter requiring that tumour cells attain several capacities, including hyper-proliferation, anchorage and growth-factor independency, evasion of apoptosis, angiogenesis and metastasis.

The continuing quest to unearth a cure or prophylactic vaccine for this formidable collection of over 200 diseases in various tissues is one which has exercised the medicinal chemistry field over the past half-century. However, progress in this area has been rendered painstakingly slow due to the high toxicity of most front-line anti-cancer drug families, non-selective killing of normal somatic cells, and increasingly, development of innate chemotherapeutic resistance, by means of drug efflux pumps and drug metabolism.[4-8] Multidrug efflux pumps, for example, p-glycoprotein, are perhaps the most important contributor to multidrug resistance and are capable of expelling multiple drug classes from within the cell environment. The expression of these pumps can also be upregulated by exposure to a single chemotherapeutic agent.[9-11]

Indolo[2,3-*a*]carbazole (ICZ) **1** was observed over the course of several screening programs to represent a privileged multiple site target scaffold (Fig. 1.1). Interest in anti-cancer ICZ drug discovery has arisen due to the untapped potential of these potent 'lead' compounds to intervene through novel mechanisms in tumourigenesis signaling pathways, cell cycle surveillance, tumour perfusion and even in mediation of multi-drug resistance reversal. The normal roles of these cellular targets are altered in some cancers, wherein dysfunctions have been related to uncontrolled proliferation.[12-20]



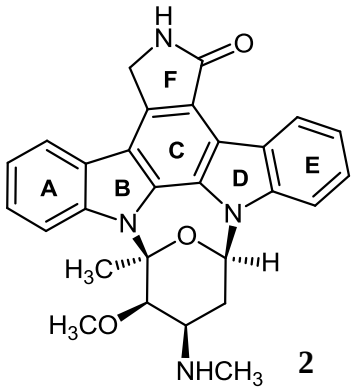
1

Fig. 1.1 Structure of indolo[2,3-*a*]carbazole **1**

1.2 Importance of indolocarbazole alkaloids

"Progress lies not in enhancing what is, but in advancing toward what will be."
- Kahlil Gibran

Initial interest in the possible use of indolocarbazole alkaloids as clinical anti-tumour agents began as a result of the discovery in 1977, by Omura and co-workers, of a natural product aminoglycoside, initially termed AM-2282, and later reclassified as staurosporine **2**, from soil samples containing the actinomycete *Streptomyces staurosporeus*, a filamentous Gram-positive microbe belonging to the phylum *Actinobacteria* (Fig. 1.2).[21]



2

Fig. 1.2

Actinomycetes are widely distributed in terrestrial and aquatic ecosystems, being involved in soil biodegradation and humus formation by the recycling of decomposing organic polymers such as keratin, lignocelluloses and chitin.[22,23] Around 23,000 bioactive microbial natural products have been reported to date; 10,000 of these compounds are produced by actinomycetes, and around 75% of these are derived from *Streptomyces* species - the primary antibiotic-producing organisms in the pharmaceutical industry.[24] Members of this group also

produce clinically useful anti-tumour drugs such as anthracyclines (aclarubicin, daunomycin and doxorubicin), peptides (bleomycin and actinomycin D), mitomycins and others.[25]

Over the last 30 years, metabolites comprising the characteristic indolo[2,3-*a*]pyrrolo[3,4-*c*]carbazole chromophore **3** have also been isolated from bacteria, fungi and invertebrates in diverse geographical locations (Fig. 1.3). In addition to fermentation of other producer strains such as *Streptomyces hygroscopicus* C39280-450-9 (ATCC 53730), *Streptomyces* sp. TP-A0274 and *Streptomyces lividus* ATCC 21178, staurosporine **2** has also been repeatedly isolated from field samples such as marine invertebrates *Eudistoma toealensis* (tunicate) and its predatory flatworm *Pseudoceros* sp.[16,26] In 1992, Kinnel and Scheuer also extracted 11-hydroxystaurosporine **4** and 3,11-dihydroxystaurosporine **5** (minor component) from the Pohnpei tunicate (*Eudistoma* sp.), which were the first ICZs isolated from a marine organism or animal. Both compounds were active against cancer cells, and 11-hydroxystaurosporine **4** was more potent than STA **2** in PKC inhibition.[16,27] K-252c **6** and arcyriaflavin A **7** are important indolo[2,3-*a*]carbazoles produced by the marine actinomycete strain Z$_2$039-2; arcyriaflavin A **7** induced almost 70% apoptosis in a human chronic myelogenous leukemia K562 cell line at 100 μM, while more active K-252c **6** was found to induce greater than 50% apoptosis at 10 μM and nearly 100% at 100 μM, in the same assay (Fig. 1.3).[25,28,29]

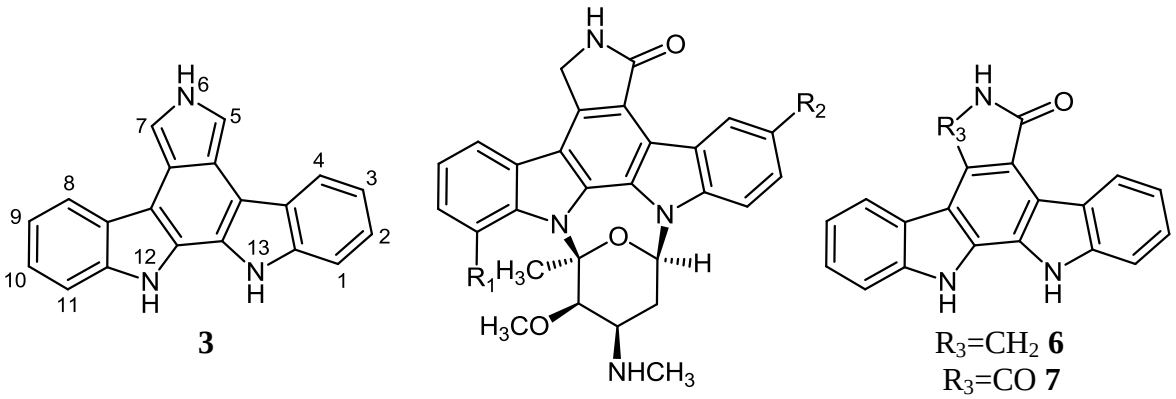
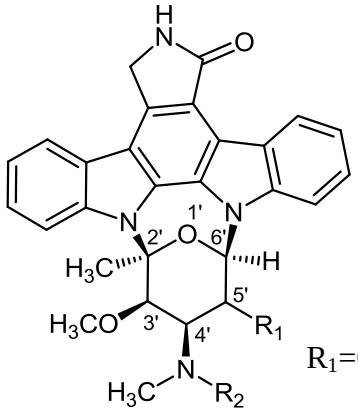


Fig. 1.3

Actinomycetes are ubiquitous from marine sources, being found in symbiosis with different invertebrates, especially sponges, or bioaccumulated through filter-feeding. The relatively unexplored marine ecosystem is a natural laboratory enveloping almost 70% of the Earth's surface and contains a multitude of microbial lifeforms with unique metabolic capabilities evolved over far longer timescales than terrestrial biology. In addition to producing metabolites with anti-tumour and other pharmacological activities, to modulate the chemical

effects of salinity, pressure and temperature in this environment, these compounds also mediate potent biochemical effects on marine eukaryotic organisms, including mammals.[25,30] Staurosporine **2** has been isolated, together with two natural analogues, 4'-*N*-methyl-5'-hydroxystaurosporine **8** and 5'-hydroxystaurosporine **9** from *Micromonospora* sp. L-31-CLCO-002, obtained from a homogenate of the sponge *Clathrina coriacea* collected from Fuerteventura Island in the Canary Islands, and were five times more active than staurosporine **2** *in vitro* against colon adenocarcinoma HT29 cell line (Fig. 1.4).[31]



R_1=R_2=H **2**
R_1=OH; R_2=CH_3 **8**
R_1=OH; R_2=H **9**

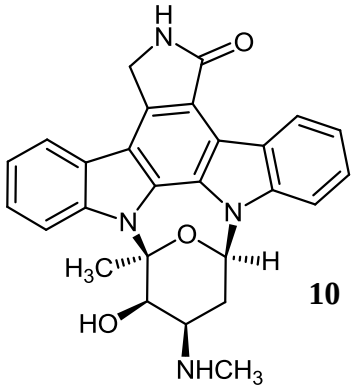
Fig. 1.4

Total synthesis of indolocarbazole analogues derived from actinomycetes is of critical importance due to ongoing pharmaceutical research into their SAR profiles, as well as practical difficulties in bioprospecting and culturing inefficient producer microorganisms, in order to access these congeners in sufficient multigram quantities for clinical trials.

1.2.1 Staurosporine – a promiscuous lead for new inhibitor development

Biosynthesis of **2** from two units of tryptophan, along with a glycosyl residue derived from glucose and methionine, is widespread among actinomycetes and has been frequently 'rediscovered' in various natural product screening assays due to the wide range of biological potencies across multiple targets displayed by this compound.[25] These effects include strong anti-fungal and hypotensive activity, inhibition of platelet aggregation and potent cytotoxicity in cell cultures of murine macrophage P388D1 (IC_{50} = 0.01 μg/mL), human lung adenocarcinoma A549 (IC_{50} = 0.0005 μg/mL) and melanoma SK-MEL-28 cell lines (IC_{50} = 0.001 μg/mL).[31] Additionally, natural and synthetic analogues of staurosporine **2** have been implicated in other mechanisms of neuroprotection, insecticidal activity, immunosuppression and reversal of multidrug resistance.[20,21,32-35] An important breakthrough in this field was achieved in 1986, when **2** was found to be a nanomolar PKC inhibitor *in vitro*, and subsequently exhibited non-specific activity against at least 12 kinase targets including GSK-3β, CDK-2, MAPKK and PI3K.[33]

This high level of nonspecific toxicity is due to the fact that the catalytic domain of PKC is highly homologous to similar domains found in other protein kinases (e.g. $pp60^{v\text{-}src}$, cAMP-dependent protein kinase A, casein kinase etc.), each of which is critical for normal cell operation.[34,36] Following determination of its absolute configuration by X-ray crystallography, staurosporine **2** was identified to closely mimic adenosine within the conserved ATP binding pocket, interfering in ATP-dependent cell homeostatic processes, and thus eliciting complex biological activity and toxicity profiles *in vivo*.[16,37,38]



10

Fig. 1.5

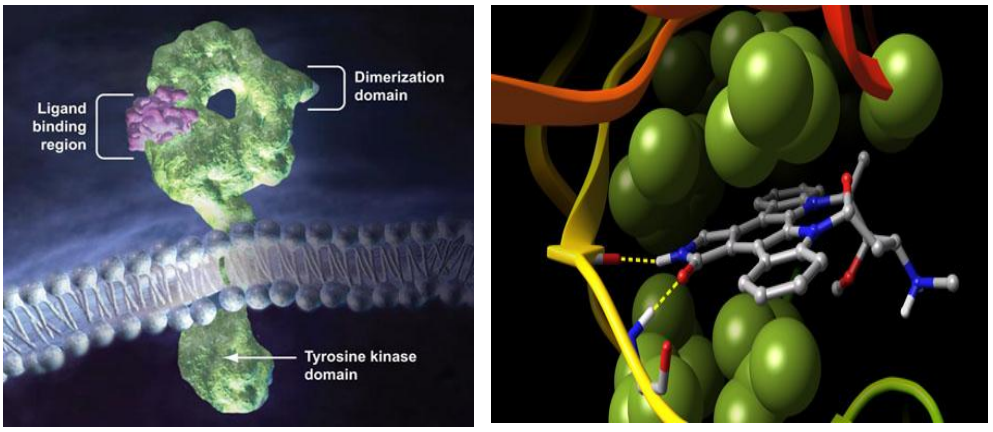
Illustrating the pharmaceutical potential derived from modified biosynthetic pathways, a blocked mutant of *S. longisporoflavus* R19 afforded 3'-desmethylstaurosporine **10** – a less potent PKC inhibitor than **2**, which selectively inhibited PKC subtypes α, β-2 and γ (Fig. 1.5).[39] Synthetic endeavours have also derived numerous active congeners with improved solubility, cell permeability and enhanced tumour cell line specificity. However, translation of indolocarbazole agents to the clinical milieu has been impaired due to an absence of complete molecular biology data for these compounds, as current deficiencies in the pharmacological profiles of these candidates extend to a lack of target enzyme specificity, as will be described, and perhaps other as yet unidentified modes of action *in vivo*.[40-43]

1.3 Mechanisms of action of indolocarbazoles at the molecular level

Active ICZ analogues possess immense potential to mediate anti-cancer effects through either kinase or topoisomerase inhibition. Since these enzymes perform a wide variety of regulatory roles orchestrating a vast repertoire of cellular responses, a discussion of how specific small-molecule inhibitors achieve desirable therapeutic outcomes is of immense benefit for design of selective ICZ analogues imparting improved therapeutic results based on these effects.

1.3.1 Protein kinase inhibition: From clinical challenges to selective candidates

In the field of target identification there has been a great deal of enthusiasm for the prospect of identifying novel drug targets based on knowledge of key signal transduction components and their links to disease. Protein kinases modulate intracellular signal transmission by phosphorylating a hydroxyl group of residues in target proteins which are involved in signal pathways, with acute relevance to cancer, diabetes, immune system disorders, neurodegenerative disorders, cardiovascular disease and inflammation (Fig. 1.6).[44,45]

(a) 

(b)

Fig. 1.6 (a) Transmembrane structure of HER (RTK); (b) Molecular model of staurosporine **2** within CDK2 binding pocket.[46,47]

Protein kinases constitute 22% of the medicinal genome, and a critical drug target in the post-genomic 21st century landscape. As knowledge of the 518 enzymes that comprise the human 'kinome' advances towards clinical applications, small-molecule kinase inhibition is now at the forefront of anti-cancer drug development, due to the current urgent need for versatile 'single-target' anti-tumour therapies to overcome resistant cancers.[45,48,49]

Signal transduction therapy achieves this aim by modulating individual upstream kinases across a number of families, discussed below, which participate in errant pathways leading to cancer progression, hyperproliferation and cell cycle evasion, with minimal interference on normal cell processes involving other kinases, and thus reducing the overall burden of systemic cytotoxicity within normally dividing somatic cells.[50,51]

1.3.1.1 Classification of protein kinases: a target for signal transduction therapy

Genes coding for protein kinases constitute 1.7% of the total number of human genes and are one of the largest and most functionally disparate gene families in nature, as they control the location and synchronised function of proteins, maintaining cellular homeostasis and orchestrating the flow of ubiquitous cellular processes. Kinases regulate normal signal

transduction from extracellular stimuli to intracellular signalling pathways by catalysing the transfer of the γ-phosphate group of adenosine triphosphate (ATP) **11** to the hydroxyl group of a peptide residue, affording a new phosphopeptide and adenosine diphosphate (ADP) **12**.[52] In the case of membrane-bound RTKs, binding of a ligand to the extracellular domain induces receptor dimerisation and ATP-mediated mutual transphosphorylation of a phosphate-acceptor tyrosine residue (E-OH→E-PO_4^{3-}). The active enzyme phosphorylates downstream signalling proteins (i.e. protein 'X' in Fig. 1.7) *via* its intracellular catalytic site and thus, elicits a vast array of cellular responses through initiation of multiple pathways. Activation of a corresponding transcription factor results in enhanced cell growth and proliferation, and in aberrant oncogene expression, this chain of events is a key influence on tumourigenesis (Fig. 1.7).[50]

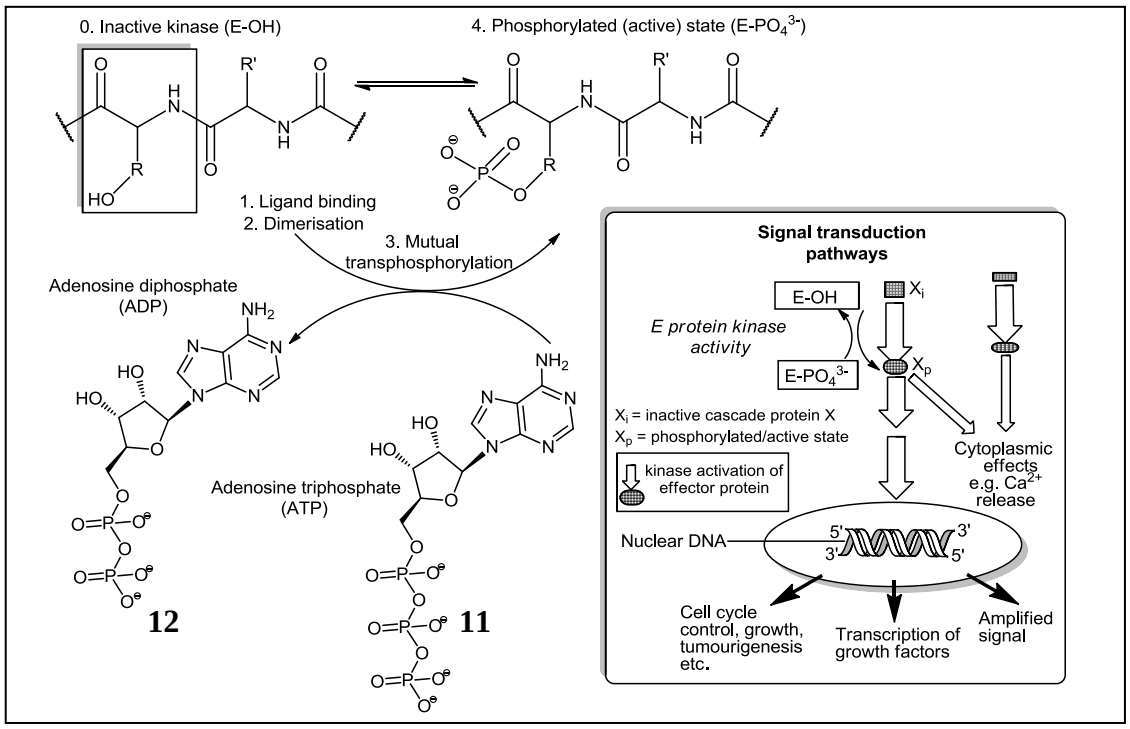


Fig. 1.7: Molecular and supramolecular regulation of signal transduction by kinase-mediated protein phosphorylation (RTK) in the presence of ATP.

The importance of kinase activity in cell metabolism was recognized in 1992, when Krebs and Fischer were awarded the Nobel Prize in physiology/medicine 'for their discoveries concerning reversible protein phosphorylation as a biological regulatory mechanism'.

The absolute indispensability of kinase functions is demonstrated by the conservation of over 50 distinct kinase families through sequence alignment between yeast, invertebrate and mammalian kinomes (Fig. 1.8). Of the 518 human protein kinases, 478 constitute the

'typical' kinase superfamily, known through sequence homology and their ability to transfer a phosphate group *via* conserved catalytic domains.

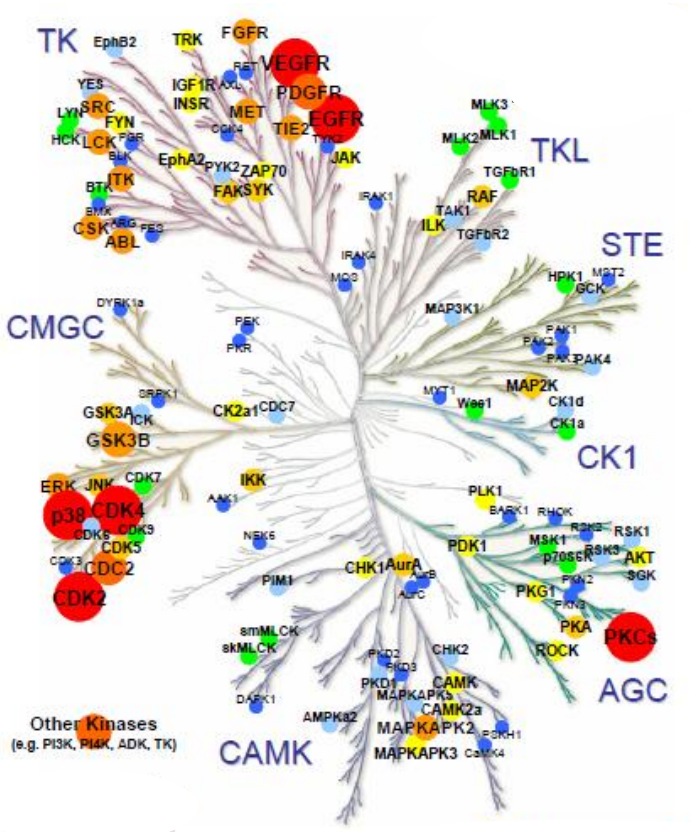


Fig. 1.8: Phylogenetic relationship between human protein kinases, illustrating the location of critical targets for kinase modulating therapy.[35]

Further phylogenetic studies led to differentiation of these kinases into 6 distinct groups catalysing phosphorylation of a Ser/Thr residue, and tyrosine kinases (TKs), that catalyse transfer of a phosphate group from ATP to a tyrosine residue of a substrate peptide (Fig. 1.8).[53]

Furthermore, each group can be sub-divided into families and sub-families, e.g. based on sequence identity, substrate type and structure of extracellular domains. A genetic map known as a dendrogram graphically illustrates this classification; the distance between two main branches correlates with mutual evolutionary divergence, and variation of catalytic site sequences. In the context of this discussion, ICZ congeners have been observed to confer inhibition across a wide variety of enzyme families, from distinct kinase groups.[33,35,38,54,55]

1.3.1.2 Structural basis of ATP-competitive protein kinase inhibition

Eukaryotic protein kinases comprise approximately 250-300 amino acid residues, and are characterised by the appearance of a number of highly conserved functional subdomains.[56]

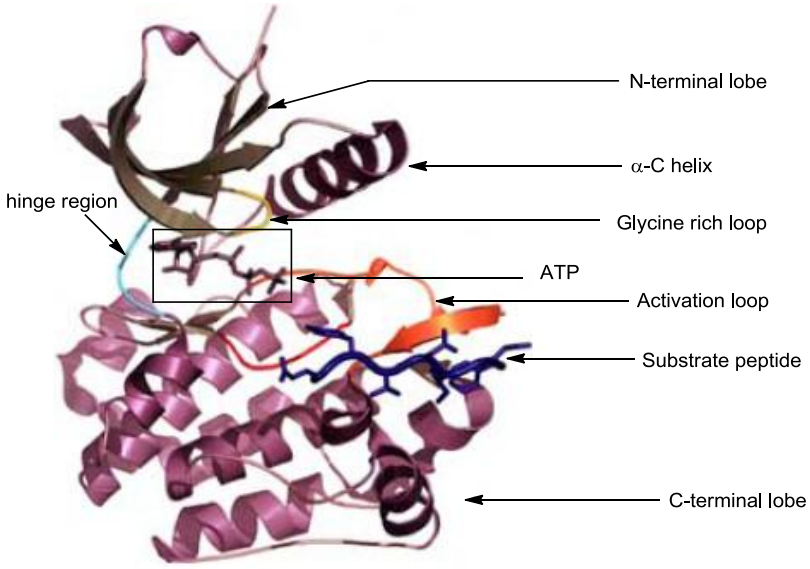


Fig. 1.9: Crystal structure of ATP **11** bound within kinase site (substrate peptide is coloured blue).[57]

Numerous X-ray crystal structures of kinases have identified discrete N and C-terminal lobes, with both ATP **11** and substrate-binding sites located in the interlobular cleft (hinge region) (Fig. 1.9).[58] Of particular interest, e.g. in PKA, is the flexible glycine-rich loop as well as Lys72 (catalytic region) and Glu91 (activation segment) residues which form a salt bridge within the enzyme active site, with an important regulatory role in correctly orientating ATP for kinase activity (Fig. 1.10).[52,53]

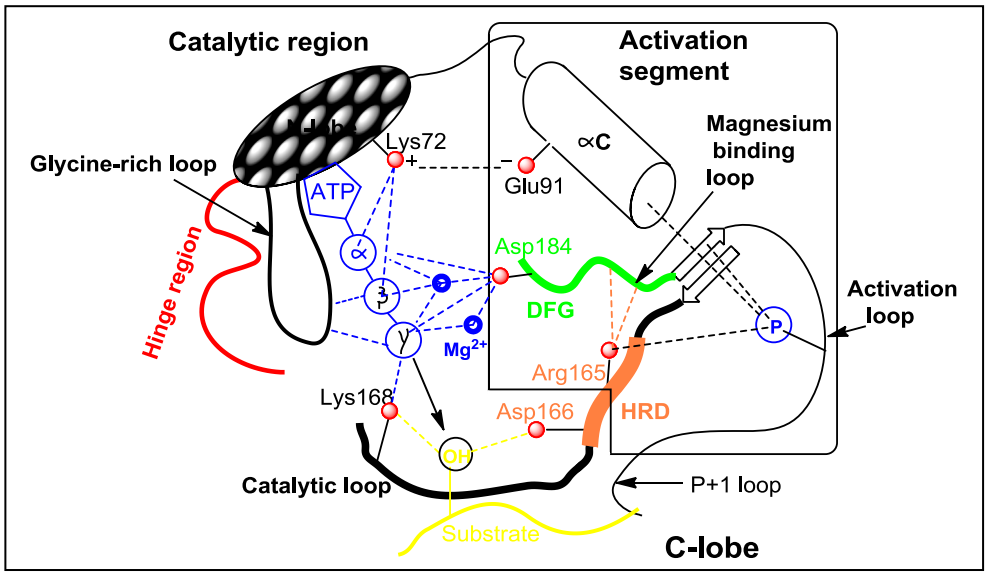


Fig. 1.10: Schematic of kinase phosphorylation activity and critical active site interactions in PKA.[52]

Other essential residues in the 'DFG' motif (magnesium binding loop), e.g. Asp184 in PKA, also confer a strong conformational influence, by co-ordinating Mg^{2+} within the ATP phosphate binding region, as illustrated in Fig. 1.10. In addition, the HRD catalytic motif (Arg165 and Asp 166 in PKA), catalytic loop and α-C helix also comprise residues

maintaining the catalytic orientation of the ATP **11** γ-phosphate, and several regulatory autophosphorylation sites are also located within the activation loop region.[52,56]

The ATP-binding pocket consists of the 38 residues known to interact with protein kinase inhibitors through multiple alignment of PDB kinase crystal structures in complex with these agents.[58] These residues are close in space but not necessarily close in primary sequence. The adenine binding region, ribose pocket and phosphate region were identified based on crystal structures containing ATP **11**. The surrounding hydrophobic pocket I, hydrophobic pocket II or 'gatekeeper' pocket, and solvent accessible regions were discovered in kinase crystal structures with ATP-competitive inhibitors (Fig. 1.11).

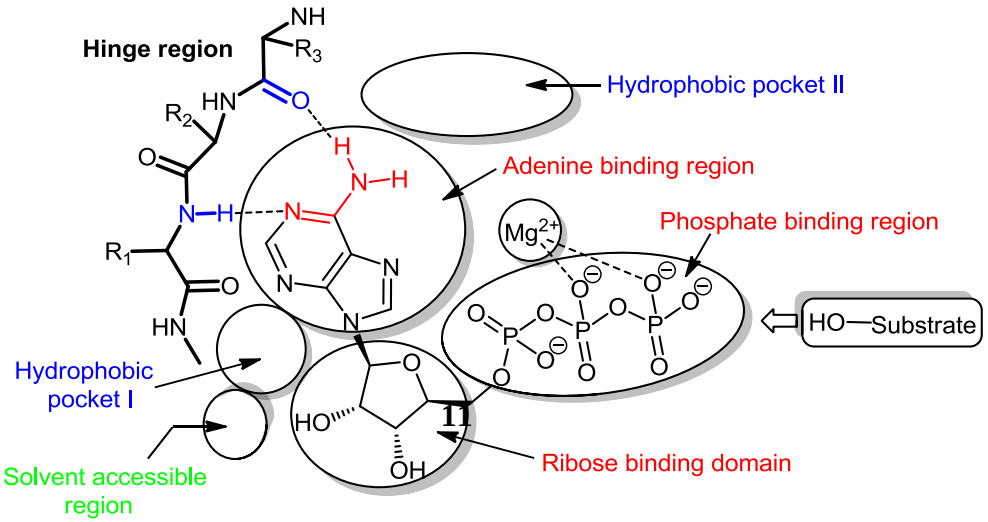


Fig. 1.11: Schematic of ATP **11** binding motif present in catalytic sites of protein kinases.[45]

An expanded region of the ATP-binding site displayed in Fig. 1.11 contains an essential adenine pocket which forms two H-bonds to the protein backbone, ribose and phosphate binding sites, and two hydrophobic regions, containing less conserved, non-polar residues.

Following initial kinase catalytic activation, docking of associated signaling proteins potentiates downstream signalling cascades, invoking their biological response.[59] In the inactive kinase conformation, residues within the activation loop motif are orientated towards the 'activation segment' and occlude ATP **11**-Mg^{2+} binding. However, ligand-induced phosphorylation may release this constraint by directing these residues away from the active site, ordering stable formation of other activating non-covalent interactions (Fig. 1.12).[45,60]

Binding of inhibitors to inactive kinase conformations is highly attractive as they incorporate more structural diversity even within kinase subfamilies than their corresponding active conformations and therefore demonstrate increased scope for innate selectivity.[61] However,

development of novel kinase inhibitors of this type has been difficult due to the lack of available binding assays and mechanistic data regarding binding sites of inactive conformations.[45]

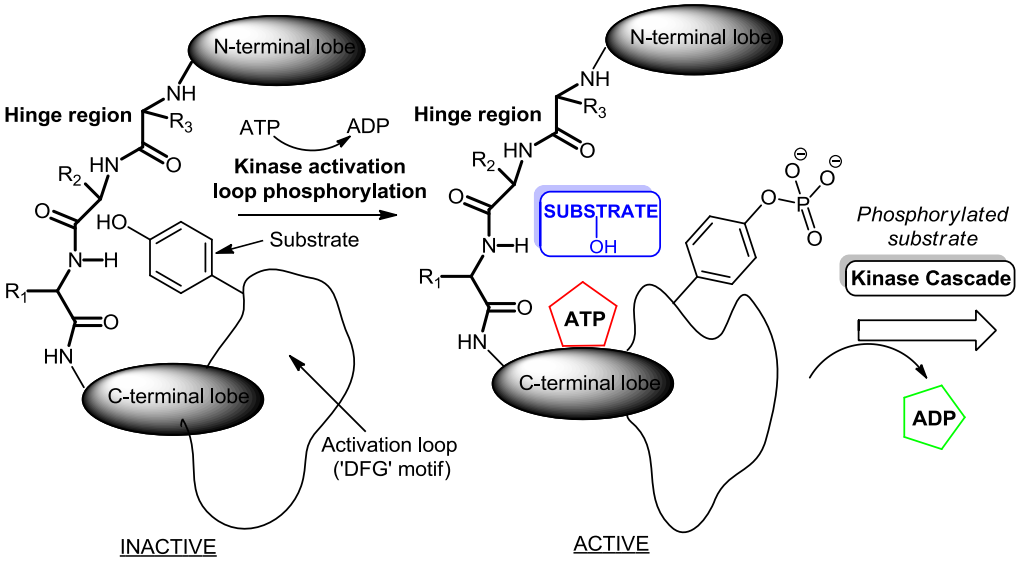


Fig. 1.12: Conformational effect of 'activation loop' phosphorylation on kinase catalysis.[45]

1.3.1.3 Structural features of staurosporine: an ICZ kinase inhibitor template

As mentioned previously, due to its extended planar chromophore and propitious hydrogen bonding network, staurosporine **2** occupies the nucleotide-binding region and closely mimics the hydrogen bonding network of adenine with conserved hinge region residues. In addition extensive hydrophobic contacts are formed with relatively variable non-polar side chains in buried domains not occupying ATP **11** (c.f. Fig. 1.11).[57]

Accommodation of optimised ligands in these unique buried regions and induced-fit interactions with flexible loop regions (activation loop, glycine-rich loop, e.g. pyranose ring O in **2** with Gly365 in the ZAP-70 complex, etc.) are the two major determinants of inhibitor selectivity.[62-64] The three nucleotide-binding (adenine, sugar and phosphate) domains are not characterized by large amino acid variability and thus constitute a poor target for obtaining overall specificity.[35,45,65]

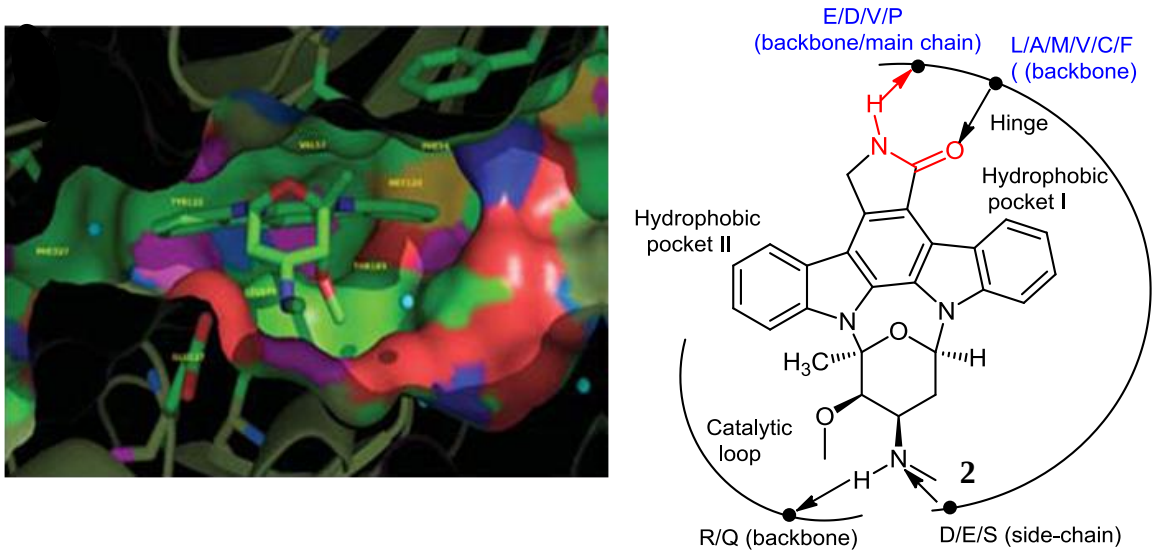


Fig. 1.13: Orientation of inhibitor **2** within ATP-binding protein kinase active site (ZAP-70).[35]

Conceptual concerns regarding enhanced specificity of staurosporine **2** analogues have been somewhat allayed by recent three-dimensional crystallographic (>40 kinase domains co-crystallised with **2** are reported in the PDB) and site-directed mutagenesis studies, illustrating universal characteristics of inhibition.[35] These highly conserved molecular interactions include hydrogen bonds involving backbone atoms (CO and NH) of two hinge residues, (one of which is highly conserved as glutamate) anchoring the lactam or maleimide ring moiety to the enzyme hinge region.[57] Other essential hydrogen bonds involve the methylamino nitrogen of the perpendicular glycosidic ring bound in its active boat conformation: one to the backbone of a catalytic loop residue, and the other to a polar side-chain from a residue C-terminal to the hinge (Fig. 1.13).[35]

1.3.1.4 Selectivity profile of staurosporine

Despite its promiscuous binding nature, staurosporine **2** also exhibits a pattern of selectivity between some closely related protein kinases, and the origin of these effects may permit design of more selective ICZ analogues.[35] The position of **2** in the ATP-binding pocket of CSK almost exactly matches the relative position of this chromophore (as well as perpendicular conformations of aminopyranose moiety) in the PKA structure described by Prade *et al.*, yet micromolar inhibitor concentrations are necessary to reduce CSK enzyme activity by 50% (IC_{50}) whereas only nanomolar concentrations of **2** are required for equipotent inhibition of PKA or CDK2 (Fig. 1.14).[47,65]

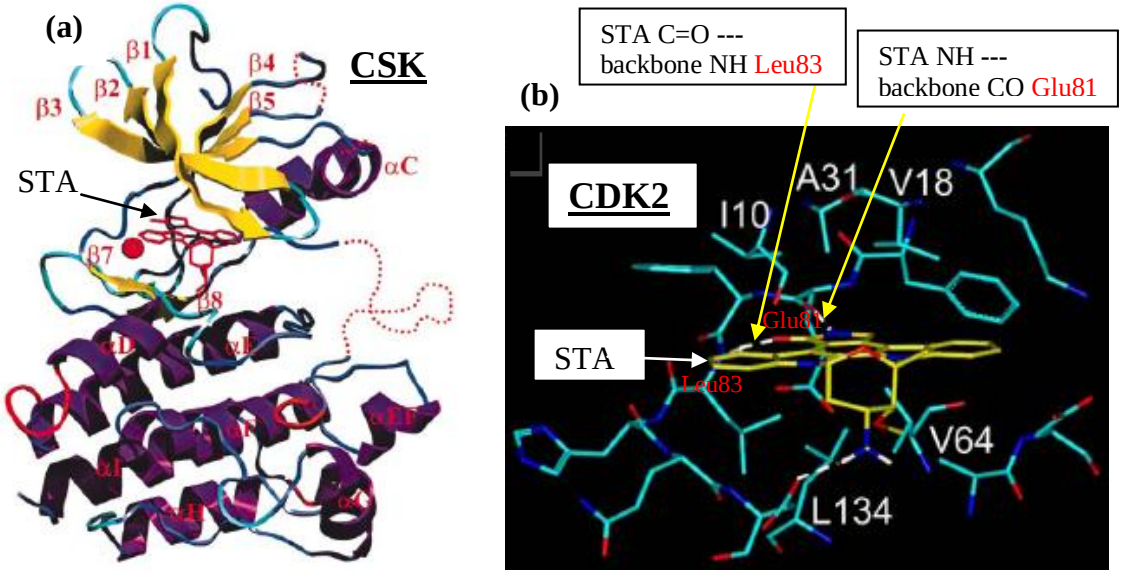


Fig. 1.14: Inhibitory binding mode of **2** within co-crystallised CSK and CDK2 protein complexes.[58,66]

The enhanced interaction energy resulting from more stable inhibitor hydrogen bonding is a fundamental contribution to $>10^3$-fold greater binding affinity in PKA. Staurosporine **2** can only make three hydrogen-bond contacts with CSK as opposed to the four possible in PKA (c.f. CSK structure (a), Fig. 1.14). These are the lactam carbonyl group O30 to the backbone amide group of Met269 (equivalent to Val123 in PKA), the N19 lactam ring amide hydrogen bond donating to the Glu267 backbone carbonyl group (equivalent to Glu121 in PKA) and the methylamino, N31 hydrogen bond donating to the Arg318 backbone carbonyl group (equivalent to Glu170 in PKA). The missing hydrogen bond would be formed between N31 and the side-chain of Glu127 in PKA and Asp86 in CDK2.[66,67]

Similarly, STA **2** is a low nanomolar inhibitor of CDK2/cyclin A (IC_{50} = 8 nM), but only inhibits casein kinase I (CKI) with an IC_{50} value of 3.4 µM (CDK2 structure (b), Fig. 1.14).[58] Structural changes in CKI, reducing STA **2** affinity, to account for this difference include:

- Substitution of bulkier Ile26 (CKI) for highly conserved Val18 (CDK2)
- Substitution of a rare and less flexible Pro69 (CKI) for Val64 (CDK2)[58]

In addition, despite substantial sequence similarity in two tyrosine kinases (EGFR and HER2), EGFR is inhibited by **2** at low nM concentrations, but HER2 remains unbound even at 10^5 nM concentration, perhaps due to conformational changes disfavouring inhibitor binding.[35]

The ability of ATP-competitive staurosporine **2** analogues to predominantly afford polar interactions with highly conserved backbone amide bonds, including an induced fit between

the backbone amide of the first glycine of a glycine-rich loop and the ether oxygen of the glycosidic ring present in **2** is a key component of its unselective inhibition.[33,57] Conversely, hydrophobic interactions within the ATP-binding region involve more variable side-chain groups, indicating that regioselective installation of lipophilic substituents at key positions of the chromophore, affirmed to interact with these recognition residues may confer optimal selectivity.[45,58,68] Thus, global analysis of kinase domains in complex with staurosporine **2** has shown that binding affinity is intimately correlated with two factors: the size of the 'gatekeeper' residue (hydrophobic pocket II), and the distance between the first Gly of the glycine-rich loop and the Asp of the DFG loop – a measure of the closure of both lobes.[35,65]

Further investigation into why staurosporine **2** does not inhibit certain kinases may also reveal how low potency can be overcome through mediation of novel structural reorganisation proximal to the ATP **11** binding site. In 2009, Shomin *et al.* reported that STA **2** covalently linked to a cyclic PKA substrate peptide displayed >60 times greater potency towards PKA, compared to staurosporine **2** alone. This bivalent linker (BL) strategy was also reported to be readily applicable to user defined warhead fragments, i.e. more selective small-molecule inhibitors, and exhibited activity employing long linkers, indicating that the peptide moiety may be binding to allosteric sites rather than an adjacent substrate site – a novel mode of inhibition with the capacity to discriminate between kinases while exploiting avid ATP-competitive binding within the ICZ chemical class.[69,70]

1.3.1.5 Non-STA indolocarbazole TK inhibitors

Due to its promiscuous kinase inhibition, staurosporine **2** possesses therapeutic limitations due to its off-target effects. However, extensive investigation of the indolocarbazole scaffold has identified several derivatives with advantageous kinase activity profiles. An important target for a number of these compounds is the TK family, comprising several kinases with dysfunctions implicated in cancer. Tyrosine kinases can be classified into receptor and non-receptor types, and over 20 members of this class are currently being evaluated for therapeutic inhibition in malignant and non-malignant diseases.[3,49,71,72]

1.3.1.5.1 K-252a – c-Met kinase inhibitor

An important RTK, c-Met, constitutes an attractive target in cancer therapy, owing to involvement in migration, angiogenesis, invasion and metastasis. An activating point mutation of the receptor has been suggested to exist in aggressive hereditary papillary renal carcinoma, as well as metastatic HNSCC and gastric carcinoma, associated with a poor

prognosis.[49] Cyclofuranosylated indolocarbazole K-252a **13** has recently been demonstrated to inhibit c-Met phosphorylation in a cellular assay, and causes reversion of tumorigenicity in fibroblasts transformed with an oncogenic form of c-Met. K-252a **13** binds in the adenine pocket of c-Met in a similar F-ring manner to structures of PKA and CDK2 co-crystallised with staurosporine **2**. However, the c-Met-K-252a **13** complex possesses three additional hydrogen bonds, unique to the ribofuranosylated fragment in contrast to the 4'-methylamino-pyranose moiety in **2**, as illustrated in Fig. 1.15. In common with STA **2** binding, the glycosyl ring oxygen also approaches within 3.7Å of the α-carbon of Gly-1085 within the catalytic glycine-rich loop, affording a possible CH-O polar interaction.[60,73]

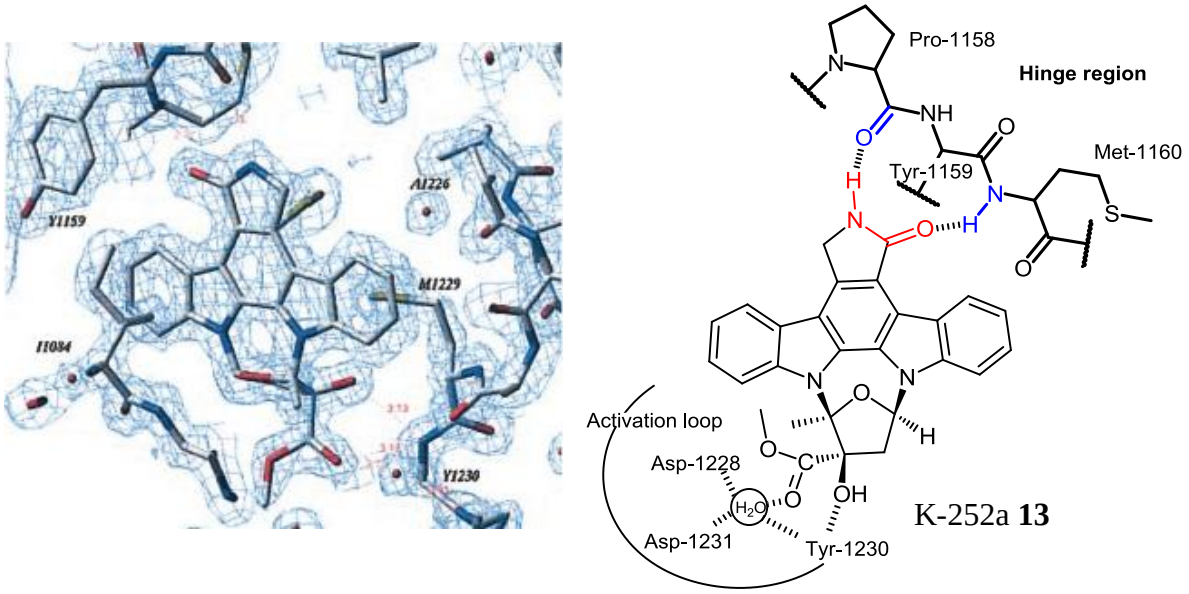


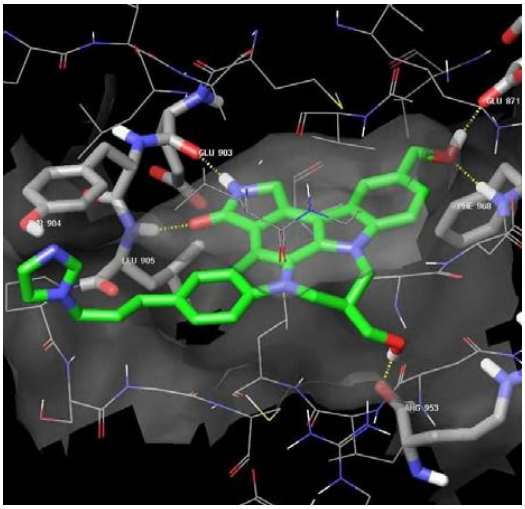
Fig. 1.15: Crystal structure of c-Met in complex with K-252a **13**[60]

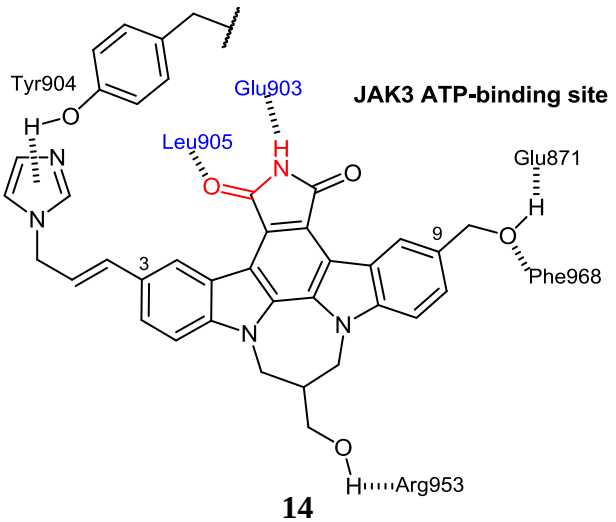
1.3.1.5.2 C-3 and C-9 substituted indolocarbazoles – JAK inhibitors

Janus kinases (JAKs) are important soluble NRTKs that play a role in cytokine-mediated lymphocyte development and correspondingly, inhibition may be therapeutically useful in immunological defects such as organ transplant rejection, allergy and asthma.[68,74] In 2006, Yang *et al.* successfully elaborated the JAK inhibitory pharmacophore of the pan-kinase inhibitor, stauosporine **2**, by means of ring simplification and indole ring substitutions (C-3 and C-9). This endeavour resulted in formation of indolocarbazole **14**, which inhibited JAK 3 with an IC_{50} value of 3 nM, albeit with poor solubility.[68]

Modeling indicated that **14** adopted a typical bidentate hydrogen-bonding mode with the JAK3 backbone at the ATP **11** adenine binding segment (hinge region); the lactam NH interacts with the carbonyl oxygen of Glu903, while the carbonyl oxygen contacts the amide

nitrogen of Leu905. The hydroxymethyl on the aliphatic ring within **14** forms a hydrogen bond with the side chain of Arg953, and the C-9 hydroxymethyl side chain was implicated with this low single digit nanomolar activity due to its orientation inside a small binding pocket to form hydrogen bonds with Glu871 and Phe968 (Fig. 1.16).[68]



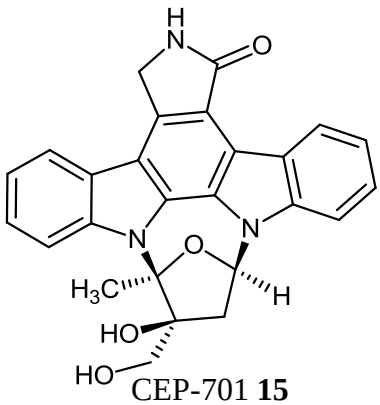


14

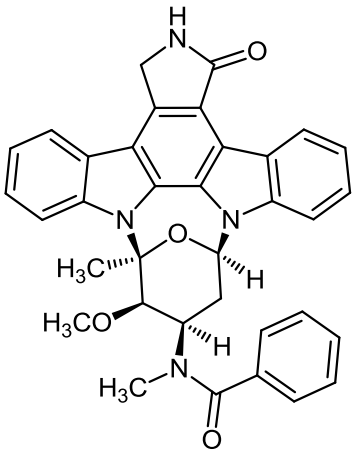
Fig. 1.16: Selectivity pattern illustrated by crystal structure of **14** in complex with JAK3 active site.[68]

1.3.1.5.3 Clinical indolocarbazole candidates as Flt3 inhibitors

Indolo[2,3-*a*]carbazoles are notably effective against several tumours characterized by genetic abnormalities, such as CML, where approximately 30% of patients, with poor prognosis, have a hyper-activating gain of function (GOF) mutation in RTK Flt3. CEP-701 **15** and midostaurin **16** are currently in phase I and II trials against AML, due to their attractive anti-proliferative activity in Flt3-mutant receptor cells, with no adverse effects on cells expressing the wild-type enzyme (Fig. 1.17).[49,75] Preliminary results also indicate that disease remission is highly successful in the presence of Flt3 dysfunction.[76] In addition, midostaurin **16** has entered phase I trials in the treatment of solid tumours.[77]



CEP-701 **15**



midostaurin **16**

Fig. 1.17

1.3.1.6 Indolocarbazole derivatives as modulators of aberrant cell cycle activity

Recognition that protein phosphorylation events underpin control of cell cycle transitions in a precisely co-ordinated and sequential fashion in dividing somatic cells dates back to the 1970s, with the ground-breaking research of Lee Hartwell, Paul Nurse and Tim Hunt.[78,79]

Cell cycle regulatory kinases display complex, synchronised roles in normal cell-cycle modulation, with cell cycle kinase perturbation having causal links to cancer (Fig. 1.18).[2,80]

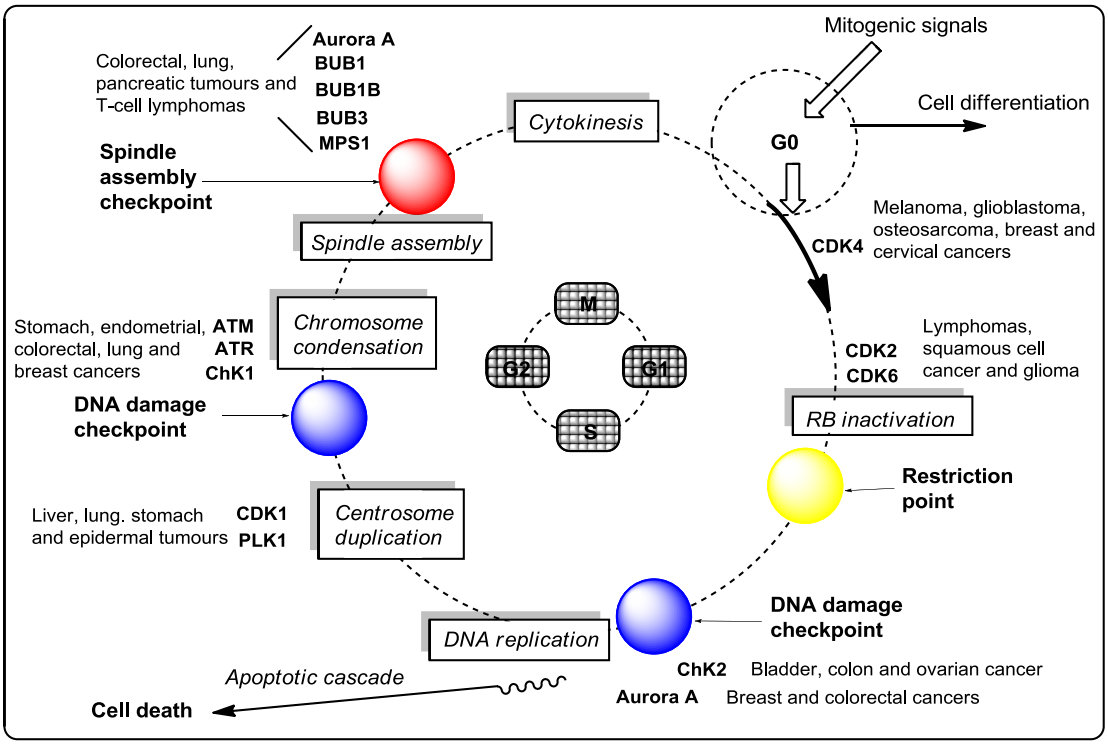


Fig. 1.18: Cancers associated with specific genetic alterations of cell cycle-related enzymes; CDK inhibitors (G1, S, G2), ChK inhibitors (G1, G2), Topo I (S), Topo II (S, G2).

Illustrating this phenomenon, inhibition of cyclin D1-CDK4 results in selective G1 arrest, prior to S phase, thus preventing replication of damaged DNA.[81] It was also reported that IC_{50} values for indolocarbazole inhibitors of purified cyclin D1-CDK4 correlated with anti-proliferative IC_{50} values against colon carcinoma cell line, HCT-116, following incubation for 24 hours.[82]

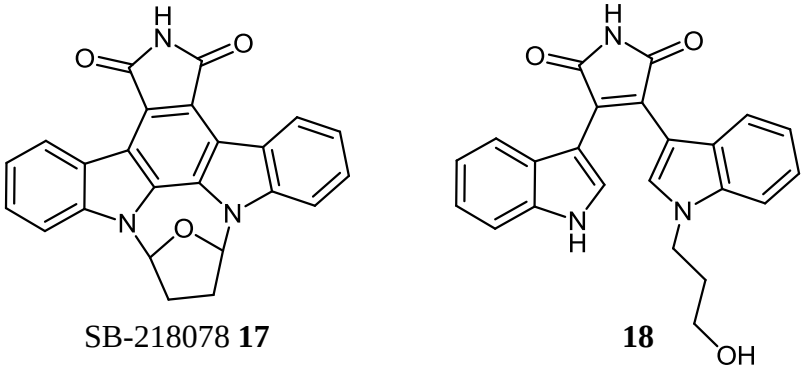
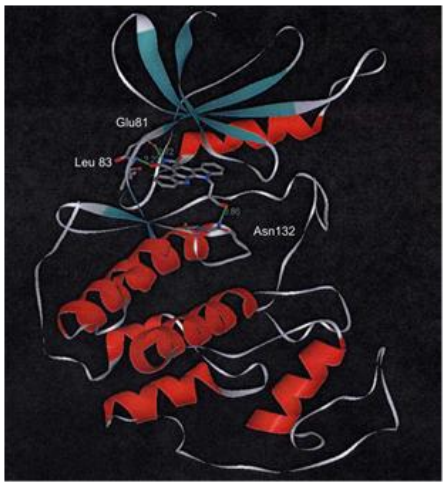
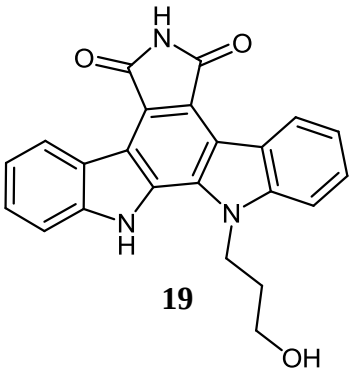


Fig. 1.19 SB-218078 **17** **18**

SB-218078 **17**, a ChK1 (K_i = 15 nM) and PKC inhibitor, also demonstrated a potent D1-CDK4 inhibitory effect (IC_{50} = 0.54 μM) (Fig. 1.19).[35] Sanchez-Martinez and co-workers also reported that aromatized ICZ congeners conferred between 8 and 42 times greater cyclin D1/CDK4 potency than their corresponding BIM analogues, e.g. 3-hydroxypropyl BIM **18** (D1/CDK4 IC_{50} = 1.17 μM), compared with the indolocarbazole derivative **19** (D1/CDK4 IC_{50} = 0.07 μM).

Flow cytometry analysis also demonstrated that active ICZs elicited G1 arrest and a decrease in S and G2/M populations, within 24 hours, whereas BIMs produced G2/M accumulation.[82] A crystal structure of the ATP binding pocket of another cell cycle kinase, CDK2, in the presence of **19** (cyclin E/CDK2 IC_{50} = 0.18 μM) revealed the bidentate hydrogen bonding between the maleimide carbonyl group and backbone NH of Leu83, as well as interaction of the imide NH with the backbone carbonyl group of Glu81 (Fig. 1.20).[82]

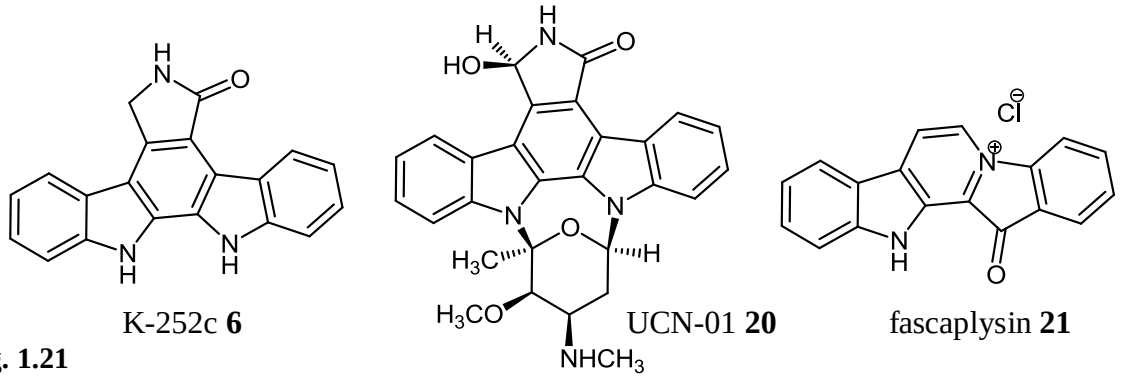




19

Fig. 1.20: Structure of CDK2 co-crystallised in the presence of hydroxypropyl ICZ analogue **19**.[82]

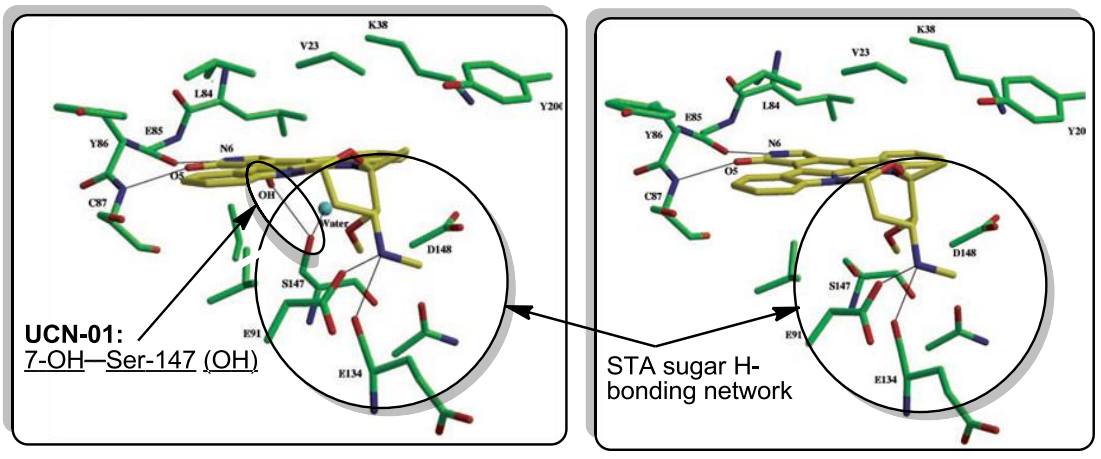
Another natural metabolite from *Streptomyces* species, 7-hydroxystaurosporine (UCN-01) **20,** is a potent PKC inhibitor (IC_{50} = 30 nM). It also selectively targets tumour suppressor p53 deficient, G1 checkpoint-defective cancer cells resulting in S or G2 checkpoint-mediated arrest and mitotic catastrophe *via* accumulation of irreparable DNA damage (Fig. 1.21). Similar to STA **2** and SB218078 **17**, UCN-01 **20** is also a potent inhibitor of ChK1 (K_i = 5.6 nM), but interestingly, confers decreased activity against CDKs (CDK1; K_i = 95 nM, CDK2; K_i = 30 nM, CDK4; K_i = 3.6 μM).[35]



K-252c **6** UCN-01 **20** fascaplysin **21**

Fig. 1.21

The origin of this selectivity is the energetically favourable hydrogen bond formed with Ser147 in ChK1.[64] This interaction is absent in both staurosporine **2** and SB-218078 **17** inhibitor complexes. In addition, the 7-OH group in **20** forms an unfavourable hydrophilic-hydrophobic contact within the CDK2 hinge region, while UCN-01 **20** is also unable to stabilise the activation loop through formation of any sugar-residue hydrogen bonds (Fig. 1.22).[35] In contrast to UCN-01 **20** and STA **2**, SB218078 **17** possesses a tetrahydrofuran ring and does not have a H-bonding methylamine group. However, SB218078 **17** is almost as potent as STA **2** in inhibiting ChK1 and CDK2 activity, indicating that retention of a lactam/maleimide H-bonding scaffold and hydrophobic planarity is most essential for efficacious inhibition.[35,63]

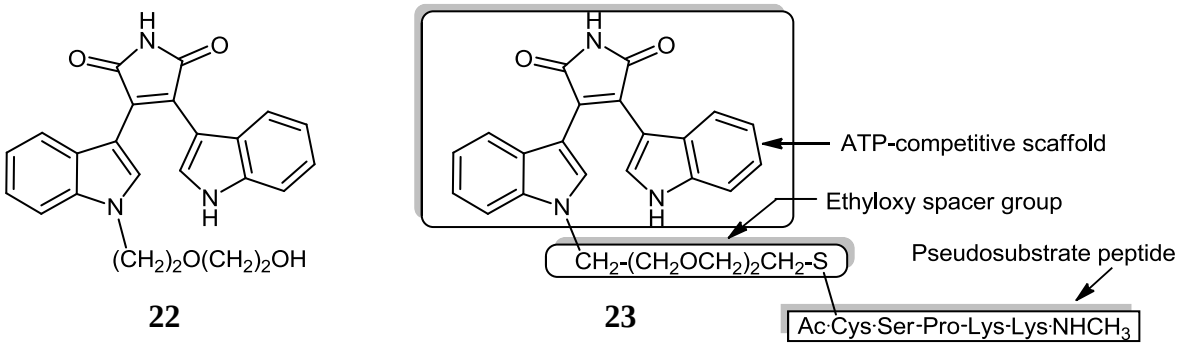


(a) (b)

Fig. 1.22:(a) Origin of UCN-01 **20** selectivity in ChK1; (b) STA **2** lacks key C7 H-bond donor.[63]

Various compounds derived from the indolo[2,3-*a*]carbazole framework present in staurosporine, e.g. K-252c **6**, have also been reported as potential CDK inhibitors, leading to significant G2 arrest, presumably due to inhibition of downstream cell cycle-related kinases.[18,82] Structurally related to this chemical series, the marine sponge pigment, fascaplysin **21**, has also been identified as a CDK4-selective inhibitor (Fig. 1.21).[83]

It may be possible to overcome the limitations of high cellular ATP concentration ($[ATP]_i$ = 3 mM) imposed upon conventional kinase inhibitors, as well as the inherent selectivity problem, by introducing bivalent inhibitors combining an active 'anchor' inhibitor tethered to a short peptide sequence incorporating a recognition motif *via* flexible spacer groups. This approach affords a dual high affinity competitive inhibitor of both ATP **11** and peptide substrates (Fig. 1.23).[69,70] Introduction of peptide pseudosubstrate into compound **22** significantly enhanced anti-CDK1 activity; *in vitro* potency of **22** (IC_{50} = 285 µM) was improved to 4.5 µM by **23**. Spacer chain length was critical for efficient inhibition, as both individual components each displayed only negligible CDK1 inhibition (IC_{50} >1 mM).[70]



22 **23**

Fig. 1.23

1.3.1.7 PKC inhibition: a new anti-tumour strategy

Members of the AGC serine/threonine kinase group constitute another class with important downstream signal capability in diverse cell growth and differentiation, following extracellular activation of RTKs. The most important family is PKC, comprising 10 isoforms, implicated in various tumour types.[84-86]

Long term activation of PKC modulates several processes such as immune response, memory/learning, and receptor desensitization. In 2010, Abrams *et al.* reported that VEGF stimulated PKC-βII activity in chronic lymphocytic leukemia cells.[87] PKC is also a key effector of ERK activation under the influence of VEGF and upregulated transcription factor activation in unabated growth responses has been reported in several malignancies *in vivo*.[77] Based on these observations, initial discovery of the nanomolar inhibitory efficacy of STA **2** towards PKC (IC_{50} = 2.7 nM) has precipitated a surge in development of important BIM and ICZ analogues, some of which have successfully progressed to clinical trials (Fig. 1.24). However, activity within these derivatives is still not known to exclusively stem from PKC inhibition, another kinase (e.g. PKA) or perhaps even a combination.[34,38,55]

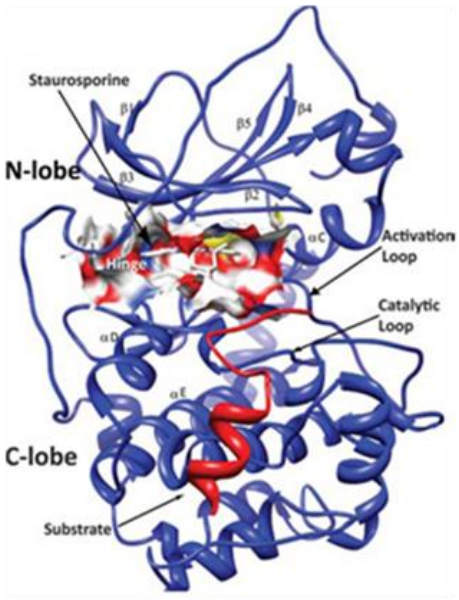


Fig. 1.24: Crystal diagram of PKC in complex with staurosporine **2**[35]

The absence of consistent inhibitor selectivity profiles is also a significant stumbling block to clinical progress. Ro-318220 **24** is a potent inhibitor of PKC isoforms α, β and μ, but only inhibits the closely related PKCξ at much higher concentrations, despite having considerable potency against less sequentially homologous kinases (Fig. 1.25).[88]

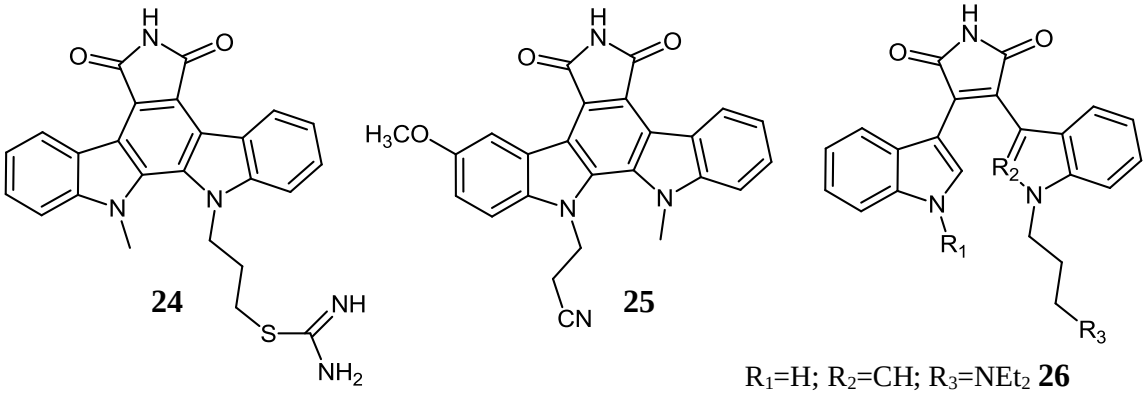
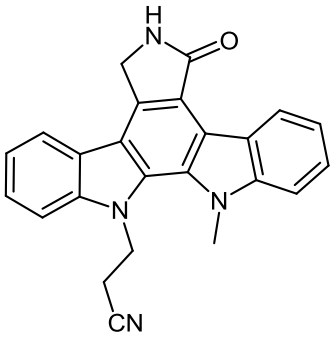


Fig. 1.25

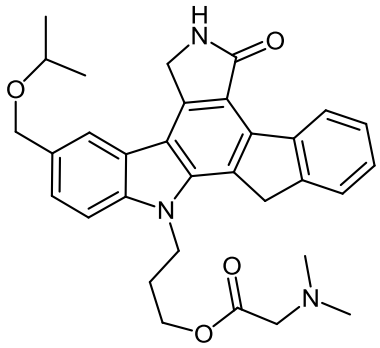
Endothelial PKC inhibition constitutes an important strategy for impairing solid tumour metastasis, due to the reduction in VEGF-induced vasculogenesis by diverse PKC inhibitors *in vitro*. In an endothelial cell co-culture assay, VEGF-induced angiogenesis was markedly inhibited by the BIM, GF-109203x **26** (PKC IC_{50} = 10 nM).[89] In 2005, BIM analogue indolylindazolylmaleimides **27** were also reported as low nanomolar inhibitors of PKC-β, blocking release of a proinflammatory cytokine IL-8, also associated with promotion of metastasis, enhanced survival, and angiogenesis, induced by PKC-βII (IC_{50} = 20-25 nM),

while possessing enviable selectivity against other PKC isoforms and structurally analogous GSK-3β (Fig. 1.25).[90]

Mechanistic studies within this inhibitor class have also confirmed that Gö7612 **25** competitively inhibited PKC, with respect to ATP **11** binding *in vitro*. Experimental K_m values were ascertained to shift to higher ATP **11** concentrations in the presence of increasing concentrations of Gö7612 **25**, while v_{max} remained relatively unchanged.[84] These workers also reported that for imide PKC inhibitors, methyl and dimethylaminohydroxypropyl groups at the indolyl nitrogens were most beneficial for potency and selectivity, and the presence of the hydroxyl group in this alkyl chain has a substantial effect in reducing off-target MLCK inhibition.[84] In 1993, synthesis of non-glycosidic indolo[2,3-*a*]carbazole, Gö6976 **28** was reported, which displayed selective PKC inhibition, as well as activity against human immunodeficiency virus 1 (HIV-1).[91,92] In addition to Gö7612 **25**, planar ring substitution has also been reported to enhance kinase inhibition in a number of ICZ derivatives possessing extremely favourable pre-clinical activity, such as CEP-7055 **29** (VEGFR) and CEP-1347 **30** (ChAT, JNK, and MLKs), due to 'gatekeeper-induced selectivity' (Fig. 1.26).[16,49,93]



Gö 6976 **28**



CEP-7055 **29**

Fig. 1.26

This phenomenon describes the nature of a single gatekeeper residue within the buried hydrophobic pocket adjacent to the ATP-binding site (Fig. 1.27); the size of this residue is a critical determinant of inhibitor selectivity. Interestingly, 50% of tyrosine kinases have a threonine gatekeeper, but only 10% of serine-threonine kinases have this residue; serine-threonine kinases are thus relatively cross-resistant to tyrosine kinase inhibitors.[45]

Further SAR work has revealed that glycosidic ICZ analogues comprising an F-ring lactam moiety rather than an imide system preferentially inhibit PKC, whereas in aglycon systems, the maleimide F-ring is more favourably indicated for activity.[16]

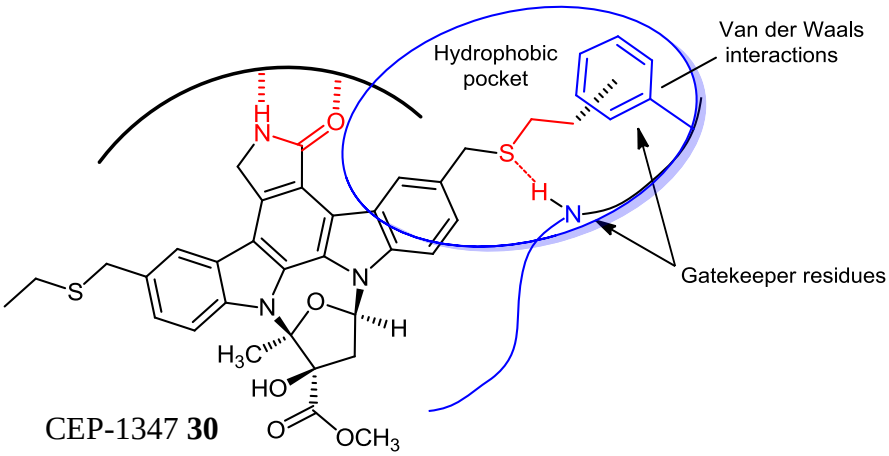


Fig. 1.27: Structural basis of the residue 'gatekeeper' mechanism for selective kinase inhibition.

Nanomolar inhibition of other serine/threonine kinases containing structural homology within the adenine-binding region, e.g. protein kinase D (PKD) associated with gastric tumours, by non-specific PKC inhibitors, such as K-252a **13**, is intriguing, but further insight into the nature of this target may be required prior to full scale clinical target identification based on these results.[94]

1.3.1.8 Indolocarbazoles as GSK-3β inhibitors

Glycogen synthase kinase (GSK) 3β - a member of the CMGC group of kinases, has an interesting range of biological effects including regulation of cardiac hypertrophy. It has also been pursued as a treatment for insulin-resistant type II diabetes due to its intrinsic role in glycogen synthesis.[95]

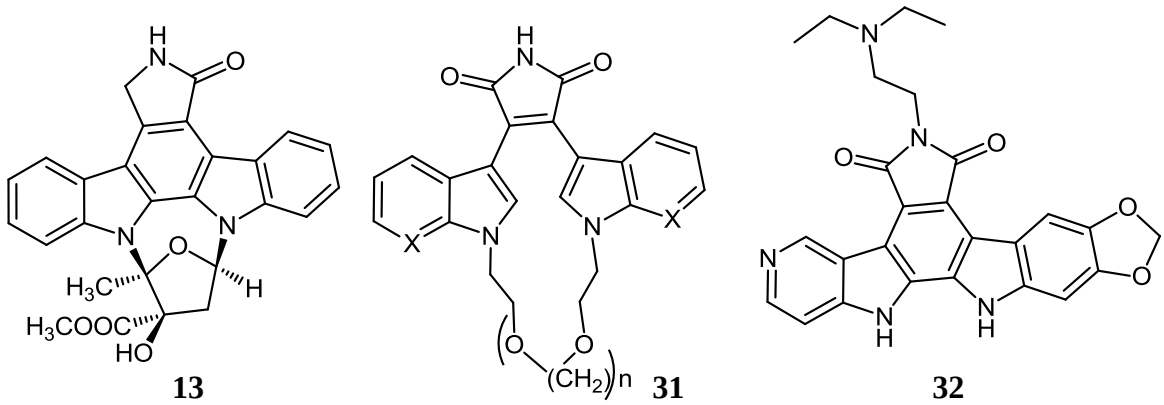


Fig. 1.28

The observation that GSK-3β activity is associated with promoting apoptosis in a protective anti-tumourigenic role, initially suggested that enzyme inhibition would be highly undesirable. However, due to complex conflicting pro-tumour effects, kinase inhibition in GSK-3β over-expressing ovarian cell lines has been demonstrated to have significant anti-proliferative effects *in vivo*. Following a study into new inhibitors of PKC-γ, Kuo *et al.*

discovered that polyoxygenated macrocyclic BIM analogues **31** conferred enviable GSK-3β potency, while replacement of both indoles with 7-azaindole moieties resulted in almost no inhibition across a panel of 50 protein kinases, but retained sub-micromolar selective activity against this GSK isoform.[96,97] In 2008, several 3-azaindolocarbazole derivatives also inhibited two cancer cell lines with activity in the submicromolar range. The synthetic lead candidate **32** inhibited the L1210 leukaemia cell line with an IC_{50} of 195 nM, while compounds with unsubstituted F-ring moieties were most active in purified ChK1 assays, possessing IC_{50} values as low as 14 nM within this series (Fig. 1.28).[98]

1.3.1.9 Conclusion

According to the Sanger Institute, over 300 proto-oncogenes associated with cancer progression exist within the genome, and many of these gene products are protein kinases or their endogenous ligands.[2] Nascent awareness of small-molecule kinase inhibition has coincided with an observation of the acute significance of aberrant protein phosphorylation and protein-protein interaction (PPI) in affecting cellular homeostasis, and therefore, its causative role in mediating several disease states.[44] At present over 30 kinase inhibitors are in clinical trials for their therapeutic applications and 8 kinase inhibitors, including AML front-line agent imitanib **3**, which demonstrates tumour regression in 90% of cases involving the Philadelphia chromosome, have achieved full FDA approval for clinical use.[49]

A fundamental limitation for ICZ congeners in their common mode of action is the competitive nature of their binding within the ATP-binding domain of the kinase hinge region.[35] Exploitation of subtle conformational differences for unique binding profiles will undoubtedly attract increasing attention as clinical success emerges in the field of small-molecule kinase inhibition. Assessment of kinase selectivity by *in vitro* screening is intrinsic to future development of novel inhibitors, but does not address critical issues of metabolic deactivation, cell permeability and adverse off-target effects.[45] IC_{50} values also vary enormously between laboratories depending on the ATP **11** concentrations employed in purified enzyme assays. Concentrations of ATP **11** *in vivo* are approximately 3 mM, while most tyrosine kinases possess extremely high affinity for ATP (K_m = 10 - 150 μM), thus highlighting the difficulty of identifying new lead chemical scaffolds eliciting significant ATP-competitive inhibitory effects. Thus, theoretical potency may be difficult to correlate with studies performed *in vivo*, with increased complexity arising from fluctuating kinase expression, endogenous inhibition and effects on alternate targets in tumourigenesis.[44,57,84] Anti-vascular inhibition of PKC, VEGFR and FGFR represents an attractive alternative to

non-selective cytotoxic drugs with a complementary spectrum of activity including improving intravenous drug delivery due to normalisation of abnormal vessel development.[99]

In addition to further elucidation of activity in individual kinases, and novel strategies for signal transduction therapy, development of markers of kinase mutation in tumour phenotypes as well as identification of germ-line mutations indicating pre-disposition to cancer, e.g. c-Met mutation in familial renal cell carcinoma, will ultimately allow administration of selective inhibitors tailored for specific kinase abnormalities.[4,45,49] Future breakthroughs in kinase research leading to successful therapeutic strategies have the potential to transform cancer from an acute crisis into a chronic disorder, where abnormal tumour growth signaling has effectively ceased by targeting individual dysregulated kinases.

1.3.2 Topoisomerase I inhibition and putative intercalative effects

The recently digitized human genome is a revolutionary genetic repository located at the forefront of biology, set to redefine the blueprint for medicine in the 21st century. The human genome comprises approximately 4 billion base pairs of DNA integrated into 44 somatic and 2 sex chromosomes. Although this genetic material is only 20 Å in diameter, if total DNA from the nuclei of all 10^{13} cells within the body were laid end-to-end, it would equal the distance of almost 70 round trips between Earth and the Sun.

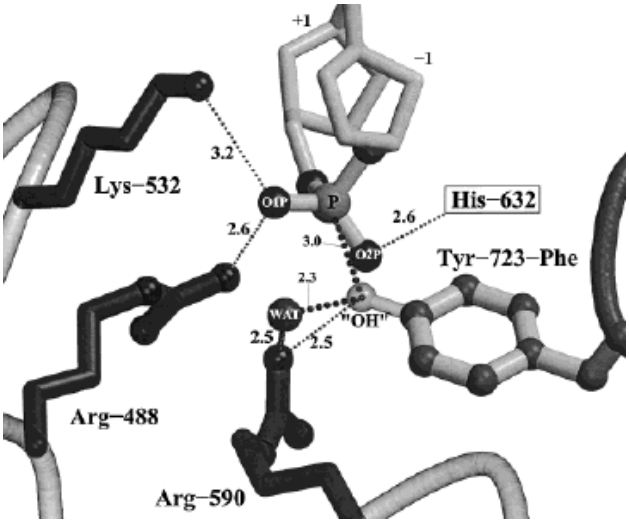


Fig. 1.29: Critical non-covalent DNA-topo I interactions involved in 'cleavage complex' formation.[100]

In order to compact this overwhelming amount of DNA more than 200,000 fold, ubiquitous eukaryotic nuclear enzymes known as DNA topoisomerases control helical torsional strain by catalysing the concerted breaking and religating of supercoiled DNA. This topological adaptability is exerted over DNA during essential metabolic processes, including

transcription, replication, recombination, chromosome condensation and mitotic chromosomal segregation.[101-105]

In humans, there are 6 topoisomerase genes coding for nuclear topoisomerase I (topo I) and mitochondrial topo Iβ, along with topoisomerases IIα, IIβ, IIIα, IIIβ.[106] Topo Iβ is a monomeric protein (765 residues), consisting of four major domains: a C-terminus catalytic region that contains the active nucleophilic tyrosine residue, a non-conserved "linker" domain, a conserved "core" domain, and an N-terminus domain that contains a nuclear localization signal (NLS).[106,107] Topo Iβ clamps DNA at its sequence recognition point, prior to relaxing local superhelical stress by nicking and rejoining a single strand of DNA, in the absence of energetic co-factors or metal ions (Fig. 1.29). In contrast, topo II enzymes are dimeric, break both strands of a duplex DNA (using catalytic Tyr residues from each monomer), and pass an intact DNA duplex through this transient double-stranded break.[101]

The catalytic cycle of eukaryotic topo I can be divided into four main steps and is initiated by the binding of the enzyme to DNA (Fig. 1.30). The second step of the cycle encompasses nicking of one DNA strand by transesterification of an active-site tyrosine (Tyr723 in human topo I) at a DNA phosphodiester bond, prefiguring formation of a covalent 3'-phosphotyrosine DNA break (cleavage complex). Base activation of the nucleophilic Tyr723 residue is required in order for it to attack the 3′-phosphate group. This activation is thought to occur by means of a deprotonated water molecule as no other residues have been found in close enough proximity to carry out this function. The third step in the catalytic cycle invokes superhelical relaxation and more than likely occurs *via* a mechanism of “controlled rotation” in which the intact strand remains stationary and the cleaved strand interacts through transient electrostatic interactions with positively charged regions of the topo I enzyme that are in close proximity to the downstream DNA.

The final step in the catalytic cycle is DNA religation and occurs when the released 5'-OH of the broken strand reattacks the phosphotyrosine intermediate in a second transesterification reaction to release the DNA constraints.[108] In kinetic terms, the rate of religation in this reversible process has been determined to be normally much faster than the initial rate of DNA uncoiling, indicating that the steady state concentration of the covalent 3'-phosphotyrosyl topo I–DNA complex is extremely low.[109] As a result of unique activity, topo I can modulate DNA underwinding and overwinding, but cannot resolve knots or tangles from double stranded DNA.[101,108]

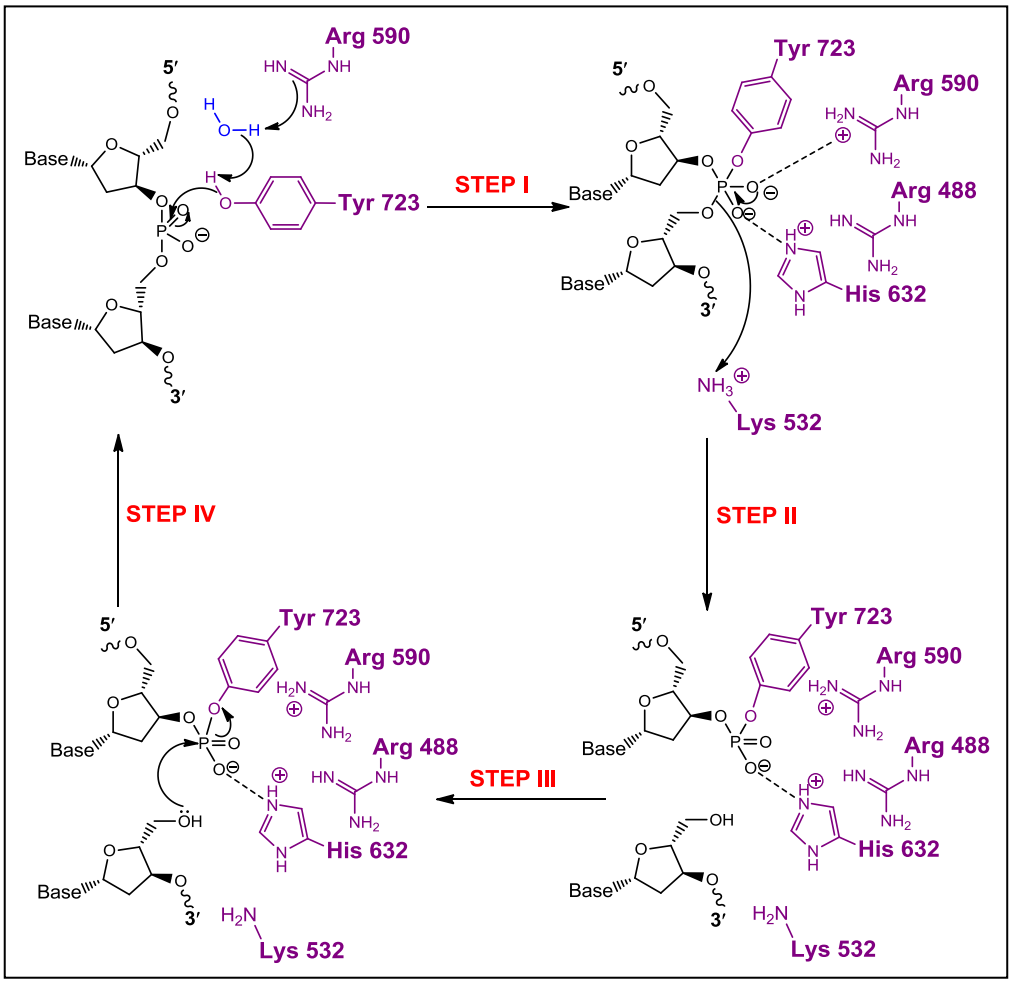


Fig. 1.30: Schematic representation of the stepwise mechanism of topo I activity in DNA (for clarity, DNA strands are represented in black, while topo I residues are coloured purple)

Several DNA mutations (e.g. mutation expressing A718T residue substitution in topo I) and inhibitory drugs have been shown to stabilize the covalent 3'-phosphotyrosyl intermediate, and induce extensive DNA strand fragmentation, *in vitro* (Fig. 1.31).[109,110] Elevated topo I expression, relative to baseline cell levels, reported by Giovanella *et al.*, in advanced human colon cancer also reinforces a link beween topo I targeting and anti-cancer therapy.[111]

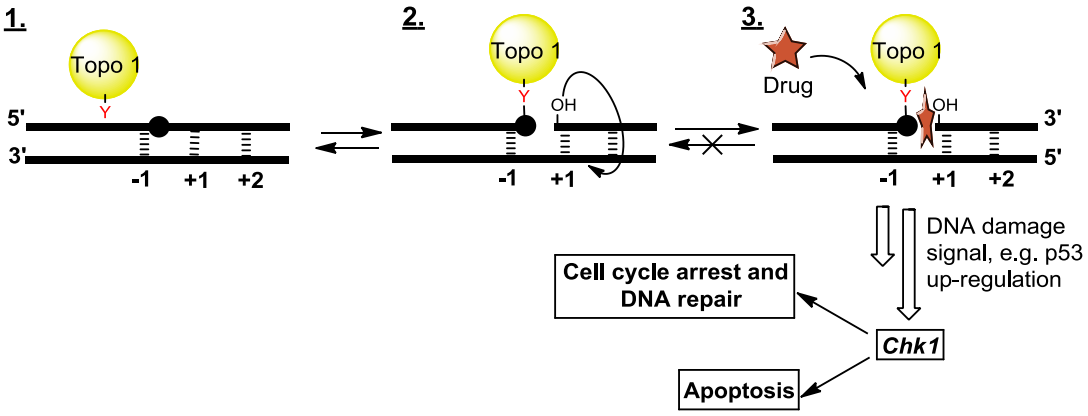


Fig. 1.31: Cellular responses to drug-mediated topo I poisoning/DNA lesion formation.

A particular classification system for the mode of action mediated by specific anti-topoisomerase agents incorporates a number of mechanistic classes based on their sites of action. Topoisomerase suppressors act on either DNA or topo I, and do not bind to the transient 'covalent complex'. Alternatively, uncompetitive inhibitors which bind to this DNA-enzyme complex are known as topo I poisons, and this approach is of acute clinical relevance to current anti-cancer research.[112,113] In each case, disruption of the catalytic cycle results in persistent strand breakage during DNA synthesis (S) phase and elicits massive DNA damage from replication fork and transcription complex collisions, leading to ultimate cell death, if not repaired (Fig. 1.31).[109,110]

1.3.2.1 Topo I 'poisons' at the DNA-enzyme interface: a potent anti-cancer lead

The DNA-topo I macromolecular complex was the intrinsic nuclear target for the potent anti-cancer natural product camptothecin **33** isolated by Wall and Wani from the Chinese tree *Camptotheca acuminata*, subsequently found to promote accumulation of DNA-topo I adducts and inhibit DNA synthesis for up to 8 hours following drug removal. The natural alkaloid **33** is the 20*S*-enantiomer which is active against topo I and experimental cancers, whereas the synthetic 20*R*-enantiomer lacks both activities (Fig. 1.32).[114]

Camptothecin **33** does not bind to either DNA or purified topo 1 alone; the uncompetitive nature of inhibitor binding to the transient cleavable complex extends some mechanistic limitations to formulation of a full binding model due to the fact that no equilibrium constants have been determined for **33** or analogues, such as silatecan **34**. However, it can be surmised that CPT-like agents must act in a concentration dependent manner, due to interaction of each drug molecule with one topo I enzyme to afford a single DNA lesion.[110]

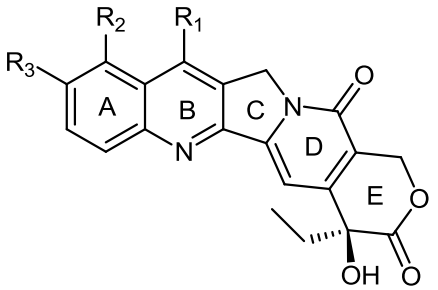


Fig. 1.32: Camptothecin **33** (R_1-R_3=H) family of topoisomerase I poisons, including silatecan **34** (R_1 = TBDMS; R_2 = H; R_3 = OH) and approved chemotherapeutic congeners, topotecan **35** (R_1 = H; R_2 = $CH_2N(CH_3)_2$; R_3 = OH**)** and irinotecan **36** (R_1 = CH_2CH_3; R_2 = H; R_3 = $OCON(CH_2)_4N(CH_2)_5$).

CPT **33** activates cell cycle S and G2 checkpoints, as well as p53/p21 pathways in response to DNA damage, halting mitosis (preferentially targeting rapidly dividing tumour cells with

over-expressed topo I), increasing DNA repair, and preventing amplification of replicative errors (c.f. Fig. 1.31).[109,112]

Two FDA-approved water soluble CPT **33** analogues are now routinely used for *intravenous* (IV) administration in human cancer therapy: topotecan **35** (Hycamtin®, GSK) in small cell lung cancer as well as for second-line treatment of advanced ovarian cancer and irinotecan **36** (CPT-11, Camptosar®, Yakult Honsha KK) used for treatment of colorectal cancers (Fig. 1.32).[20] Haemotological toxicity is a common side effect of camptothecin derivatives due to the destruction of bone marrow progenitors. However, the major clinical limitation of these analogues relates to the rapid metabolic inactivation of the lactam E-ring to the inactive serum protein-sequestered carboxylate form.[5,115]

1.3.2.2 Indenoisoquinolines – polycyclic non-CPT intercalatory topo I inhibitors

A number of topo I inhibitors from a range of chemical classes share close target analogy with CPT **33** analogues, and thus, may possess different spectra of clinical activity, with complementary efficacy against diverse tumour types *in vivo*. Over 300 indenoisoquinoline (IIQ) derivatives such as MJ-238 **37** have been synthesised to date, following investigation into agents resembling CPT **33** in their activity profiles against 60 human cancer cell lines.[114]

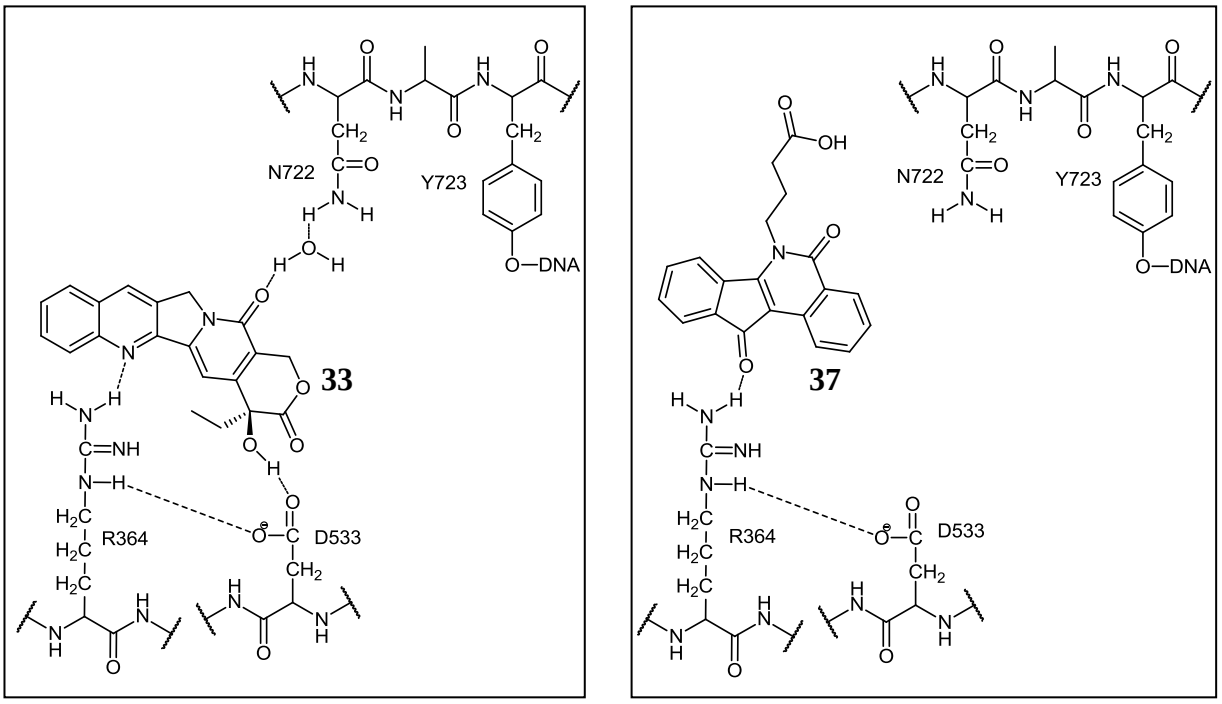
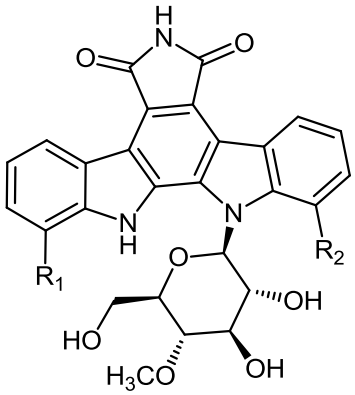


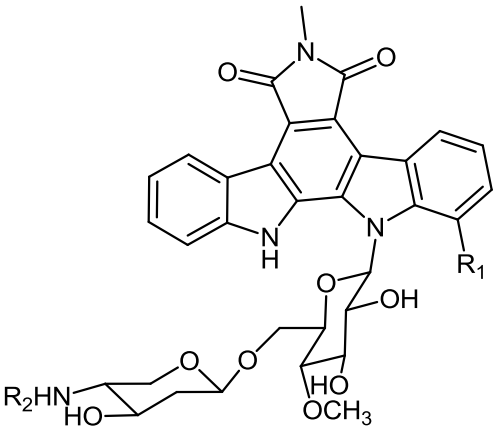
Fig. 1.33: Schematic representation of key hydrogen bond networks between two interfacial inhibitors (CPT **33**; MJ-238 **37**) and catalytic topo I amino acid residues in drug-topo I-DNA complexes.[114]

In contrast to camptothecin **33**, IIQs, e.g. **37,** are chemically stable and do not contain the labile hydroxylactone E-ring characteristic of CPTs. In addition, 'trapped' ternary complexes within this series are much more stable than those formed by CPTs (Fig. 1.33). Key hydrophobic stacking (intercalation) between successive base pairs flanking the DNA cleavage site and formation of critical hydrogen bonds with topo I amino acid residues, also reveals a common interfacial binding mode between CPT **33** and IIQ **37** inhibition.[114]

1.3.2.2 DNA binding and topo I poisoning activities of rebeccamycin-type ICZs

Indolocarbazoles represent the most advanced non-CPT topo I inhibitor class encountered to date, with a well studied mechanism of action and a number of derivatives in current clinical development.[14,112] Interest in this field began in 1985, when a new ICZ possessing the conserved indolo[2,3-*a*]carbazole framework was isolated from cultures of *Lechevalieria aerocolonigenes*, so termed rebeccamycin (REB) **38** for the daughter of the scientist who isolated the compound.[116] It is arguably the most important derivative of the indolo[2,3-*a*]carbazole family, due to the vast amount of synthesis, relating to design of novel clinical congeners based on this privileged topo I inhibitory lead, reported in scientific literature.[14,40,41,117-122]





R_1=R_2=Cl **38**
R_1=H; R_2=Cl **39**
R_1=Br; R_2=Br **40**
R_1=Cl; R_2=CH_3 **41**
R_1=H; R_2=CH_3 **43**
R_1=Cl; R_2=H **42**
R_1=R_2=H **44**

Fig. 1.34

This water insoluble compound was found to inhibit topo I with an IC_{50} value of 1.75 μM, but unlike STA **2**, is virtually inactive towards topo II and PKC (IC_{50} >100 μM).[41,122] The primary structural features of REB **38** and its anti-cancer analogue, 11-dechlororebeccamycin **39**, also isolated from this microbial source, include the presence of a carbohydrate moiety (4-*O*-methylglucose) attached in an 'open' orientation *via* a β-*N*-glucosyl bond to a single indole nitrogen and unsubstituted maleimide F-ring (Fig. 1.34).

In 1987, rebeccamycin **38** was reported to induce prolongation of survival of leukaemic mice (P388 leukaemia/ L1210 leukaemia) at a wide dose range, from 8 – 256 mg/ kg. *In vitro* anti-proliferative activities against murine B16 melanoma and P388 leukaemia cell lines were 0.48 μM and 1.22 μM, respectively, while growth of human lung adenocarcinoma cells was also suppressed *via* topo I inhibition and production of single DNA strand breaks.[117,122] Although structurally related to other microbial indolocarbazoles, rebeccamycin **38** is unusual in that it can be isolated in large quantities from fermentation, e.g. in a 30 L fermentor, a yield of 663 mg/L was observed.[41] In 1991, the water soluble, potent anti-tumour derivative, bromorebeccamycin **40** was also successfully cultured in the presence of bromide ions.[123]

Tight intercalation and the observation of growth inhibition in leukaemic cell lines, discovered by Facompre *et al.*, stemming from DNA complexation within the AT2433 aminodisaccharides (AT2433-A_1 **41**, AT2433-A_2 **42**, AT2433-B_1 **43** and AT2433-B_2 **44**), isolated from *Actinomadura melliaura*, comprising an *N*-methylimide, also represent a novel DNA unwinding lead within this series.[124] These derivatives **41-44** were investigated in clinical trials for the treatment of a wide range of malignancies, including refractory pediatric neuroblastoma, advanced renal cell carcinoma, metastatic or locally recurrent colorectal and stage IIIB or IV breast cancer.[125] Two anti-topo I compounds, BMS-250749 **45** and edotecarin **46**, from the mono-*N*-glycosidic indolo[2,3-*a*]carbazole class are also currently in phase III human clinical trials; full disclosure as to their future therapeutic applicability is currently being awaited (Fig. 1.35).[126,127]

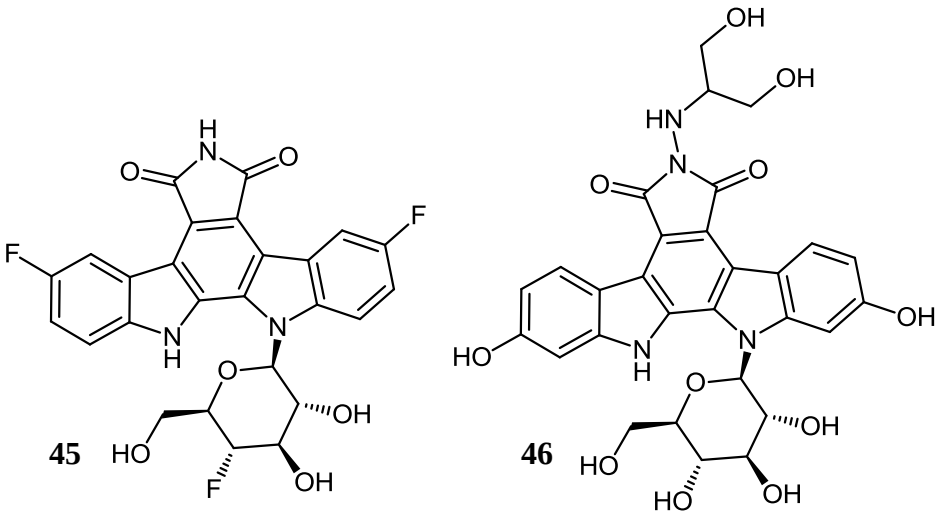
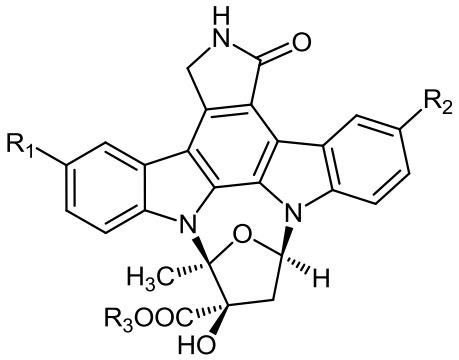


Fig. 1.35

Interestingly, development of topo I inhibitors in the ICZ series retains a high degree of structural fidelity to the indolopyrrolocarbazole **3** glycoside template represented by REB **38**; kinase inhibition based on STA **2** tolerates structural diversity to a much larger extent.

However, there is also evidence of exploitable structural overlap between these drug targets, as the proportion of persistent 'nicked' DNA produced by the PKC active, K-252a **13** derivative, KT-6006 **47** was >50% of substrate DNA or comparable to CPT **33**, with DNA relaxation and cleavage activities also being similar to the camptothecins **33, 35-36** (i.e. no cleavage observed in absence of topo I or in the presence of topo II) (Fig. 1.36).[14,114,128]



R_1=R_2=H; R_3=CH_3 **13** K-252a
R_1=R_2=OH; R_3=CH_3 **47** KT-6006

Fig. 1.36

The reduction in this DNA cleavage, following thermal denaturation (65°C) indicates the involvement of a disrupted reversible DNA-enzyme complex, i.e. 'poisoning' effect.[28] The weakly intercalating lactam ICZ compound **48** reported by Yamashita *et al.* also induced topo I-mediated DNA cleavage in a dose-dependent manner up to 50 μM, at comparable levels, *in vitro*, to camptothecin (Fig. 1.37).[128]

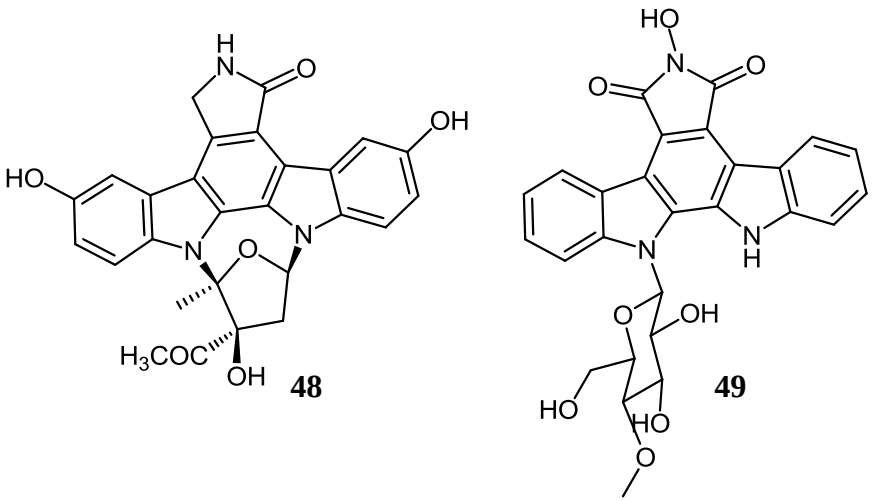


Fig. 1.37

Additionally, topo I confers dual activity as it has recently been shown to phosphorylate serine/arginine (S/R) residues in substrate proteins. As well as having DNA affinity and CPT-like topo I poisoning, ICZ compound R-3 **49** displays discrete anti-topo I kinase activity in the absence of DNA (IC_{50} = 1-2 μM), independently of its DNA cleavage capacity in a knockout Y723F mutant (Fig. 1.37). Interestingly, CPT **33** required DNA to inhibit topo

I kinase function, and could not confer inhibition in the absence of DNA even at concentrations as high as 500 μM. This DNA-independent anti-kinase activity may evolve to be a fertile new target for pharmaceutical mediation due to its prodigious selectivity (R-3 **49** is 10^4 times less potent than STA **2** for PKC), as it exhibits a differential pharmacological trait between ICZ agents and CPT analogues **33**, **35-36** that interact *via* analogous binding modes within DNA.[129]

In alternative indications, staurosporine **2** aglycon, K-252c **6** and arcyriaflavin A **7**, containing a maleimide F-ring, also diminished relative resistance of cells transfected with ABCG2 - a drug transporter comprising an ATP-binding motif, strongly implicated in cancer chemoresistance, to irinotecan **36** *in vitro*.[130] This observation may be important for future adjuvant therapies as topotecan **35** and irinotecan **36** are also substrates of drug efflux pumps such as P-glycoprotein (P-gp) and breast cancer resistant protein (BCRP) *in vivo*.[112,130]

1.3.2.3 Overview of SAR in ICZ topo I inhibition

The semi-synthetic, but only sparingly water-soluble rebeccamycin analogue, NB-506 **50**, discovered from natural product screening of a Streptoverticillium culture, and endowed with *in vivo* anti-cancer activity has undergone clinical trials, with positive clinical Phase I results, especially against taxol-resistant breast and ovarian cancers, as well as lung and colon cancer indications.[131] Based on work by Ohkubo *et al.*, it is now postulated that NB-506 **50**, as a prime exemplar of this class, contains three indispensable functional domains for anti-topo I activity (Fig. 1.38).[132]

These structural segments facilitate maleimide ring DNA major groove and protein side-chain contacts, interfacial intercalation between successive DNA bases at GC-rich sites (cleaving TG linkages), through an extended planar chromophore and DNA accommodation of a glycosyl side-chain by means of minor groove insertion.[133-137]

Observed tumour sensitivity to ICZ glycosides may also be due to the crucial role of the glycosyl residue in mediating cellular uptake *via* passive diffusion through the plasma membrane.[138] In addition, hydrophilic F-ring *N*-imide substituents are also necessary for effective topo I inhibition.[121,132] Despite profound structural differences, glycosylated ICZs, IIQs and camptothecin classes share common steric and electronic features, recognising similar structural elements to specifically stabilise the topo I-DNA-drug ternary complex.[114]

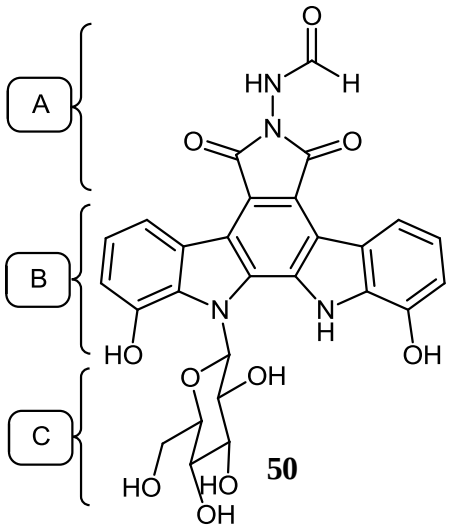


Fig. 1.38: Three functional domains of NB-506 **50**, a model glycosidic ICZ topo I inhibitor.
A = Enzyme-interacting domain.
B = Planar DNA-binding domain.
C = Minor groove DNA-binding domain.

This conclusion was supported by X-ray crystallographic analysis of the topo I-DNA complex bound to either CPT **33,** IIQ congener, MJ-238 **37** or the 2,10-dihydroxylated, SA315F **51**, which demonstrated that distinct intercalative modes prevailed for each class, along with common features including mimicking of a DNA base pair at the cleavage site and multiple contact stabilisation of the ternary complex. Co-axial interfacial stacking interactions between -1 (nucleotide covalently linked to topo I) and +1 (nucleotide at free 5'-OH terminus) base pairs at the topo I cleavage site following binding of SA315F **51** results in DNA unwinding due to the increased distance between flanking base pairs required to accommodate the intercalated molecule. It was also observed that the protein-interacting maleimide ring was orientated into the major groove of DNA, while the hydrophilic deoxyribose unit was accommodated in the minor groove (Fig. 1.39).[114]

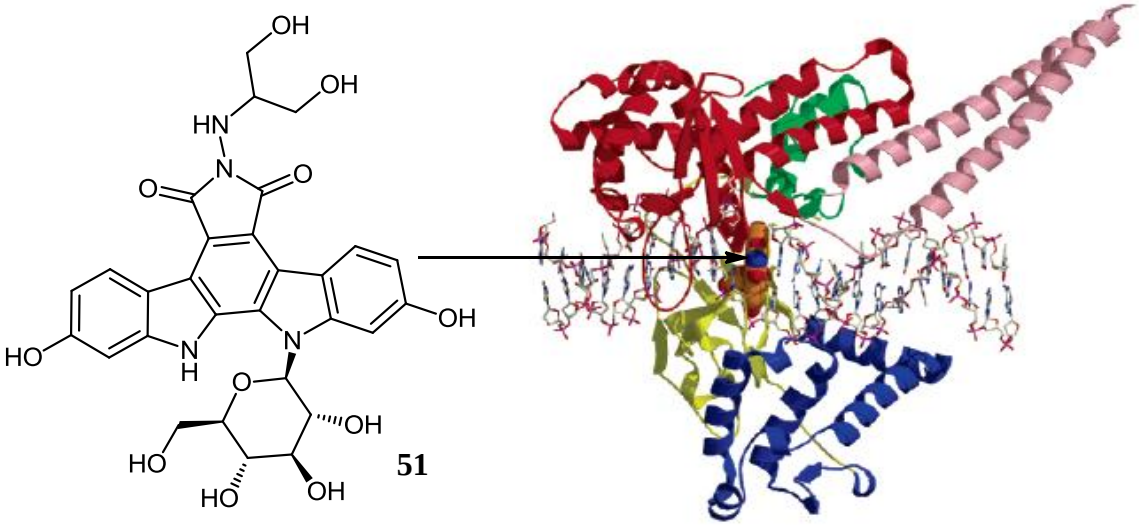


Fig. 1.39: Crystal structure of SA315F **51** bound to a stabilised DNA-topo I covalent complex.[139]

The glycosylated indole ring stacked with bases on the intact strand, while the unsubstituted ring intercalated with the cleaved DNA complement. Essential active site residues also interacted with a hydroxyl of the sugar moiety, with one of the carbonyls at the maleimide ring, and with both hydroxyl substituents of the planar ring system.[114] Additionally, it was determined that alkyl-substitution of the non-glycosylated indole nitrogen totally abolished topo I inhibition; in addition, peripheral ring substituents have also been shown to either abolish or enhance anti-topo I activity, and are also highly correlated with DNA intercalation and anti-tumour cell line selectivity.[40,136,140]

Thus, ED-110 **53**, a glucosylated derivative of a 1,11-dihydroxylated dual topo I/II inhibitor (both IC_{50} = 2 µM), BE-13793c **52**, exhibited *in vitro* cytotoxicity across a wide spectrum of cancer cell lines and pre-clinical *in vivo* activity in xenotransplanted nude mice (Fig. 1.40).[141-144]

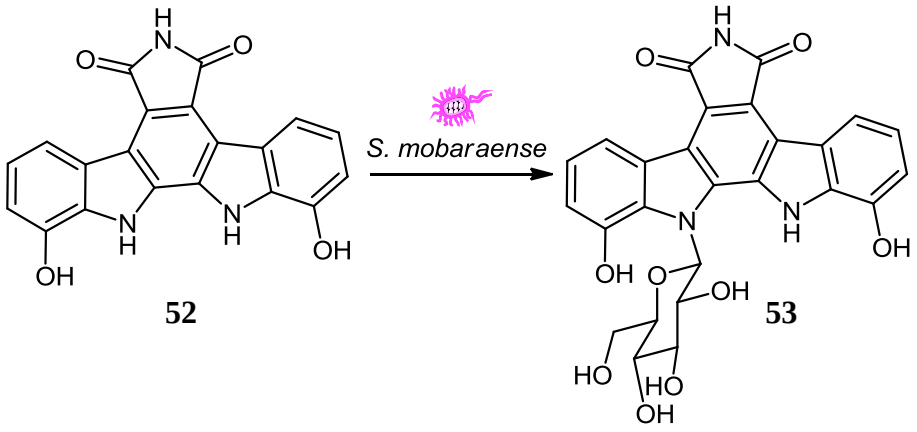


Fig. 1.40: Enzymatic transformation of BE-13793c **52** to D-glucosylated derivative ED-110 **53**.

As displayed in Fig. 1.41, a regioisomeric derivative **54** was reported to be ten-fold more active than ED-110 **53** against topo I and 5 to 35 times more active against cancer cell lines, such as colon HT29 (IC_{50} = 0.84 µM; **54**, c.f. >10 µM; **53**) and prostate DU-145 (IC_{50} = 0.067 µM (**54**), c.f. 2.3 µM (**53**)).[145] In 1999, Bailly *et al.* also reported how ICZ analogues with ten-fold greater DNA binding affinities exhibited no improvement on topo I inhibition, illustrating that intercalation and topo I poisoning comprise two distinct modes of action.[135,140,146]

The action of ICZ inhibitors is also similar to camptothecin **33** with respect to the stability of the drug-induced cleavable complex, and in a comparison study of camptothecin with the intercalating R-3 **49** both preferred binding sites were in the 361-364 amino acid 'lip' region of topo I.

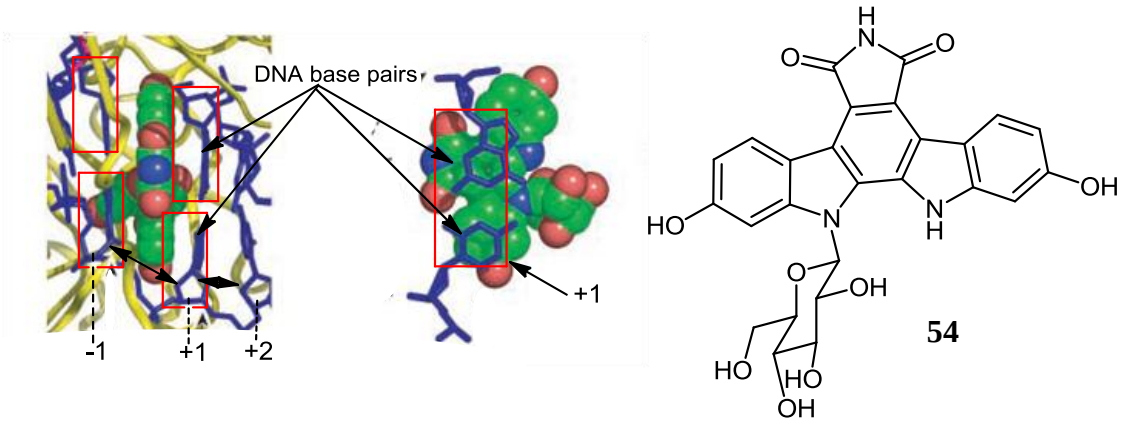


Fig. 1.41: DNA cleavage site of topo I in the presence of co-axial DNA intercalator SA315F **51**, illustrating planar intercalating motif and DNA supercoil unwinding effect (increased distance between -1 and +1, compared with +1 to +2), and structure of topo I intercalatory inhibitor **54**.[114]

This region is essential for covalent and non-covalent contacts in DNA cleavage activity, and cross-resistance to derivative **49** was also demonstrated following alteration of a common critical residue in a F361S topo I mutant.[147] The absolutely essential requirement of correct orientation for the sugar linkage is necessary for an appreciable DNA binding affinity.[148] In fact, inversion of configuration at C1 of a galactose residue attached to a close rebeccamycin **38** analogue has been reported to abolish effective minor-groove DNA binding *in vitro*, based on fluorescence energy-transfer experiments.[147]

1.3.2.4 Conclusion

In summary, previously asserted structural differences between different chemical classes of topoisomerase I inhibitors, such as CPTs, IIQs and ICZs may now be exploited for novel pharmacophore design, based on converging stereochemical features.[114] Rational design of more potent topo I inhibitors as clinical agents and valuable mechanistic probes has accelerated following the advent of powerful *in silico* techniques, along with insights arising from isolation of crystal structures of small-molecule inhibitors in complex with topo I.[40,41,147,148] Cleavage site mapping studies have also recently been employed for estimating *in vivo* anti-tumour activity from the electrophoretic properties of structurally related derivatives possessing closely aligned DNA cleavage capacities, and thus, similar sites of action.[149]

Important work must also complete the full SAR profile determining how topoisomerase disruption, conferred by novel indolocarbazole compounds containing hydrophilic maleimide F-ring substituents can be clinically exploited. Various substitutions, in addition

to attractive imide substitutions have also been exhibited to exert potent effects on cytotoxicity.[41]

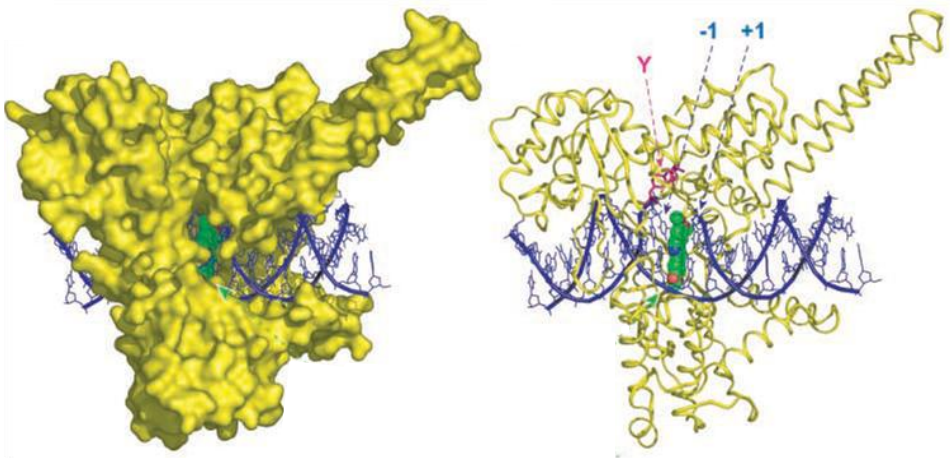


Fig. 1.42: Intercalative binding mode of anti-cancer indolocarbazole topo I inhibitors.[114]

Anti-proliferative effects of topo I inactive ICZ analogues must be attributable to alternative cellular targets such as DNA interaction and phosphotransferase activity; this has been corroborated by assays where actual cytotoxicity for members of this series could not be correlated with *in vitro* topo I inhibitory efficacy in CPT-resistant (expressing low topo I levels) murine leukaemic cell lines (CPT **33** = 10^5 loss of activity, c.f. NB-506 **50** = 2-10 fold reduction). It has also been established that 2'-aminoglucose substituted ICZ **55** reinforces much stronger affinity for DNA than 2'-OH congener **56**, at low pH, yet both possess similar ability to inhibit topo I. Thus, DNA intercalation and topo I inhibition are not necessarily inter-related and can both contribute to an overall anti-cancer activity profile (Fig. 1.42).[129]

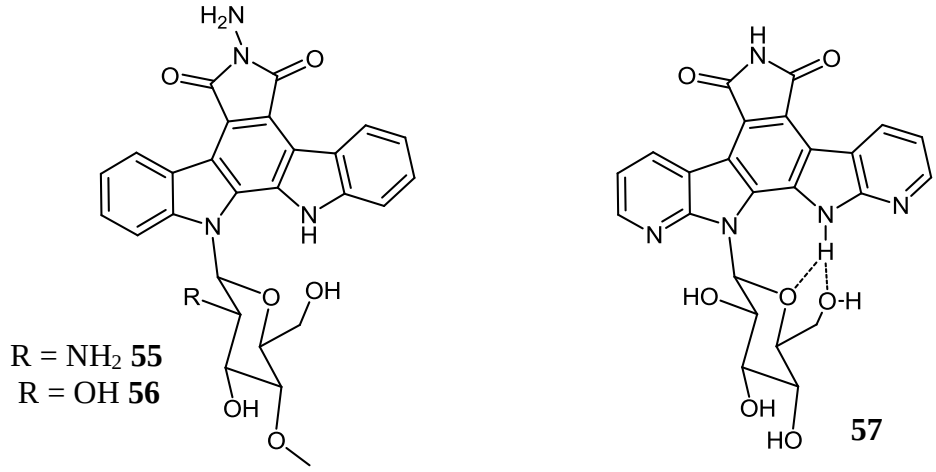


Fig. 1.43

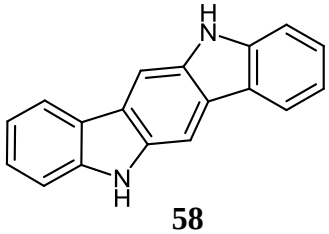
In fact, tight binding to DNA can be detrimental for trapping the covalent DNA-topo I complexes.[118,140] In addition, the mode of binding of the carbohydrate moiety rather than the binding affinity may be a crucial determinant, as evident from the incorporation of a

methylaminoxylose carbohydrate unit which reinforced DNA interaction but abolished anti-topo I activity, whereas modifying an inactive disaccharide unit to another epimer may induce the correct drug-enzyme contacts to stabilise the transient ternary complex.[147,148]

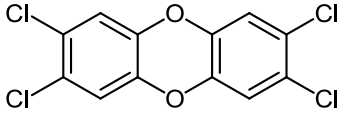
Future work in this series may elaborate on the unique biological properties of 1,11-aza-rebeccamycin derivatives. Marminon and co-workers have recently reported that an anti-proliferative derivative **57,** for which 66% of cells in the L1210 murine leukemic cell line were arrested in G2/M at a concentration of 0.25 µM (IC_{50} = 0.067 µM), was much more active than rebeccamycin **38** (IC_{50} = 0.14 µM) yet possessed diminished activity against other cell lines (A549 IC_{50} = 41.5 µM; **57**), suggesting that related analogues may have improved toxicity profiles *in vivo* (Fig. 1.43).[150] Also, alkyl substitution of the non-glycosidic nitrogen in most REB-like anti-topo I ICZs is not tolerated, due to active β-*N*-glycosidic conformations comprising a bifurcated intramolecular H-bonding network between donor NH and pyranose oxygen/6'-OH positions.[136] In the corresponding mono-azaindole series, it was also disclosed that incorporation of the sugar on the indolic ring confers higher affinity for DNA and improved anti-topo I capacities than on the 7-azaindole moiety, within aza-rebeccamycin congeners.[140]

1.4 Significant milestones in ICZ research

The indolocarbazole family consists of 5 isomeric classes, of which the indolo[2,3-*a*]carbazole **1** series is the most important as most indolocarbazole alkaloids isolated from natural sources to date, exist in this orientation. Isomeric analogues mimicking other bioactive compounds, such as aza-derivatives of indolo[3,2-*b*]carbazole **58** have also been reported to display affinity for the aryl hydrocarbon (Ah) or 2,3,7,8-tetrachlorodibenzo-*p*-dioxin **59** (TCDD) receptor, possibly due to the presence of a shared planar, polycyclic binding motif (Fig. 1.44).[151]



58



59

Fig. 1.44

In this overview, the initial development of classical indolo[2,3-*a*]pyrrolo[3,4-*c*]carbazoles as improved congeners of STA **2** and REB **38** in terms of their topo I, kinase inhibition or other modes of action, will be assessed. Biological activity of the closely related, unaromatised bisindolylmaleimide family will then be described, as well as heterocyclic modifications accomplished on the indolo[2,3-*a*]carbazole **1** template in order to

contextualize the synthetic work undertaken during this project. The following section will then explore the status of up to date research on therapeutic candidates within these classes undergoing clinical phase I-III trials.

1.4.1 Introduction to the structure-bioactivity paradigm within ICZs

Following initial identification of the exceptional biological potency of ICZ alkaloids in nature, it was also deemed beneficial to characterize the provenance of specific biological roles *via* SAR patterns of critically conserved structural motifs. On comparison of cytotoxicity data from this class, it was noted that target enzyme selectivity seemed to derive from two significant structural differences between REB **38** (topo I active, without efficacy towards PKA/PKC) and STA **2** (non-selective PKC inhibitor, topo I inactive) congeners:

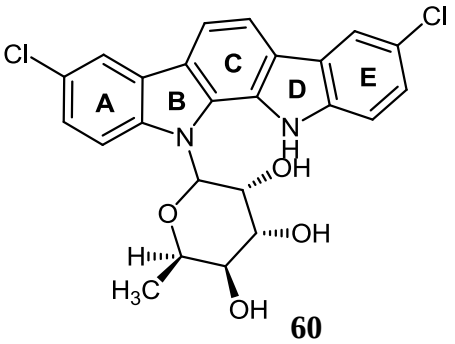
- imide H-bonding network for active REB **38** derivatives, replacing lactam functionality within potent PKC inhibitor STA **2** analogues, in the F-ring position.
- glycosyl moiety linked to only one indole nitrogen in REB **38** (c.f. doubly linked *N*-glycosidic linkage in STA **2**), essential for DNA minor groove binding and cell permeability.[15]

A recently enhanced awareness of how more subtle changes in molecular functionality within the indolo[2,3-*a*]pyrrolo[3,4-*c*]carbazole framework **3** can potentiate an extraordinary range of biological activities through its polyheterocyclic framework derives from an array of sources. Fermentation (actinomycetes, cyanobacteria, β-proteobacteria etc.), combinatorial biosynthesis, collection of eukaryotic field samples (myxomycetes, slime moulds, marine invertebrates), and an explosion of synthetic endeavour in the last 15 years, have all assisted compilation of the tantalizing SAR within this chemical family over that time.[16,152,153] In the following sub-sections, the properties of several important ICZ classes distinct from the STA **2** and REB **38** template, including those derivatives bearing no F-ring, a cyclofuranosylated/ modified pyranose sugar linkage and the clinically attractive non-planar bisindolylmaleimide scaffold will be discussed with respect to distinct bioactivity profiles within selected members of each series.

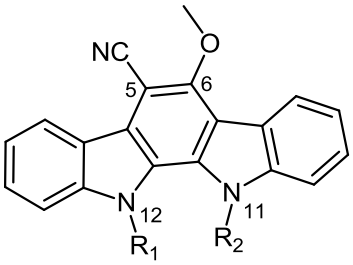
1.4.1.1 Bioactivity of ICZs lacking an F-ring

The necessity of an annelated pyrrolo[3,4-*c*] structural motif for biological effects associated with STA **2** congeners has been investigated by several workers. Thus, glycosidic tjipanazole A1 **60** which lacks any indolo[2,3-*a*]carbazole F-ring has been demonstrated to be PKC-

inactive and lack cytotoxic activity, but has been reported to possess phytopathogenic anti-fungal action (Fig. 1.45).[154]



60

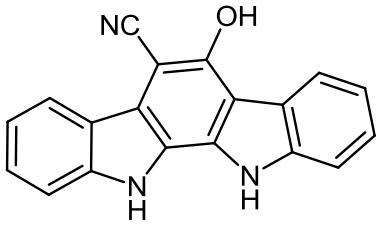


R_1 = H; R_2 = CH_3 **61**
R_1 = CH_3; R_2 = H **62**
R_1 = H; R_2 = H **63**

Fig. 1.45

In 1990, ICZ metabolites were isolated for the first time from cyanobacteria (blue-green algae). Extracts from cultures of *Nostoc sphaericum* EX-5-1 possessed moderate antiviral activity against herpes simplex virus type 2 (HSV-2) and weak, non-selective cytotoxicity against human cancer cell lines. This biological activity was attributable to the presence of 5-cyano-6-methoxy-11-methylindolo[2,3-*a*]carbazole **61** (major product), its regioisomer **62**, and desmethyl analogue **63** (Fig. 1.45).[155,156]

In 2009, Guo and co-workers synthesised a panel of these derivatives and reported their anti-bacterial activity against *B. anthracis* and *M. tuberculosis*. The necessity of indole methyl substitution, as well as the nature of substituents at both 5 and 6-positions were also investigated, and activity within novel analogues was compared to that of **61** against both bacterial strains. The results of SAR within this series confirmed that inhibitory activity was improved where R_4 = H, and was adversely affected by alkyl substitution on R_1 (Fig. 1.46).



64

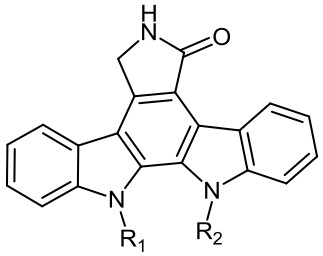
Fig. 1.46

The most active congener in this screen was determined to be **64** (MIC_{50} *B. anthracis* = 1.6 µM; MIC_{50} *M. tuberculosis* = 15.0 µM), compared with reduced inhibitory activity in the natural product **61** (MIC_{50} *B. anthracis* = >200 µM; MIC_{50} *M. tuberculosis* = >128 µM).

1.4.1.2 F-ring variants of ICZs with bridged ribofuranose linkages

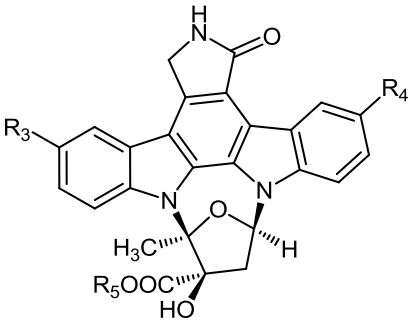
In 1986, the isolation of a series of novel ICZs, K-252a **13**, K-252b **65** and STA aglycon K-252c **6**, was reported from *Nocardiopsis* sp. K-290 providing further insight into the preponderance of the indolo[2,3-*a*]carbazole scaffold **1** as an immutable and diversifiable biological motif (Fig. 1.47).[157] These three compounds were strongly cytotoxic and conferred weak anti-microbial capacities; K-252a **13** possessed a 3'-ester substituted ribofuranose ring and mediated weak anti-bacterial and anti-fungal effects, including a prophylactic effect on rice plants against bacterial infection, in addition to potent PKC inhibition, also observed in K-252b **65**.[151,158]

Indolocarbazole platforms offer unique opportunities for imbuing specific biological capacities with subtly graduated alterations to overall molecular structure. Due to this property, indocarbazostatin **66** was successfully identified as a potent inhibitor of NGF-induced neuronal outgrowth from PC12 cells, yet remarkably, while K-252a **13** was a weaker inhibitor, STA **2** actually induced neurite outgrowth in the same cell line.[159,160]

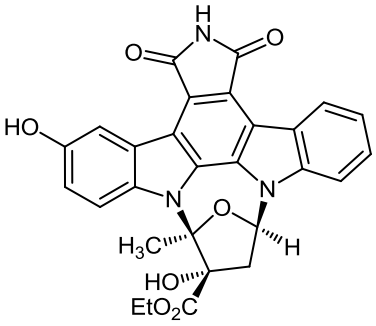


R_1=R_2= **2**

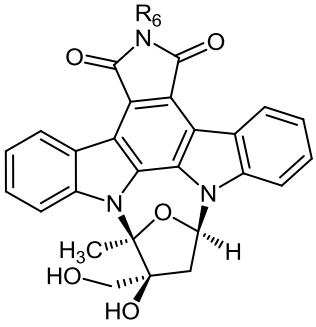
R_1=R_2=H K-252c **6**



R_3=R_4=H; R_5=CH_3 K-252a **13**
R_3=R_4=OH; R_5=CH_3 KT-6006 **47**
R_3=R_4=H; R_5=H K-252b **65**



66
Indocarbazostatin



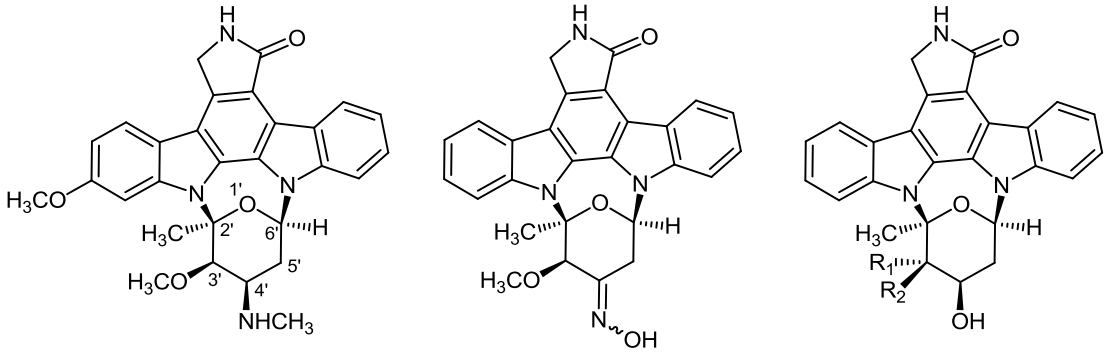
R_6=NH_2 **67** KT-6124
R_6=OH **68** KT-6528

Fig. 1.47

Prudhomme *et al.* also described in 1996 the development of a K-252a **13** structural congener, KT-6006 **47**, with competitive antagonism at the ATP-binding site of PKC, while similar ribofuranosylated analogues to KT-6006 **47**, differing only in F-ring imide substitution, KT-6124 **67** and KT-6528 **68** displayed much less potent PKC activity, but exhibited broad spectrum anti-proliferative activity against human tumour cell lines *in vitro* due to their attractive topo I inhibition profiles (Fig. 1.47).[161,162]

1.4.1.3 STA analogues containing modified pyranose moieties

In the mid-1990's, interesting work from several groups produced structures for two biologically relevant STA derivatives, namely, the PKC-active anti-tumour metabolite 10-methoxystaurosporine, TAN-999 **69**, derived from the soil bacterium *Nocardiopsis dassonvillei*, as well as a 4'-oxime analogue, (-)-TAN-1030a **70**, from *Streptomyces* sp. C-71799, with both possessing significant macrophage activation ability.[17] The synthetic derivative (+)-RK-286c **71** was equipotent to STA **2** as an inhibitor of platelet aggregation, and differs from staurosporine **2** *via* its 4'-hydroxy substitution, yet was only a weak inhibitor of PKC, as was its epimeric PKC inhibitor RK-1409B **72** (Fig. 1.48).[163,164]

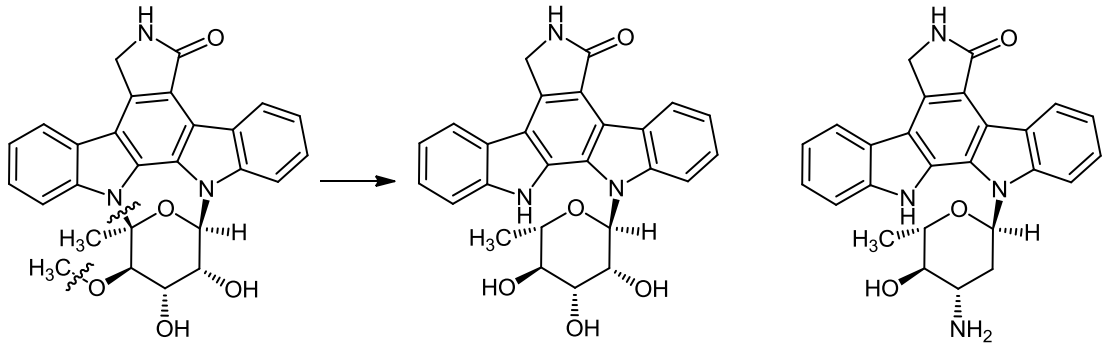


TAN-999 **69** (-)-TAN-1030a **70** R_1=H; R_2=OCH_3 (+)-RK-286c **71**
R_1=OCH_3; R_2=H RK-1409B **72**

Fig. 1.48

Thus, when a corresponding rhamnose sugar was inserted into the STA framework, **(+)-**MLR-52 **73** afforded almost identical *in vitro* platelet inhibitory activity to (+)-RK-286c **71** and STA **2**, as well as conferring micromolar PKC inhibition.[165] In addition, a natural 3'-demethylated analogue of (+)-MLR-52 **73**, K-252d **74** lacked the doubly linked sugar configuration, and contained a REB-type mono-α-L-rhamnose linkage, yet also conserved kinase inhibitory activity (Fig. 1.49).[157]

In 1999, a 5'-deoxyaminohexose derivative of K-252d **74** isolated from the marine actinomycete strain N96C-47, holyrine A **75**, was also reported to exhibit potent and quite selective kinase inhibition.[166]

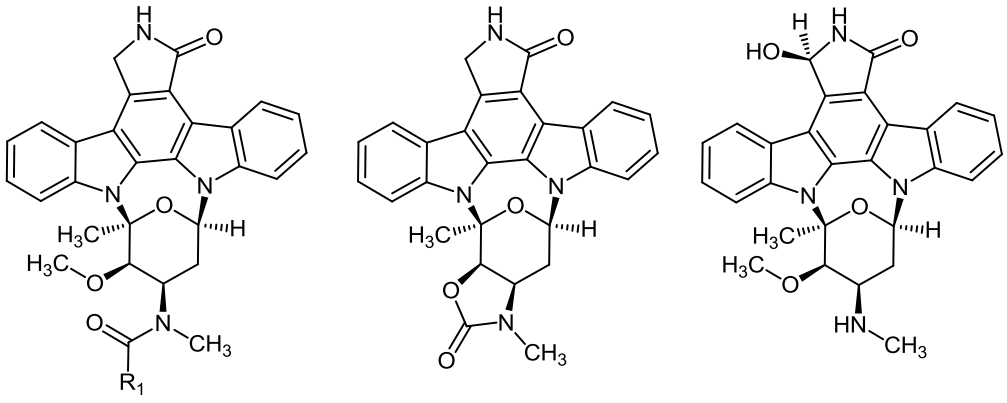


MLR-52 **73** K-252d **74** holyrine A **75**

Fig. 1.49: Deconvolution of sugar configuration in active mono and di-*N*-glycosidic indolocarbazole natural product kinase inhibitors conserving a lactam F-ring heterocyclic moiety.

An interesting result in this area concerns the recent isolation of the 4'-*N*-formyl **76** and 4'-*N*-carboxamido **77** derivatives of STA **2** from *Streptomyces* sp. QD518 and testing against a number of solid tumour cell lines. 4'-*N*-Carboxamido staurosporine **77** was determined to be the most active compound with a mean IC_{50} of 0.016 µg/mL, while 4'-*N*-formyl-staurosporine **76** was also highly active *in vitro* (IC_{50} = 0.063 µg/mL) (Fig. 1.50).[167]

It may also be possible to constrain and align certain optimised sugar orientations, with the goal of creating potent kinase inhibitors through novel non-covalent stabilising contacts with residues in the hydrophilic region of the ATP-binding domain. A putative lead compound which could be exploited through this strategy is the novel oxazolone-fused pyran system (perhaps mimicking a backbone interaction in the kinase ATP pocket) in the naturally occurring marine indolo[2,3-*a*]carbazole ZHD-0501 **78** from *Actinomadura* sp. 007.[25]



R_1=H **76** ZHD-0501 **78** UCN-01 **20**

Fig. 1.50 R_1=NH_2 **77**

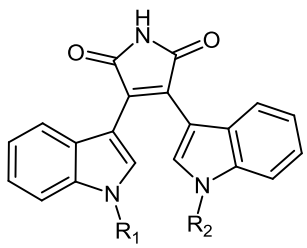
At 1 µM concentration, this metabolite **78** inhibited the proliferation of human lung adenocarcinoma A549 and pro-myelocytic leukemia HL60 cancer cell lines with inhibition rates of 82.6% and 76.1%. It also exhibited strong anti-proliferative activity against mouse

mammary cancer tsFT210 cells by eliciting mitotic catastrophe *via* accumulation of cells in the G2/M phase.[168] This spectrum of activity is similar to the previously discussed anti-cancer agent, UCN-01 **20**, potent in p53-deficient (G1-evading) tumours due to inhibition of various cell cycle-related kinases such as ChK1, PDK1 and various CDKs (Fig. 1.50).[35]

1.4.1.4 Heterocyclic ring modifications in ICZs

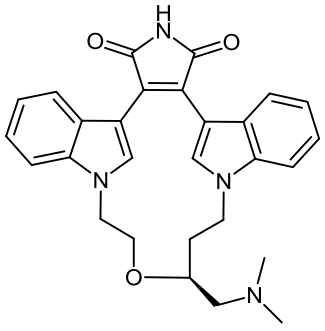
1.4.1.4.1 Bisindolylmaleimide (BIM) derivatives: acyclic C-ring analogues

As previously discussed, the broad spectrum of biological activity displayed by STA **2** was rationalized in 1986 to be due to its behaviour as a non-specific ATP-competitive kinase inhibitor, exhibiting strong cytotoxic activity against cancer cell lines due to its nanomolar PKC activity, as well as CDK inhibition, *in vitro*.[33,38] As biogenetic ICZ precursors, the bisindolylmaleimide (3,4-di-1*H*-indol-3-yl-1*H*-pyrrole-2,5-dione) scaffold based on the anti-fungal metabolite arcyriarubin A **79**, which was isolated as the pigment from myxomycetes such as *Arcyria denudata* and *A. nutans*, may also represent a novel template for selective PKC inhibition and anti-angiogenesis activity *via* effects on VEGFR.[169,170]

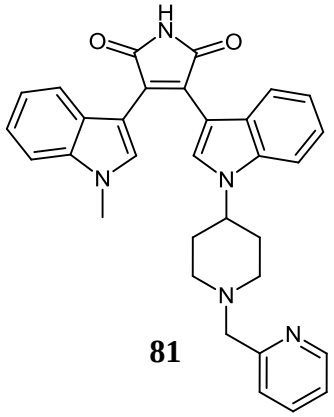


$R_1 = R_2 = H$ **79**

$R_1 = H$; $R_2 = (CH_2)_3N(CH_3)_2$ **26**



80



81

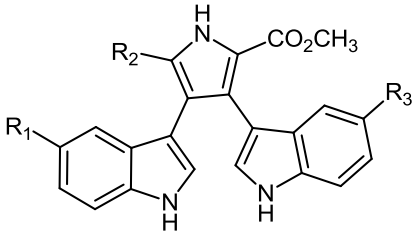
Fig. 1.51

Compounds of this type are also associated with suppression of cultured cancer cell line progression, while displaying a narrow therapeutic window, as well as having vast clinical potential for treatment of autoimmune diseases.[171,172] As will be discussed in Section 1.5, selective PKC-β inhibitors ruboxistaurin **80** and enzastaurin **81** possess extremely attractive potential as clinical agents against cancer and other indications (Fig. 1.51). Bisindolylmaleimide congener GF109203x **26** was also identified to display extremely potent activity against PKC (IC_{50} = 10 nM), although kinase selectivity issues later emerged.[173-175] In terms of overcoming innate chemotherapeutic resistance, active bisindolylmaleimides (BIMs) have also been described as ABCG2 transporter inhibitors, thus increasing the oral bioavailability of co-administered ABCG2 substrate cytotoxic

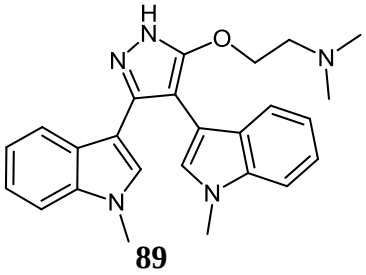
agents, in order to potentiate an effective therapeutic response and significantly improve subsequent clinical outcome.[130]

Due to their close biosynthetic and structural relationships with ICZs and BIMs, a number of other related alkaloids with interesting biological applications have been encountered from natural product screening. Lynamycin E **82** is a member of a family of bisindole pyrroles related to BIMs that all demonstrate potent anti-microbial activity against staphylococci and enterococci and was initially isolated from *Marinispora* sp. NPS12745, present in marine sediment collected off the coast of San Diego, California.[25,176,177] Its dechloro derivative, lycogarubin C **83** was isolated in the slime mold *Lycogala epidendrum*, and possessed moderate anti-viral activity against human simplex virus type 1 (HSV-1) (Fig. 1.52).[178,179]

Several complex analogues of simple indole alkaloids are also formed from alternative minor biosynthesis pathways *via* oxygenation and cyclisation steps.[16] Thus, cinereapyrroles A **84** and B **85** were present, together with arcyriarubin A **79**, in *Arcyria cinerea*, and regioisomeric annelation product arcyriacyanin A **86** was isolated, along with arcyriarubin A **79**, aromatised arcyriaflavin A **7**, dihydroarcyriarubin B **87** and arcyriaverdin C **88**, in the brightly coloured slime mold *Arcyria denudata* (Figs. 1.52 and 1.53).[16,169,180]



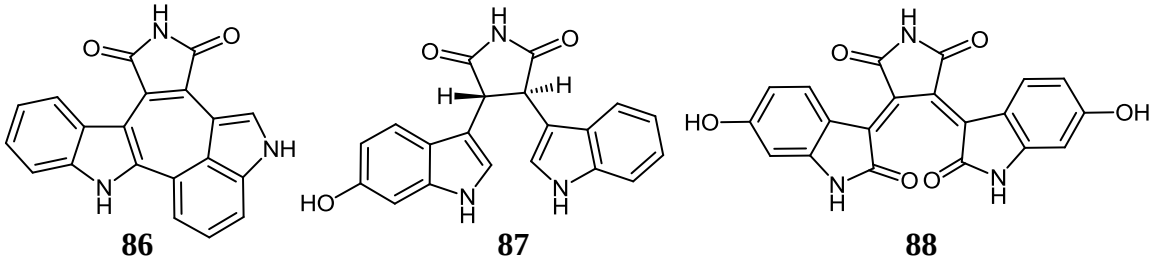
R_1=H; R_2=CO_2CH_3; R_3=Cl **82** R_1=H; R_2=OH; R_3=OH **84**
R_1=R_3=H; R_2=CO_2CH_3 **83** R_1=H; R_2=H; R_3=OH **85**



89

Fig. 1.52

Anti-cancer effects were reported by Brãna *et al.* within BIM analogue *N*,*N*-dimethylaminoethyl-substituted pyrazolone **89**, which induced 43% apoptosis within HeLa cells at 100 μM.[181] Interestingly, arcyriacyanin A **86** also exhibited anti-proliferative effects on several human tumour cell lines, as well as inhibiting PKC and protein tyrosine kinase.[182] Thus, initial condensation of two tryptophan units and F-ring diversity affords a disparate variety of bisindolyl metabolites with attractive medicinal characteristics, in which the indolo[2,3-*a*]carbazoles are present within modified heterocyclic scaffolds (Fig. 1.53).[16,30,183]

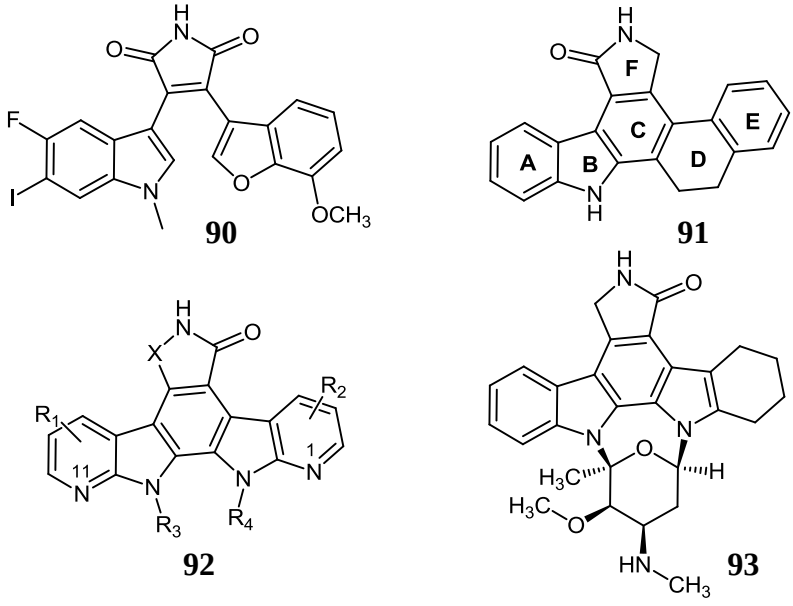


86 **87** **88**

Fig. 1.53

1.4.1.4.2 Peripheral ring modification: substituted D/E-rings in BIMs and ICZs

In addition to non-carbazole (acyclic) BIM derivatives, recent work, has revealed that chemical modification of advanced bisindolylethene chromophores may derive unique ligand binding interactions within an ATP-binding pocket, with enhanced target selectivity, due to increased conformational flexibility.[184,185] Thus, replacement of an indolic ring with a benzofuran heterocycle in **90** has been reported to confer potent GSK-3β inhibition.[186] SAR also revealed that lactam regiochemistry and retention of aryl rings B and E are important in development of potent cell-permeable MLK1/3 family selective inhibitors. Accordingly, the non-planar fused pyrrolocarbazole dihydronaphthyl[3,4-*a*]pyrrolo[3,4-*c*]carbazole-7-one **91** was determined to be a comparable MLK1/MLK3 inhibitor to K-252a **13**, and was 3 times more active than K-252c **6** (Fig. 1.54).[187]



90 **91**

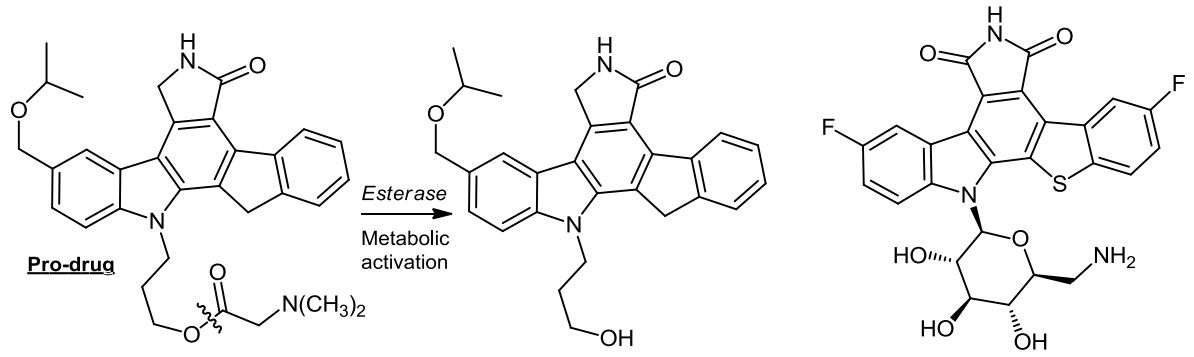
92 **93**

Fig. 1.54

Maintaining the arcyriaflavin A **7** framework, several workers have also recently synthesised other related fused carbazole analogues retaining either maleimide or imide F-ring systems, including naphtho and phenylcarbazoles, while the development of 1,11-azaindolocarbazoles **92**, including anti-topo I derivative **57** will have important future significance in cognisance

of their reported biological effects to date.[98,152,188,189] The attractive, partially hydrogenated 4*H*-tetrahydrostaurosporine **93** is a more soluble non-planar STA **2** analogue, possessing reduced aromatic E-ring character (Fig. 1.54). It has also been co-crystallised with Abl kinase and JAK3, binding in a distinct mode deep in the ATP pocket.[35,74]

A water-soluble 5-oxoindeno[2,1-*a*]pyrrolo[3,4-*c*]carbazole derivative CEP-7055 **29** was also observed to exhibit anti-angiogenic properties through metabolic esterase activation of the prodrug to the VEGF inhibitor CEP-5214 **94** (Fig. 1.55). CEP-7055 **29** entered phase I/II clinical trials for solid tumours but pre-clinical assessment of the drug apparently ceased in 2005.[16,93]



CEP-7055 **29** CEP-5214 **94** BMS-251873 **95**

Fig. 1.55: Metabolic conversion of CEP-7055 **29** to its active form, CEP-5214 **94** and structure of topo I inhibitor **95**.

Finally, to demonstrate the utility of indolic ring replacement for non-kinase targeting agents, Saulnier and co-workers recently reported synthesis of a putative clinical target – the highly active fluorinated rebeccamycin **38** analogue, BMS-251873 **95**, containing a contiguous thiophene-fused carbazole core and 6'-aminoglycosylated system, which possessed potent *in vitro* anti-tumour activity due to efficient promotion of topo I-mediated DNA cleavage.[126,190]

1.4.2 Conclusion

In conclusion, it seems that, in the case of a non-glycosylated system, any specific structure–activity relationships seem to operate only for a particular protein kinase and a given ICZ type, and are also limited in scope by the non-specific basis of their understood modes of action.[16] Specific biological functions within this series may be encoded within distinct structural domains, and perhaps, the ability to decouple structural ('modular') traits corresponding to anti-tumour or immunosuppressive ability may lead to less toxic, mono-purpose clinical agents incorporating a rationally designed indolo[2,3-*a*]carbazole **1**

skeleton. These results suggest that major alterations to the initial aminohexose configuration of STA **2**, (including mono-*N*-linkage, ring contraction and 3'-$NHCH_3$ replacement) could selectively modulate interesting biological effects (e.g. neurological treatment), but does not constitutively abolish PKC inhibition; the corresponding aglycon K-252c **6** still conferred significant PKC inhibition, if slightly weaker than both glycosides, K-252a **13** and K-252b **65**.[34,157,164,165,191]

Analysis of the activity of biosynthetic precursors may also benefit SAR within this series, due to the large number of closely related structures isolated in nature to date. In the case of clinical development of K-252c **6**, therefore, the vital necessity for *N*-glycosylation should be explored, as aqueous solubility of the non-glycosylated kinase-inhibitory pharmacophore could also be enhanced *via* efficacious alkylation/ carbohydrate modification.[120,190]

The synthetic endeavours encountered herein feature comprehensive efforts to apply synergistic advantages from the exciting strategies which underpin current research in relation to cancer. Thus, K-252c **6** and 3,4-diarylmaleimide (e.g. arcyriaflavin A **7**) investigation will culminate in design and synthesis of novel anti-cancer agents incorporating unique heterocyclic F-ring and indole ring subunits, with well defined biological potential. Unique opportunities arising from elaboration of a basic 1,2-bisindolyl-*cis*-ethene pharmacophore will thus be exploited to afford novel bioactive 'bridge-head' structural motifs, fully consistent with the basic indolo[2,3-*a*]pyrrolo[3,4-*c*]carbazole template **3**.

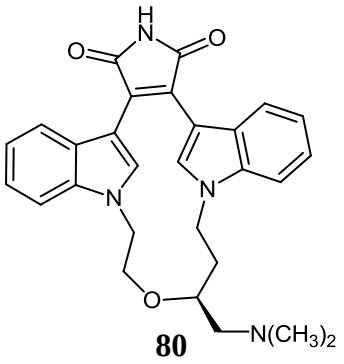
1.5 Current development of indolocarbazoles as clinical therapeutic agents

In recent years, several industrial indolocarbazole derivatives have been developed in order to optimize their intrinsic pharmacological activity, while limiting undesirable activity at other target sites.[13,15,152,192] Following a number of pre-clinical studies on REB **38** and STA **2** analogues, advanced candidates were investigated to possess attractive therapeutic and physicochemical characteristics (log P, molecular weight etc.). Based on these results, effective congeners which possessed low toxicity through enviable selectivity profiles, effective dosage regimens and acceptable drug metabolic fates in target tissue have now progressed to current clinical trials.[16,193]

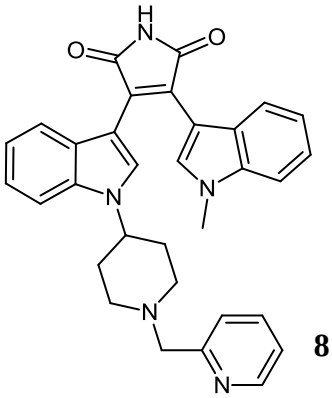
1.5.1 Bisindolylmaleimides (BIMs)

Recent progress in the development of PKC isoform-selective inhibitors has been highlighted by the drug application submitted to the FDA by Eli Lilly, in February 2006,

following successful clinical phase III trials, for the macrocyclic bisindolylmaleimide, ruboxistaurin mesylate (Arxxant®) **80** (Fig. 1.56).[16,194]



80



81

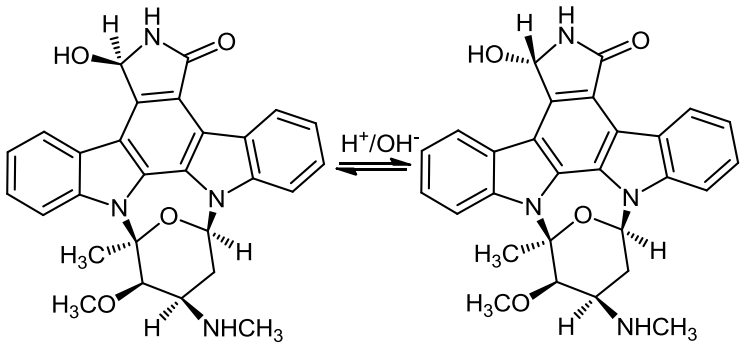
Fig. 1.56

Interestingly, compound **80** was reported to confer quite discrete enzyme selectivity; IC_{50} values for PKC-β1 and β2 (4.7 and 5.9 nM, respectively), are more than 40-fold greater than for other PKC isoforms, and thousands-fold more potent than against other ATP-dependent kinases, e.g. Src tyrosine kinase.[195,196] This clinical candidate possesses attractive efficacy in reducing vision loss in patients with diabetic peripheral retinopathy, and is currently defined as the first chemotherapeutic treatment for this serious complication of diabetes.[85,197] The orally-administered enzastaurin **81** has also been evaluated favorably in clinical trials for the treatment of glioblastoma and colo-rectal cancer, and is described to operate *via* induction of apoptosis and inhibition of VEGF-mediated angiogenesis.[198,199] Preliminary phase I/II data published to date also supports the potential of **81** as a component of adjuvant therapies for diffuse large B-cell lymphoma and refractive Akt-mediated diseases, such as breast and ovarian cancers due to its highly attractive PKCβ and AKT/PI3 activity (Fig. 1.56).[200-202]

1.5.2 Staurosporine derivatives

In 1987, Takahashi and co-workers isolated the epimeric 7-hydroxystaurosporine UCN-01 **20** from *Streptomyces* sp. N-126 – which is unique as the only natural indolo[2,3-*a*]carbazole to be in current clinical trials.[203,204] This compound is now finding application against haematological and advanced solid tumours, melanoma, and small-cell lung cancer, especially in combination with DNA-damaging agents, topo I poisons or radiotherapy, due to synergistic inhibition of various PKCs and cell cycle-related kinases.[77,205-208] The stereochemical configuration of the hydroxyl group in **20** is unstable in low or high pH solution and is found to exist in equilibrium with epimeric UCN-02 **96** (Fig. 1.57).[209] Active UCN-01 **20**, possesses poor tissue distribution and a prolonged half-life of elimination

(600h) following 72h infusion, due to high affinity for α_1-acid glycoprotein. Additional refinement may be required in order to overcome this pharmacokinetic limitation.[204,209-211]

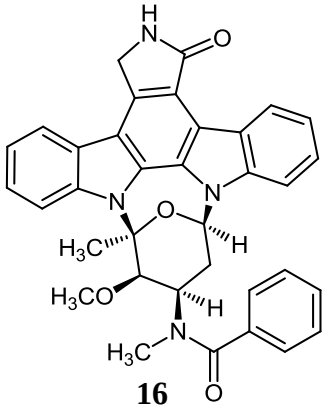


20 **96**

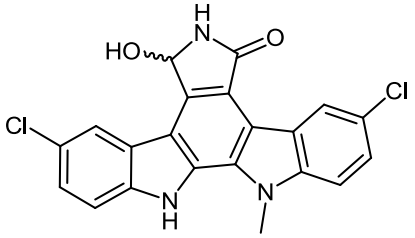
Fig. 1.57: Configurational instability of UCN-01 **20** in aqueous acidic or basic media.

Based on crystallographic data, the ability of **20** to potently inhibit ChK1 (K_i = 5.6 nM), PDK (IC_{50} = 5 nM) and PKC-β (IC_{50} = 10 nM) and abrogate G2/M checkpoint induced by DNA-damaging agents was ascertained by flexible conformational interactions in the adenine domain, glycine-rich and activation loops and hydrophobic pockets.[35,63,64]

Furthermore, UCN-01 **20** polypharmacology may also extend to anti-tumour activity based on disruption of Akt pathways arising from upstream PDK-1 inhibition.[212] In addition, UCN-01 **20** exhibits enhanced cytotoxicity in commonly refractory HT-29 and CA-46 cancer cell lines due to a down-regulated or mutated p53 tumour suppressor gene. G1 phase cell cycle arrest in a head and neck carcinoma cell line (HN12) has also been reported for **20**, but does not seem to be associated with p53, or maintaining hypophosphorylation of Rb protein, based on the conclusions of Shimizu *et al.*, following a review of its effects in lung cancer.[204,213] Future exploration of the pyrrolo[3,4-*c*]ring ring system present in UCN-01 **20** may also focus on semi-synthetic and chemical derivatisation of tjipanazole J **97**, a fungicidal indolo[2,3-*a*]carbazole produced by the blue-green alga, *tolypothrix tjiapanasensis*, which has relatively little biological data reported to date (Fig. 1.58).[16,154]



16



tjipanazole J **97**

Fig. 1.58

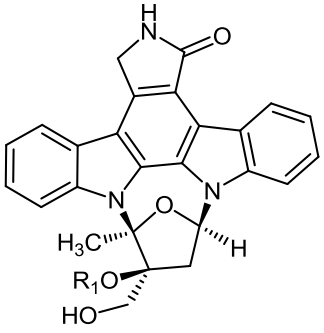
The relatively non-specific kinase inhibitor and orally administered midostaurin **16**, has entered phase I/II trial in patients with acute myeloid leukaemia, due to its potent inhibition of Flt-3, which is mutated in approximately 30% of these cancers.[12,214-216] Its use has also been positively indicated in clinical phase I/II trials for B-chronic lymphocytic leukaemia, acute myeloid leukemia (AML) and non-cancer disorders such as diabetic macular edema, based upon the recognised ability of midostaurin **16** to potently inhibit kinases including VEGFR2, PDGFR and c-Kit, involved in development of aberrant microvascularisation associated with this complication of diabetes (Fig. 1.58).[16,76,217]

1.5.3 K-252a derivatives

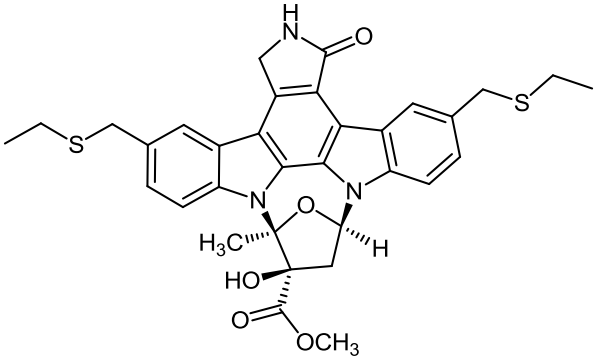
Lestaurtinib (CEP-701) **98** and CEP-751 **99** have also been found to possess intrinsic anti-tumour activity via inhibition of neurotrophin-specific trk-receptors, in addition to kinases including PDGFR and Flt-3, and have entered phase II/ III clinical trials against refractive AML in patients with mutated copies of Flt-3.[218-220]

In April 2006, lestaurtinib **98** was granted orphan drug designation against AML, and is currently undergoing various trial protocols for additional treatment of myelofibrosis and prostate cancer, in addition to early human trials in children with high risk neuroblastoma and patients with severe psoriasis (Fig. 1.59).[16,35]

A 3,9-bis(ethylthiomethyl) derivative of K-252a **13**, orally active CEP-1347 **30** was also found to possess pre-clinical neuroprotective activity due to its inhibition of MLK kinases, which are key modulators within the JNK signalling pathway implicated in neurodegeneration and apoptosis.[221,222]



R_1=H **98** lestaurtinib
R_1=CH_3 **99** CEP-751



CEP-1347 **30**

Fig. 1.59

CEP-1347 **30** thus represents a rational target for suppression of Parkinson's disease, *via* disruption of pathogenesis.[16] Subsequently, in May 2005, clinical studies were discontinued

due to the lack of an observable therapeutic dividend arising from **30** (Fig. 1.59). However, it is still an intriguing development and further research could elucidate precise neuroprotective pathways affected by similar compounds. Perhaps, more effective ICZ derivatives could be found through combination therapy with another inhibitory agent or improving pharmacokinetics within this poorly aqueous soluble drug class by engineering a prodrug containing a labile water-soluble fragment, increasing bioavailability, prior to enzymatic cleavage and localisation of the active moiety within the target site.

1.5.4 Rebeccamycin derivatives

Due to the aqueous insolubility of rebeccamycin **38**, subsequent structural analogues of clinical relevance within this series have incorporated improved hydrophilic functionality, in addition to their enhanced spectra of activity and improved toxicity profiles.[41,120,138]

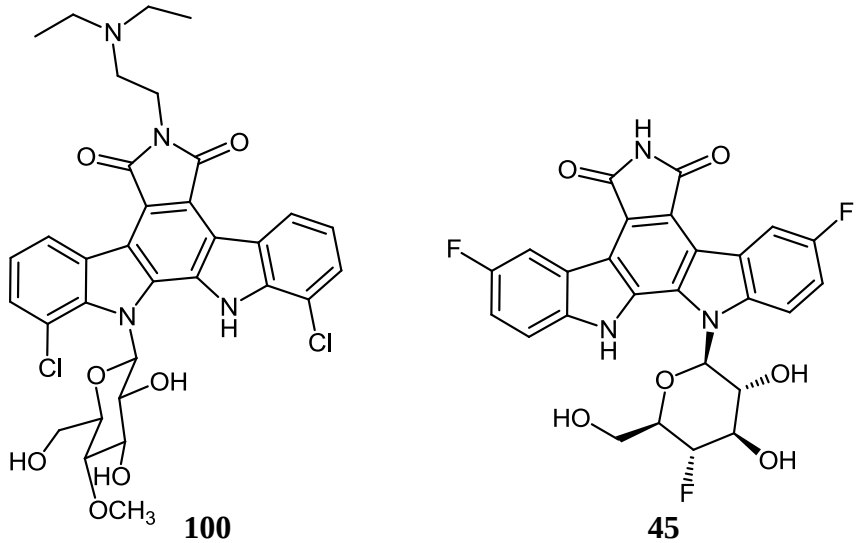


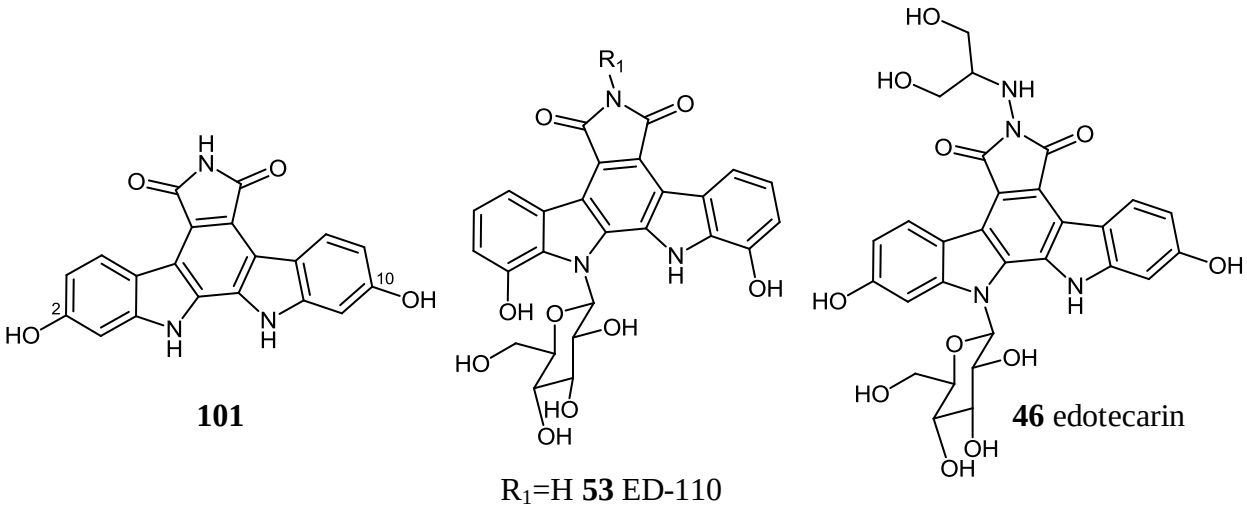
Fig. 1.60 **100** **45**

This anti-cancer compound, becatecarin **100**, unlike REB **38**, can act through tight DNA intercalation. Thus, it is active as a topo I poison mediating extensive strand fragmentation, and potently inhibits topo II by preventing correct DNA binding of the enzyme. In addition, **100** also induces expression of ABCG2 drug transporter, implicated in mechanisms of cancer chemoresistance against other ABCG2 substrate drugs.[120,223] A fluorinated analogue, BMS-250749 **45**, entered human trials as a result of effective topo I-mediated DNA cleavage, following a biocombinatorial study involving addition of starting fluorotryptophans to a culture of *L. aerocolonigenes*, to afford the corresponding fluoroindolocarbazoles (Fig. 1.60).[126,190]

The difficulty of predicting putative modes of action of *de novo* synthetic indolocarbazoles can be encapsulated by the unique biological characteristics of the 2,10-dihydroxylated

congener, arcyriaflavin C **101**, produced by the slime mold, *Tubifera casparyi*.[224] Arcyriaflavin C **101** induced cell-cycle arrest at lower concentrations, while displaying cytotoxicity at higher concentrations, along with no observable effect on bacterial topo 1 activity. Interestingly, the arcyriaflavin C **101** 1,11-dihydroxylated regioisomer and potent dual topo I/II inhibitor, BE-13793C **52** (aglycon of ED-110 **53**) also overcomes conventional drug resistance phenomena in that it inhibits the growth of P388/ADR cells, which are refractive towards doxorubicin, part of a well-known family of DNA intercalating topo II suppressors (Fig. 1.61).[144]

Due to its hydrophobic, polyheteroaromatic core, derivative **52** demonstrated the significant drawback of low water solubility, and thus a clinical study set about evaluating analogues with improved physico-chemical parameters, through glycosylation and imide substitution. The resultant glucosylated anti-cancer derivative ED-110 **53** also possessed a significantly lower log P value and interestingly, inhibited topo I while being topo II inactive (Fig. 1.61).[141-143]



101 **46** edotecarin

R_1=H **53** ED-110

Fig. 1.61 R_1=NHCHO **50** NB-506

In 1994, another more soluble, semi-synthetic 6-*N*-formylamino derivative, NB-506 **50** progressed to clinical trials for treatment of solid tumours.[131,225] This 1,11-dihydroxylated ICZ **50** was an effective anti-topo I congener, preserving its capacity for DNA binding, in addition to inhibition of its dual DNA relaxing and SR kinase activity.[16] These multiple mechanisms contribute to the limited resistance seen for **50** on camptothecin-resistant cancer cell lines; it was observed that camptothecin **33** induced greater than 100-fold reduction in anti-cancer activity, while NB-506 **50** only elicited less than 10-fold decrease in cytotoxicity against cell strains also resistant to NB-506 **50** topo I inhibition.[226] Developmental work culminated in a positive phase I outcome for NB-506 **50** against estrogen sensitive ovarian

and breast cancers resistant to vinca alkaloid anti-mitotics, but further advanced clinical trials were ultimately unsuccessful.[131]

Another cytotoxic derivative of **50**, edotecarin **46**, also afforded topo I-mediated persistent single strand breakage and DNA lesion formation more effectively than either camptothecin **33** or NB-506 **50**, and improved its pharmacokinetic and efficacy profile further by replacing the formylamino group of **50** with a more hydrophilic 1,3-dihydroxyisopropylamino moiety, and adjusting the hydroxylation pattern of the planar chromophore (2-OH and 10-OH).[112,227] These structural alterations result in non-covalent stabilisation of H-bonding interactions within the DNA stacking or protein side-chain regions of the drug-DNA-topo I ternary complex. Following initial human tumour xenograft testing against CNS, colon and breast neoplasms, edotecarin **46** was revealed to exert dose-limiting haematologic toxicity and subsequently entered advanced clinical trials as an intravenous infusion, for the treatment of breast, gastric and metastatic colo-rectal cancer, and is currently in phase III studies against glioblastoma multiforme.[228-230]

1.6 Final perspective on future indolocarbazole development

Critical insights from the validated bioactivity of natural product and synthetic ICZs denote an exciting launching pad for new chemical research into formation of diverse analogues as a potential new anti-cancer class with a multitude of biological applications.

Originally isolated from microbial sources, indolocarbazoles display important effects in morphogenesis and developmental processes, such as cell differentiation within marine actinomycetes; it has been speculated that potent activity at discrete eukaryotic targets also confers an acute defence mechanism against attack.[16] The primary biological targets probed by current novel indolo[2,3-*a*]pyrrolo[3,4-*c*]carbazole development are inhibition of protein kinases (characterised by an unsubstituted lactam/maleimide F-ring), which constitute 22% of the total medicinal genome, as well as distinct topo I poisoning using hydrophilic, branched F-ring analogues, unrelated to tyrosine kinase inhibition.

Stabilisation of the DNA-topoisomerase covalent catalytic intermediate or ‘cleavable complex’ and avid DNA binding by 2,10-dihydroxylated (A/E-ring) indolocarbazoles also disrupts critical cell processes such as transcription and replication, in a relatively complex fashion, also possibly related to intrinsic topo I kinase (phosphotransferase) inhibition.[129] The contribution of other mechanisms to overall anti-cancer activity was also illustrated by

only partial correlation between the *in vitro* S-phase cytotoxicity and G2-M cell cycle arrest induced by rebeccamycin **38** derivatives and their corresponding topo I inhibitory activity or magnitude of drug-DNA binding.[41,112,226] Thus, it is evident that no mono-modal or single target activity paradigm underpins the fusion of biological effects transmitted by the diverse spectrum of indolo[2,3-*a*]carbazole agents.

Indolocarbazole derivatives possessing an essential bidentate hydrogen bonding network and hydrophobic heterocyclic scaffold, are now fully recognised as constituting a versatile anti-cancer class with novel synthetic congeners yielding noteworthy success in a multitude of clinical trials within the last 15 years, against diverse cancer states, with successful BIM investigational compounds ruboxistaurin **80** and enzastaurin **81**, attracting intense clinical interest within diabetic retinopathy chemotherapy and Parkinson's disease, due to specifically targeting PKC-β and MLK, respectively.[16,77] Relatively structurally diverse indolocarbazole scaffolds have also been employed to derive relatively specific PKC inhibitors, with possible application to non-cytotoxic anti-angiogenesis therapies, as well as cell cycle modulating roles due to inhibition of CDK, PDK1 and ChK1 enzymes. With respect to carbohydrate substitution, the necessity of an active mono-glycosyl conformation with an adjacent indole NH, for topo I inhibition within this series was outlined by Facompre and co-workers. However, for general kinase inhibition, active glycosidic derivatives favour the presence of a lactam F-ring moiety, while non-glycosidic congeners comprising an imide heterocyclic nucleus generally exhibit enhanced activity.

Kinase inhibition is more tolerant of functional group variation and simplification; acyclic bisindolylmaleimide analogues are believed to bind in a more flexible mode within the adenosine-binding hinge region of the ATP pocket, in unique conformations exploiting selective non-covalent ligand interactions.[82,136,185] In concert with the enviable pre-clinical activity observed for UCN-01 **20** (containing a modified 5-hydroxypyrrol-2-one F-ring system) against a range of solid and haematological tumours, these underpinning structural relationships clearly demonstrate how bisindolylmaleimide and indolocarbazole derivatives possessing desirable pyrrol-2-one (maleimide/lactam) isosteres may impart improved anti-cancer potency and target selectivity. However, few workers to date have comprehensively investigated heterocyclic modification of the crucial F-ring pyrrole moiety and its associated potential for accessing new molecular targets, or an enhanced array of anti-cancer properties.

The illustrious history of indolocarbazole anti-cancer research and underlying clinical benefits accruing from defining new robust analogues within this privileged bioactive 1,2-

bis(indol-3-yl)-*cis*-ethene scaffold offers unique opportunities ripe for exploration over the course of this work.

1.7 References

1. Cancer in Ireland 1994-2007 *National Cancer Institute Ireland* **2009**, *Annual Statistical Report*.
2. Lapenna, S.; Giordano, A. *Nat.Rev.Drug Discovery* **2009**, *8*, 547-566.
3. Shawver, L. K.; Slamon, D.; Ullrich, A. *Cancer Cell* **2002**, *1*, 117-123.
4. Carter, S. K. *Oncologist* **2000**, *5*, 51-54.
5. Garcia-Carbonero, R.; Supko, J. G. *Clin.Cancer Res.* **2002**, *8*, 641-661.
6. Ghoul, A.; Serova, M.; Bieche, I.; Videau, M.; Benhadji, K. A.; Faivre, S.; Raymond, E. *Eur.J.Cancer* **2008**, *6*, 157.
7. Janne, P. A.; Gray, N.; Settleman, J. *Nat.Rev.Drug Discovery* **2009**, *8*, 709-723.
8. Merritt, J. E.; Sullivan, J. A.; Drew, L.; Khan, A.; Wilson, K.; Mulqueen, M.; Harris, W.; Bradshaw, D.; Hill, C. H.; Rumsby, M.; Warr, R. *Cancer Chemother.Pharmacol.* **1999**, *43*, 371-378.
9. Kanzawa, F.; Nishio, K.; Kubota, N.; Saijo, N. *Cancer Res.* **1995**, *55*, 2806-2813.
10. Utz, I.; Hofer, S.; Regenass, U.; Hilbe, W.; Thaler, J.; Grunicke, H.; Hofmann, J. *Int.J.Cancer* **1994**, *57*, 104-110.
11. Conseil, G.; Perez-Victoria, J. M.; Jault, J. M.; Gammaro, F.; Goffeau, A.; Hofmann, J.; Di Pietro, A. *Biochemistry (Mosc).* **2001**, *40*, 2564-2571.
12. Meyer, T.; Regenass, U.; Fabbro, D.; Alteri, E.; Rosel, J.; Muller, M.; Caravatti, G.; Matter, A. *Int.J.Cancer* **1989**, *43*, 851-856.
13. Akinaga, S.; Sugiyama, K.; Akiyama, T. *Anticancer.Drug Des.* **2000**, *15*, 43-52.
14. Bailly, C.; Riou, J. F.; Colson, P.; Houssier, C.; Rodrigues-Pereira, E.; Prudhomme, M. *Biochemistry (Mosc).* **1997**, *36*, 3917-3929.
15. Prudhomme, M. *Curr.Pharm.Des.* **1997**, *3*, 265-290.
16. Sanchez, C.; Mendez, C.; Salas, J. A. *Nat.Prod.Rep.* **2006**, *23*, 1007-1045.
17. Tanida, S.; Takizawa, M.; Takahashi, T.; Tsubotani, S.; Harada, S. *J.Antibiot.* **1989**, *42*, 1619-1630.
18. Zhu, G. X.; Conner, S. E.; Zhou, X.; Shih, C.; Li, T. C.; Anderson, B. D.; Brooks, H. B.; Campbell, R. M.; Considine, E.; Dempsey, J. A.; Faul, M. M.; Ogg, C.; Patel, B.; Schultz, R. M.; Spencer, C. D.; Teicher, B.; Watkins, S. A. *J.Med.Chem.* **2003**, *46*, 2027-2030.
19. Zimmermann, A.; Wilts, H.; Lenhardt, M.; Hahn, M.; Mertens, T. *Antiviral Res.* **2000**, *48*, 49-60.
20. Oikawa, T.; Shimamura, M.; Ashino, H.; Nakamura, O.; Kanayasu, T.; Morita, I.; Murota, S. *J.Antibiot.* **1992**, *45*, 1155-1160.
21. Omura, S.; Iwai, Y.; Hirano, A.; Nakagawa, A.; Awaya, J.; Tsuchiya, H.; Takahashi, Y.; Masuma, R. *J.Antibiot.* **1977**, *30*, 275-282.
22. McCarthy, A. J.; Williams, S. T. *Gene* **1992**, *115*, 189-192.
23. Wilkins, K. *Chemosphere* **1996**, *32*, 1427-1434.
24. Berdy, J. *J.Antibiot.* **2005**, *58*, 1-26.
25. Olano, C.; Mendez, C.; Salas, J. A. *Marine Drugs* **2009**, *7*, 210-248.
26. Schupp, P.; Steube, K.; Meyer, C.; Proksch, P. *Cancer Lett.* **2001**, *174*, 165-172.
27. Kinnel, R. B.; Scheuer, P. J. *J.Org.Chem.* **1992**, *57*, 6327-6329.
28. Horton, P. A.; Longley, R. E.; McConnell, O. J.; Ballas, L. M. *Experientia* **1994**, *50*, 843-845.
29. Liu, R.; Zhu, T. J.; Li, D. H.; Gu, J. Y.; Xia, W.; Fang, Y. C.; Liu, H. B.; Zhu, W. M.; Gu, Q. Q. *Arch.Pharm.Res.* **2007**, *30*, 270-274.
30. Pindur, U.; Lemster, T. *Curr.Med.Chem.* **2001**, *8*, 1681-1698.
31. Hernandez, L. M. C.; Blanco, J. A. D.; Baz, J. P.; Puentes, J. L. F.; Millan, F. R.; Vazquez, F. E.; Fernandez-Chimeno, R. I.; Gravalos, D. G. *J.Antibiot.* **2000**, *53*, 895-902.

32. Oka, S.; Kodama, M.; Takeda, H.; Tomizuka, N.; Suzuki, H. *Agric.Biol.Chem.* **1986**, *50*, 2723-2727.
33. Omura, S.; Sasaki, Y.; Iwai, Y.; Takeshima, H. *J.Antibiot.* **1995**, *48*, 535-548.
34. Tamaoki, T.; Nomoto, H.; Takahashi, I.; Kato, Y.; Morimoto, M.; Tomita, F. *Biochem.Biophys.Res.Commun.* **1986**, *135*, 397-402.
35. Gani, O.; Engh, R. *Nat.Prod.Rep.* **2010**, *27*, 489-498.
36. Nakano, H.; Kobayashi, E.; Takahashi, I.; Tamaoki, T.; Kuzuu, Y.; Iba, H. *J.Antibiot.* **1987**, *40*, 706-708.
37. Funato, N.; Takayanagi, H.; Konda, Y.; Toda, Y.; Harigaya, Y.; Iwai, Y.; Omura, S. *Tetrahedron Lett.* **1994**, *35*, 1251-1254.
38. Ruegg, U. T.; Burgess, G. M. *Trends Pharmacol.Sci.* **1989**, *10*, 218-220.
39. Hoehn, P.; Ghisalba, O.; Moerker, T.; Peter, H. H. *J.Antibiot.* **1995**, *48*, 300-305.
40. Moreau, P.; Gaillard, N.; Marminon, C.; Anizon, F.; Dias, N.; Baldeyrou, B.; Bailly, C.; Pierre, A.; Hickman, J.; Pfeiffer, B.; Renard, P.; Prudhomme, M. *Bioorg.Med.Chem.* **2003**, *11*, 4871-4879.
41. Prudhomme, M. *Eur.J.Med.Chem.* **2003**, *38*, 123-140.
42. Sancelme, M.; Fabre, S.; Prudhomme, M. *J.Antibiot.* **1994**, *47*, 792-798.
43. Bailly, C.; Dassonneville, L.; Colson, P.; Houssier, C.; Fukasawa, K.; Nishimura, S.; Yoshinari, T. *Cancer Res.* **1999**, *59*, 2853-2860.
44. Cohen, P. *Nat.Rev.Drug Discovery* **2002**, *1*, 309-315.
45. Sawa, M. *Mini Rev.Med.Chem.* **2008**, *8*, 1291-1297.
46. Burgess, A. W.; Cho, H. S.; Eigenbrot, C.; Ferguson, K. M.; Garrett, T. P.; Leahy, D. J.; Lemmon, M. A.; Sliwkowski, M. X.; Ward, C. W.; Yokoyama, S. *Mol.Cell* **2003**, *12*, 541-552.
47. Lawrie, A. M.; Noble, M. E. M.; Tunnah, P.; Brown, N. R.; Johnson, L. N.; Endicott, J. A. *Nat.Struct.Biol.* **1997**, *4*, 796-801.
48. Powis, G. *Trends Pharmacol.Sci.* **1991**, *12*, 188-194.
49. Pearson, M.; Garcia-Echeverria, C.; Fabbro, D. *Protein Tyrosine Kinases: From Inhibitors to Useful Drugs*; Edited by Fabbro, D.; McCormick, F., Eds.; Humana Press: Totowa, NJ, 2006; pp 1-31.
50. Noble, M. E. M.; Endicott, J. A.; Johnson, L. N. *Science* **2004**, *303*, 1800-1805.
51. Blume-Jensen, P.; Hunter, T. *Nature* **2001**, *411*, 355-365.
52. Kornev, A. P.; Haste, N. M.; Taylor, S. S.; Eyck, L. F. T. *Proc.Natl.Acad.Sci.U.S.A.* **2006**, *103*, 17783-17788.
53. Manning, G.; Whyte, D. B.; Martinez, R.; Hunter, T.; Sudarsanam, S. *Science* **2002**, *298*, 1912-1934.
54. Gescher, A. *Gen.Pharm.Vascular System* **1998**, *31*, 721-728.
55. Mizuno, K.; Saido, T. C.; Ohno, S.; Tamaoki, T.; Suzuki, K. *FEBS Lett.* **1993**, *330*, 114-116.
56. Hanks, S. K.; Hunter, T. *FASEB J.* **1995**, *9*, 576-596.
57. Stout, T. J.; Foster, P. G.; Matthews, D. J. *Curr.Pharm.Des.* **2004**, *10*, 1069-1082.
58. Vulpetti, A.; Bosotti, R. *Farmaco* **2004**, *59*, 759-765.
59. Ono, Y.; Fujii, T.; Igarashi, K.; Kuno, T.; Tanaka, C.; Kikkawa, U.; Nishizuka, Y. *Proc.Natl.Acad.Sci.U.S.A.* **1989**, *86*, 4868-4871.
60. Schiering, N.; Knapp, S.; Marconi, M.; Flocco, M. M.; Cui, J.; Perego, R.; Rusconi, L.; Cristiani, C. *Proc.Natl.Acad.Sci.U.S.A.* **2003**, *100*, 12654-12659.
61. Li, B.; Liu, Y.; Uno, T.; Gray, N. *Combinatorial Chemistry & High Throughput Screening* **2004**, *7*, 453-472.
62. Jin, L.; Pluskey, S.; Petrella, E. C.; Cantin, S. M.; Gora, J. C.; Rynkiewicz, M. J.; Pandey, P.; Strickler, J. E.; Babine, R. E.; Weaver, D. T.; Seidl, K. J. *J.Biol.Chem.* **2004**, *279*, 42818-42825.

63. Zhao, B.; Bower, M. J.; McDevitt, P. J.; Zhao, H. Z.; Davis, S. T.; Johanson, K. O.; Green, S. M.; Concha, N. O.; Zhou, B. B. S. *J.Biol.Chem.* **2002**, *277*, 46609-46615.
64. Komander, D.; Kular, G. S.; Bain, J.; Elliott, M.; Alessi, D. R.; Van Aalten, D. M. F. *Biochem.J.* **2003**, *375*, 255-262.
65. Prade, L.; Engh, R. A.; Girod, A.; Kinzel, V.; Huber, R.; Bossemeyer, D. *Structure* **1997**, *5*, 1627-1637.
66. Lamers, M. B.; Antson, A. A.; Hubbard, R. E.; Scott, R. K.; Williams, D. H. *J.Mol.Biol.* **1999**, *285*, 713-725.
67. Gray, N.; Lénaïck, D.; Doerig, C.; Meijer, L. Curr.Med.Chem. **1999**, *6*, 859-875
68. Yang, S. M.; Malaviya, R.; Wilson, L. J.; Argentieri, R.; Chen, X.; Yang, C. M.; Wang, B. B.; Cavender, D.; Murray, W. V. *Bioorg.Med.Chem.Lett.* **2007**, *17*, 326-331.
69. Shomin, C. D.; Meyer, S. C.; Ghosh, I. *Bioorg.Med.Chem.* **2009**, *17*, 6196-6202.
70. Sasaki, S.; Hashimoto, T.; Obana, N.; Yasuda, H.; Uehara, Y.; Maeda, M. *Bioorg.Med.Chem.Lett.* **1998**, *8*, 1019-1022.
71. Traxler, P.; Bold, G.; Buchdunger, E.; Caravatti, G.; Furet, P.; Manley, P.; O'Reilly, T.; Wood, J.; Zimmermann, J. *Med.Res.Rev.* **2001**, *21*, 499-512.
72. Grimminger, F.; Schermuly, R. T.; Ghofrani, H. A. *Nat.Rev.Drug Discovery* **2010**, *9*, 956-970.
73. Ma, P. C.; Maulik, G.; Christensen, J.; Salgia, R. *Cancer Metastasis Rev.* **2003**, *22*, 309-325.
74. Boggon, T. J.; Li, Y. Q.; Manley, P. W.; Eck, M. J. *Blood* **2005**, *106*, 996-1002.
75. Brown, P.; Levis, M.; McIntyre, E.; Griesemer, M.; Small, D. *Leukemia* **2006**, *20*, 1368-1376.
76. Stone, R. M.; DeAngelo, D. J.; Klimek, V.; Galinsky, I.; Estey, E.; Nimer, S. D.; Grandin, W.; Lebwohl, D.; Wang, Y. F.; Cohen, P.; Fox, E. A.; Neuberg, D.; Clark, J.; Gilliland, D. G.; Griffin, J. D. *Blood* **2005**, *105*, 54-60.
77. Marengo, B.; De, C.; Ricciarelli, R.; Pronzato, M.; Marinari, U. M.; Domenicotti, C. *Cancers* **2011**, *3*, 531-567.
78. Nurse, P. *Cell* **1997**, *91*, 865-867.
79. Weinert, T.; Lydall, D. *Semin.Cancer Biol.* **1993**, *4*, 129-140.
80. Malumbres, M.; Barbacid, M. *Nat.Rev.Cancer* **2009**, *9*, 153-166.
81. Landberg, G. *Adv.Cancer Res.* **2002**, 35-56.
82. Sanchez-Martinez, C.; Shih, C.; Zhu, G. X.; Li, T. C.; Brooks, H. B.; Patel, B. K. R.; Schultz, R. M.; Dehahn, T. B.; Spencer, C. D.; Watkins, S. A.; Ogg, C. A.; Considine, E.; Dempsey, J. A.; Zhang, F. M. *Bioorg.Med.Chem.Lett.* **2003**, *13*, 3841-3846.
83. Soni, R.; Muller, L.; Furet, P.; Schoepfer, J.; Stephan, C.; Zumstein-Mecker, S.; Fretz, H.; Chaudhuri, B. *Biochem.Biophys.Res.Commun.* **2000**, *275*, 877-884.
84. Kleinschroth, J.; Hartenstein, J.; Rudolph, C.; Schachtele, C. *Bioorg.Med.Chem.Lett.* **1995**, *5*, 55-60.
85. Grant, S.; Tran, P.; Zhang, Q.; Zou, A.; Dinh, D.; Jensen, J.; Zhou, S.; Kang, X.; Zachwieja, J.; Lippincott, J.; Liu, K.; Johnson, S. L.; Scales, S.; Yin, C.; Nukui, S.; Stoner, C.; Prasanna, G.; Lafontaine, J.; Wells, P.; Li, H. *Eur.J.Pharmacol.* **2010**, *627*, 16-25.
86. Gonelli, A.; Mischiati, C.; Guerrini, R.; Voltan, R.; Salvadori, S.; Zauli, G. *Mini Rev.Med.Chem.* **2009**, *9*, 498-509.
87. Abrams, S. T.; Brown, B. R. B.; Zuzel, M.; Slupsky, J. R. *Blood* **2010**, *115*, 4447-4454.
88. Cohen, P. *Curr.Opin.Chem.Biol.* **1999**, *3*, 459-465.
89. Gliki, G.; Wheeler-Jones, C.; Zachary, I. *Cell Biol.Int.* **2002**, *26*, 751-759.

90. Zhang, H. C.; Derian, C. K.; McComsey, D. F.; White, K. B.; Ye, H.; Hecker, L. R.; Li, J.; Addo, M. F.; Croll, D.; Eckardt, A. J.; Smith, C. E.; Li, Q.; Cheung, W. M.; Conway, B. R.; Emanuel, S.; Demarest, K. T.; Andrade-Gordon, P.; Damiano, B. P.; Maryanoff, B. E. *J.Med.Chem.* **2005**, *48*, 1725-1728.
91. Martinybaron, G.; Kazanietz, M. G.; Mischak, H.; Blumberg, P. M.; Kochs, G.; Hug, H.; Marme, D.; Schachtele, C. *J.Biol.Chem.* **1993**, *268*, 9194-9197.
92. Qatsha, K. A.; Rudolph, C.; Marme, D.; Schachtele, C.; May, W. S. *Proc.Natl.Acad.Sci.U.S.A.* **1993**, *90*, 4674-4678.
93. Gingrich, D. E.; Reddy, D. R.; Iqbal, M. A.; Singh, J.; Aimone, L. D.; Angeles, T. S.; Albom, M.; Yang, S.; Ator, M. A.; Meyer, S. L.; Robinson, C.; Ruggeri, B. A.; Dionne, C. A.; Vaught, J. L.; Mallamo, J. P.; Hudkins, R. L. *J.Med.Chem.* **2003**, *46*, 5375-5388.
94. Sinnett-Smith, J.; Jacamo, R.; Kui, R.; Wang, Y. Z. M.; Young, S. H.; Rey, O.; Waldron, R. T.; Rozengurt, E. *J.Biol.Chem.* **2009**, *284*, 13434-13445.
95. Fischer, P. M. *Chem.Biol.* **2003**, *10*, 1144-1146.
96. Kuo, G. H.; Prouty, C.; DeAngelis, A.; Shen, L.; O'Neill, D. J.; Shah, C.; Connolly, P. J.; Murray, W. V.; Conway, B. R.; Cheung, P.; Westover, L.; Xu, J. Z.; Look, R. A.; Demarest, K. T.; Emanuel, S.; Middleton, S. A.; Jolliffe, L.; Beavers, M. P.; Chen, X. *J.Med.Chem.* **2003**, *46*, 4021-4031.
97. Zhang, H. C.; Ye, H.; Conway, B. R.; Derian, C. K.; Addo, M. F.; Kuo, G. H.; Hecker, L. R.; Croll, D. R.; Li, J.; Westover, L.; Xu, J. Z.; Look, R.; Demarest, K. T.; Andrade-Gordon, P.; Damiano, B. P.; Maryanoff, B. E. *Bioorg.Med.Chem.Lett.* **2004**, *14*, 3245-3250.
98. Lefoix, M.; Coudert, G.; Routier, S.; Pfeiffer, B.; Caignard, D. H.; Hickman, J.; Pierre, A.; Golsteyn, R. M.; Leonce, S.; Bossard, C.; Merour, J. Y. *Bioorg.Med.Chem.* **2008**, *16*, 5303-5321.
99. Rosen, L. S. *Oncologist* **2005**, *10*, 382-391.
100. Redinbo, M. R.; Champoux, J. J.; Hol, W. G. *Biochemistry (Mosc).* **2000**, *39*, 6832-6840.
101. Champoux, J. J. *Annu.Rev.Biochem.* **2001**, *70*, 369-413.
102. Gupta, M.; Fujimori, A.; Pommier, Y. *Biochim.Biophys.Acta, Gene Struct.Expression* **1995**, *1262*, 1-14.
103. Nitiss, J. L. *Biochim.Biophys.Acta, Gene Struct.Expression* **1998**, *1400*, 63-81.
104. Topcu, Z. *J.Clin.Pharm.Ther.* **2001**, *26*, 405-416.
105. Wang, J. C. *Annu.Rev.Biochem.* **1996**, *65*, 635-692.
106. Wang, J. C. *Nat.Rev.Mol.Cell Biol.* **2002**, *3*, 430-440.
107. Ahuja, H. G.; Felix, C. A.; Aplan, P. D. *Blood* **1999**, *94*, 3258-3261.
108. Stewart, L.; Redinbo, M. R.; Qiu, X.; Hol, W. G. J.; Champoux, J. J. *Science* **1998**, *279*, 1534-1541.
109. Pourquier, P.; Pommier, Y. *Adv.Cancer Res.* **2001**, 189-216.
110. Burgin, A. B.; Feese, M. D.; Staker, B. L.; Stewart, L. *Camptothecins in Cancer Therapy*; Edited by Adams, V. R.; Burke, T. G., Eds.; Humana Press: Totowa, N.J, 2005; pp 23-38.
111. Giovanella, B. C.; Stehlin, J. S.; Wall, M. E.; Wani, M. C.; Nicholas, A. W.; Liu, L. F.; Silber, R.; Potmesil, M. *Science* **1989**, *246*, 1046-1048.
112. Teicher, B. *Biochem.Pharmacol.* **2008**, *75*, 1262-1271.
113. Meng, L. H.; Liao, Z. Y.; Pommier, Y. *Curr.Top.Med.Chem.* **2003**, *3*, 305-320.
114. Marchand, C.; Antony, S.; Kohn, K. W.; Cushman, M.; Ioanoviciu, A.; Staker, B. L.; Burgin, A. B.; Stewart, L.; Pommier, Y. *Mol.Cancer Ther.* **2006**, *5*, 287-295.
115. Burke, T. G.; Mi, Z. H. *J.Med.Chem.* **1994**, *37*, 40-46.
116. Nettleton, D. E.; Doyle, T. W.; Krishnan, B.; Matsumoto, G. K.; Clardy, J. *Tetrahedron Lett.* **1985**, *26*, 4011-4014.

117. Bush, J. A.; Long, B. H.; Catino, J. J.; Bradner, W. T. *J.Antibiot.* **1987**, *40*, 668-678.
118. Anizon, F.; Moreau, P.; Sancelme, M.; Laine, W.; Bailly, C.; Prudhomme, M. *Bioorg.Med.Chem.* **2003**, *11*, 3709-3722.
119. Faul, M. M.; Sullivan, K. A.; Grutsch, J. L.; Winneroski, L. L.; Shih, C.; Sanchez-Martinez, C.; Cooper, J. T. *Tetrahedron Lett.* **2004**, *45*, 1095-1098.
120. Kaneko, T.; Wong, H.; Utzig, J.; Schurig, J.; Doyle, T. W. *J.Antibiot.* **1990**, *43*, 125-127.
121. Moreau, P.; Anizon, F.; Sancelme, M.; Prudhomme, M.; Bailly, C.; Carrasco, C.; Ollier, M.; Severe, D.; Riou, J. F.; Fabbro, D.; Meyer, T.; Aubertin, A. M. *J.Med.Chem.* **1998**, *41*, 1631-1640.
122. Prudhomme, M. *Curr.Med.Chem.* **2000**, *7*, 1189-1212.
123. Lam, K. S.; Schroeder, D. R.; Veitch, J. M.; Matson, J. A.; Forenza, S. *J.Antibiot.* **1991**, *44*, 934-939.
124. Facompre, M.; Carrasco, C.; Colson, P.; Houssier, C.; Chisholm, J. D.; Van Vranken, D. L.; Bailly, C. *Mol.Pharmacol.* **2002**, *62*, 1215-1227.
125. Chisholm, J. D.; Van Vranken, D. L. *J.Org.Chem.* **2000**, *65*, 7541-7553.
126. Saulnier, M. G.; Balasubramanian, B. N.; Long, B. H.; Frennesson, D. B.; Ruediger, E.; Zimmermann, K.; Eummer, J. T.; St Laurent, D. R.; Stoffan, K. M.; Naidu, B. N.; Mahler, M.; Beaulieu, F.; Bachand, C.; Lee, F. Y.; Fairchild, C. R.; Stadnick, L. K.; Rose, W. C.; Solomon, C.; Wong, H.; Martel, A.; Wright, J. J.; Kramer, R.; Langley, D. R.; Vyas, D. M. *J.Med.Chem.* **2005**, *48*, 2258-2261.
127. Denny, W. A. *Idrugs* **2004**, *7*, 173-177.
128. Yamashita, Y.; Fujii, N.; Murakata, C.; Ashizawa, T.; Okabe, M.; Nakano, H. *Biochemistry (Mosc).* **1992**, *31*, 12069-12075.
129. Labourier, E.; Riou, J. F.; Prudhomme, M.; Carrasco, C.; Bailly, C.; Tazi, J. *Cancer Res.* **1999**, *59*, 52-55.
130. Robey, R. W.; Shukla, S.; Steadman, K.; Obrzut, T.; Finley, E. M.; Ambudkar, S. V.; Bates, S. E. *Mol.Cancer Ther.* **2007**, *6*, 1877-1885.
131. Arakawa, H.; Iguchi, T.; Morita, M.; Yoshinari, T.; Kojiri, K.; Suda, H.; Okura, A.; Nishimura, S. *Cancer Res.* **1995**, *55*, 1316-1320.
132. Bailly, C.; Qu, X. G.; Chaires, J. B.; Colson, P.; Houssier, C.; Ohkubo, M.; Nishimura, S.; Yoshinari, T. *J.Med.Chem.* **1999**, *42*, 2927-2935.
133. Fukasawa, K.; Komatani, H.; Hara, Y.; Suda, H.; Okura, A.; Nishimura, S.; Yoshinari, T. *Int.J.Cancer* **1998**, *75*, 145-150.
134. Ohkubo, M.; Kawamoto, H.; Ohno, T.; Nakano, M.; Morishima, H. *Tetrahedron* **1997**, *53*, 585-592.
135. Bailly, C.; Qu, X. G.; Anizon, F.; Prudhomme, M.; Riou, J. F.; Chaires, J. B. *Mol.Pharmacol.* **1999**, *55*, 377-385.
136. Facompre, M.; Carrasco, C.; Vezin, H.; Chisholm, J. D.; Yoburn, J. C.; Van Vranken, D. L.; Bailly, C. *ChemBioChem* **2003**, *4*, 386-395.
137. Chaires, J. B. *Anticancer.Drug Des.* **1996**, *11*, 569-580.
138. Goossens, J. F.; Henichart, J. P.; Anizon, F.; Prudhomme, M.; Dugave, C.; Riou, J. F.; Bailly, C. *Eur.J.Pharmacol.* **2000**, *389*, 141-146.
139. Staker, B. L.; Feese, M. D.; Cushman, M.; Pommier, Y.; Zembower, D.; Stewart, L.; Burgin, A. B. *J.Med.Chem.* **2005**, *48*, 2336-2345.
140. Messaoudi, S.; Anizon, F.; Leonce, S.; Pierre, A.; Pfeiffer, B.; Prudhomme, M. *Eur.J.Med.Chem.* **2005**, *40*, 961-971.
141. Arakawa, H.; Iguchi, T.; Yoshinari, T.; Kojiri, K.; Suda, H.; Okura, A. *Jpn.J.Cancer Res.* **1993**, *84*, 574-581.
142. Tanaka, S.; Ohkubo, M.; Kojiri, K.; Suda, H.; Yamada, A.; Uemura, D. *J.Antibiot.* **1992**, *45*, 1797-1798.

143. Yoshinari, T.; Yamada, A.; Uemura, D.; Nomura, K.; Arakawa, H.; Kojiri, K.; Yoshida, E.; Suda, H.; Okura, A. *Cancer Res.* **1993**, *53*, 490-494.
144. Kojiri, K.; Kondo, H.; Yoshinari, T.; Arakawa, H.; Nakajima, S.; Satoh, F.; Kawamura, K.; Okura, A.; Suda, H.; Okanishi, M. *J.Antibiot.* **1991**, *44*, 723-728.
145. Zembower, D. E.; Zhang, H. P.; Lineswala, J. P.; Kuffel, M. J.; Aytes, S. A.; Ames, M. M. *Bioorg.Med.Chem.Lett.* **1999**, *9*, 145-150.
146. Bailly, C.; Goossens, J. F.; Laine, W.; Anizon, F.; Prudhomme, M.; Ren, J. S.; Chaires, J. B. *J.Med.Chem.* **2000**, *43*, 4711-4720.
147. Bailly, C.; Carrasco, C.; Hamy, F.; Vezin, H.; Prudhomme, M.; Saleem, A.; Rubin, E. *Biochemistry (Mosc).* **1999**, *38*, 8605-8611.
148. Bailly, C.; Qu, X. G.; Graves, D. E.; Prudhomme, M.; Chaires, J. B. *Chem.Biol.* **1999**, *6*, 277-286.
149. Hsiang, Y. H.; Liu, L. F. *J.Biol.Chem.* **1989**, *264*, 9713-9715.
150. Marminon, C.; Pierre, A.; Pfeiffer, B.; Perez, V.; Leonce, S.; Renard, P.; Prudhomme, M. *Bioorg.Med.Chem.* **2003**, *11*, 679-687.
151. Knolker, H. J.; Reddy, K. R. *Chem.Rev.* **2002**, *102*, 4303-4427.
152. Bergman, J.; Janosik, T.; Wahlstrom, N. *Adv.Heterocycl.Chem.* **2001**, *80*, 1-71.
153. Sanchez, C.; Mendez, C.; Salas, J. A. *J.Ind.Microbiol.Biotechnol.* **2006**, *33*, 560-568.
154. Bonjouklian, R.; Smitka, T. A.; Doolin, L. E.; Molloy, R. M.; Debono, M.; Shaffer, S. A.; Moore, R. E.; Stewart, J. B.; Patterson, G. M. L. *Tetrahedron* **1991**, *47*, 7739-7750.
155. Knubel, G.; Larsen, L. K.; Moore, R. E.; Levine, I. A.; Patterson, G. M. L. *J.Antibiot.* **1990**, *43*, 1236-1239.
156. Guo, S.; Tipparaju, S. K.; Pegan, S. D.; Wan, B.; Mo, S.; Orjala, J.; Mesecar, A. D.; Franzblau, S. G.; Kozikowski, A. P. *Bioorg.Med.Chem.* **2009**, *17*, 7126-7130.
157. Nakanishi, S.; Matsuda, Y.; Iwahashi, K.; Kase, H. *J.Antibiot.* **1986**, *39*, 1066-1071.
158. Kase, H.; Iwahashi, K.; Nakanishi, S.; Matsuda, Y.; Yamada, K.; Takahashi, M.; Murakata, C.; Sato, A.; Kaneko, M. *Biochem.Biophys.Res.Commun.* **1987**, *142*, 436-440.
159. Rasouly, D.; Rahamim, E.; Lester, D.; Matsuda, Y.; Lazarovici, P. *Mol.Pharmacol.* **1992**, *42*, 35-43.
160. Ubukata, M.; Tamehiro, N.; Matsuura, N.; Nakajima, N. *J.Antibiot.* **1999**, *52*, 921-924.
161. Pereira, E. R.; Belin, L.; Sancelme, M.; Prudhomme, M.; Ollier, M.; Rapp, M.; Severe, D.; Riou, J. F.; Fabbro, D.; Meyer, T. *J.Med.Chem.* **1996**, *39*, 4471-4477.
162. Akinaga, S.; Ashizawa, T.; Gomi, K.; Ohno, H.; Morimoto, M.; Murakata, C.; Okabe, M. *Cancer Chemother.Pharmacol.* **1992**, *29*, 266-272.
163. Koshino, H.; Osada, H.; Amano, S.; Onose, R.; Isono, K. *J.Antibiot.* **1992**, *45*, 1428-1432.
164. Osada, H.; Takahashi, H.; Tsunoda, K.; Kusakabe, H.; Isono, K. *J.Antibiot.* **1990**, *43*, 163-167.
165. McAlpine, J. B.; Karwowski, J. P.; Jackson, M.; Mullally, M. M.; Hochlowski, J. E.; Premachandran, U.; Burres, N. S. *J.Antibiot.* **1994**, *47*, 281-288.
166. Williams, D. E.; Bernan, V. S.; Ritacco, F. V.; Maiese, W. M.; Greenstein, M.; Andersen, R. J. *Tetrahedron Lett.* **1999**, *40*, 7171-7174.
167. Wu, S. J.; Fotso, S.; Li, F.; Qin, S.; Kelter, G.; Fiebig, H. H.; Laatsch, H. *J.Antibiot.* **2006**, *59*, 331-337.
168. Han, X. X.; Cui, C. B.; Gu, Q. Q.; Zhu, W. M.; Liu, H. B.; Gu, J. Y.; Osada, H. *Tetrahedron Lett.* **2005**, *46*, 6137-6140.
169. Steglich, W. *Pure Appl.Chem.* **1989**, *61*, 281-288.

170. Bit, R. A.; Davis, P. D.; Elliott, L. H.; Harris, W.; Hill, C. H.; Keech, E.; Kumar, H.; Lawton, G.; Maw, A.; Nixon, J. S.; Vesey, D. R.; Wadsworth, J.; Wilkinson, S. E. *J.Med.Chem.* **1993**, *36*, 21-29.
171. Courage, C.; Snowden, R.; Gescher, A. *Br.J.Cancer* **1996**, *74*, 1199-1205.
172. Birchall, A. M.; Bishop, J.; Bradshaw, D.; Cline, A.; Coffey, J.; Elliott, L. H.; Gibson, V. M.; Greenham, A.; Hallam, T. J.; Harris, W.; Hill, C. H.; Hutchings, A.; Lamont, A. G.; Lawton, G.; Lewis, E. J.; Maw, A.; Nixon, J. S.; Pole, D.; Wadsworth, J.; Wilkinson, S. E. *J.Pharmacol.Exp.Ther.* **1994**, *268*, 922-929.
173. Toullec, D.; Pianetti, P.; Coste, H.; Bellevergue, P.; Grandperret, T.; Ajakane, M.; Baudet, V.; Boissin, P.; Boursier, E.; Loriolle, F.; Duhamel, L.; Charon, D.; Kirilovsky, J. *J.Biol.Chem.* **1991**, *266*, 15771-15781.
174. Davies, S. P.; Reddy, H.; Caivano, M.; Cohen, P. *Biochem.J.* **2000**, *351*, 95-105.
175. Alessi, D. R. *FEBS Lett.* **1997**, *402*, 121-123.
176. McArthur, K. A.; Mitchell, S. S.; Tsueng, G.; Rheingold, A.; White, D. J.; Grodberg, J.; Lam, K. S.; Potts, B. C. M. *J.Nat.Prod.* **2008**, *71*, 1732-1737.
177. Gullo, V. P.; McAlpine, J.; Lam, K. S.; Baker, D.; Petersen, F. *J.Ind.Microbiol.Biotechnol.* **2006**, *33*, 523-531.
178. Hashimoto, T.; Yasuda, A.; Akazawa, K.; Takaoka, S.; Tori, M.; Asakawa, Y. *Tetrahedron Lett.* **1994**, *35*, 2559-2560.
179. Frode, R.; Hinze, C.; Josten, I.; Schmidt, B.; Steffan, B.; Steglich, W. *Tetrahedron Lett.* **1994**, *35*, 1689-1690.
180. Kamata, K.; Kiyota, M.; Naoe, A.; Nakatani, S.; Yamamoto, Y.; Hayashi, M.; Komiyama, K.; Yamori, T.; Ishibashi, M. *Chem.Pharm.Bull.* **2005**, *53*, 594-597.
181. Brana, M. F.; Gradillas, A.; Ovalles, A. G.; Lopez, B.; Acero, N.; Llinares, F.; Mingarro, D. M. *Bioorg.Med.Chem.* **2006**, *14*, 9-16.
182. Murase, M.; Watanabe, K.; Yoshida, T.; Tobinaga, S. *Chem.Pharm.Bull.* **2000**, *48*, 81-84.
183. Meksuriyen, D.; Cordell, G. A. *J.Nat.Prod.* **1988**, *51*, 893-899.
184. Gassel, M.; Breitenlechner, C. B.; Konig, N.; Huber, R.; Engh, R. A.; Bossemeyer, D. *J.Biol.Chem.* **2004**, *279*, 23679-23690.
185. Grodsky, N.; Li, Y.; Bouzida, D.; Love, R.; Jensen, J.; Nodes, B.; Nonomiya, J.; Grant, S. *Structure* **2006**, 13970-13981.
186. Gaisina, I. N.; Gallier, F.; Ougolkov, A. V.; Kim, K. H.; Kurome, T.; Guo, S.; Holzle, D.; Luchini, D. N.; Blond, S. Y.; Billadeau, D. D.; Kozikowski, A. P. *J.Med.Chem.* **2009**, *52*, 1853-1863.
187. Hudkins, R. L.; Johnson, N. W.; Angeles, T. S.; Gessner, G. W.; Mallamo, J. P. *J.Med.Chem.* **2007**, *50*, 433-441.
188. Pindur, U.; Kim, Y. S.; Mehrabani, F. *Curr.Med.Chem.* **1999**, *6*, 29-69.
189. Routier, S.; Ayerbe, N.; Merour, J. Y.; Coudert, G.; Bailly, C.; Pierre, A.; Pfeiffer, B.; Caignard, D. H.; Renard, P. *Tetrahedron* **2002**, *58*, 6621-6630.
190. Balasubramanian, B. N.; Laurent, D. R. S.; Saulnier, M. G.; Long, B. H.; Bachand, C.; Beaulieu, F.; Clarke, W.; Deshpande, M.; Eummer, J.; Fairchild, C. R.; Frennesson, D. B.; Kramer, R.; Lee, F. Y.; Mahler, M.; Martel, A.; Naidu, B. N.; Rose, W. C.; Russell, J.; Ruediger, E.; Solomon, C.; Stoffan, K. M.; Wong, H.; Zimmermann, K.; Vyas, D. M. *J.Med.Chem.* **2004**, *47*, 1609-1612.
191. Kase, H.; Iwahashi, K.; Matsuda, Y. *J.Antibiot.* **1986**, *39*, 1059-1065.
192. Moffat, D.; Nichols, C. J.; Riley, D. A.; Simpkins, N. S. *Org.Biomol.Chem.* **2005**, *3*, 2953-2975.
193. Butler, M. S. *Nat.Prod.Rep.* **2005**, *22*, 162-195.

194. Aiello, L. P.; Clermont, A.; Arora, V.; Davis, M. D.; Sheetz, M. J.; Bursell, S. E. *Invest.Ophthalmol.Vis.Sci.* **2006**, *47*, 86-92.
195. Jirousek, M. R.; Gillig, J. R.; Gonzalez, C. M.; Heath, W. F.; McDonald, J. H.; Neel, D. A.; Rito, C. J.; Singh, U.; Stramm, L. E.; Melikian-Badalian, A.; Baevsky, M.; Ballas, L. M.; Hall, S. E.; Winneroski, L. L.; Faul, M. M. *J.Med.Chem.* **1996**, *39*, 2664-2671.
196. Way, K. J.; Chou, E.; King, G. L. *Trends Pharmacol.Sci.* **2000**, *21*, 181-187.
197. Joy, S. V.; Scates, A. C.; Bearelly, S.; Dar, M.; Taulien, C. A.; Goebel, J. A.; Cooney, M. J. *Ann.Pharmacother.* **2005**, *39*, 1693-1699.
198. Keyes, K. A.; Mann, L.; Sherman, M.; Galbreath, E.; Schirtzinger, L.; Ballard, D.; Chen, Y. F.; Iversen, P.; Teicher, B. A. *Cancer Chemother.Pharmacol.* **2004**, *53*, 133-140.
199. Kreisl, T. N.; Kotliarova, S.; Butman, J. A.; Albert, P. S.; Kim, L.; Musib, L.; Thornton, D.; Fine, H. A. *Neuro-Oncology* **2010**, *12*, 181-189.
200. Querfeld, C.; Rizvi, M. A.; Kuzel, T. M.; Guitart, J.; Rademaker, A.; Sabharwal, S. S.; Krett, N. L.; Rosen, S. T. *J.Invest.Dermatol.* **2006**, *126*, 1641-1647.
201. Rademaker-Lakhai, J. M.; Beerepoot, L. V.; Mehra, N.; Radema, S. A.; van Maanen, R.; Vermaat, J. S.; Witteveen, E. O.; Visseren-Grul, C. M.; Musib, L.; Enas, N.; van Hal, G.; Beijnen, J. H.; Schellens, J. H. M.; Voest, E. E. *Clin.Cancer Res.* **2007**, *13*, 4474-4481.
202. Robertson, M. J.; Kahl, B. S.; Vose, J. M.; de Vos, S.; Laughlin, M.; Flynn, P. J.; Rowland, K.; Cruz, J. C.; Goldberg, S. L.; Musib, L.; Darstein, C.; Enas, N.; Kutok, J. L.; Aster, J. C.; Neuberg, D.; Savage, K. J.; LaCasce, A.; Thornton, D.; Slapak, C. A.; Shipp, M. A. *J.Clin.Oncol.* **2007**, *25*, 1741-1746.
203. Takahashi, I.; Kobayashi, E.; Asano, K.; Yoshida, M.; Nakano, H. *J.Antibiot.* **1987**, *40*, 1782-1784.
204. Senderowicz, A. M. *Cancer Chemother.Pharmacol.* **2003**, *52 Suppl 1*, S61-S73.
205. Graves, P. R.; Yu, L. J.; Schwarz, J. K.; Gales, J.; Sausville, E. A.; O'Connor, P. M.; Piwnica-Worms, H. *J.Biol.Chem.* **2000**, *275*, 5600-5605.
206. Busby, E. C.; Leistritz, D. F.; Abraham, R. T.; Karnitz, L. M.; Sarkaria, J. N. *Cancer Res.* **2000**, *60*, 2108-2112.
207. Kortmansky, J.; Shah, M. A.; Kaubisch, A.; Weyerbacher, A.; Yi, S.; Tong, W.; Sowers, R.; Gonen, M.; O'Reilly, E.; Kemeny, N.; Ilson, D. I.; Saltz, L. B.; Maki, R. G.; Kelsen, D. P.; Schwartz, G. K. *J.Clin.Oncol.* **2005**, *23*, 1875-1884.
208. Hotte, S. J.; Oza, A.; Winquist, E. W.; Moore, M.; Chen, E. X.; Brown, S.; Pond, G. R.; Dancey, J. E.; Hirte, H. W. *Ann.Oncol.* **2006**, *17*, 334-340.
209. Fuse, E.; Kuwabara, T.; Sparreboom, A.; Sausville, E. A.; Figg, W. D. *J.Clin.Pharmacol.* **2005**, *45*, 394-403.
210. Sausville, E. A.; Arbuck, S. G.; Messmann, R.; Headlee, D.; Bauer, K. S.; Lush, R. M.; Murgo, A.; Figg, W. D.; Lahusen, T.; Jaken, S.; Jing, X. X.; Roberge, M.; Fuse, E.; Kuwabara, T.; Senderowicz, A. M. *J.Clin.Oncol.* **2001**, *19*, 2319-2333.
211. Fuse, E.; Hashimoto, A.; Sato, N.; Tanii, H.; Kuwabara, T.; Kobayashi, S.; Sugiyama, Y. *Pharm.Res.* **2000**, *17*, 553-564.
212. Sato, S.; Fujita, N.; Tsuruo, T. *Oncogene* **2002**, *21*, 1727-1738.
213. Shimizu, E.; Zhao, M. R.; Nakanishi, H.; Yamamoto, A.; Yoshida, S.; Takada, M.; Ogura, T.; Sone, S. *Oncology* **1996**, *53*, 494-504.
214. Fabbro, D.; Buchdunger, E.; Wood, J.; Mestan, J.; Hofmann, F.; Ferrari, S.; Mett, H.; O'Reilly, T.; Meyer, T. *Pharmacol.Ther.* **1999**, *82*, 293-301.
215. Fabbro, D.; Ruetz, S.; Bodis, S.; Pruschy, M.; Csermak, K.; Man, A.; Campochiaro, P.; Wood, J.; O'Reilly, T.; Meyer, T. *Anticancer.Drug Des.* **2000**, *15*, 17-28.

216. Weisberg, E.; Boulton, C.; Kelly, L. M.; Manley, P.; Fabbro, D.; Meyer, T.; Gilliland, D. G.; Griffin, J. D. *Cancer Cell* **2002**, *1*, 433-443.
217. Ganeshaguru, K.; Wickremasinghe, R. G.; Jones, D. T.; Gordon, M.; Hart, S. M.; Virchis, A. E.; Prentice, H. G.; Hoffrand, A. V.; Man, A.; Champain, K.; Csermak, K.; Mehta, A. B. *Haematologica* **2002**, *87*, 167-176.
218. Camoratto, A. M.; Jani, J. P.; Angeles, T. S.; Maroney, A. C.; Sanders, C. Y.; Murakata, C.; Neff, N. T.; Vaught, J. L.; Isaacs, J. T.; Dionne, C. A. *Int.J.Cancer* **1997**, *72*, 673-679.
219. Strock, C. J.; Park, J. I.; Rosen, M.; Dionne, C.; Ruggeri, B.; Jones-Bolin, S.; Denmeade, S. R.; Ball, D. W.; Nelkin, B. D. *Cancer Res.* **2003**, *63*, 5559-5563.
220. Strock, C. J.; Park, J. I.; Rosen, D. M.; Ruggeri, B.; Denmeade, S. R.; Ball, D. W.; Nelkin, B. D. *J.Clin.Endocrinol.Metab.* **2006**, *91*, 79-84.
221. Murakata, C.; Kaneko, M.; Gessner, G.; Angeles, T. S.; Ator, M. A.; O'Kane, T. M.; McKenna, B. A. W.; Thomas, B. A.; Mathiasen, J. R.; Saporito, M. S.; Bozyczko-Coyne, D.; Hudkins, R. L. *Bioorg.Med.Chem.Lett.* **2002**, *12*, 147-150.
222. Kaneko, M.; Saito, Y.; Saito, H.; Matsumoto, T.; Matsuda, Y.; Vaught, J. L.; Dionne, C. A.; Angeles, T. S.; Glicksman, M. A.; Neff, N. T.; Rotella, D. P.; Kauer, J. C.; Mallamo, J. P.; Hudkins, R. L.; Murakata, C. *J.Med.Chem.* **1997**, *40*, 1863-1869.
223. Rewcastle, G. W. *Idrugs* **2005**, *8*, 838-847.
224. Nakatani, S.; Naoe, A.; Yamamoto, Y.; Yamauchi, T.; Yamaguchi, N.; Ishibashi, M. *Bioorg.Med.Chem.Lett.* **2003**, *13*, 2879-2881.
225. Yoshinari, T.; Matsumoto, M.; Arakawa, H.; Okada, H.; Noguchi, K.; Suda, H.; Okura, A.; Nishimura, S. *Cancer Res.* **1995**, *55*, 1310-1315.
226. Urasaki, Y.; Laco, G.; Takebayashi, Y.; Bailly, C.; Kohlhagen, G.; Pommier, Y. *Cancer Res.* **2001**, *61*, 504-508.
227. Cavazos, C. M.; Keir, S. T.; Yoshinari, T.; Bigner, D. D.; Friedman, H. S. *Cancer Chemother.Pharmacol.* **2001**, *48*, 250-254.
228. Ciomei, M.; Croci, V.; Ciavolella, A.; Ballinar, D.; Pesenti, E. *Clin.Cancer Res.* **2006**, *12*, 2856-2861.
229. Hurwitz, H. I.; Cohen, R. B.; McGovren, J. P.; Hirawat, S.; Petros, W. P.; Natsumeda, Y.; Yoshinari, T. *Cancer Chemother.Pharmacol.* **2007**, *59*, 139-147.
230. Saif, M. W.; Sellers, S.; Diasio, R. B.; Douillard, J. Y. *Anticancer.Drugs* **2010**, *21*, 716-723.

Chapter 2

Chemical Introduction

Contents

2.0 Chemical Introduction 68
2.1 Development of chemical routes to indolo[2,3-*a*]carbazoles 68
2.2 Overview of current strategies for indolocarbazole synthesis 69
2.2.1 Early efforts in synthesis of indolo[2,3-a]carbazoles 69
2.2.2 C-Ring forming routes 70
2.2.2.1 Electrophilic strategies to ICZs 70
2.2.2.2 Base-mediated synthesis of indolo[2,3-a]carbazole analogues 75
2.2.3 B and D-Ring forming routes 80
2.2.3.1 Cadogan cyclisation 80
2.2.3.2 Fischer indole synthesis 83
2.2.4 F-Ring Routes 86
2.2.4.1 Perkin condensation approach 86
2.2.4.2 Iodine-mediated indole coupling reactions 88
2.2.5 Successful multiple ring forming strategies 89
2.2.5.1 [4+2] Diels-Alder cycloaddition in B/D/F-ring formation 89
2.2.5.2 B/C-ring formation employing Diels-Alder cycloaddition 89
2.2.5.3 Retro Diels-Alder route: C-ring formation 90
2.2.5.4 Tandem conjugate addition reactions 91
2.2.5.5 Transition metal-mediated routes 92
2.3 Strategies for synthesis of *N*-glycosidic linkages in natural ICZs 97
2.3.1 Importance of sugars in indolocarbazole alkaloids 97
2.3.2 Biosynthetic origin of indolocarbazole sugar moieties 97
2.3.3 Semi-synthesis of natural bioactive indolocarbazole glycosides 99
2.3.4 Chemical routes to mono-*N*-glycosides 100
2.3.4.1 Total synthesis of rebeccamycin 100
2.3.4.2 Synthesis of rebeccamycin analogues: NB-506, ED-110 and J-109 404 103
2.3.5 Chemical routes to di-*N*-glycosides 105
2.3.5.1 Total synthesis of staurosporine 105
2.3.5.2 Total synthesis of K-252a 107
2.4 Chemical modification of the indolo[2,3-*a*]carbazole nucleus 111
2.4.1 Sugar substitution: synthesis of ICZ-bridged cyclopentanes 111
2.4.2 Indolocarbazole A/E ring substitution 114
2.4.3 1-Azaindolocarbazoles 115
2.5 Synthesis of arylindolyl derivatives related to indolocarbazoles 117
2.5.1 Synthesis of 3,4-bisarylmaleimides via Perkin condensation 117
2.5.2 Planar ring modification: formation of heteroarylcarbazole derivatives 118
2.5.3 Granulatimide cycloaddition 121
2.6 Conclusion 122
2.7 References 124

2.0 Chemical Introduction

2.1 Development of chemical routes to indolo[2,3-*a*]carbazoles

Indolo[2,3-*a*]carbazoles comprise a core pentacyclic scaffold consisting of a carbazole moiety fused to an indole ring unit *via* its five-membered ring.[1] Privileged approaches to derivatisation of this skeleton utilising a multitude of heterocyclic strategies involving ICZ ring assembly and B/C/D/F-ring annulation have propelled the ongoing quest for synthetic analogues with attractive biological applications.[2-4]

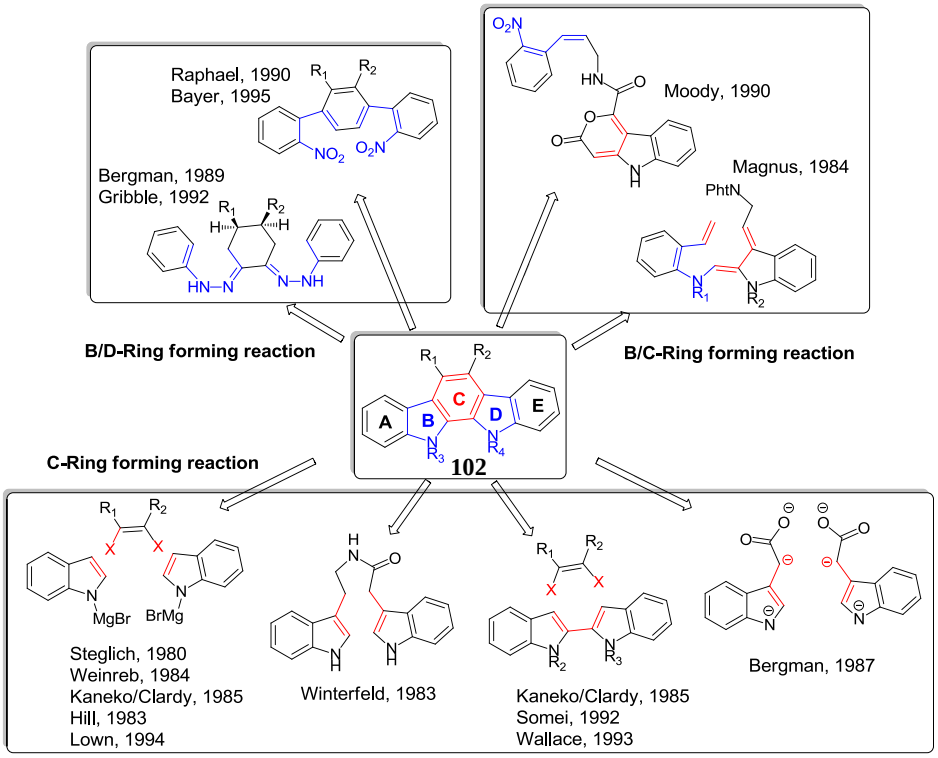


Fig. 2.1: Classical methods of indolo[2,3-*a*]carbazole **102** synthesis

As illustrated in Fig. 2.1, retrosynthetic routes to construction of the indolo[2,3-*a*]carbazole nucleus (**102**) can be classified according to the site of final ICZ ring formation. Several workers have reported Fischer cyclisation and Cadogan nitrene insertion processes as peripheral B and D-ring forming methodologies while Diels-Alder cycloaddition has also been employed by several workers in B/C-ring annulation, in addition to targeting versatile carbon-carbon bond formation within advanced ICZ intermediates.[5,6] A wide diversity of C-ring routes is characterised by coupling of indole moieties to activated F-ring precursors, followed by oxidative ring closure, or ring dehydrogenation in the case of a 2,2-biindolyl dienophile tandem cyclisation approach. It should also be remarked that this review primarily addresses the study of current methodologies available for synthesising regio-

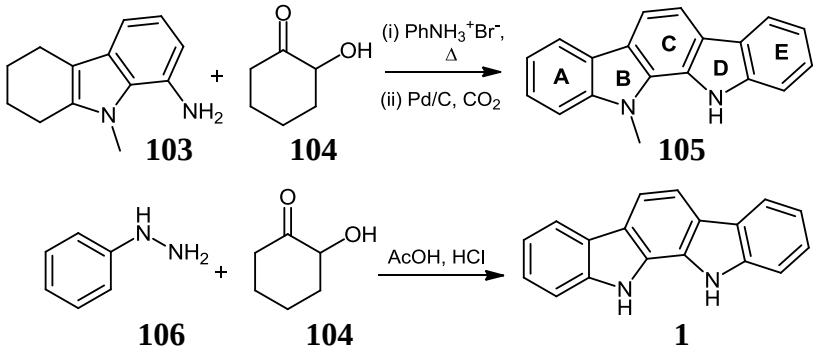
analogues of indolo[2,3-*a*]carbazoles bearing diverse F-ring functionality, and will serve as a critical launching pad for our novel investigations in this relatively unexplored field.

2.2 Overview of current strategies for indolocarbazole synthesis

Chemical diversity observed within complex indolo[2,3-*a*]carbazole natural products reflect the wide range and overwhelming impact of biological roles mediated by this chemical class (Section 1.0; Biological Introduction).[7-9] Discussion of these strategies will comprise initial approaches to the indolocarbazole nucleus as well as F-ring containing derivatives, prior to investigating individual C, B/D and F-ring forming reaction types classified by means of their highlighted ring cyclisation step.

2.2.1 Early efforts in synthesis of indolo[2,3-a]carbazoles

Prior to initial isolation of these alkaloids from natural sources and discovery of their biological potential, derivatisation of the conserved indolo[2,3-*a*]carbazole scaffold received scant attention from medicinal chemists.



103 **104** **105**

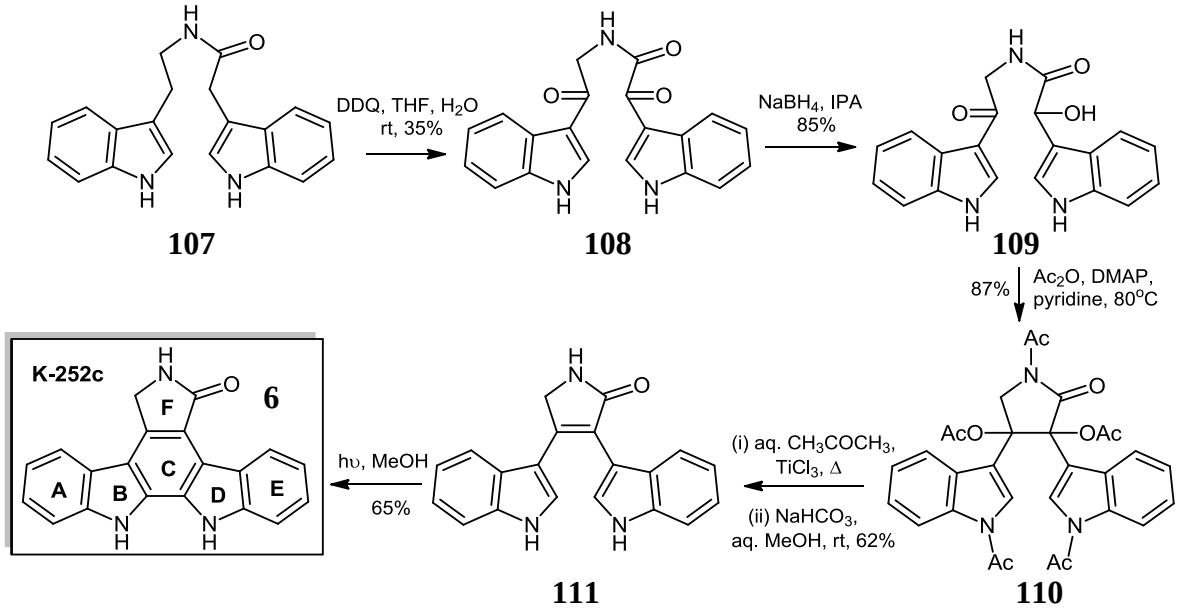
106 **104** **1**

Scheme 2.1

In 1956, Tomlinson reported the first synthesis of the indolo[2,3-*a*]carbazole core as an *N*-methyl derivative **105**, following condensation of 8-amino-1,2,3,4-tetrahydro-9-methyl-9*H*-carbazole **103** with acyloin **104**, followed by dehydrogenation (Scheme 2.1).[10] However, an analogous approach to form the demethylated indolo[2,3-*a*]carbazole **1** was unsuccessful. However, Mann and co-workers employed stepwise Fischer indolisation of acyloin **104** with phenylhydrazine **106** to afford the unsubstituted skeleton, following cyclisation of both indole rings, prior to final aromatisation to yield **1**.[11]

Winterfeldt and co-workers reported the first synthesis of pyrrolo[3,4-*c*] analogue, K-252c **6**, paving the way for continuing synthetic endeavours in the field of F-ring head group derivatisation.[12,13] Starting from bisindolyl amide **107**, DDQ oxidation in aqueous THF afforded intermediate trione **108**, which was partially reduced following treatment with

$NaBH_4$, to **109**. Polyacetylation was then carried out to form intermediate **110**, prior to titanium-induced reduction. Following indole deacetylation to afford **111** under basic conditions, final oxidative ring closure was performed under photocyclisation conditions to afford compound **6** in 65% yield (Scheme 2.2).



Scheme 2.2

2.2.2 C-Ring forming routes

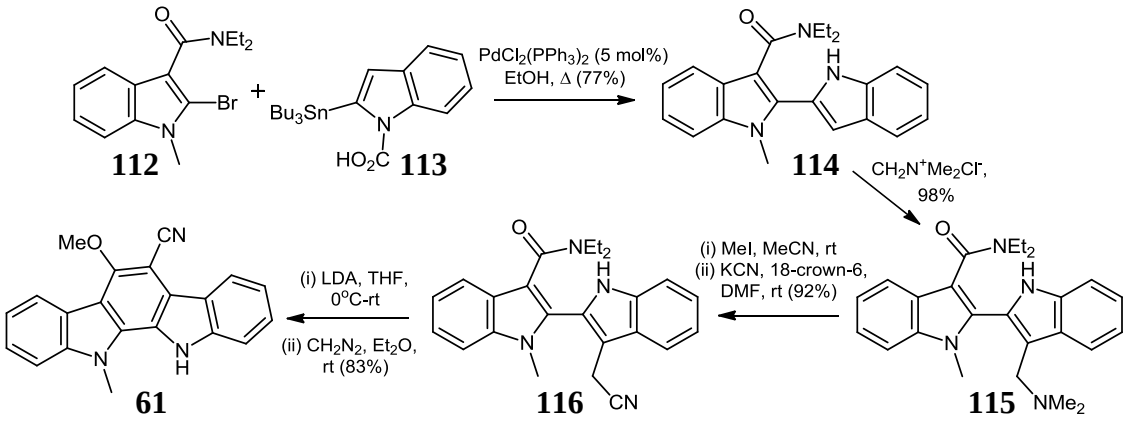
2.2.2.1 Electrophilic strategies to ICZs

These reaction types exploit the nucleophilic C-3 reactivity of indole with electrophilic reagents, in order to afford advanced intermediates which can subsequently be cyclised to form the indolo[2,3-*a*]carbazole core.

2.2.2.1.1 Indole C-3 electrophilic addition

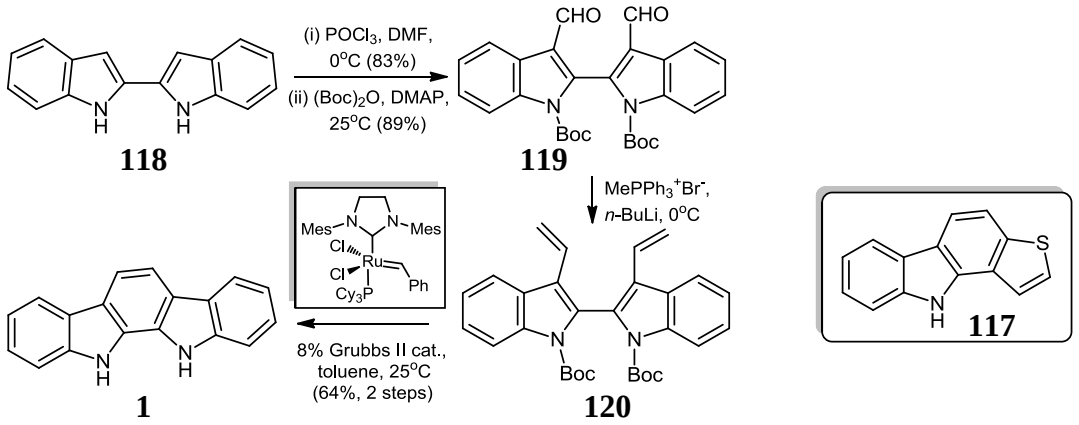
Cai and Snieckus reported an elegant C-ring condensation approach, invoking early 2,2'-bond formation *via* Stille cross-coupling of both indolic fragments **112** and **113**.[14] 2,2'-Biindolyl **114** then undergoes C-3 attack from a dialkyliminium electrophile on treatment with Eschenmoser's salt, to provide gramine derivative **115** (Scheme 2.3).

Methylation and cyanide addition then resulted in formation of key nitrile intermediate **116**, which, following base-induced ring closure and diazomethane-mediated etherification, completed synthesis of cytotoxic 5-cyano-6-methoxy-11-methylindolo[2,3-*a*]carbazole **61**, lacking an F-ring moiety (Section 1.4.1.1).[15]



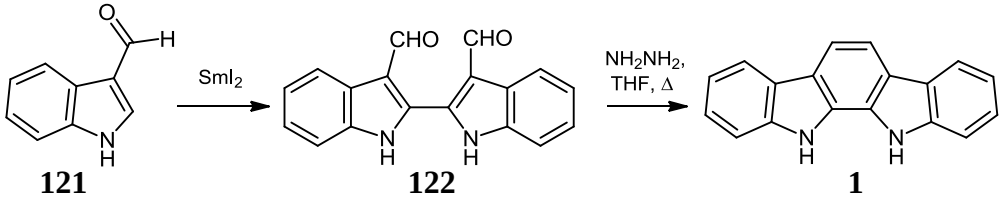
Scheme 2.3

Recently, a ruthenium catalysed indolocarbazole synthesis has been published which is based on Grubbs' celebrated metathesis reaction. This rather limited approach to indolocarbazole design was fully realised by Pelly *et al.* in 2005, when synthesis of the pentacyclic indolocarbazole core **1** and a sulfur analogue of furostifoline **117** were completed (Scheme 2.4).[16]



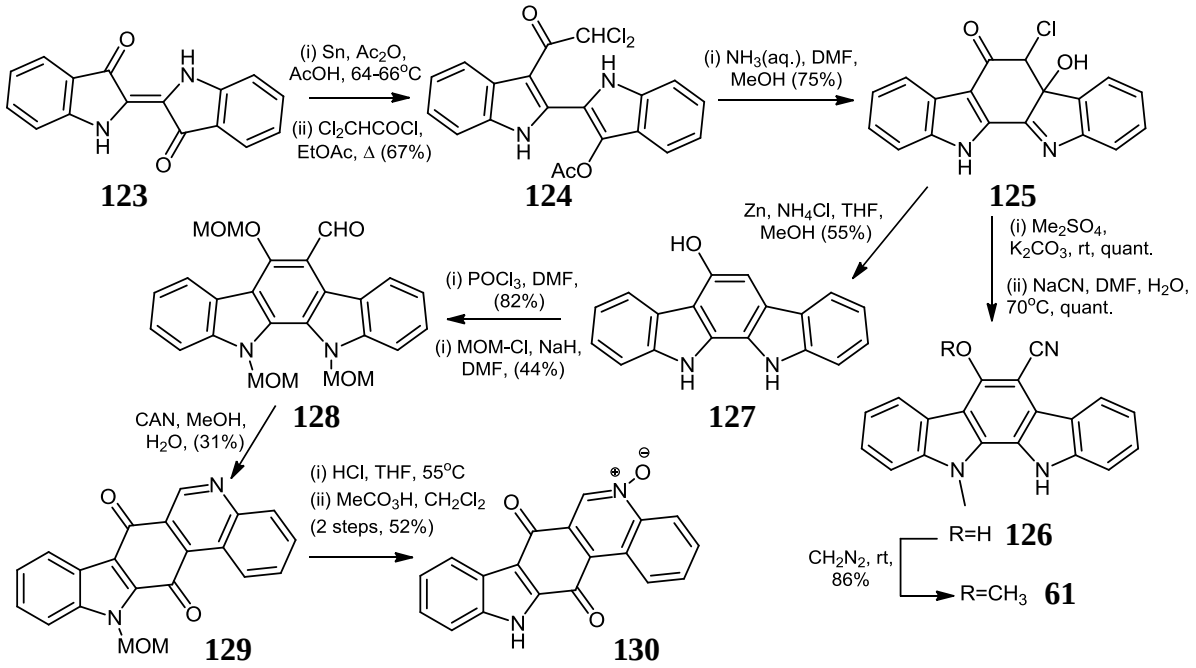
Scheme 2.4

Similar to other benzannulation approaches, a feature of this method is the early formation of the 2,2'-biindolyl bond; the central carbocyclic ring is then rendered by ring-closing metathesis (RCM) reaction. Conversion of starting biindolyl **118** to dialdehyde **119** was achieved using the Vilsmeier-Haack protocol and, following double Boc-protection, converted to the corresponding diene **120**, by means of a Wittig reaction. Exposure of **120** to the Grubbs second-generation catalyst in toluene at 80°C for 24 hours gave the anticipated product **1** in overall combined yield of 47%.



Scheme 2.5

A more straightforward route has recently been suggested, involving 2,2'-dimerisation of indole-3-carboxaldehyde **121** with the single-electron transfer reagent, SmI_2, followed by annulation of the resulting product **122** with hydrazine in refluxing THF, leading to indolocarbazole **1** *via* ultimate extrusion of nitrogen (Scheme 2.5).[17,18]

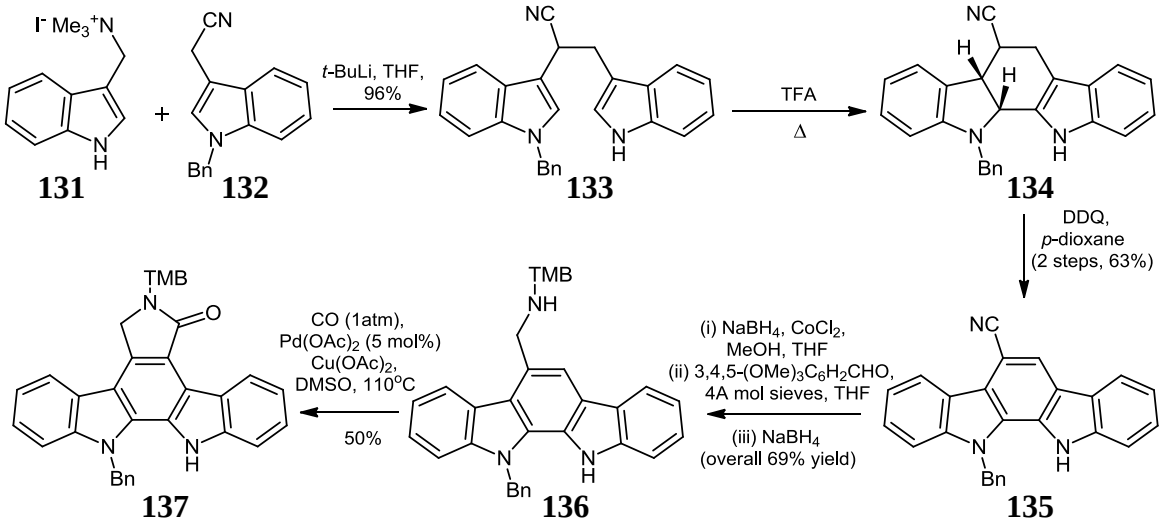


Scheme 2.6

An alternative route to interesting polycyclic analogues involving a readily available, symmetrical starting material and critical C3 electrophilic aromatic substitution step was reported by Somei *et al*, in 59% yield over six steps.[19,20] Starting from indigo **123**, initial reduction by tin in acetic acid/acetic anhydride afforded an initial 3-acetoxylated precursor, which was heated with dichloroacetyl chloride to form the C-3 acylated 2,2'-bisindolyl derivative **124** (67% yield over two steps); treatment with ammonia to form **125**, followed by *N*-methylation, cyanation and *O*-methylation of **126**, provided natural product 5-cyano-6-methoxy-11-methylindolo[2,3-*a*]carbazole **61**, which was identical to the anti-viral compound synthesised by Cai *et al.*, and originally isolated from a blue-green alga by Moore and co-workers in 1990.[14,15] In 2007, McErlean *et al.* co-opted this route for a biomimetic synthesis of a structurally related pentacyclic indolo[3,2-*j*]phenanthridine natural product, calothrixin A **130**.[21,22] Reduction of intermediate **125** to 5-hydroxyindolo[2,3-*a*]carbazole **127** was followed by Vilsmeier-Haack formylation and universal MOM-protection steps. CAN-induced rearrangement of intermediate **128** to **129** was then performed in a yield of 31%, prior to HCl deprotection and mild peroxyacid oxidation to afford **130** (Scheme 2.6).

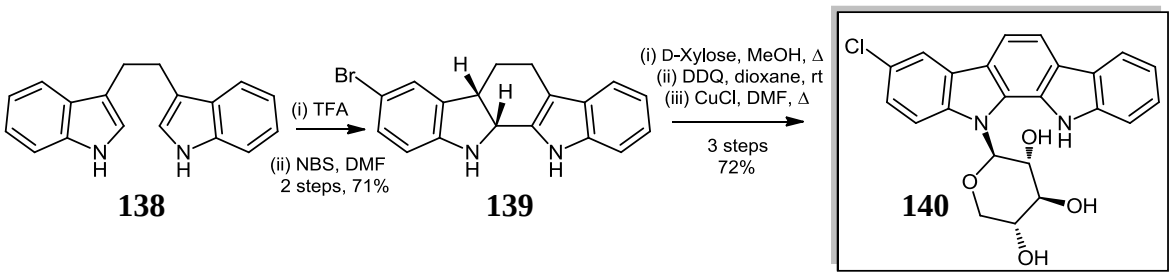
2.2.2.1.2 Mannich cyclisation of 1,2-bisindolylethane derivatives

An efficient biomimetic route to indolocarbazole construction involved base-mediated condensation of gramine methiodide **131** and *N*-protected indole-3-acetonitrile **132**, to afford bisindole derivative **133**; TFA-induced Mannich cyclisation and subsequent DDQ oxidation of the non-aromatic **134** produced indolocarbazole **135** (Scheme 2.7).[23]



Scheme 2.7

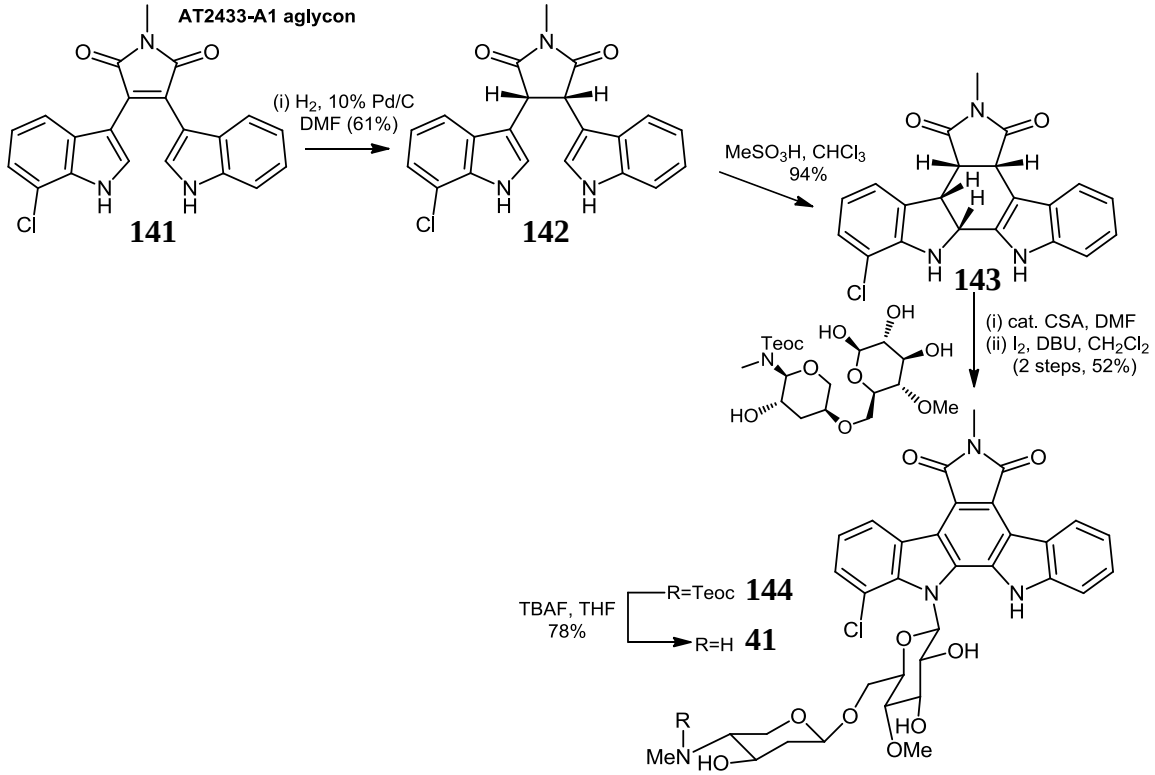
Reduction of the aryl nitrile **135**, followed by reductive amination employing 3,4,5-trimethoxybenzaldehyde afforded 5-aminomethyl substituted derivative **136**, which was employed to access the lactam-bearing indolo[2,3-*a*]pyrrolo[3,4-*c*]carbazole ring system **137**, *via* palladium-catalysed carbonylation reaction, in the presence of copper acetate and carbon monoxide, in DMSO, at 110°C (50%). This rection step also represents a significant improvement on the route of Magnus *et al.* that employed gaseous phosgene along with a strong Lewis acid, $TiCl_4$, in order to complete F-ring pyrrol-2-one synthesis (c.f. Section 2.2.5.2).[24]



Scheme 2.8

The key TFA-promoted Mannich cyclisation step is a versatile approach to the partially saturated polyheteroaromatic nucleus, being essential to Van Vranken's tjipanazole F2 **140** synthesis *via* 1,2-bis(indol-3-yl)ethane **138**, which was transformed to **139** under acidic

conditions, prior to mono-*N*-glycosylation, aromatisation and chlorination, to furnish **140**, in 72% yield over three steps (Scheme 2.8).[25]



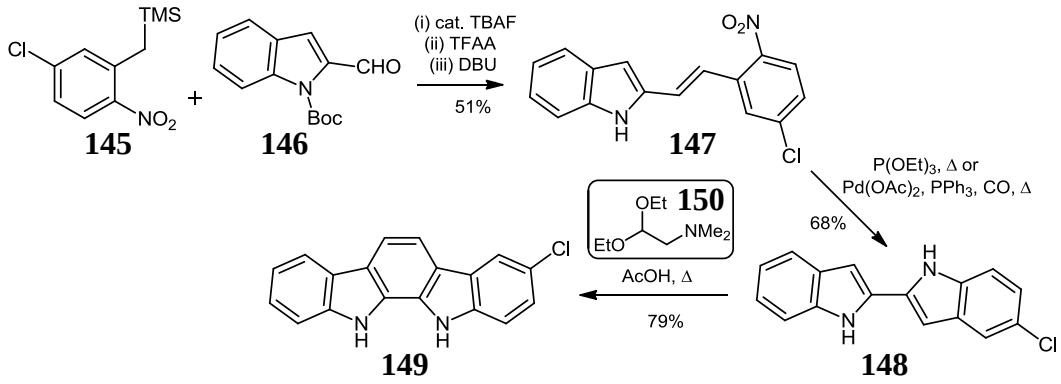
Scheme 2.9

In 2000, a similar method was applied in order to derive a total synthesis of AT-2433-A_1 **41**, comprising linked methylglucose and deoxyaminopyranose moieties, featuring hydrogenation of the corresponding aglycon **141** to Mannich substrate bisindolylsuccinimide **142**, prior to methanesulfonic acid-induced cyclisation to provide the hexacyclic derivative **143**.[26,27] This indoline derivative constitutes a privileged aminodisaccharide coupling precursor, and readily undergoes acid-promoted regioselective β-*N*-glycosylation.[28] Final treatment with DBU and iodine thus afforded the fully aromatised silyl-protected analogue **144**, which was converted to glycoside **41**, on reaction with TBAF, in 78% yield (Scheme 2.9).[27]

2.2.2.1.3 Electrophilic cyclisation of 2,2'-biindolyl derivatives

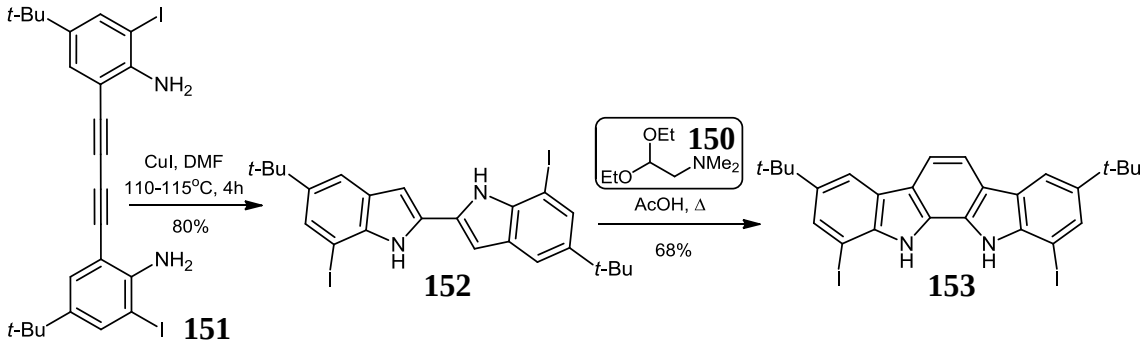
Synthesis of the central C-ring within unsymmetrical indolo[2,3-*a*]carbazoles has been facilitated by recent developments, characterised by heterocyclic elaboration of simple precursors containing desired functionality.[5] An elegant contribution was reported by Bartoli *et al.* following condensation of TMS-substituted nitrotoluene derivative **145** with indole-2-

carboxaldehyde **146**, in the presence of TBAF, prior to base-induced elimination, affording styrene intermediate **147** (Scheme 2.10).[29,30]



Scheme 2.10

Conversion to the hetero-substituted 2,2-biindolyl **148** was smoothly achieved under Cadogan conditions, and was subsequently annulated to the chlorinated tjipanazole I **149** on heating with dimethyl aminoacetaldehyde diethyl acetal **150** in acetic acid.[30,31] Application of reagent **150** in the ultimate central ring formation step derived from intermediate **152**, to afford **153** was also demonstrated by Chang *et al.*, following initial copper-mediated double intramolecular cyclisation of diyne **151** (Scheme 2.11).[32]



Scheme 2.11

2.2.2.2 Base-mediated synthesis of indolo[2,3-a]carbazole analogues

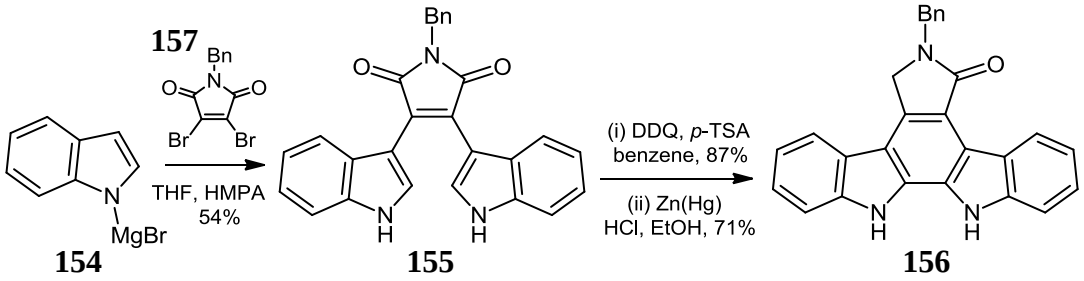
These reaction types constitute a type of indole electrophilic substitution reaction, where initial indole reaction with an organometallic base or LiHMDS results in enhanced C-3 nucleophilicity prior to stepwise substitution reaction with 3,4-dihalomaleimide reactants, and subsequent C-ring aromatisation.

2.2.2.2.1 Grignard-mediated 3,4-dihalomaleimide substitution

The majority of versatile syntheses of K-252c **6** (and related congeners) employing a key base-promoted indole coupling strategy can be classified into two carbon-carbon bond forming stages:[33]

- Formation of a 3,4-bisindolyl substituted pyrrol-2-one/pyrrol-2,5-dione scaffold by nucleophilic substitution of an electrophilic F-ring precursor.
- Oxidative cyclisation to form the ultimate biindolyl 2,2'-bond, with concomitant formation of the planar indolocarbazole chromophore.

The classical base-mediated route employed by Weinreb[34] in 1984 utilised indole coupling reaction, under Grignard conditions, in the presence of *N*-benzyl-3,4-dibromomaleimide **157**, to provide intermediate bisindolylmaleimide **155**, as well as pioneering F-ring desymmetrisation by means of Clemmensen reduction, also encountered by Hughes and Raphael[35], to afford benzylated lactam **156**. However, in an improvement on the palladium-mediated oxidative cyclisation route of Hill[36], the penultimate ring-closing step was accomplished by reaction with DDQ, along with *p*-TSA, in an aromatic hydrocarbon as solvent. Under these optimised conditions, Joyce and co-workers employed indolylmagnesium bromide **154**, along with HMPA, heated in the presence of **157** for 44 hours, and high-yielding DDQ cyclisation to isolate ICZ **156** (Scheme 2.12).

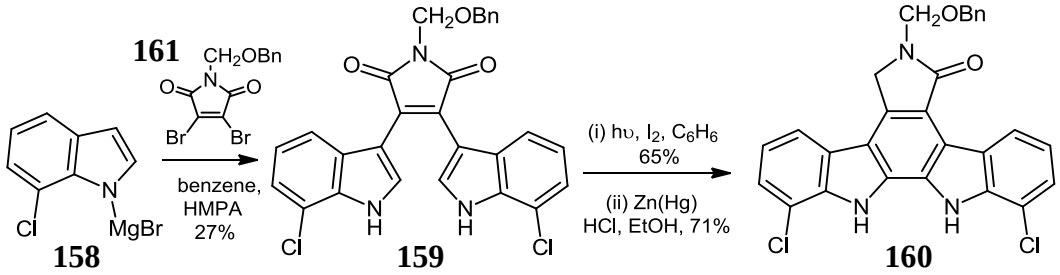


Scheme 2.12

In an investigation of the oxidative cycliation step, Faul and Sullivan also evaluated alternative mild conditions utilising PIFA, in combination with $BF_3.Et_2O$, for aromatisation of *N*-benzyl bisindolylmaleimide **155** and demonstrated that C-ring formation occurred at best in modest yields only, and with a limited scope for substrate applicability (c.f. Section 4.7.1).[37] In 2005, Witulski *et al.* also successfully cyclised *N*-benzyl-3,4-bisindolylmaleimide **155** using the catalyst, $RhCl_3.3H_2O$ (10 mol%), in the presence of 1.1 equiv of $Cu(OAc)_2.H_2O$, in reproducibly high yields.[38] Excellent results have also been reported for annulations of similar substrates with $Pd(OAc)_2$ (5 mol%) and $CuCl_2$ (1 equiv), heated in DMF in the presence of air.[39]

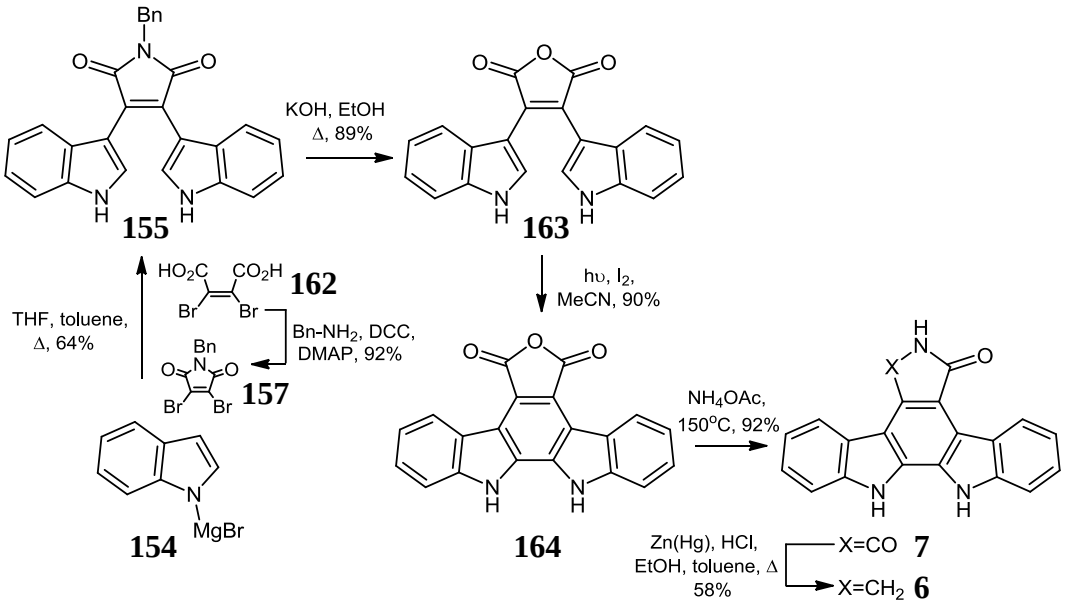
Kaneko and Clardy also utilised similar base methodology employing 7-chloroindolylmagnesium bromide **158** and BOM-protected dibromomaleimide **161** to

prepare the appropriately protected bisindolylmaleimide analogue **159**, which was subsequently cyclised and reduced to the corresponding *N*-protected REB aglycon **160**, bearing a lactam BOM substituent and 1,11-dichlorinated chromophore, by U.V. irradiation in benzene followed by Clemmensen reduction (Scheme 2.13).[40]



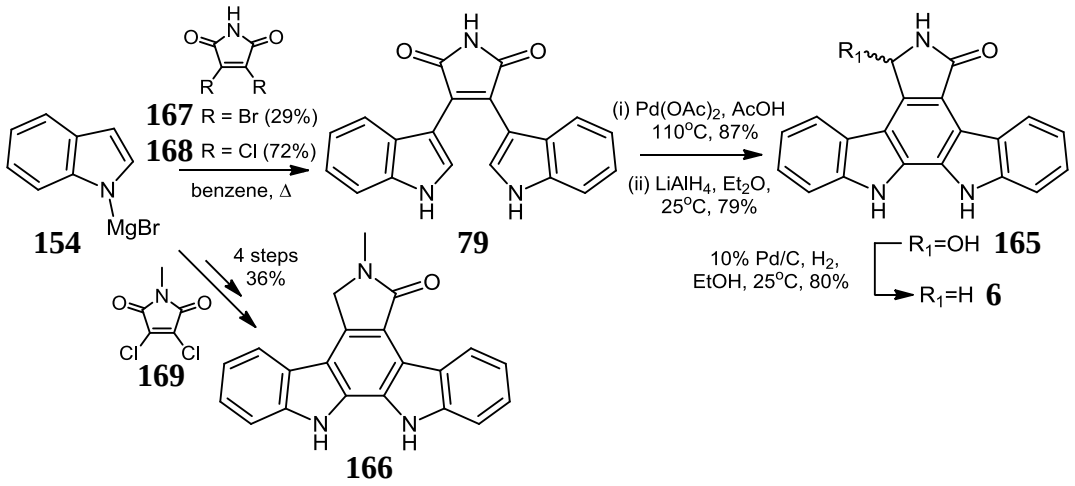
Scheme 2.13

In 1994, Xie and Lown also demonstrated this procedure to form *N*-benzylstaurosporinone **156**, from acyclic precursor **155**, *via* reaction of starting **154**, along with an improved synthesis of *N*-benzyl-3,4-dibromomaleimide **157** in a yield of 92% by condensation of dibromomaleic acid **162** with benzylamine, in the presence of DCC, and catalytic DMAP.[41] Kirilovsky's modification of the Weinreb approach involved KOH-mediated conversion of benzylated arcyriarubin A analogue **155** to the corresponding maleic anhydride **163**.[42] This step was followed by U.V-mediated conversion to **164**, prior to treatment with ammonium acetate at 150°C, affording **7**, and final reduction with Zn amalgam. K-252c **6** was obtained in a yield of 25%, over six steps, from dibromomaleic acid **162** (Scheme 2.14).[41]



Scheme 2.14

As previously mentioned, an alternative approach to the penultimate acyclic precursor was proposed by Hill and co-workers, where aromatisation of arcyriarubin A **79**, constituted the key step towards K-252c **6** formation. Synthesis of **79** was realised in a single step without protection of the imide nitrogen by heating of dibromomaleimide (R = Br; **167**) with 4 equivalents of indolylmagnesium bromide **154** in benzene (Scheme 2.15).[36]



Scheme 2.15

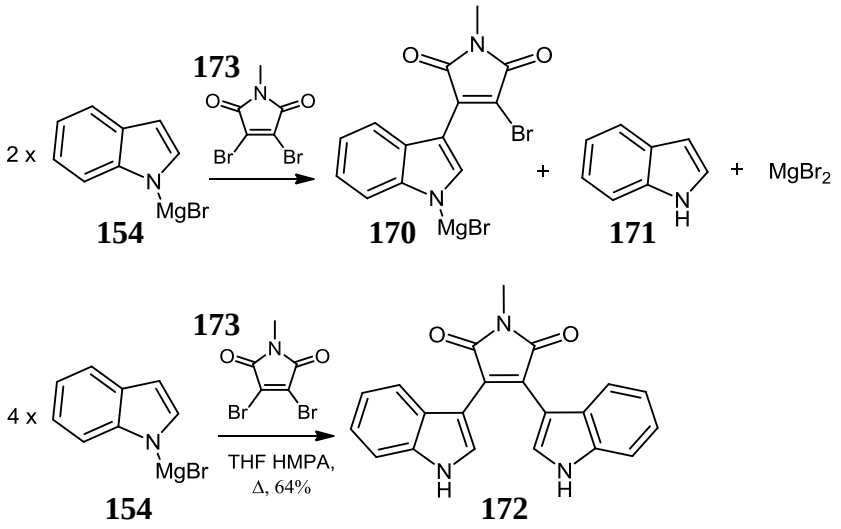
Oxidative cyclisation employing 1 eq. of palladium acetate in acetic acid and careful hydride reduction ($LiAlH_4$) to afford monohydroxy intermediate **165** followed by hydrogenation afforded K-252c **6** in an overall yield of 14%, over 4 steps. In 1995, Faul *et al.* disclosed an optimised route to K-252c **6** based on the Hill protocol, replacing dibromomaleimide **167** with dichloromaleimide (R = Cl; **168**) to produce **6** in an enhanced yield of 34% over these four steps.[43] In 2000, Burtin and co-workers also applied Hill's route to synthesise the KT-5823 aglycon **166** from *N*-methyl-3,4-dichloromaleimide **169** and indolylmagnesium bromide **154**, in four steps and 36% cumulative yield (Scheme 2.15).[44]

2.2.2.2.2 LiHMDS-mediated route to arcyriaflavin B

During the course of research into the reactivity of indole **171** as Grignard acceptor, activating the C3 position towards electrophilic substitution, it was apparent that two-fold molar excess of reactant **154** was required in order to afford synthesis of indolocarbazole precursors such as 6-methylarcyriarubin A **172**, arising from a competing side-reaction.[45]

Formation of monoindolyl substituted intermediate **170** is postulated to occur following initial bromide displacement from **173** by indolylmagnesium bromide **154**. However, another equivalent of this nucleophilic indole Grignard reagent has limited reactivity in displacement of the second bromine leaving group from **170** (Scheme 2.16). Successful

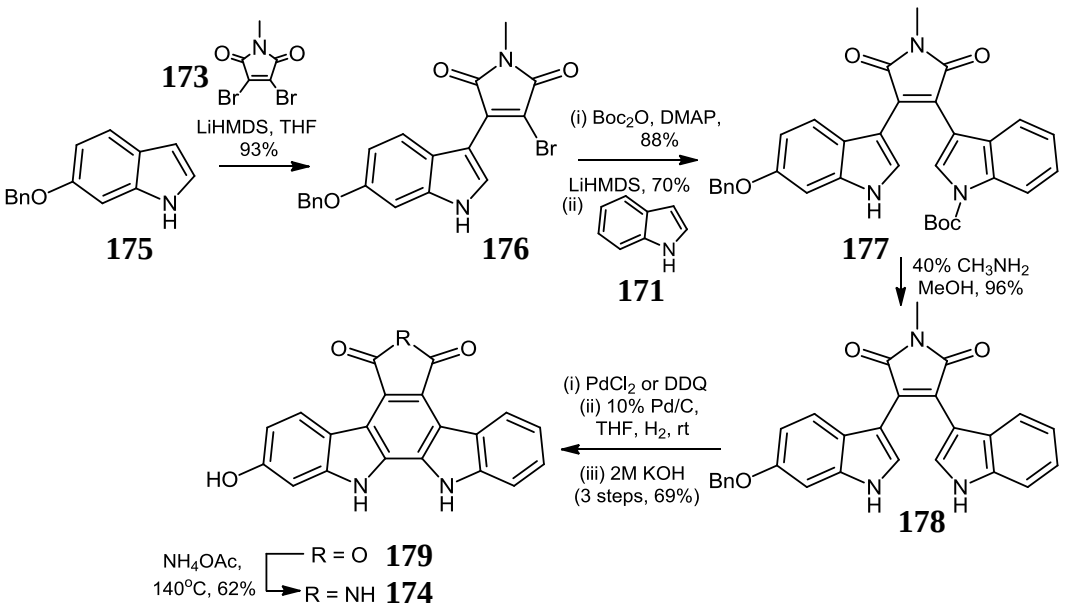
reactions of this type are thus characterised by several drawbacks such as extended reflux, inefficient excess of coupling reagent, as well as necessity for additives such as carcinogenic HMPA. Therefore, an alternative milder base methodology was sought in order to form indole derivatives activated towards electrophilic C-3 attack.[34,40,42,45]



Scheme 2.16

In 1996, Ohkubo *et al*. reported an optimised Grignard-mediated route to unsymmetrical arcyriaflavin B **174**, eliminating the problems associated with indolylmagnesium bromide **154**, and which was derived from initial formation of precursor bisindolylmaleimide *via* reaction of a lithiated indole salt, followed by oxidative 2,2'-bond formation as the terminal ring-closing step. In an application of this approach utilising reaction of 6-benzyloxyindolyl **175** anion with *N*-methyl-3,4-dibromomaleimide **173**, clean monoindolylation to afford **176** was achieved in 93% yield, under stoichiometric conditions.[46]

Following Boc-protection of monoindolyl derivative **176**, the second LiHMDS-mediated indolylation to form **177** was accomplished in 70% yield, prior to high yielding amine-promoted protecting group removal. Cyclisation of **178** was accomplished by exposure to DDQ, prior to *O*-debenzylation. Employing Kirilovsky conditions, arcyriaflavin B **174** was afforded *via* initial alkaline imide hydrolysis, followed by amination of the resultant maleic anhydride moiety **179** with ammonium acetate at 140^{o}C, in a yield of 62% (Scheme 2.17).[46] Interestingly, smooth one-pot conversion to the corresponding *N*-benzyl-3,4-bisindolylmaleimide **155** has also been reported following heating of the lithium salt of indole **171** in the presence of *N*-benzyl-3,4-dibromomaleimide **157** for 12 hours at reflux.[38]



Scheme 2.17

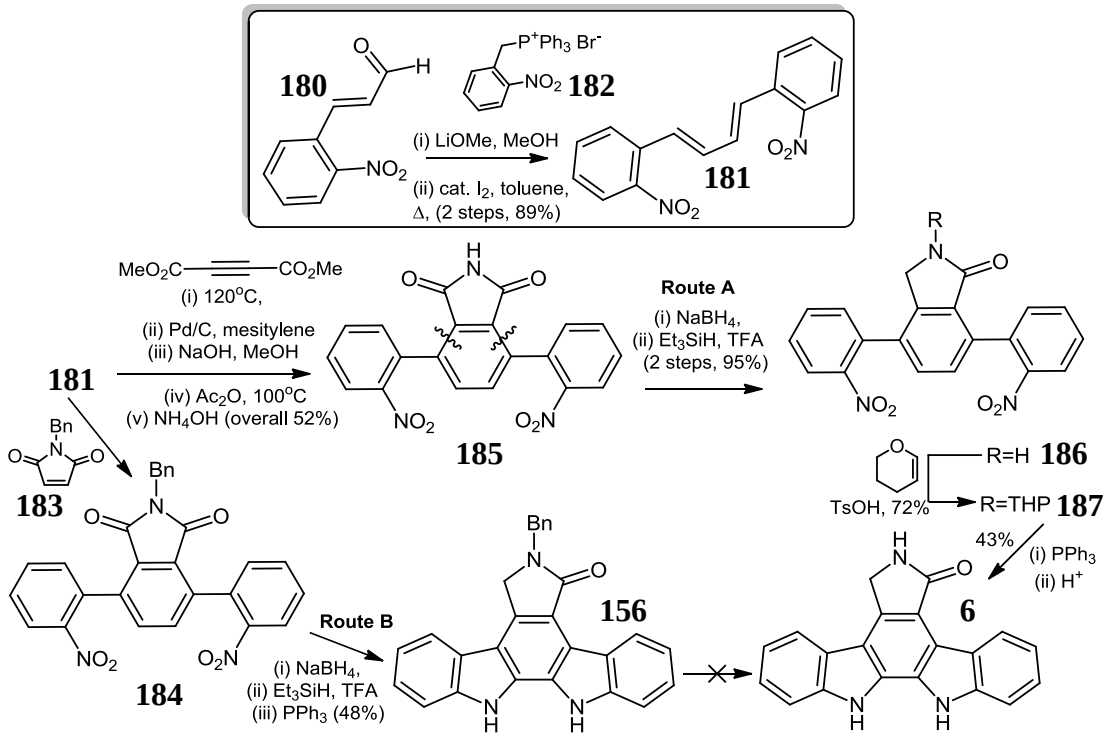
2.2.3 B and D-Ring forming routes

2.2.3.1 Cadogan cyclisation

These routes are characterised by a nitrated biphenyl ICZ precursor, which undergoes nitrene insertion to the central C-ring to yield the full carbazole ring moiety.

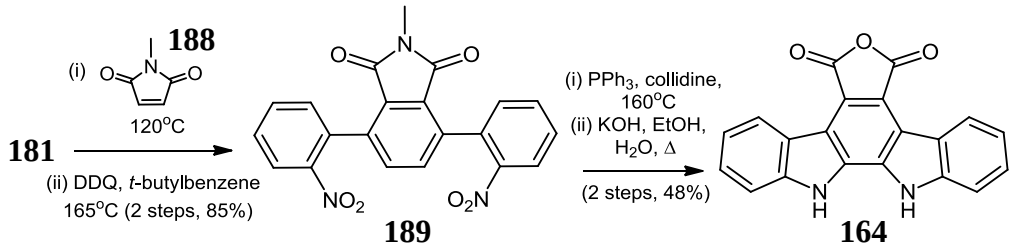
In 1990, Raphael and co-workers proffered a modification of their earlier plan towards formation of K-252c **6** incorporating cycloaddition of *N*-benzylmaleimide **183** to 1,4-diarylbutadiene **181** derived from Wittig reaction of **180** and **182**, to afford terphenyl imide **184**. Subsequent conversion to **6** was unsuccessful due to the resistance of the *N*-benzyl imide protecting group within **156** to facile cleavage conditions (Scheme 2.18; Route B).[35]

Employing DMAD as dienophile, conversion of the resultant anhydride to the unprotected imide **185** and subsequent 7-deoxygenation by $NaBH_4$/triethylsilylhydride treatment to lactam **186** prefigured final cyclisation by a Cadogan double nitrene insertion.[47] Unfortunately, only an inseparable complex of K-252c **6** and triphenylphosphine oxide could be formed at the conclusion of this route; attachment of a THP protecting group (**187**) prior to bisannulation, and final acidic deprotection afforded K-252c **6** (Scheme 2.18; Route A).[35]



Scheme 2.18

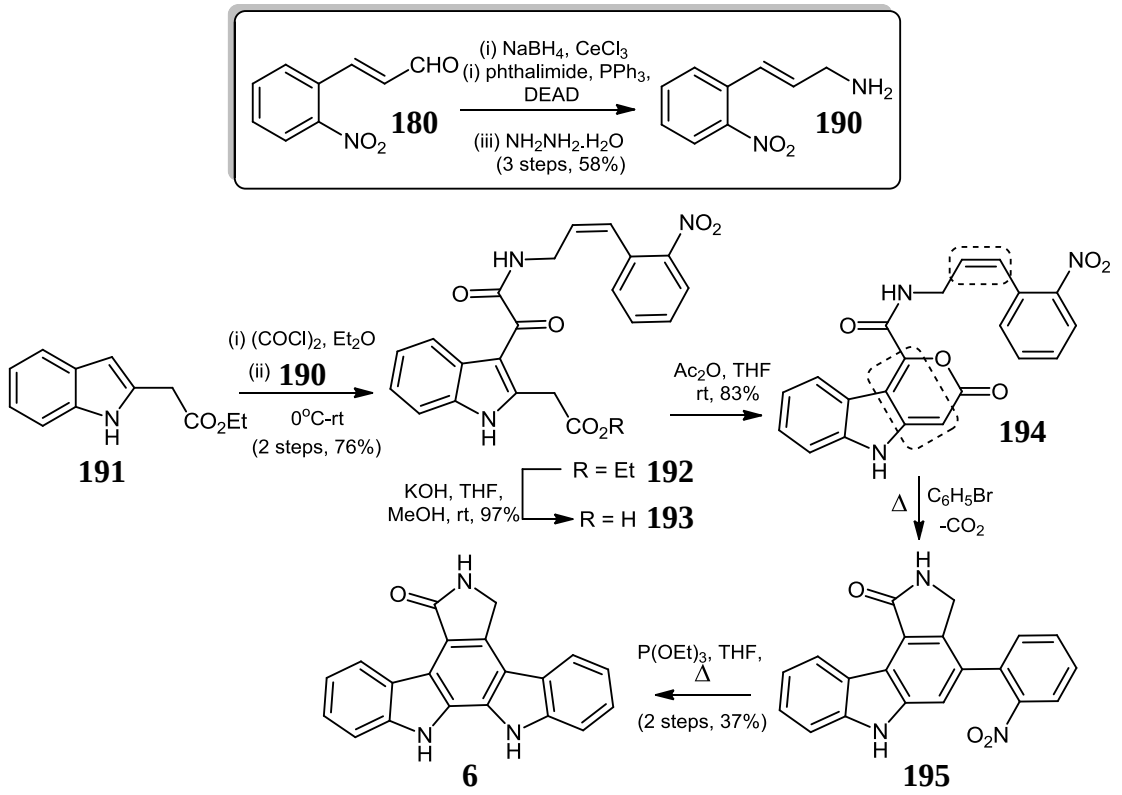
Lowinger and co-workers at Bayer subsequently improved Kirilovsky-type conversion to maleic anhydride **164**, by initial cycloaddition of *N*-methylmaleimide **188** prior to refluxing of triaryl **189** in the presence of triphenylphosphine and collidine, and basic hydrolysis, to complete the ICZ scaffold, easily ammonolysed to arcyriaflavin A **7** (Scheme 2.19).[48]



Scheme 2.19

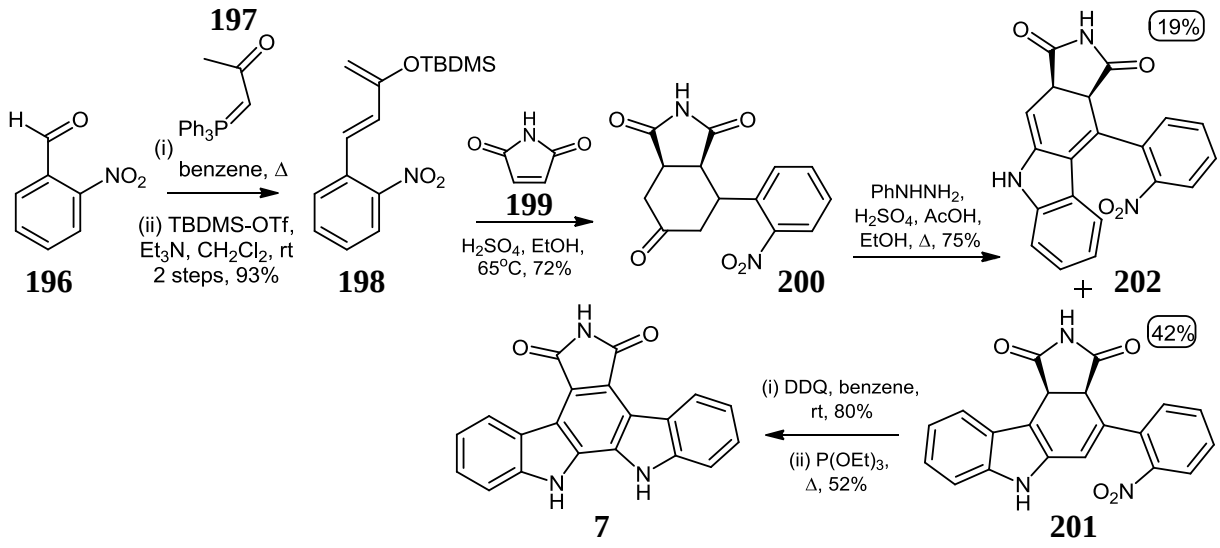
Also in 1990, Moody and Rahimtoola disclosed intramolecular Diels-Alder reaction of pyrano[4,3-*b*]indol-3-one **194** in bromobenzene, with subsequent aromatization to key intermediate **195**, *via* CO_2 extrusion and air oxidation.[49] Cinnamylamine **190** was initially prepared in three steps from commercial 2-nitrocinnamaldehyde **180**; reaction of ethyl indole-2-acetate **191** with oxalyl chloride, followed by condensation with **190** afforded glyoxamide **192**, which was hydrolysed in virtually quantitative yield to **193**, and cyclised in the presence of acetic anhydride to form **194** (Scheme 2.20). A final nitrene insertion step following triethylphosphite-induced deoxygenation then afforded K-252c **6**, in an overall

yield of 23% over six steps. Interestingly, this route is distinguished by a substitution pattern capable of differentiating both indole nitrogens and thus, may also allow regioselective introduction of a carbohydrate moiety.[50]



Scheme 2.20

In 2000, the intensely studied model indolo[2,3-*a*]pyrrolo[3,4-*c*]carbazole, arcyriaflavin A **7** was prepared by Tomé *et al.* by means of an elegant route from 2-nitrobenzaldehyde **196**, involving stepwise Diels-Alder cycloaddition, Fischer methodology and nitrene insertion (Scheme 2.21).[51,52]



Scheme 2.21

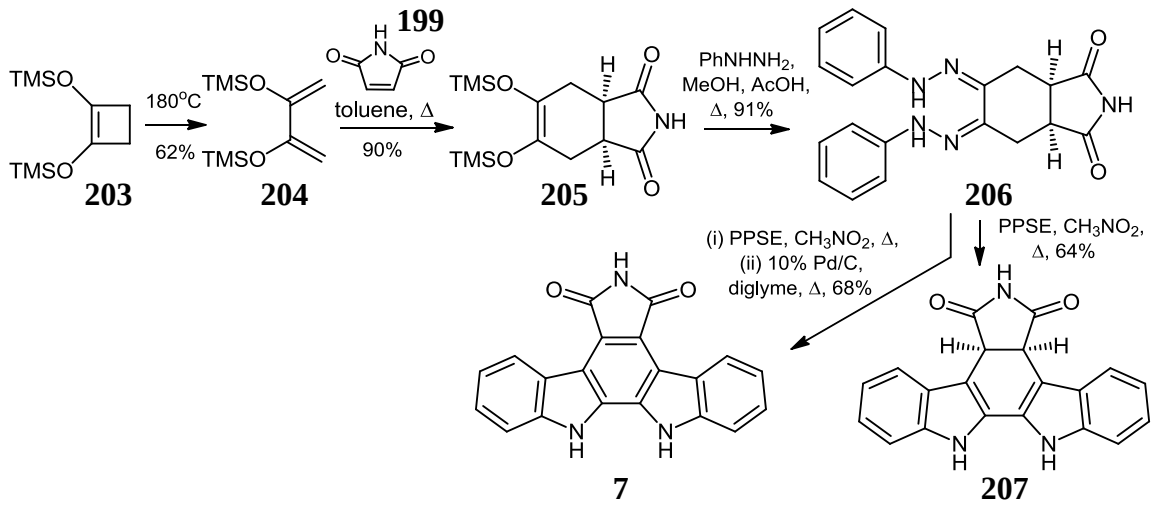
Wittig reaction of 2-nitrobenzaldehyde **196** with ketone **197**, followed by carbonyl group protection to TBDMS-enol derivative **198** preceded [4+2] cycloaddition with maleimide **199** to afford the initial cycloaddition adduct, in quantitative yield; acidic hydrolysis then afforded desilylated cyclohexanone derivative **200**, which was configured for Fischer indolisation with phenylhydrazine, providing correct regioisomer **201** and undesirable **202** in a 2:1 ratio, under acidic conditions. DDQ-induced oxidation of major isomer **201**, followed by Cadogan annulation in the presence of triethyl phosphite gave access to arcyriaflavin A **7** in a yield of 42% over two steps.[52]

2.2.3.2 Fischer indole synthesis

This synthetic approach targets the fully aromatised indolo[2,3-*a*]carbazole ring system *via* reaction of phenylhydrazine with cyclohexanone derivatives. As the C-ring structure is already established, these routes efficiently target B/D ring formation.

Synthesis of indolo[2,3-*a*]carbazole **1** was initially reported by Bhide and Mann derived from one-pot bisphenylhydrazone (osazone) formation and acid-promoted oxidation of 2-hydroxycyclohexanone **104** (Scheme 2.1).[11,53] In 1989, Bergman and Pelcman disclosed how their strategy employing double Fischer methodology resulted in synthesis of arcyriaflavin A **7** scaffold, over four steps.[54]

These workers also demonstrated the potential of this process for facile synthesis of a panel of unsymmetrical indolocarbazole alkaloids, based on the nature of these bis-phenylhydrazone derivatives.[54,55]

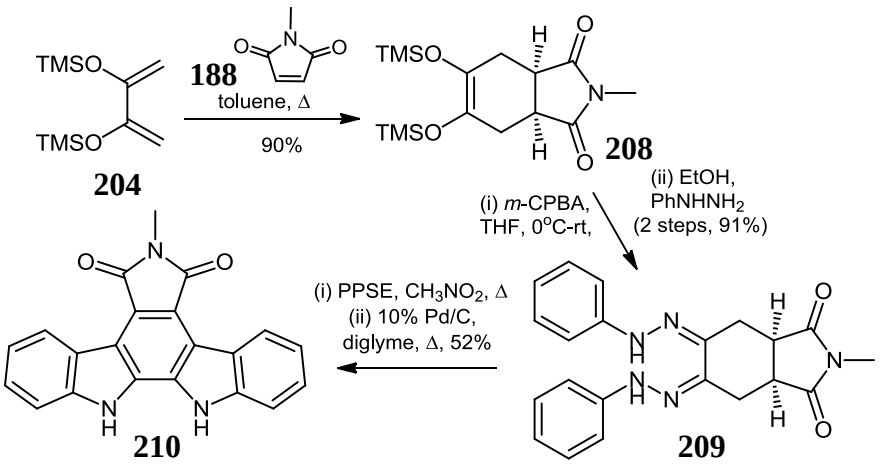


203 **204** **205** **206** **7** **207**

Scheme 2.22

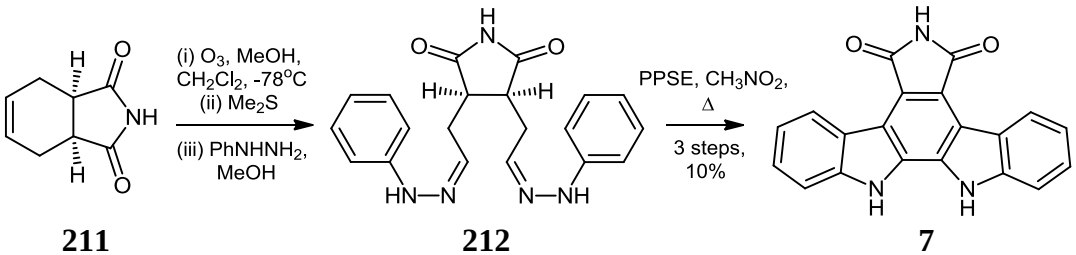
Preparation of the TMS-protected dione **205** substrate was achieved *via* [4+2] cycloaddition of 2,3-bis(trimethysilyloxy)butadiene **204**, prepared by thermal ring-opening of **203**, with maleimide **199** (90%), and condensed with phenylhydrazine under acidic conditions to afford osazone **206** (91%).[56]

Double Fischer indolisation employing PPSE in nitromethane led to dihydroarcyriaflavin A **207**, which could be dehydrogenated *in situ* to arcyriaflavin A **7** (Scheme 2.22).[54,57] Gribble and co-workers independently developed a variant of this route to form 6-methylarcyriaflavin A **210** (aglycon of synthetic AT2433-B topo I inhibitor class), by Diels-Alder reaction of **204** with *N*-methylmaleimide **188** to provide intermediate **208**, prior to hydrazone formation (**209**) and conversion to 6-methylarcyriaflavin A **210** in almost identical overall yield to that achieved by Bergman (Scheme 2.23).[55]



Scheme 2.23

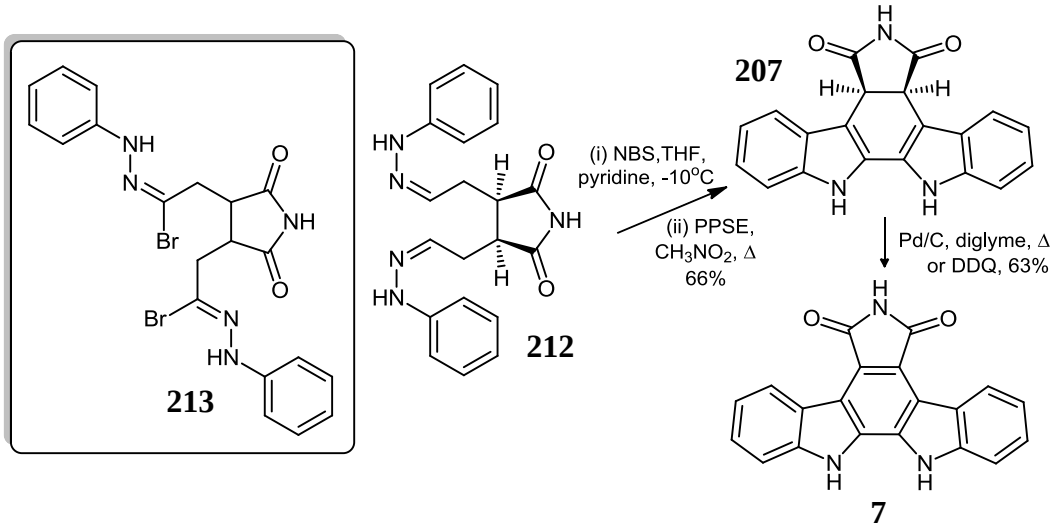
In 1992, Gribble and Berthel also described a shorter but lower yielding two-step route to both arcyriaflavin A **7** and **210**. Reductive ozonolysis of the commercial tetrahydrophthalimide **211** resulted in formation of a labile dialdehyde, prior to conversion with 2 equivalents of phenylhydrazine to afford bis(phenyl)hydrazone **212** (Scheme 2.24).[55]



Scheme 2.24

Following treatment with other arylhydrazines, it was noted that considerable stability issues were present. Exposure to Lewis acid catalyst, polyphosphoric acid trimethylsilyl ester (PPSE) in refluxing nitromethane, resulted predominantly in decomposition, but in the case

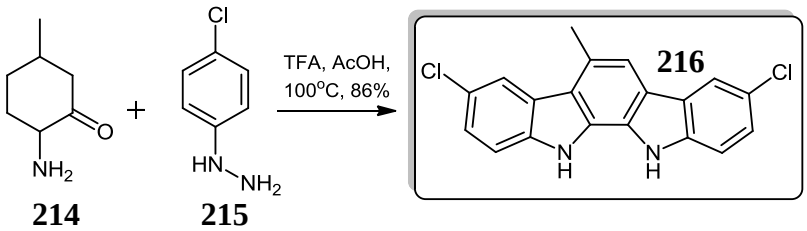
of unsubstituted phenylhydrazine, the fully aromatised indolocarbazole **7** could be isolated in 10% yield, following chromatography.[55]



Scheme 2.25

Interestingly, an ultimately unsuccessful attempt to block the premature cyclisation of bisphenylhydrazone **212** (leading to decomposition products) was carried out by means of NBS treatment in THF to give the putative bis-hydrazonyl bromide **213**. However, when applied to the succinimide derivative **212** in THF/ pyridine at −10°C, this route afforded an enhanced, high-yielding route to dihydroarcyriaflavin A **207** (66%) and thus, following PPSE-induced indolisation and full cyclodehydrogenation, employing 10% Pd/C in refluxing diglyme (63%), elicited a novel pathway to indolo[2,3-*a*]carbazoles congeners, under Bergman cyclisation conditions (PPSE, $MeNO_2$), as displayed in Scheme 2.25.[54,55]

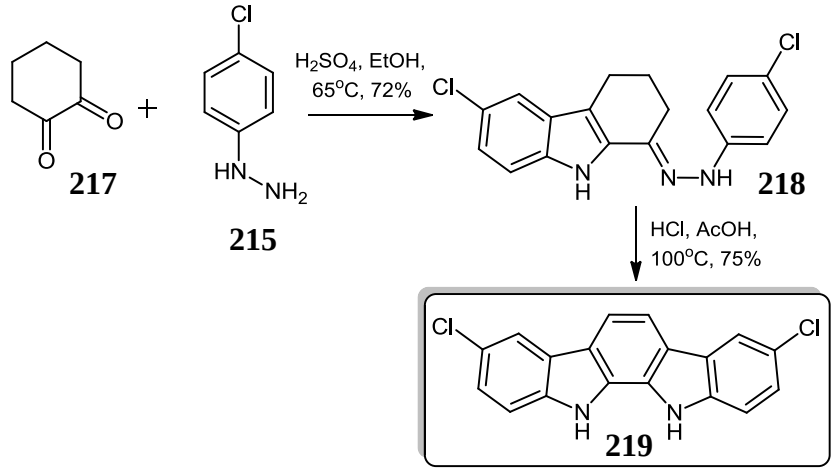
In 2005, Hu and Chen demonstrated that exposure of amino-substituted cyclohexanone **214** to 4-chlorophenylhydrazine **215** in a mixture of acetic acid and TFA yielded the corresponding modified indolo[2,3-*a*]carbazole **216** (Scheme 2.26).[58]



Scheme 2.26

Similarly, the double Fischer indolisation between cyclohexane-1,2-dione derivatives and substituted hydrazines may also constitute a key route to construction of symmetric 3,8 or 1,10-disubstituted indolo[2,3-*a*]carbazoles, *via* a protocol initially proposed by Curiel *et al.*[59]

This approach was also utilised by Bonjouklian and co-workers in order to introduce the 3,8-dichloro substitution pattern present within tjipanazole D **219**, without the need for any protecting groups or regioselectivity concerns.[31]



Scheme 2.27

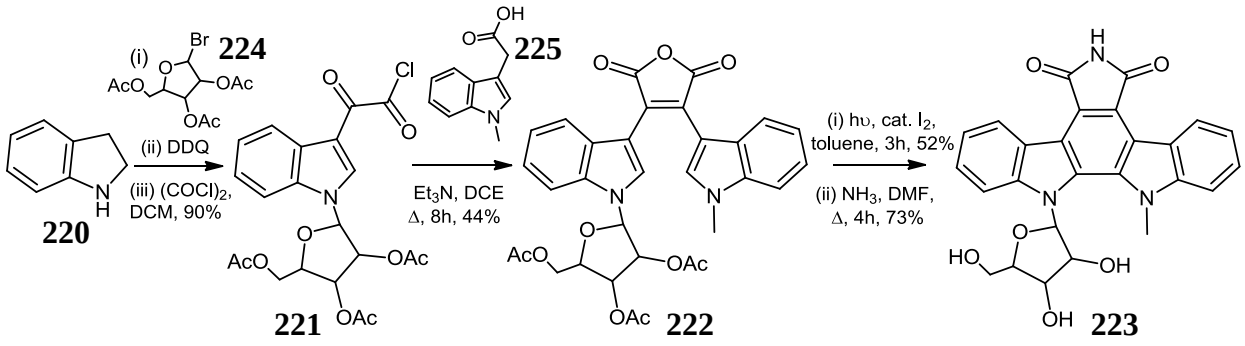
In this route, cyclohexane-1,2-dione **217** was condensed with 4-chlorophenylhydrazine **215** in the presence of H_2SO_4 to afford the hydrazone derivative **218** (72%), which was then converted under acidic conditions to the desired natural product **219** (Scheme 2.27).

2.2.4 F-Ring Routes

2.2.4.1 Perkin condensation approach

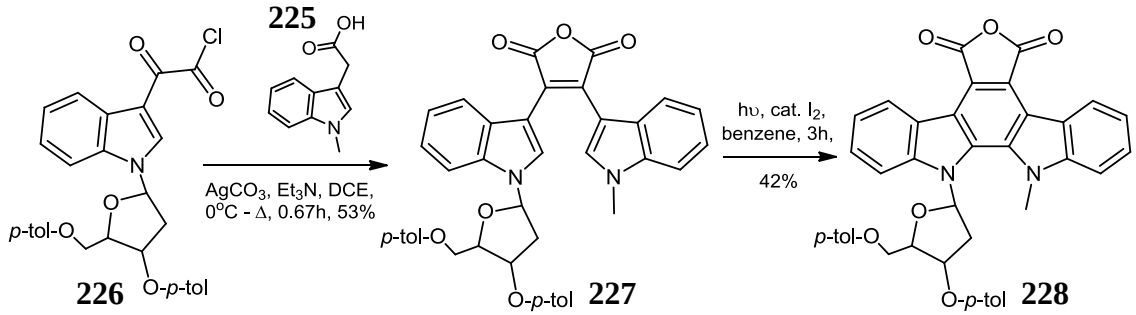
These reaction types involve either the combination of an indole-3-glyoxylate or related glyoxylyl chloride with an indole-3-acetic acid derivative, or homocoupling reaction of an indole-3-acetic acid followed by amidation.

In 2003, Garaeva and co-workers published an efficient synthesis of indolocarbazole β-*N*-ribofuranoside **223**, starting from indoline **220** and 2,3,5-triacetylated bromofuranose derivative **224**, was then converted to a 1-(2,3,5-tri-*O*-acetyl)-β-D-ribofuranosylated indole precursor, in the presence of DDQ.[60]



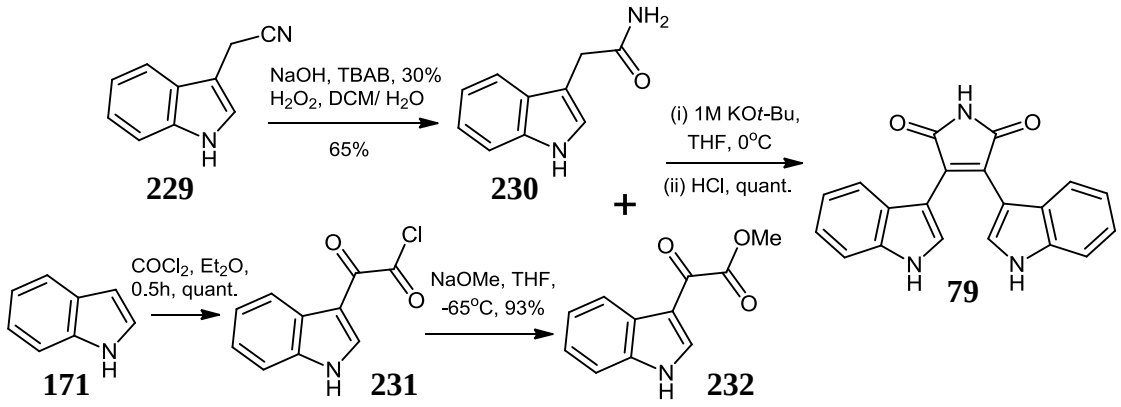
Scheme 2.28

Following oxalyl chloride-mediated glyoxylyl chloride **221** synthesis, base-induced condensation with *N*-methyl indole-3-acetic acid **225** resulted in formation of tri-*O*-acetylated bisindolylfuran-2,5-dione **222**, in a yield of 44%. Following oxidative cyclisation, exposure to ammonia provided access to deacetylated pyrrole-2,5-dione **223** in a yield of 73% (Scheme 2.28). These workers also investigated the biological nature of novel sugars possessing distinct hydrogen bonding character, attached to the indolocarbazole nucleus. In the case of 2-deoxyribofuranoside derivatives, initial 1-(β-D-2-deoxyribofuranosyl)indole-3-glyoxylyl chloride analogue **226** condensation with **225** also effected anomerisation, yielding a 1:1 diastereomeric mixture of furanosylation products due to *in situ* generation of HCl. Fortunately, addition of silver carbonate to the reaction mixture was reported to suppress this phenomenon, and subsequent cyclisation of the 2'-deoxy-β-*N*-glycoside **227** afforded the corresponding indolocarbazole **228** in moderate yield (Scheme 2.29).[60]



Scheme 2.29

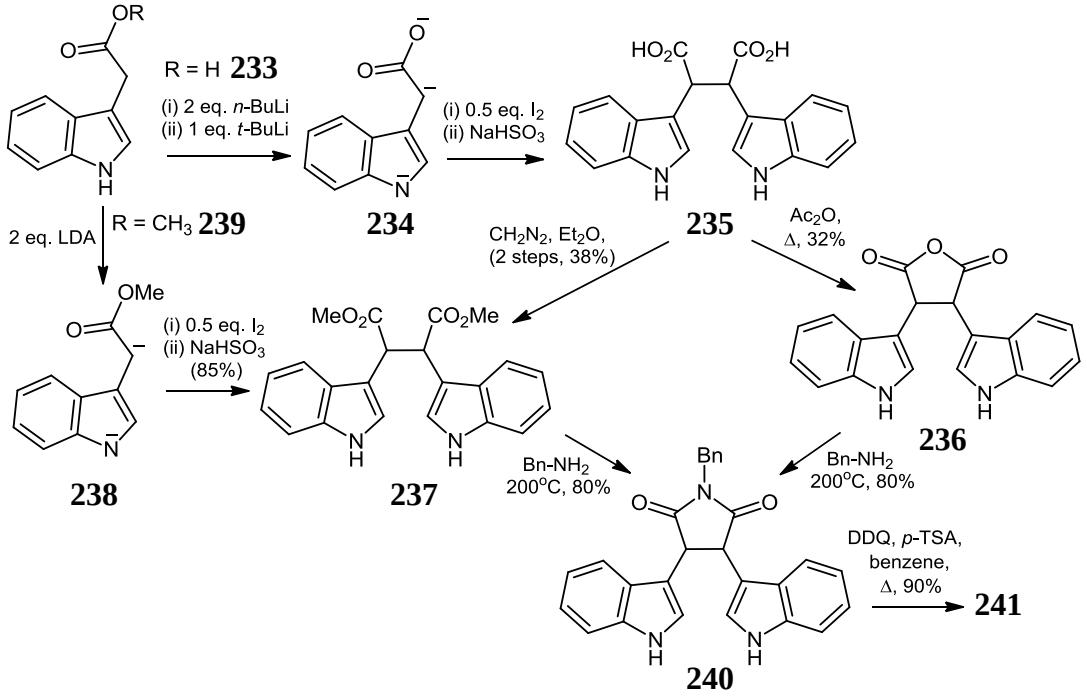
Faul's methodology permitted one-pot synthesis of a range of disubstituted maleimides and avoided any ammonolysis step.[61] These reactions have also been shown to be highly tolerant to substrate variation and affords quantitative conversion to arcyriarubin A **79**, without the need for protecting groups. Addition of strong base to a reaction mixture in THF at 0°C, comprising indole-3-acetamide **230**, isolated following hydrolysis of the corresponding nitrile **229**, along with labile glyoxylate ester **232**, formed in two steps, from indole **171** *via* glyoxylyl chloride **231** afforded **79** in quantitative yield (Scheme 2.30).[61,62]



Scheme 2.30

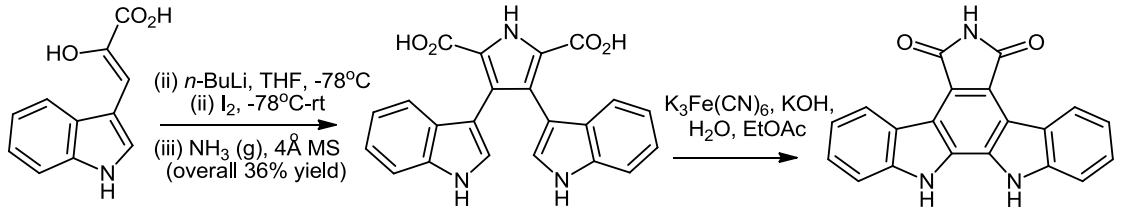
2.2.4.2 Iodine-mediated indole coupling reactions

Employing this biomimetic approach, deprotonation of **233** with 2 equivalents of *n*-butyllithium and 1 equivalent of *tert*-butyllithium successively, enabled formation of the indole-3-acetic acid trianion **234**, prior to oxidative coupling to form **235**.[63,64] Refluxing in acetic anhydride afforded derivative **236**, whereas diazomethane treatment resulted in formation of diester **237**. Iodine-promoted dimerisation of dianion **238** obtained from methyl indole-3-acetate **239** following addition of 2 equiv of LDA constituted an improved yield of this ester **237** (85%). Reaction of succinic anhydride **236** or diester **237** with benzylamine resulted in isolation of *N*-benzyl bisindolyl analogue **240** in a yield of 80%, which could then be efficiently oxidised by DDQ in benzene to the corresponding fully aromatised pyrrolo[3,4-*c*]carbazole product **241** in a yield of 90% (Scheme 2.31).[63,65]



Scheme 2.31

In 2007, Hinze *et al.* reported a related biomimetic oxidative annulation sequence involving *n*-butyllithium/iodine radical dimerisation of pyruvic acid **242** at −78°C, prior to condensation with gaseous ammonia, to afford 3,4-bisindolylpyrrole-2,5-dicarboxylic acid **243** (36%). Subsequent oxidative ring-closure in aqueous KOH, in the presence of potassium ferricyanide resulted in formation of arcyriaflavin A **7**; however, no yield was reported for this final cyclisation step (Scheme 2.32).[66]



Scheme 2.32

2.2.5 Successful multiple ring forming strategies

2.2.5.1 [4+2] Diels-Alder cycloaddition in B/D/F-ring formation

Numerous workers have reported Diels-Alder carbon-carbon bond forming reactions as key points in diverse syntheses of ICZs. Recent examples of this versatile C-ring forming process for intermediate steps are illustrated in Fig. 2.2, and include Moody's ICZ route involving decarboxylative carbazole ring aromatisation[49] within **194** (Scheme 2.20), Raphael's dienophile addition[35] to 1,4-bisarylbutadiene precursor **181** (Scheme 2.18), Tomé's strategy[52] employing cycloaddition of maleimide **199** to 2-nitrostyrene derivative **198** (Scheme 2.21), and Bergman's Fischer route from 2,3-bis(trimethylsilyloxy)butadiene **204** (Scheme 2.22).[55]

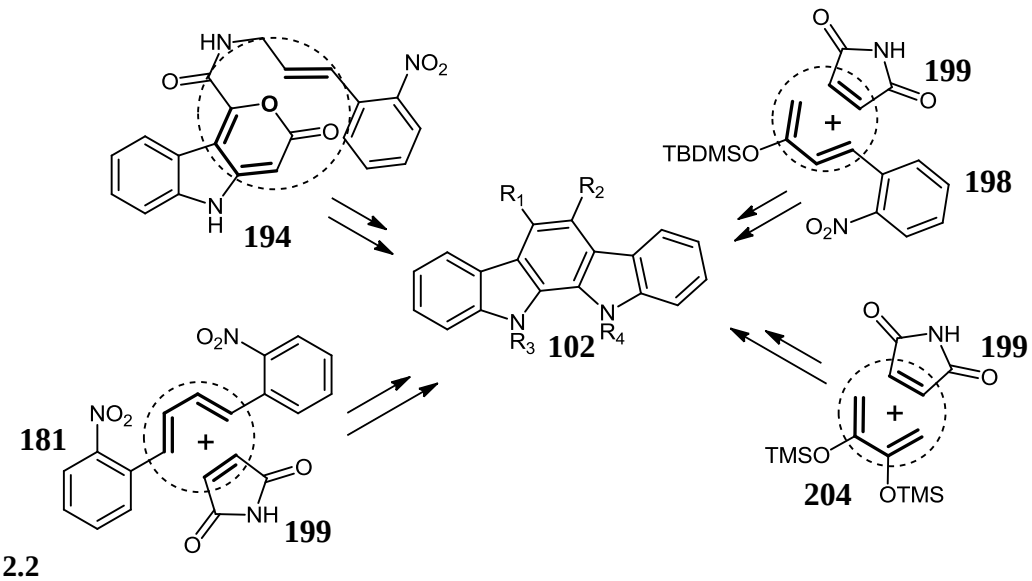
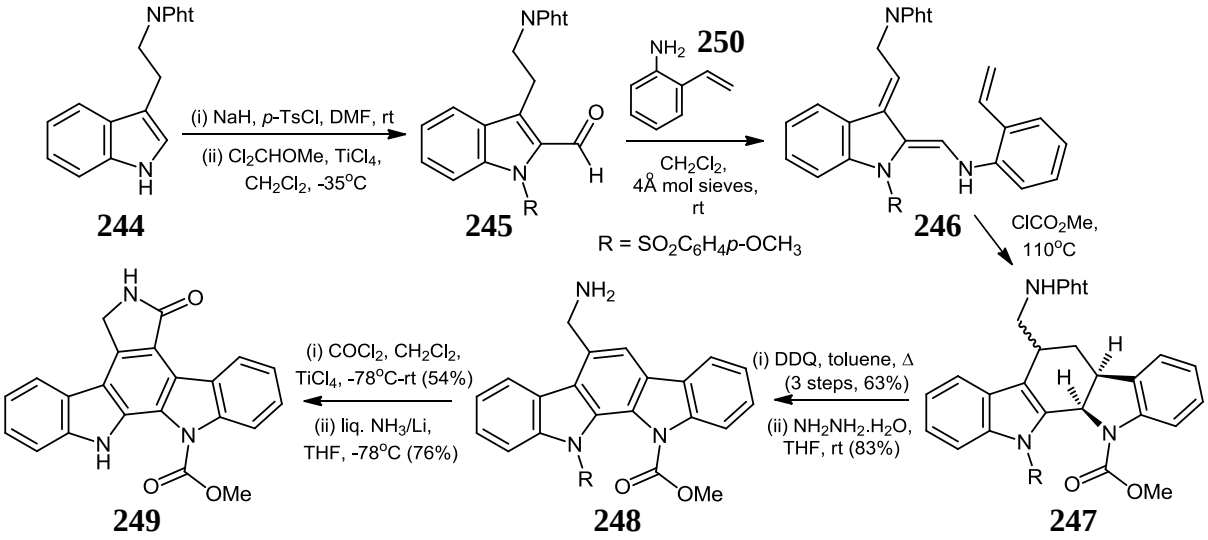


Fig. 2.2

2.2.5.2 B/C-ring formation employing Diels-Alder cycloaddition

In 1983, Magnus and co-workers reported the first synthesis of more complex F-ring substituted ICZs by intramolecular Diels-Alder cycloaddition of indole-2,3-quinodimethane analogue **246**, formed following initial conversion of tryptamine derivative **244** to *N*-protected 2-formyl analogue **245** and subsequent 2-aminostyrene **250** condensation.[24]

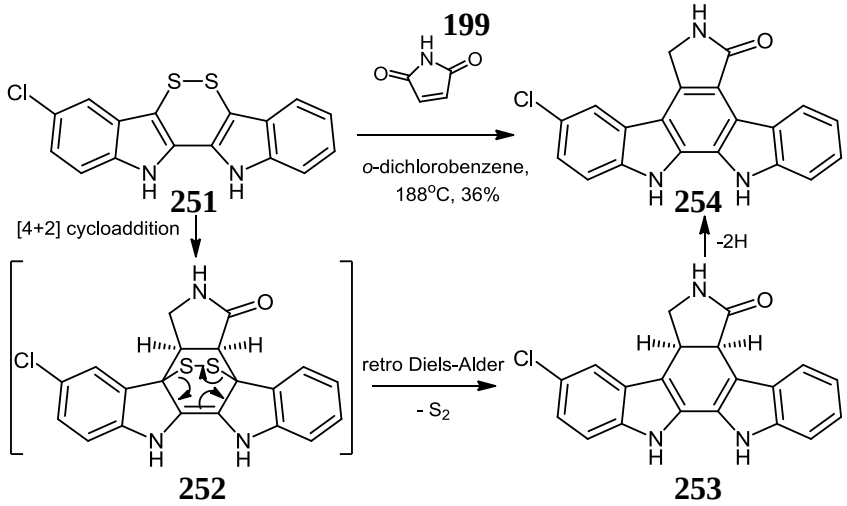
Formation of target compound **249** then occurred in 5 steps from **246**; intramolecular Diels-Alder ring-closure occurred under thermal conditions to provide carbamate-protected intermediate **247**, which then underwent DDQ-induced aromatisation and phthalimide deprotection forming **248**, prior to successive phosgene-mediated cyclocarbonylation in the presence of a Ti(IV) Lewis acid catalyst and final detosylation, to provide lactam **249**, in a yield of 65% over the final two steps (Scheme 2.33).[24]



Scheme 2.33

2.2.5.3 Retro Diels-Alder route: C-ring formation

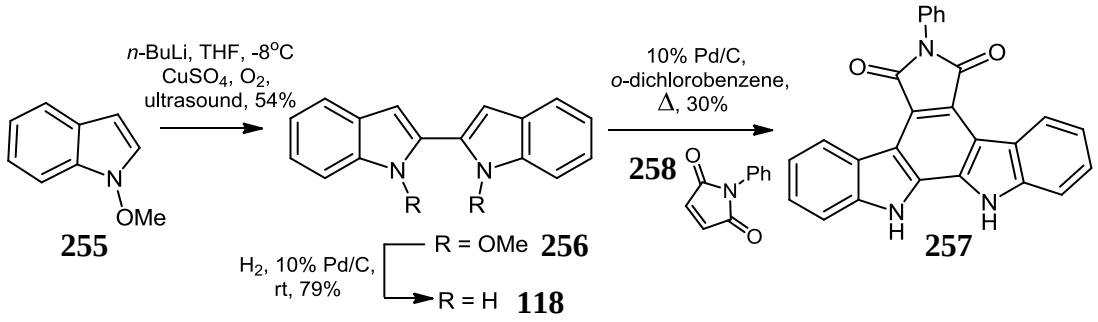
In 1999 and 2000, Lobo and co-workers disclosed two methods employing electrocyclic removal of S_2 as a key step in their synthetic procedure.[67,68] A one-step synthesis of 3-chlorinated K-252c derivative **254** in 36% yield, following treatment of 2,2'-biindolyl-3,3'-dithiete **251** with maleimide **199** in 1,2-dichlorobenzene at high temperature. This reaction is believed to feature initial Diels Alder cycloadduct **252**, followed by elegant retro Diels-Alder formation of intermediate **253**, prior to air oxidation to aromatised **254** (Scheme 2.34).[67]



Scheme 2.34

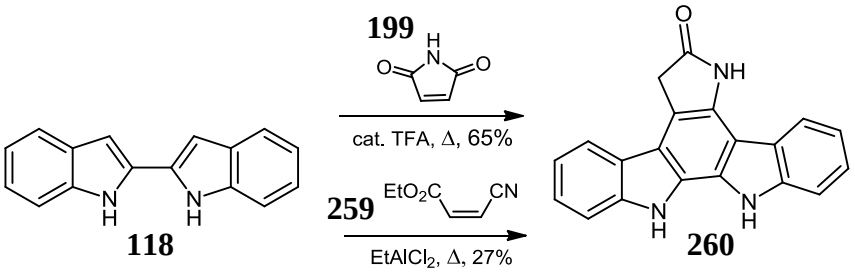
2.2.5.4 Tandem conjugate addition reactions

The involvement of 6π-electrocyclisation events within diverse routes to ICZ formation and closely related Michael addition/cyclisation reactions of 2,2'-biindolyl **118**, have been disclosed as a relatively unversatile C-ring forming reaction for generation of the indolo[2,3-*a*]carbazole nucleus **1**. In 1992, Somei and Kodama employed this [4+2] cycloaddition-type strategy utilising *N*-phenylmaleimide **258** to afford an intermediate adduct, which was subsequently dehydrogenated to 6-phenylarcyriaflavin A **257**, in a yield of 30%.[69]



Scheme 2.35

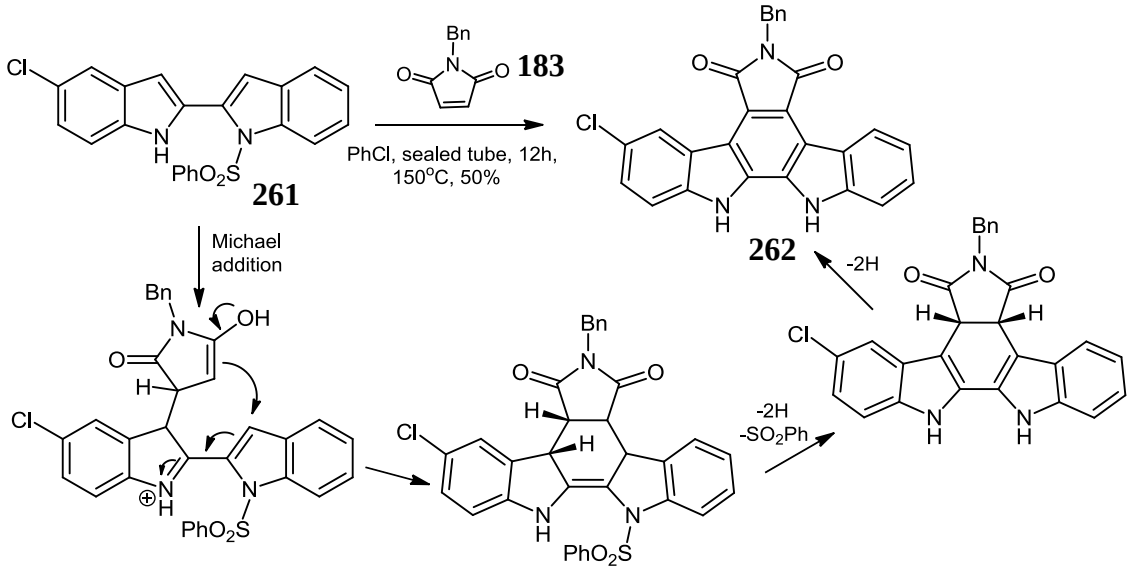
These workers also employed a novel ultrasound-induced oxidative coupling of 2-lithiated *N*-methoxyindole **255**, with anhydrous copper(II) sulfate under oxygen atmosphere to provide 2,2-biindolyl **118**, following reductive demethoxylation of **256**, in overall 43% yield (Scheme 2.35). Unfortunately, subsequent attempts by several workers to effect facile cycloaddition between a panel of functionalised dienophiles and 2,2'-biindolyl **118**, in order to develop a direct route to indolo[2,3-*a*]carbazoles have been beset by low yields and limited success under conventional high-temperature conditions.[5,69-72]



Scheme 2.36

In the case of unsubstituted biindolyl **118**, Hudkins and Diebold also reported unanticipated formation of a K-252c **6** regio-analogue, **260** *via* acid-catalysed tandem Michael addition, following exposure to either maleimide **199** or ethyl *cis*-β-cyanoacrylate **259** in the presence of trifluoroacetic acid or ethylaluminium dichloride, respectively (Scheme 2.36).[73] These reactions are thus believed to progress *via* a mechanism of conjugate 1,4-addition, followed by nucleophilic addition and dehydrogenation, rather than formal concerted [4+2] electrocyclization. Exploiting this stepwise Michael condensation-cyclisation rationale,

Kuethe *et al.* also recently developed an innovative one-pot route to the unprotected indolo[2,3-*a*]carbazole scaffold within **262** by heating mono-*N*-protected 2,2'-biindolyl **261** to high temperature in the presence of *N*-benzylmaleimide **183**.[74]



Scheme 2.37

Under these harsh conditions, thermal cyclisation of **261** is facilitated by the electron-withdrawing *N*-substituent; dehydrogenation to form 9-chloro-*N*-benzylarcyriaflavin A **262** then proceeds with *in situ* elimination of the *N*-phenylsulfonyl group (Scheme 2.37).[74] In terms of analogous glycosidic chemistry, Somei *et al.* illustrated that mono-*N*-glucopyranosylated 2,2'-biindolyls also exhibit moderate reactivity with DMAD in nitrobenzene, to afford the corresponding indolo[2,3-*a*]carbazoles in low yields.[75] Consequently, these non-facile cycloaddition approaches are limited in scope, due to the absence of robust chemistry to diverse chemical scaffolds, application of harsh reaction conditions and requirement for auxiliary indole functionality to enhance reactivity.[68,74,76]

2.2.5.5 Transition metal-mediated routes

Although stringently limited in substrate scope and product derivatisation capacity, few constructions of the central indolocarbazole core still display such elegance as the diverse range of transition metal-mediated routes, employing relatively mild conditions as well as one-pot conversion of simple starting materials to complex polycyclic products through regioselective control of concerted bond-forming reactions.[77-82] Up to relatively recent times, three alternative strategies were adopted through this methodology:

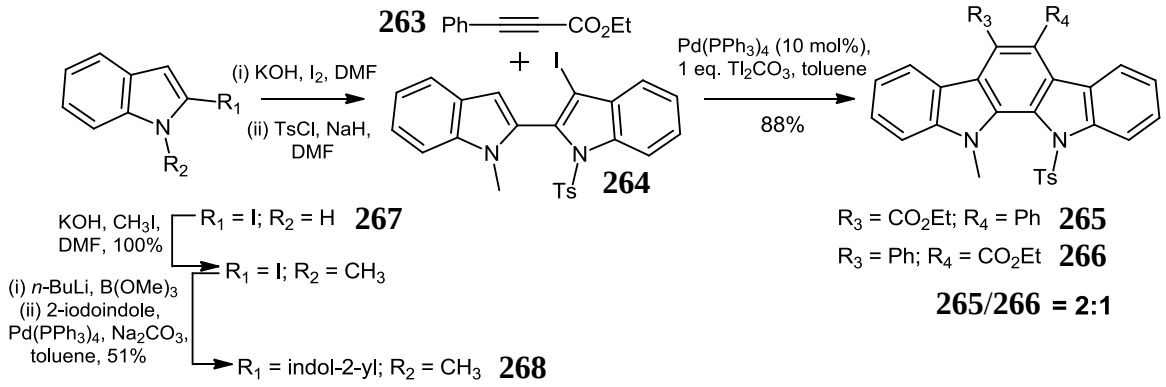
(i) Pd(0)-catalysed benzannulation route

(ii) Annulation of Fischer carbene intermediates

(iii) Pd(0)-mediated 1,3-diacetylene double cyclisation

2.2.5.5.1 C-Ring formation: Benzannulation route

Merlic and colleagues disclosed regioisomeric synthesis of indolocarbazole analogues **265** and **266**, derived from indole utilising a key Pd-induced benzanulation step.[83] Following the Bergman/Venemalm strategy, quantitative *N*-methylation of readily available 2-iodoindole **267** was performed, prior to conversion *in situ* to the corresponding indole-2-boronic ester. Suzuki cross-coupling with 2-iodoindole **267** in the presence of $Pd(PPh_3)_4$ (**268**), prior to 3'-iodination and tosylation of the NH unsubstituted indole ring then provided access to 3-iodo-2,2'-bisindolyl derivative **264**.[76,84-86] Unsymmetrical intermediate **264** afforded a mixture of ICZ regioisomers **265** and **266** in a ratio of 2:1, in moderate yields, *via* palladium(0)-catalysed benzannulation reaction with phenylacetylene ester reactant **263** (Scheme 2.38).[83]

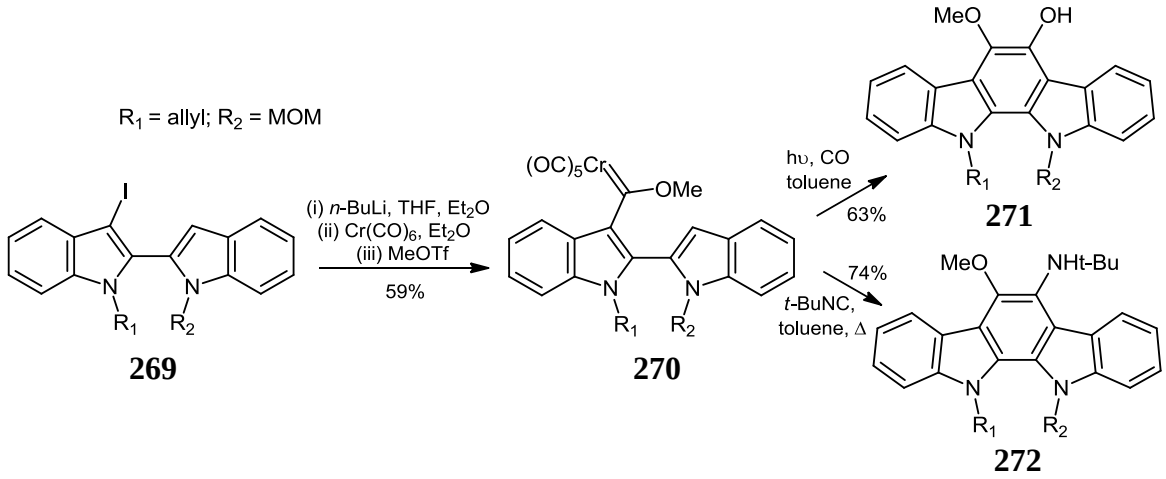


Scheme 2.38

2.2.5.5.2 C-Ring formation: annulation of Fischer carbene intermediates

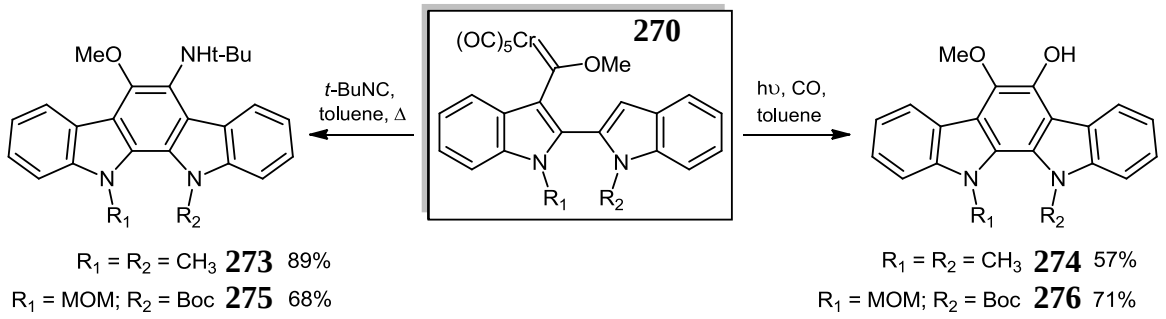
Fischer chromium carbene methodology also constitutes an important transition metal route involving benzannulation of 2,2'-biindolyl chromium carbene complexes, also derived from 3-iodo-2,2'-bisindolyl precursors to form products in a single step.[83,87]

Preparation of carbene complex **270** from corresponding **269**, was readily accomplished by means of standard metal-halogen exchange with *n*-butyllithium, followed by addition to chromium hexacarbonyl and methylation with methyl triflate.



Scheme 2.39

Cyclisation of **270** (R_1=allyl, R_2=MOM) to yield the desired benzannulation products was accomplished by a photochemical method in the presence of carbon monoxide, employing toluene or THF as solvent *via* a ketene intermediate to form **271** in 63% yield or conversely, following aminobenzannulation reaction occurring with *tert*-butylisocyanide – forming an intermediate ketenimine complex capable of undergoing thermal 6π-electrocyclisation to provide **272** in a yield of 74%. (Scheme 2.39).[77,87] Comparative yields reported in this study were 71% (photochemical) for **276** as opposed to 68% in boiling toluene for **275**; R_1=MOM, R_2=Boc, and 57% for irradiated reaction to afford **274**, along with a highest yield of 89% for thermal transformation to **273** (R_1=R_2=CH_3; Scheme 2.40).[87]

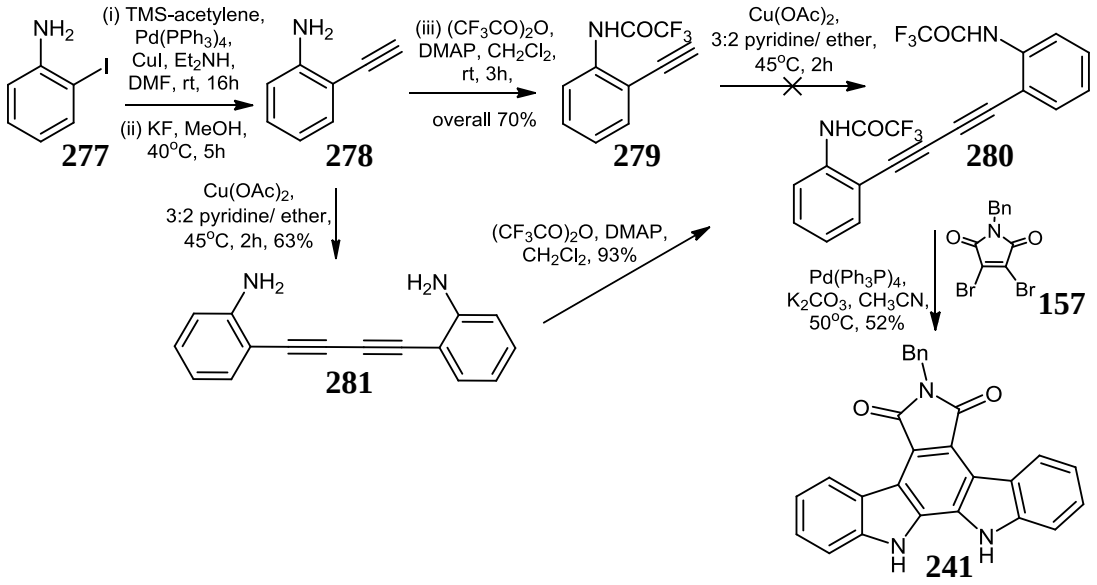


Scheme 2.40

2.2.5.5.3 B/C/D-ring formation: 1,3-diacetylene double cyclisation

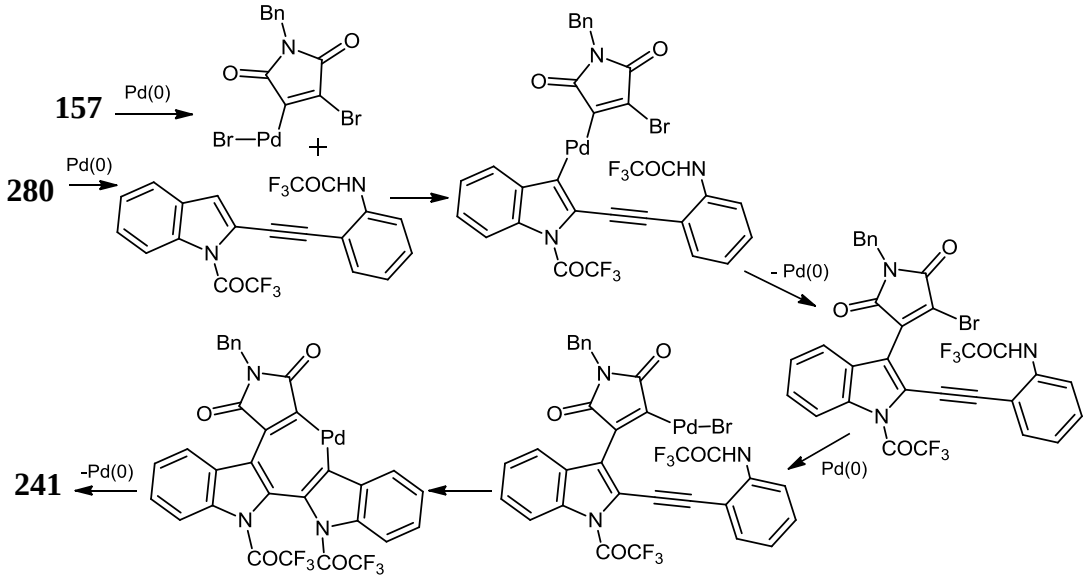
This strategy developed by Saulnier and co-workers involves assembly of the indolo[2,3-*a*]carbazole framework *via* a polyannulation methodology wherein both indole B and D-rings, and central C-ring are formed in a one-pot process from the 1,3-diacetylene precursor **280**.[88,89]

Starting from 2-iodoaniline **277**, this was readily converted to 2-ethynylaniline **278** and then to trifluoroacetanilide **279**, under Cacchi conditions, in reported 70% yield (Scheme 2.41).[79]



Scheme 2.41

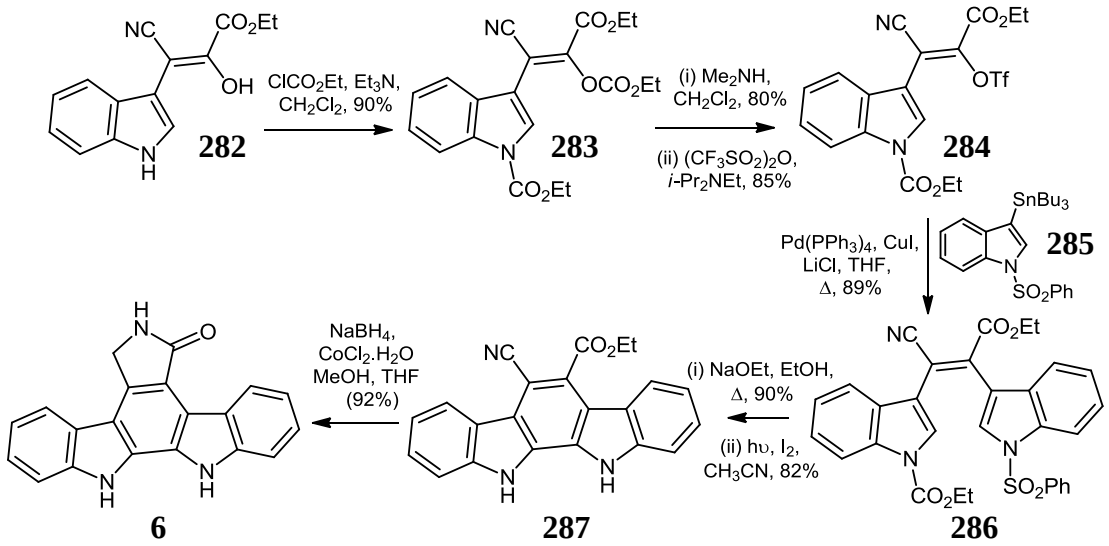
However, under typical Sondheimer conditions none of the desired **280** could be obtained. Fortunately, direct transformation of **278** to intermediate **281** under similar coupling conditions (63%), followed by trifluoroacetylation provided access to the desired bistrifluoroacetanilide **280** in 93% yield for this step.[88]



Scheme 2.42

Coupling of **280** with **157** in the presence of potassium carbonate and tetrakis(triphenylphosphine)palladium (7 mol%) at 50°C overnight, afforded the corresponding 6-benzylarcyriaflavin A **241** in 52% yield. The putative mechanism for this polyannulation implicates the activity of the readily cleavable trifluoroacetyl group in attenuating nitrogen nucleophilicity – thus favouring subsequent C(3)-Pd attack (Scheme 2.42).[88]

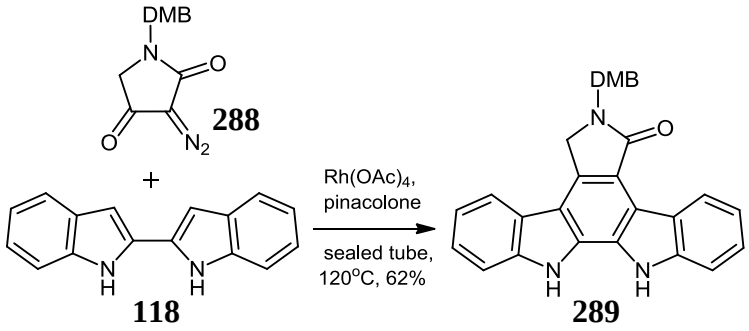
In other work, Beccalli *et al.* disclosed a route to K-252c **6** incorporating a pivotal palladium-mediated Stille reaction step. Starting from readily accessible ethyl 3-cyano-2-hydroxy-3-(1*H*-indol-3-yl)acrylate **282**, reaction with ethyl chloroformate to form **283** and selective *O*-deprotection under mildly basic conditions, followed by trifylation employing Hunig's base provided the Stille precursor **284**.[90]



Scheme 2.43

Coupling of triflate **284** with 1-phenylsulfonyl-3-tributylstannylindole **285** led to 1,2-bisindolyl-*cis*-alkene **286** in 89% yield. Following indolic deprotection and U.V. aromatisation, reductive amidation of **287** in a methanolic mixture containing $NaBH_4$ and $CoCl_2$ gave lactam **6** (92%), as illustrated in Scheme 2.43.[90,91]

Finally, according to the elegant carbenoid protocol of Wood *et al.*, treatment of 2,2'-biindolyl **118** with the diazo compound **288** in the presence of catalytic $Rh_2(OAc)_4$ and degassed pinacolone as solvent, directly afforded K-252c analogue **289** in a yield of 62%.[92] This reaction has been postulated to proceed by sequential C-H insertion, electrocyclization, and aromatization (Scheme 2.44).[93]



Scheme 2.44

2.3 Strategies for synthesis of *N*-glycosidic linkages in natural ICZs

2.3.1 Importance of sugars in indolocarbazole alkaloids

Indolocarbazole glycosides possessing modified sugar units possess a wider range of biological activity than their corresponding aglycon analogues, due to the increased aqueous solubility of these derivatives, as well as the recognised ability of these glycosyl units to mediate important structural interactions within target enzyme active sites.[7,94] These compounds can be broadly classified into two classes based on the mode of sugar attachment. Single β-*N*-glycosidic ICZ linkages, as present in rebeccamycin **38**, are essential to topo I-mediated DNA strand breakage and intercalatory capacity, with the sugar moiety being accommodated within the minor groove of DNA and greatly contributing to energetic stabilisation of the drug-DNA-topo I cellular 'poison'.[95-97] The ability of a sugar unit to form hydrogen bonds with the unsubstituted indole nitrogen within these systems also potentiates an active warhead alignment of the enzyme-interacting F-ring within the topo I pocket.[98]

In addition, double β-*N*-glycosidic linkages, such as those present in cycloglycosylated staurosporine **2** and K-252a **13** have also been described to enhance ATP-competitive kinase inhibition within this class, due to the formation of an extended non-covalent bonding network where the glycosyl residue mimics important ATP phosphate contacts within the kinase ATP-binding domain.[99,100] Crystallographic data also indicates that sugar moieties may adopt a binding mode perpendicular to the planar indolocarbazole ring, and interact with several residues within the activation loop, in a unique phenomenon also contributing to attractive kinase selectivity.[100-102] Thus, derivatisation work within glycosidic congeners constitutes a crucial element within overall design of more potent ICZs. Isolation of these compounds has been achieved by fermentation, based on modification of natural biosynthetic pathways, as well as total synthesis of complex analogues bearing a range of sugar sub-units. These innovative chemical glycosidation strategies will now be discussed for important analogues within a highlighted panel of mono and di-β-*N*-glycosidic derivatives.

2.3.2 Biosynthetic origin of indolocarbazole sugar moieties

Endogenous functionalisation of natural products provides important clues for biocombinatorial synthesis of novel derivatives, as well as for innovative synthetic strategies capable of mimicking critical enzymic transformations *in vivo*.[4,103,104]

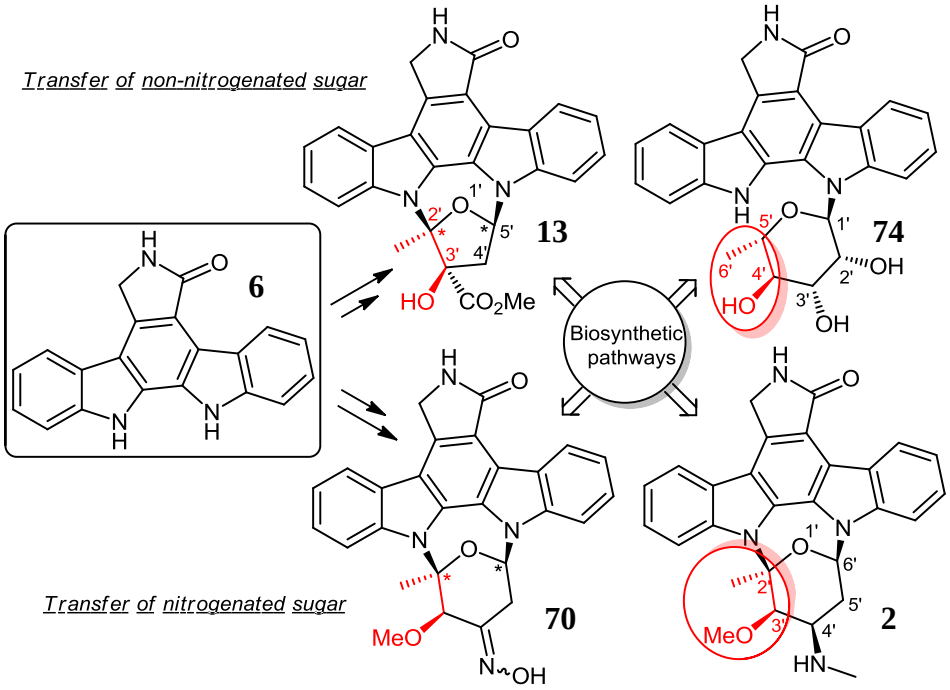
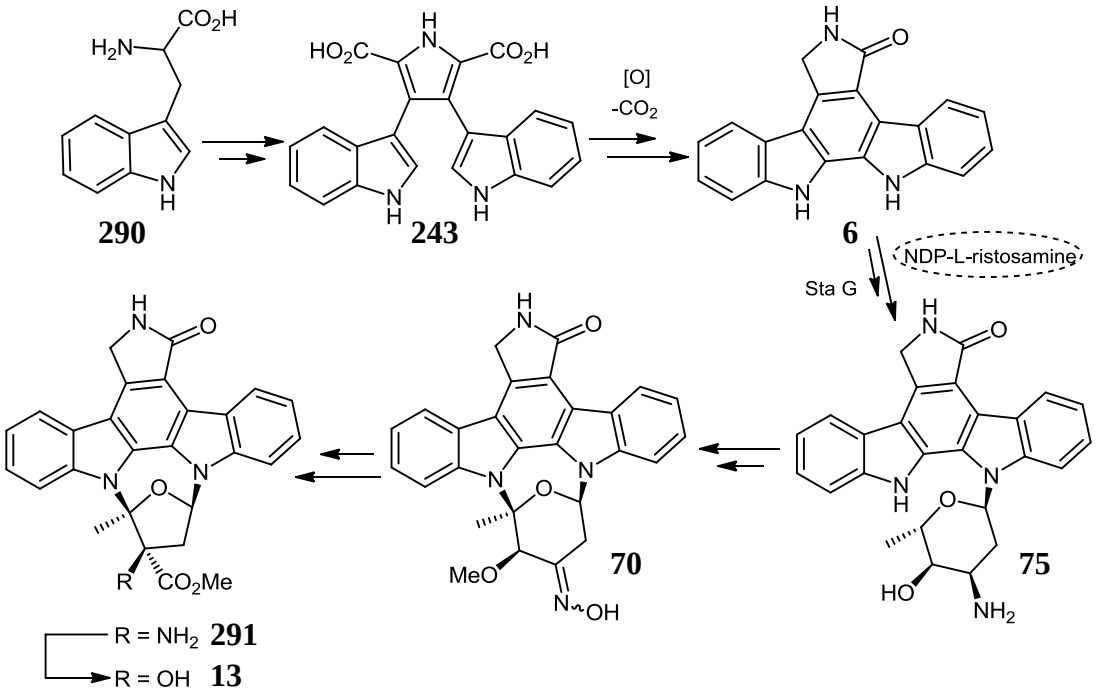


Fig. 2.3

Recent insights into the biosynthetic gene clusters of ICZ producing microorganisms have revealed several conserved features within their glycosidation strategies: (a) close alignment of absolute configurations of sugar moieties within co-produced ICZ metabolites possessing disparate indole-*N*-glycosidic linkages, e.g. stereochemistry at positions C-4' and C-5' of L-rhamnose in K252d **74** is identical to C-3' and C-2' of the deoxyaminopyranose moiety in staurosporine **2**, and (b) TAN-1030a **70** and staurosporine **2** retain identical absolute stereochemistry as ribofuranosylated K-252a **13** at the bridging anomeric carbons (Fig. 2.3). In addition, synthetic studies have also determined that carbohydrate moieties undergo remarkably stereoselective ring modification pathways.[4,105-107]

An important transition enabling commitment of indolocarbazole precursors to a specific metabolic fate occurs within the biosynthetic pathway starting from tryptophan **290**-derived chromopyrrolic acid **243** following production of K-252c **6** (Scheme 2.45).[108,109]

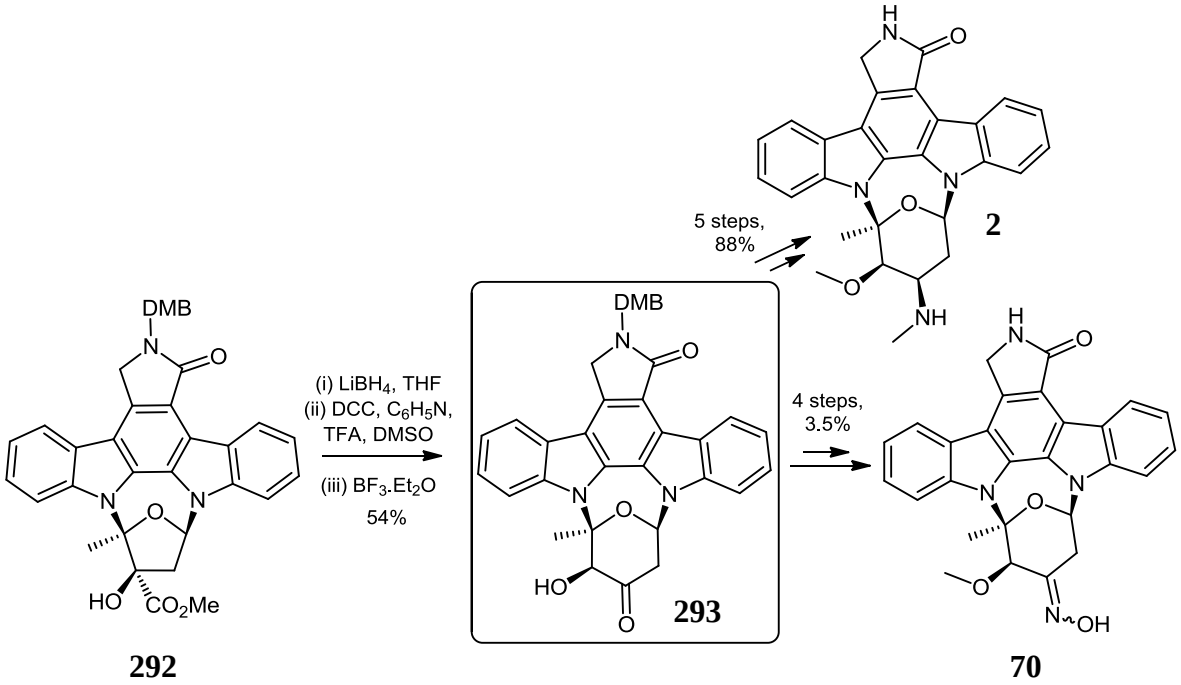


Scheme 2.45

Under the influence of the gene product of StaG, regiospecific incorporation of a mono-*N*-glycosylated aminosugar (e.g. NDP-L-ristosamine) results in formation of precursor holyrine A **75** and may subsequently permit formation of a second glycosidic linkage *via* enzymatic C-N bond formation. Alternatively, following initial transfer of a non-nitrogenated carbohydrate unit, analogues such as K-252d **74** may be produced, in addition to ring-contraction leading to ribofuranosylated derivatives related to K-252a **13**. Six-carbon carboxyfuranosylated derivatives are thus postulated to be formed from rearrangement of six-membered pyranose derivatives such as TAN-1030a **70** – a K-252a **13** biosynthetic precursor *via* an intermediate 3'-amino analogue **291** (Scheme 2.45).[4]

2.3.3 Semi-synthesis of natural bioactive indolocarbazole glycosides

Wood and co-workers established an elegant derivatisation protocol towards a panel of indolo[2,3-*a*]carbazole analogues including (+)-**2** and (-)-**70** based on biomimetic diversification of a common precursor, α-hydroxy ketone (+)-**293**, possessing all essential stereogenic centres in place.[106,110] Final imide deprotection of each DMB-protected congener was performed in a mixture of TFA and anisole to afford the parent natural compound in each case (Scheme 2.46).



Scheme 2.46

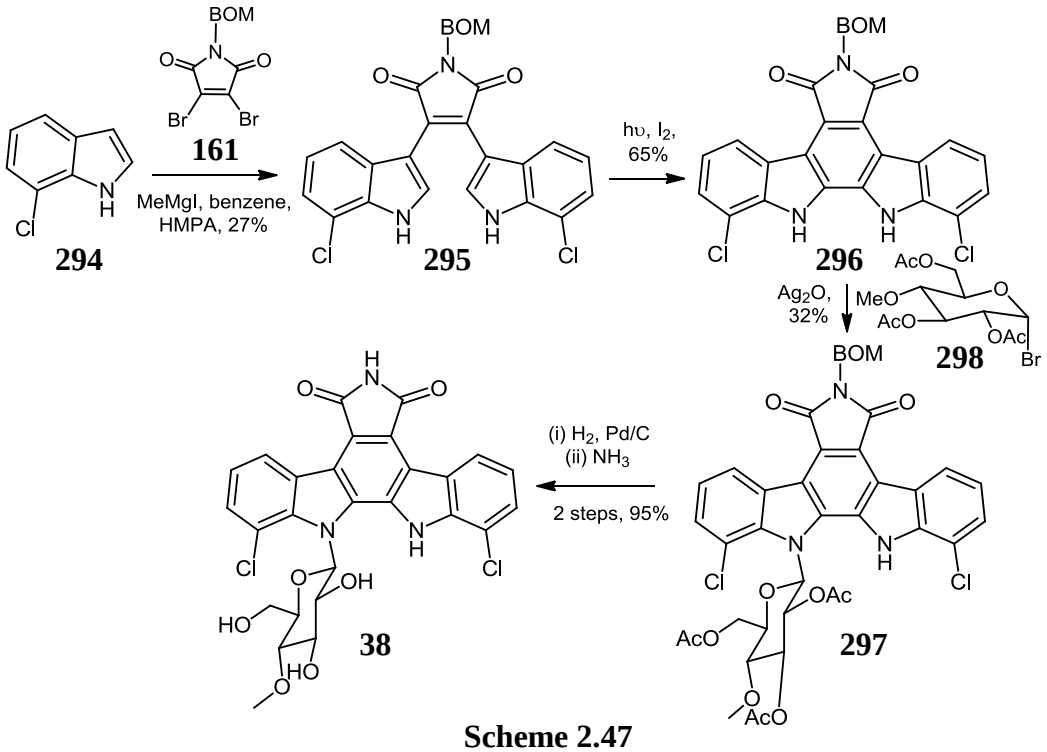
Regioselective reduction of K-252a derivative **292** followed by regioselective Lewis acid-mediated Demjanov-Tiffeneau-type ring expansion provided intermediate α-hydroxy ketone **293** over three steps. Semi-synthetic routes involving key reductive amination of this glycosylated precursor afforded staurosporine **2** in 88% yield over 5 steps, while regioselective *O*-methylation and oxime transformation also led to synthesis of TAN-1030a **70**, in 4 steps and in overall yield of 3.5%, due to difficult DMB group removal (Scheme 2.46).[110]

2.3.4 Chemical routes to mono-*N*-glycosides

Development of chemical strategies to mono-*N*-glycosylated ICZ congeners involve application of classical routes to the correspsonding aglycon prior to a stereoselective sugar coupling step to afford the target compound.

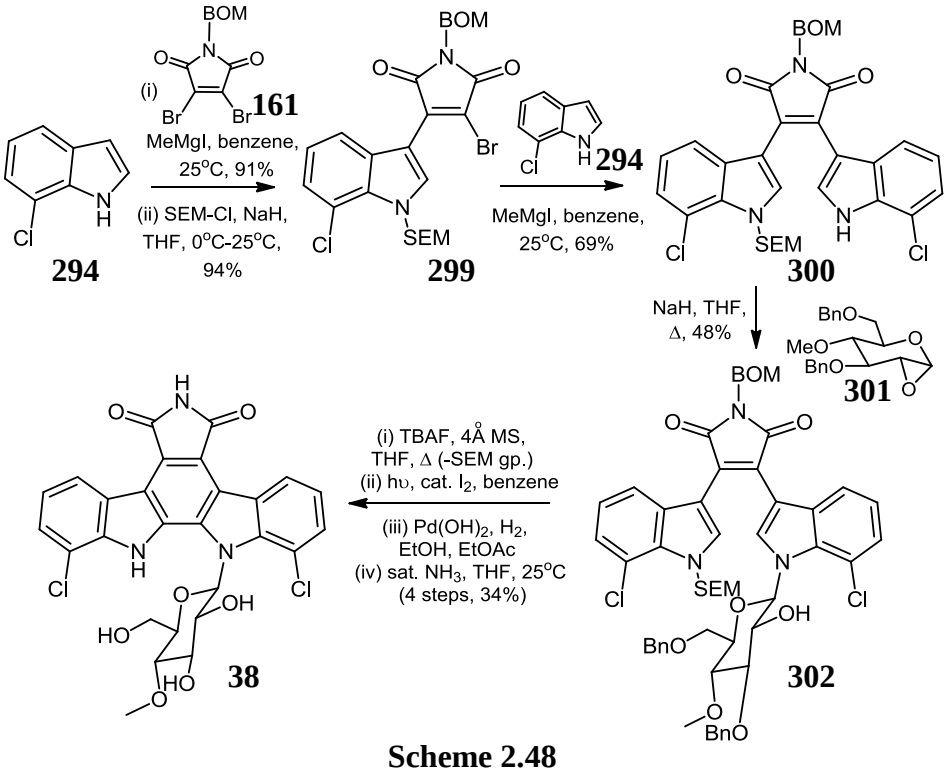
2.3.4.1 Total synthesis of rebeccamycin

In 1985, Kaneko and co-workers reported the first total synthesis of topo I inhibitory natural product rebeccamycin **38**, according to a strategy involving double 7-chloroindole **294** substitution of BOM-protected dibromomaleimide **161**, to afford bisindolylmaleimide **295** according to Weinreb's Grignard base-mediated procedure, followed by iodine-induced photocyclisation in a yield of 65% (Scheme 2.47).[40]



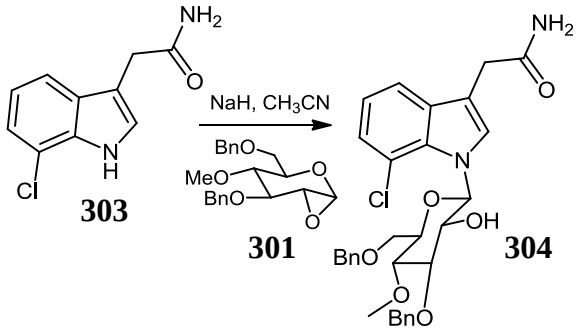
Scheme 2.47

Koenigs-Knorr coupling of aglycon **296** with 1-bromo-2,3,6-tri-*O*-acetyl-4-*O*-methylglucose **298**, in the presence of Ag_2O afforded **297**, and was transformed to the title *N*-glycosidic compound **38** in 30% yield, upon removal of the BOM group by hydrogenolysis and full ammonolytic 2,3,6-tri-*O*-deacetylation (Scheme 2.47).[40]



Scheme 2.48

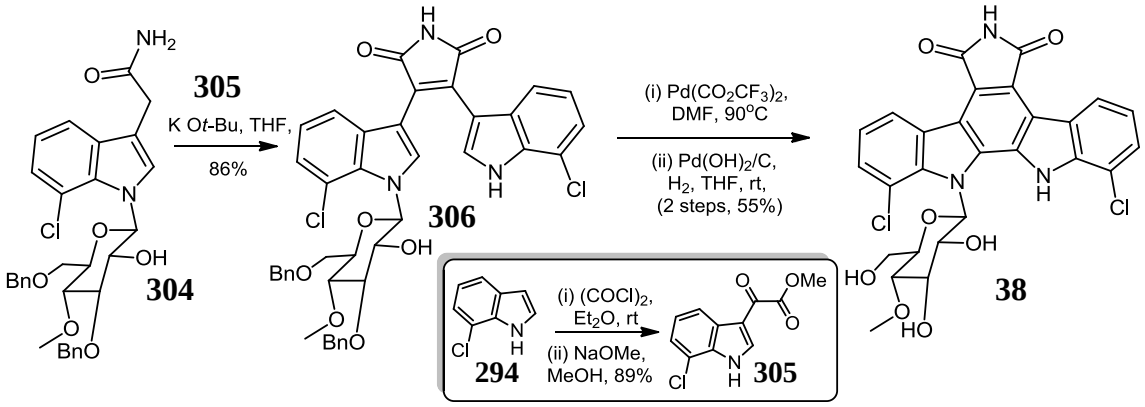
In 1993, Danishefsky reported development of glycal chemistry as an improved strategy towards formation of analogues comprising an *N*-glycosidic monolinkage (Scheme 2.48).[111] Initial monosubstitution of Kaneko precursor, BOM-protected dibromomaleimide **161**, formed in an excellent yield of 91% at room temperature, permitted selective indole nitrogen SEM-protection (**299**), prior to bromine displacement with another equivalent of the Grignard salt of 7-chloroindole **294** in benzene. Glycosidation of the sodium salt of **300** with α-1,2-anhydrosugar **301,** obtained from commercially available tri-*O*-acetyl-D-glucal, gave access to the β-glucopyranoside **302** in 48% yield. Following fluoride-induced SEM deprotection, construction of the central carbocyclic ring was achieved by U.V.-irradiation. The final two steps in this synthesis comprised BOM hydrogenolysis employing Pearlman's $Pd(OH)_2$ catalyst and ammonolysis to afford **38**. The monochlorinated ICZ side-product was also reported in 14% yield under these hydrogenation conditions. The major advantage of this method involves the novel application of stereoselective glycal epoxide ring-opening to form intermediate **302**, as well as utilising the bisindolylmaleimide precursor **300**, prior to photocyclisation, as a superior glycosyl acceptor (44% yield), compared with Kaneko's pathway employing the aromatised indolocarbazole core within **296** (Scheme 2.48).[40,111]



Scheme 2.49

Subsequent to discovery of their condensation method for bisindolylmaleimide synthesis, Faul *et al.* also published their total synthesis of rebeccamycin **38** including application of their pioneering step involving reaction of *N*-glycosylated 7-chloroindole-3-acetamide **304** with methyl 7-chloroindole-3-glyoxylate **305** to afford the anticipated di-*O*-benzyl derivative **306**.[61,112] The carbohydrate-linked acetamide **304** was stereoselectively synthesised *via* Danishefsky's methodology; reaction of the 1-indolyl anion of **303** with dibenzylated precursor **301** proceeded in a yield of 40%, and the desired β-epimer **304** (16:1 β/α-selectivity) was isolated in >98% diastereomeric purity (Scheme 2.49).[111,112] Following condensation to afford β-*N*-glucosylated bisindolylmaleimide in 86% yield, oxidative cyclisation employing palladium(II) trifluoroacetate at high temperature, followed by

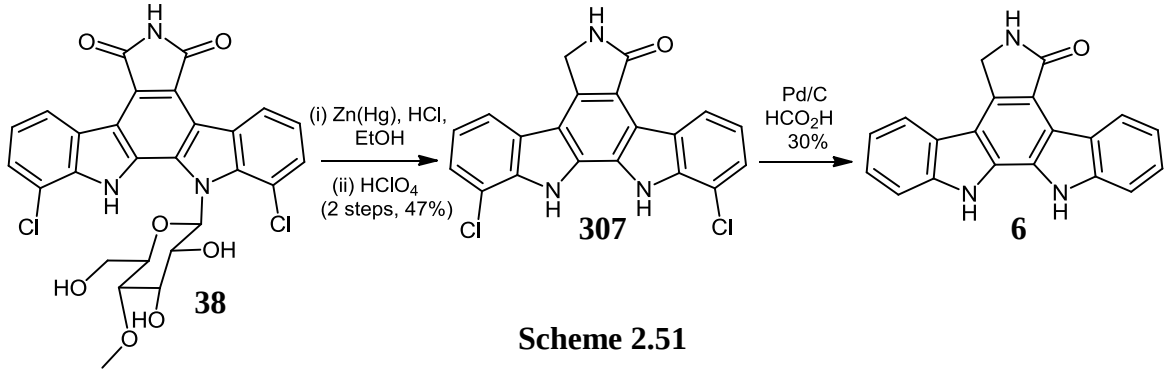
debenzylation revealed the natural product rebeccamycin **38** in three steps and 47% cumulative yield (Scheme 2.50).[112]



Scheme 2.50

This base-promoted route also constitutes a more efficient synthesis of **38**, compared with those of Danishefsky or Kaneko, as it requires no maleimide protection, obviating indole deprotection or imide deprotection steps, necessary for masking acidic sites under Grignard-mediated coupling routes to furnishing BIM compounds.

In addition, Prudhomme described a route envisaged as degradation of this natural product **38**, to afford K-252c **6**, in two steps. Reduction of the 7-oxo functionality followed by perchlorate-induced carbohydrate cleavage resulted in formation of 1,11-dichlorostaurosporinone analogue **307**, in a yield of 47%. Palladium-mediated dechlorination under acidic conditions then provided **6** in 30% yield (Scheme 2.51).[113]

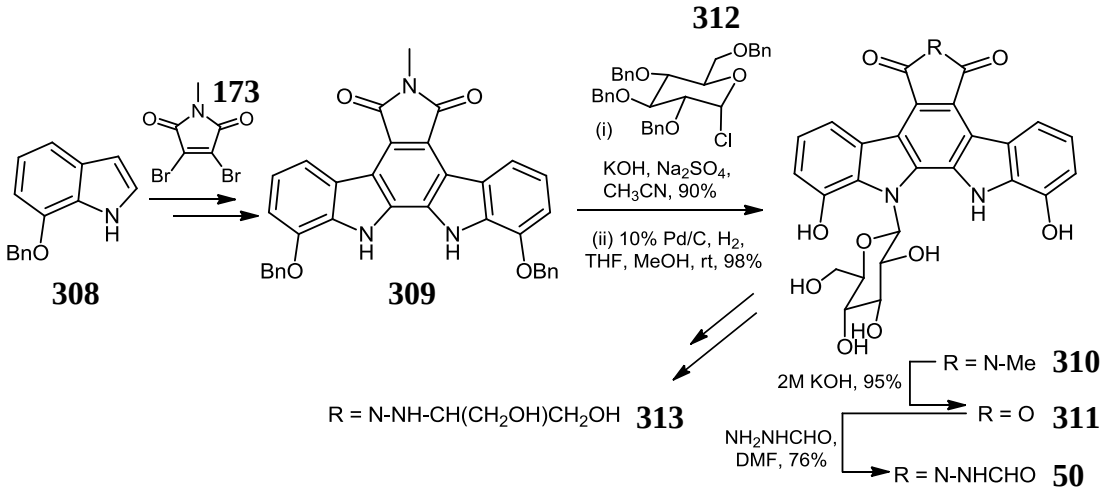


Scheme 2.51

2.3.4.2 Synthesis of rebeccamycin analogues: NB-506, ED-110 and J-109 404

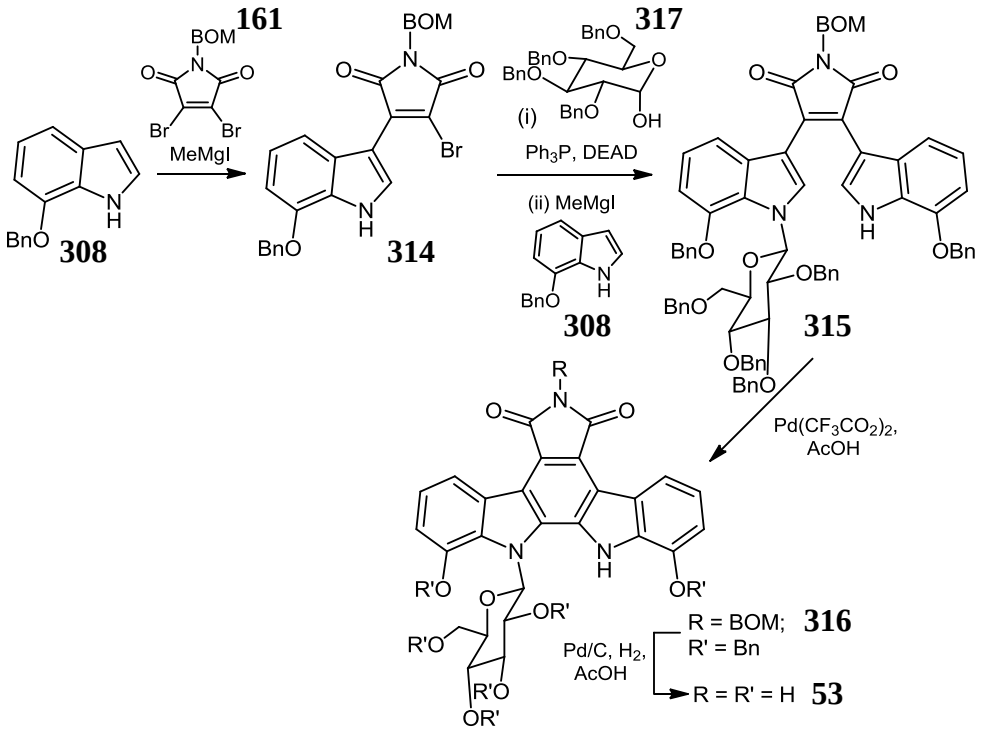
Ohkubo and co-workers utilised initial indole coupling chemistry to develop a route to the aglycon precursor of the clinical analogue, NB-506 **50**, from 7-benzyloxyindole **308** and 3,4-dibromo-*N*-methylmaleimide **173**, in five steps and 34% yield.[46]

Glycosylation of the potassium salt of precursor **309** with 2,3,4,6-tetra-*O*-benzyl-α-D-glucopyranosyl chloride **312** was accomplished with enviable stereoselectivity (α/β = 1:37). Following full debenzylation to intermediate **310** and imide hydrolysis, exposure of **311** to formic hydrazide provided NB-506 **50** in a final step yield of 76% (Scheme 2.52).[114]



Scheme 2.52

Alternatively, treatment of the electrophilic precursor **311** with hydrazine or amine derivatives resulted in 6-*N*-amino substituted analogues of **50**, including the anti-cancer compound, J-109 404 **313**, with a 1,3-dihydroxyisopropyl group in place of the *N*-formyl group, and formation of a panel of dihydroxylated anti-topo I congeners.[115-117]



Scheme 2.53

ED-110 **53** synthesis reported by Zembower *et al.* in 1999 employed Danishefsky's stepwise formation of BOM-protected bis(1,11-dibenzyloxyindolyl)maleimide **315** *via* successive Grignard-mediated 3-indolylation steps (Scheme 2.53).[111,118] Transformation of monoindolylbromomaleimide **314** to the corresponding bisindole-*N*-glycoside **315** was accomplished with 2,3,4,6-tetra-*O*-benzyl-α-D-glucose **317**, under Mitsunobu conditions, prior to bromine displacement by addition of the Grignard salt of 7-benzyloxyindole **308**.[119] Palladium-mediated oxidation of **315** under acidic conditions afforded derivative **316**, which could be deprotected by hydrogenolysis to access ED-110 **53** (Scheme 2.53).

2.3.5 Chemical routes to di-*N*-glycosides

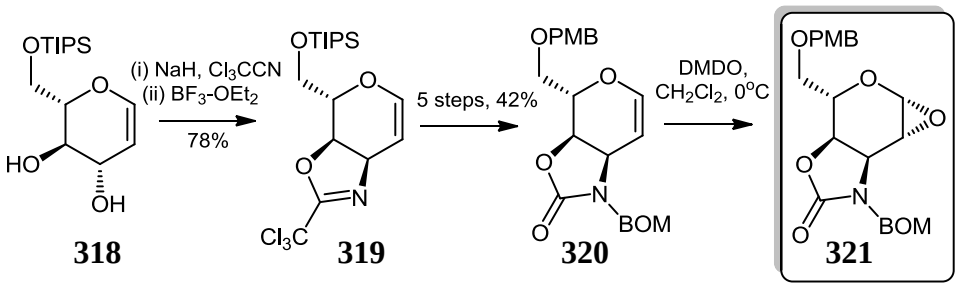
A common feature of strategies for natural product di-β-*N*-glycoside ICZ formation is the initial indole coupling of a complex electrophilic sugar derivative to a protected BIM or ICZ intermediate. These complex, multi-step routes also require activation of mono-*N*-glycosylated precursors prior to late-stage chemistry to furnish the second C-N linkage.

2.3.5.1 Total synthesis of staurosporine

Elegant contributions to steresoselctive carbohydrate synthesis in the field of ICZ research have been instrumental concerning preparation of the aminohexose ring system in **2** from simple starting blocks. Employing these carbohydrate synthons requires several steps to afford the final ICZ natural product culminating in aglycon formation, mono-*N*-glycosylation and subsequent intramolecular electrophilic cyclisation *via* attack of the unsubstituted indole nitrogen on the modified sugar moiety.

2.3.5.1.1 Staurosporine carbohydrate development

In 1993, Danishefsky reported that base-induced epoxysugar ring opening constituted an effective *N*-glycosylation methodology towards preparation of **2**.[120]



318 **319** **320** **321**

Scheme 2.54

Subsequently, in 1995, L-glucal derivative **318** was utilised as a key starting material for total synthesis of **2** based on stepwise formation of oxazoline **319** *via* Schmidt reaction,

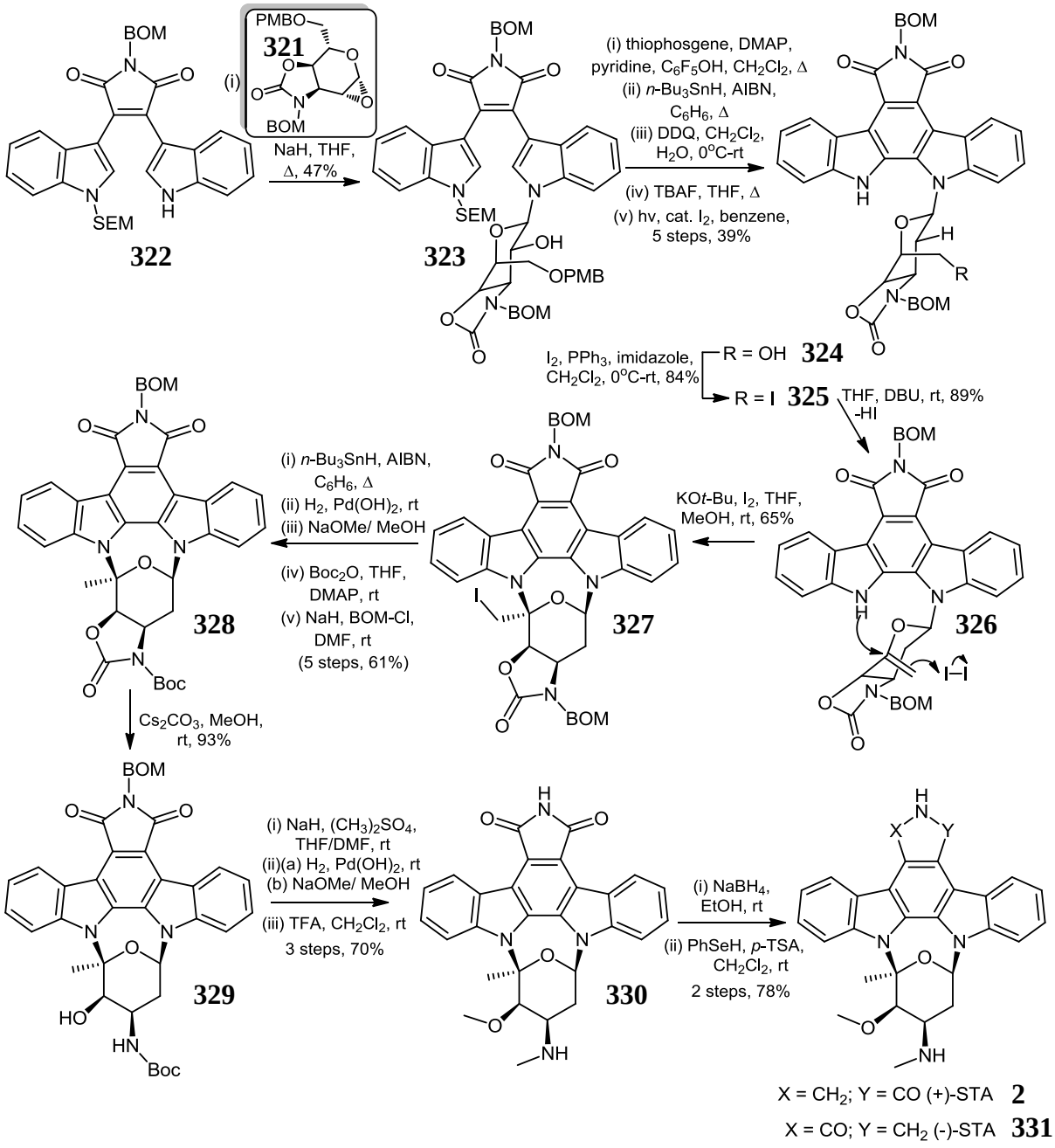
conversion to oxazolidinone **320** and treatment of this intermediate with Murry's dioxirane reagent, to yield the glycal epoxide derivative **321**. This compound **321** has subsequently gained application as an effective glycosyl donor in further elaboration of the staurosporine **2** indolocarbazole skeleton (Scheme 2.54).[120,121]

2.3.5.1.2 Sugar-aglycon coupling route for total synthesis of staurosporine

Synthesis of the selectively protected aglycon **322** was initially achieved in three steps and 57% yield.[111] Formation of the first *N*-glycosidic linkage occurred by reaction of the sodium salt of **322** with sugar precursor **321**, to afford **323**, prior to C2'-hydroxyl removal from the glycosyl moiety by Barton deoxygenation.[120-122] Two-step elimination of the PMB and SEM protecting groups was followed by photocyclisation, in order to provide *N*-protected imide congener **324** (73%).[123] Conversion of C6'-hydroxyl group to the iodo derivative **325** enabled dehydroiodination under the influence of DBU, to provide *exo*-glycal derivative **326**.

Base-induced intramolecular coupling of this activated mono-β-*N*-glycosyl derivative **326** *via* attack of indole nitrogen on C5' of the electrophilic terminal alkene in the presence of iodine afforded cyclopyranosylated indolocarbazole intermediate **327**, which was initially deiodinated under radical hydrodehalogenation conditions.[120-122] Subsequent oxazolidinone ring cleavage to form **329** necessitated a three-step protection strategy. BOM hydrogenolysis over Pearlman's catalyst, followed by regioselective oxazolidinone Boc protection and concluding imide BOM-reprotection achieved initial conversion to analogue **328**.[124] Smooth hydrolysis of the labile Boc-protected oxazolidinone ring moiety was subsequently accomplished by stirring with cesium carbonate to provide the corresponding deoxyaminosugar **329** in a yield of 93%.

A series of functional group modifications involving *N*,*O*-dimethylation with dimethylsulfate, followed by BOM-deprotection and Boc removal resulted in formation of 7-oxostaurosporine **330** in 70% yield over three steps. Transformation by $NaBH_4$ reduction to the intermediate lactol ring followed by deoxygenation with phenylselenol in the presence of a catalytic amount of *p*-TSA, resulted in non-stereospecific desymmetrisation of the 7-oxo precursor and formation of equivalent amounts of both desired (+)-STA **2** (39%) and isomeric isostaurosporine **331** (39%), in combined 78% yield from **330** (Scheme 2.55).[121,125]



Scheme 2.55

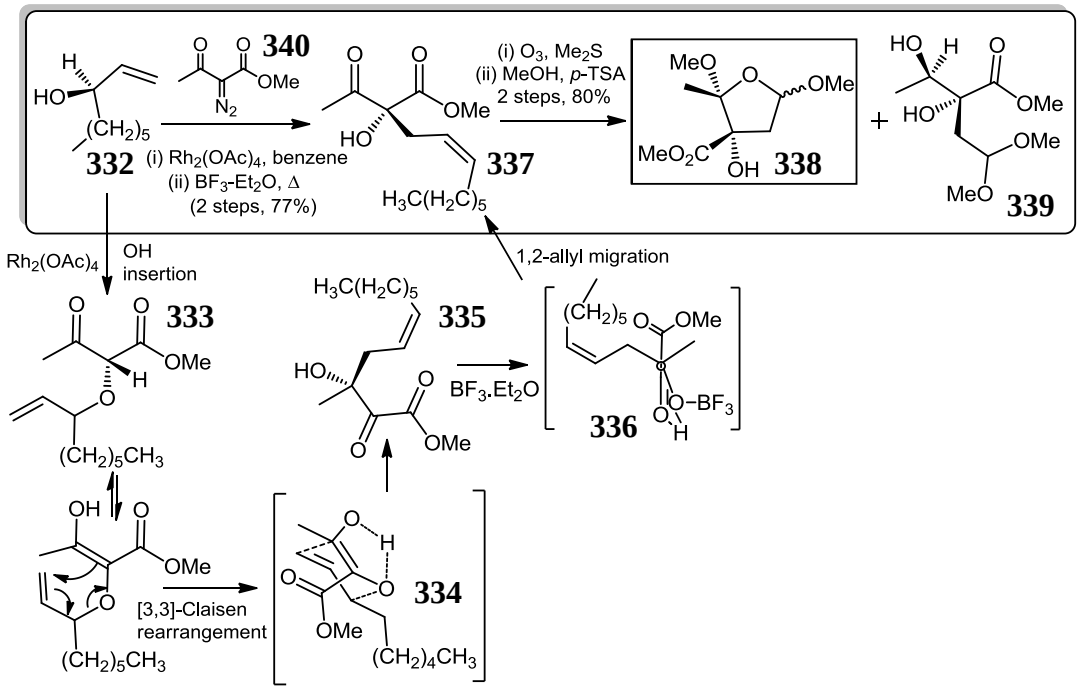
2.3.5.2 Total synthesis of K-252a

Synthetic cyclofuranosylation methodologies have also been developed to access bioactive ICZ, K-252a **13**. In this section, two alternative approaches, employing electrophilic dimethoxyfuranose coupling and modified Danishefsky cycloglycosylation will be discussed.

2.3.5.2.1 Route to electrophilic K-252a furanose precursor

An asymmetric synthesis of the (-)-diastereomer of dimethoxyfuranose **338**, starting from a transformation of (*R*)-(-)-1-nonen-3-ol **332** to intermediate acetoacetate **337**, was initially

accomplished following treatment with methyl 2-diazo-3-oxobutyrate **340**, in the presence of $Rh_2(OAc)_4$, *via* tandem [3,3]-Claisen rearrangement of initial O-H insertion product α-allyloxy ketone **333** to form the *R*-enantiomer of α-ketoester **335** (ee = 95%) and final Lewis acid-promoted α-ketol rearrangement (Scheme 2.56).[92,126]



Scheme 2.56

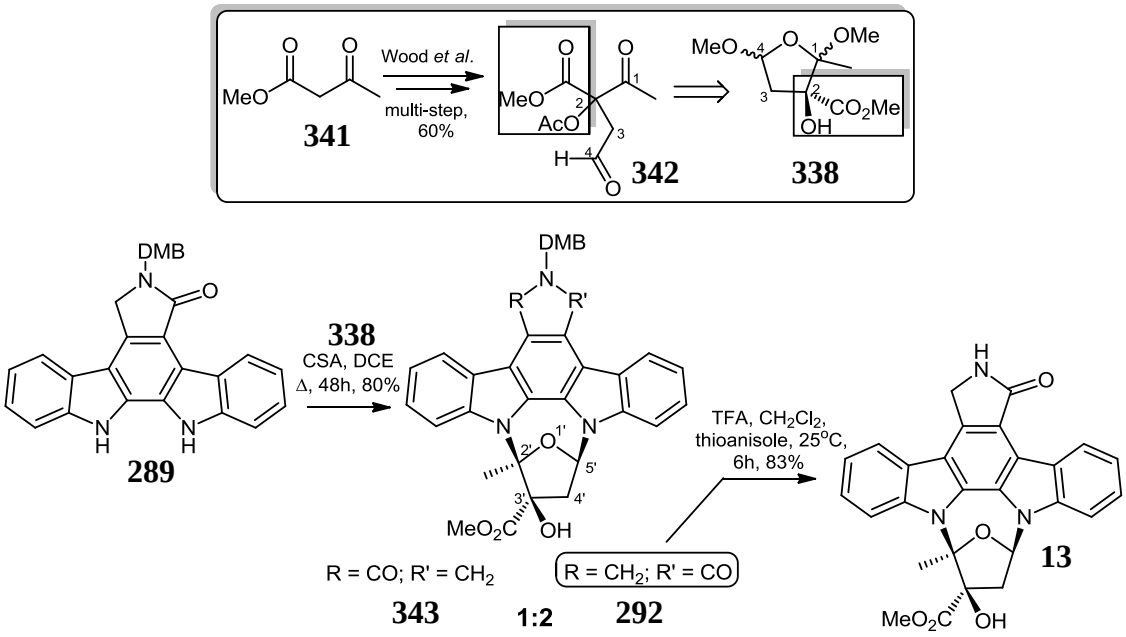
Induction of the observed stereochemical outcome is thought to be mediated by a preferred Z-enol chair conformation, avoiding unfavourable steric interactions present within the [3,3]-transition state **334**. Similarly, the necessity for a syn-periplanar relationship between the hydroxyl and α-carbonyl groups within **335** also correlates with a high degree of (*S*)-stereoselectivity within **337** (ee = 92%). Hydroxyl group activation by $BF_3.Et_2O$ complexation is thought to promote intramolecular carbonyl protonation through enhancing alcohol acidity, thus favouring the 'pseudo-chelated' transition state maintained in **336**.

One-pot synthesis of the desired K-252a sugar residue was effected by reductive ozonolysis, followed by acid-mediated cyclisation, to afford a mixture of carbohydrate synthon, (-)-**338** and side product (+)-**339** in an overall yield of 80%.[127]

2.3.5.2.2 Acid-mediated cyclofuranosylation route to K-252a

According to McCombie's original procedure, acid-catalysed cyclofuranosylation is hypothesised to proceed *via* stepwise formation of an aminoacetal intermediate, which then undergoes further nucleophilic indole nitrogen attack and acid-promoted intramolecular cyclisation.[128] Exposure of DMB-protected **289** to carbohydrate precursor **338**, generated

from methyl acetoacetate **341** *via* intermediate **342**, as per the route outlined in Scheme 2.57, in the presence of CSA, afforded a regioisomeric mixture of K-252a analogues **292** and **343**, in a ratio of 2:1, and overall yield of 80%.



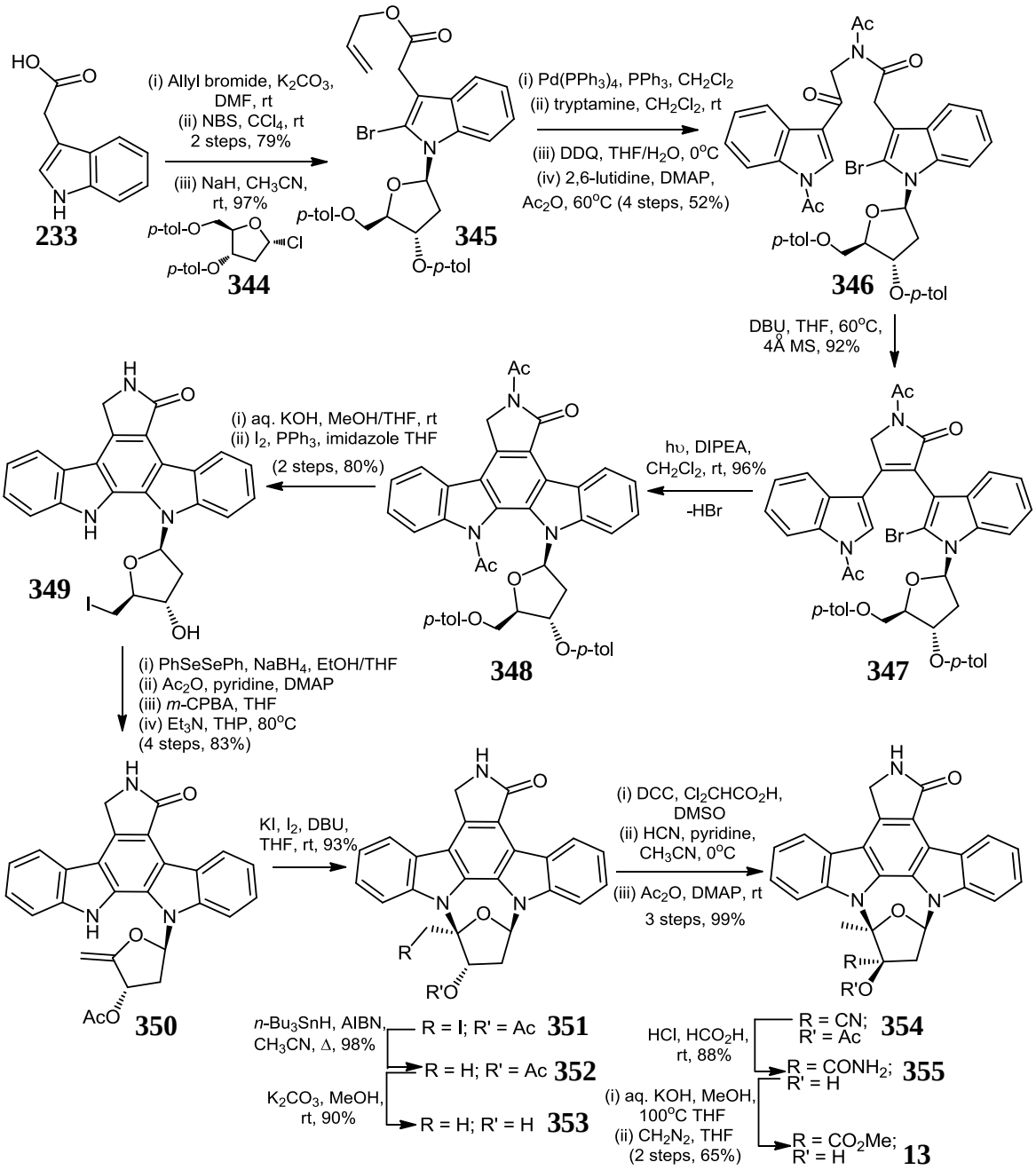
Scheme 2.57

Following chromatographic purification, final imide protecting group removal similar to the 2,4-DMB peptidic deprotection procedure initially refined by Steglich *et al.*, was carried out to afford natural product (+)-K-252a **13**, in 83% yield following treatment of major regioisomer **292** with TFA, for 6 hours (Scheme 2.57).[92,127,129]

2.3.5.2.3 Fukuyama total synthesis of K-252a employing Danishefsky glycosidation strategy

In 1999, Fukuyama and co-workers reported an elegant total synthesis of (+)-K-252a **13** starting from indole-3-acetic acid **233**.[130] Initial *O*-allylation was then followed by indole C-2 bromination at room temperature, in 79% yield over two steps. Employing an analogous approach to the NB-506 **50** methodology developed by Ohkubo *et al.*, initial deprotonation, followed by addition of *p*-toluoyl protected furanose derivative **344** then provided β-*N*-glycoside **345** as sole product in 97% yield.[131] Diacetylated compound **346** was produced in four steps and 52% yield following allyl ester hydrolysis, amide formation, regioselective benzylic oxidation to ketone and *N*-acetylation of both indole and amide nitrogens. DBU-catalysed formation of lactam **347** in the presence of 4Å molecular sieves proceeded in 92% yield, prior to annulation by irradiation in the presence of DIPEA, leading to the dehydrobrominated pyrrolo[3,4-*c*]carbazole analogue **348** in almost quantitative yield (96%). Complete masking group deprotection under alkaline conditions followed by chemoselective

iodination of the resultant primary alcohol also provided access to intermediate **349** in high yield (Scheme 2.58).[130,132]



Scheme 2.58

Four-step conversion to alkene **350** employed initial diphenylselenide treatment, followed by reacetylation, oxidation and triethylamine-induced elimination/olefination steps. Application of Danishefsky's di-*N*-glycoside cyclisation method, employing iodine, KI, and DBU as base (**351**), followed by radical deiodination afforded cyclofuranosylated congener **352**.[133] Conventional K_2CO_3-mediated deacetylation of the C3'-hydroxy group to fully deprotected **353**, prior to regioselective Moffatt-Pfitzner oxidation was then followed by addition of

HCN and acetic anhydride to afford elegant conversion to the single acetylcyanohydrin diastereoisomer **354**, under mild conditions.

Following acidic conversion to amide **355**, KOH hydrolysis elicited formation of the corresponding acid, which was finally esterified to give (+)-K-252a **13** in 23 steps and cumulative yield of 10% starting from indole-3-acetic acid **233** (Scheme 2.58).[130]

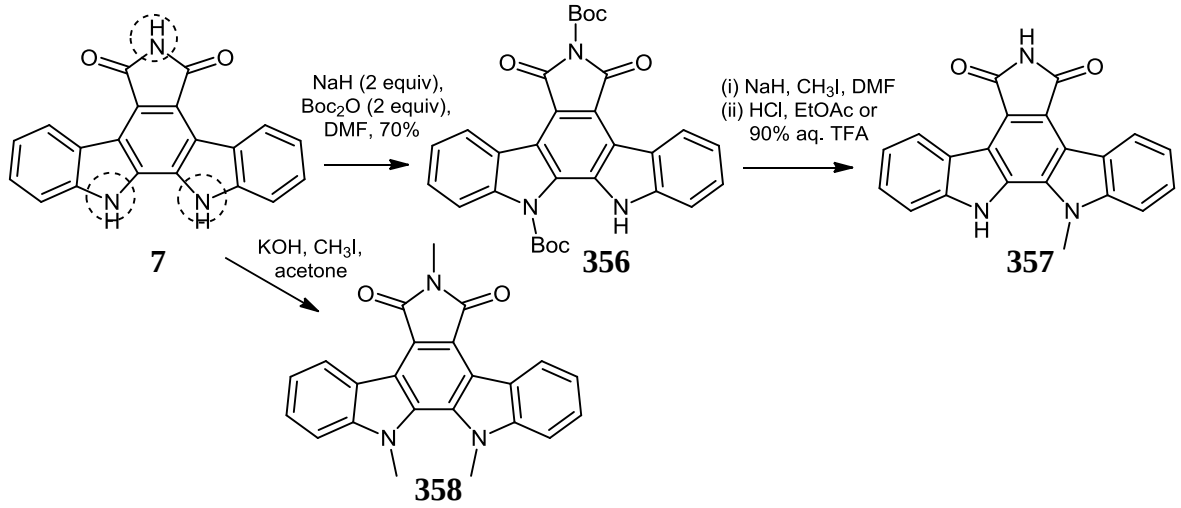
2.4 Chemical modification of the indolo[2,3-*a*]carbazole nucleus

During the course of this project, chemical studies based on ICZ heterocyclic replacement were of paramount importance. Literature results based on sugar modification, indolocarbazole A/E-ring substitution and indole B/D-ring replacement with 7-azaindole isosteres are important contributions in this area. Derivatisation routes focusing on F-ring diversity remain relatively unexplored, but will be addressed in the present work (*vide infra*).

2.4.1 Sugar substitution: synthesis of ICZ-bridged cyclopentanes

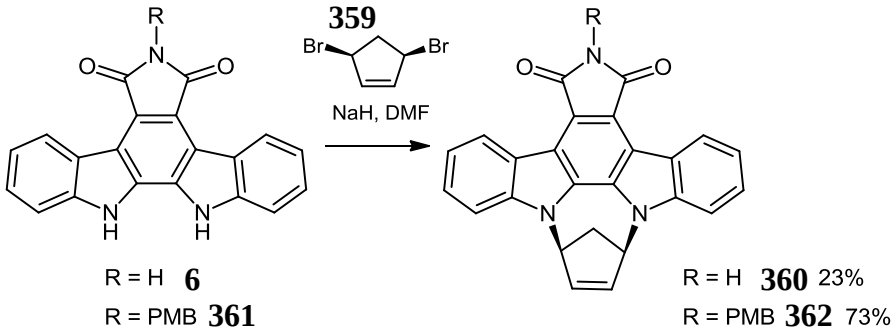
In order to investigate the effects of regioselective non-glycosidic alkylations on specific kinase activity, much synthetic effort has also been concerned with structural modifications of the indolocarbazole glycosyl moiety, leading to clinical development of functionalised macrocyclic analogues possessing attractive PKC activity.[42,134-136]

Alkylation of indolo[2,3-*a*]pyrrolo[3,4-*c*]carbazoles, comprising all three unprotected nitrogens constitutes a formidable challenge, with respect to regioselective mono-*N*-alkylation. In the course of accessing *N*-alkylated indolocarbazoles as effective inhibitors of human cytomegalovirus replication, it was reported that treatment of arcyriaflavin A **7** with Boc anhydride in the presence of NaH, afforded the regioselectively diprotected compound **356** in 70% yield.[137] Subsequent indolic nitrogen alkylation and full deprotection, forming 12-methyl analogue **357** thus represented a privileged route to a panel of monoalkylated derivatives.[137] Interestingly, application of less electrophilic alkylating agents gave more complex mixtures, postulated to be due to protecting group instability under harsher conditions.[138] Application of **7** along with KOH/iodomethane in acetone also afforded the corresponding tri-alkylated congener **358** (Scheme 2.59).[139]



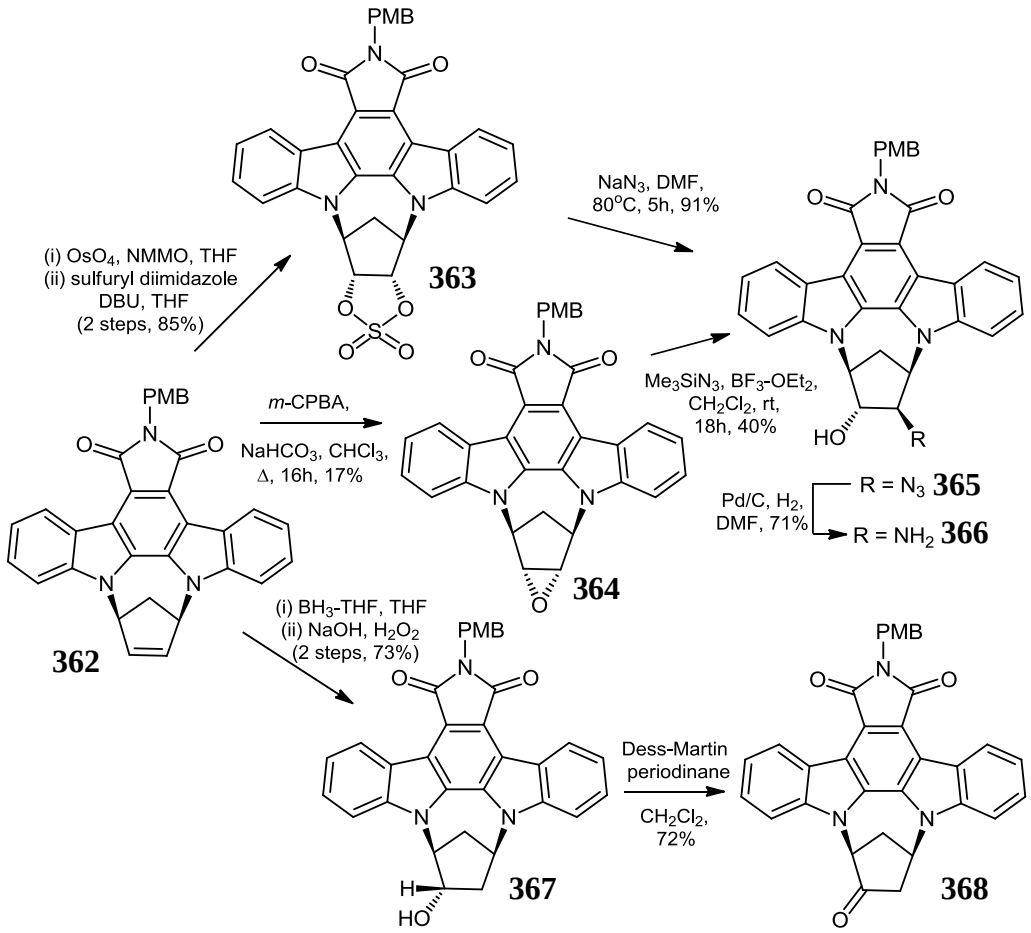
Scheme 2.59

In addition, reaction of arcyriaflavin A **7** with *cis*-dibromocyclopentene **359** only afforded a modest amount of the anticipated cyclic derivative **360**, whereas following attachment of a 6-PMB group, the analogous reaction of **361** proceeded to give cyclopentene-bridged **362** in a yield of 73% (Scheme 2.60). Masking of the reactive imide group is an important feature of indolocarbazole chemistry, due to the reagent incompatibility and poor solubility of the corresponding N-H analogues under a wide range of synthetic conditions.[140] Introduction of the readily cleavable, modified PMB group has also been described by many groups, including Wood and Moffat, to be beneficial due to its stability and increased solubility, as well avoiding the exigencies associated with removal of the *N*-Bn group.



Scheme 2.60

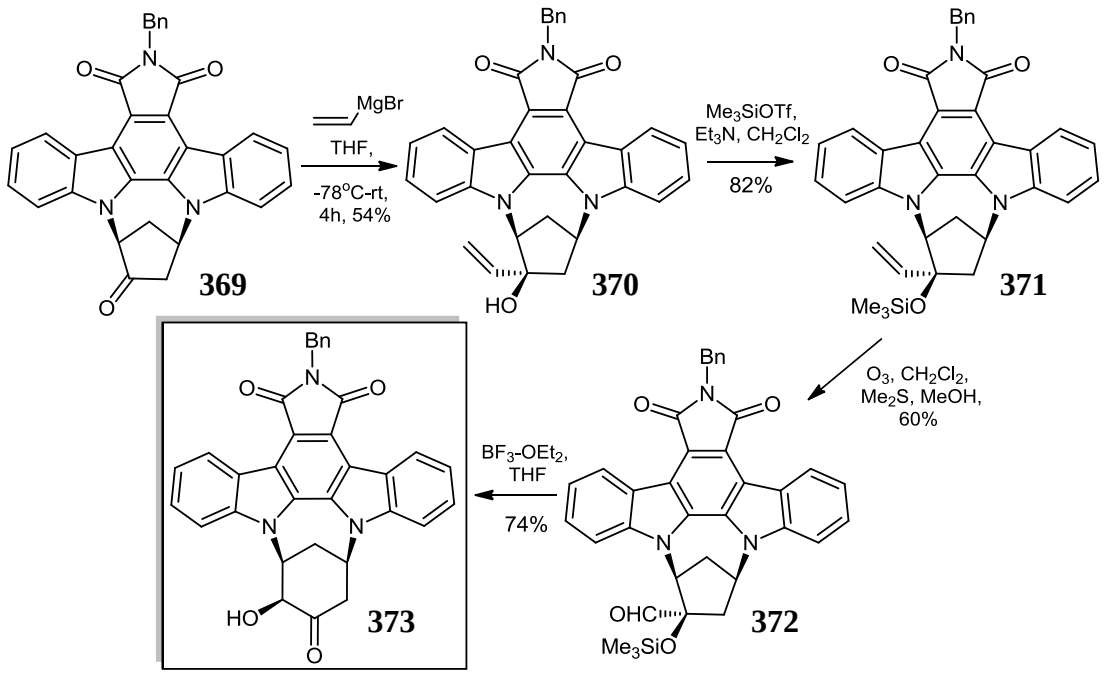
In 2005, Moffat and co-workers reported transformations based on alkene **362** leading to construction of a range of ICZ-bridged cyclopentane congeners (Scheme 2.61).[140]



Scheme 2.61

Azidoalcohol **365** formation could be realised by either *m*-CPBA epoxidation of starting **362**, to yield epoxide **364** followed by addition of TMS-azide and $BF_3.Et_2O$, in overall 40% yield, or alternatively, dihydroxylation of **362** with OsO_4, followed by treatment of the resulting diol with sulfuryl diimidazole, gave the cyclic sulfate derivative **363**, which could be further converted to the desired azidoalcohol **365**. This intermediate **365** was readily convertible to the corresponding amino derivative **366** following hydrogenation. Diastereoselective hydroboration to form precursor alcohol **367**, prior to Dess-Martin periodinane-mediated oxidation also afforded cyclopentanone intermediate **368** (Scheme 2.61).[140]

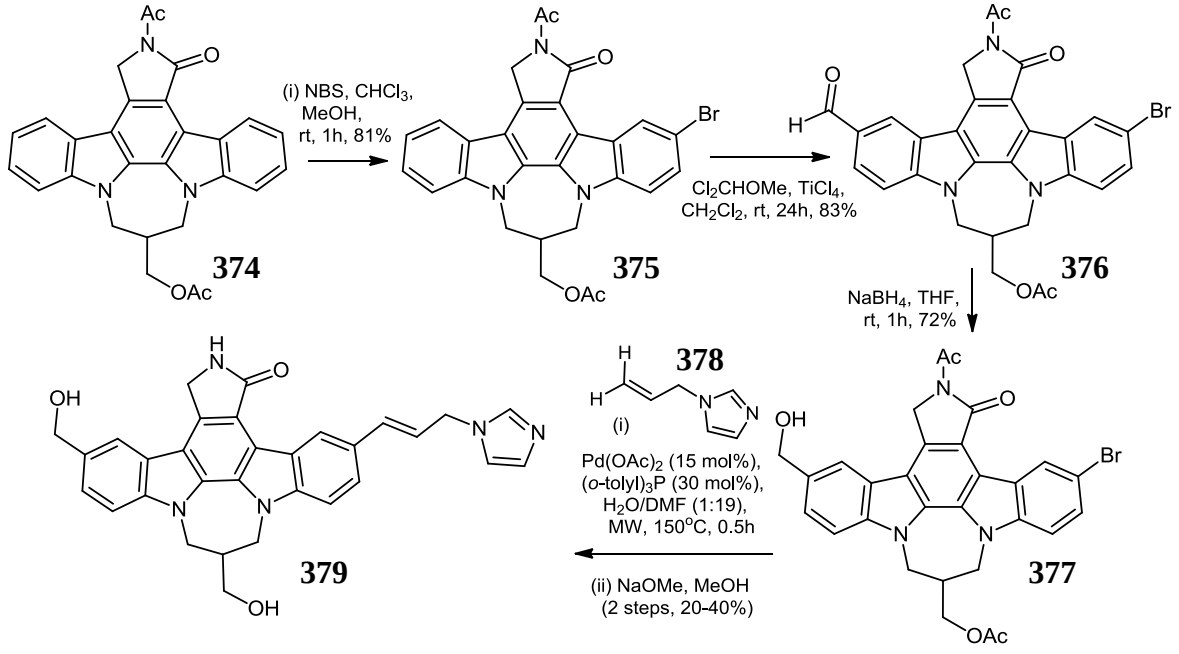
An innovative route to novel *N*,*N*-cyclohexyl analogues of staurosporine **2**, was also elucidated by cyclopentanone ring-expansion to form a key α-hydroxyketone product **373** derived from vinylmagnesium bromide addition to ketone **369**, subsequent TMS protection of alcohol **370**, ozonolysis of alkene **371** and Lewis acid-mediated α-ketol rearrangement of aldehyde **372** (Scheme 2.62; c.f. Section 2.10.5.2.1).[106,110,140]



Scheme 2.62

2.4.2 Indolocarbazole A/E ring substitution

A convenient means to directly functionalise ICZs usually involves incorporation of appropriately substituted indole units in conventional Fischer indolisation routes, incorporation of substituted indoles in dibromomaleimide coupling or Diels-Alder cycloaddition/tandem electrocyclisation of substituted 2,2-biindolyl analogues[46,112,118] However, an important transformation concerns electrophilic indole substitution and subsequent modifications investigated to refine bioactivity and improve solubility.[4,141-143]

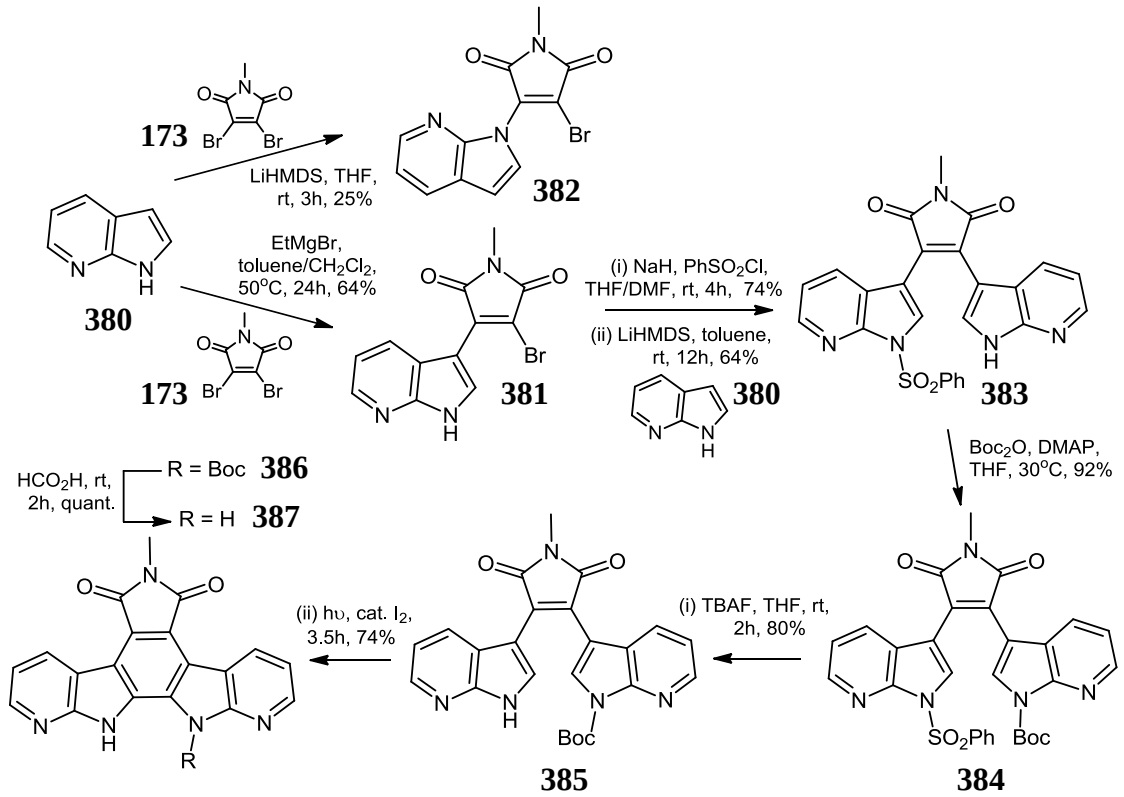


Scheme 2.63

In 2007, development of elegant synthetic methodology for targeted modification of critical C-3 and C-9 indole positions within JAK3 inhibitors structurally related to phase II/III VEGFR-active analogues, was reported by Yang *et al*.[4,62] Regioselective NBS bromination of ICZ pyrrol-2-one **374** occurs preferentially at C-3, followed by Lewis acid-mediated formylation of **375** employing dichloromethyl methyl ether proceeds at C-9 to afford intermediate **376** (83%). Hydride reduction of unsymmetrical aldehyde **376** then afforded C-9 hydroxymethyl bromo-derivative **377** (72%), which was converted, on reaction with **378**, to the corresponding C-3 allyl imidazole-substituted compound **379** (JAK3; IC_{50} = 3 nM) in moderate yield under Heck microwave conditions (Scheme 2.63).[62,80]

2.4.3 1-Azaindolocarbazoles

Synthetic efforts in the field of indole ring isosteric replacement have also recently described desirably selective cytotoxicity profiles associated with a panel of 1-azarebeccamycin analogues.[144-146]

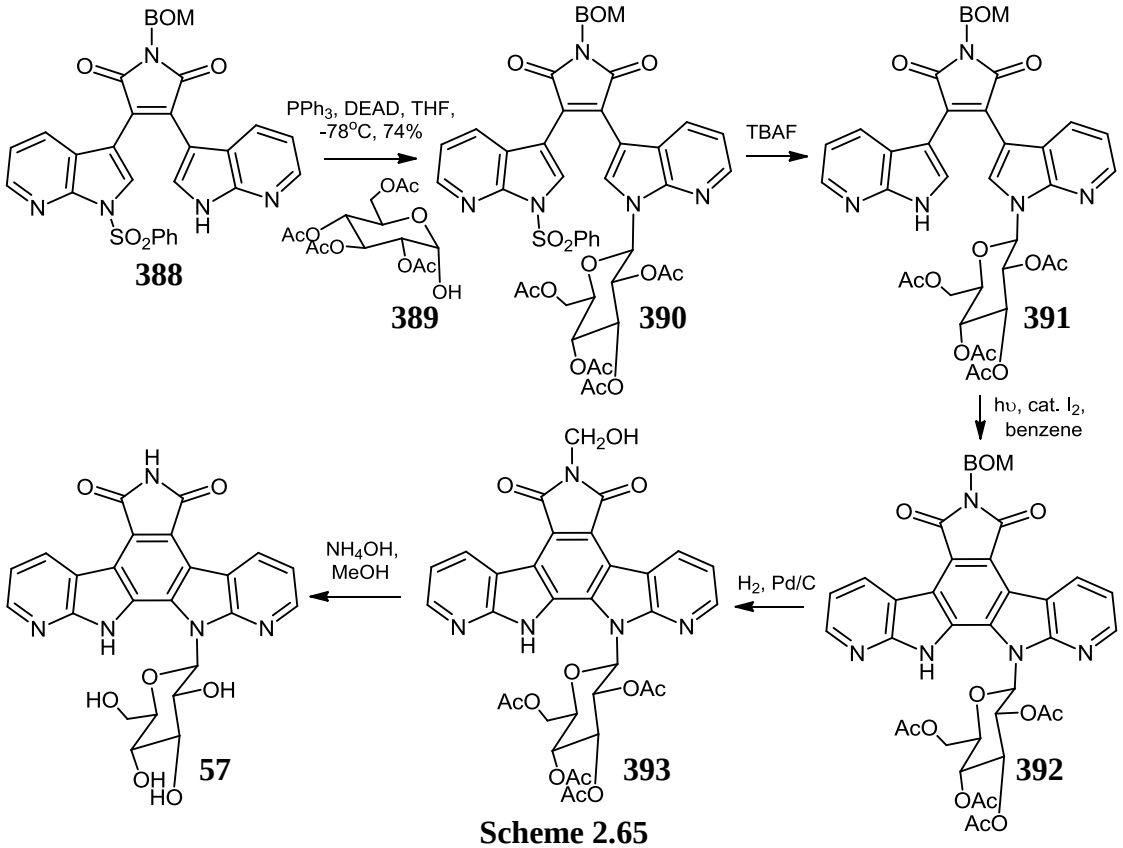


Scheme 2.64

Replacement of an indole unit with an azaindole moiety introduces novel basic character capable of modifying inherent pharmacological properties of ICZs, while also enhancing drug-complex affinity by formation of hydrogen bonds orientated within the active site of target enzymes and/or DNA.[147,148] Symmetrical 1,11-azaindolocarbazole synthesis was reported by Routier *et al.* under Grignard conditions, starting from 7-azaindole **380** reaction

with 3,4-dibromo-*N*-methylmaleimide **173** at 50°C for 24 hours, to afford **381** in 64% yield. Interestingly, this transformation was strongly base-dependent and the regioisomeric *N*-substituted analogue **382** was formed in 25% yield, following stirring of **380** along with **173** in LiHMDS, for 3 hours. However, following *N*-phenylsulfonyl protection, sterically favoured C-3 substitution of the 7-azaindole lithium salt rapidly provided bis(7-azaindolyl)maleimide **383**, then transformed to protected **384**, prior to selective deprotection to the mono-Boc derivative **385**. Following subsequent U.V. ring-closure, **386** was treated with formic acid to afford indolocarbazole **387** in 74% yield, over two steps (Scheme 2.64).[145,146]

In 2003, Marminon and co-workers introduced a carbohydrate moiety within BOM-protected 1,11-azarebeccamycin **392** following reaction of BOM-protected bisazaindolylmaleimide **388** with 2,3,4,6-penta-*O*-acetyl-α-D-glucopyranose **389** under standard Mitsunobu coupling conditions to give **390**, and overall accessed β-*N*-glycosidic ICZ **57** following initial $PhSO_2$ group removal (**391**), cyclisation (**392**), BOM hydrogenation to yield compound **393** and ammonolysis to provide the potent anti-proliferative compound **57** (Scheme 2.65).[147]



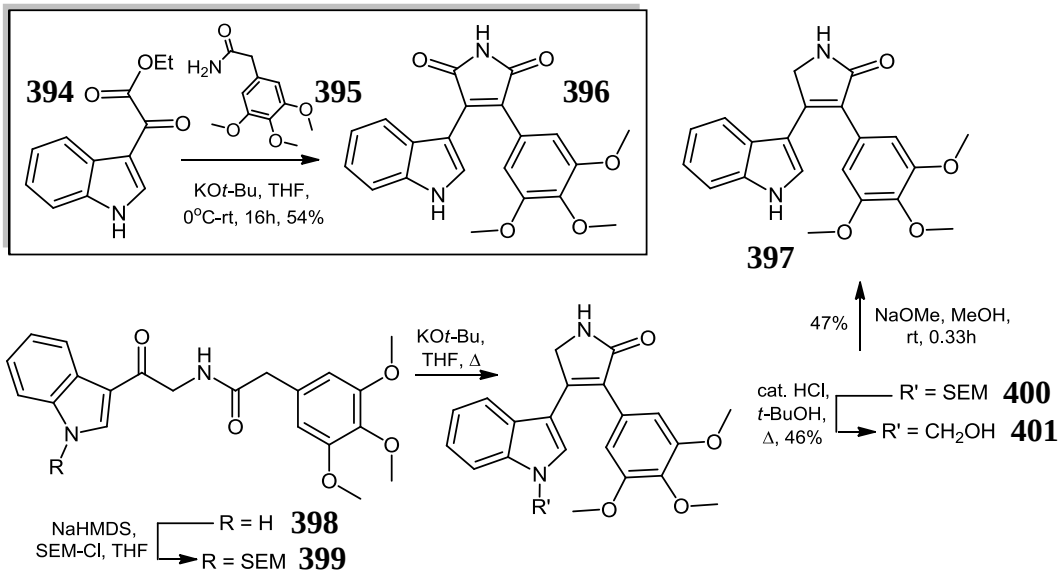
Scheme 2.65

2.5 Synthesis of arylindolyl derivatives related to indolocarbazoles

Due to vast interest in development of novel bioactive compounds structurally related to staurosporine **2**, incorporation of diverse arylindolylmaleimide heterocyclic functionality has become an essential target for current research related to the ability of modified indolocarbazole chromophores to exhibit potent kinase inhibition.[16,149-154]

2.5.1 Synthesis of 3,4-bisarylmaleimides *via* Perkin condensation

In 1998, a new and robust preparation of arcyriarubin A **79** was revealed, utilising base-induced Perkin-type condensation; this versatile methodology has also been successfully applied to synthesis of unsymmetrical bisindolyl analogues, as well as diverse arylindolylmaleimides (Section 2.2.4.1).[61,62,155] In 2006, Peifer and co-workers efficiently employed this approach in order to synthesise a panel of asymmetrically substituted 3,4-bisarylmaleimides, as potent VEGFR2 inhibitors.[156,157] In each case, one-pot condensation of acetamide and an excess of an indole glyoxylate ester, prepared *via* Friedel-Crafts acylation or treatment of indolylmagnesium bromide **154** with diethyl oxalate at low temperature, occurred following reaction in the presence of potassium *tert*-butoxide in THF. Application of this method involving ethyl indole-3-glyoxylate **394** and 3,4,5-trimethoxyphenylacetamide **395** afforded 3-(indol-3-yl)-4-(3,4,5-trimethoxyphenyl)-1*H*-pyrrole-2,5-dione **396**, subsequently determined to inhibit VEGFR2 (IC_{50} of 2.5 nM), in 54% yield (Scheme 2.66).[157] Based on molecular modelling rationale, this group subsequently published the synthesis of lactam **397**, conserving a critical pyrrole-2-one H-bonding motif.[158]

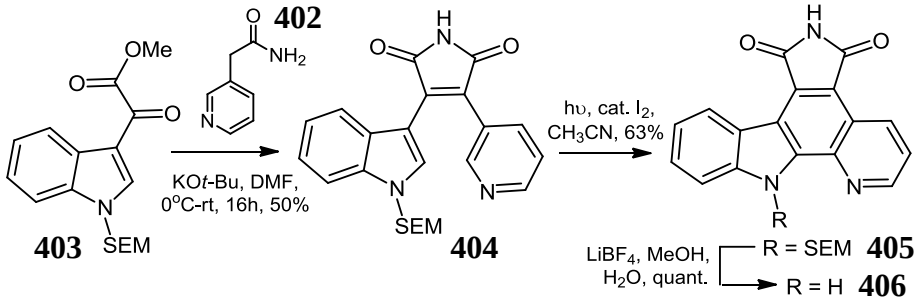


Scheme 2.66

Due to the reported difficulty associated with regiospecific maleimide carbonyl reduction of compound **396** to derivative **397**, a modified Knoevenagel condensation of precursor **399,** isolated following SEM-protection of **398**, afforded the aldol precursor, which was self-condensed, to yield the corresponding pyrrole-2-one **400**. Heating of **400** along with a catalytic amount of HCl, resulted in isolation of hemiaminal **401** (46%). The desired analogue **397**, was then synthesised following elimination of formaldehyde, in 47% yield. Interestingly, while reaction of **400** under acidic catalysis afforded predominantly **401**, 10% of the target pyrrole-2-one **397** was also detected as the minor component of the final product mixture (Scheme 2.66).[158]

2.5.2 Planar ring modification: formation of heteroarylcarbazole derivatives

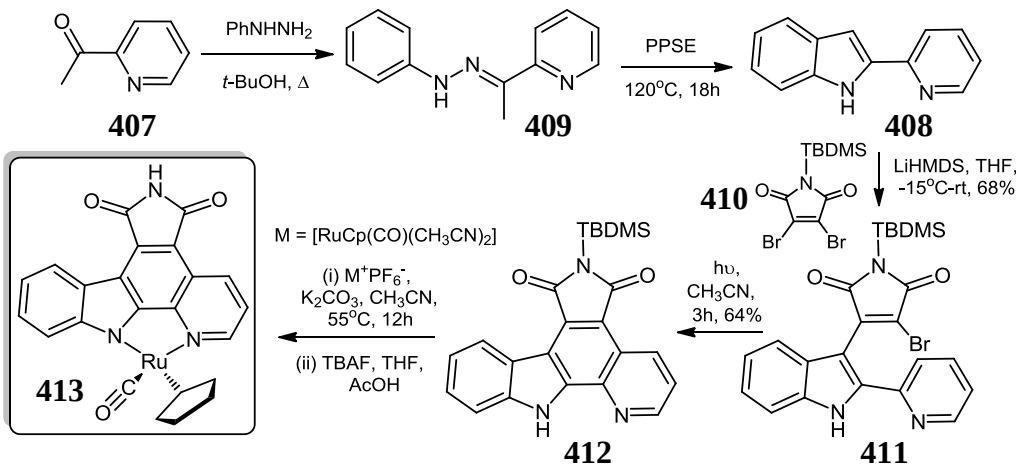
In 2005, Meggers and co-workers suggested that application of pentacyclic pyrido[2,3-*a*]pyrrolo[3,4-*c*]carbazoles constituted an interesting bioisostere of active classical indolo[2,3-*a*]carbazole analogues.[155]



Scheme 2.67

The initial route selected for synthesis of compound **406**, involved Faul-type condensation to yield **404**, utilising pyridine-3-acetamide **402** and SEM-protected methyl indole-3-glyoxylate **403**, followed by photoinduced annulation to finally give **406** after ultimate deprotection (Scheme 2.67).[155]

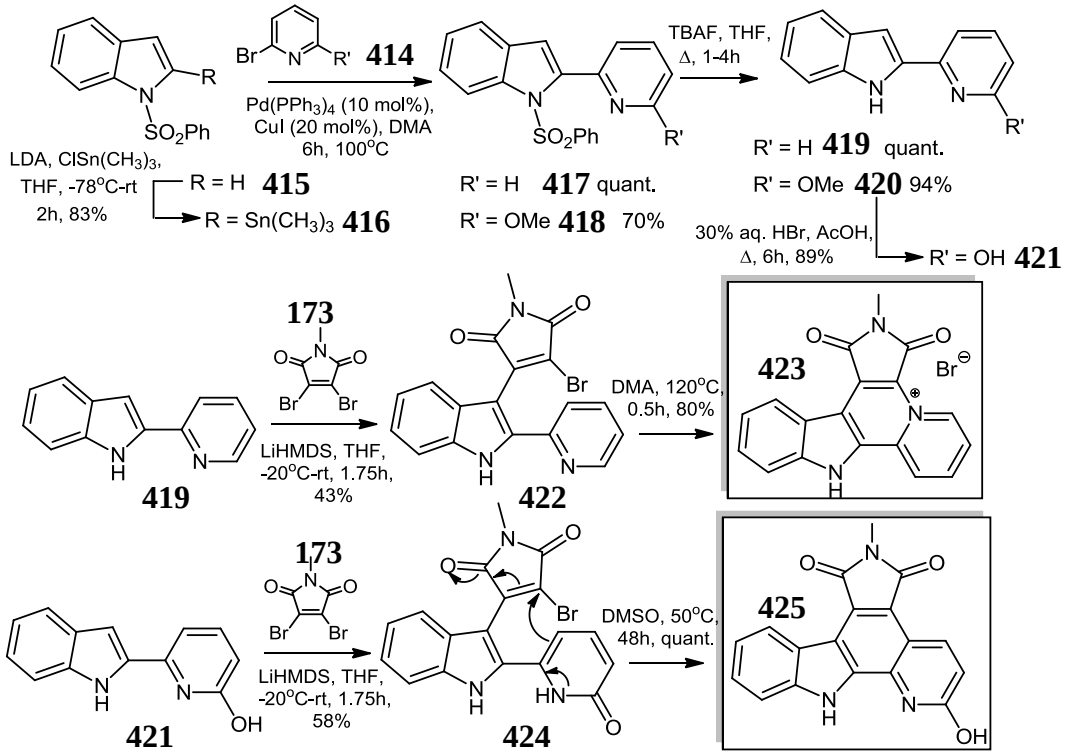
However, due to the insolubility of **406** in most organic solvents, an alternative strategy was developed, which avoided the necessity for indole nitrogen protection, and was analogous to the 2,2'-biindolyl **118** cycloaddition approach. This method encompassed initial hydrazone formation between 2-acetylpyridine **407** and phenylhydrazine **106**, resulting in formation of 2,2'-pyridoindole **408**, following exposure of intermediate **409** to PPSE at reflux (Scheme 2.68).[155] However, addition of TBDMS-protected dibromomaleimide **410** does not proceed *via* the thermal one-pot cyclisation mechanism proposed by Bergman *et al.* similar to the bisindolyl series; in this case, LiHMDS-mediated indole-maleimide C-C bond formation (**411**) is followed by U.V.-induced oxidative dehydrobromination, to form **412**.[5,155]



Scheme 2.68

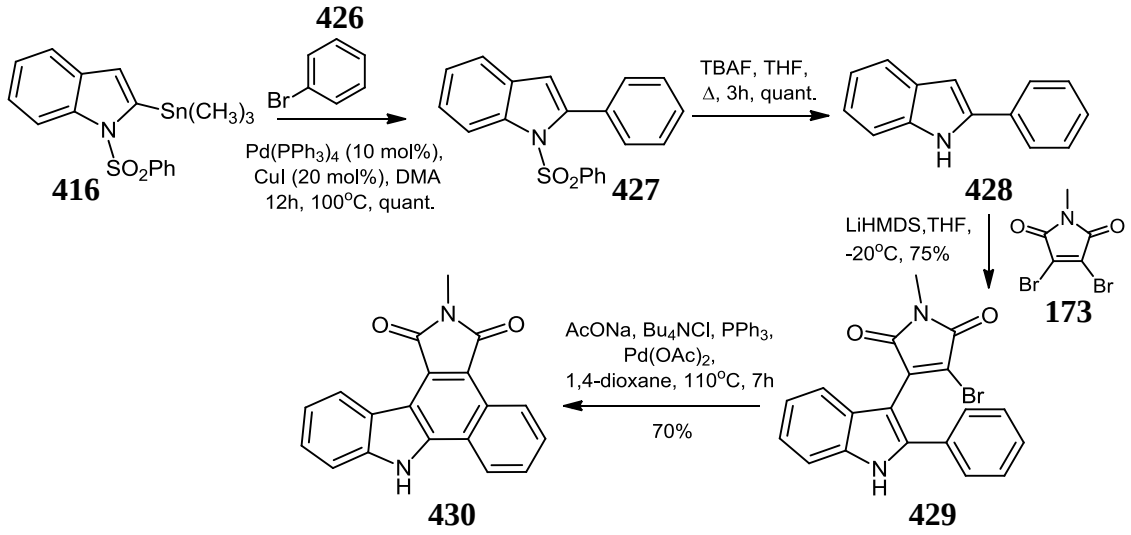
These workers also designed an elaborate cyclometalation strategy, permitting formation of a unique ligand sphere within a water and air-stable metal complex capable of potent interactions with specific ATP-binding site residues.[159] Heating of TBDMS-protected intermediate **412** with $[RuCp(CO)(CH_3CN)_2]^+PF_6^-$ complex, along with K_2CO_3, formed a ruthenium complex **413**, which, following TBS deprotection, possessed prodigious IC_{50} activity against GSK-3α (0.3 nM); formation of **413** proceeded *via* co-ordination of the pyridyl nitrogen, followed by indole attack and subsequent deprotonation.[155]

In 2008, Bourderioux *et al.* developed an alternative and versatile palladium-mediated route to pyrido- and other heteroarylcarbazoles, beginning from trimethylstannylation of 1-phenylsulfonylindole **415** to form precursor **416** in 83% yield, prior to Stille coupling with a 2-bromopyridine derivative **414** (R'=H, OMe) in the presence of 10 mol% of $Pd(PPh_3)_4$, and CuI, in DMA at high temperature, to afford unsubstituted **417** and methoxy analogue **418**, respectively.[154] The corresponding intermediate 2,2-pyridoindoles **419** and **420**, were then isolated in >90% yields following TBAF deprotection. Following formation of the maleimide-fused intermediate **422** *via* reaction of **419** and **173** under basic conditions, nucleophilic formation of a ring-constrained pyridinium salt **423**, was also reported by these workers. In addition, 2-hydroxypyridine derivative **421**, initially formed by HBr-acetic acid demethylation of 2-methoxypyridine derivative **420** (89%) could be thermally cyclised to pyrido[2,3-*a*]carbazole congener **425** by a facile addition-elimination mechanism *via* its pyridone tautomer **424** (Scheme 2.69).[154]



Scheme 2.69

Reaction of bromobenzene **426** with 2-trimethylstannylindole **416** resulted in formation of 2-phenylated analogue **427**, which was desulfonylated in quantitative yield (**428**), prior to LiHMDS-mediated 1,4-conjugate addition with *N*-methyl-3,4-dibromomaleimide **173** to produce 2,3-disubstituted indole derivative **429**.[74] Heck arylation of bromoalkene **429** was successfully achieved, in the presence of stoichiometric $Pd(OAc)_2$, to afford annulated benzo[*a*]carbazole **430** in a yield of 70% after 7 hours (Scheme 2.70).

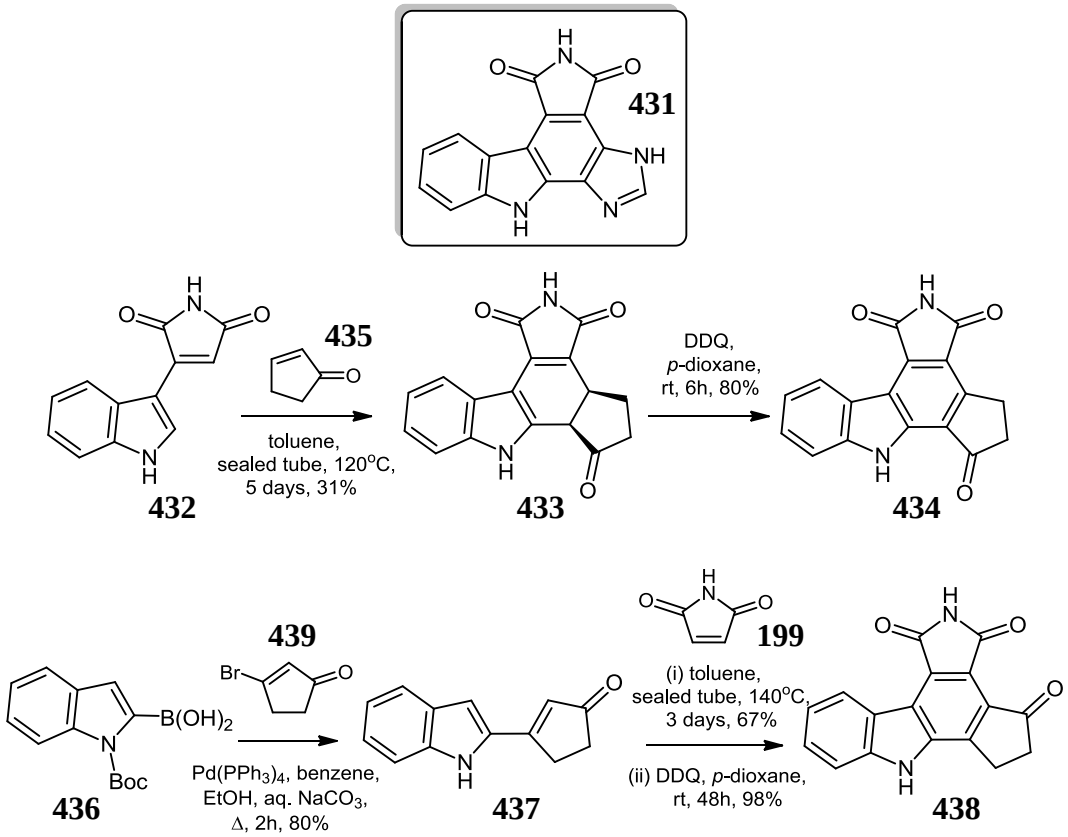


Scheme 2.70

These workers also reported that strongly electron-withdrawing phenyl substituents retarded the progress of this reaction; presumably, the nature of this phenomenon is due to the deactivating influence of these groups on the critical C-Pd bond insertion step within the Pd-induced intramolecular Heck reaction.[80,154]

2.5.3 Granulatimide cycloaddition

In 2007, Prudhomme demonstrated novel applications involving Diels-Alder cycloaddition of 3-indolylmaleimide **432** and cyclopent-2-enone **435** to form cyclised non-carbazole precursor **433**, which was subsequently dehydrogenated to the carbocyclic pyrrolo[3,4-*c*]carbazole **434** (25%), based on the structure of the ChK1 inhibitor granulatimide **431** (Scheme 2.71).[160,161]



Scheme 2.71

In addition, palladium-mediated Suzuki coupling of Boc-protected 2-indoleboronic acid **436** with 3-bromocyclopent-2-enone **439** afforded 2-substituted indole **437**. Condensation with maleimide **199** as Diels-Alder dienophile, at 140°C for 3 days provided cycloadduct **438**, following DDQ-induced aromatisation in a two-step yield of 66%, and thus providing the regioisomeric carbonyl group orientation to **434** (Scheme 2.71).[161]

2.6 Conclusion

The observed structural complexity present in the indolopyrrolocarbazole chemical class has given rise to diverse strategies for versatile construction of a wide range of structural congeners.[2,5,6] However, a number of critical carbon-carbon bond forming events such as tandem conjugate cycloaddition, base-mediated indole coupling and palladium-catalysed diyne cyclisation have been described as attractive routes to indolo[2,3-*a*]pyrrolo[3,4-*c*]carbazole analogues.[65,74,78,138] Fischer indolisation methodologies suffer from a regiochemical limitation of employing only 2 or 4-substituted phenylhydrazine substrates as indolocarbazole precursors, while in many routes, poor organic solubility of unmasked polar heterocyclic functionality, as well as non-facile central benzene ring closure issues have also been recognised as significant challenges towards formation of this heterocyclic scaffold.[38,54,155,162]

Other recent routes to indolocarbazole aglycon precursors also include base-mediated Perkin condensation to afford an attractive one-pot route to unsymmetrical bisindolylmaleimides.[61] Biomimetic approaches have also been reported based on complex enzymatic pathways to indolocarbazole alkaloids, illustrated by iodine-mediated oxidative coupling of indole-3-acetic acid trianion **234**, as well as diverse semi-synthetic routes from versatile common intermediates such as ketone derivatives **293** and **373**, analogous to compounds isolated from biosynthetic pathways.[63,107,110,140]

In addition, application of disparate glycosidation strategies exploit the nucleophilic reactivity of indole moieties in order to couple electrophilic sugar units capable of subsequent transformation to a range of mono and di-*N*-glycosidic derivatives. Danishefsky and co-workers utilised a glycal intermediate **321** as a key staurosporine **2** aminohexose synthon, which could then be converted to a doubly linked carbohydrate unit, following base-mediated electrophilic cyclisation of an alkene intermediate **326**.[120,121] This group also employed similar 1,2-anhydrosugar methodology to synthesise the β-*N*-glycosidic mono-linkage within an anti-topo I lead natural product, rebeccamycin **38**.[111] In these cases, the conventional base-induced 3,4-dibromomaleimide substitution initially developed by Steglich and Weinreb was demonstrated to efficiently furnish the bisindolylmaleimide precursor prior to regioselective sugar coupling.[33,34] An important feature of these routes also concerned the enhanced reactivity of bisindole intermediates compared with the corresponding indolocarbazoles, as initial glycosyl acceptors, prior to aromatisation.

Synthetic challenges were also overcome in the synthesis of cyclofuranosylated K-252a **13**; Fukuyama's elegant stereoselective route employed halosugar substitution, DBU-mediated

lactam ring formation and oxidative dehydrobromination steps, as well as displaying Danishefsky's di-*N*-glycosylation protocol.[130] Wood and co-workers also demonstrated synthesis of **13** by means of a multi-step route to a dimethoxyfuranose derivative **338** that was subsequently coupled to an N6-protected K-252c derivative **289** *via* CSA-promoted cyclofuranosylation.[127,163] Utilisation of stereoselectively β-*N*-glycosylated indoline precursors subsequently oxidised to the corresponding indole analogues within routes to novel sugar-linked indolo[2,3-*a*]carbazole compounds have also been recently reported by Garaeva *et al*., but this approach is hindered by the lack of functionalised starting materials, as well as having an extra oxidation step.[60]

Based on the wide spectrum of biological profiles of natural indolocarbazole alkaloids, as described in Section 1, recent synthetic focus has also shifted to altered heteroarylcarbazole derivatives maintaining a central polyheteroaromatic system, fused to a hydrogen-bonding pyrrole head group.[145,154] Synthetic strategies employed to investigate these peripheral molecular characteristics include incorporation of 7-azaindole **380** moieties within unique topo I inhibitors and application of Meggers' elegant organometallic ruthenium-complexed pyridocarbazole nucleus **413** with attractive GSK-3α kinase inhibition.[147,148,155] However, it can be noted that few workers in this area have attempted to derivatise the constituent pyrrole-2,5-dione F-ring, to explore its potential effects on kinase inhibition or conferring novel modes of biological activity based on enhanced solubility or new hydrogen bonding profiles.[145]

In order to fully contextualise these major pharmaceutical advances with respect to innovation of unique biological profiles within this chemical family, it is also necessary to identify new opportunities for synthetic exploitation which may not be sufficiently addressed by workers in this field, to date. Thus, a beneficial requirement for extensive derivatisation work, designed to evoke new structural insights into the bioactive indolocarbazole aglycon still behoves continuing development of a wide array of innovative strategies supporting their total synthesis, especially for novel F-ring analogues, currently unexplored in pre-clinical cancer chemotherapy.

2.7 References

1. Steglich, W. *Pure Appl.Chem.* **1989**, *61*, 281-288.
2. Prudhomme, M. *Curr.Pharm.Des.* **1997**, *3*, 265-290.
3. Pindur, U.; Kim, Y. S.; Mehrabani, F. *Curr.Med.Chem.* **1999**, *6*, 29-69.
4. Sanchez, C.; Mendez, C.; Salas, J. A. *Nat.Prod.Rep.* **2006**, *23*, 1007-1045.
5. Bergman, J.; Janosik, T.; Wahlstrom, N. *Adv.Heterocycl.Chem.* **2001**, *80*, 1-71.
6. Knolker, H. J.; Reddy, K. R. *Chem.Rev.* **2002**, *102*, 4303-4427.
7. Prudhomme, M. *Eur.J.Med.Chem.* **2003**, *38*, 123-140.
8. Akinaga, S.; Sugiyama, K.; Akiyama, T. *Anticancer.Drug Des.* **2000**, *15*, 43-52.
9. Kodach, L. L.; Bos, C. L.; Duran, N.; Peppelenbosch, M. P.; Ferreira, C. V.; Hardwick, J. C. H. *Carcinogenesis* **2006**, *27*, 508-516.
10. Brunton, R. J.; Drayson, F. K.; Plant, S. G. P.; Tomlinson, M. L. *J.Chem.Soc.* **1956**, 4783-4785.
11. Mann, F. G.; Willcox, T. J. *J.Chem.Soc.* **1958**, 1525-1529.
12. Bruning, J.; Hache, T.; Winterfeldt, E. *Synthesis* **1994**, 25-27.
13. Sarstedt, B.; Winterfeldt, E. *Heterocycles* **1983**, *20*, 469-476.
14. Cai, X. W.; Snieckus, V. *Org.Lett.* **2004**, *6*, 2293-2295.
15. Knubel, G.; Larsen, L. K.; Moore, R. E.; Levine, I. A.; Patterson, G. M. L. *J.Antibiot.* **1990**, *43*, 1236-1239.
16. Pelly, S. C.; Parkinson, C. J.; van Otterlo, W. A. L.; de Koning, C. B. *J.Org.Chem.* **2005**, *70*, 10474-10481.
17. Lin, S. C.; Yang, F. D.; Shiue, J. S.; Yang, S. M.; Fang, J. M. *J.Org.Chem.* **1998**, *63*, 2909-2917.
18. Banerji, A.; Bandyopadhyay, D.; Basak, B.; Biswas, P. K.; Banerji, J.; Chatterjee, A. *Chem.Lett.* **2005**, *34*, 1500-1501.
19. Hayashi, H.; Suzuki, Y.; Somei, M. *Heterocycles* **1999**, *51*, 1233-1235.
20. Somei, M.; Hayashi, H.; Ohmoto, S. *Heterocycles* **1997**, *44*, 169-176.
21. McErlean, C. S. P.; Sperry, J.; Blake, A. J.; Moody, C. J. *Tetrahedron* **2007**, *63*, 10963-10970.
22. Sperry, J.; McErlean, C. S. P.; Slawin, A. M. Z.; Moody, C. J. *Tetrahedron Lett.* **2007**, *48*, 231-234.
23. Wada, Y.; Nagasaki, H.; Tokuda, M.; Orito, K. *J.Org.Chem.* **2007**, *72*, 2008-2014.
24. Magnus, P. D.; Exon, C.; Sear, N. L. *Tetrahedron* **1983**, *39*, 3725-3729.
25. Gilbert, E. J.; Van Vranken, D. L. *J.Am.Chem.Soc.* **1996**, *118*, 5500-5501.
26. Matson, J. A.; Claridge, C.; Bush, J. A.; Titus, J.; Bradner, W. T.; Doyle, T. W.; Horan, A. C.; Patel, M. *J.Antibiot.* **1989**, *42*, 1547-1555.
27. Chisholm, J. D.; Van Vranken, D. L. *J.Org.Chem.* **2000**, *65*, 7541-7553.
28. Gilbert, E. J.; Ziller, J. W.; Van Vranken, D. L. *Tetrahedron* **1997**, *53*, 16553-16564.
29. Bartoli, G.; Bosco, M.; Dalpozzo, R.; Todesco, P. E. *J.Org.Chem.* **1986**, *51*, 3694-3696.
30. Kuethe, J. T.; Wong, A.; Davies, I. W. *Org.Lett.* **2003**, *5*, 3721-3723.
31. Bonjouklian, R.; Smitka, T. A.; Doolin, L. E.; Molloy, R. M.; Debono, M.; Shaffer, S. A.; Moore, R. E.; Stewart, J. B.; Patterson, G. M. L. *Tetrahedron* **1991**, *47*, 7739-7750.
32. Chang, K. J.; Chae, M. K.; Lee, C.; Lee, J. Y.; Jeong, K. S. *Tetrahedron Lett.* **2006**, *47*, 6385-6388.
33. Steglich, W.; Steffan, B.; Kopanski, L.; Eckhardt, G. *Angew.Chem.* **1980**, *19*, 459-460.
34. Weinreb, S. M.; Garigipati, R. S.; Gainor, J. A. *Heterocycles* **1984**, *21*, 309-324.
35. Hughes, I.; Nolan, W. P.; Raphael, R. A. *J.Chem.Soc., Perkin Trans.1* **1990**, 2475-2480.

36. Harris, W.; Hill, C. H.; Keech, E.; Malsher, P. *Tetrahedron Lett.* **1993**, *34*, 8361-8364.
37. Faul, M. M.; Sullivan, K. A. *Tetrahedron Lett.* **2001**, *42*, 3271-3273.
38. Witulski, B.; Schweikert, T. *Synthesis* **2005**, 1959-1966.
39. Wang, J. J.; Rosingana, M.; Watson, D. J.; Dowdy, E. D.; Discordia, R. P.; Soundarajan, N.; Li, W. S. *Tetrahedron Lett.* **2001**, *42*, 8935-8937.
40. Kaneko, T.; Wong, H.; Okamoto, K. T.; Clardy, J. *Tetrahedron Lett.* **1985**, *26*, 4015-4018.
41. Xie, G. J.; Lown, J. W. *Tetrahedron Lett.* **1994**, *35*, 5555-5558.
42. Toullec, D.; Pianetti, P.; Coste, H.; Bellevergue, P.; Grandperret, T.; Ajakane, M.; Baudet, V.; Boissin, P.; Boursier, E.; Loriolle, F.; Duhamel, L.; Charon, D.; Kirilovsky, J. *J.Biol.Chem.* **1991**, *266*, 15771-15781.
43. Faul, M. M.; Sullivan, K. A.; Winneroski, L. L. *Synthesis* **1995**, 1511-1516.
44. Burtin, G. E.; Madge, D. J.; Selwood, D. L. *Heterocycles* **2000**, *53*, 2119-2122.
45. Brenner, M.; Rexhausen, H.; Steffan, B.; Steglich, W. *Tetrahedron* **1988**, *44*, 2887-2892.
46. Ohkubo, M.; Nishimura, T.; Jona, H.; Honma, T.; Morishima, H. *Tetrahedron* **1996**, *52*, 8099-8112.
47. Cadogan, J. I. G.; Cameron-Wood, M.; Mackie, R. K.; Searle, R. J. G. *J.Chem.Soc.* **1965**, 4831-4837.
48. Lowinger, T. B.; Chu, J. X.; Spence, P. L. *Tetrahedron Lett.* **1995**, *36*, 8383-8386.
49. Moody, C. J.; Rahimtoola, K. F. *J.Chem.Soc., Chem.Commun.* **1990**, 1667-1668.
50. Moody, C. J.; Rahimtoola, K. F.; Porter, B.; Ross, B. C. *J.Org.Chem.* **1992**, *57*, 2105-2114.
51. Adeva, M.; Caballero, E.; Garcia, F.; Medarde, M.; Sahagun, H.; Tome, F. *Tetrahedron Lett.* **1997**, *38*, 6893-6896.
52. Adeva, M.; Buono, F.; Caballero, E.; Medarde, M.; Tome, F. *Synlett* **2000**, 832-834.
53. Bhide, G. V.; Tikotkar, N. L.; Tilak, B. D. *Chem.Ind.* **1957**, 363.
54. Bergman, J.; Pelcman, B. *J.Org.Chem.* **1989**, *54*, 824-828.
55. Gribble, G. W.; Berthel, S. J. *Tetrahedron* **1992**, *48*, 8869-8880.
56. Anderson, D. R.; Koch, T. H. *J.Org.Chem.* **1978**, *43*, 2726-2728.
57. Yamamoto, K.; Watanabe, H. *Chem.Lett.* **1982**, 1225-1228.
58. Hu, Y. Z.; Chen, Y. Q. *Synlett* **2005**, 42-48.
59. Curiel, D.; Cowley, A.; Beer, P. D. *Chem.Commun.* **2005**, 236-238.
60. Garaeva, L. D.; Bakhmedova, A. A.; Yartseva, I. V.; Melnik, S. Y.; Adanin, V. M. *Russ.J.Bioorg.Chem.* **2003**, *29*, 160-167.
61. Faul, M. M.; Winneroski, L. L.; Krumrich, C. A. *J.Org.Chem.* **1998**, *63*, 6053-6058.
62. Yang, S. M.; Malaviya, R.; Wilson, L. J.; Argentieri, R.; Chen, X.; Yang, C. M.; Wang, B. B.; Cavender, D.; Murray, W. V. *Bioorg.Med.Chem.Lett.* **2007**, *17*, 326-331.
63. Bergman, J.; Pelcman, B. *Tetrahedron Lett.* **1987**, *28*, 4441-4444.
64. Bergman, J.; Koch, E.; Pelcman, B. *J.Chem.Soc., Perkin Trans.1* **2000**, 2609-2614.
65. Joyce, R. P.; Gainor, J. A.; Weinreb, S. M. *J.Org.Chem.* **1987**, *52*, 1177-1185.
66. Hinze, C.; Kreipl, A.; Terpin, A.; Steglich, W. *Synthesis* **2007**, 608-612.
67. Marques, M. M. B.; Lobo, A. M.; Prabhakar, S.; Branco, P. S. *Tetrahedron Lett.* **1999**, *40*, 3795-3796.
68. Marques, M. M. B.; Santos, M. M. M.; Lobo, A. M.; Prabhakar, S. *Tetrahedron Lett.* **2000**, *41*, 9835-9838.
69. Somei, M.; Kodama, A. *Heterocycles* **1992**, *34*, 1285-1288.
70. Somei, M.; Hayashi, H.; Izumi, T.; Ohmoto, S. *Heterocycles* **1995**, *41*, 2161-2164.
71. Barry, J. F.; Wallace, T. W.; Walshe, N. D. A. *Tetrahedron Lett.* **1993**, *34*, 5329-5330.

72. Barry, J. F.; Wallace, T. W.; Walshe, N. D. A. *Tetrahedron* **1995**, *51*, 12797-12806.
73. Hudkins, R. L.; Diebold, J. L. *Tetrahedron Lett.* **1997**, *38*, 915-918.
74. Kuethe, J. T.; Davies, I. W. *Tetrahedron Lett.* **2004**, *45*, 4009-4012.
75. Somei, M.; Yamada, F.; Kato, J.; Suzuki, Y.; Ueda, Y. *Heterocycles* **2002**, *56*, 81-84.
76. Bergman, J.; Koch, E.; Pelcman, B. *Tetrahedron* **1995**, *51*, 5631-5642.
77. Merlic, C. A.; Xu, D. Q. *J.Am.Chem.Soc.* **1991**, *113*, 7418-7420.
78. Merlic, C. A.; McInnes, D. M. *Tetrahedron Lett.* **1997**, *38*, 7661-7664.
79. Arcadi, A.; Cacchi, S.; Marinelli, F. *Tetrahedron Lett.* **1989**, *30*, 2581-2584.
80. Heck, R. F. *Acc.Chem.Res.* **1979**, *12*, 146-151.
81. Larock, R. C.; Berriospena, N.; Narayanan, K. *J.Org.Chem.* **1990**, *55*, 3447-3450.
82. Trost, B. M. *Tetrahedron* **1977**, *33*, 2615-2649.
83. Merlic, C. A.; McInnes, D. M.; You, Y. *Tetrahedron Lett.* **1997**, *38*, 6787-6790.
84. Bocchi, V.; Palla, G. *Synthesis* **1982**, 1096-1097.
85. Bergman, J.; Venemalm, L. *J.Org.Chem.* **1992**, *57*, 2495-2497.
86. Miyaura, N.; Suzuki, A. *Chem.Rev.* **1995**, *95*, 2457-2483.
87. Merlic, C. A.; You, Y.; McInnes, D. M.; Zechman, A. L.; Miller, M. M.; Deng, Q. *Tetrahedron* **2001**, *57*, 5199-5212.
88. Saulnier, M. G.; Frennesson, D. B.; Deshpande, M. S.; Vyas, D. M. *Tetrahedron Lett.* **1995**, *36*, 7841-7844.
89. Abbiati, G.; Arcadi, A.; Beccalli, E.; Bianchi, G.; Marinelli, F.; Rossi, E. *Tetrahedron* **2006**, *62*, 3033-3039.
90. Beccalli, E. M.; Gelmi, M. L.; Marchesini, A. *Tetrahedron* **1998**, *54*, 6909-6918.
91. Heinzman, S. W.; Ganem, B. *J.Am.Chem.Soc.* **1982**, *104*, 6801-6802.
92. Wood, J. L.; Stoltz, B. M.; Dietrich, H. J.; Pflum, D. A.; Petsch, D. T. *J.Am.Chem.Soc.* **1997**, *119*, 9641-9651.
93. Tamaki, K.; Huntsman, E. W. D.; Petsch, D. T.; Wood, J. L. *Tetrahedron Lett.* **2002**, *43*, 379-382.
94. Prudhomme, M. *Curr.Med.Chem.* **2000**, *7*, 1189-1212.
95. Bailly, C.; Qu, X. G.; Graves, D. E.; Prudhomme, M.; Chaires, J. B. *Chem.Biol.* **1999**, *6*, 277-286.
96. Bailly, C.; Qu, X. G.; Anizon, F.; Prudhomme, M.; Riou, J. F.; Chaires, J. B. *Mol.Pharmacol.* **1999**, *55*, 377-385.
97. Facompre, M.; Carrasco, C.; Colson, P.; Houssier, C.; Chisholm, J. D.; Van Vranken, D. L.; Bailly, C. *Mol.Pharmacol.* **2002**, *62*, 1215-1227.
98. Facompre, M.; Carrasco, C.; Vezin, H.; Chisholm, J. D.; Yoburn, J. C.; Van Vranken, D. L.; Bailly, C. *ChemBioChem* **2003**, *4*, 386-395.
99. Omura, S.; Sasaki, Y.; Iwai, Y.; Takeshima, H. *J.Antibiot.* **1995**, *48*, 535-548.
100. Schiering, N.; Knapp, S.; Marconi, M.; Flocco, M. M.; Cui, J.; Perego, R.; Rusconi, L.; Cristiani, C. *Proc.Natl.Acad.Sci.U.S.A.* **2003**, *100*, 12654-12659.
101. Furet, P.; Caravatti, G.; Lydon, N.; Priestle, J. P.; Sowadski, J. M.; Trinks, U.; Traxler, P. *J.Comput.Aided Mol.Des.* **1995**, *9*, 465-472.
102. Komander, D.; Kular, G. S.; Bain, J.; Elliott, M.; Alessi, D. R.; Van Aalten, D. M. F. *Biochem.J.* **2003**, *375*, 255-262.
103. Salas, J. A.; Mendez, C. *Curr.Opin.Chem.Biol.* **2009**, *13*, 152-160.
104. Sanchez, C.; Zhu, L. L.; Brana, A. F.; Salas, A. P.; Rohr, J.; Mendez, C.; Salas, J. A. *Proc.Natl.Acad.Sci.U.S.A.* **2005**, *102*, 461-466.
105. Fredenhagen, A.; Peter, H. H. *Tetrahedron* **1996**, *52*, 1235-1238.
106. Stoltz, B. M.; Wood, J. L. *Tetrahedron Lett.* **1995**, *36*, 8543-8544.
107. Stoltz, B. M.; Wood, J. L. *Tetrahedron Lett.* **1996**, *37*, 3929-3930.
108. Salas, A. P.; Zhu, L. L.; Sanchez, C.; Brana, A. F.; Rohr, J.; Mendez, C.; Salas, J. A. *Mol.Microbiol.* **2005**, *58*, 17-27.
109. Sanchez, C.; Mendez, C.; Salas, J. A. *J.Ind.Microbiol.Biotechnol.* **2006**, *33*, 560-568.

110. Wood, J. L.; Stoltz, B. M.; Goodman, S. N.; Onwneme, K. *J.Am.Chem.Soc.* **1997**, *119*, 9652-9661.
111. Gallant, M.; Link, J. T.; Danishefsky, S. J. *J.Org.Chem.* **1993**, *58*, 343-349.
112. Faul, M. M.; Winneroski, L. L.; Krumrich, C. A. *J.Org.Chem.* **1999**, *64*, 2465-2470.
113. Fabre, S.; Prudhomme, M.; Rapp, M. *Bioorg.Med.Chem.Lett.* **1992**, *2*, 449-452.
114. Ohkubo, M.; Kawamoto, H.; Ohno, T.; Nakano, M.; Morishima, H. *Tetrahedron* **1997**, *53*, 585-592.
115. Bailly, C.; Qu, X. G.; Chaires, J. B.; Colson, P.; Houssier, C.; Ohkubo, M.; Nishimura, S.; Yoshinari, T. *J.Med.Chem.* **1999**, *42*, 2927-2935.
116. Ohkubo, M.; Nishimura, T.; Honma, T.; Nishimura, I.; Ito, S.; Yoshinari, T.; Arakawa, H.; Suda, H.; Morishima, H.; Nishimura, S. *Bioorg.Med.Chem.Lett.* **1999**, *9*, 3307-3312.
117. Yoshinari, T.; Ohkubo, M.; Fukasawa, K.; Egashira, S.; Hara, Y.; Matsumoto, M.; Nakai, K.; Arakawa, H.; Morishima, H.; Nishimura, S. *Cancer Res.* **1999**, *59*, 4271-4275.
118. Zembower, D. E.; Zhang, H. P.; Lineswala, J. P.; Kuffel, M. J.; Aytes, S. A.; Ames, M. M. *Bioorg.Med.Chem.Lett.* **1999**, *9*, 145-150.
119. Ohkubo, M.; Nishimura, T.; Jona, H.; Honma, T.; Ito, S.; Morishima, H. *Tetrahedron* **1997**, *53*, 5937-5950.
120. Link, J. T.; Gallant, M.; Danishefsky, S. J.; Huber, S. *J.Am.Chem.Soc.* **1993**, *115*, 3782-3783.
121. Link, J. T.; Raghavan, S.; Danishefsky, S. J. *J.Am.Chem.Soc.* **1995**, *117*, 552-553.
122. Link, J. T.; Raghavan, S.; Gallant, M.; Danishefsky, S. J.; Chou, T. C.; Ballas, L. M. *J.Am.Chem.Soc.* **1996**, *118*, 2825-2842.
123. Liu, L. B.; Yang, B. W.; Katz, T. J.; Poindexter, M. K. *J.Org.Chem.* **1991**, *56*, 3769-3775.
124. Danishefsky, S.; Berman, E.; Clizbe, L. A.; Hirama, M. *J.Am.Chem.Soc.* **1979**, *101*, 4385-4386.
125. Link, J. T.; Danishefsky, S. J. *Tetrahedron Lett.* **1994**, *35*, 9135-9138.
126. Gao, Y.; Hanson, R. M.; Klunder, J. M.; Ko, S. Y.; Masamune, H.; Sharpless, K. B. *J.Am.Chem.Soc.* **1987**, *109*, 5765-5780.
127. Wood, J. L.; Stoltz, B. M.; Dietrich, H. J. *J.Am.Chem.Soc.* **1995**, *117*, 10413-10414.
128. McCombie, S. W.; Bishop, R. W.; Carr, D.; Dobek, E.; Kirkup, M. P.; Kirschmeier, P.; Lin, S. I.; Petrin, J.; Rosinski, K.; Shankar, B. B.; Wilson, O. *Bioorg.Med.Chem.Lett.* **1993**, *3*, 1537-1542.
129. Nakanishi, S.; Yamada, K.; Iwahashi, K.; Kuroda, K.; Kase, H. *Mol.Pharmacol.* **1990**, *37*, 482-488.
130. Kobayashi, Y.; Fujimoto, T.; Fukuyama, T. *J.Am.Chem.Soc.* **1999**, *121*, 6501-6502.
131. Girgis, N. S.; Cottam, H. B.; Robins, R. K. *J.Heterocycl.Chem.* **1988**, *25*, 361-366.
132. Classon, B.; Liu, Z. C.; Samuelsson, B. *J.Org.Chem.* **1988**, *53*, 6126-6130.
133. Kuivila, H. G.; Menapace, L. W. *J.Org.Chem.* **1963**, *28*, 2165-2167.
134. Gani, O.; Engh, R. *Nat.Prod.Rep.* **2010**, *27*, 489-498.
135. Marengo, B.; De, C.; Ricciarelli, R.; Pronzato, M.; Marinari, U. M.; Domenicotti, C. *Cancers* **2011**, *3*, 531-567.
136. Podar, K.; Raab, M. S.; Zhang, J.; McMillin, D.; Breitkreutz, I.; Tai, Y. T.; Lin, B. K.; Munshi, N.; Hideshima, T.; Chauhan, D.; Anderson, K. C. *Blood* **2007**, *109*, 1669-1677.
137. Slater, M. J.; Baxter, R.; Bonser, R. W.; Cockerill, S.; Gohil, K.; Parry, N.; Robinson, E.; Randall, R.; Yeates, C.; Snowden, W.; Walters, A. *Bioorg.Med.Chem.Lett.* **2001**, *11*, 1993-1995.
138. Janosik, T.; Wahlstrom, N.; Bergman, J. *Tetrahedron* **2008**, *64*, 9159-9180.

139. Nakazono, M.; Nanbu, S.; Uesaki, A.; Kuwano, R.; Kashiwabara, M.; Zaitsu, K. *Org.Lett.* **2007**, *9*, 3583-3586.
140. Moffat, D.; Nichols, C. J.; Riley, D. A.; Simpkins, N. S. *Org.Biomol.Chem.* **2005**, *3*, 2953-2975.
141. Moreau, P.; Anizon, F.; Sancelme, M.; Prudhomme, M.; Severe, D.; Riou, J. F.; Goossens, J. F.; Henichart, J. P.; Bailly, C.; Labourier, E.; Tazzi, J.; Fabbro, D.; Meyer, T.; Aubertin, A. M. *J.Med.Chem.* **1999**, *42*, 1816-1822.
142. Mucke, H. A. M. *Idrugs* **2003**, *6*, 377-383.
143. Gingrich, D. E.; Reddy, D. R.; Iqbal, M. A.; Singh, J.; Aimone, L. D.; Angeles, T. S.; Albom, M.; Yang, S.; Ator, M. A.; Meyer, S. L.; Robinson, C.; Ruggeri, B. A.; Dionne, C. A.; Vaught, J. L.; Mallamo, J. P.; Hudkins, R. L. *J.Med.Chem.* **2003**, *46*, 5375-5388.
144. Marminon, C.; Pierre, A.; Pfeiffer, B.; Perez, V.; Leonce, S.; Joubert, A.; Bailly, C.; Renard, P.; Hickman, J.; Prudhomme, M. *J.Med.Chem.* **2003**, *46*, 609-622.
145. Routier, S.; Ayerbe, N.; Merour, J. Y.; Coudert, G.; Bailly, C.; Pierre, A.; Pfeiffer, B.; Caignard, D. H.; Renard, P. *Tetrahedron* **2002**, *58*, 6621-6630.
146. Routier, S.; Coudert, G.; Merour, J. Y.; Caignard, D. H. *Tetrahedron Lett.* **2002**, *43*, 2561-2564.
147. Marminon, C.; Pierre, A.; Pfeiffer, B.; Perez, V.; Leonce, S.; Renard, P.; Prudhomme, M. *Bioorg.Med.Chem.* **2003**, *11*, 679-687.
148. Messaoudi, S.; Anizon, F.; Leonce, S.; Pierre, A.; Pfeiffer, B.; Prudhomme, M. *Eur.J.Med.Chem.* **2005**, *40*, 961-971.
149. Caballero, E.; Adeva, M.; Calderon, S.; Sahagun, H.; Tome, F.; Medarde, M.; Fernandez, J. L.; Lopez-Lazaro, M.; Ayuso, M. J. *Bioorg.Med.Chem.* **2003**, *11*, 3413-3421.
150. Ciganek, E.; Schubert, E. M. *J.Org.Chem.* **1995**, *60*, 4629-4634.
151. de Koning, C. B.; Michael, J. P.; Rousseau, A. L. *J.Chem.Soc., Perkin Trans.1* **2000**, 1705-1713.
152. Deslandes, S.; Chassaing, S.; Delfourne, E. *Marine Drugs* **2009**, *7*, 754-786.
153. Narasimhan, N. S.; Gokhale, S. M. *J.Chem.Soc., Chem.Commun.* **1985**, 86-87.
154. Bourderioux, A.; Kassis, P.; Merour, J.-V.; Routier, S. *Tetrahedron* **2008**, *64*, 11012-11019.
155. Bregman, H.; Williams, D. S.; Meggers, E. *Synthesis* **2005**, 1521-1527.
156. Peifer, C.; Krasowski, A.; Hammerle, N.; Kohlbacher, O.; Dannhardt, G.; Totzke, F.; Schachtele, C.; Laufer, S. *J.Med.Chem.* **2006**, *49*, 7549-7553.
157. Peifer, C.; Stoiber, T.; Unger, E.; Totzke, F.; Schachtele, C.; Marme, D.; Brenk, R.; Klebe, G.; Schollmeyer, D.; Dannhardt, G. *J.Med.Chem.* **2006**, *49*, 1271-1281.
158. Peifer, C.; Selig, R.; Kinkel, K.; Ott, D.; Totzke, F.; Schachtele, C.; Heidenreich, R.; Rocken, M.; Schollmeyer, D.; Laufer, S. *J.Med.Chem.* **2008**, *51*, 3814-3824.
159. Toledo, L. M.; Lydon, N. B. *Structure* **1997**, *5*, 1551-1556.
160. Berlinck, R. G. S.; Britton, R.; Piers, E.; Lim, L.; Roberge, M.; da Rocha, R. M.; Andersen, R. J. *J.Org.Chem.* **1998**, *63*, 9850-9856.
161. Conchon, E.; Anizon, F.; Aboab, B.; Prudhomme, M. *J.Med.Chem.* **2007**, *50*, 4669-4680.
162. Roy, S.; Eastman, A.; Gribble, G. W. *Synth.Commun.* **2005**, *35*, 595-601.
163. Tamaki, K.; Shotwell, J. B.; White, R. D.; Drutu, I.; Petsch, D. T.; Nheu, T. V.; He, H.; Hirokawa, Y.; Maruta, H.; Wood, J. L. *Org.Lett.* **2001**, *3*, 1689-1692

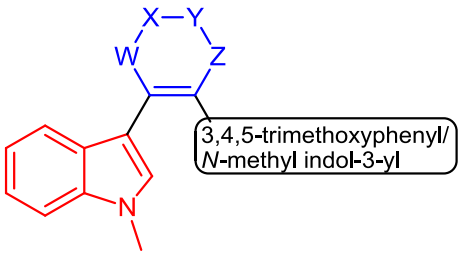
Chapter 3

Aims and Objectives

3.0 Aims and Objectives

3.1 Project outline

Nature can be envisaged as a useful ally to the intrepid medicinal chemist, providing a wide range of active compounds from ubiquitous sources. Natural bisindole alkaloids have recently been revealed to constitute an important class, based on their ability to modulate important biological functions, often with interesting activity profiles.

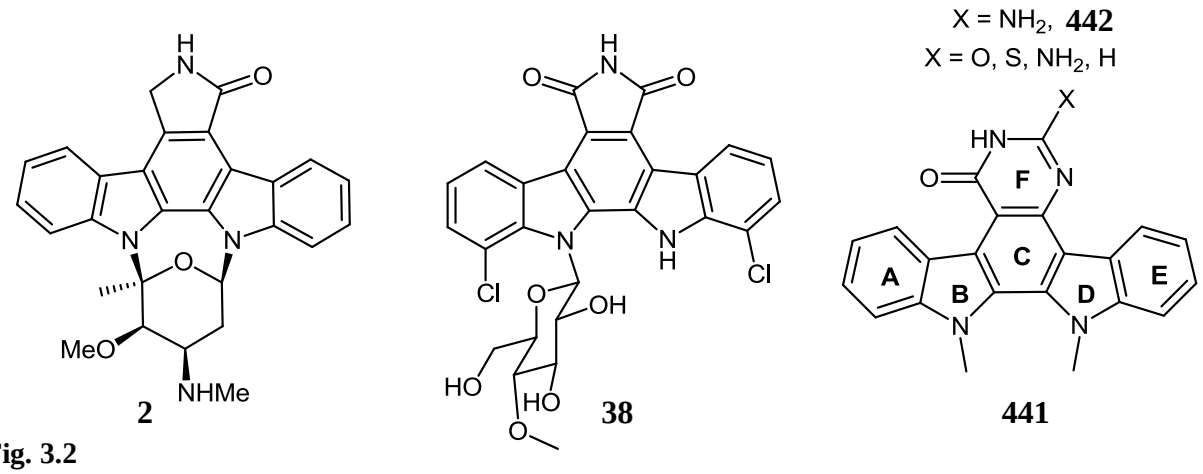


440

Fig. 3.1: General structure of heterocyclic scaffold utilised for design of novel anti-cancer derivatives

Preliminary screening work within the group has identified a group of compounds based on the natural product indolo[2,3-*a*]carbazoles, staurosporine **2** and rebeccamycin **38**, incorporating five or six-membered heterocyclic ring systems (**440**) between the two indole rings as a lead structure capable of delivering novel anti-cancer activity. In addition, a rational approach to diversity-oriented synthesis (DOS) has the potential to yield new small molecule kinase inhibitors, overcoming the low availability and dose-limiting side-effects of current agents (Fig. 3.1).[1-6]

Refinement of this pharmacophore is envisaged to generate multiple biochemical hits against an array of validated molecular targets in cancer and other disorders, with beneficial effects in potency and enzyme selectivity. Derivatisation of this H-bonding protein-interacting scaffold will also achieve improvements in physico-chemical parameters such as enhancement of aqueous solubility, by introduction of biologically relevant polar functionality.[7]



2 **38** **441**

Fig. 3.2

Statement of aims:

At the outset of this work, a synthetic strategy was outlined which incorporated the following project output goals:

(a) Design and synthesis of novel 5,6-bisindolylpyrimidin-4(3*H*)-ones as potential bisindolylmaleimide analogues and investigation of routes to the planar *indolo[2,3-*a*]pyrimido[5,4-*c*]carbazol-4(3*H*)-one* **441** series.

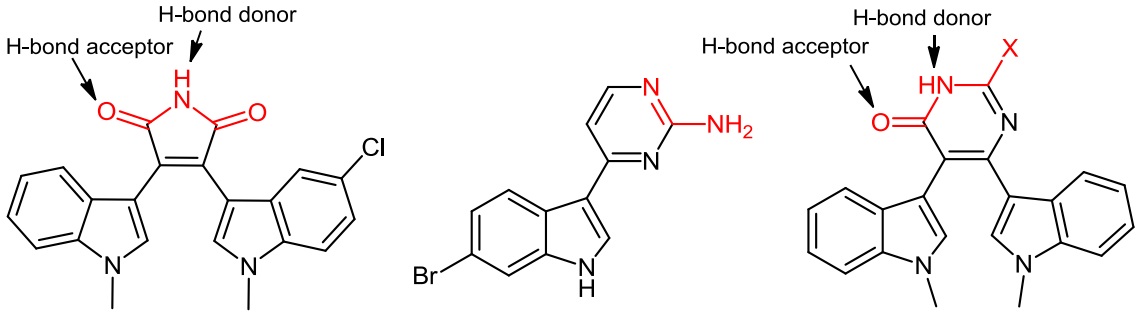
(b) Exploration of heterocyclic derivatisation methodology towards development of novel anti-cancer activity and topoisomerase inhibition by isosteric replacement of inhibitory structural motifs.

(c) Evaluation of optimal routes and key intermediates for future development of novel heterocyclic derivatives in related aryl/bisindolyl compound screening panels.

Overview of objectives

In the following section, a brief SAR background to the aims of this project will be provided. In summary, the known chemical diversity of kinase inhibitors, and related ability of a wide number of indolocarbazole derivatives to exhibit biological versatility underpins this project. Following investigation of literature in this area, a number of structural leads for enzyme inhibition by modified structures have been identified. In addition, very little work has been carried out by workers in the area of modifying the key H-bonding lactam/maleimide ring within active aglycons of STA **2** and REB **38**. This insight has led us to develop several strategies targeting innovative F-ring installation in new bioactive BIMs and ICZs.

Bisindolylmaleimide **443** was demonstrated by Davis *et al.* to inhibit PKC with an IC_{50} value of 0.11 µM, while monoindolyl Meridianin D **444**, isolated from the marine tunicate *Aplidium meridianum*, displayed modest cytotoxicity towards LMM3 (murine mammarian adenocarcinoma cell line), with an IC_{50} value of 33.9 µM, as well as being an inhibitor of several protein kinases.[8,9] Extrapolating from this structural evidence, novel bisindolyl heterocycles related to compound **445**, where X = NH_2, containing a 1,2-(bisindolyl)-*cis*-ethene scaffold and H-bonding pyrimidinone core would be of immense interest as elaborate isosteres containing a similar bidentate acceptor-donor heterocyclic H-bond motif (Fig. 3.3).

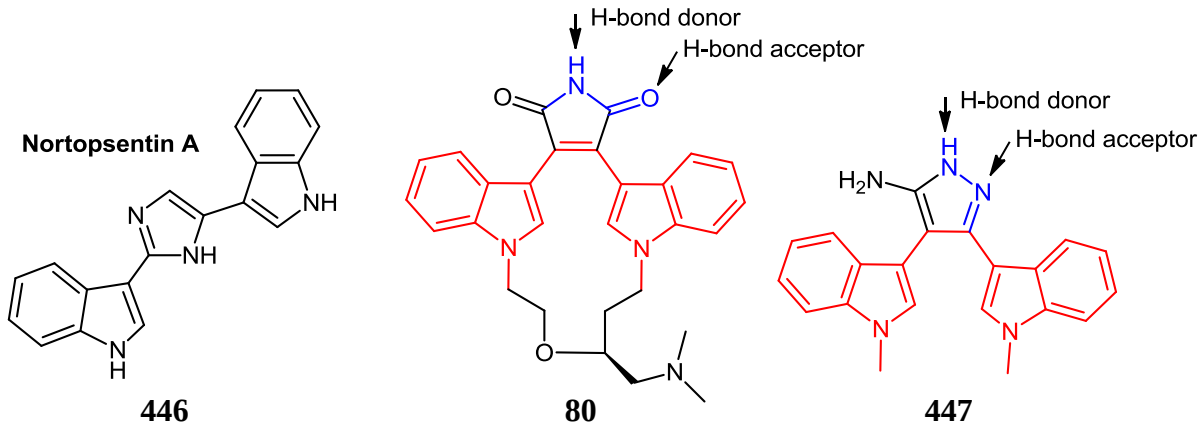


443 **444** X = NH_2; **445**
X = SH, OH, H

Fig. 3.3

Investigation of conformationally rigid heterocycles and alkylated analogues would also extensively probe the molecular space within proposed binding pockets. As a benchmark compound, the new planar indolo[2,3-*a*]carbazole structure **441** would allow us determine if new interactions with enzyme residues by this six-membered ring series correlates with improved inhibitory activity, in comparison to the highly active, five-membered indolo[2,3-*a*]pyrrolo[3,4-*c*]carbazoles. In particular, the 2-aminopyrimidine-4-one (isocytosine) subunit fused to the indolocarbazole (X = NH_2; **442**), would be appealing since analogous pyrimidine moieties form a component of nucleoside bases, which play a powerful role in biological systems (Fig. 3.2).[10-12]

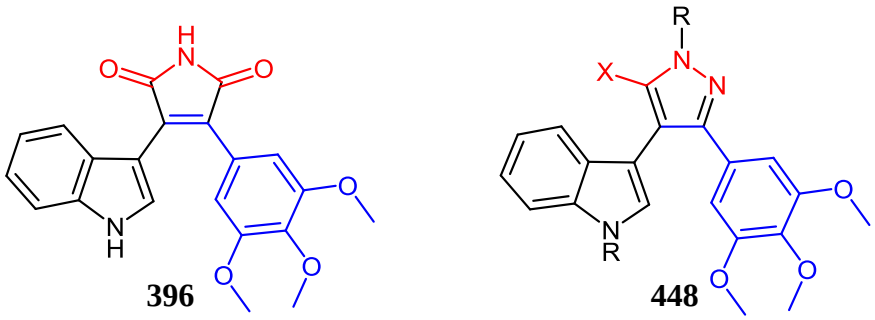
A major objective of this work was transfer of distinct structural features of related heterocyclic compounds into emerging lead architectures obtainable from key intermediates. This concept has been pursued by targeting modification of the cytotoxic marine bisindole pyrrole alkaloid – nortopsentin A **446**.[13] Synthesis of 3,4-bisindolylpyrazol-5-amine **447** and complementary analogues have not been previously described, and this chimeric system has the potential to augment the attractive H-bonding network within bioactive anti-cancer bisindolylmaleimide derivatives such as ruboxistaurin **80** (Fig. 3.4).[14-16]



446 **80** **447**

Fig. 3.4

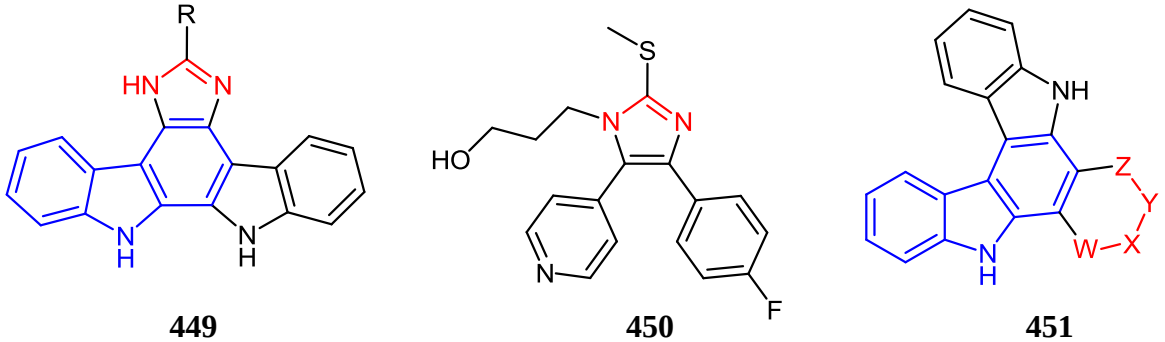
It was anticipated that work based on the VEGFR2 inhibitor 3-(indol-3-yl)-4-(3,4,5-trimethoxyphenyl)-1*H*-pyrrole-2,5-dione **396** would also afford a number of novel congeners of general structure **448**, retaining an arylindolyl system, while comprising a new H-bonding enzyme-interacting template with immense biological potential in this series (Fig. 3.5).[17,18]



396 **448**

Fig. 3.5

The final element of this work involved initiating development of routes to novel chemical classes attracting future research within the group. Development of a new route to *imidazo[4,5-c]indolo[2,3-a]carbazoles* ***449*** - a new synthetic template based on the 3,4-diarylimidazole class reported by Laufer *et al.*, and exemplified by the p38 MAP kinase inhibitor **450** (Fig. 3.6).[19,20] Devising new approaches to indolo[2,3-*c*]carbazoles **451** and preliminary investigation of heterocyclic variation within this regio-series constituted work focused on the future identification of diverse ICZ leads with enviable biological activity.



449 **450** **451**

Fig. 3.6

3.2 References

1. Gani, O.; Engh, R. *Nat.Prod.Rep.* **2010**, *27*, 489-498.
2. Hosoya, T.; Yamamoto, Y.; Uehara, Y.; Hayashi, M.; Komiyama, K.; Ishibashi, M. *Bioorg.Med.Chem.Lett.* **2005**, *15*, 2776-2780.
3. Kamata, K.; Kiyota, M.; Naoe, A.; Nakatani, S.; Yamamoto, Y.; Hayashi, M.; Komiyama, K.; Yamori, T.; Ishibashi, M. *Chem.Pharm.Bull.* **2005**, *53*, 594-597.
4. Pindur, U.; Lemster, T. *Curr.Med.Chem.* **2001**, *8*, 1681-1698.
5. Sancelme, M.; Fabre, S.; Prudhomme, M. *J.Antibiot.* **1994**, *47*, 792-798.
6. Bergman, J.; Janosik, T.; Wahlstrom, N. *Adv.Heterocycl.Chem.* **2001**, *80*, 1-71.
7. Prudhomme, M. *Eur.J.Med.Chem.* **2003**, *38*, 123-140.
8. Davis, P. D.; Hill, C. H.; Lawton, G.; Nixon, J. S.; Wilkinson, S. E.; Hurst, S. A.; Keech, E.; Turner, S. E. *J.Med.Chem.* **1992**, *35*, 177-184.
9. Casar, Z.; Bevk, D.; Svete, J.; Stanovnik, B. *Tetrahedron* **2005**, *61*, 7508-7519.
10. Cohen, P. *Curr.Opin.Chem.Biol.* **1999**, *3*, 459-465.
11. Traxler, P.; Bold, G.; Buchdunger, E.; Caravatti, G.; Furet, P.; Manley, P.; O'Reilly, T.; Wood, J.; Zimmermann, J. *Med.Res.Rev.* **2001**, *21*, 499-512.
12. Pourquier, P.; Gioffre, C.; Kohlhagen, G.; Urasaki, Y.; Goldwasser, F.; Hertel, L. W.; Yu, S. Y.; Pon, R. T.; Gmeiner, W. H.; Pommier, Y. *Clin.Cancer Res.* **2002**, *8*, 2499-2504.
13. Sanchez, C.; Mendez, C.; Salas, J. A. *Nat.Prod.Rep.* **2006**, *23*, 1007-1045.
14. Courage, C.; Snowden, R.; Gescher, A. *Br.J.Cancer* **1996**, *74*, 1199-1205.
15. Bit, R. A.; Davis, P. D.; Elliott, L. H.; Harris, W.; Hill, C. H.; Keech, E.; Kumar, H.; Lawton, G.; Maw, A.; Nixon, J. S.; Vesey, D. R.; Wadsworth, J.; Wilkinson, S. E. *J.Med.Chem.* **1993**, *36*, 21-29.
16. Brehmer, D.; Godl, K.; Zech, B.; Wissing, J.; Daub, H. *Molecular & Cellular Proteomics* **2004**, *3*, 490-500.
17. Peifer, C.; Krasowski, A.; Hammerle, N.; Kohlbacher, O.; Dannhardt, G.; Totzke, F.; Schachtele, C.; Laufer, S. *J.Med.Chem.* **2006**, *49*, 7549-7553.
18. Peifer, C.; Stoiber, T.; Unger, E.; Totzke, F.; Schachtele, C.; Marme, D.; Brenk, R.; Klebe, G.; Schollmeyer, D.; Dannhardt, G. *J.Med.Chem.* **2006**, *49*, 1271-1281.
19. Peifer, C.; Wagner, G.; Laufer, S. *Curr.Top.Med.Chem.* **2006**, *6*, 113-149.
20. Peifer, C.; Abadleh, M.; Bischof, J.; Hauser, D.; Schattel, V.; Hirner, H.; Knippschild, U.; Laufer, S. *J.Med.Chem.* **2009**, *52*, 7618-7630.

Chapter 4

Chemical Results and Discussion

Contents

4.0 Chemical Results and Discussion 136
4.1 Synthesis of 3,4-bisindolylmaleimides 136
4.1.1 Indole substitution reactions 136
4.1.2 Perkin condensation 138
4.2 Modified classical routes to 5,6-bisindolyl-substituted pyrimidin-4-ones 139
4.2.1 Diels-Alder reaction 139
4.2.2 Base-mediated indole coupling 140
4.3 Synthesis of indolo[2,3-c]carbazoles 141
4.3.1 Synthesis of 3,3-biindolyl 142
4.3.2 Diels-Alder [4+2] cycloadditions 142
4.3.3 Attempted derivatisation of indolo[2,3-*c*]carbazole 143
4.3.4 Attempted Curtius rearrangement 144
4.4 Formation of β-ketoesters 145
4.4.1 Esterification of indole-3-acetic acid (IAA) 146
4.4.2 Synthesis of indole-3-carbonyl chloride 147
4.4.3 Synthesis of 2,3-bisindolyl methyl-3-oxopropionate 149
4.4.5 Attempted reductive amination 150
4.4.6 Synthesis of methyl 3-chloro-2,3-bisindolylacrylate 152
4.5 Cyclocondensation with urea 153
4.5.1 Attempted microwave-mediated synthesis of uracils 153
4.5.2 Reaction of urea with β-ketoesters in routes to 5,6-bisindolyluracils 154
4.6 Other cyclocondensations in routes to bisindolyl heterocycles[45] 157
4.6.1 Reaction with hydrazines 158
4.6.2 Reaction with thiourea 159
4.6.3 Thiouracil derivatisation routes to 5,6-bisindolylpyrimidin-2,4-dione 161
4.6.4 Reaction with guanidine carbonate 164
4.6.5 Attempted reaction with panel of bidentate *N*-nucleophiles 167
4.7 Oxidative cyclisation of bisindolylpyrimidinone series 170
4.7.1 Indolo[2,3-*a*]pyrimido[5,4-*c*]carbazol-4(3*H*)-one synthesis *via* 2,2'-ring closure of 5,6-bisindolyl-2-aminopyrimidin-4-one 170
4.7.2 Attempted photocyclisation of other novel heterocycles 175
4.8 Spectroscopic analysis of the heteroaromatic region of novel bisindolyl heterocyclic derivatives 177
4.9 Synthesis of 3,4-bisindolyl-5-aminopyrazoles 183
4.9.1 Synthesis of 2,3-bis(1-methyl-1*H*-indol-3-yl)-3-oxopropanenitrile 184
4.9.2 Synthesis of 3,4-bis(1-methyl-1*H*-indol-3-yl)-5-aminopyrazole 185
4.9.3 Reactivity of 3,4-bis(1-methyl-1*H*-indol-3-yl)-5-aminopyrazole 186
4.10 Synthesis of aryl-substituted indolyl-heterocycles 190

4.10.1 Synthesis of 4-(1-methyl-1*H*-indol-3-yl)-5-(3,4,5-trimethoxyphenyl)-pyrazol-3-one 191
4.10.2 Synthesis of 4-(1-methyl-1*H*-indol-3-yl)-3-(3,4,5-trimethoxyphenyl)-5-aminopyrazole 192
4.10.3 Derivatisation of 4-(1-methyl-1*H*-indol-3-yl)-5-(3,4,5-trimethoxyphenyl)-5-aminopyrazole 193
4.11 Synthesis of 4,5-bisindolyl-2-substituted imidazoles 196
4.11.1 Synthesis of 1,2-bis(1*H*-indol-3-yl)ethane-1,2-dione 197
4.11.2 A potential one-pot condensation route to 4,5-bisindolylimidazoles 197
4.11.3 Photochemical synthesis of imidazolo[4,5-*c*]indolo[2,3-*a*]carbazoles 198
4.12 Conclusion 199
4.13 References 203

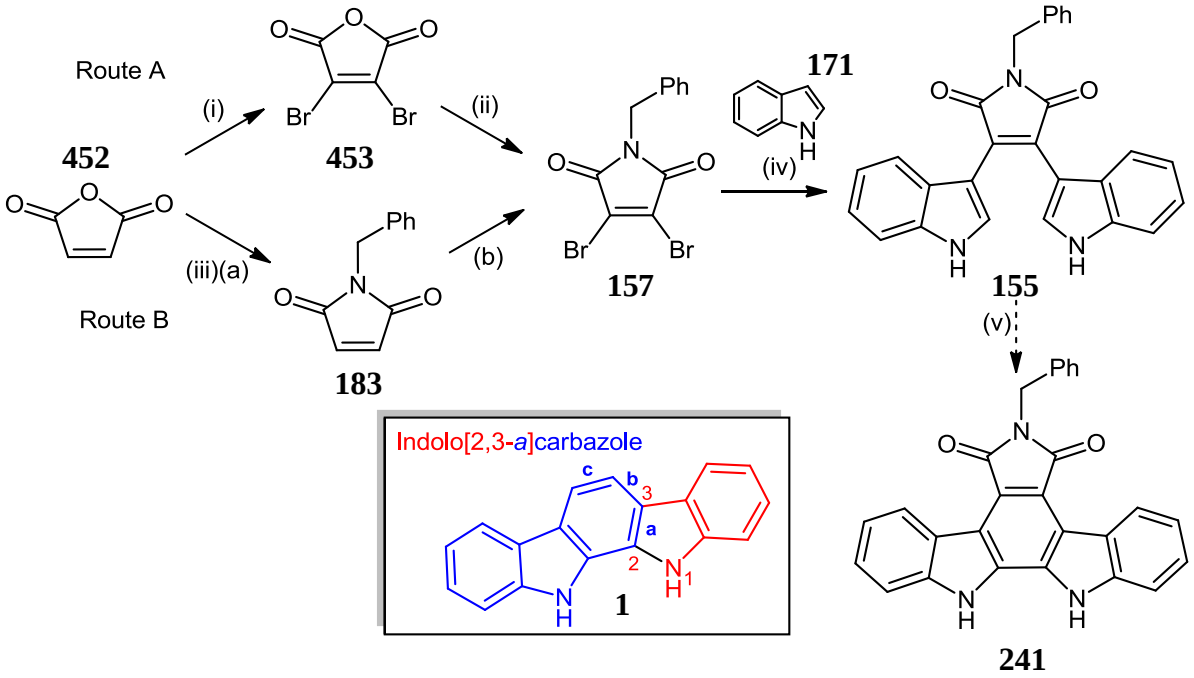
4.0 Chemical Results and Discussion

4.1 Synthesis of 3,4-bisindolylmaleimides

Any individual method for the construction of the indolo[2,3-*a*]pyrrolo[3,4-*c*]carbazole **3** core, as well as regio-analogues, must be selected according to the structural nature of the target of interest. In recent times, a number of versatile approaches to these systems have been exploited, with a common motif observed for these routes including the late-stage bisindolylmaleimide ring closure to form the central carbocyclic ring.[1-3]

4.1.1 Indole substitution reactions

A classical approach to indolo[2,3-*a*]carbazole **1** alkaloids involves oxidative cyclisation of an appropriately derivatised 3,4-bisindolylmaleimide intermediate **155** *via* double coupling of preformed indole **171** to a dihalo substituted maleimide precursor **157**.[4,5]



Reagents and conditions: (i) Br_2, $AlCl_3$, 120°C, 16h, **453** = 90%; (ii) Bn-NH_2, AcOH, 120°C, 3h, **157** = 60%; (iii)(a) Bn-NH_2, AcOH, 120°C, 2h, (b) Br_2, NaOAc, 0°C - 120°C, 2h, **157** = 60%; (iv) LiHMDS, -78°C - 100°C, toluene, 16h, **155** = 42% (crude); (v) DDQ, cat. *p*-TSA, toluene, 100°C, 1h

Scheme 4.1

As an initial effort to develop a versatile method of indolocarbazole formation, a trial route was initiated with *N*-benzyl-3,4-dibromomaleimide **157** as electrophile, with a view to its replacement by other dihalogenated heterocycles within new chemical series (Section 4.2.2).[6]

Dibromination of maleic anhydride **452**, using 1.5 equivalents of bromine in DMF, stirred for 3 days at 55°C was attempted with limited success. Consequently, according to the approach outlined by Dubernet *et al.* (Route A), a mixture containing precursor **452** and bromine, along with a catalytic amount of aluminium chloride, was heated in a sealed vessel at 120°C for 16 hours. Following work-up, 2,3-dibromomaleic anhydride **453** was isolated in a yield of 90%. Conversion of this intermediate to *N*-benzyl-3,4-dibromomaleimide **157** was achieved through amination with 1.1 equivalents of benzylamine, and following chromatography, the desired product **157** was isolated, as an off-white solid, in a yield of 60% (Scheme 4.1).[6,7]

Interestingly, another method employed to good synthetic effect was the one-pot preparation of **157**, *via* intermediate **183**, first reported by Choi *et al.* (Route B), which afforded **157** in a yield of 60%, in our hands. However, the non-facile issue of the efficient open-vessel heating of volatile bromine limited this route in comparison to Dubernet's robust methodology.[8]

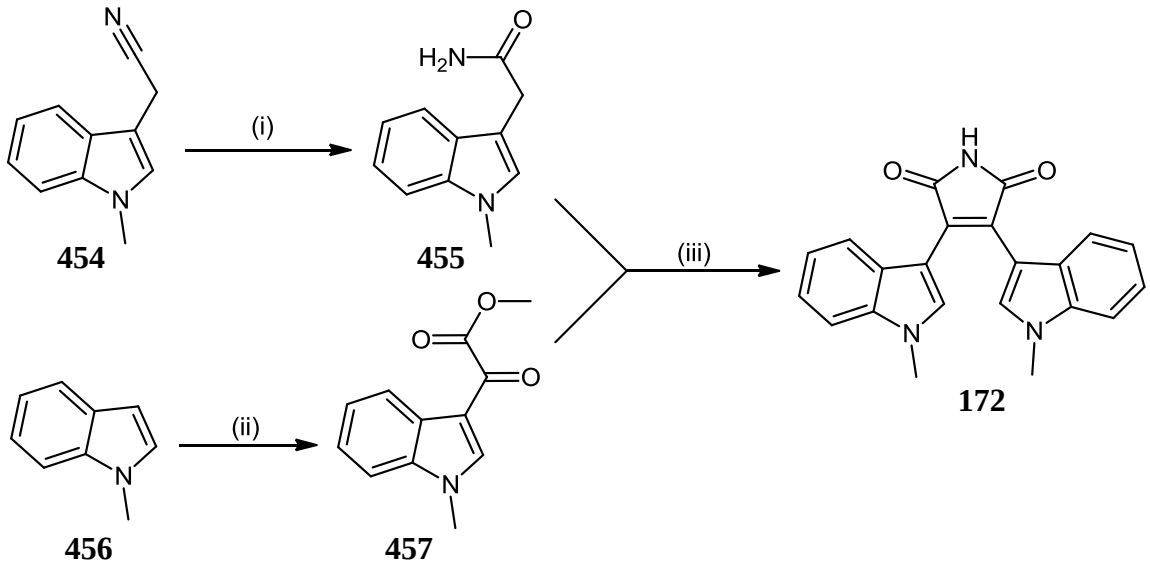
The penultimate step consisted of the nucleophilic displacement of both bromine atoms in intermediate **157**, by two indolyl anions, to yield the acyclic bisindolylmaleimide core **155**.[9,10] Heating of a mixture of 2.5 equivalents of indolemagnesium bromide and the *N*-benzyl-3,4-dibromomaleimide **157**, in the presence of transmetallating $ZnCl_2$ solution, in diethyl ether, did not yield **155**, under these conditions. However, other workers attempting this transformation have also employed LiHMDS, to furnish this bisindolylmaleimide **155**. To a solution of LiHMDS formed *in situ*, at 0°C, 2 equivalents of **171** in toluene were added, at −78°C. On addition of a solution of protected dibrominated maleimide **157** to the flask, a dark blue colour initially appeared, that changed to a red mixture following heating overnight. The resultant crude yield of the bisindolylmaleimide product **155** was 42%, but unfortunately, this process was strongly affected by product solubility and work-up issues.[11]

The final stage in this process required full aromatisation of the indolocarbazole nucleus, *via* oxidative cyclisation. Applying the method of Joyce *et al.*, oxidative cyclisation was carried out by heating a mixture of DDQ and crude bisindolylmaleimide **155**, along with a catalytic amount of *p*-TSA, in toluene.[9] Fractions containing a fluorescent spot consistent with *N*-benzyl indolocarbazole **241** formation were observed, but could only be recovered in a yield of <5%, on a 100 mg scale reaction. Several complex fractions were also collected, indicating that perhaps competing side-reactions suppressed the formation of indolocarbazole **241**; this result suggested that it may be necessary to adopt alternative

milder aromatisation methodologies in order to provide access to analogous compounds in higher yields.[2,12,13] The poor profile of this route also necessitated further work on an efficacious route to classical indolo[2,3-*a*]pyrrolo[3,4-*c*]carbazole derivatives.

4.1.2 Perkin condensation

Given the inherent difficulties and lack of versatility of the indolic substitution approach, a further route to derive di-*N*-methyl protected arcyriarubin A **172** was explored *via* a base-mediated Perkin condensation of *N*-methyl indole-3-acetamide **455** and *N*-methyl indole-3-glyoxylate **457**, according to the procedure reported by Faul *et al.*[14-16] Treatment of 3-indolylacetonitrile **454** with 30% hydrogen peroxide and 1M aqueous NaOH solution, along with TBAB, in DCM overnight at room temperature was thus found to afford acetamide **455** in a yield of 52%, following purification (Scheme 4.2).[15]



Reagents and conditions: (i) 30% H_2O_2, aq. NaOH, cat. TBAB, DCM, rt, 16h; (ii) (a)$(COCl)_2$, Et_2O, 30 min.; (b) 25% NaOMe, -65°C - rt; (c) H_2O; (iii)(a) 3 eq. 1M KO*t*-Bu, THF, rt, 3h; (b) 5% HCl, 0°C

Scheme 4.2

Reaction of *N*-methylindole **456** with 1.1 equivalents of oxalyl chloride at -65°C, followed by addition of sodium methoxide solution, and work-up involving water quenching, successfully isolated the corresponding *N*-methyl methyl indole-3-glyoxylate ester **457** in a yield of 42%. Following stirring of a bright-red suspension of acetamide **455** and glyoxylate **457**, in THF at 0°C, in the presence of potassium *tert*-butoxide, bisindolylmaleimide derivative **172** was afforded as an amorphous red powder in a yield of 67% (Scheme 4.2).

Formation of arcyriarubin A derivative **172** represented an attractive indolo[2,3-*a*]carbazole **1** 'benchmark' compound, important as a standard in order to assess the relative potency and modes of action of structurally related novel bisindolyl analogues, referenced during this investigation.[4,5,14,17-19]

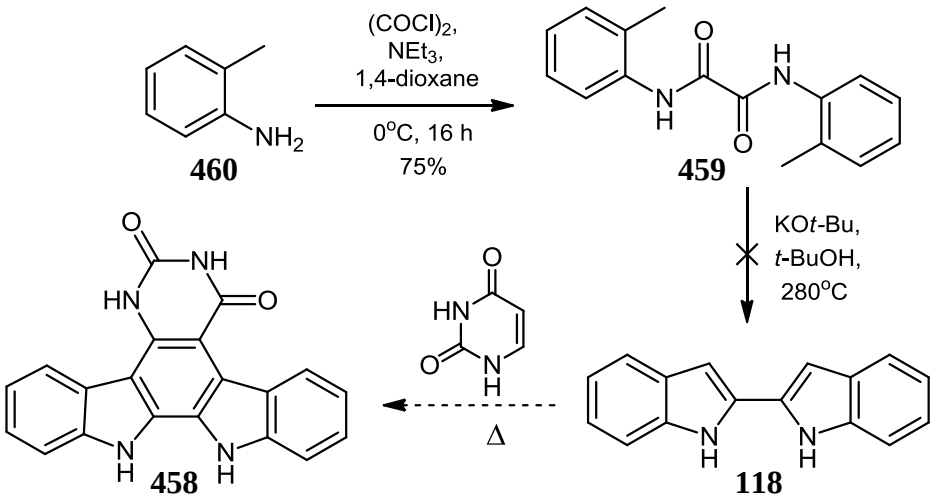
4.2 Modified classical routes to 5,6-bisindolyl-substituted pyrimidin-4-ones

Due to the non-versatile nature of the Perkin condensation, initial investigation of alternate BIM-forming methodologies which could be modified for accessing 5,6-bisindolylpyrimidin-4-one congeners classified Diels-Alder cycloaddition and base-mediated indole coupling to 5,6-dihalouracil derivatives as potential routes to this new chemical class.

4.2.1 Diels-Alder reaction

An alternative methodology was considered for the formation of indolo[2,3-*a*]carbazole **458**, which involved the Diels-Alder [4+2] cycloaddition reaction of 2,2'-biindolyl **118** and maleimide **199**, as a heterocyclic dienophile. Unfortunately, while literature references to the preparation of **118** are surprisingly rare and constitute a series of uniformly unattractive routes, its potential procurement from commercial sources was also deemed to be prohibitively expensive. Madelung cyclisation of an *N*,*N'*-bis(*O*-tolyl)oxamide **459** under extremely forcing conditions (>300°C) was known to provide **118** in moderate yield.[20]

The bisamide intermediate **459** was prepared in a facile fashion following reaction of a mixture of *o*-toluidine **460**, triethylamine and oxalyl chloride in 1,4-dioxane, maintained at 0^{o}C. Following work-up, the reaction mixture was filtered to cleanly isolate the toluidide **459** in a yield of 75% as an off-white solid.[21] Treatment of **459** with 5 equivalents of potassium *tert*-butoxide, in the presence of *tert*-butanol, at 280°C, only resulted in the recovery of starting material. This reaction has not been documented to proceed below 300°C and the apparatus at our disposal could not achieve the necessarily harsh conditions required (Scheme 4.3). The capricious nature of this indole-forming reaction has been previously documented, yet few improvements, in achieving this conversion under milder conditions have been described to date.[22]

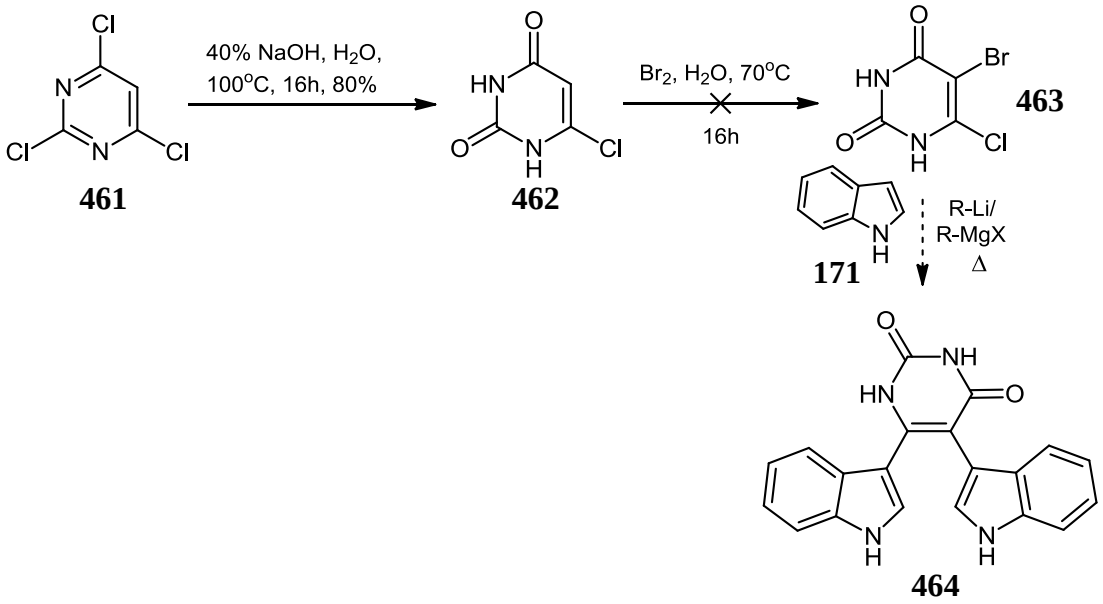


Scheme 4.3

This route was therefore abandoned due to the high degree of difficulty in obtaining starting material and potential lack of viability of the Diels-Alder method. Due to the absence of an array of heterocycles capable of behaving as effective dienophiles, the scope of this methodology would also be incapable of sustaining a wider program of indolocarbazole derivatisation. Following completion of this work, Tsuchimoto and co-workers have reported the utilisation of Fischer indole cyclisation, *via* 1-(indol-2-yl)ethanone phenylhydrazone, in 28% yield, while 2,2'-biindolyl formation has also been accomplished by transition metal-mediated routes not investigated in the present work.[23,24]

4.2.2 Base-mediated indole coupling

In contrast to 2,2-biindolyl **118**, 2,4,6-trichloropyrimidine **461** could be cheaply sourced and hydrolysed readily to 6-chlorouracil **462**, under aqueous alkaline conditions at 100°C. Employing a protocol derived from the work of Murray *et al.*, reaction of **462** in the presence of bromine water at 60°C, did not yield any of the anticipated 5-brominated derivative **463** (Scheme 4.4).[25] On detailed inspection of the literature in this area, it was noted that use of 5,6-dihalouracils, in general, was exceedingly rare. No work-up was available in any available scientific literature, and interestingly, while *C*-6 attack by pyridine to form pyridinium salts etc. have been previously documented, no references were found to any reaction in which nucleophilic attacks have been reported occurring simultaneously on both the C-5 and C-6 positions of the uracil ring. Therefore, it was established that an innovative retrosynthetic plan was required for accessing novel 5,6-bisindolyluracil **464** derivatives.



Scheme 4.4

4.3 Synthesis of indolo[2,3-*c*]carbazoles

Different arrangements of indole **171** and carbazole moieties have been reported to form 5 possible isomeric ring systems. However, the vast preponderance of indolocarbazoles isolated from natural sources are indolo[2,3-*a*]carbazoles **1** and therefore, most research attention in this area has been focused on analogues which comprise this heterocyclic system.

It was decided that two congeners bearing the indolo[2,3-*c*]carbazole **465** chromophore would initially be produced in order to effect direct comparison with a panel of indolo[2,3-*a*]carbazole derivatives, as well as for the development of novel indolocarbazole analogues within this series. These compounds could be formed *via* cycloaddition of 3,3-biindolyl **466** and maleimide **199** for synthesis of **468**, or with maleic anhydride **452** as dienophile in order to access compound **467**, as reported by Bergman *et al.* (Fig. 4.1).[26]

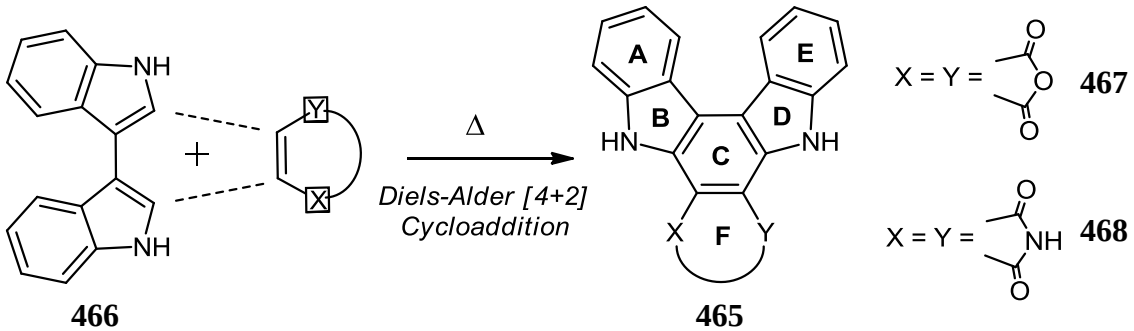
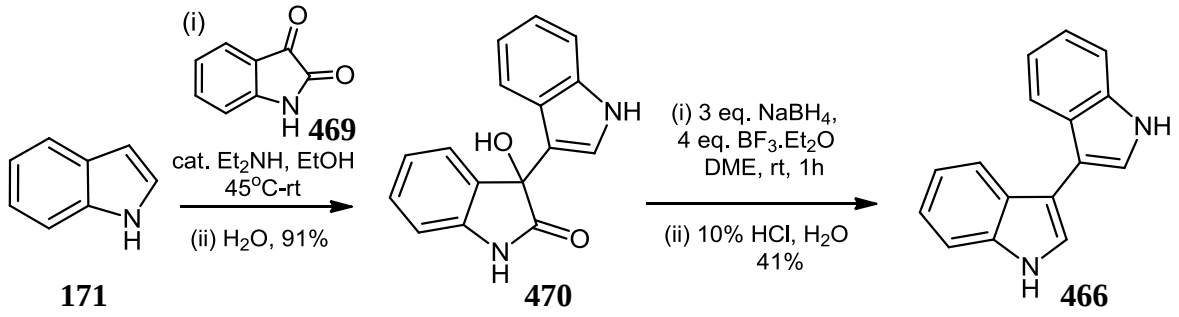


Fig. 4.1: Cycloaddition route to indolo[2,3-*c*]carbazoles

4.3.1 Synthesis of 3,3-biindolyl

Based on Bergman's procedure, to a mixture of indole **171** and an equivalent amount of isatin **469**, was added a small volume of 98% diethylamine solution, along with absolute ethanol. Following overnight reaction and addition of water during work-up, 3-(3'-hydroxyindolin-2'-one)indole **470**, was isolated by filtration and recrystallised from methanol, to afford a single crop of **466**, as light pink crystals, in a yield of 91%.[27]

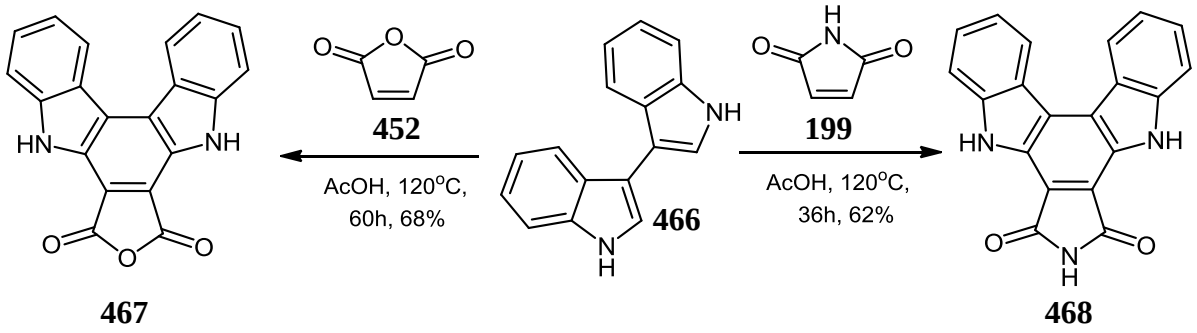
3-(3'-Hydroxyindolin-2'-one)indole **470** was initially charged to a mixture of sodium borohydride and 1,2-dimethoxyethane (DME). A solution of $BF_3.Et_2O$ complex in DME solution was then added to the beige-coloured, vigorously stirred reaction over 30 minutes. During this period, the flask initially assumed a light-green appearance, which transformed into a straw-coloured slurry on full reagent addition. Following work-up and cooling to 0^oC, the slurry was filtered and washed with DCM, to yield 3,3'-biindolyl **466**, as silver plate-like crystals, in a yield of 41% (Scheme 4.5).[26,27]



Scheme 4.5

4.3.2 Diels-Alder [4+2] cycloadditions

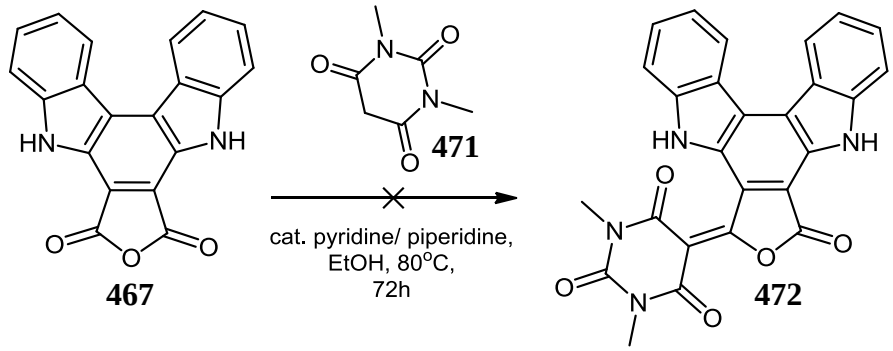
Thermal electrocyclisation of 3,3'-biindolyl **466** with a heterocyclic dienophile was reported to successfully generate indolo[2,3-*c*]carbazole **465** functionality, and unlike Diels-Alder approaches for the corresponding indolo[2,3-*a*]carbazole **1** series, was detailed to proceed in excellent yield, under relatively mild conditions (Section 4.2.1). Following heating of maleic anhydride **452** and 3,3-biindolyl **466**, in the presence of glacial acetic acid, for 60 hours at 120^oC, the dark red mixture was filtered to yield furo[3,4-*a*]indolo[2,3-*c*]carbazole-6,8(5*H*,9*H*)-dione **467** (68%). Under similar reaction conditions, employing 2 equivalents of maleimide **199** stirred in acetic acid for 36 hours at 120^oC, 5*H*-indolo[2,3-*c*]pyrrolo[3,4-*a*]carbazole-6,8(7*H*,9*H*)-dione **468** was isolated after work-up, as a dark-red amorphous solid, in a yield of 62% (Scheme 4.6).[26]



Scheme 4.6

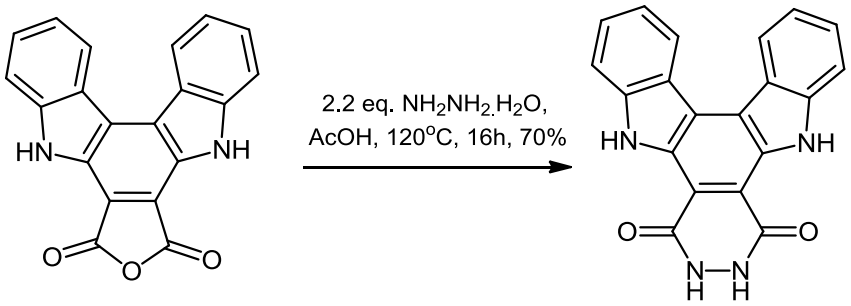
4.3.3 Attempted derivatisation of indolo[2,3-*c*]carbazole

A Knoevenagel reaction was attempted between **467** and 1,3-dimethylbarbituric acid **471**, carried out by stirring one equivalent of each reactant at 80°C, in the presence of ethanol containing a catalytic amount of either pyridine or piperidine, acting as base (Scheme 4.7).



Scheme 4.7

Unfortunately, no reaction to form **472** occurred under these conditions, and only starting material could be detected even after 72 hours. Nucleophilic ring-opening of **467** utilising hydrazine in acetic acid, heated at reflux overnight, successfully afforded 7,8-dihydroindolo[2,3-*c*]pyridazino[4,5-*a*]carbazole-6,9(5*H*,10*H*)-dione **473**, as a brown powder, in a yield of 70%, following addition of water, and filtration of the reaction mixture (Scheme 4.8).[28] This novel indolocarbazole **473** represents the first example of a six-membered F-ring moiety within this series and future work in this area will exploit this route for further derivatisation.



467 **473**

Scheme 4.8

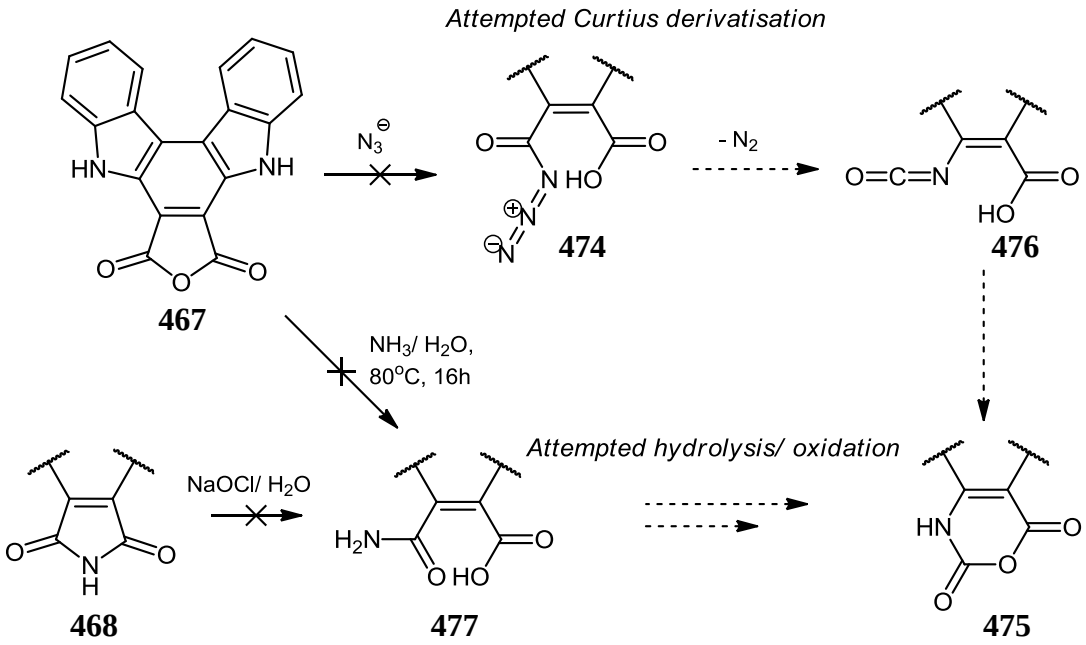
4.3.4 Attempted Curtius rearrangement

Based on literature precedent in this area and the initial success of hydrazine-mediated pyridazin-3,6-dione **473** formation, it was postulated that azide-induced Curtius rearrangement of **467** proffered a route to other novel heterocyclic derivatives.[29] However, reaction of **467** with a number of nucleophilic azide donors, in polar aprotic solvents, known to mediate this transformation, failed to yield the desired acyl azide **474** intermediate or final oxazine product **475**, *via* Curtius product **476,** after 24 hours (Table 4.1). Ammonolysis of **467** in aqueous ammonia solution overnight at 80°C, in order to produce the corresponding carboxyamide **477** was attempted, but could not be effected under these hydrolytic degradation conditions. Indolocarbazole **468** was also stirred along with a solution of sodium hypochlorite, at 0°C, for 2 hours, followed by heating at 70°C overnight; however, only starting material was recovered, due to the poor oxidative efficiency of this transformation (Scheme 4.9).

Table 4.1: Conditions employed for attempted indolo[2,3-*c*]carbazole (467)* Curtius rearrangement to yield a novel oxazine intermediate (475)

Reagent	***Equiv.***	***ICZ reactant***	***Solvent***	***Reflux***	***Product†***
NaN_3	10	**467**	DMF	110°C/ 24h	n.r
NaN_3	10	**467**	DMSO	150°C/ 24h	n.r
NaN_3#	20	**467**	DMF	110°C/ 24h	n.r
TMS-N_3	10	**467**	DMF	110°C/ 24h	n.r
TMS-N_3	10	**467**	DMSO	150°C/ 24h	n.r

*Reaction monitored by TLC and ESI-MS analysis.
†Predominantly starting material was recovered after completion of each reaction run, with minor degradation evident (n.r = no reaction).
#In the presence of a catalytic amount of activated azide donor reagent, TMS-N_3 (trimethylsilyl azide).



Scheme 4.9

4.4 Formation of β-ketoesters

At the outset of this work, an optimal retrosynthetic strategy was investigated for assembly of novel 5 and 6-membered H-bonding frameworks **441** as new analogues of bioactive BIMs (c.f. Section 4.1).

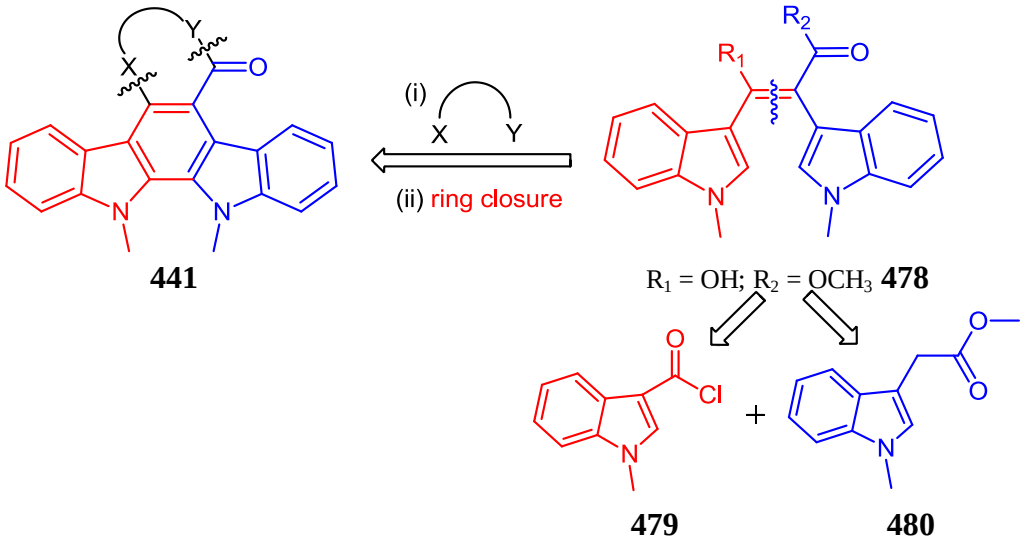


Fig. 4.2: Retrosynthetic strategy employed for design of novel indolocarbazoles

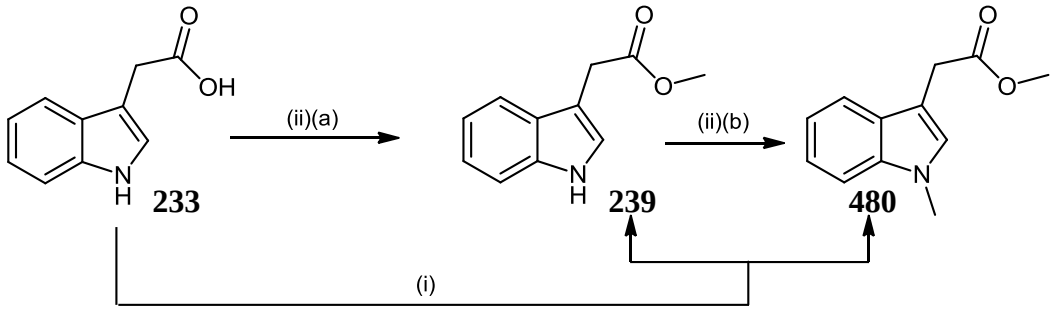
Initial investigation revealed that modification of pre-existing, classical indolocarbazole routes was impractical; a new strategy was devised, gaining access to advanced dicarbonyl precursors, prior to ring condensation and formation of the central carbocyclic ring, as final steps (Fig. 4.2). This putative route was also deemed attractive as a versatile method for the

preparation of unsymmetrically substituted indolocarbazoles, which are of keen interest within the research group. Chemical studies carried out to fully validate bi-nucleophile addition to an β-ketoester intermediate **478**, formed by condensation between **480** and **479**, as a viable new route to a panel of novel 5,6-bisindolylpyrimidin-4-ones will now be discussed.

4.4.1 Esterification of indole-3-acetic acid (IAA)

Starting from the commercially available indole-3-acetic acid **233**, the one-pot preparation of the *N*-methyl protected methyl indole-3-acetic acid ester **480**, as a dark yellow oil, was achieved in satisfactory yield of 82%, *via* use of dimethyl carbonate as methylating agent, along with potassium carbonate, stirred in dry DMF, at 130°C overnight.[30]

The conditions for this reaction were reported by Zhang *et al*. as a clean, efficient method, which avoided the use of toxic dimethyl sulfate or iodomethane, and avoided a two-step esterification/protection strategy.[30] The literature conditions were initially optimised, as a stoichiometric amount of potassium carbonate was used in our case, rather than the 50 mol% reported (due to reduction of yields of **480** to 45-50%, when those conditions prevailed), and the reaction time, at 130°C, was extended from 3 to 20 hours, in order to maximise conversion to the desired ester **480**. It was also determined that methyl indol-3-yl acetate **239** was formed as a recyclable side-product, in a proportion that could be minimised to approximately 10%, by employing **233** along with 3 equivalents of dimethyl carbonate (Scheme 4.10).



Reagents and conditions: (i) K_2CO_3, $(CH_3)_2CO_3$, DMF, 130°C, 12h, **480** = 82%, **239** = 10%; (ii)(a) $SOCl_2$, MeOH, -65°C – rt, 16h, **239** = 99%; (b) NaH, MeI, DMF, 0°C – rt, 16h, **480** = 92%

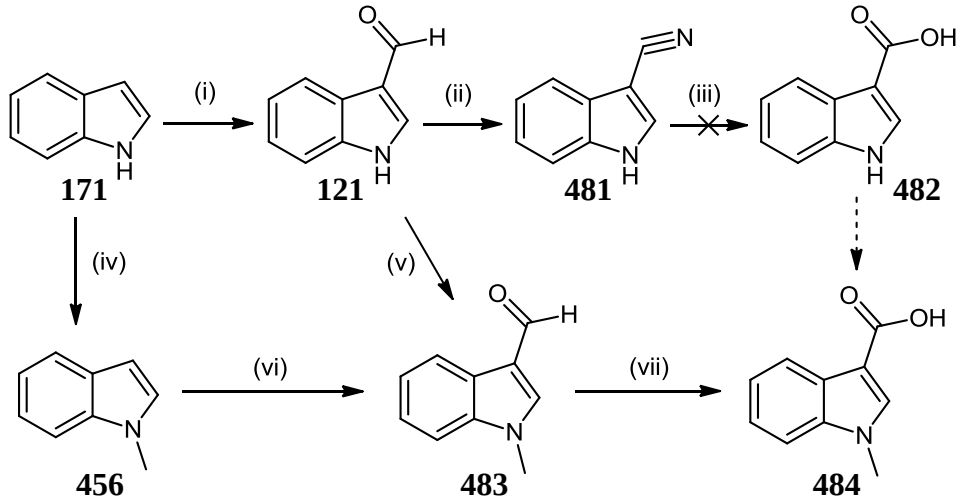
Scheme 4.10

The corresponding two-step sequence to the protected ester **480** involved reaction of acid **233** and thionyl chloride, in distilled methanol at −65°C for one hour, prior to warming to 20°C overnight, to form mono *O*-methylated **239** as a violet oil in a yield of 99%.

Alternatively, when this reaction was attempted at room temperature for 3 hours, a small amount of starting material persisted, leading to a poorer overall product profile. Intermediate **239** was then reacted with NaH, at 0°C, followed by addition of iodomethane, in dry DMF; stirring of the light green mixture at room temperature yielded ester **480**, isolated by chromatography, in an overall yield of 90% (Scheme 4.10).[31]

4.4.2 Synthesis of indole-3-carbonyl chloride

Following a series of literature preparations, synthesis of *N*-methyl indol-3-yl carbonyl chloride **479** began with the standard Vilsmeier-Haack formylation of indole **171** at the *C*-3 position, carried out by the addition of a solution of indole **171** in DMF at 5°C to a mixture of $POCl_3$ and DMF cooled to 0°C for 35 minutes. Following successive basification and acidification steps, the light orange crude indole-3-carboxaldehyde **121** was filtered and recrystallised as light-yellow needles, from a mixture of DMF/H_2O in a yield of 79% (Scheme 4.11). Formation of 3-cyanoindole **481** was carried out by reaction of aldehyde **121** with hydroxylamine hydrochloride, in DMF, at 90°C, for 15 minutes (61%).[32] However, derivative **481** could not be hydrolysed to the acid **482**, following heating under a range of strongly basic or acidic conditions, as determined by IR spectroscopy.



Reagents and conditions: (i) $POCl_3$, DMF, 0°C - 45°C, 2h, **121** = 79%; (ii) $NH_2OH.HCl$, DMF, 130°C, 16h, **481** = 61%; (iii) OH^- or H^+, Δ, 16h, n.r; (iv) K_2CO_3, $(CH_3)_2CO_3$, DMF, 130°C, 12h, **456** = 88%; (v) NaH/ MeI, DMF, 0°C - rt, 16h, **483** = 92%; (vi) $POCl_3$, DMF, 0°C - 45°C, 2h, **483** = 28%; (vii)(a) 40% aq. $KMnO_4$, acetone, rt, 16h; (b) H_2O_2, **484** = 83%

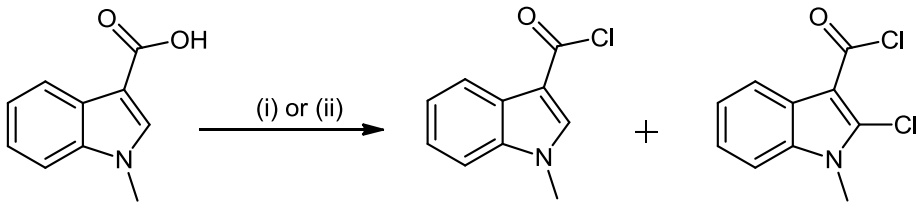
Scheme 4.11

As an alternative strategy, initial *N*-methylation of **121** was accomplished by NaH/MeI reaction, in order to afford *N*-methyl indol-3-yl carboxaldehyde **483** as a viscous dark oil (92%). The synthesis of this precursor **483** was also successful following treatment of indole

171 with potassium carbonate along with dimethyl carbonate, in DMF at 130°C for 5 hours, to provide *N*-methyl indole **456**, as a dark brown oil, in a yield of 88%. Formation of **483** could then be achieved by direct 3-formylation of **456,** under Vilsmeier-Haack conditions, in a yield of 28% for this step.[32] Oxidation of aldehyde **483** to the corresponding *N*-methyl indol-3-yl carboxylic acid **484** was attempted with sodium chlorite, stirred in 1,4-dioxane overnight, in the presence of TBAB, but this yielded only starting material **483** after 24 hours (Scheme 4.11).[33]

Fortunately, on stirring of aldehyde **483** with a 40% aqueous solution of potassium permanganate in acetone at 35°C for 20 hours, a dark mixture was obtained, from which *N*-methyl indol-3-yl carboxylic acid **484** was filtered as an off-white powder (83%), following acidic work-up and readily identified by its characteristic IR carbonyl stretch at 1750 cm^{-1}. Unfortunately, this reaction worked well at sub-gram scales but was not amenable to up-scaling, due to the use and disposal of large potassium permanganate/hydrogen peroxide volumes and subsequent low yields of product.

Synthesis of *N*-methyl indol-3-yl carbonyl chloride **479**, from **484**, in quantitative yield, was reported by Braña and co-workers, employing 20 equivalents of thionyl chloride as solvent, along with stirring of **484** for 24 hours, at ambient temperature (Scheme 4.12; Method A).[34] Under these conditions, an unusual chlorine fragmentation pattern in the mass spectrum of the resultant crude acid chloride **479** was observed, consistent with incorporation of another chlorine atom at the C-2 indole position. According to a literature procedure, this *N*-methyl 2-chloro indol-3-yl carbonyl chloride **485** derivative could be synthesised by heating of **484** in neat thionyl chloride, at 80°C for 24 hours prior to evaporation to a light red residue.[34] The appearance of this 2-chloro impurity **485**, in addition to **479**, at room temperature, in our work, suggests that regioselective temperature control of this step may be more problematic than initially proposed.



484 **479** **485**

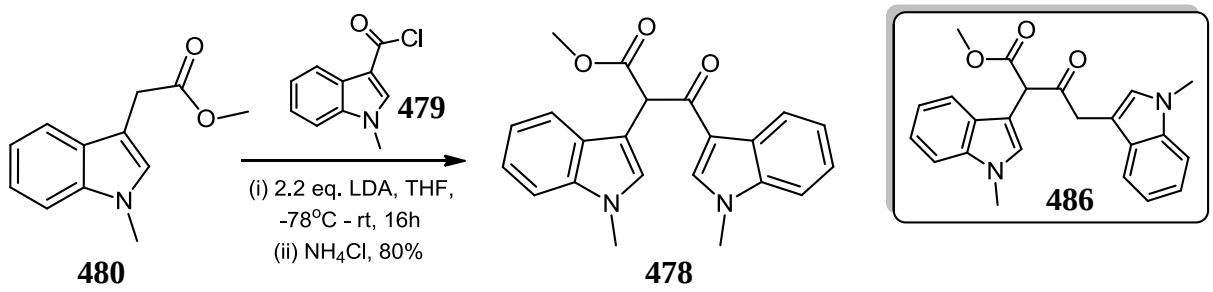
Reagents and conditions: Method A: (i) 20 eq. $SOCl_2$, rt, 24h, **479+485** = 99%; **Method B:** (ii) 1.1 eq. $COCl_2$, DCM, rt, 1.25h, **479** = 99%

Scheme 4.12

Future work in the research group may focus on the synthetic applications of this useful intermediate **485** as both an electrophile and novel halo-aryl substrate for palladium-mediated arylation chemistry.[35,36] In any case, this desired transformation was finally achieved under mild conditions, when the procedure of Hutchins *et al.* was adopted; **484** was thus successfully converted to **479**, abolishing any side-formation of **485**, in quantitative yield (99%), following stirring with oxalyl chloride in dry DCM, at room temperature, for 75 minutes (Scheme 4.12; Method B).[37] The resultant pink solid residue was used successfully in further reactions without any purification, and was identified by its characteristic IR carbonyl stretch which was altered from that in acid **484** to 1850 cm^{-1}.

4.4.3 Synthesis of 2,3-bisindolyl methyl-3-oxopropionate

Construction of the novel advanced β-dicarbonyl intermediate **478** was achieved *via* the α-deprotonated ester of **480**, which underwent modified Claisen reaction with **479** to yield the corresponding β-ketoester **478** (Scheme 4.13).



Scheme 4.13

A solution of the methyl ester **480** was slowly charged to a flask containing 2.2 equivalents of LDA in dry THF, maintained at −78°C; the resultant α-anion remained stable *in situ* at this temperature, while the dark mixture was allowed to stir for 90 minutes to ensure full deprotonation had occurred. Formation of the self-condensation side-product **486**, was effectively suppressed under these conditions, but it was observed that if an unreactive or poorly soluble electrophile was present under identical conditions, **486** could be detected in low yields (<10%). Fortunately, no solubility issues were encountered with acid chloride **479**, and a solution of **479** in THF was added dropwise over several minutes to the reaction vessel, while maintaining an internal temperature of below −65°C. The dark mixture was allowed to warm to room temperature over 16 hours, at which point the desired β-ketoester **478** was formed exclusively, in the absence of any starting **480**. Following work-up and

chromatography, product fractions were combined and evaporated to form a brown foam, which upon drying afforded title compound **478** as a golden crystalline solid (Scheme 4.13).

The optimisation protocols developed for this process are outlined below in Table 4.2. Following work carried out to investigate the conditions for this route, the anticipated reaction yield for this step was increased from 53%, as recently described for analogous literature conditions, to 80%.[34]

Table 4.2: Optimisation study of conditions employed in formation of 2,3-bisindolyl alkyl-3-oxopropionate (478)*

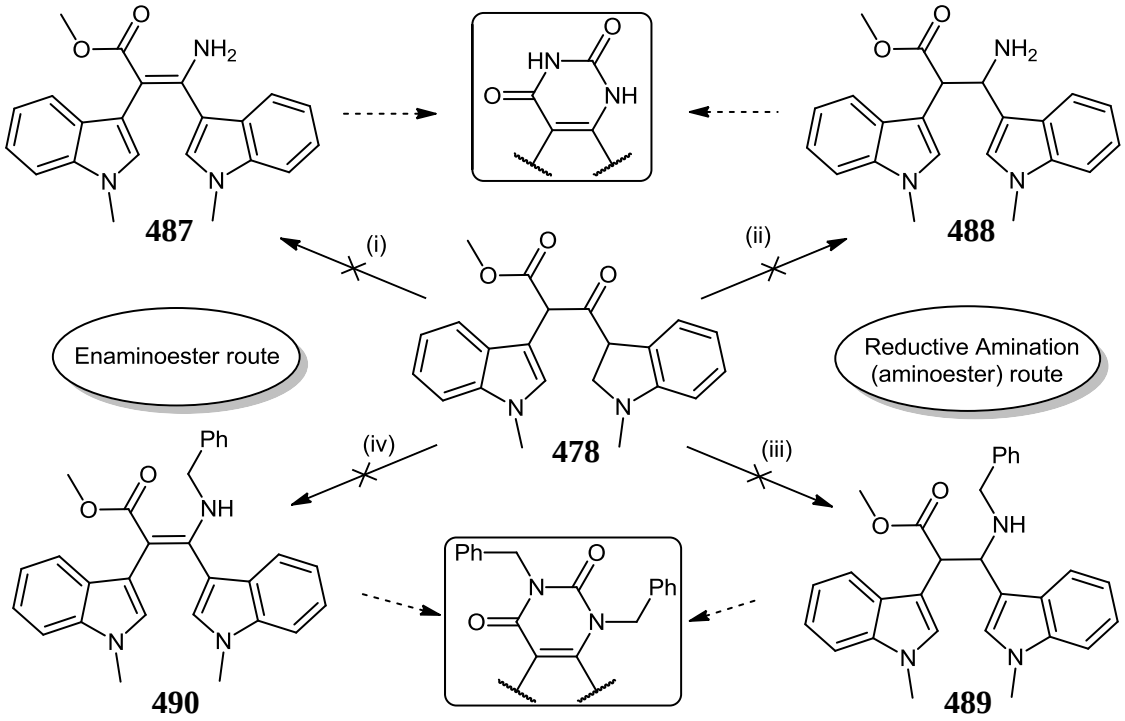
Reaction property	***Original conditions (lit.)[34]***	***Optimised conditions***
*Acid chloride **479** formation*	$SOCl_2$, rt, 24h	$(COCl)_2$, DCM, rt, 1.25h
*Ester **480** deprotonation; <-70°C*	1h	1.5h
Initial reactant concentration[#]	1 mmol: 4 mL THF	1 mmol: 1.8 mL THF
Aq. reaction quench (work-up)	H_2O	NH_4Cl/ H_2O
Rate of acid chloride addition[‡]	1.1 eq./ 30 min	1.3 eq./ 15 min
Chromatographic purification	30% ethyl acetate/ 70% hexane	10% - 100% ethyl acetate

* Reaction successfully performed up to 10 g scale (**480**); optimal yield (80%): 6 g ester **480**.
[#] Dilution of *N*-methyl methyl indole-3-acetic acid ester **480** in initial volume of THF, prior to addition of LDA.
[‡] Added as acid chloride **479** (1 g)/7 mL THF, based on full conversion of *N*-methyl indole-3-carboxylic acid **484**.

4.4.5 Attempted reductive amination

A number of reactions were carried out in order to convert β-ketoester **478** to its corresponding β-enaminoester **487**, *via* imine formation. Reaction of **478** with 10 equivalents of ammonium acetate in dry ethanol, was carried out in the presence of 1.1 equivalents of tetraethyl orthosilicate – a Lewis acid catalyst and water scavenger, shifting the equilibrium position of this reaction towards β-enaminoester **487** formation. Unfortunately, following heating for 24 hours, only starting material **478** could be detected (Scheme 4.14).

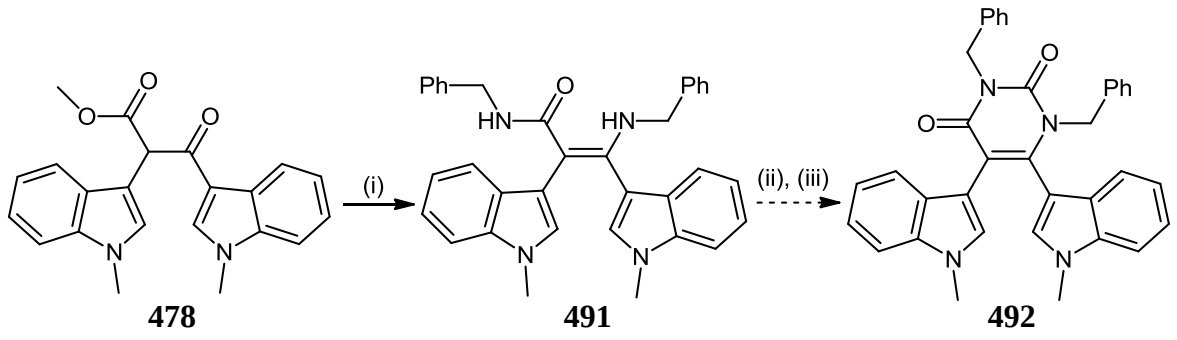
Similarly, reaction of **478** with 10 equivalents of ammonium acetate, stirred in ethanol, in the presence of 3 equivalents of sodium triacetoxyborohydride for 16 hours at reflux, afforded none of the reduced β-aminoester **488**. Reaction with benzylamine under identical reductive amination conditions, yielded only starting material **478**, in the absence of anticipated **489**, following heating for 24 hours.



Reagents and conditions: (i) 10 eq. NH_4OAc, 1.1 eq. $Si(OEt)_4$, EtOH, N_2, Δ, 24h; (ii) 10 eq. NH_4OAc, 3 eq. $NaBH(OAc)_3$, EtOH, N_2, Δ, 16h; (iii) 10 eq. Bn-NH_2, 3 eq. $NaBH(OAc)_3$, EtOH, Δ, 16h; (iv) 10 eq. Bn-NH_2, 1.1 eq. $Si(OEt)_4$, EtOH, Δ, 24h

Scheme 4.14

Interestingly, when β-ketoester **478** was heated in neat benzylamine along with a catalytic amount of tetraethyl orthosilicate overnight in order to produce **490**, starting material **478** was fully consumed, along with appearance of a dark brown, fluorescent material with a significantly higher Rf value (Scheme 4.15). This property was consistent with incorporation of aromatic substituents and corresponded to formation of the dibenzyl protected analogue **491**, as confirmed by HRMS analysis (m/z = 525).



Reagents and conditions: 1 eq. $Si(OEt)_4$, Bn-NH_2, 120°C, 16h, **491** = 50%; (ii) 1 eq. $(CCl_3)_2CO_3$, DCE, 80°C, 24h; (iii) NH_2CONH_2, 170°C, 20h

Scheme 4.15

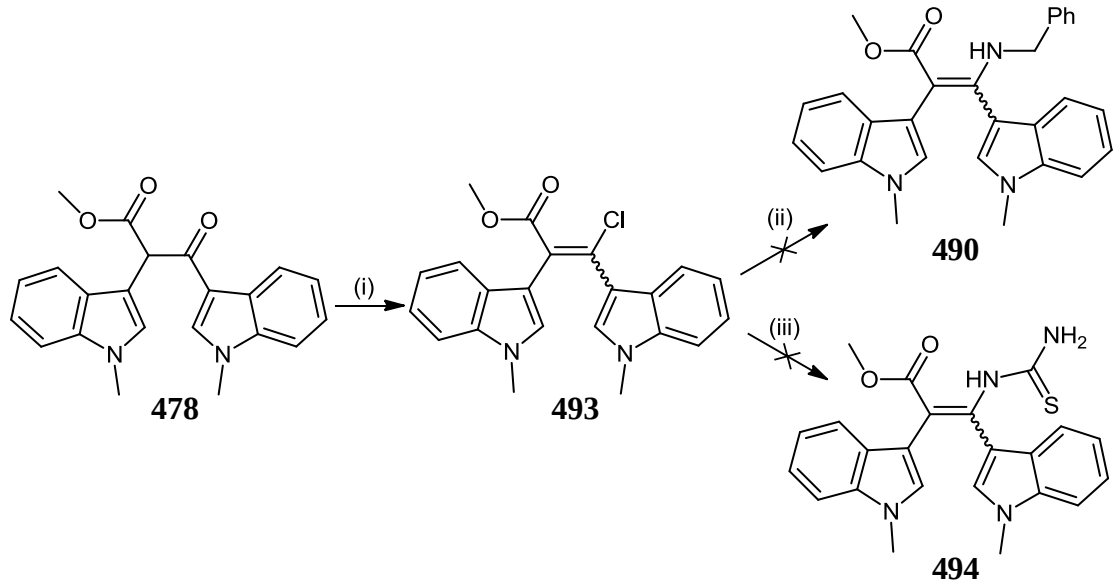
Unfortunately, β-enaminoamide **491** could not be isolated pure, as a result of its decomposition during silica gel chromatography. Reaction of crude **491** with 1 equivalent of

triphosgene (a safer, solid alternative to the use of gaseous phosgene), in 1,2-dichloroethane, at 80°C, for 24 hours, could not successfully form any of the desired 1,3-benzylated uracil analogue **492**.[38] Reaction of **491** under solvent-free conditions along with urea at 170°C similarly yielded only decomposition products. However, future applications of this approach to related systems may provide an accessible route to new compounds. Application of new electrophiles and further investigation of the stability of these enaminoamide synthetic intermediates will also be necessary.

4.4.6 Synthesis of methyl 3-chloro-2,3-bisindolylacrylate

In order to modulate the apparent limited reactivity of the ketoester nucleus, a strategy was adopted whereby **478** was converted to novel β-chloroacrylate **493**, formed as an inseparable mixture of *E* and *Z*-isomers as identified by NMR analysis, in a yield of 65%, following reaction with PCl_5, in DMF overnight at 110°C (Scheme 4.16).

As the stated synthetic goals necessitated introduction of heterocyclic character into an advanced bisindolyl precursor, modification of this intermediate **493** was attempted by heating with benzylamine to form **490** or thiourea in order to afford **494**; however, only starting material **493** could be recovered in each case. Reactivity at the β-chloro site is postulated to be diminished due to the bulk steric effects of both indolyl substituents blocking access to the electrophilic sp^2 carbon centre. Future work will also employ superior nucleophiles in order to maximise reactivity. In this regard, utilisation of reactants such as hydrazine or azide may proffer distinct advantages in pursuing the full potential of this route.



Reagents and conditions: (i) 1.5 eq. PCl_5, DMF, 110°C, 20h, **493** = 65%; (ii) 5 eq. Bn-NH_2, Et_3N, EtOH, reflux, 24h; (iii) 2.2 eq. NH_2CSNH_2, Et_3N, EtOH, reflux, 24h

Scheme 4.16

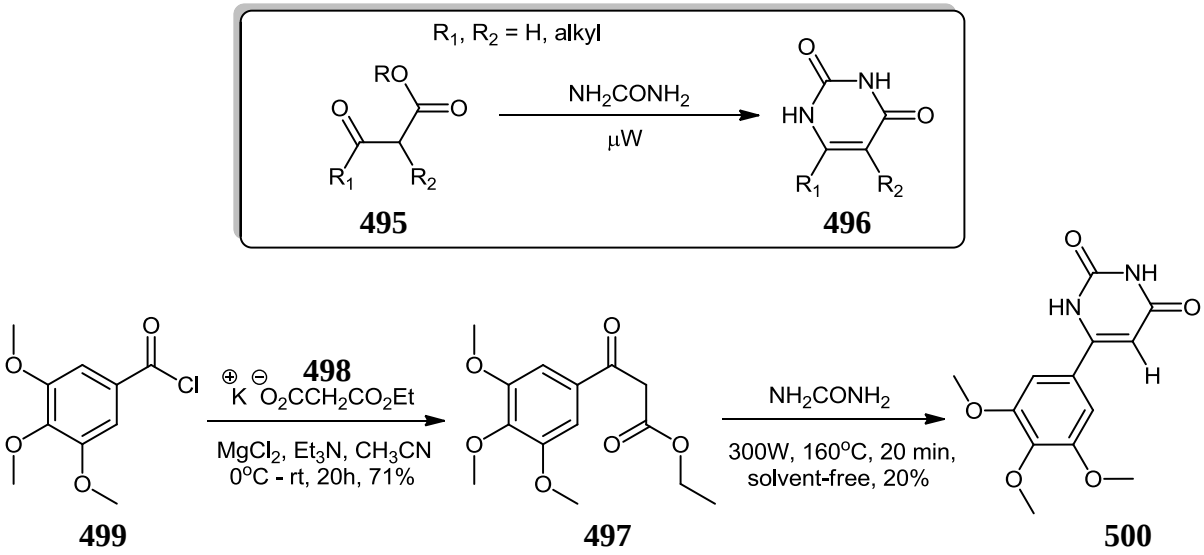
4.5 Cyclocondensation with urea

Employing urea as a primary nucleophile, conditions for corresponding uracil synthesis were studied under a range of conditions, in the presence of electrophilic bisindolyl derivatives. As discussed, solvent-free thermal heating of urea along with β-enaminoamide **491** was unsuccessful, and thus, similar conversion of dicarbonyl intermediates by efficient microwave heating, and thermal heating of urea in the presence of base were investigated.

4.5.1 Attempted microwave-mediated synthesis of uracils

The primary method for converting a nominal alkyl β-ketoester **495** to the corresponding pyrimidin-2,4-dione **496** moiety involves exposure of the substrate to either urea or thiourea, in the presence of sodium alkoxide in alcohol, and heating of this mixture for an extended period.[39,40] Microwave-assisted organic synthesis (MAOS) represents a recent alternative to conventional (convection) heating, and constitutes an important new methodology in the area of heterocycle synthesis, with a major advantage deriving from efficient thermal heating and enhanced concentration effects. Therefore, yields and impurity profiles can be improved across a range of reaction types, while reaction times are also typically short. In 2002, it was first reported that simple β-ketoester **495** precursors could be transformed directly to the respective 5,6-alkyl substituted uracils **496** by conventional microwave irradiation in the presence of urea, under solvent-free conditions.[41]

Unfortunately, successful reaction conditions could not be easily prescribed for development of a robust, versatile microwave protocol, due to the quite disparate nature of the 5,6-alkyl substituents in the study by Mojtahedi *et al.*, and so the versatility of this technique to allow formation of 5,6-bis(aryl) pyrimidin-2,4-diones such as **464** remains uncertain.[41]



Scheme 4.17

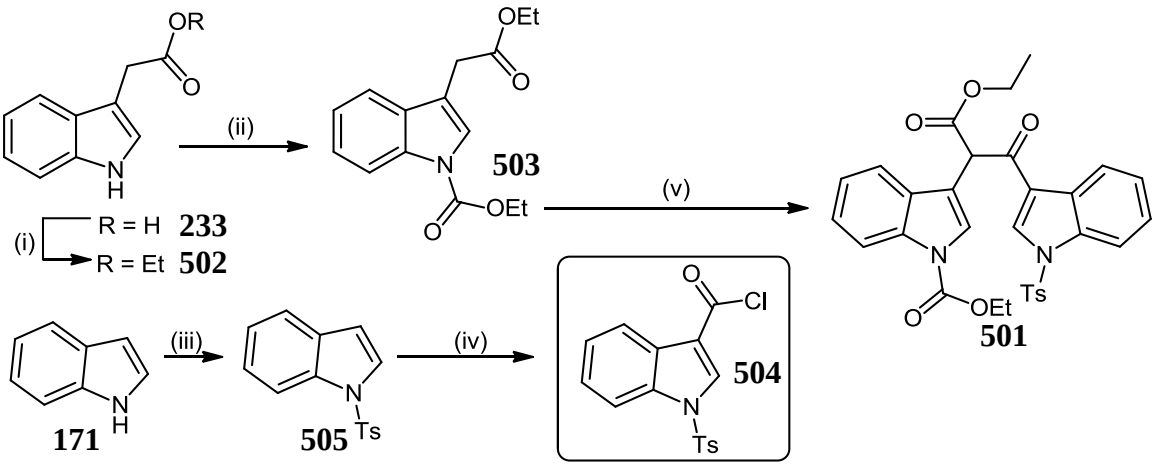
Preliminary data indicates that this method may be fruitful, but possesses critical limitations including thermal decomposition, low electrophilic reactivity and poor reaction reproducibility.

In order to validate this microwave route, the synthesis of novel 3,4,5-trimethoxyphenyl ethyl 3-oxoalkanoate **497** was carried out and its reactivity under trial microwave conditions was investigated. Following initial KOH-mediated conversion of diethyl malonate to potassium monoethyl malonate **498**, 2 equivalents of this salt were then stirred at 15^{o}C in acetonitrile, along with triethylamine and anhydrous magnesium chloride, at which point the suspension was warmed to room temperature and maintained for 2.5 hours. The resultant milky slurry was cooled to 0^{o}C and a solution of 3,4,5-trimethoxybenzoyl chloride **499** in acetonitrile was added dropwise over 15 minutes. Following further triethylamine addition, the reaction mixture was then stirred for 20 hours at room temperature. Following acidic work-up, novel β-ketoester **497** was isolated as an off-white solid in a yield of 71% (Scheme 4.17).

Employing harsh microwave conditions, intermediate **497** was pre-mixed with 5 equivalents of urea, and heated under solvent-free conditions, at a power level of 300W, at 170°C for 25 minutes, including a 5 minute ramp time. On completion, the resultant urea 'melt' was dissolved in water; the resultant white crystalline precipitate was then filtered and washed with diethyl ether in order to fully eliminate starting material **497**. Following recrystallisation from absolute ethanol, novel 6-(3,4,5-trimethoxyphenyl)uracil **500** was successfully isolated in high purity, as an off-white crystalline solid, in a moderate yield of 20% (Scheme 4.17).

4.5.2 Reaction of urea with β-ketoesters in routes to 5,6-bisindolyluracils

Following this initial success, synthesis of a novel bisindolyl β-ketoester derivative **501** containing labile protecting groups was carried out, as an analogous substrate for pyrimidin-2,4-dione ring formation. Ethyl indol-3-yl acetate **502** was simply derived from the corresponding indole-3-acetic acid **233**, which was initially stirred in dry ethanol, in the presence of thionyl chloride, at -60°C, and then allowed to warm to 20^{o}C overnight. Protection of the indolic nitrogen of ester **502** was then completed under phase-transfer conditions. Conversion to *N*-carbamate ester **503**, was accomplished by treatment with aqueous NaOH in DCM, in the presence of ethyl chloroformate, along with catalytic TBAB, and then stirred at 0^{o}C for one hour, prior to warming to room temperature overnight. The crude residue was then purified to afford **503** as a colourless oil in 76% yield (Scheme 4.18).[42]



Reagents and conditions: (i) $SOCl_2$, dry EtOH, -78°C - rt, 16h, **502** = quant; (ii) 1.1 eq. $ClCO_2Et$, 30% aq. NaOH, cat. TBAB, DCM, 0°C - rt, 16h, **503** = 76%; (iii) 1.5 eq. *p*-$TolSO_2Cl$, 50% aq. NaOH, 0.2 eq. TBAHS, toluene, 0°C - rt, 16h, **505** = 96%; (iv) 3 eq. $(COCl)_2$, 1 eq. $AlCl_3$, DCM, 0°C - 20°C, 3h, **504** = quant; (v) 2.2 eq. 1.8M LDA, **504**, THF, -78°C - rt, 20h, **501** = 25%.

Scheme 4.18

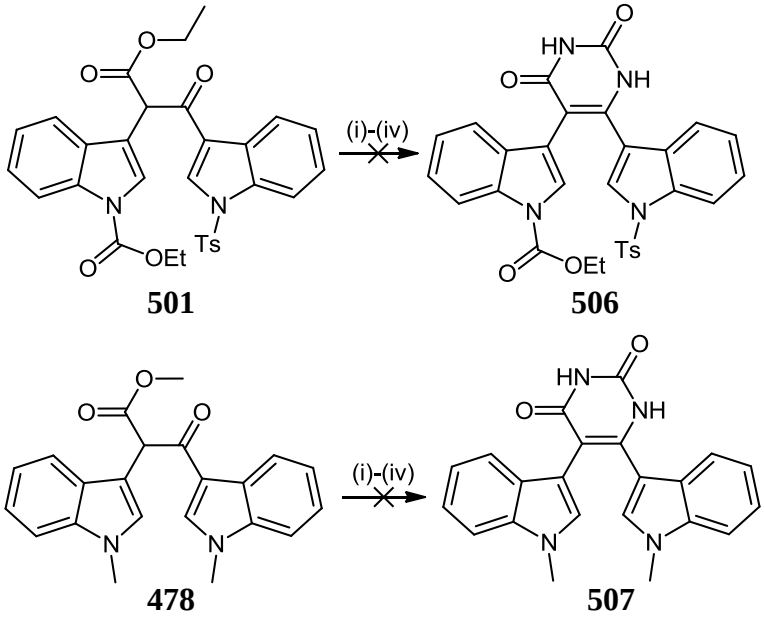
Synthesis of *N*-toluenesulfonyl indole-3-carbonyl chloride **504** required initial formation of *p*-toluenesulfonyl indole **505**, by addition of a 50% aqueous NaOH solution to indole **171**, which was stirred in toluene, in the presence of TBAHS. *p*-Toluenesulfonyl chloride was then added to the mixture at 0°C, prior to stirring at room temperature overnight. On work-up, *p*-toluenesulfonyl indole **505** was identified by means of its characteristic IR spectroscopic SO_2 bond stretches at 1168 and 1379 cm^{-1} and was isolated as a light pink solid in a yield of 96%. Under Friedel-Crafts conditions, acid chloride **504** was formed quantitatively, upon addition of **505** to a mixture of 3 equivalents of oxalyl chloride and $AlCl_3$ stirred at 0°C and stirring of the subsequent black suspension for a further 3 hours at room temperature. The crude acid chloride **504** was isolated as a viscous brown oil following work-up, and was used directly in the following step (Scheme 4.18).[43,44]

The corresponding bisindolyl β-ketoester **501** was isolated as a light brown crystalline solid in a yield of 25%, by reaction of precursors **503** and **504** under optimised Claisen conditions, followed by ammonium chloride quench. Purification of crude **501** could be effected either by ethyl acetate/ hexane column chromatography or by direct crystallisation from a mixture of 95% ethanol and water.

Unfortunately, the success of microwave reaction for simple alkyl (**495**) and monoaryl (**497**) compounds to afford corresponding pyrimidine-2,4-diones **496** and **500** respectively, could not be replicated for **501** following solvent-free microwave heating with urea at 150°C for 20 minutes (Scheme 4.19). The dark brown reaction 'melt' was not found to contain any uracil

506, but a mixture of starting material and assorted decomposition products formed by loss of the cleavable carbamate and tosyl *N*-protecting groups. The desired transformation also did not occur when these reactants were subjected to conventional heating at reflux for 16 hours in ethanol, in the presence of excess sodium ethoxide. Alternatively, microwave irradiation of **478** in the presence of 10 equivalents of urea avoided certain limitations due to incorporation of very stable *N*-methyl groups, but also failed to yield any trace of the anticipated pyrimidin-2,4-dione product **507** (Scheme 4.19).

Unfortunately, application of *p*-TSA and camphoric acid, in order to activate the reactant towards nucleophilic urea attack also failed to yield benefits for this microwave synthesis.



501 **506**

478 **507**

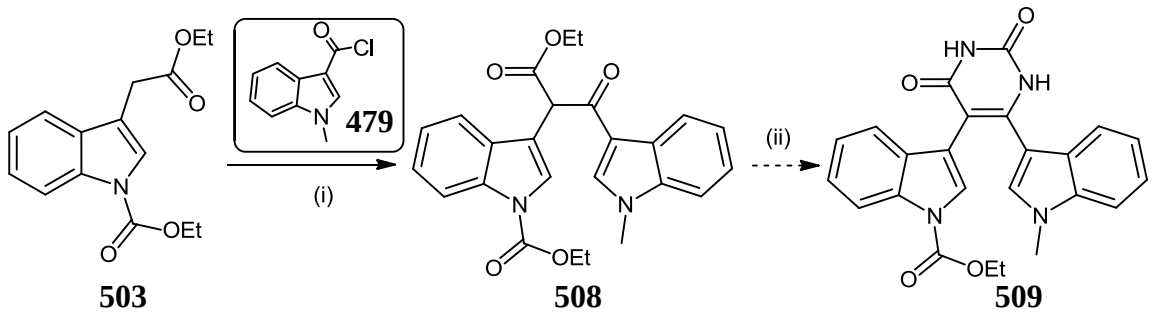
Reagents and conditions: (i) 10 eq. NH_2CONH_2, 300W, 160°C, 20 min (μW); (ii) 10 eq. NH_2CONH_2, 300W, 160°C, 2.2 eq. camphoric acid, 20 min (μW); (iii) 10 eq. NH_2CONH_2, 2.2 eq. *p*-TSA, 300W, 160°C, 20 min (μW); (iv) 10 eq. NH_2CONH_2, NaOMe, MeOH, reflux, 16h

Scheme 4.19

Under forcing microwave conditions, heating of excess urea along with **478** and 2.2 equivalents of acid resulted in only decomposition in each case, and it was evident that under harsh conditions, side-reactions predominate over the desired cyclisation process (Scheme 4.19). Interestingly, reaction of an alternative protected β-ketoester **508**, derived from base-mediated reaction of **479** and **503** (with reduced conformational and steric bulk compared to **501**) employing optimised microwave settings, with 10 equivalents of urea and 2.2 equivalents of *p*-TSA, under solvent-free conditions resulted in isolation of a trace amount of the desired uracil derivative **509**, as identified by mass spectroscopic analysis, along with

disappearance of the characteristic β-ketoester α-proton in the crude ^{1}H spectrum in the region of 5.7 ppm (Scheme 4.20).

This reaction has been found to be relatively non-reproducible, largely due to the capricious nature of a 'reaction melt', and whether these intense conditions can suppress decomposition pathways relative to attractive product formation. Future work in this area will optimise individual reaction parameters in order to yield a single-step, versatile and robust method for gaining access to novel heterocyclic analogues, following this template. In the next section, the thermal reactivity of more nucleophilic bidentate nitrogen nucleophiles will be thoroughly explored, in the context of fully realising the rich potential of transformations of this type.



Reagents and conditions: (i) 2.2 eq. 1.8M LDA, THF, -78°C - rt, 20h, **508** = 34% (ii) 10 eq. NH_2CONH_2, 2.2 eq. *p*-TSA, 300W, 160°C, 20 min (μW)

Scheme 4.20

4.6 Other cyclocondensations in routes to bisindolyl heterocycles[45]

In pursuit of the synthesis of new bioactive 1,2-bisindolyl-*cis*-ethene heterocycles with novel bridgehead functionality (general structure **441**), development of cyclocondensation chemistry involving bisindolyl dicarbonyl intermediate **478** was deemed highly attractive. Following initial indication of the poor reactivity of urea as a potential nitrogen nucleophile, comprehensive studies into the utility of a panel of substituted urea analogues to produce novel conversions of this type were undertaken (Fig. 4.3).

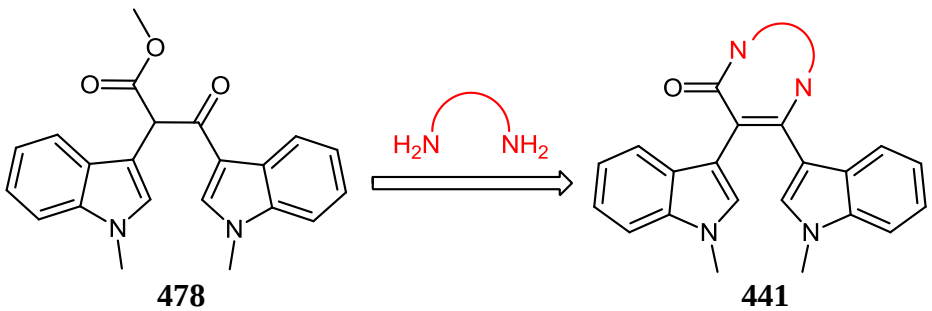
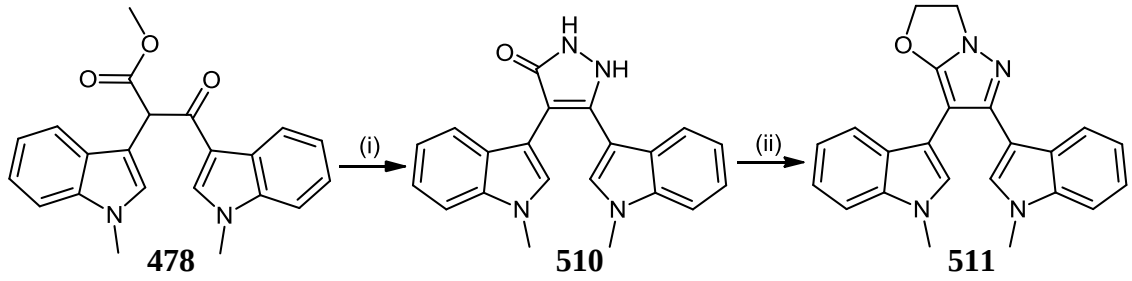


Fig. 4.3

4.6.1 Reaction with hydrazines

4.6.1.1 Synthesis of pyrazolone derivatives

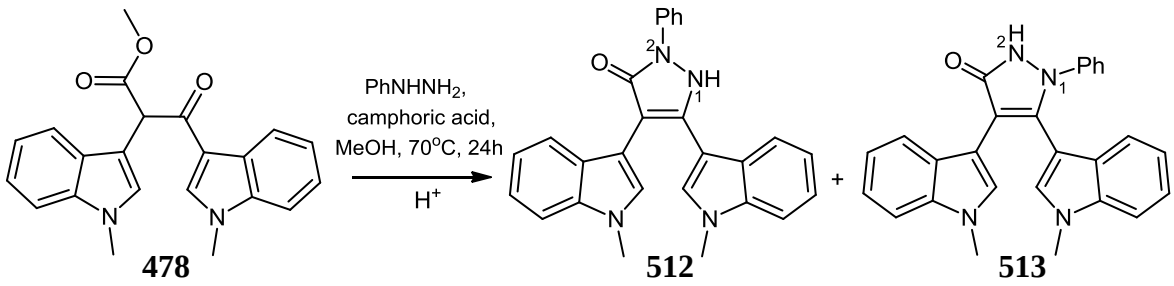
During the course of this work, conditions for the efficient synthesis of 4,5-bisindolyl pyrazol-3-one **510** from reaction of the ethyl ester derivative of **478** with hydrazine were reported by Braña and co-workers, following their research into potential anti-cancer activity within *N*,*N*-diethylaminoalkyl *O*-substituted analogues derived from Mitsunobu reaction of parent diarylpyrazolones.[34] As an initial test reaction in our study, β-ketoester **478** was stirred along with hydrazine hydrate and camphoric acid, at reflux temperature for 3 hours, prior to addition of excess hydrazine hydrate and subsequent heating for 21 hours. Chromatography afforded the fluorescent, polar pyrazolone product **510** as a grey crystalline product in a yield of 68%. The *N*,*O*-cycloalkylated product **511** was synthesised in 57% yield under mild conditions following treatment of **510** in 1,4-dioxane, containing potassium carbonate, 1,2-dibromoethane and TBAB, at 30°C for 20 hours.[46] Novel heterocyclic derivative **511** was then isolated as a pale yellow solid yield of 55% (Scheme 4.21).



Reagents and conditions: (i) 4 eq. $NH_2NH_2.H_2O$, 1 eq. camphoric acid, MeOH, reflux, 24h, **510** = 68%; (ii) 2.5 eq. K_2CO_3, 1.2 eq. $BrCH_2CH_2Br$, 1,4-dioxane, 30°C, 20h, **511** = 57%

Scheme 4.21

Reaction of β-ketoester **478** with phenylhydrazine under identical conditions resulted in successful formation of an inseparable isomeric mixture of novel *N*-phenyl substituted pyrazolone analogues (**512**, **513**) in overall 65% yield, with product distribution under thermodynamic control. NMR studies illustrated that compounds **512** and **513** were formed in the ratio of approximately 2:1, under these reaction conditions (Scheme 4.22).

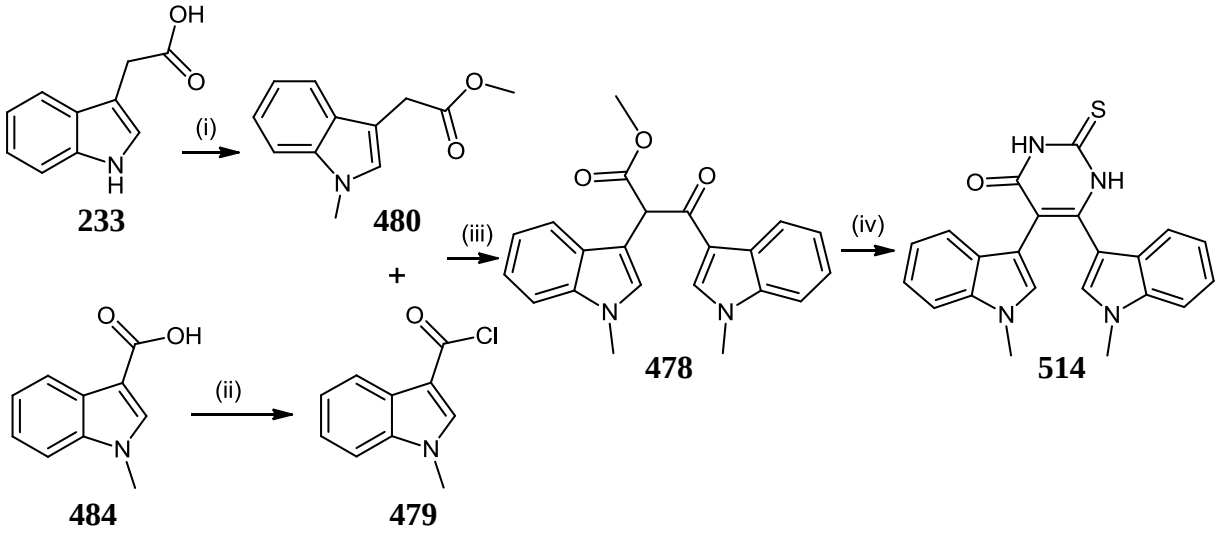


Scheme 4.22

4.6.2 Reaction with thiourea

4.6.2.1 Formation of 5,6-bisindolyl-2-thiopyrimidin-4-one

As a landmark reaction, 2,3-bisindolyl methyl-3-oxopropionate **478** was successfully converted, in the presence of methanolic sodium methoxide (10 equivalents) and excess thiourea (5 equivalents), to the corresponding novel thiouracil **514**, following reflux for 24 hours. On solvent removal, the crude gummy residue was suspended in water and acidified to pH 3 with 10% aq. HCl solution. Gravity filtration of the resultant aqueous slurry was inefficient and time-consuming, due to the gummy nature of the dark-orange precipitate. Fortunately, it was subsequently observed that decanting of the supernatant layer in place of filtration was successful, even on multi-gram scale (Scheme 4.23).



Reagents and conditions: (i) 1 eq. K_2CO_3, 3 eq. $(CH_3)_2CO_3$, DMF, 130°C, 12h, **480** = 82%; (ii)(a) 1.1 eq. $(COCl)_2$, DCM, 75 min, **479** = 100%; (iii)(a) 2.2 eq. LDA, 1.5 eq. **479**, THF, -78°C - rt, 16h, (b) NH_4Cl/ H_2O, **478** = 80%, (iv) 10 eq. NaOMe, 5 eq. NH_2CSNH_2, MeOH, reflux, (b) 10% HCl, **514** = 24%.

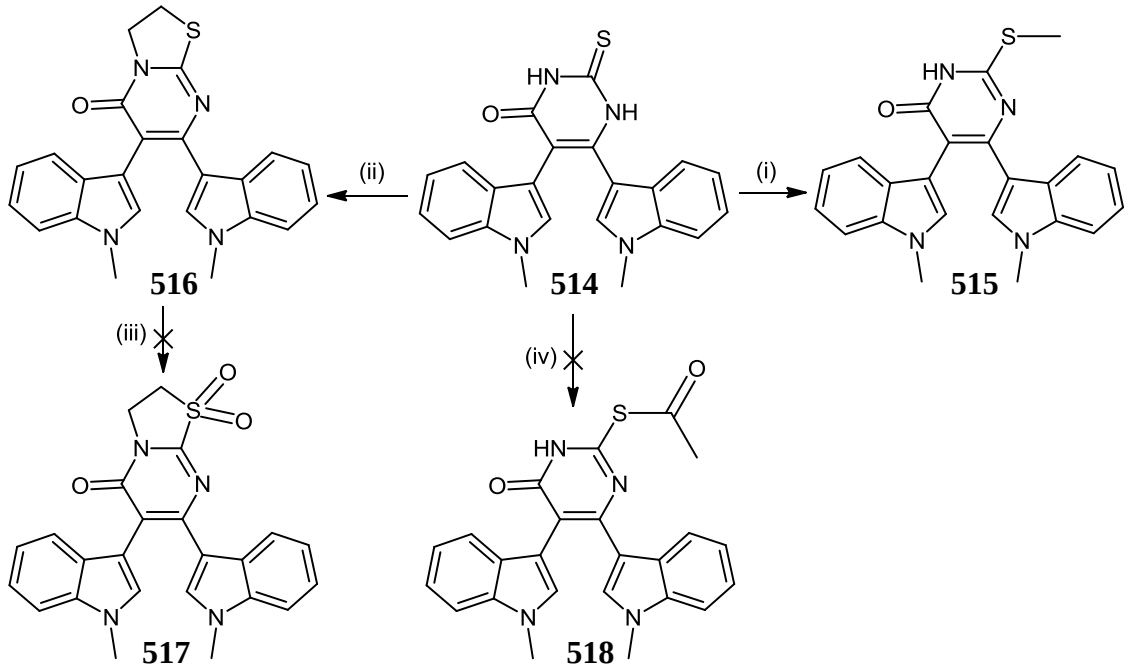
Scheme 4.23

Initial purification of target compound **514** could be achieved by chromatography employing DCM/methanol as eluent. Fortunately, in the course of process optimisation, it was found that trituration of crude **514** with boiling absolute ethanol, prior to cooling to 35°C, obviated any need for chromatography, and novel **514**, could be isolated pure, as a pale yellow powder, following filtration of the dark brown slurry and washing with diethyl ether (Scheme 4.23). The overall yield for this reaction was found to be 20-24%, irrespective of whether the reaction time was extended to 72 hours or if a larger excess of base (20 equivalents) was employed.

4.6.2.2 Derivatisation of 5,6-bisindolyl-2-thiopyrimidin-4-one

In order to resolve principal difficulties associated with the poor organic solubility of the parent thiopyrimidinone **514,** it was established that a panel of alkylated analogues could be synthesised under extremely mild phase-transfer conditions (Scheme 4.24).[46]

Reaction of title compound **514** with iodomethane in methanol stirred at 30°C, in the presence of potassium carbonate isolated sulfide **515** as a straw-coloured powder in a moderate yield of 35% following chromatography.



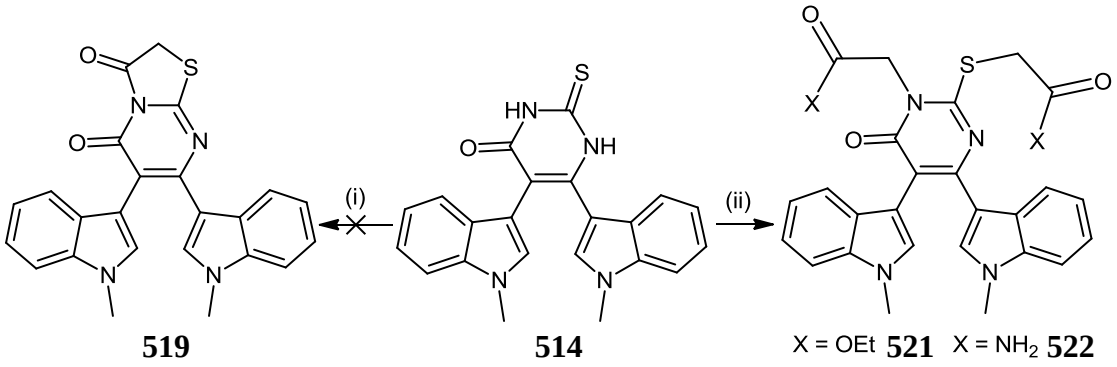
Reagents and conditions: (i) 1.2 eq. CH_3I, 1.5 eq. K_2CO_3, MeOH, 30°C, 20h, **515** = 35%; (ii) 1.1 eq. $Br(CH_2)_2Br$, 3 eq. K_2CO_3, cat. TBAB, 1,4-dioxane, rt, 16h, **516** = 66%; (iii) 20 eq. *m*-CPBA, DCM, reflux, 72h; (iv) 1.5 eq. $(CH_3CO)_2O$, C_6H_5N, 90°C, 20h

Scheme 4.24

Thiouracil **514** was also reacted with 1,2-dibromoethane in the presence of potassium carbonate and TBAB, for 16 hours, at room temperature, to yield thiazolo[3,2-*a*]pyrimidin-5-one **516**; this was identified to be the *S,N*-dialkylated derivative due to the characteristic amide carbonyl absorption occurring at 1644 cm^{-1}. Following washing of the crude residue with hexane in order to remove unreacted 1,2-dibromoethane and crystallisation with 95% ethanol, **516** was isolated as an amorphous yellow powder in 66% yield. Attempted oxidation of **516** to the sulfone **517** following reaction in DCM, in the presence of excess *m*-CPBA did not proceed even after 3 days at elevated temperature.

The thioacetylated compound **518** could not be formed, perhaps due to instability and *in situ* deacetyation of the initially formed derivative, following heating of parent thiouracil **514** with acetic anhydride in pyridine, at 90°C.

Interestingly, the corresponding synthesis of a lactam derivative **519** by reaction of **514** with chloroacetyl chloride **520** under identical conditions as for synthesis of **516**, was unsuccessful. Similarly, reaction of ethyl bromoacetate failed to form any of the anticipated thiazolidinone **519**, but instead afforded the novel bisalkylated congener **521** (Scheme 4.25, (ii); X = OEt) in a yield of 45%. Employing this insight, synthesis of the *S,N*-bisacetamido-thiouracil **522** (Scheme 4.25, (ii); X = NH_2), was also effected in a yield of 40%, following reaction of **514** with α-chloroacetamide **523**, a light beige solid, initially prepared by treatment of chloroacetyl chloride **520** with aqueous ammonia, for 16 hours.



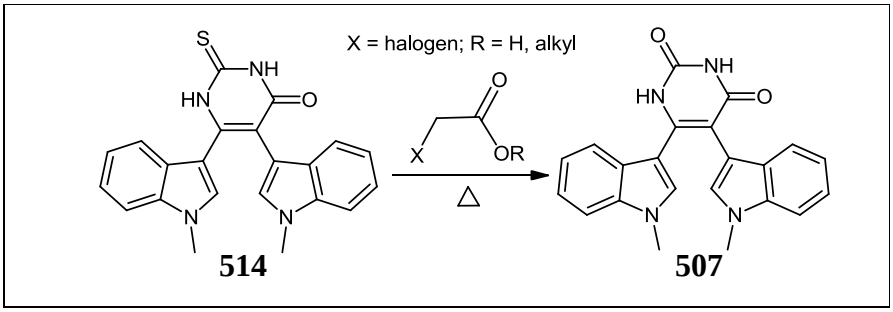
Reagents and conditions: (i) 2.2 eq. $ClCH_2COCl$ (**520)**, 3.5 eq. K_2CO_3, cat. TBAB, 1,4-dioxane, rt, 16h, (ii) 2.2 eq. $BrCH_2CO_2Et$ or $ClCH_2CONH_2$ (**523)**, 3.5 eq. K_2CO_3, cat. TBAB, 1,4-dioxane, rt, 16h , **521** = 45%, **522** = 40%

Scheme 4.25

4.6.3 Thiouracil derivatisation routes to 5,6-bisindolylpyrimidin-2,4-dione

Chemistry was undertaken in order to convert thiouracil **514,** to the attractive pyrimidine-2,4-dione or uracil ring system **507**, which is present in several drug families, e.g. pyrimidine anti-metabolites and barbiturates, and whose design was envisaged as a bioisosteric replacement of the lactam ring/imide motifs (Section 3.0, Aims and Objectives).[47-52] Surprisingly, as far as we are aware, this was the first investigation of the necessary conditions for converting a 5,6-bis(heteroaryl)-2-thiopyrimidin-4-one substrate to the corresponding 5,6-bis(heteroaryl)pyrimidin-2,4-dione. This transformation involved considerable optimisation, with solvent choice being critical; the issue of reaction heterogeneity impaired this process until the final resolution was achieved. A summary of some oxidative conditions which were investigated for this transformation, and the results of these runs are outlined in Table 4.3.

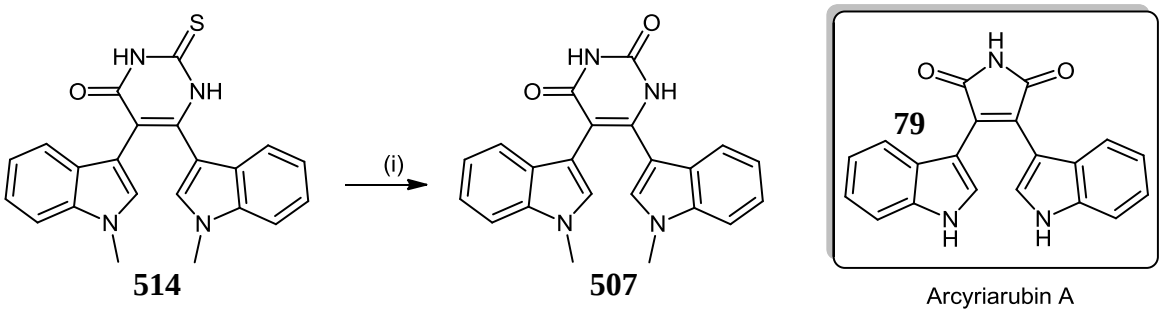
Table 4.3: Study of conditions for conversion of 2-thiopyrimidin-4-one (514) to pyrimidin-2,4-dione (507)



Reagent	*Quantity*	*Solvent*	*Conditions*	*Product formation*	
				514	**507**
$ClCH_2CO_2H$	10% w/v	H_2O	72h/ reflux	√	√
$ClCH_2CO_2H$	10% w/v	AcOH	72h/ reflux	√	√
$ClCH_2CO_2H$	10% w/v	DMF	72h/ 110°C	√	√
$ClCH_2CO_2H$	5 eq.	MeOH	72h/ reflux	√	-
aq. H_2O_2	30% w/v	H_2O	20h/ 70°C	√	-
$BrCH_2CO_2Et$	1.1 eq.	MeOH	20h/ reflux	-	**17%**
$BrCH_2CO_2Et$	1.5 eq.	DMF	24h/ 110°C	√	-
$BrCH_2CO_2Et$	2.5 eq.	$MeOH/H_2O$	48h/ reflux	-	**45%**

Based on previous literature, this conversion, known as oxidative desulfurisation, is known to be carried out under aqueous oxidative conditions, in the presence of 10% w/v chloroacetic acid, at high temperatures, to routinely convert simple 5,6-alkyl substituted thiouracils to the corresponding uracils in moderate to excellent yields.[53] Unfortunately, aqueous chloroacetic acid could not effect full conversion of thiouracil **514** to the desired pyrimidin-2,4-dione **507**, even with a prolonged reflux of 72 hours. In most cases, only inseparable product mixtures were formed – displaying a set of characteristic peaks from ^{13}C NMR corresponding to both compounds, thiouracil (**514**): 161.3 and 174.3 ppm, and uracil (**507**): 151.1 and 164.3 ppm, and also confirmed by mass spectrometry (see Section 4.8). It was postulated that heterogeneous conditions prevented full conversion of the sulfur analogue **514** to the desired **507**, and even when solvent conditions were changed to increase thiouracil **514** solubility (DMF, methanol), the non-aqueous conditions then seemed to inhibit the oxidative desulfurisation process. Utilisation of 30% aqueous hydrogen peroxide as an alternative oxidant yielded only starting material following heating at 70°C overnight (Table 4.3).

However, following an intensive study, it was discovered that the use of a stoichiometric quantity of ethyl bromoacetate - an alternative α-haloacetic acid derivative and a liquid reagent at room temperature, in dry methanol, which was heated at reflux for 16 hours, yielded the product **507**, exclusively, in a moderate yield of 17%, following recrystallisation from a mixture of DMF/H_2O (5:1).[54] This process was improved by heating 2.5 equivalents of ethyl bromoacetate in the presence of thiouracil **514**, in methanol containing a few drops of water, for 48 hours. Following solvent removal, the residue was crystallised to yield uracil **507** exclusively in an enhanced yield of 45% (Scheme 4.26).



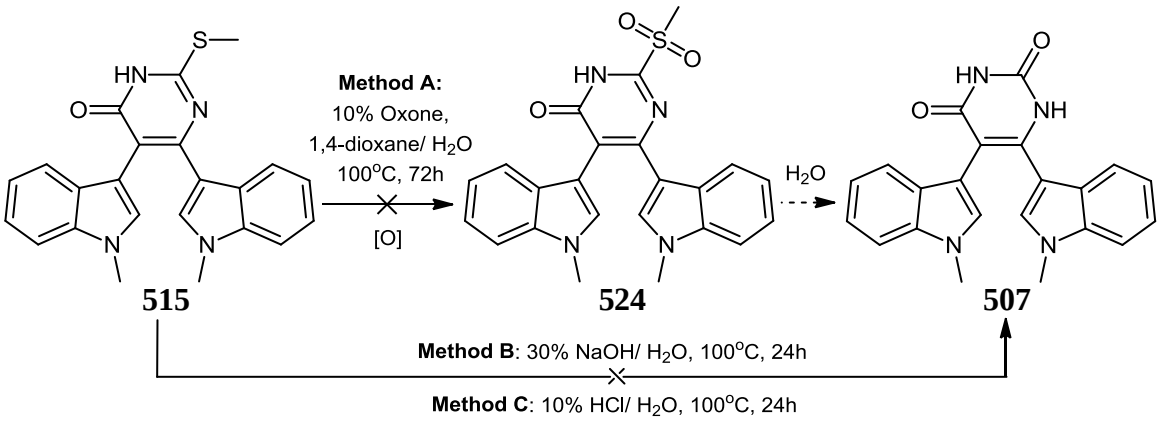
514 **507**

Reagents and conditions: (i)(a) 2.5 eq. $BrCH_2CO_2Et$, MeOH, reflux, 48h, (b) H_2O, **507** = 45%

Scheme 4.26

As an alternative strategy, the hydrolytic conversion of *S*-methylthiopyrimidin-4-one **515** to bisindolyluracil **507** was also attempted under similar conditions to those reported by Gibson *et al.* for chemistry carried out on a solid support (Scheme 4.27; Method A).[55] Reaction with 10 equivalents of oxone® in aqueous 1,4-dioxane for 3 days at 70°C, involved the putative oxidation of sulfide **515** to its corresponding 4-sulfonyl derivative **524** prior to hydrolysis affording **507**. Sulfone **524** would be envisaged to readily undergo hydrolytic cleavage as a result of the greater electrophilicity at the carbon centre (*C*-2), due to an inductive electron withdrawing effect. Unfortunately, no trace of sulfone **524** was detected following heating with oxone® under these conditions and thus, subsequent hydrolysis to form **507** did not occur.

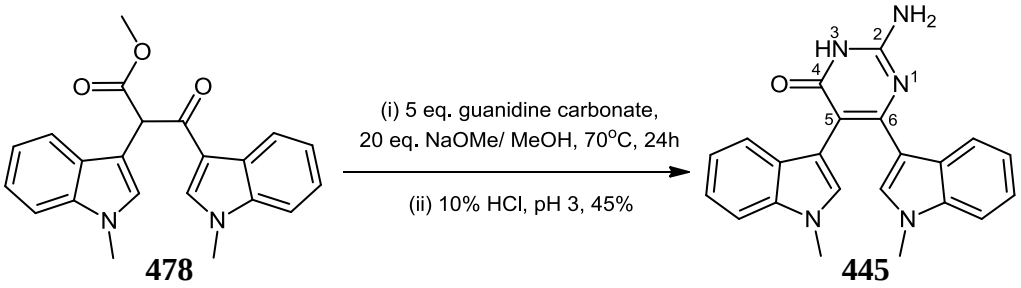
According to the procedure of Lu *et al.*, **515** was also heated along with aqueous 30% NaOH (Scheme 4.27; Method B) or 10% HCl (Method C); however, transformation to the corresponding pyrimidin-2,4-dione **507** did not occur and only starting material **515** could be isolated.[56] Future work in this area should countenance that *S*-oxidation and hydrolysis be attempted in a stepwise manner, in order to fully elucidate the limitations of this strategy.



Scheme 4.27

4.6.4 Reaction with guanidine carbonate

Synthesis of 5,6-bisindolyl substituted 2-aminopyrimidin-4-one **445**, constituted a highly interesting target with potential biological activity.[40,47] As illustrated in Scheme 4.28, this novel bisindolyl-substituted isocytosine derivative **445** was produced from base-mediated cyclocondensation of guanidine - liberated *in situ* from the reaction of guanidine carbonate with excess sodium methoxide, with β-ketoester **478**. The reaction contents were stirred under inert atmosphere, at reflux temperature, for 24 hours, followed by solvent evaporation, acidic work-up, filtration and careful chromatography employing DCM/methanol in order to elute title compound **445**, in an overall yield of 45%.



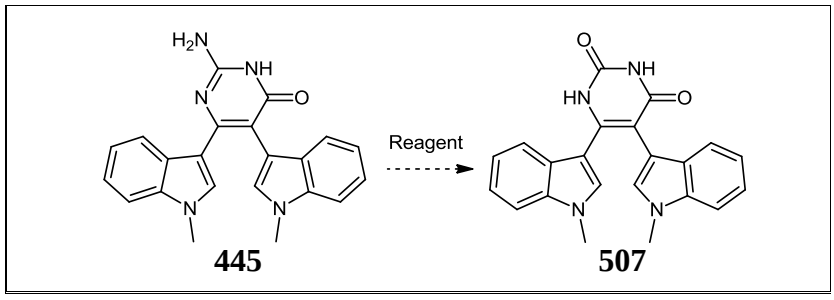
Scheme 4.28

4.6.4.1 Derivatisation of 5,6-bisindolyl-2-aminopyrimidin-4-one

A conventional diazotisation route was initially rationalised to introduce a hydroxyl group in place of aryl amine functionality within isocytosine derivative **445**.[57] Attempted reaction of the amino group of **445** with sodium nitrite/excess HCl, *t*-butyl nitrite/ acetic acid or *t*-butyl nitrite/ aqueous 2-propanol, to form a diazonium salt, yielded unreacted **445,** in each case, following stirring overnight at 0°C and warming gradually to room temperature. Similarly, hydrolytic reaction of **445** with aqueous 10% HCl at 80°C for 7 days resulted in formation of

only decomposition products. Treatment of **445** with freshly generated nitrosylsulfuric acid under aqueous conditions at 70°C or heating of **445** with 40 equivalents of *t*-butyl nitrite in DMF at 100°C, also resulted in detection of a complex mixture of degradation material (Table 4.4).

Table 4.4: Attempted diazotisation/ hydrolysis of bisindolyl-2-aminopyrimidin-4-one congener (445) to form uracil derivative (507) †



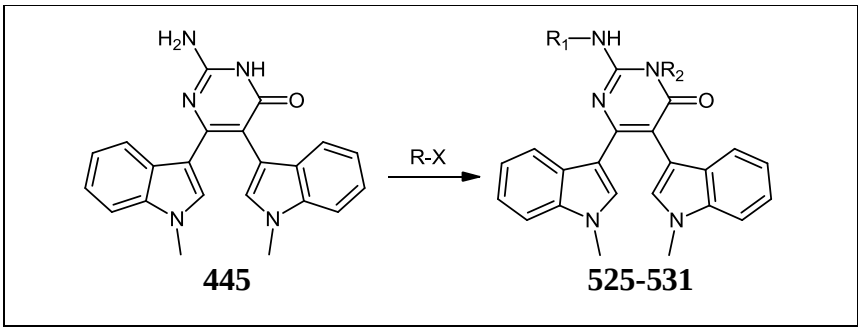
445 **507**

Reagent	*Amount*	*Conditions*	*Time*	*Result*
$NaNO_2$	5.0 eq.	AcOH, 0°C - rt	20h	S.M
$NaNO_2$	5.0 eq.	10% HCl/ H_2O, 0°C - 70°C	24h	S.M
***t*-BuONO**	5.0 eq.	AcOH, 0°C - rt	20h	S.M
***t*-BuONO**	5.0 eq.	IPA/ H_2O, 0°C - rt	24h	S.M
$[NO]HSO_4$	>100 eq.	H_2SO_4/ H_2O, 0°C - 70°C	20h	decomp.
***t*-BuONO**	40 eq.	DMF, 100°C	20h	decomp.
10% HCl	>100 eq.	H_2O, 80°C	7d	S.M

† In each case, reaction was performed on 150 mg scale. Qualitative ^{13}C and ESI-MS analysis was used to determine product formation

Exploration of the potent nature of subtle changes within the parent H-bonding framework to modulate key biological activity was also undertaken; a wide range of conditions for substitution of the isocytosine nucleus within **445** were assessed, as outlined in Table 4.5. The use of potassium carbonate/methanesulfonyl chloride (**525**), NaH/methanesulfonyl chloride (**525**) or NaH/methyl isothiocyanate (**526**) mixtures, in DMF at high temperature was observed to be ineffective. Reaction with acetic anhydride in pyridine provided the acetylated derivative **527**, as an amorphous light yellow powder, in a yield of 35% (Table 4.5). Interestingly, if pyridine was employed as solvent, sulfonamide **525** could not be formed following reaction with methanesulfonyl chloride.

Table 4.5: Condition employed for attempted synthesis of N^2-alkylated 5,6-bisindolylisocytosine derivatives (525-531)



R_1	R_2	I.D	Conditions	Temp	Time*	Yield
SO_2CH_3	H	**525**	1.5 eq. K_2CO_3, 1.2 eq. CH_3SO_2Cl, DMF	90°C	24h	S.M
SO_2CH_3	H	**525**	5 eq. NaH, 2.2 eq. CH_3SO_2Cl, DMF	90°C	24h	S.M
$CSNH(CH_3)$	H	**526**	10 eq. NaH, 3.5 eq. CH_3NCS, DMF	110°C	48h	S.M
SO_2CH_3	H	**525**	1.5 eq. CH_3SO_2Cl, C_6H_5N	90°C	24h	S.M
$COCH_3$	H	**527**	1.5 eq. $(CH_3CO)_2O$, C_6H_5N	90°C	24h	**35%**
$COCF_3$	H	**528**	$(CF_3CO)_2O$, CF_3CO_2H (3:1)	75°C	20h	**45%**
$COCF_3$	H	**528**	1.5 eq. $(CF_3CO)_2O$, Et_3N, CH_3CN	80°C	24h	S.M
$=C(CF_3)-CH=C(CF_3)-$		**529**	5 eq. $CF_3COCH_2COCF_3$, AcOH	120°C	24h	S.M
-CO-NH-CO-		**530**	1.1 eq. ClCONCO, Et_3N, DCM	20°C	20h	S.M
$=C(CH_3)-CH=C(CH_3)-$		**531**	3.3 eq. $CH_3COCH_2COCH_3$, 5% HCl/ H_2O	100°C	24h	S.M

† In each case, reaction was performed on 150 mg scale. Qualitative ^{13}C and ESI-MS analysis was used to determine product formation

However, reaction of isocytosine **445** with a mixture of trifluoroacetic anhydride and trifluoroacetic acid (5:1), stirred at 90°C for 20 hours, afforded the corresponding trifluoroacetamide **528** as light orange crystals in a yield of 45% following column chromatography. The importance of trifluoroacetic acid behaving as a catalyst, protonating the carbonyl group of trifluoroacetic anhydride, thus activating it towards nucleophilic attack, is illustrated by the lack of any reaction when trifluoroacetic anhydride was instead stirred with **445**, in acetonitrile, containing a few drops of triethylamine, at 80°C for 24 hours.

A series of reactions with pharmaceutically relevant bidentate electrophiles in order to yield a library of cycloalkylated analogues were also unsuccessful in our hands. Employing efficacious conditions for aminopyrazole derivatisation (Section 4.9), the parent isocytosine **445** was reacted with chlorocarbonyl isocyanate, in DCM, containing triethylamine,

overnight.[58] Following addition of water, the residue was filtered but was found to comprise only starting material, with no trace of the anticipated triazinedione derivative **530**. Attempted routes to pyrimido[1,5-*a*]pyrimidine analogues **529** and **531** were also unsuccessful under the reaction conditions outlined in Table 4.5.

4.6.5 Attempted reaction with panel of bidentate *N*-nucleophiles

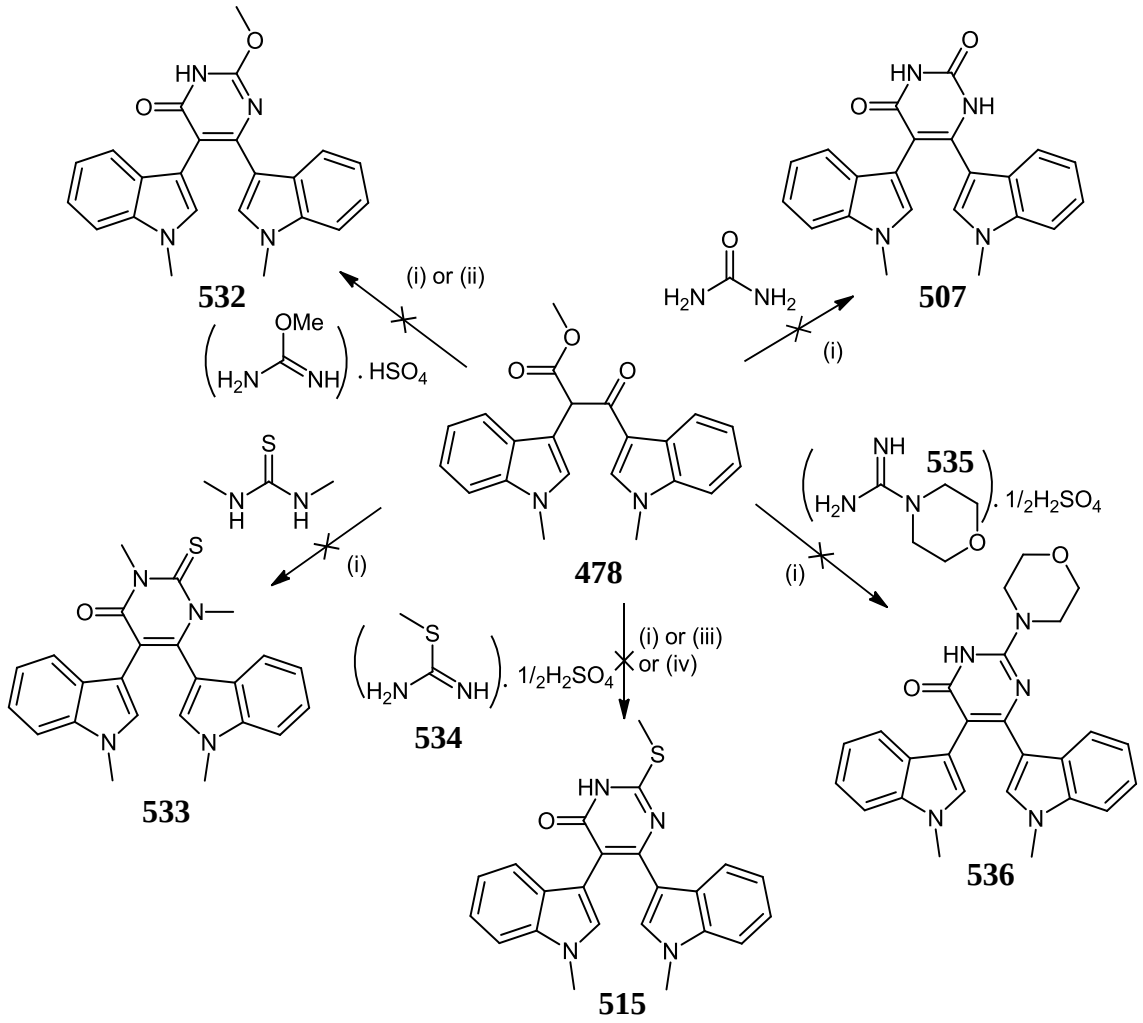
It has been established that base-mediated cyclocondensation of a dicarbonyl precursor with an appropriate nucleophile represents a viable route to heterocyclic systems bearing a pyrimidine sub-unit. The versatility of this reaction with related ureas of varying nucleophilicity was studied, and the results of this reactant study are described in Scheme 4.29. Reactions of **478** with hydrazine, thiourea and guanidine carbonate have already been discussed and the resulting bisindolyl heterocyclic derivatives represent a validated route to this novel class of compounds.

As a baseline starting point for accessing bisindolyluracil **507**, reaction of 5 equivalents of urea, freshly recrystallised from absolute ethanol, with intermediate **478**, heated to reflux temperature, in the presence of excess sodium methoxide did not yield any anticipated product **507** upon acid work-up, even after 72 hours.

Reaction of 5 equivalents of *O*-methyl isourea under identical reaction conditions also yielded only starting material **478** following stirring for 36 hours at 70^{o}C. Utilising aqueous inorganic base-mediated conditions, as reported by Botta *et al.*, conversion to uracil **532** was investigated following reaction of **478**, but no reaction had occurred.[59]

Reaction of *N*,*N'*-dimethyl thiourea also failed to provide any **533**, resulting in isolation of only starting material **478** following reaction for 48 hours under these conditions (Scheme 4.29).

S-Methylisothiouronium hemisulfate **534** was synthesised by heating of thiourea with dimethyl sulfate in ethanol, for 2 hours. Following cooling to 0^{o}C, filtration and successive washing with water and diethyl ether, produced the white crystalline hemisulfate salt **534** in a yield of 53%. Unfortunately, reaction of 5 equivalents of **534** with **478** under standard methoxide conditions did not result in formation of any product **515**, following extended reflux for 72 hours. Similarly, when reaction of 5 equivalents of the salt **534**, along with ketoester **478**, in a 10% aqueous KOH solution, was carried out, no reaction was observed.



Reagents and conditions: (i) 20 eq. NaOMe/ MeOH, 5 eq. $NH_2(CX)=NH$ reagent, reflux, 24-72h; (ii) $Ca(OH)_2$, 5 eq. $NH_2(NH)$-X reagent, aq. H_2SO_4, 80°C, 36h; (iii) 10% KOH/ H_2O, 5 eq. $NH_2(NH)$-X reagent, r.t, 24h; (iv) 20 eq. KOH, 5 eq. $NH_2(NH)$-X reagent, THF, reflux, 24h

Scheme 4.29

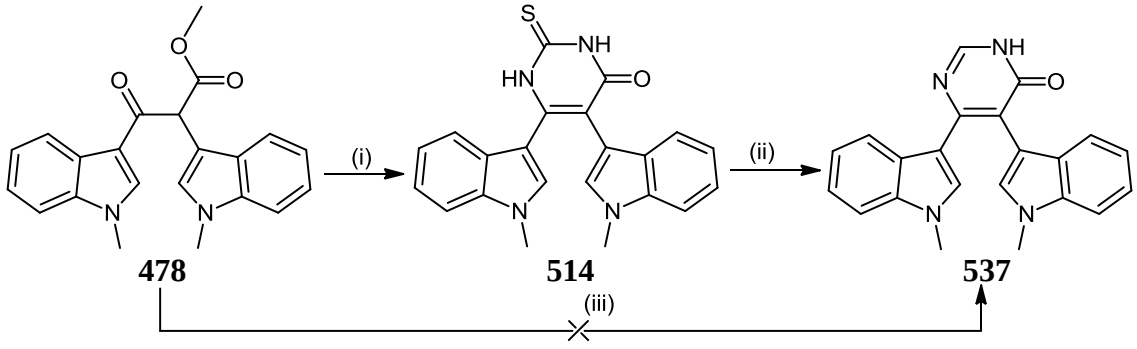
Due to concerns over these heterogeneous reaction conditions, a modified reaction involving heating of KOH along with isothiouronium salt **534** and intermediate **478**, in THF, for 16 hours, was attempted, but without any success.[40] Synthesis of 4-morpholinocarboxamidine hemisulfate **535** was carried out in a yield of 78%, by one-pot reaction of *S*-methylisothiouronium salt **534** with 1.1 equivalents of morpholine, stirred in 1,4-dioxane for 20 hours at 90°C. However, none of the anticipated morpholino product **536** was formed under standard base conditions (Scheme 4.29).

Based on these data, thiourea and guanidine possessed superior nucleophilicity compared with alternative urea derivatives. In qualitative terms, this is accounted for by the lower electronegativity of the C=N and C=S groups, with respect to the electron withdrawing C=O within urea. It was also necessary to be cognisant of the severe problems associated with the

apparent lack of reactivity of β-ketoester **478** compared with simple alkyl substituted analogues, in many instances. To this end, conversion of **478** to more electrophilic or nucleophilic intermediates such as enaminoamide **491** or β-chloroester **493** respectively, has been successfully achieved; however, no major advantages have manifested from application of these analogues to date. Thus, it can be confirmed that bidentate reactants imbued with strong nitrogen nucleophilicity as well as relatively harsh initial ring-forming conditions are required for effective heterocycle formation.

The failure of alternate substituted urea analogues to yield the desired products **532-536** in the majority of cases was also illuminating with respect to devising an effective derivatisation strategy. The critical conclusion to be deduced from this study was that major synthetic issues encountered within the pyrimidine derivative series could not be satisfactorily resolved through targeting the primary base-mediated condensation step, but could instead be undertaken by secondary modification of pre-existing pyrimidine functionality.

This provident strategy was clearly demonstrated when confronting challenges associated with the formation of a highly interesting lactam derivative - 5,6-bis(1-methyl-1*H*-indol-3-yl)pyrimidin-4(3*H*)-one **537**, incorporating an amide H-bonding functionality, similar to staurosporine **2**, rather than the imide motif conserved in pyrimidin-2,4-dione **507**, or in the closely related thioimide congener **514**. Putative reaction of **478** with formamidine acetate and sodium methoxide was initially attempted, but unfortunately, only starting material **478** was present after 48 hours, in the absence of any desired compound **537** (Scheme 4.30).



Reagents and conditions: (i) 10 eq. NaOMe, 5 eq. NH_2CSNH_2, MeOH, reflux, 24h (b) 10% HCl, **514** = 24%**;** (ii) 5 eq. $NiBr_2$, 15 eq. $NaBH_4$, MeOH, 20°C, 16h, **537** = 55%; (iii) 10 eq. NaOMe, 5 eq. $NHCHNH_2.HOAc$, MeOH, reflux, 48h, n.r

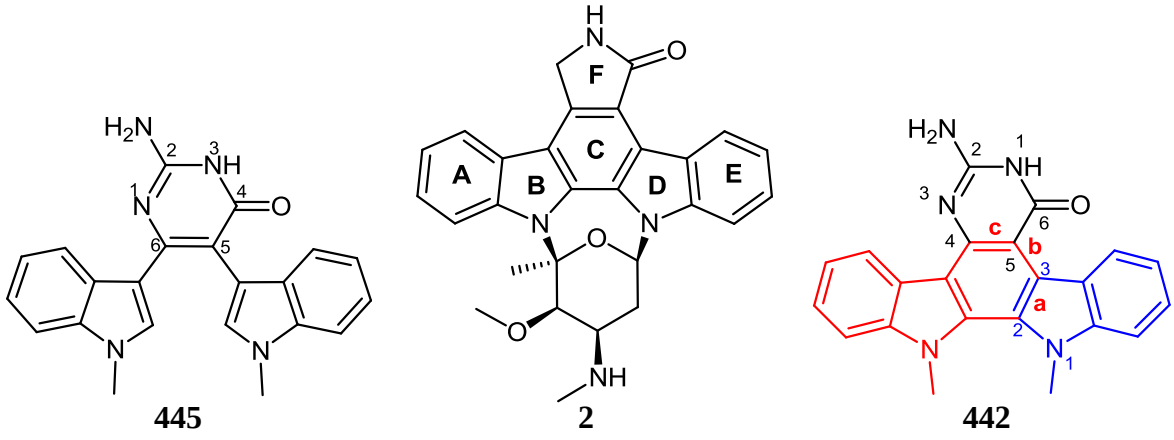
Scheme 4.30

Conversely, stirring of a dark suspension of **514** and 5 equivalents of nickel bromide in distilled methanol, to which was added portionwise, 15 equivalents of sodium borohydride,

under ambient conditions, successfully yielded the desulfurised pyrimidinone analogue **537**, through reductive cleavage of the thiocarbonyl (C=S) bond, in a yield of 55%.[60]

4.7 Oxidative cyclisation of bisindolylpyrimidinone series

Novel bisindolyl derivatives, represented by 5,6-bisindolyl-2-aminopyrimidin-4-one **445**, constitute an interesting bioisosteric modification of the intrinsic heterocyclic (F ring) H-bonding network within bisindolylmaleimides (BIMs) known to confer potent anti-PKC activity (Section 1; Biological Introduction). The ultimate step in generation of a direct staurosporine **2** aglycon analogue within this series was now investigated and involves aromatisation of the acyclic precursor **445** to novel, fully planar indolo[2,3-*a*]pyrimido[5,4-*c*]carbazol-4(3*H*)-one **442** (Fig. 4.4).[61-65]



445 **2** **442**

Fig. 4.4

4.7.1 Indolo[2,3-*a*]pyrimido[5,4-*c*]carbazol-4(3*H*)-one synthesis *via* 2,2'-ring closure of 5,6-bisindolyl-2-aminopyrimidin-4-one

Following synthesis of the isocytosine derivative **445**, attention turned towards the final C-C bond formation step, *via* oxidative cyclisation, to yield fully aromatised (1-methyl-1*H*-indolyl)[2,3-*a*](2-aminopyrimidin-4-one)[5,6-*c*]carbazole **442**. The three most commonly employed oxidants employed in transformations of this type within classical bisindolylmaleimide chemistry are (i) DDQ[9,10,66], (ii) Pd(II)-mediated oxidation[3,67,68] and (iii) U.V. photocyclisation.[6,42,69]

Unfortunately, DDQ oxidations are reported to be of limited utility and do not routinely prevail in instances where the indole nitrogens are alkyl-protected, as in our case. Due to its limited substrate scope, DDQ was discounted at an early stage from our cyclisation study.

4.7.1.1 Attempted transition metal-mediated route

Positive results have been reported in the chemical literature, with palladium-based reagents acting as oxidants for the aromatisation of bisindolylmaleimides furnished with a mono-*N*-protected indolic nitrogen, and most commonly, for mono-*N*-glycosylated analogues. Palladium(II) acetate is an effective mediator of this type of conversion, and oxidative ring-closure was attempted under a series of conditions reported in chemical literature. One equivalent of this Pd complex was added to dry DMF, containing **445**, under inert atmosphere, and stirred at 110^{o}C for 24 hours. However, no evidence of indolocarbazole formation could be detected by LCMS under these conditions. Similarly, reaction of bisindolyl precursor **445** with 5 equivalents of $Pd(OAc)_2$ in acetic acid, at 110^{o}C for 24 hours, in the presence of air, yielded no product formation. Disappointingly, the application of the more reactive $Pd(CF_3CO_2)_2$, also failed to achieve this oxidative cyclisation, following heating in DMF overnight, under aerobic conditions.

On consideration of transition metal mediated cyclisations, adverse solubility and compatibility issues related to palladium chemistry proffered an obvious obstacle to subsequent diversification of any chemical route. An alternative route employing $K_3[Fe(CN_6)]$, which is known to operate as an oxidant under aqueous alkaline conditions, afforded only starting material **445** following an extended reaction time.[70] Similarly, the recently reported utility of the hypervalent iodine (V) reagent, [bis(trifluoroacetoxy)iodo]benzene (PIFA), to achieve oxidative transformations in a number of polycyclic heterocyclic systems did not translate into any success with conversion of bisindolyl isocytosine compound **445** to the corresponding indolo[2,3-*a*]carbazole **442**, following stirring at room temperature, along with 2.2 equivalents of the oxidative reagent in DCM, for 24 hours.[13]

4.7.1.2 U.V Photocyclisation route

A photocyclisation route was deemed to be an attractive method for achieving the final step in this synthetic pathway for design of novel heterocyclic compounds. Previous work indicated a wide application for iodine/U.V. light-mediated carbazole cyclisation, tolerating a wide range of protected indolic systems; it is also economical and readily applicable to diverse chemistry. Initially, following conditions outlined by Garaeva *et al*., reaction of **445**, suspended in toluene (1 mg/0.5 mL) in the presence of 1 equivalent of iodine, and irradiated for 24 hours with a medium-pressure mercury lamp was carried out (Fig. 4.5).[71] Analysis of the crude residue yielded evidence of a small amount of product formation, but

predominantly starting material, presumably due to the low solubility of 5,6-bisindolyl-2-aminopyrimidin-4-one **445** in toluene.

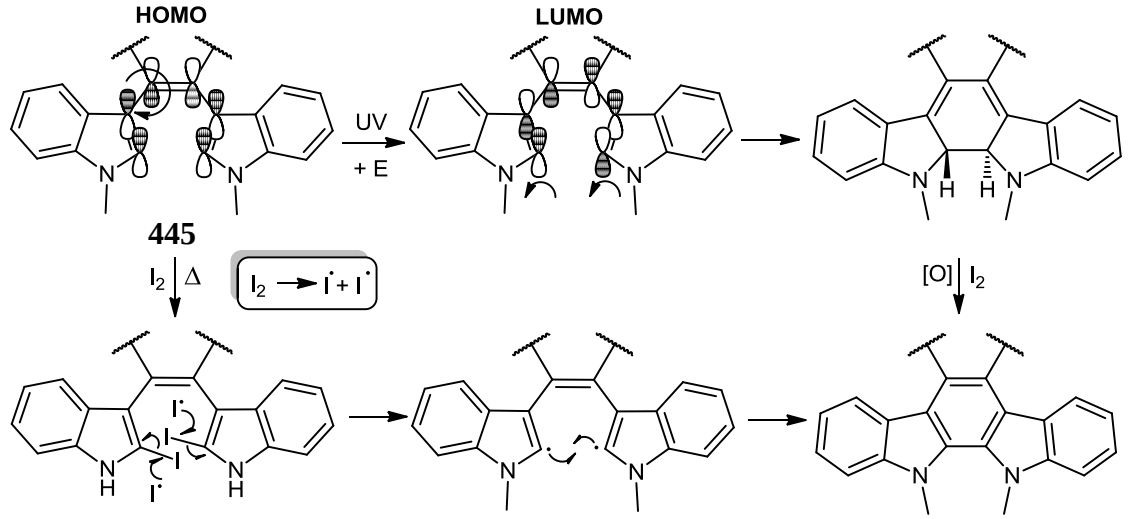


Fig. 4.5: Mechanisms proposed for U.V.-photocyclisation of bisindolyl precursors.

An important feature of this transformation concerns the initial conformation of both indolyl substituents - anticipated to initially display a 'non-cisoid' hexatriene orientation, and thus could disfavour the corresponding transition state. The relative ease of U.V.-promoted isomerisation of this system may thus contribute to the difference in reactivity observed for individual members across the bisindolylpyrimidinone series. A number of workers have reported different mechanisms accounting for the final light-mediated oxidative cyclisation step to access indolocarbazole derivatives, as illustrated in Fig. 4.5. Based on Woodward-Hoffmann criteria, a photochemically induced electrocyclic reaction may be realised *via* conrotatory ring closure of the acyclic precursor. Interestingly, electron releasing substituents at the C-2 position (e.g. NH_2, **442** or H, **537**) were successful candidates for this transformation, and this may be due to partial resonance contributions that stabilise both indole moieties in a beneficial less hindered, co-planar relationship (Fig. 4.5). Application of iodine as oxidant then results in conversion to the fully oxidized product.

Alternatively, homolytic fission of iodine may be necessary to afford a radical cyclisation methodology, in which initial 2,2'-iodination is followed by double radical abstraction and indolyl radical dimerisation to provide the central benzene C-ring. In the case of improving these final-step strategies, use of Pd/C as final oxidant, in place of iodine has been reported in non-radical routes, and future advantages may thus be conferred by performing this modification on unreactive bisindolylpyrimidinone analogues.

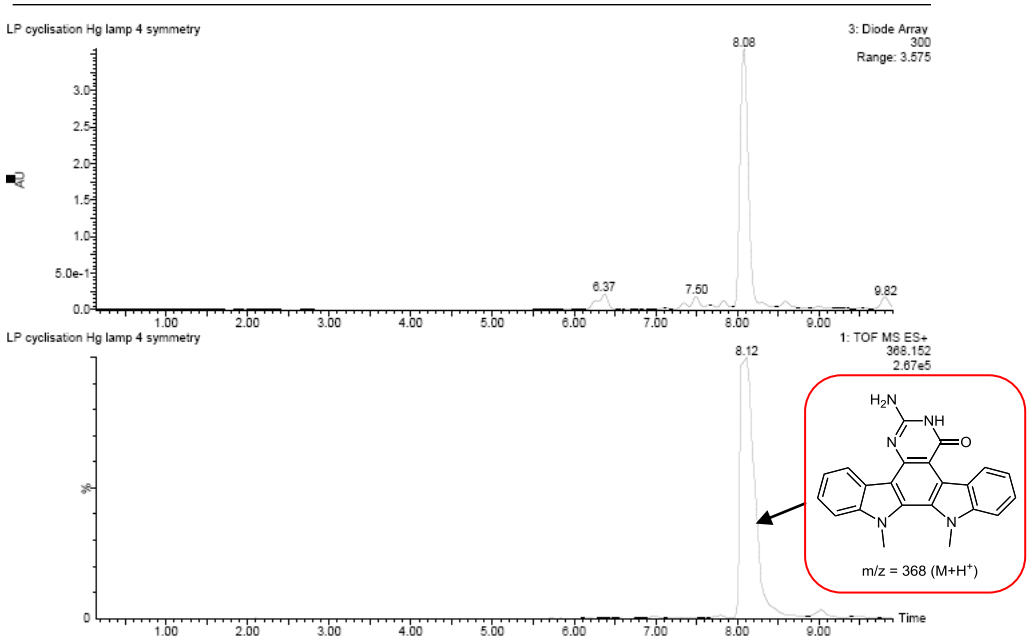
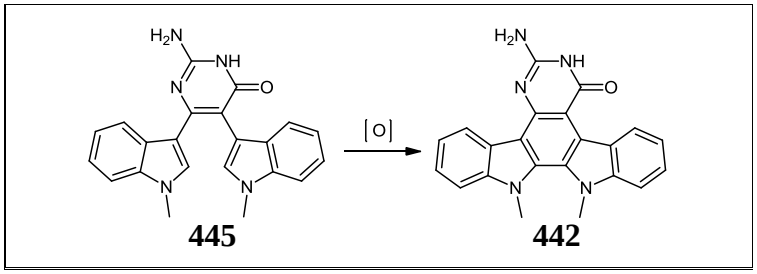


Fig. 4.6: LCMS analysis of planar indolo[2,3-*a*]pyrimido[5,4-*c*]carbazole **442**

In the course of our work, optimisation of the encouraging photocyclisation strategy as a viable route to the fully aromatized indolocarbazole **442** determined that an acetonitrile/ methanol (3:2) solvent system yielded maximum solubility of the 5,6-disubstituted isocytosine **445**, at a dilution of 1 mg substrate/2.5 mL solvent mixture. Conditions were also varied in order to investigate how oxidation proceeded in the presence or absence of air. In the absence of atmospheric oxygen, no reaction occurred when **445** was allowed to stir vigorously, while U.V. irradiated for 20 hours, in the presence of catalytic iodine.

Final product formation was carried out successfully on a 100 mg scale, following reaction overnight in an open vessel under our optimized reaction conditions, affording the fully aromatized congener **442** exclusively, in 55% yield, following gradient column chromatography with DCM/methanol. The reaction was also carried out with a constant stream of air being bubbled through the solvent over the course of the reaction. However, no difference in yield or reaction profile could be identified by excessive aeration of the reaction media by this method – thus, stirring under normal atmospheric conditions was deemed to be sufficient for full oxidative cyclisation to reach completion, as outlined in Table 4.6.

Table 4.6: Summary of cyclisation study for novel pyrimidinoindolocarbazole (442) synthesis from acyclic 5,6-bisindolyl-2-aminopyrimidin-4-one (445)



Reagent	Stoichiometry	Conditions	Time	Product	Yield
$Pd(OAc)_2$	1.0 eq.	DMF, 130°C‡	20h	**445**	-
$Pd(OAc)_2$	5.0 eq.	AcOH, 110°C	20h	**445**	-
$Pd(CF_3CO_2)_2$	3.0 eq.	DMF, 100°C‡	20h	**445**	-
$K_3[Fe(CN)_6]$	1.0 eq.	10% KOH / H_2O, 100°C‡	24h	**445**	-
PIFA	2.5 eq.	DCM, rt‡	36h	**445**	-
hυ / I_2	1.0 eq.#	toluene, rt, air	72h	**445+442**	-
hυ / I_2	0.5 eq.#	CH_3CN/MeOH (3:2), rt‡	24h	**445**	-
hυ / I_2	0.5 eq.#	CH_3CN/MeOH (3:2), rt, air§	16h	**442**	**53%**
hυ / I_2	0.5 eq.#	CH_3CN/MeOH (3:2), rt, air¥,§	16h	**442**	**55%**

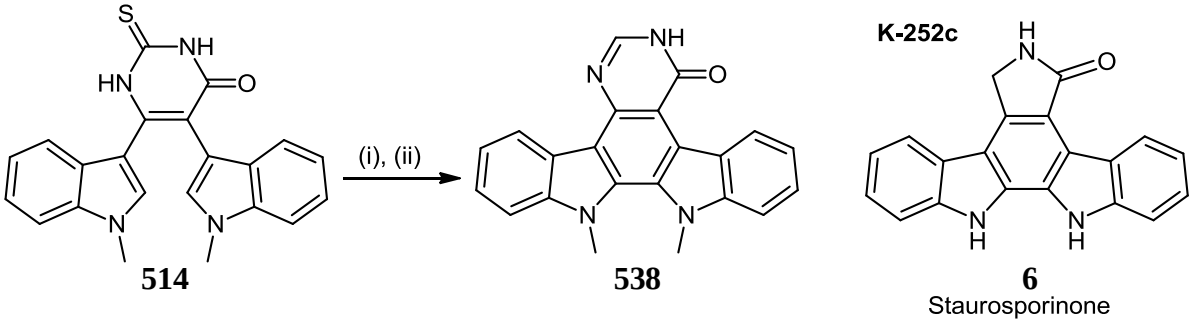
Abbreviations: PIFA = $PhI(OCF_3CO)_2$
‡ Anoxic conditions / N_2 atmosphere.
# Refers to stoichiometry of iodine
¥ Air-bubbling (solvent aeration)
§ Dilution: 1.0 mg substrate / 2.5 mL solvent

At the conclusion of this work, full conversion of precursor **445** to the contiguous heteroaromatic indolo[2,3-*a*]pyrimido[5,4-*c*]carbazole **442** is described. Utilisation of an acetonitrile/ methanol solvent system, in place of previously reported benzene or toluene[10], as reaction medium, also represents an optimisation of the overall efficacy of this photochemical route. A robust method for purification and characterization of these reactions has been developed, using LCMS; under these effective conditions, the novel indolocarbazole **442**, was synthesised, in the absence of starting material **445** or oxidation side-products (Fig. 4.6).

4.7.2 Attempted photocyclisation of other novel heterocycles

Following development of a successful aromatisation strategy, conditions were applied to a number of bisindolyl pyrazole and pyrimidinone derivatives, in order to generate a panel of corresponding indolocarbazoles, with limited success. In each case, the acyclic substrate was dissolved in a mixture of acetonitrile/methanol (3:2), along with a catalytic amount of iodine, and irradiated with U.V. light for 20 hours, under atmospheric conditions (Table 4.7).[42]

Employing this procedure, U.V. photocyclisation of the acyclic pyrimidine-4-one precursor **537**, formed initially from thiouracil intermediate **514** provided novel indolocarbazole **538** as a light-yellow powder, in a yield of 60% (Scheme 4.31). Interestingly, **538** incorporates a 6-membered lactam F-ring and bears close similarity to K-252c **6** (staurosporinone) – a cytotoxic anti-PKC microbial alkaloid derived from *Nocardiopsis* sp. K-290.[48,72,73]

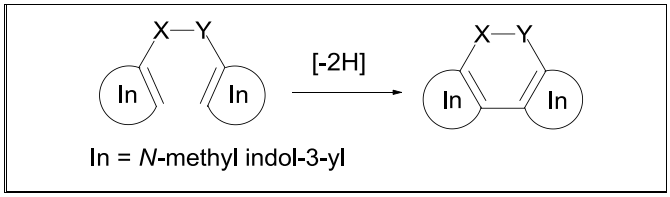


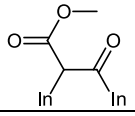
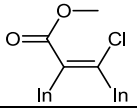
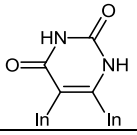
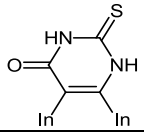
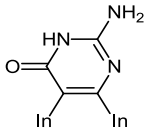
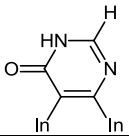
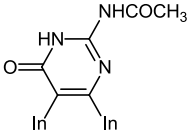
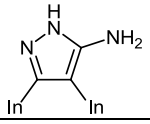
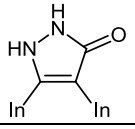
Reagents and conditions: 5 eq. $NiBr_2$, 15 eq. $NaBH_4$, MeOH, 20°C, 16h, **537** = 55%; (ii) hυ, cat. I_2, CH_3CN/ MeOH (3:2), 16h, **538** = 60%

Scheme 4.31

As illustrated in Table 4.7, a panel of other related 1,2-bisindolyl-*cis*-ethene analogues, containing diverse bridgehead functionality were also investigated for their potential to undergo U.V. and $Pd(CO_2CF_3)_2$-mediated oxidative cyclisation. In the case of β-ketoester **478** and chloroacrylate derivative **493**, as well as uracil **507**, thiouracil **514** and *N*-acetylisocytosine **527** heterocyclic congeners, no reaction was observed. Pyrazolone **510** and novel 5-aminopyrazole **447** derivatives were also unreactive under U.V. conditions. The successful conversion of isocytosine **445** and pyrimidin-4(3*H*)-one **537** to the corresponding ICZs demonstrates the utility of this route, and future work will seek to optimize conditions to successfully achieve oxidative ring closure within less reactive acyclic substrates, as well as investigating the enhanced potential of demethylated indole analogues within this step.

Table 4.7: Conditions for U.V. photocyclisation of novel bisindolyl heterocycles to indolo[2,3-*a*]carbazoles



Compound	X-Y	Conditions/ [Ox]	Product	HRMS	Yield
478		**A**	SM	-	-
493		**A**	SM	-	-
507		**A** **B**	SM decomp.	- -	- -
514		**A** **B**	SM decomp.	- -	- -
445		**A**	**442**	368.1511 ($C_{22}H_{18}N_5O$)	**55%**
537		**A**	**538**	353.1396 ($C_{22}H_{17}N_4O$)	**60%**
527		**A**	SM	-	-
447*		**A**	SM	-	-
510		**A**	SM	-	-

Method A: Substrate (100 mg), 3:2 acetonitrile/ MeOH (1 µmol/mL), hυ (254 nm), 16h
Method B: 300 mol% $Pd(CF_3CO_2)_2$, DMF, 110°C, 24h
*__447__ = Section 4.9.2.

4.8 Spectroscopic analysis of the heteroaromatic region of novel bisindolyl heterocyclic derivatives

In this section, characteristic differences in electronic environments between individual 5,6-bisindolylpyrimidin-4-one analogues will be probed *via* chemical shift perturbations within indole ring systems, attributable to the nature of the pyrimidin-4-one substituent. Synthesis of complex pyrimidine-fused bicyclic compounds **539** and **540**, not discussed in this section, will be described in detail in Sections 4.9 and 4.10, respectively (Fig. 4.7).

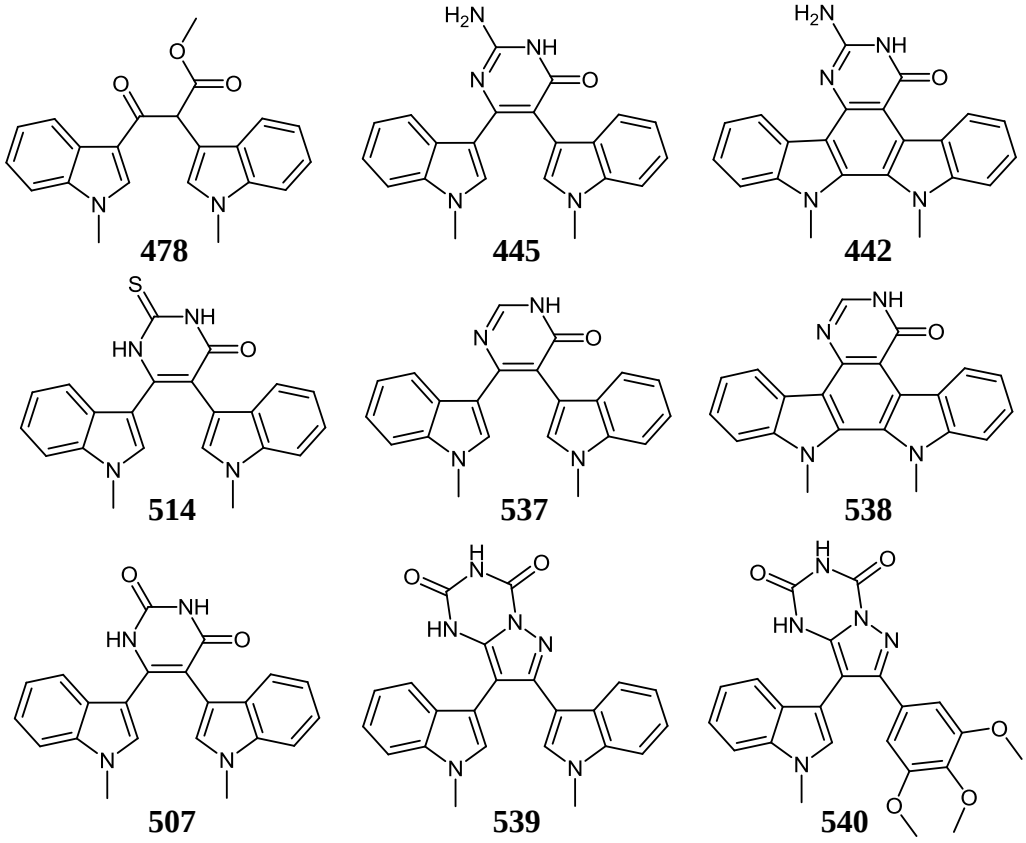


Fig. 4.7

Initial synthesis of β-ketoester **478** was confirmed by IR spectroscopic analysis from the appearance of absorption bands relating to carbonyl group stretching appearing at 1644 cm^{-1} (C=O) and 1732 cm^{-1} (CO_2Me). Investigation by ^1H NMR spectroscopy also reaffirmed this structure, and deshielded sharp 1H singlet signal at 5.70 ppm was also observed, corresponding to the presence of its characteristic alpha proton (CO-C<u>H</u>-CO_2Me).

Synthesis of the panel of 5,6-bisindolylpyrimidin-4-one analogues was successfully undertaken, and an overview of the unique NMR properties of a selected panel of novel indolocarbazole derivatives can be seen in Tables 4.8 and 4.9.

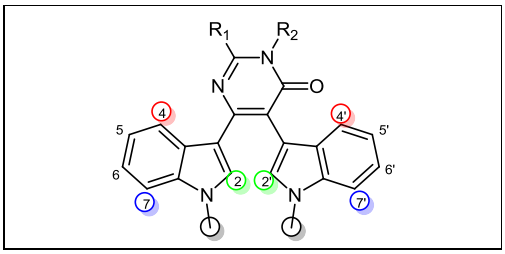
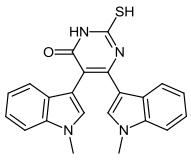
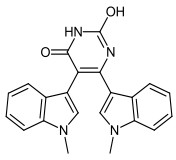
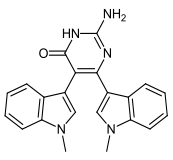
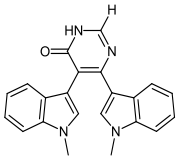


Table 4.8: Selected ^{1}H NMR analysis of novel 5,6-bisindolylpyrimidin-4-ones

R_1	R_2	N-CH_3	^{1}H NMR (C-$H_{2'}$)	^{1}H NMR (C-H_2)	^{1}H NMR (C-$H_{4'}$)	^{1}H NMR (C-H_4)	^{1}H NMR (C-$H_{7'}$)	^{1}H NMR (C-H_7)
SH	H	3.63	7.21	7.65	7.24-7.27	7.30-7.33	6.95-7.01	6.95-7.01
(**514**)		3.70	(1H, s)	(1H, s)	(1H, d)	(1H, d)	(1H, m)	(1H, m)
J (Hz)		-	-	-	8.2	8.2	-	-
OH	H	3.63	7.11	7.50	7.24-7.27	7.30-7.33	6.96-7.08	6.96-7.08
(**507**)		3.67	(1H, s)	(1H, s)	(1H, d)	(1H, d)	(1H, m)	(1H, m)
J (Hz)		-	-	-	8.2	8.2	-	-
NH_2	H	3.40	6.62	7.11	7.37-7.39	8.31-8.34	7.02-7.07	7.24-7.26
(**445**)		3.80	(1H, s)	(1H, s)	(1H, d)	(1H, d)	(1H, m)	(1H, m)
J (Hz)		-	-	-	6.9	7.8	-	-
H	H	3.38	6.80	7.35	7.33-7.35	7.95-7.98	6.84-6.86	7.23-7.25
(**537**)		3.74	(1H, s)	(1H, s)	(1H, d)	(1H, d)	(1H, d)	(1H, d)
J (Hz)		-	-	-	5.9	7.9	7.9	8.0
-SCH_2CH_2-		3.52	6.89	7.39	7.47-7.50	7.97-8.00	7.02-7.04	7.36-7.39
(**516**)		3.87	(1H, s)	(1H, s)	(1H, d)	(1H, d)	(1H, d)	(1H, d)
J (Hz)		-	-	-	8.2	8.0	7.9	8.2
SCH_3	H	3.46	6.87	7.37	7.41-7.44	8.06-8.09	6.93-7.95	7.32-7.35
(**515**)		3.82	(1H, s)	(1H, s)	(1H, d)	(1H, d)	(1H, d)	(1H, d)
J (Hz)		-	-	-	8.2	8.0	7.9	8.1
SCH_2CO_2Et	CH_2CO_2Et	3.36	6.73	7.32	7.49-7.52	8.16-8.19	7.13-7.21	7.36-7.39
(**521**)		3.84	(1H, s)	(1H, s)	(1H, d)	(1H, d)	(1H, m)	(1H, d)
J (Hz)		-	-	-	8.2	7.9	-	8.1
SCH_2CONH_2	CH_2CONH_2	3.47	6.78	7.39	7.48-7.51	8.13-8.16	7.12-7.26	7.35-7.37
(**522**)		3.84	(1H, s)	(1H, s)	(1H, d)	(1H, d)	(1H, m)	(1H, d)
J (Hz)		-	-	-	8.4	7.8	-	8.0
$NHCOCH_3$	H	3.43	6.74	7.35	7.43-7.46	8.36-8.38	6.93-6.96	7.32-7.35
(**527**)		3.84	(1H, s)	(1H, s)	(1H, d)	(1H, d)	(1H, d)	(1H, m)
J (Hz)		-	-	-	8.2	8.0	7.8	-

†NMR measurements were made in DMSO-d_6 solvent; HRMS data agreed with proposed structures

Table 4.9: Selected ^{13}C NMR and IR data of 5,6-bisindolylpyrimidin-4-ones

Structure				
Compound No.	**514**	**507**	**445**	**537**
^{13}C NMR/ppm δ (C=C-CO-NH)	161.3	164.3	161.8	161.7
^{13}C NMR/ppm δ (N=CX-NH)	174.3	151.1	152.7	155.7
$\upsilon_{C=O}$/ cm^{-1}	1651	1639, 1703	1686	1633

†NMR measurements were made in DMSO-d_6 solvent; IR spectra measured as KBr discs

A major question posed at the outset of this study was whether these constitutively similar compounds could be differentiated *via* facile spectroscopic methodology, and determine how discrete chemical shift patterns could be ascertained, based on modulation of electron delocalisation, as illustrated in Fig. 4.8.

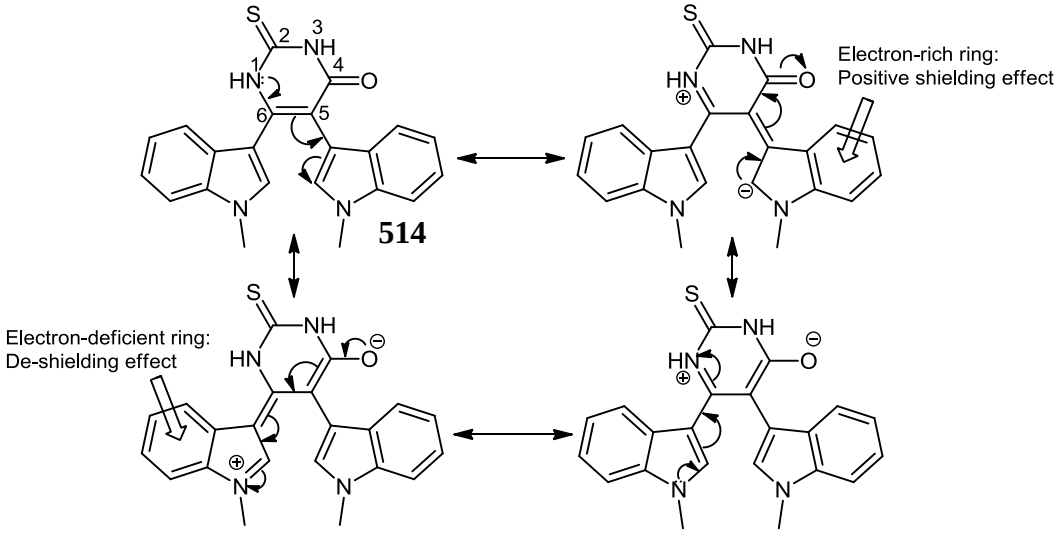


Fig. 4.8: Select resonance canonical structures for inequivalent indole substituents in **514**

Employing this effect, the distinct chemical environments of the both 5 and 6-indolyl substituents on the pyrimidinone ring can be deconvoluted, in addition to providing a framework for explaining NMR changes that occur between the acyclic and corresponding fully aromatised indolocarbazole derivatives.

For 5,6-bisindolyl-2-thiopyrimidin-4-one **514**, differential shielding/deshielding effects act to 'desymmetrise' both indole substituents, thus permitting full assignment of the otherwise

much more complex ^{1}H NMR spectrum. As observed in Table 4.8, the 1H singlet for C-H_2, occurred at 7.21 ppm, while the corresponding signal for C-H_2 was significantly shifted downfield to a position of 7.65 ppm (300 MHz; DMSO-d_6). On investigation of its ^{13}C NMR spectrum, a signal was detected for the carbon of the thiocarbonyl (C=S) group at 174.3 ppm, while the amide carbonyl C_4 occurred at 161.3 ppm (Table 4.9). As observed in Fig. 4.7, the thiocarbonyl group is adjacent to inductively electron-withdrawing N^1 and N^3 thiouracil ring positions and is thus strongly deshielded in this environment. Conversely, even though oxygen also exerts a considerable deshielding influence, the amide position is subject to inward electron donation *via* conjugation with the indole nitrogen lone pair and partial negative charge localised on the oxygen atom, accounting for its relative upfield shift. Several workers have also proposed that systems related to thioimide-bearing thiouracil **514** may exist predominantly in the 'enol' or '2-mercaptolactam' tautomeric form, analogous to the 2-aminopyrimidin-4-one and pyrimidin-4(3*H*)-one derivatives consistently reported within scientific literature in this form.[40,46] Characteristic ^{13}C chemical shift differences observed within diverse pyrimidin-4-one ring compounds are also displayed in Fig. 4.9.

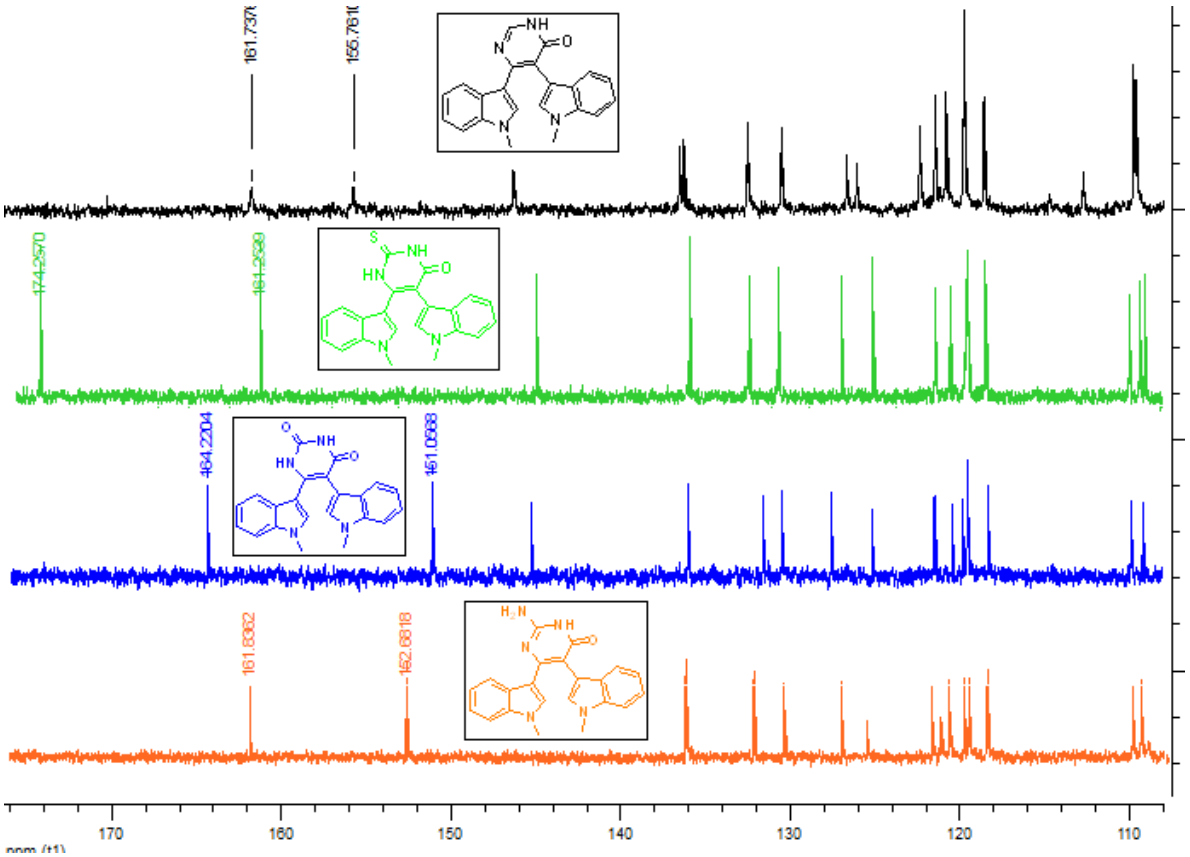


Fig. 4.9: Downfield C-2 and C-4 pyrimidinone fingerprint signals in ^{13}C NMR of 5,6-bisindolylpyrimidin-4-ones: pyrimidin-4(3*H*)-one **537** = black; thiouracil **514** = green; uracil **507** = blue; isocytosine **445** = orange

In the case of 5,6-bisindolyl-2-aminopyrimidin-4-one **445**, a large shielding phenomenon was observed due to the release of electron density *via* the lone pair of electrons delocalised from the 2-amino group of the isocytosine ring. The 1H singlet for C-$H_{2'}$ was identified upfield at 6.62 ppm, due to this effect, while C-H_2 was located at a chemical shift of 7.11 ppm (Table 4.8). This isocytosine derivative **445** possessed a $\Delta\delta_H$ of 0.49 ppm, between these two proton environments, which could be rationalised in terms of the increased electron density localised at C-$H_{2'}$, and the additional electron-withdrawing effect due to resonance stabilization on the deshielded indole ring substituent (Fig. 4.10).

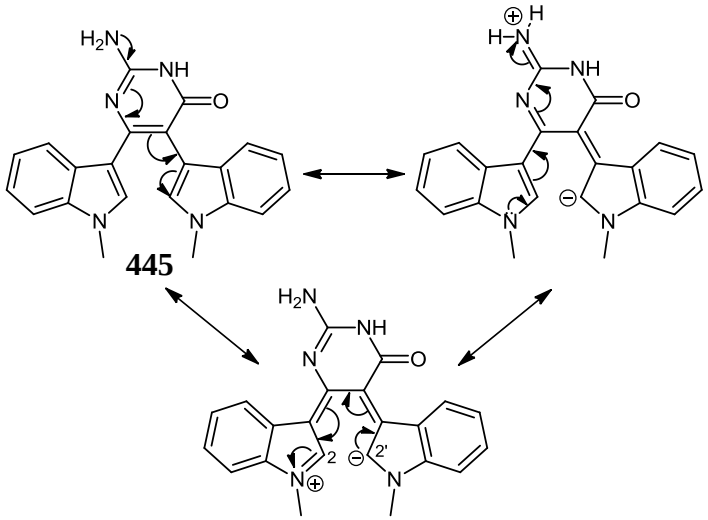


Fig. 4.10: Resonance effects on unsymmetrical indole rings within isocytosine derivative **445**

The ^{1}H NMR spectrum of planar compound **442**, containing a 2-aminoindolo[2,3-*a*]pyrimido[5,4-*c*]carbazole ring system confirmed that successful oxidative cyclisation had occurred, due to the absence of any 1H singlet signals in the C-H_2 region.

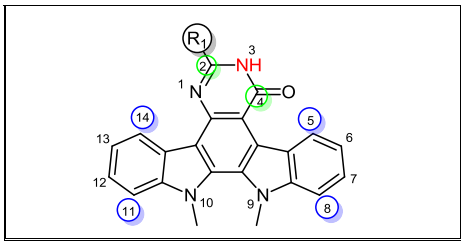


Table 4.10: Selected NMR analysis of novel indolo[2,3-*a*]pyrimido[5,4-*c*]carbazoles

R_1	N-CH_3	^{1}H NMR (C-H_5)	^{1}H NMR (C-H_8)	^{1}H NMR (C-H_{11})	^{1}H NMR (C-H_{14})	^{1}H NMR N<u>H</u>-CO	^{1}H NMR (R_1)	^{13}C NMR (R_1-<u>C</u>=N)	^{13}C NMR (NH-<u>C</u>=O)
NH_2 (**442**)	4.15 4.23	9.06-9.09 (1H, d)	7.64-7.67 (1H, d)	7.71-7.74 (1H, d)	9.68-9.70 (1H, d)	10.93 (1H, bs)	6.41 (2H, s NH_2)	**151.5**	**162.0**
J (Hz)	-	10.5	8.8	8.8	7.0	-	-		
H (**538**)	4.24 4.28	8.98-9.01 (1H, d)	7.71-7.74 (1H, d)	7.76-7.79 (1H, d)	9.72-9.75 (1H, d)	12.33 (1H, bs)	8.32-8.33 (1H, d, C-H)	**144.0**	**160.7**
J (Hz)		7.8	8.1	8.2	8.3	-	3.6		

†NMR measurements were made in DMSO-d_6 solvent; HRMS data agreed with proposed structures.

The 2-amino group was observed as a broad singlet at 6.40 ppm. In the downfield region, the secondary amide (N^3) proton was also detected as a characteristic broad singlet at 10.93 ppm (Table 4.10). In the ^{13}C DEPT 90 NMR spectrum of **442**, only 8 signals were present, corresponding to the benzenoid ring protons of the indolocarbazole scaffold, and also confirming that ring closure had occurred (Fig. 4.11).

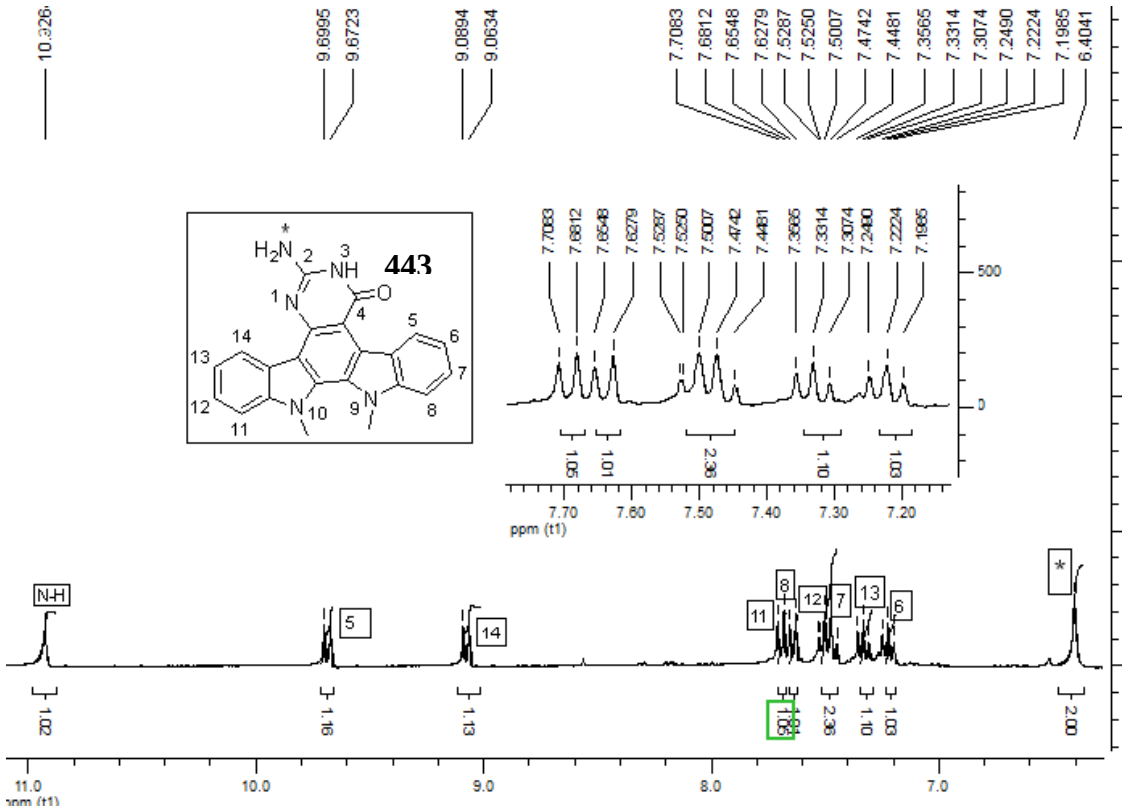


Fig. 4.11: Partial ^1H NMR spectrum of 2-aminoindolo[2,3-*a*]pyrimido[5,4-*c*]carbazol-4(3*H*)-one **442**

When the corresponding bisindolyl **537** and aromatised pyrimidin-4(3*H*)-one **538** derivatives were analysed, similar effects to those reported for other members of this series were observed. In the ^1H NMR spectrum of acyclic **537**, the 1H singlet corresponding to C-H_2 was observed at 7.35 ppm, while the C-$H_{2'}$ signal was located as a 1H singlet at 6.80 ppm.

^1H NMR analysis of the novel indolocarbazole **538** located the characteristic pyrimidin-4(3*H*)-one N=C-H signal as a weakly split doublet at 8.32-8.33 ppm, which was confirmed by means of a COSY 2D-NMR experiment, identifying a cross-peak with the broad N-H singlet appearing at 12.33 ppm (Fig. 4.12). Signals corresponding to C-H_7 and C-H_{12} were also identified as a 2H quartet occurring at 7.52-7.60 ppm, which is the result of an overlap of two triplets, each integrating for a single proton (Fig. 4.12).

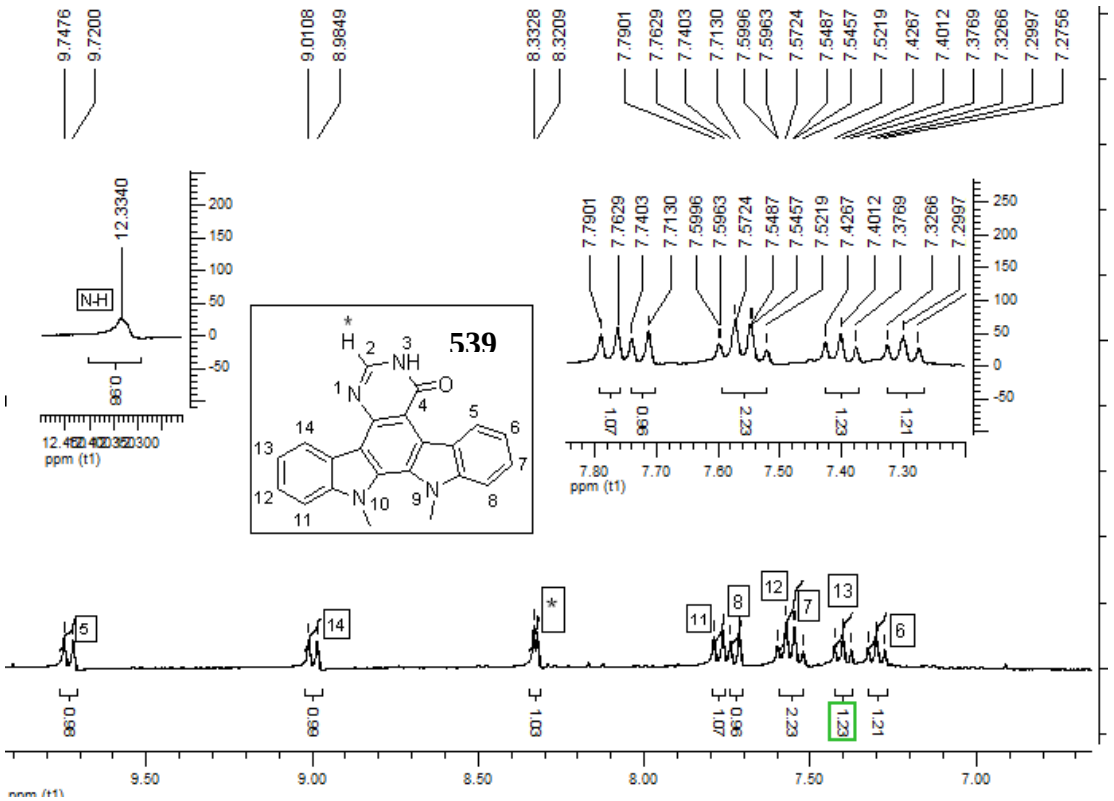
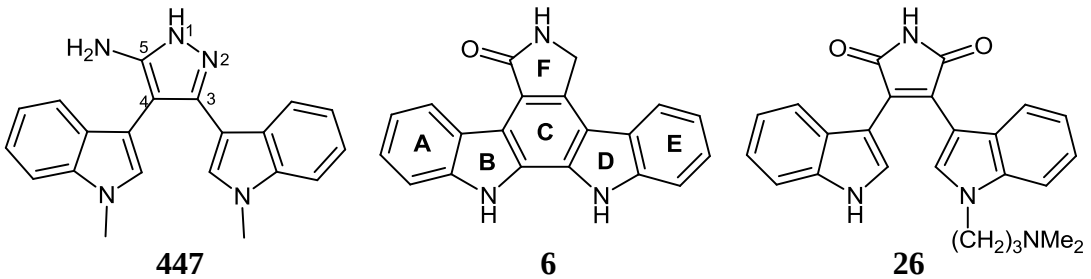


Fig. 4.12: [1]H NMR aromatic spectrum of indolo[2,3-*a*]pyrimido[5,4-*c*]carbazol-4(3*H*)-one **538**

4.9 Synthesis of 3,4-bisindolyl-5-aminopyrazoles

During the course of chemical studies on incorporating new heterocyclic diversity derived from the 3,4-bisindolylpyrrol-2,5-dione/bisindolylmaleimide molecular template, several novel bisindolyl-5-aminopyrazole **447** derivatives of biological interest have also been synthesised. This strategy complements the approach adopted to modifying the F-ring protein-interacting pharmacophore within six-membered pyrimidine analogues (*vide infra*), by incorporating attractive H-bonding characteristics, constrained in a conventional five-membered ring system – structurally similar to K-252c **6**, a natural product derived from *Nocardiopsis* strains, and the selective PKC inhibitor, GF109203x **26** (Fig. 4.13).[65,72,74,75]



447 **6** **26**

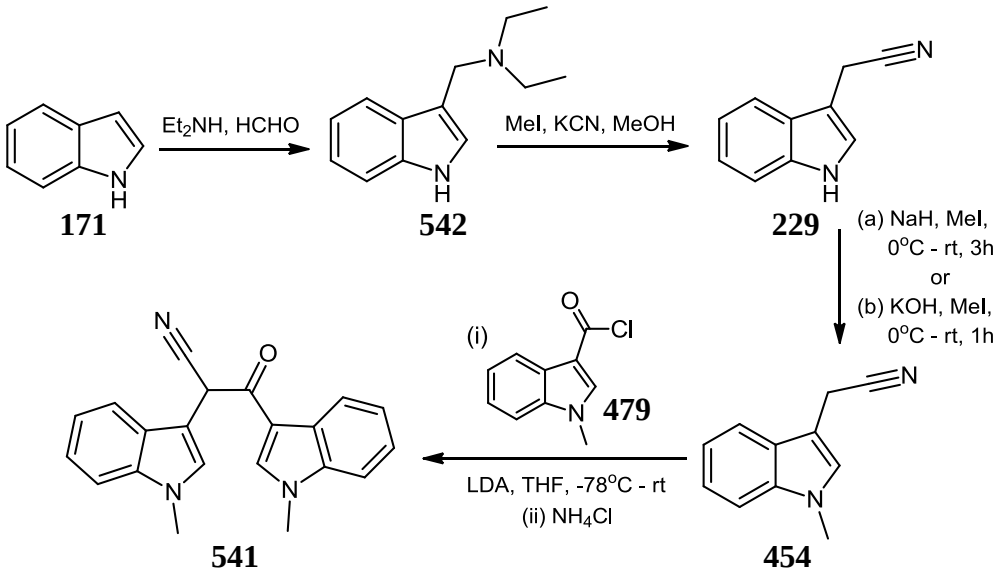
Fig. 4.13

4.9.1 Synthesis of 2,3-bis(1-methyl-1*H*-indol-3-yl)-3-oxopropanenitrile

In order to pursue the development of diverse bisindolyl-5-aminopyrazoles as a new chemical class with important biological potential, the initial synthesis of novel 2,3-bis(1-methyl-1*H*-indol-3-yl)-3-oxopropanenitrile **541** constituted a key electrophilic precursor to title compound **447**.

Synthesis of **541** began from indole **171**, substituted under standard Mannich conditions, employing diethylamine and formaldehyde to afford gramine **542**, as an off-white powder, in 62% yield, following crystallisation. 3-Indolylacetonitrile **229** was derived from cyanolysis of **542** in methanol, in the presence of potassium cyanide and iodomethane, and was isolated as an off-white solid, following chromatography (67%). Appearance of a characteristic weak absorption band in the middle IR region (~2200 cm^{-1}) confirmed the presence of an aryl-substituted acetonitrile C≡N stretch.

Following reaction of **229** with NaH and iodomethane in anhydrous DMF, initially at 0^oC, prior to warming to room temperature, *N*-methyl indole-3-acetonitrile **454**, was isolated as a violet coloured oil, in quantitative yield (100%). A similar result was accomplished by employing powdered KOH base system, in DMF, to afford **454** cleanly, in a yield of 99%, within one hour, at room temperature. The *N*-methylated arylacetonitrile **454** was sufficiently pure to be used without any further purification following acidic work-up (Scheme 4.32).[15]



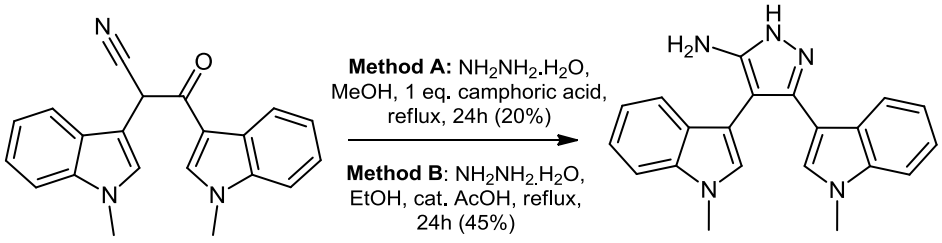
Scheme 4.32

Formation of the corresponding β-ketonitrile **541** was initially attempted by stirring of **454** in the presence of triethylamine, in DMF, at room temperature, along with *N*-methylindol-3-yl

carbonyl chloride **479**, and which resulted in only starting material present after 24 hours. However, when LDA was stirred along with precursor **454** in THF, maintained at −78°C, subsequent dropwise addition of a solution of *N*-methyl indol-3-yl carbonyl chloride **479** in THF, followed by warming of the reaction to room temperature overnight, successfully achieved this transformation. The dark orange intermediate **541** was purified by careful gradient ethyl acetate/hexane chromatography in a yield of 76% from **454** (Scheme 4.32).

4.9.2 Synthesis of 3,4-bis(1-methyl-1*H*-indol-3-yl)-5-aminopyrazole

Heterocyclic functionalisation of appropriate precursors represents a versatile and robust general method for the delivery of a large number of distinct compound types. A cyclocondensation route was chosen in order to access parent 3,4-bisindolylpyrazol-5-amine **447**; no special conditions or protecting groups were required, as the key heterocyclic nucleus was furnished in the final step. This conversion was initially realised by stirring **541** in distilled methanol, along with addition of one equivalent of camphoric acid and three equivalents of hydrazine, initially refluxed for 2 hours, at which point a further three equivalents of hydrazine were added to the reaction flask and reflux was extended for 24 hours. However, only 600 mg of the polar, fluorescent compound **447** could be isolated when this route was performed on a 3 gram scale (20%).[34] Fortunately, aminopyrazole **447** formation proceeded in enhanced yields of 40-45% when β-ketonitrile precursor **541** was heated with catalytic glacial acetic acid and excess hydrazine monohydrate in absolute ethanol for 24 hours, prior to isolating as a light brown powder, characteristically identified as the final fraction during column chromatography with 100% ethyl acetate (Scheme 4.33).

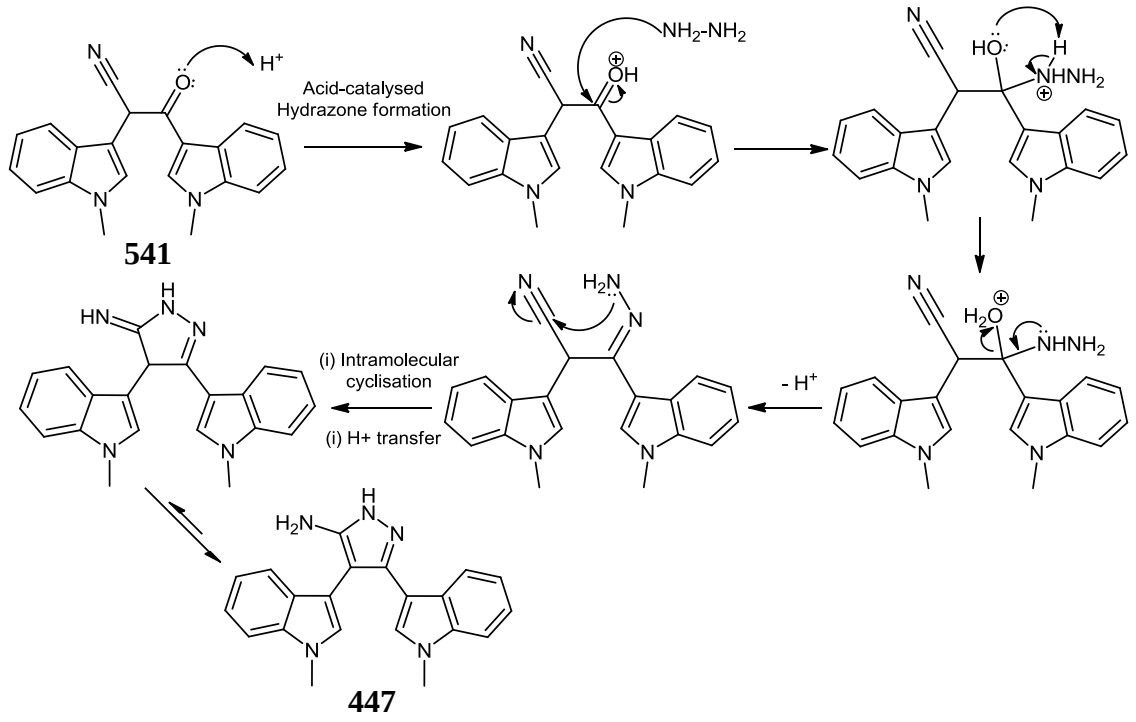


541 **447**

Scheme 4.33

The nature of this synthesis depended on the acid catalyst employed; addition of a few drops of acetic acid demonstrated a substantial yield enhancement (and observed darkening of the reaction mixture following catalyst addition), when compared with catalyst-free reaction (no reaction after 24 hours), or utilising camphoric acid. The apparent mechanism of this reaction is outlined in Fig. 4.14, and the addition of acid clearly promotes initial hydrazone formation prior to cyclisation. The predominant product of this reaction after 24 hours was

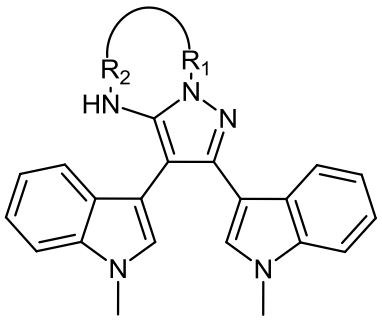
447, along with minimal unreacted **541**; prolonged reflux for 72 hours offered no further yield dividend.



Scheme 4.34

4.9.3 Reactivity of 3,4-bis(1-methyl-1*H*-indol-3-yl)-5-aminopyrazole

A series of pharmaceutically relevant derivatisation studies were conducted in order to expand the library of bisindolyl-5-aminopyrazoles available for biological study. A number of routes were thus developed in order to access novel derivatives of parent compound **447**.[76]



R_1,R_2 = H = **447**

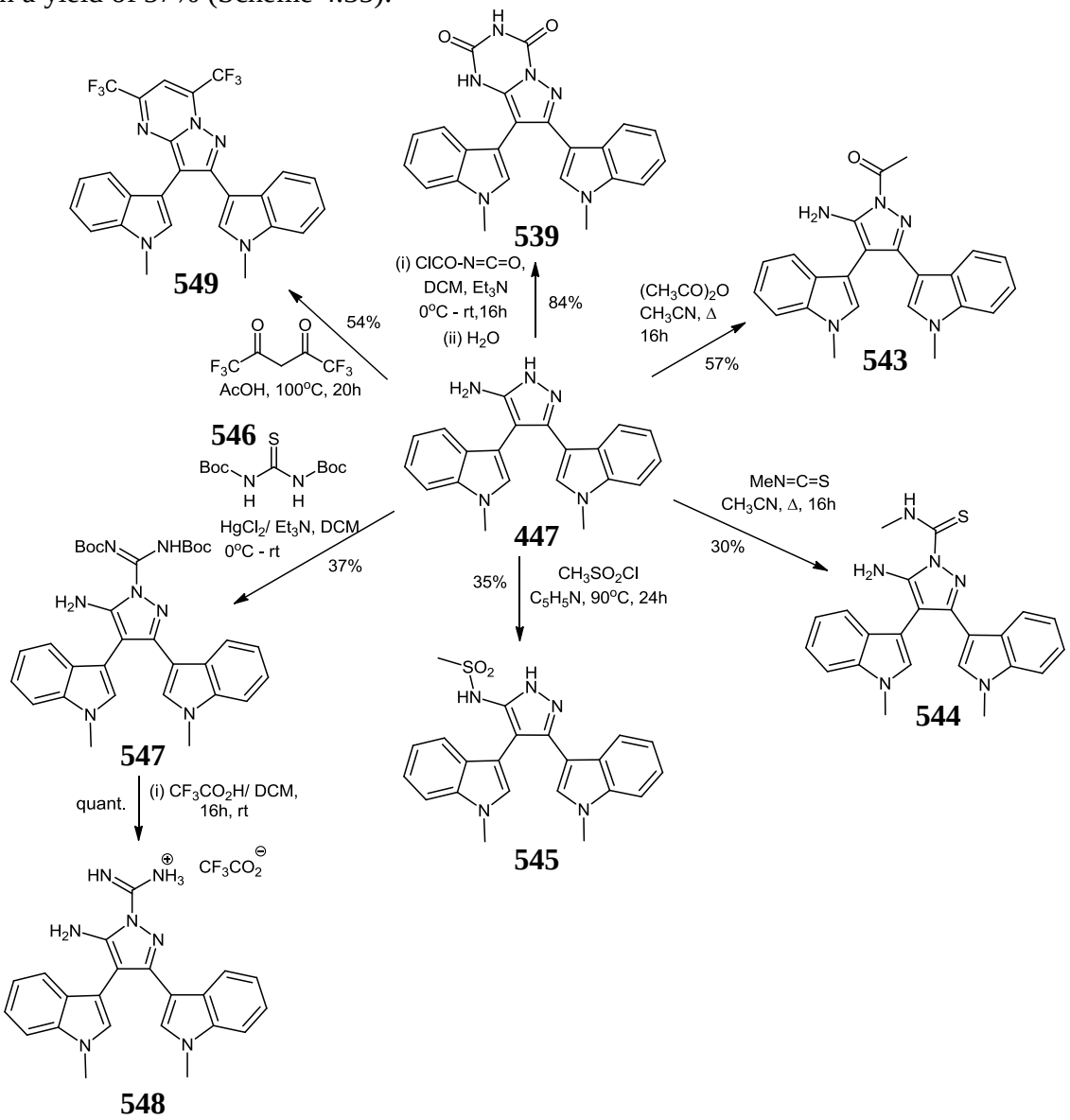
Fig. 4.14: General structure of substituted 3,4-bisindolyl-5-aminopyrazoles

Chemical routes based on a dual strategy of pyrazole ring substitution and cycloalkylation with appropriate electrophiles were chosen to assess H-bonding and potential enzyme binding domains of the 5-aminopyrazole ring system (**447**; Fig. 4.14) within its putative binding pocket. Potency and selectivity may also be improved by incorporating diverse

chemical functionality in order to create new non-covalent enzyme-inhibitor contacts within this series.

*4.9.3.1 Mono-*N*-substitution of aminopyrazole ring*

Initial *N*-acetylation of the aminopyrazole nucleus within **447** was successfully achieved by reaction with acetic anhydride in acetonitrile, at reflux, for 20 hours. Following work-up and chromatography, the N^1-acetylated product **543** was isolated as an off-white crystalline solid in a yield of 57% (Scheme 4.35).



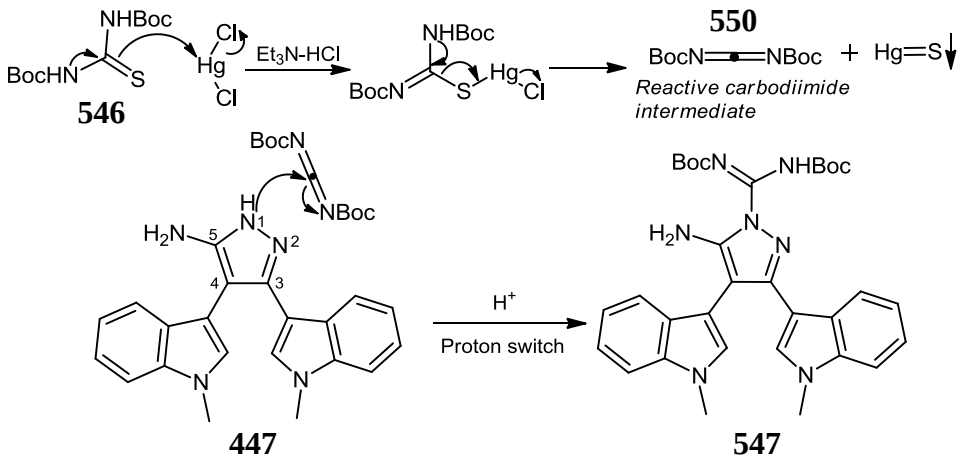
Scheme 4.35: *Target synthetic routes employed for chemical derivatisation of 3,4-bisindolyl-5-aminopyrazole* **447** nucleus.

Following ongoing work to incorporate novel H-bonding networks into these novel anti-cancer classes, unique thioamide functionality was efficiently introduced following heating of aminopyrazole **447** with 1.1 equivalents of methyl isothiocyanate, in refluxing

acetonitrile, for 20 hours. The reaction was then quenched with water and stored at 0°C for a further hour, at which point the light-brown residue was filtered, washed with water and diethyl ether, and dried to afford the pure crystalline compound **544** (30%).

Attempted *N*-sulfonylation employing 1.2 equivalents of methanesulfonyl chloride along with triethylamine in DCM, afforded only starting material following stirring at room temperature for 48 hours. However, harsher conditions utilising methanesulfonyl chloride in pyridine as solvent, stirred at reflux for 20 hours successfully converted **447** to the corresponding amino-substituted sulfonamide as a dark brown solid, in a yield of 35%, following chromatography.

Expansion of the acetyl (C=O) and thiourea (C=S) themes led to synthesis of a substituted pyrazolic derivative **548** bearing the complementary guanidine functional motif (urea analogue). Preparation of the pyrazolyl-guanidine core was successfully carried out by initial coupling of **447** and (*N*,*N'*-di-*tert*-butoxycarbonyl)thiourea **546**, (generated from reaction of thiourea and di-*tert*-butyl carbonate in 93% yield), in the presence of mercuric chloride, and triethylamine, in DCM, warmed from 0°C to room temperature overnight, provided the relatively non-polar **547**, as a beige powder, in overall 37% yield, following work-up and chromatography.



Scheme 4.36: *Mechanism of guanylated-pyrazole* **547** *formation* via *electrophilic carbodiimide reactive intermediate* **550**

This mechanism of N^1-guanylation is believed to proceed through initial formation of a reactive Boc-protected carbodiimide species **550** – derived from attack of the nucleophilic sulfur of thiourea **546** on mercuric chloride to generate a mercury complex (thermodynamically driven by the high affinity of sulfur for mercury in the bond-forming

event), which then undergoes concerted intramolecular cleavage to produce the final electrophilic carbodiimide intermediate **550** and insoluble side-product (Fig. 4.16).
Final deprotection of compound **547** was carried out with a mixture of TFA in DCM, stirred at room temperature for 16 hours; the title trifluoroacetate salt **548** was isolated following drying under high vacuum overnight, in quantitative yield (Scheme 4.35).[77]

*4.9.3.2 Pyrazolo[1,5-*a*]pyrimidine heterocycle formation*

Development of routes to bisindolyl-substituted pyrazolopyrimidine derivatives was undertaken, due to their resemblance to the adenine moiety, within ATP, and thus to investigate the biological potential underpinning the application of bicyclic 1,2-bisindolyl-*cis*-ethene bridging ring systems within future anti-cancer compounds (Section 6.0, Biological Results and Discussion).

Heating of **447** with excess HFAA in acetic acid at 120^{o}C for 20 hours characteristically resulted in rapid and persistent appearance of a dark red colour during the reaction. After this time, the target pyrazolo[1,5-*a*]pyrimidine **549** was isolated as a red powder in a satisfactory yield of 54% (Scheme 4.35).
The final derivatisation undertaken in this study was the transformation of aminopyrazole **447** to the attractive triazinedione congener **539**. This derivative was anticipated to be highly useful, both as it constitutes a novel planar H-bonding pharmacophore, and also as an investigative tool to ascertain whether overall larger ring size or relative spatial distortion of the uracil motif (pyrazolo[1,5-*a*]pyrimidine orientation), within this bicyclic derivative **539** has any biological effect in comparison to the analogous 6-membered uracil ring system of 5,6-bisindolylpyrimidin-2,4-dione **507**.

Reaction with 2.2 equivalents of chlorosulfonyl isocyanate in DCM, containing triethylamine, at room temperature for 16 hours provided only starting material **447** following aqueous quenching of the dark reaction mixture. Fortunately, the reaction proceeded well once the conditions were altered to employ chlorocarbonyl isocyanate in DCM at 0^{o}C, in the presence of **447**, along with a few drops of triethylamine, followed by gentle stirring at room temperature for 16 hours.[58] Addition of water resulted in precipitation of the novel triazinedione product **539**, in an excellent yield of 84% following filtration (Scheme 4.35).

4.9.3.3 Regiochemistry of 5-aminopyrazole monosubstitution

The observed pattern of electrophile addition to the aminopyrazole ring was observed to be strongly dependent on the nature of the electrophile and reaction conditions, and was investigated by means of ^{1}H NMR spectroscopy. Evidence of N-5 or N-1 substitution is given from the presence or absence of signals relating to the amine (2H, broad peak between 4.5-6.5 ppm) as well as confirmatory evidence from single crystal X-ray structure analysis (see Section 4.10.2.1). Consequently it is seen that the amine is functionalized in the case of the trifluoroacetamide and the methanesulfonamide, whereas in all other cases the ring nitrogen was substituted. Interestingly, in the case of methanesulfonylation, reaction of **447** with methanesulfonyl chloride in refluxing acetonitrile, containing Et_3N was unsuccessful, amino substituted derivative **545** was formed in the presence of pyridine at 90^{o}C - indicating that thermal conditions may have a role in defining the preferred site of ring attack.

4.10 Synthesis of aryl-substituted indolyl-heterocycles

Recognition of how privileged H-bonding characteristics within diverse aryl-substituted indolyl heterocycles may be translated into design of new 3,4-diarylpyrrole protein-interacting analogues has attracted notable success in the area of kinase inhibition (Fig. 4.15). Preliminary compound screening by Peifer and co-workers recently identified indolylarylmaleimide derivative **396** with an IC_{50} value of 2.5 nM for VEGFR2, while a simplified pyrrole-2-one **397**, also exhibited potent VEGF-R2 inhibitory activity (IC_{50} = 31 nM).[78,79] The potential for enzyme selectivity arising from strategic modification of the H-bonding pyrrole ring system was also confirmed by diminished VEGFR2 inhibition within regioisomeric pyrrol-5-one **551** (IC_{50} = 11 µM), resulting from altered orientation of the lactam ring in the ATP-binding pocket, and sets the platform for maleimide ring bioisosteric replacement in order to achieve complementary biological activity within this series.

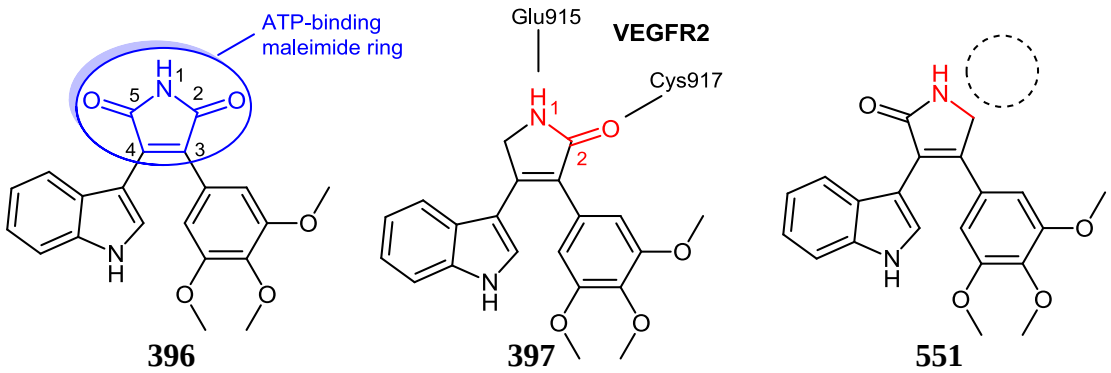


Fig. 4.15: Structures of arylindolyl-substituted PKIs for rational design of new pyrrole analogues.

Based on this discovery, novel asymmetrically substituted 4-(indol-3-yl)-3-(3,4,5-trimethoxyphenyl)-substituted analogues (pyrazol-5-one **552**; pyrazol-5-amine **553**) were valuable due to their ability to mimic the binary N^1 H-bond donor – N^2 acceptor motif, as well as introducing auxiliary H-bonding functionality at the C-5 position (Fig. 4.16). Work was also carried out to attempt a convergent cyclocondensation route to novel H-bonding 6-membered pyrimidin-4-one **554** derivatives.

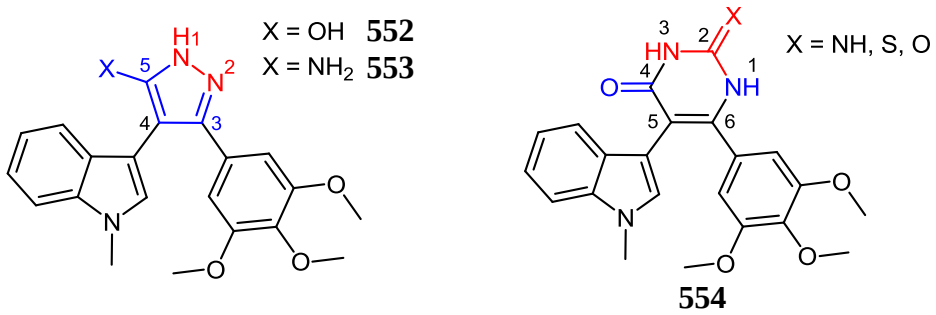


Fig. 4.16: Potential 3,4-diarylmaleimide binding motif in novel analogues of VEGFR inhibitor **397**.

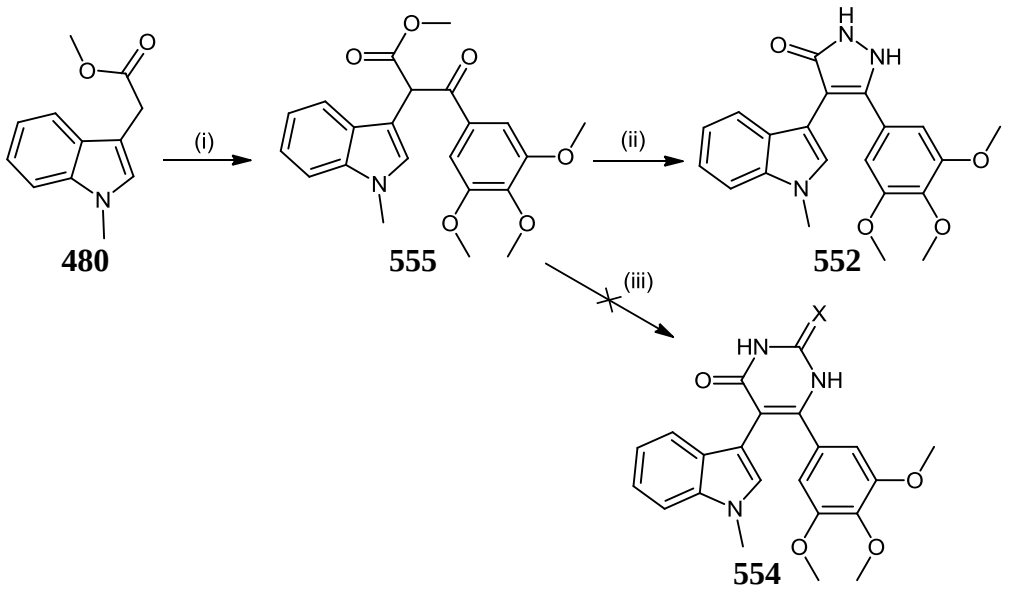
4.10.1 Synthesis of 4-(1-methyl-1*H*-indol-3-yl)-5-(3,4,5-trimethoxyphenyl)-pyrazol-3-one

Reaction of methyl 2-(1-methyl-1*H*-indol-3-yl)acetate **480**, under LDA-mediated conditions with a slight excess of 3,4,5-trimethoxybenzoyl chloride **499** in THF at −78°C**,** afforded access to light orange crystalline methyl 2-(1-methyl-1*H*-indol-3-yl)-3-oxo-3-(3,4,5-trimethoxyphenyl)propanoate **555** in a yield of 35% following chromatography. This intermediate **555** was then heated with hydrazine, along with camphoric acid, in methanol at reflux for 24 hours, to provide the novel dark brown pyrazolone derivative **552** in a yield of 60%, employing 0.5% methanol/DCM chromatography (Scheme 4.37).[34]

Unfortunately, pyrimidin-4-one **554** transformation could not be completed for this series; reaction under conventional methoxide-mediated conditions with thiourea or guanidine carbonate yielded only starting material **555** following acidic work-up of the crude reaction mixture after heating for 48 hours. In combination, the resonance effects of several -OCH_3 groups was theorized to increase the electron density at the carbonyl site, thus significantly decreasing or negating its electrophilic reactivity with moderate nucleophiles under these conditions (Scheme 4.37). Attempted microwave conversion to **554** under harsh conditions was also unsuccessful, in the presence of 2.5 equivalents of camphoric acid, following solvent-free heating of **555** and excess thiourea or urea for 25 minutes at 160°C.[41]

The observed order of reactivity (NH_2NH_2 >> thiourea/urea) is consistent with literature data, and accounts for the initial success in pyrazolone **552** formation, due to the superior

nitrogen nucleophilicity associated with hydrazine attack on the relatively electron rich carbonyl group in this system. In addition to the poor reactivity of urea and thiourea, it was also postulated that a high barrier to rotation of both flexible aryl substituents may exist, due to steric repulsion, in order to prevent desired 5-(indol-3-yl)-6-(3,4,5-trimethoxyphenyl)-pyrimidin-4-one **554** formation (Scheme 4.37). Future work in this area will investigate this phenomenon in order to devise an alternative route to these attractive molecular templates.



Reagents and conditions: (i) 2.2 eq. LDA, 1.5 eq. 3,4,5-$(O\text{-}CH_3)_3C_6H_2$-COCl, THF, -78°C - rt, 20h, **3** = 35%; (ii) 4 eq. $NH_2NH_2.H_2O$, 1 eq. camphoric acid, MeOH, reflux, 24h, **4** = 60%; (iii) 20 eq. NaOMe, 5 eq. $NH_2(C=S)NH_2$ or $[NH_2(C=NH_2)NH_2]_2CO_3$, MeOH, reflux, 24h, n.r

Scheme 4.37: Formation and reactivity of methyl 2-(1-methyl-1*H*-indol-3-yl)-3-oxo-3-(3,4,5-trimethoxyphenyl)propanoate **555**.

4.10.2 Synthesis of 4-(1-methyl-1*H*-indol-3-yl)-3-(3,4,5-trimethoxyphenyl)-5-aminopyrazole

The identification of new potential bioisosteres for 4-(indol-3-yl)-3-(3,4,5-trimethoxyphenyl)-pyrrole-2,5-dione **396** and 4-(indol-3-yl)-3-(3,4,5-trimethoxyphenyl)-pyrrole-2-one **397** agents as protein kinase drug targets, resulted in development of a successful synthetic route to the parent 3,4-diaryl-5-aminopyrazole **553** system (Fig. 4.17).

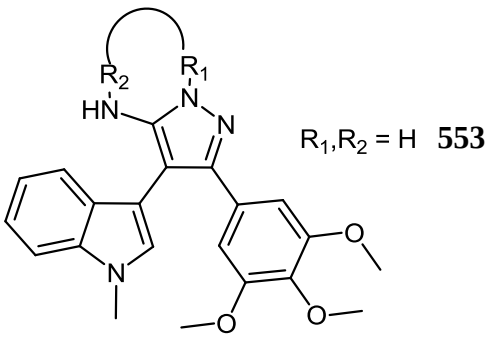
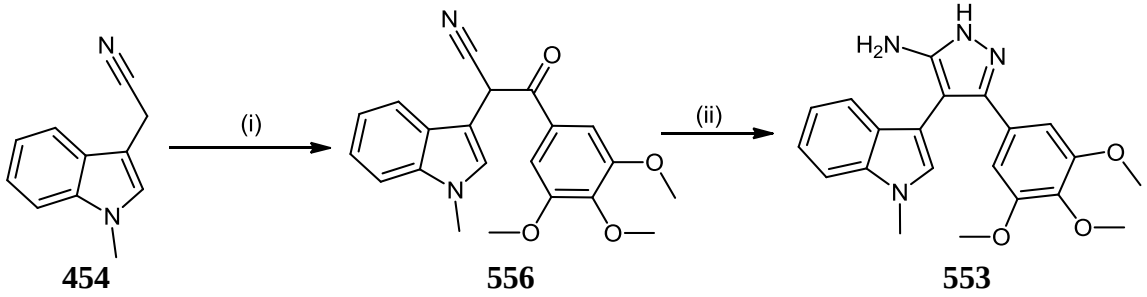


Fig. 4.17: General structure of substituted 4-(indol-3-yl)-3-(3,4,5-trimethoxyphenyl) pyrazol-5-amine **553** core

In the initial step, *N*-methyl indole-3-acetonitrile **454** was cooled to −78°C in the presence of LDA, and stirred for 1.5 hours, prior to addition of 3,4,5-trimethoxybenzoyl chloride **499**. On work-up and chromatography, the novel light orange, crystalline 2-(1-methyl-1*H*-indol-3-yl)-3-oxo-3-(3,4,5-trimethoxyphenyl)propanenitrile **556** was formed in a yield of 35% (Scheme 4.35). Following reaction of β-ketonitrile **556** with hydrazine monohydrate in absolute ethanol, containing a few drops of acetic acid, at 80°C for 24 hours, compound **553** was isolated as a brown powder in a yield of 23% (Scheme 4.38).



454 **556** **553**

Reagents and conditions: (i)(a) 1.8M LDA, 3,4,5-$(OMe)_3C_6H_2COCl$ (**499**), THF, -78°C - rt, 20h (b) NH_4Cl, **556** = 35%; (ii) 5 eq. $NH_2NH_2.H_2O$, 1 eq. camphoric acid, MeOH, reflux, 24h, **553** = 62%

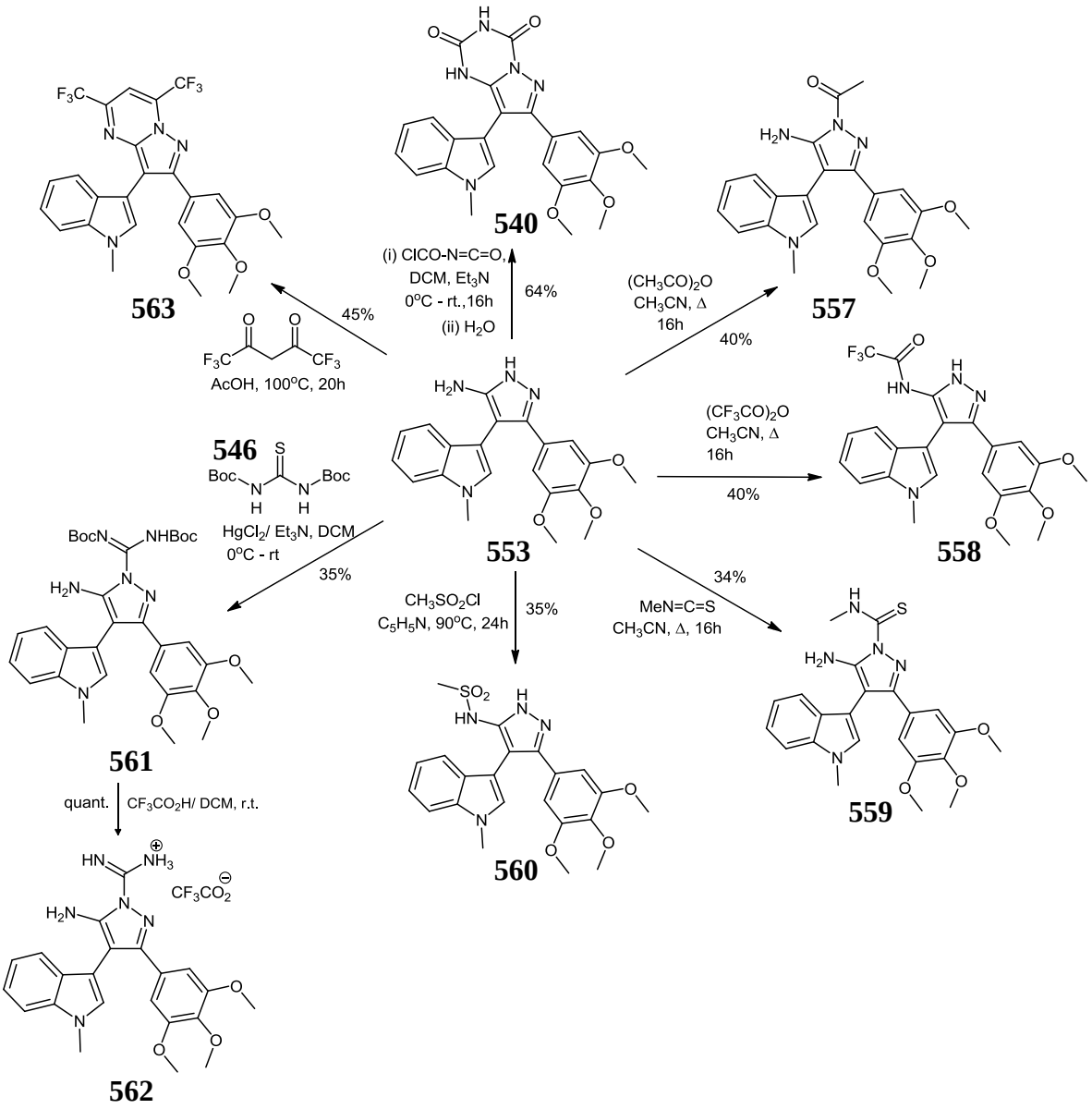
Scheme 4.38

In order to overcome improve the yield of this reaction, transformation of intermediate **556** was also investigated in the presence of one equivalent of hydrazine, along with camphoric acid in methanol for 3 hours at reflux. At this point, a small amount of desired product **553**, was detectable by TLC, along with a large proportion of starting material **556**. Following rapid addition of 4 equivalents of hydrazine to the reaction flask and vigorous reflux of the dark mixture for 24 hours, basic work-up and chromatography of the crude residue afforded 5-aminopyrazole **553** in a satisfactory yield of 62%, on multi-gram scale.[34]

4.10.3 Derivatisation of 4-(1-methyl-1*H*-indol-3-yl)-5-(3,4,5-trimethoxyphenyl)-5-aminopyrazole

A full comparative library of substituted 4-(1-methyl-1*H*-indol-3-yl)-3-(3,4,5-trimethoxyphenyl)-5-aminopyrazole **553** analogues was obtained by diversity-oriented methodology (c.f. Section 4.9). This synthetic work has exploited the versatile rationale proposed by Peifer *et al.*, by engineering a panel of novel congeners possessing the indole-substituted combretastatin A-4 stilbene scaffold and diverse heterocyclic bridgehead systems in order to explore the chemical space between the H-bonding pyrrole ring and kinase backbone, with the potential for accessing new binding modes and attractive biological activity (Scheme 4.39).[78-81]

*4.10.3.1 Mono-*N*-substitution of aminopyrazole ring*

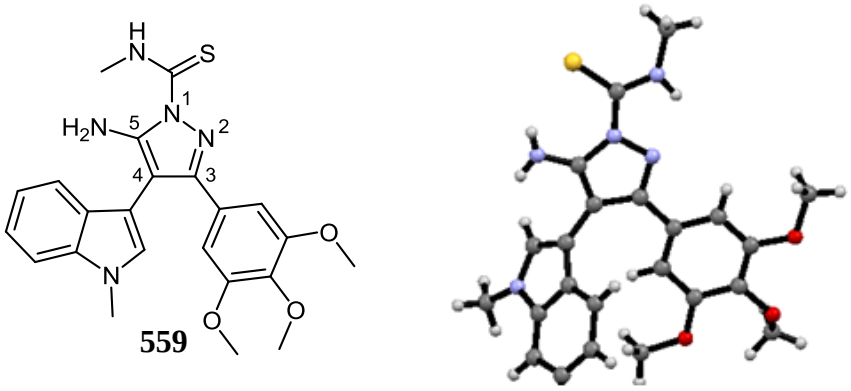


Scheme 4.39: Target synthetic routes employed for chemical derivatisation of 4-(indol-3-yl)-3-(3,4,5-trimethoxyphenyl)-5-aminopyrazole **553**

Utilising chemistry previously encountered in the bisindolyl series, the acetyl substituted analogue **557** was derived from reaction of acetic anhydride, which was stirred along with aminopyrazole **553** in refluxing acetonitrile, overnight. Following basic work-up, compound **557** was purified by chromatography as an off-white crystalline solid in a yield of 40% (Scheme 4.39). Reaction of trifluoroacetic anhydride with parent **553** under similar conditions afforded the pyrazolic trifluoroacetamide **558**, in identical yield of 40%, as a beige crystalline solid.

Synthesis of a derivative furnishing attractive thioamide functionality was accomplished by heating of **553** with methyl isothiocyanate, in acetonitrile for 20 hours.[76] The reaction was

quenched by addition of water and stored at 0°C for a further hour. Filtration of the resultant slurry afforded a crop of compound **559** as fine orange crystals. Evaporation of the mother liquor followed by chromatography of the light brown residue resulted in isolation of N^1-carbothioamide **559** in a cumulative yield of 34% (Scheme 4.39). In addition to observing the presence of the NH_2 signal in ^1H NMR, N^1-substitution within this compound was also proven by obtaining a single crystal X-ray structure of this novel product (Fig. 4.18). The influence of conjugation observed in this structure also confirms the phenomenon of unequal electron distribution within these heterocyclic systems, consistent with NMR data.



559

Fig. 4.18: Molecular structure of N^1-substituted aminopyrazole derivative **559**

Heating of **553** and methanesulfonyl chloride in neat pyridine for 20 hours afforded arylsulfonamide **560**, which was isolated following acidic work-up and chromatography, in a moderate yield of 35%, as a clay-coloured powder (Scheme 4.39).

Synthesis of novel congener **562** possessing a warhead guanidine subunit neatly complemented our strategy for targeting bioactivity within compounds comprising varied H-bonding and diverse enzyme-binding properties.

Reaction of aminopyrazole **553** with (*N*,*N'*-di-*tert*-butoxycarbonyl)thiourea **546**, mercuric chloride, and triethylamine, in DCM, for 1 hour at 0°C, prior to stirring at room temperature overnight, afforded non-polar *tert*-butyl-[(5-amino-4-{1-methyl-1*H*-indol-3-yl}-3-(3,4,5-trimethoxyphenyl)-1*H*-pyrazol-1-yl)({*tert*-butoxycarbonyl}amino)methylene] carbamate **561** (35%), as the first fraction, eluting with 10% ethyl acetate/hexane. Deprotection of **561** was subsequently carried out employing 10% TFA in DCM, in order to liberate the trifluoroacetate salt **562**, following drying (Scheme 4.39).[77]

4.10.3.2 Pyrazolo[1,5-a]pyrimidine heterocycle formation

Formation of the bicyclic pyrazolo[1,5-*a*]pyrimidine derivative **563** was accomplished by heating of **553** with HFAA in acetic acid, at 120°C, for 16 hours. Following stirring of the dark red reaction mixture overnight, TLC analysis indicated formation of an intense red spot, corresponding to the heterocyclic product **563**. Successful isolation of the pure derivative **563**, as a red crystalline solid, was achieved following hexane/ethyl acetate chromatography, in a yield of 45% (Scheme 4.39).

The final reaction in this derivatisation study was undertaken in order to incorporate the novel planar H-bonding pyrazolo[1,5-*a*][1,3,5]triazine-2,4-dione nucleus, following conversion of **553** to cyclised congener **540**, comprising the biologically relevant uracil structural motif.[58]

Addition of the unsubstituted aminopyrazole **553** to chlorocarbonyl isocyanate, in DCM, along with a few drops of triethylamine, for 16 hours, afforded a heterogeneous dark brown slurry, and subsequently filtered in order to isolate novel congener **540**, as a light brown powder, following successive washing with water and diethyl ether. Pure 8-(1-methyl-1*H*-indol-3-yl)-7-(3,4,5-trimethoxyphenyl)pyrazolo[1,5-*a*][1,3,5]triazine-2,4(1*H*,3*H*)-dione **540** was synthesised in an excellent yield of 64%, and required no further purification, under these conditions (Scheme 4.39).

4.11 Synthesis of 4,5-bisindolyl-2-substituted imidazoles

Synthesis of 1,2-bisindolyl-*cis*-ethene compounds bearing a novel substitution pattern (**564**) was also implemented, following initial design of imidazole bridgehead heterocycles incorporating novel indolocarbazole functionality **449** (Fig. 4.18).[12] Major advantages of this route include incorporation of non-protected indole units, rapid access to dione precursor **565**, and the combinatorial nature of the final three-component imidazole-forming reaction.[82] Further study to extend the undoubted utility of this chemistry towards imidazo[4,5-*c*]indolo[2,3-*a*]carbazole **449** synthesis is also being undertaken within our research group.

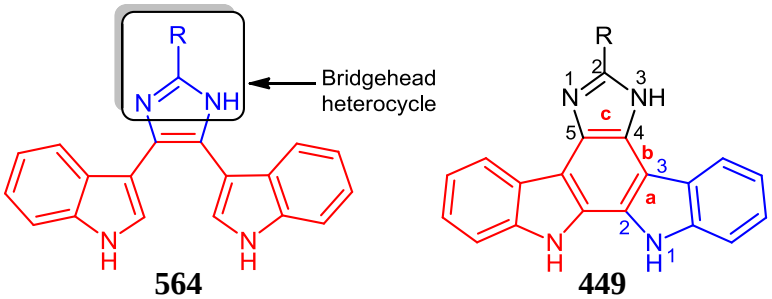
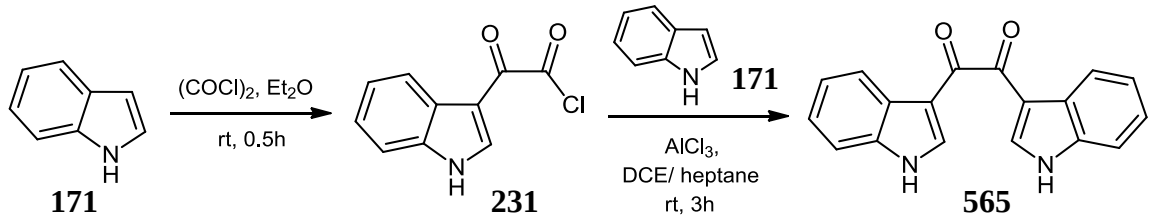


Fig. 4.19: Design of a new imidazole-based indolocarbazole compound class

4.11.1 Synthesis of 1,2-bis(1*H*-indol-3-yl)ethane-1,2-dione

The successful route to bisindolyl ethanedione **565**, was accomplished following reaction of oxalyl chloride with indole **171,** in diethyl ether as solvent, at room temperature, for 30 minutes, to yield light orange 2-(1*H*-indol-3-yl)-2-oxoacetyl chloride **231** in a yield of 90%. This labile intermediate was prepared and used on the same day, as it could not be stored for more than a few hours at room temperature prior to degradation. Employing the conditions of Krayushkin *et al.*, glyoxylyl chloride **231** was initially charged portionwise to a mixture of heptane and DCE, containing $AlCl_3$. Following vigorous stirring of the heterogeneous dark red suspension at room temperature, a solution of **171** in DCE was added dropwise, and stirred for 3 hours.[83]

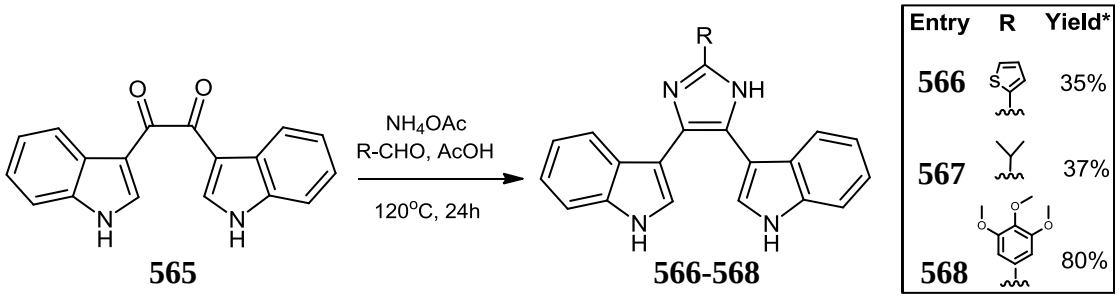


Scheme 4.40

The yield of compound **565** in this step became variable during up-scaling, but was successfully maintained in the range of 45-65%, and could not be improved by extending reaction time to 24 hours or by replacement of DCE with DCM. Trituration with ether/ethanol (20:1) isolated the desired intermediate **565** as a light brown powder in high purity, on multi-gram scale (Scheme 4.40).

4.11.2 A potential one-pot condensation route to 4,5-bisindolylimidazoles

With a scalable method to synthesise dione **565** in hand, one-pot thermal condensation offered a viable one-pot route to the novel 4,5-bisindolyl-2-substituted imidazole **564** template. Reaction of dione **565** with ammonium acetate, along with an appropriate aldehyde, in refluxing acetic acid, for 24 hours, yielded a dark-red solution in each case, which, following chromatography, supplied the crude products (**566**-**568**) (Scheme 4.41).[82]

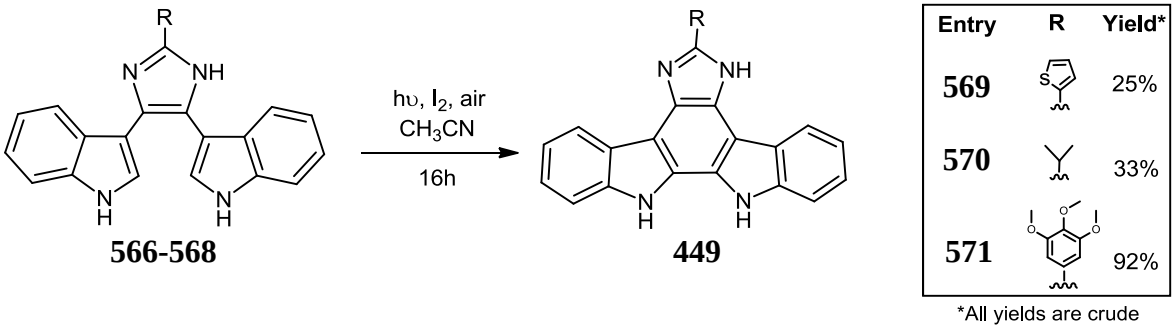


Scheme 4.41

Using thiophene-2-carboxaldehyde, the product imidazole **566** was isolated as a red powder in a yield of 35%, following elution with 1% methanol/DCM. In the case of isobutyraldehyde, these conditions yielded 4,5-bisindolyl-2-isopropyl-imidazole **567**, as a light brown solid (37%) following chromatography. Full purification of these derivatives was extremely challenging, and is the subject of current development, including investigation of reaction conditions and modes of crystallisation.

4.11.3 Photochemical synthesis of imidazo[4,5-*c*]indolo[2,3-*a*]carbazoles

Following identification of an efficient route to the acyclic bisindolyl imidazole framework **564**, a photochemical cyclisation step successfully furnished crude indolo[2,3-*a*]carbazoles in moderate yields.



Scheme 4.42

Irradiation of 4,5-bisindolyl-2-(thien-2-yl)-substituted imidazole **566** in HPLC-grade acetonitrile (1 mg/2.5 mL), containing iodine (50 mol%), for 16 hours afforded cyclised **569** in a crude yield of 25%. Exposure of 2-isopropyl imidazole **567** to U.V. irradiation, afforded indolocarbazole **570** in 33% yield (Scheme 4.42).

Synthesis of a 2-(3,4,5-trimethoxyphenyl)-imidazole analogue was also deemed interesting as Caballero *et al.* previously reported 4-arylpyrrolo[3,4-*c*]carbazole-1,3-dione **572**, with an IC_{50} value of 0.8 μM against mouse lymphoma cancer cell line P-388, with enhanced *in vitro* activity due to introduction of the 3,4,5-trimethoxyphenyl moiety as the key aryl subunit.[84] As illustrated in Scheme 4.41, imidazole **568** was initially formed as a red crystalline solid in a yield of 80%, prior to U.V. irradiation for 16 hours, to isolate aromatised congener **571** as a dark-red crystalline solid, semi-pure, in a yield of 92% after chromatography, along with an inseparable variable proportion of contaminating side material which resisted all attempts at removal, in order to furnish the fully pure final indolocarbazole derivative (Scheme 4.42).

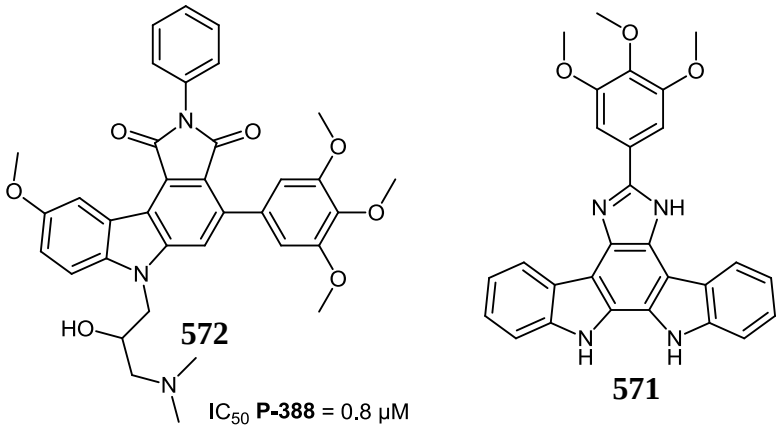


Fig. 4.20: Comparison beween a novel imidazole compound and anti-cancer **572**

This attractive methodology represents an original and economical route to access complex substituted indolocarbazole derivatives from indole **171** as a simple building block. Preliminary optimisation was carried out on the photocyclisation step, by determining the appropriate solvent, dilution level and reaction time. However, full characterization could not be achieved for these compounds, due to their difficult purification and LCMS purification of these compounds will be undertaken in future research.

4.12 Conclusion

Protein kinase inhibitors are an attractive goal for new drug therapy (especially in cancer chemotherapy). Inhibitors vary widely in structure and have inherent selectivity problems due to the wide abundance of the highly conserved ATP-binding pocket in which they bind. One of the templates used for kinase inhibition is based on the 3,4-bisindolylmaleimide structural motif, illustrated by the clinical PKC-β inhibitor ruboxistaurin **80**, which comprises a critical enzyme-interacting pyrrol-2,5-dione moiety. The reduced lactam ring is also present in several bioactive indolo[2,3-*a*]carbazoles such as K-252c **6** and in arylindolyl systems such as **397** with prodigious inhibitory activity against VEGFR2 (Fig. 4.21). These structural classes represent the anti-cancer diarylpyrrole heterocyclic templates which were effectively modified over the course of this work.

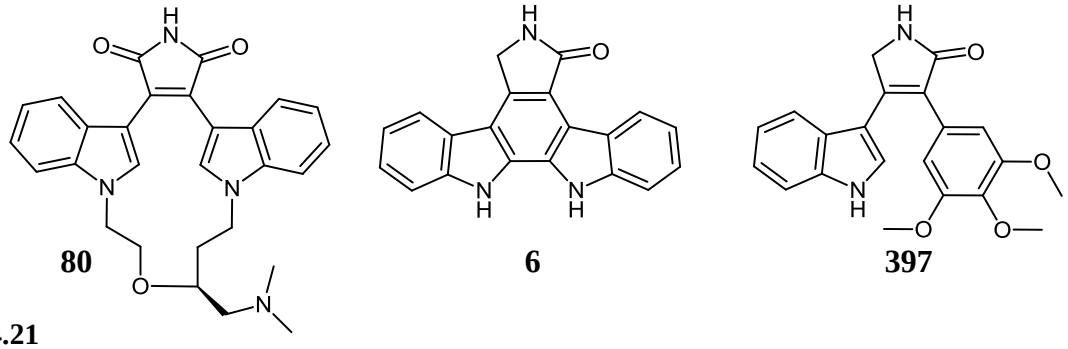


Fig. 4.21

Extensive investigations were carried out into establishing a complete protocol for the preparation of indolo[2,3-*a*]pyrimido[5,4-*c*]carbazole **441** derivatives *via* a convergent route; it was found that a β-ketoester intermediate **478** allowed access to a wide number of pyrimidine analogues structurally related to ruboxistaurin **80** *via* base-mediated cyclocondensation (Fig. 4.22; **A**).

Following work on optimisation of this route, a yield of 80% can now be achieved for β-ketoester intermediate **478**; the novel bisindolylthiouracil compound **514** was subsequently formed in 24% yield, by methoxide-induced reaction of **478** with thiourea. Following extensive investigation, the thiouracil moiety was oxidatively desulfurised to yield the bisindolyl uracil congener **507**, following heating with ethyl bromoacetate, in methanol. Additionally, formation of the reduced pyrimidin-4(3*H*)-one (lactam) **537** system by $NaBH_4/NiBr_2$ reaction, along with subsequent oxidative cyclisation, afforded an interesting indolo[2,3-*a*]carbazole analogue **538** with close structural similarity to the selective PKC-inhibitory natural product K-252c **6** (Fig. 4.22; **C**).

5,6-Bisindolyl-2-aminopyrimidin-4-one **445** was produced in 45% yield by means of a similar base-mediated conversion of **478**, in the presence of guanidine carbonate.[2] The ultimate aromatisation of this bisindolyl congener **445** to form novel 2-aminoindolocarbazol-4(3*H*)-one **442** was studied under a number of reaction conditions which have been previously utilised in oxidative ring-closure within classical bisindolylmaleimide compounds. It has now been successfully achieved through U.V. irradiation (mercury lamp: 254 nm/ Pyrex glassware) of a dilute mixture (2.5 mL/mg) of the acyclic isocytosine **445** in a 3:2 acetonitrile/methanol solvent system, along with a catalytic amount of iodine, in air, for 16 hours (Fig. 4.22; **C**).

Based on preliminary molecular modelling studies, new H-bonding networks were explored, which conserved key elements of the heterocyclic indolocarbazole pharmacophore. Resolving this challenge led to the design of a panel of novel 3,4-bisindolyl-5-aminopyrazole derivatives within a new anti-cancer class (Fig. 4.22; **A**). Protection of 3-indolylacetonitrile **229** as its *N*-methyl derivative **454** was achieved with NaH/iodomethane in 97% yield, which, on reaction with *N*-methyl indole-3-carbonyl chloride **479**, under our modified Claisen conditions, enabled synthesis of the corresponding advanced β-ketonitrile precursor **541**. Final 5-aminopyrazole **447** synthesis involved treatment of intermediate **541** with excess hydrazine hydrate overnight, in refluxing ethanol, containing an acid catalyst.

Complementary work was undertaken to furnish (3,4,5-trimethoxyphenyl)-substituted indolylpyrazolone **552** and aminopyrazole **553**, closely related to the potent arylindolyl VEGFR2 inhibitor **397,** by initially employing a modifying Claisen route, along with 3,4,5-trimethoxyphenyl carbonyl chloride **499** as acylating agent. Synthetic derivatisation of this 5-aminopyrazole ring moiety was also investigated, in order to explore different pyrazolic H-bonding orientations with potential anti-kinase activity resulting from enhanced protein backbone interactions (Fig. 4.22; **B**).

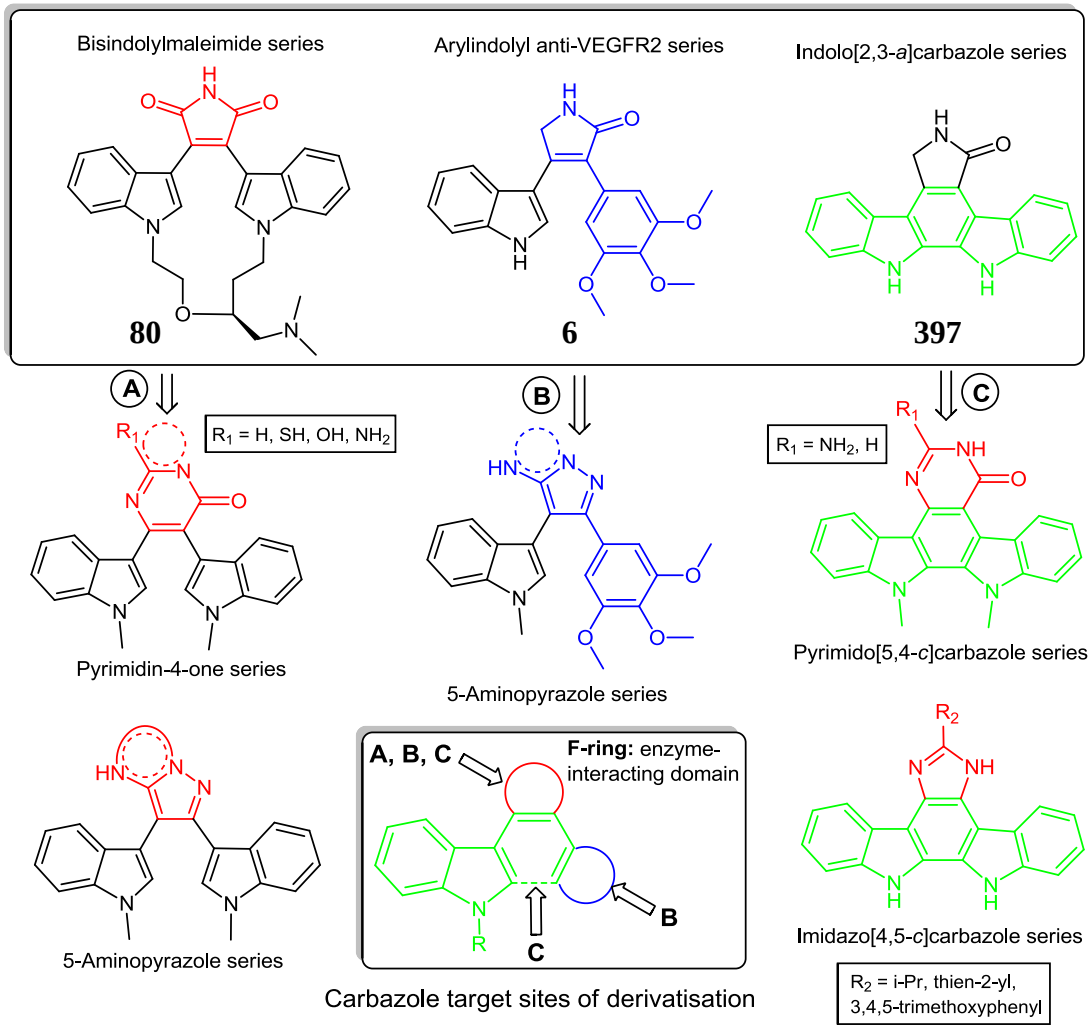


Fig. 4.22: General structures of heterocyclic fused indolo[2,3-*a*]carbazole derivatives

This work also identified a novel synthetic route towards heteroaryl-substituted bisindolyl imidazoles **566-567, 573**, which were converted to the corresponding indolo[2,3-*a*]carbazoles under optimised U.V. conditions, in the presence of air. However, solubility and purification issues have so far precluded their full isolation in high purity (Fig. 4.22; **C**).

During the course of this work, over 50 novel compounds have been synthesised by means of a range of chemistry previously unreported for the indolo[2,3-*a*]carbazole class, as well as

initiating successful chemistry for exploring the regioisomeric indolo[2,3-*c*]carbazole series *via* nucleophilic ring-opening, to afford attractive pyridazinedione **473** formation.

Development of a novel route towards formation of 5,6-bisindolylpyrimidin-4-one derivatives, prior to transformation of this acyclic template to the fully planar pyrimido[5,4-*c*]carbazole chromophore has been completed and dissemination of this work is underway through publication in peer-reviewed scientific literature. In order to probe the structural basis for arylindolyl kinase activity, constituent heteroaryl character was rationally varied, in order to access diverse substituted 4,5-bisindolyl, as well as 4-(*N*-methyl indol-3-yl)-3-(3,4,5-trimethoxyphenyl)-5-aminopyrazole congeners.

Finally, a valuable study of the factors affecting successful oxidative closure of novel bisindolyl heterocyclic precursors, to yield the final fully contiguous indolo[2,3-*a*]carbazole ring system was successfully accomplished, and this desirable transformation has been successfully rendered on a number of novel acyclic bisindolyl substrates by means of optimised photochemical methodology.

4.13 References

1. Knolker, H. J.; Reddy, K. R. *Chem.Rev.* **2002**, *102*, 4303-4427.
2. Wang, J. J.; Rosingana, M.; Watson, D. J.; Dowdy, E. D.; Discordia, R. P.; Soundarajan, N.; Li, W. S. *Tetrahedron Lett.* **2001**, *42*, 8935-8937.
3. Harris, W.; Hill, C. H.; Keech, E.; Malsher, P. *Tetrahedron Lett.* **1993**, *34*, 8361-8364.
4. Brenner, M.; Rexhausen, H.; Steffan, B.; Steglich, W. *Tetrahedron* **1988**, *44*, 2887-2892.
5. Steglich, W.; Steffan, B.; Kopanski, L.; Eckhardt, G. *Angew.Chem.* **1980**, *19*, 459-460.
6. Xie, G. J.; Lown, J. W. *Tetrahedron Lett.* **1994**, *35*, 5555-5558.
7. Dubernet, M.; Caubert, V.; Guillard, J.; Viaud-Massuard, M. C. *Tetrahedron* **2005**, *61*, 4585-4593.
8. Choi, D. S.; Huang, S. L.; Huang, M. S.; Barnard, T. S.; Adams, R. D.; Seminario, J. M.; Tour, J. M. *J.Org.Chem.* **1998**, *63*, 2646-2655.
9. Joyce, R. P.; Gainor, J. A.; Weinreb, S. M. *J.Org.Chem.* **1987**, *52*, 1177-1185.
10. Weinreb, S. M.; Garigipati, R. S.; Gainor, J. A. *Heterocycles* **1984**, *21*, 309-324.
11. Witulski, B.; Schweikert, T. *Synthesis* **2005**, 1959-1966.
12. Janosik, T.; Wahlstrom, N.; Bergman, J. *Tetrahedron* **2008**, *64*, 9159-9180.
13. Faul, M. M.; Sullivan, K. A. *Tetrahedron Lett.* **2001**, *42*, 3271-3273.
14. Steglich, W. *Pure Appl.Chem.* **1989**, *61*, 281-288.
15. Faul, M. M.; Winneroski, L. L.; Krumrich, C. A. *J.Org.Chem.* **1998**, *63*, 6053-6058.
16. Yang, S. M.; Malaviya, R.; Wilson, L. J.; Argentieri, R.; Chen, X.; Yang, C. M.; Wang, B. B.; Cavender, D.; Murray, W. V. *Bioorg.Med.Chem.Lett.* **2007**, *17*, 326-331.
17. Kramer, H. J.; Kessler, D.; Hipler, U. C.; Irlinger, B.; Hort, W.; Bodeker, R. H.; Steglich, W.; Mayser, P. *ChemBioChem* **2005**, *6*, 2290-2297.
18. Lakatosh, S. A.; Balzarini, J.; Andrei, G.; Snoeck, R.; De Clercq, E.; Preobrazhenskaya, M. N. *J.Antibiot.* **2002**, *55*, 768-773.
19. Sancelme, M.; Fabre, S.; Prudhomme, M. *J.Antibiot.* **1994**, *47*, 792-798.
20. Bergman, J.; Koch, E.; Pelcman, B. *Tetrahedron* **1995**, *51*, 5631-5642.
21. Barry, J. F.; Wallace, T. W.; Walshe, N. D. A. *Tetrahedron* **1995**, *51*, 12797-12806.
22. Merlic, C. A.; You, Y.; McInnes, D. M.; Zechman, A. L.; Miller, M. M.; Deng, Q. *Tetrahedron* **2001**, *57*, 5199-5212.
23. Tsuchimoto, T.; Matsubayashi, H.; Kaneko, M.; Nagase, Y.; Miyamura, T.; Shirakawa, E. *J.Am.Chem.Soc.* **2008**, *130*, 15823-15835.
24. Hudkins, R. L.; Diebold, J. L.; Marsh, F. D. *J.Org.Chem.* **1995**, *60*, 6218-6220.
25. Murray, P. E.; McNally, V. A.; Lockyer, S. D.; Williams, K. J.; Stratford, I. J.; Jaffar, M.; Freeman, S. *Bioorg.Med.Chem.* **2002**, *10*, 525-530.
26. Desarbre, E.; Bergman, J. *J.Chem.Soc., Perkin Trans.1* **1998**, 2009-2016.
27. Bergman, J. *Acta Chem.Scand.* **1971**, *25*, 1277-1280.
28. Bouffard, J.; Eaton, R. F.; Muller, P.; Swager, T. M. *J.Org.Chem.* **2007**, *72*, 10166-10180.
29. Brouillette, Y.; Martinez, J.; Lisowski, V. *Eur.J.Org.Chem.* **2009**, *2009*, 3487-3503.
30. Jiang, X. L.; Tiwari, A.; Thompson, M.; Chen, Z. H.; Cleary, T. P.; Lee, T. B. K. *Org.Process Res.Dev.* **2001**, *5*, 604-608.
31. Bergman, J.; Norrby, P. O.; Sand, P. *Tetrahedron* **1990**, *46*, 6113-6124.
32. Tyson, F. T.; Shaw, J. T. *J.Am.Chem.Soc.* **1952**, *74*, 2273-2274.
33. Mouaddib, A.; Joseph, B.; Hasnaoui, A.; Merour, J. Y. *Synthesis* **2000**, 549-556.
34. Brana, M. F.; Gradillas, A.; Ovalles, A. G.; Lopez, B.; Acero, N.; Llinares, F.; Mingarro, D. M. *Bioorg.Med.Chem.* **2006**, *14*, 9-16.

35. Merlic, C. A.; McInnes, D. M. *Tetrahedron Lett.* **1997**, *38*, 7661-7664.
36. Bourderioux, A.; Kassis, P.; Merour, J.-V.; Routier, S. *Tetrahedron* **2008**, *64*, 11012-11019.
37. Hutchins, M.; Sainsbury, M.; Scopes, D. *Tetrahedron* **1984**, *40*, 1511-1515.
38. Player, M. R.; Sowell, J. W. *J.Heterocycl.Chem.* **1995**, *32*, 1537-1540.
39. Orzeszko, B.; Kazimierczuk, Z.; Maurin, J. K.; Laudy, A. E.; Starosciak, B. J.; Vilpo, J.; Vilpo, L.; Balzarini, J.; Orzeszko, A. *Il Farmaco* **2004**, *59*, 929-937.
40. Larsen, J. S.; Christensen, L.; Ludvig, G.; Jorgensen, P. T.; Pedersen, E. B.; Nielsen, C. *J.Chem.Soc., Perkin Trans.1* **2000**, 3035-3038.
41. Mojtahedi, M. M.; Saidi, M. R.; Shirzi, J. S.; Bolourtchian, M. *Synth.Commun.* **2002**, *32*, 851-855.
42. Beccalli, E. M.; Gelmi, M. L.; Marchesini, A. *Tetrahedron* **1998**, *54*, 6909-6918.
43. Ketcha, D. M.; Gribble, G. W. *J.Org.Chem.* **1985**, *50*, 5451-5457.
44. Silvestri, R.; De Martino, G.; La Regina, G.; Artico, M.; Massa, S.; Vargiu, L.; Mura, M.; Loi, A. G.; Marceddu, T.; La Colla, P. *J.Med.Chem.* **2003**, *46*, 2482-2493.
45. Pierce, L. T.; Cahill, M. M.; McCarthy, F. *Tetrahedron* **2010**, *66*, 9754-9761.
46. Hassan, M. A.; Mohamed, M. M.; Shiba, S. A.; Abou El-Regal, M. K.; Khalil, A. *Phosphorus, Sulfur Silicon Relat.Elem.* **2003**, *178*, 2497-2504.
47. Casar, Z.; Bevk, D.; Svete, J.; Stanovnik, B. *Tetrahedron* **2005**, *61*, 7508-7519.
48. Horton, P. A.; Longley, R. E.; McConnell, O. J.; Ballas, L. M. *Experientia* **1994**, *50*, 843-845.
49. Argade, A.; Carroll, D.; Singh, R.; Li, H.; Catalano, S.; Hitoshi, Y.; Grossbard, E. *International Patent* **2008**, WO/2008-061201, PCT/US2007-084855.
50. Heathcote, D. A.; Patel, H.; Kroll, S. H. B.; Hazel, P.; Periyasamy, M.; Alikian, M.; Kanneganti, S. K.; Jogalekar, A. S.; Scheiper, B.; Barbazanges, M.; Blum, A.; Brackow, J.; Siwicka, A.; Pace, R. D. M.; Fuchter, M. J.; Snyder, J. P.; Liotta, D. C.; Freemont, P. S.; Aboagye, E. O.; Coombes, R. C.; Barrett, A. G. M.; Ali, S. *J.Med.Chem.* **2010**, *53*, 8508-8522.
51. Jiang, B.; Yang, C. G.; Xiong, W. N.; Wang, J. *Bioorg.Med.Chem.* **2001**, *9*, 1149-1154.
52. Traxler, P.; Bold, G.; Buchdunger, E.; Caravatti, G.; Furet, P.; Manley, P.; O'Reilly, T.; Wood, J.; Zimmermann, J. *Med.Res.Rev.* **2001**, *21*, 499-512.
53. Macchia, M.; Barontini, S.; Bertini, S.; Di Bussolo, V.; Fogli, S.; Giovannetti, E.; Grossi, E.; Minutolo, F.; Danesi, R. *J.Med.Chem.* **2001**, *44*, 3994-4000.
54. Aal, M. T. A. *Synth.Commun.* **2002**, *32*, 1365-1377.
55. Gibson, C. L.; La Rosa, S.; Suckling, C. J. *Org.Biomol.Chem.* **2003**, *1*, 1909-1918.
56. Lu, Y. L.; Xiang, T. J.; Bartberger, M. D.; Bernard, C.; Bostick, T.; Huang, L.; Liu, L. B.; Siegmund, A.; Sukay, G.; Guo, G.; Elipe, M. S.; Tormos, W.; Dominguez, C.; Koch, K.; Burgess, L. E.; Basil, T. C.; Ibrahim, P.; Hummel, C. *Tetrahedron* **2006**, *62*, 11714-11723.
57. Holmes, R. E.; Robins, R. K. *J.Am.Chem.Soc.* **1964**, *86*, 1242-1245.
58. Elgemeie, G. H.; El Ezbawy, S. R.; Ali, H. A. *Synth.Commun.* **2001**, *31*, 3459-3467.
59. Botta, M.; Artico, M.; Massa, S.; Gambacorta, A. *J.Heterocycl.Chem.* **1989**, *26*, 883-884.
60. Khurana, J. M.; Agrawal, A.; Kukreja, G. *Heterocycles* **2006**, *68*, 1885-1892.
61. Gani, O.; Engh, R. *Nat.Prod.Rep.* **2010**, *27*, 489-498.
62. Marengo, B.; De, C.; Ricciarelli, R.; Pronzato, M.; Marinari, U. M.; Domenicotti, C. *Cancers* **2011**, *3*, 531-567.
63. Mizuno, K.; Saido, T. C.; Ohno, S.; Tamaoki, T.; Suzuki, K. *FEBS Lett.* **1993**, *330*, 114-116.

64. Podar, K.; Raab, M. S.; Zhang, J.; McMillin, D.; Breitkreutz, I.; Tai, Y. T.; Lin, B. K.; Munshi, N.; Hideshima, T.; Chauhan, D.; Anderson, K. C. *Blood* **2007**, *109*, 1669-1677.
65. Toullec, D.; Pianetti, P.; Coste, H.; Bellevergue, P.; Grandperret, T.; Ajakane, M.; Baudet, V.; Boissin, P.; Boursier, E.; Loriolle, F.; Duhamel, L.; Charon, D.; Kirilovsky, J. *J.Biol.Chem.* **1991**, *266*, 15771-15781.
66. Mahboobi, S.; Eibler, E.; Koller, M.; Kumar, S.; Popp, A.; Schollmeyer, D. *J.Org.Chem.* **1999**, *64*, 4697-4704.
67. Zembower, D. E.; Zhang, H. P.; Lineswala, J. P.; Kuffel, M. J.; Aytes, S. A.; Ames, M. M. *Bioorg.Med.Chem.Lett.* **1999**, *9*, 145-150.
68. Roy, S.; Eastman, A.; Gribble, G. W. *Org.Biomol.Chem.* **2006**, *4*, 3228-3234.
69. Link, J. T.; Raghavan, S.; Danishefsky, S. J. *J.Am.Chem.Soc.* **1995**, *117*, 552-553.
70. Hinze, C.; Kreipl, A.; Terpin, A.; Steglich, W. *Synthesis* **2007**, 608-612.
71. Garaeva, L. D.; Bakhmedova, A. A.; Yartseva, I. V.; Melnik, S. Y.; Adanin, V. M. *Russ.J.Bioorg.Chem.* **2003**, *29*, 160-167.
72. Nakanishi, S.; Matsuda, Y.; Iwahashi, K.; Kase, H. *J.Antibiot.* **1986**, *39*, 1066-1071.
73. Yasuzawa, T.; Iida, T.; Yoshida, M.; Hirayama, N.; Takahashi, M.; Shirahata, K.; Sano, H. *J.Antibiot.* **1986**, *39*, 1072-1078.
74. Thomas, D.; Hammerling, B. C.; Wimmer, A. B.; Wu, K. Z.; Ficker, E.; Kuryshev, Y. A.; Scherer, D.; Kiehn, J.; Katus, H. A.; Schoels, W.; Karle, C. A. *Cardiovasc.Res.* **2004**, *64*, 467-476.
75. Komander, D.; Kular, G. S.; Schuttelkopf, A. W.; Deak, M.; Prakash, K. R. C.; Bain, J.; Elliott, M.; Garrido-Franco, M.; Kozikowski, A. P.; Alessi, D. R.; Van Aalten, D. M. F. *Structure* **2004**, *12*, 215-226.
76. Fakhry, H.; Hilmy, M. *Reactions* **2009**, *2009*, 198-250.
77. Exposito, A.; Fernandez-Suarez, M.; Iglesias, T.; Munoz, L.; Riguera, R. *J.Org.Chem.* **2001**, *66*, 4206-4213.
78. Peifer, C.; Stoiber, T.; Unger, E.; Totzke, F.; Schachtele, C.; Marme, D.; Brenk, R.; Klebe, G.; Schollmeyer, D.; Dannhardt, G. *J.Med.Chem.* **2006**, *49*, 1271-1281.
79. Peifer, C.; Selig, R.; Kinkel, K.; Ott, D.; Totzke, F.; Schachtele, C.; Heidenreich, R.; Rocken, M.; Schollmeyer, D.; Laufer, S. *J.Med.Chem.* **2008**, *51*, 3814-3824.
80. Heidel, F. H.; Lipka, D. B.; Mirea, F. K.; Markova, B.; Peifer, C.; Kramp, J. P.; Plutizki, S.; Huber, C.; Dannhardt, G.; Fischer, T. *Blood* **2007**, *110*, 1605.
81. Peifer, C.; Krasowski, A.; Hammerle, N.; Kohlbacher, O.; Dannhardt, G.; Totzke, F.; Schachtele, C.; Laufer, S. *J.Med.Chem.* **2006**, *49*, 7549-7553.
82. Krayushkin, M. M.; Sedishev, I. P.; Yarovenko, V. N.; Zavarzin, I. V.; Vorontsova, L. G.; Starikova, Z. A.; Nabatov, B. V. *Russ.J.Org.Chem.* **2005**, *41*, 1349-1353.
83. Krayushkin, M. M.; Yarovenko, V. N.; Sedishev, I. P.; Zavarzin, I. V.; Vorontsova, L. G.; Starikova, Z. A. *Russ.J.Org.Chem.* **2005**, *41*, 875-883.
84. Caballero, E.; Adeva, M.; Calderon, S.; Sahagun, H.; Tome, F.; Medarde, M.; Fernandez, J. L.; Lopez-Lazaro, M.; Ayuso, M. J. *Bioorg.Med.Chem.* **2003**, *11*, 3413-3421.

Chapter 5

Experimental

Contents

5.0 Experimental 207
5.1 General Procedures 207
5.2 Chemical Data 208
5.2.1 Initial routes to bisindolylmaleimides 208
5.2.2 Synthesis of indolo[2,3-*c*]carbazole analogues 212
5.2.3 Formation and derivatisation of 5,6-bisindolylpyrimidin-4-one derivatives 216
5.2.4 Synthesis of a 3,4-bisindolyl-5-aminopyrazole compound series 245
5.2.5 Derivatisation of 4-(indol-3-yl)-3-(trimethoxyphenyl)-5-aminopyrazoles 254
5.2.6 Synthesis of imidazo[4,5-*c*]indolo[2,3-*a*]carbazoles 263
5.2.7 Synthesis of miscellaneous 3-substituted indole compounds 266
5.2.8 Single crystal X-ray diffraction studies in 5-aminopyrazole series 272
5.3 References 274

5.0 Experimental

5.1 General Procedures

All solvents were distilled prior to use as follows: DCM was distilled from phosphorus pentoxide, ethyl acetate was distilled from potassium carbonate, hexane was distilled prior to use, ethanol and methanol were distilled from magnesium in the presence of iodine and THF was distilled from benzophenone ketal. Diethyl ether was obtained pure from Riedel de Haen. All commercial reagents, anhydrous DMF and 1,4-dioxane were obtained from Aldrich and were used without further purification unless otherwise stated. Molecular sieves were dried by heating at >100^{o}C overnight. Organic phases were dried using anhydrous magnesium sulfate. Thin layer chromatography (TLC) was carried out on precoated silica gel 60 (Merck PF_{254}) plates and compounds were visualised either by UV (254 nm) light detection, vanillin staining or ceric sulfate staining. Column 'dry flash' chromatography was carried out using Merck PF_{254} silica gel 60A.

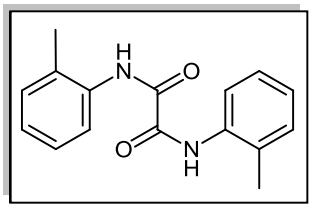
Melting points were measured in a Thomas Hoover Capillary Melting Point apparatus. Infrared (IR) spectra were recorded on a Perkin-Elmer FT-IR Paragon 1000 spectrophotometer. Liquid samples were examined as thin films interspersed between sodium chloride plates. Solid samples were dispersed in potassium bromide and recorded as pressed discs. Mass spectra were recorded on a Waters Quattro Micro (QAA1202) in ESI positive or negative modes. High resolution mass spectra (HRMS) were recorded on a Waters Micromass LCT Premier mass spectrometer (Instrument number KD 160) in ESI positive and negative modes. An external reference standard of Leucine enkephalin was infused in order to confirm mass accuracy of the MS data acquired and a sulfadimethoxine concentration test was performed to ensure the accuracy of peaks in the ion count range 1 x e^3 to 1 x e^6.

^{1}H (300 MHz) and ^{13}C NMR (75 MHz) were recorded on a Bruker Avance 300 NMR spectrometer. All spectra were recorded at 20^{o}C in deuterated chloroform ($CDCl_3$) or DMSO (DMSO-d_6) with tetramethylsilane (TMS) as internal standard unless otherwise specified. Chemical shifts (δ_H and δ_C) are expressed in parts per million (ppm), positive shift being downfield from TMS; coupling constants (J) are expressed in Hertz (Hz). Splitting patterns in ^{1}H NMR spectra are designated as s (singlet), bs (broad singlet), d (doublet), dd (doublet of doublets), t (triplet), q (quartet) and m (multiplet). For ^{13}C NMR spectra, the number of attached protons for each signal was determined using the DEPT-90 and DEPT-135 modes.

5.2 Chemical Data

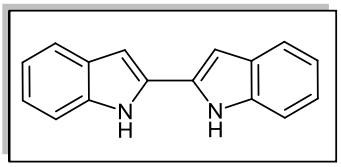
5.2.1 Initial routes to bisindolylmaleimides

5.2.1.1 *N,N'*-Bis(*o*-tolyl)oxalamide 459[1]



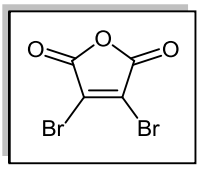
Oxalyl chloride (6.1 mL, 70 mmol) was syringed carefully into a reaction vessel containing 1,4-dioxane (20 mL), at 0°C. To this solution stirred under nitrogen atmosphere, was added *o*-toluidine **460** (15 mL, 140 mmol) and triethylamine (19.5 mL, 140 mmol) in 1,4-dioxane (30 mL) dropwise, over 30 minutes. The mixture was allowed to stir in the ice-bath for a further 2 hours, after which it was warmed up to room temperature. Deionised water (100 mL) was added slowly to the reaction, and the contents were then transferred to a conical flask. Hot ethyl acetate (100 mL) was added to dissolve the slurry and the aqueous layer removed by very careful agitation, in a 500 mL separating funnel. The crude bisamide was then filtered and washed successively with several cold aliquots of hexane, yielding crystals of an off-white solid product, *o*-toluidide **459** (9.811 g, 75%); m.p. 217-220°C (lit.[2] 215-216°C); ν_{max}/ cm^{-1} (KBr) 3100, 1725, 1590; δ_H (300 MHz, $CDCl_3$) 2.38 [6H, s, 2 × CH_3], 6.96-7.16 [2H, m, aromatic C-H], 7.23-7.30 [4H, m, aromatic C-H], 8.34-8.37 [2H, d, *J* 7.5, aromatic C-H], 9.67 [2H, bs, 2 × N-H]; δ_C (75 MHz, $CDCl_3$) 17.6 ($2CH_3$, 2 × CH_3), 124.9 (2CH, 2 × aromatic CH), 126.2 (4CH, 4 × aromatic CH), 130.4 (2CH, 2 × aromatic CH), 132.3 (C, 2 × aromatic C), 135.0 (C, 2 × aromatic C), 158.5 (C, 2 × C=O); m/z (ES+) 269.0 $[M+H]^+$ (10%), 114.9 (50%).

5.2.1.2 2,2'-Biindolyl 118[1]



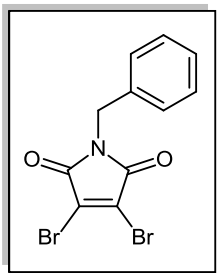
Potassium *tert*-butoxide (1.052 g, 9.34 mmol) was added to the *o*-toluidide **459** (0.503 g, 1.87 mmol) in *tert*-butanol (5 mL). The mixture was heated vigorously and a micro-distillation apparatus was employed to remove the solvent, along with heating up to 250°C. A white frothy solid was sublimated at this point. Heating could not be sustained to 280°C, at which point the cake melts. At maximum heating, achieved *via* sand bath, for 1 hour, the mixture was allowed to cool to room temperature. Water (5 mL) was then added and the resulting cake crushed. Ethanol (3 mL) was added to the residue and then heated to its boiling point. The solution was then cooled and filtered, prior to suction drying. However, the product 2,2'-biindolyl **118** could not be produced under these conditions and this route was abandoned, without any further optimisation.

5.2.1.3 3,4-Dibromomaleic anhydride 453[3]



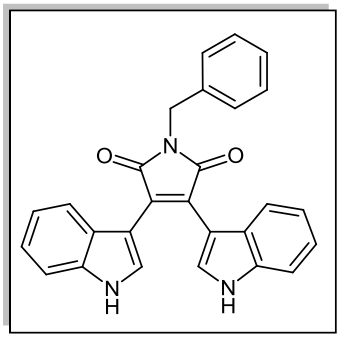
In a pressure-resistant microwave tube was placed a solution of maleic anhydride (1.503 g, 15.3 mmol), along with a catalytic amount of aluminium chloride (0.028 g, 0.21 mmol) and bromine (1.5 mL, 30.6 mmol, 2 eq.). The tube was then sealed and heated to 120°C for 16 hours. On cooling to room temperature, the mixture was taken up in ethyl acetate, filtered and the dark brown filtrate concentrated *in vacuo* to afford 2,3-dibromomaleic anhydride **453** as a beige solid (3.520 g, 90%); m.p. 105-107°C (lit.[3] 113-114°C); ν_{max}/ cm^{-1} (KBr) 1735, 1466; δ_C (75 MHz, $CDCl_3$) 131.8 (2C, 2 × C-Br), 152.1 (2C, 2 × C=O); m/z (ES-) 274.8 $[M+H_2O-H]^-$ (5%), 194.9, 192.9 $[M+H_2O-HBr]^-$ (60%).

5.2.1.4 1-Benzyl 3,4-dibromomaleimide 157[3]



3,4-Dibromomaleic anhydride **453** (1.004 g, 4.43 mmol) was dissolved in acetic acid (20 mL) in a nitrogen purged flask. To the stirring solution was added benzylamine (0.5 mL, 4.7 mmol, 1.1 eq.) added dropwise over a few minutes. Reflux at 120 °C was then applied to the vessel for 3 hours. After removal of the solvent under reduced pressure, flash column chromatography using 15% ethyl acetate/ hexane as the eluent yielded a pure fraction, confirmed by TLC analysis to be the maleimide product **157** (0.900 g, 60%); m.p. 115-118°C (lit.[3] 107-108°C); ν_{max}/ cm^{-1} (KBr) 2916, 1740, 1623, 1438; δ_H (300 MHz, $CDCl_3$) 4.75 [2H, s, CH_2], 7.30-7.37 [5H, m, 5 × aromatic C-H]; δ_C (75 MHz, $CDCl_3$) 43.2 (CH_2, N-CH_2), 128.4 (CH, aromatic CH), 128.8 (2CH, 2 × aromatic CH), 128.9 (2CH, 2 × aromatic CH), 129.5 (C, aromatic C), 135.2 (2C, 2 × C-Br), 163.6 (2C, 2 × C=O); m/z (ES+) 114.9 (100%), (ES-) 78.7, 80.8 (100%).

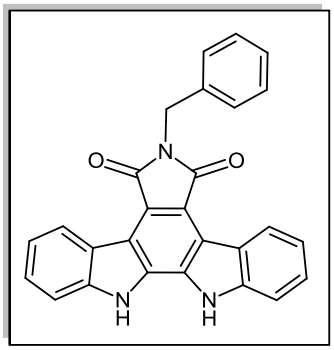
5.2.1.5 1-Benzyl-3,4-bis(1*H*-indol-3-yl)-1*H*-pyrrole-2,5-dione 155[4]



A solution of hexamethyldisilazane (0.5 mL, 2.32 mmol), in dry toluene (10 mL), was cooled to −78°C, under inert atmosphere, prior to the dropwise addition of 2.5 M *n*-butyllithium (1 mL, 2.4 mmol) over 10 minutes. The stirring mixture was then placed in an ice-bath for 10 minutes, followed by the addition of indole **171** (0.268 g, 2.32 mmol) in toluene

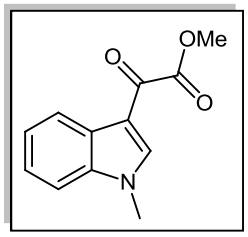
(10 mL), and stirred for a further 30 minutes at −78°C. *N*-Benzyl 3,4-dibromomaleimide **157** (0.400 g, 1.16 mmol) was then dissolved in toluene (10 mL) and added to the vessel, eliciting formation of a blue solution, then kept at room temperature for 20 minutes. The reaction was refluxed for 16 hours and then poured into 0.2 M aqueous HCl (50 mL), followed by extraction with ethyl acetate. Following washing with sodium bicarbonate, water and brine solution, the dried filtrate was passed through a pad of celite. The mother liquor was then concentrated and washed with ethyl acetate to yield a red solid in a yield of 42%, but which could only be identified by nominal mass spectrometry as containing bisindolylmaleimide **155** (along with degradation of starting material); m/z (ES+) 418 $[M+H]^+$ (100%).

5.2.1.6 2-Benzyl-8,9-dihydro-1*H*-indolo[2,3-*a*]pyrrolo[3,4-*c*]carbazole-1,3(2*H*)-dione 241[5]



Crude bisindolyl intermediate **155** (0.101 g, 0.342 g) was added to dry toluene (30 mL), along with DDQ (0.085 g, 0.374 mmol). A catalytic amount of *p*-TSA was then added to the stirring mixture. The vessel was then heated to reflux for one hour. The solvent was then removed under reduced pressure to yield a residue, which was redissolved in ethyl acetate, adsorbed on celite® and purified by flash chromatography. Employing 25% ethyl acetate/ hexane as eluent, fractions containing a yellow fluorescent material were isolated, but produced only a negligible amount of the fully aromatised indolocarbazole **241**, which could not be isolated for further study and was not optimised.

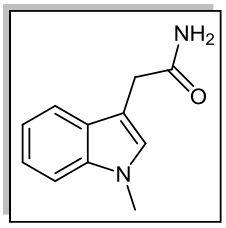
5.2.1.7 1-Methyl methyl 1*H*-indol-3-yl glyoxylate 457[6]



To a solution of *N*-methyl indole **456** (2.011 g, 15.2 mmol) in diethyl ether (20 mL), at 0°C, oxalyl chloride (3 mL, 34.4 mmol) was added dropwise, over 10 minutes. The yellow slurry was stirred at 0°C for 30 minutes, and then cooled to −65°C prior to slow addition of a 25% methanolic sodium methoxide solution (15.6 mL, 68.2 mmol) to the reaction mixture, while maintaining the internal temperature below −60°C. The reaction was allowed to warm to room temperature and then quenched by the addition of water (10 mL). The precipitated solid was isolated by filtration and dried under vacuum to give the product *N*-methyl glyoxylate ester **457** as a light brown amorphous powder (1.380 g, 42%); m.p. 102-104°C (lit.[7] 96-97°C); ν_{max}/ cm^{-1} (KBr) 2953, 1736, 1634, 1621, 1581, 1509, 1419; δ_H

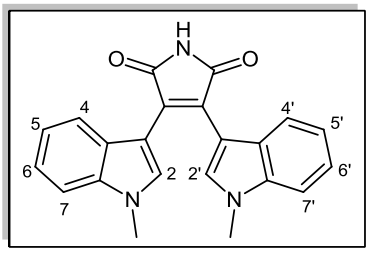
(300 MHz, DMSO-d_6) 3.90 [3H, s, O-CH_3], 3.92 [3H, s, N-CH_3], 7.30-7.35 [1H, td, *J* 7.2, 1.3, aromatic C-H_5], 7.35-7.40 [1H, td, *J* 7.2, 1.5, aromatic C-H_6], 7.61-7.64 [1H, dd, *J* 6.9, 1.5, aromatic C-H_7], 8.17-8.20 [1H, m, aromatic C-H_4], 8.51 [1H, s, aromatic C-H_2]; δ_C (75 MHz, DMSO-d_6) 33.5 (CH_3, N-CH_3), 52.5 (CH_3, O-CH_3), 111.2 (CH, aromatic CH), 111.2 (C, aromatic C), 121.3 (CH, aromatic CH), 123.2 (CH, aromatic CH), 123.9 (CH, aromatic CH), 125.9 (C, aromatic C), 137.4 (C, aromatic C), 141.6 (CH, aromatic CH), 163.9 (C, $\underline{C}O_2CH_3$), 178.0 (C, C=O); m/z (ES+) 218.0 $[M+H]^+$ (20%).

5.2.1.8 1-Methyl 1*H*-indol-3-yl acetamide 455[6]



To a solution of *N*-methyl 3-indolylacetonitrile **454** (2.010 g, 11.8 mmol) and TBAB (0.507 g, 1.6 mmol) in DCM (12 mL), at 0°C, was added 30% aqueous hydrogen peroxide solution (5 mL), followed by 20% aqueous NaOH solution (4 mL). The mixture was stirred at room temperature for 20 hours. DCM (80 mL) was then added to the reaction and washed with 5% aqueous HCl (70 mL), water (70 mL), dried over magnesium sulfate and filtered. Following solvent removal, hexane (30 mL) was added to the viscous beige slurry and this was then filtered under vacuum. Rinsing the acetamide **455** with DCM/ hexane (1:1) (15 mL) afforded the final purified product as a yellow powder (1.151 g, 52%); m.p. 181-184°C (lit.[8] 182-184 °C); ν_{max}/ cm^{-1} (KBr) 3437, 3190, 1650, 1623, 1475; δ_H (300 MHz, $CDCl_3$) 3.47 [2H, s, CH_2], 3.74 [3H, s, N-CH_3], 6.87 [1H, bs, NH], 7.00-7.05 [1H, t, *J* 7.8, aromatic C-H_5], 7.12-7.17 [1H, t, *J* 7.2, aromatic C-H_6], 7.17 [1H, s, aromatic C-H_2], 7.35 [1H, bs, NH], 7.37-7.40 [1H, d, *J* 8.2, aromatic C-H_7], 7.55-7.58 [1H, d, *J* 7.8, aromatic C-H_4]; m/z (ES+) 189.1 $[M+H]^+$ (40%).

5.2.1.9 3,4-Bis(1-methyl-1*H*-indol-3-yl)-1*H*-pyrrole-2,5-dione 172[6]

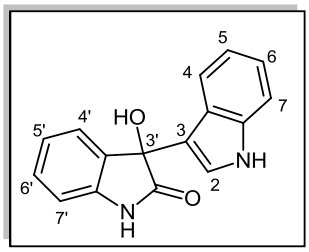


To a suspension of the *N*-methyl indole-3-acetamide **455** (0.333 g, 1.77 mmol) and *N*-methyl methyl indole-3-glyoxylate **457** (0.460 g, 2.12 mmol) in dry THF (5 mL), at 0°C, was added 1M potassium *tert*-butoxide in THF (5.3 mL, 5.3 mmol). The reaction was then allowed to stir at room temperature for 3 hours, and subsequently quenched by addition of 5% HCl (10 mL). The resultant slurry was then cooled to 0°C and the purified bisindolylmaleimide **172** was isolated by vacuum filtration to yield a bright red crystalline solid. The mother liquor was then recovered, recooled and filtered to afford a second crop of *N*-methyl arcyriarubin A derivative **172** (0.230 g), and in an overall yield of 0.420 g (67%); m.p. >300°C (lit.[9] 357-

359°C); ν_{max}/ cm^{-1} (KBr) 3411, 1709, 1608, 1523; δ_H (300 MHz, DMSO-d_6) 3.85 [6H, s, 2 × N-CH_3], 6.63-6.68 [2H, t, *J* 7.3, aromatic C-$H_{5,5'}$], 6.76-6.79 [2H, d, *J* 8.0, aromatic C-$H_{7,7'}$], 7.02-7.06 [2H, t, *J* 7.3, aromatic C-$H_{6,6'}$], 7.41-7.44 [2H, d, *J* 8.2, aromatic C-$H_{4,4'}$], 7.80 [2H, s, aromatic C-$H_{2,2'}$], 10.91 [1H, bs, NH]; δ_C (75 MHz, DMSO-d_6) 31.7 ($2CH_3$, 2 × N-CH_3), 103.6 (2C, 2 × aromatic C), 108.9 (2CH, 2 × aromatic CH), 118.4 (2CH, 2 × aromatic CH), 120.0 (2CH, 2 × aromatic CH), 120.5 (2CH, 2 × aromatic CH), 124.8 (2C, 2 × aromatic C), 125.9 (2C, 2 × aromatic C), 131.9 (2CH, 2 × aromatic CH), 135.3 (2C, 2 × aromatic C), 171.8 (2C, 2 × C=O); m/z (ES+) 356.0 $[M+H]^+$ (25%).

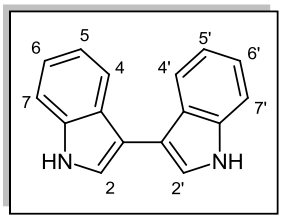
5.2.2 Synthesis of indolo[2,3-*c*]carbazole analogues

5.2.2.1 3-(3'-Hydroxyindolin-2'-one)indole 470[10]



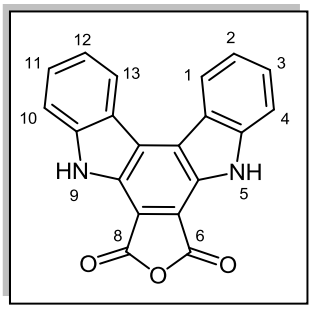
A mixture of indole **171** (5.854 g, 50 mmol), isatin (7.356 g, 50 mmol), 98% diethylamine solution (1 mL) and absolute ethanol (75 mL) was heated at 45°C for 3 hours. The dark red solution was then stirred vigorously at 25°C for a further 20 hours. The reaction was then heated to 45°C for a further hour, prior to cooling to room temperature. Water (200 mL) was added to the clear, red solution and some turbidity was observed at this point. Following further cooling to 0°C, crystallisation was complete and the crude solid (13.723 g) was filtered under vacuum. Recrystallisation of **470** was achieved from methanol, to afford a crop of light pink crystals (10.821 g, 91%); m.p. 124-127°C (lit.[10] 122-123°C); ν_{max}/ cm^{-1} (KBr) 3415, 3208, 3056, 1708, 1617, 1470; δ_H (300 MHz, DMSO-d_6) 6.37 [1H, s, OH], 6.85-6.90 [1H, t, *J* 6.9, aromatic C-$H_{5'}$], 6.90-6.93 [1H, d, *J* 7.5, aromatic C-$H_{7'}$], 6.93-6.99 [1H, t, *J* 7.5, aromatic C-$H_{6'}$], 7.00-7.06 [1H, t, *J* 7.4, aromatic C-H_5], 7.08-7.09 [1H, d, *J* 2.5, aromatic C-H_2], 7.23-7.26 [1H, d, *J* 7.4, aromatic C-$H_{4'}$], 7.23-7.28 [1H, t, *J* 7.3, aromatic C-H_6], 7.33-7.38 [2H, m, aromatic C-$H_{4,7}$], 10.36 [1H, bs, indolic NH], 11.00 [1H, bs, N<u>H</u>-CO]; δ_C (75 MHz, DMSO-d_6) 74.9 (C, <u>C</u>-OH), 109.6 (CH, aromatic CH), 111.5 (CH, aromatic CH), 115.4 (C, aromatic C), 118.4 (CH, aromatic CH), 120.3 (CH, aromatic CH), 121.0 (CH, aromatic CH), 121.7 (CH, aromatic CH), 123.5 (CH, aromatic CH), 124.7 (CH, aromatic CH), 124.9 (C, aromatic C), 129.0 (CH, aromatic CH), 133.4 (C, aromatic C), 136.8 (C, aromatic C), 141.6 (C, aromatic C), 178.4 (C, C=O); m/z (ES+) 247.1 $[M-H_2O+H]^+$ (100%). (ES-) 263.1 $[M-H]^-$ (100%).

5.2.2.2 3,3'-Biindolyl 466[10]



1,2-Dimethoxyethane (30 mL) was charged into a nitrogen-purged flask containing finely ground sodium borohydride (2.285 g, 60 mmol) and indolin-2-one derivative **470** (5.611 g, 20 mmol). A solution of boron trifluoride-diethyl etherate complex (9.9 mL, 80 mmol) in 1,2-dimethoxyethane (10 mL) was then added slowly via dropping funnel to the straw-coloured, vigorously stirred, reaction mixture. On half-addition, the mixture assumed a viscous, light green appearance, but following total addition, a beige coloured slurry was observed. At this point, the reaction was allowed to stir for a further hour at room temperature; 10% HCl (25 mL) was then added, and the resulting suspension was diluted with water (120 mL). The formed solids were filtered, redissolved in THF (30 mL) at 50^{o}C, and rapidly filtered at this temperature. DCM (60 mL) was slowly added to the filtrate solution, until turbidity became apparent. On cooling to 0^{o}C, the light green 3,3'-biindolyl **466** precipitated immediately. This was then filtered under vacuum, washed with DCM (2 × 5 mL), and dried in air, to yield the product **466** as fine plate crystals (1.925 g, 41%); m.p. 287-290^{o}C (lit.[10] 285-287^{o}C); ν_{max}/ cm^{-1} (KBr) 3396, 1615, 1586, 1456, 1410; δ_H (300 MHz, DMSO-d_6) 7.06-7.11 [2H, t, *J* 6.8, aromatic C-H$_{5,5'}$], 7.15-7.20 [2H, t, *J* 7.0, aromatic C-H$_{6,6'}$], 7.48-7.51 [2H, d, *J* 7.9, aromatic C-H$_{7,7'}$], 7.68 [2H, d, *J* 2.4, aromatic C-H$_{2,2'}$], 7.81-7.84 [2H, d, *J* 7.7, aromatic C-H$_{4,4'}$], 11.19 [2H, bs, 2 × NH]; δ_C (75 MHz, DMSO-d_6) 109.7 (2C, 2 × aromatic C), 111.6 (2CH, 2 × aromatic CH), 118.8 (2CH, 2 × aromatic CH), 119.6 (2CH, 2 × aromatic CH), 121.2 (2CH, 2 × aromatic CH), 121.8 (2CH, 2 × aromatic CH), 126.1 (2C, 2 × aromatic C), 136.4 (2C, 2 × aromatic C); m/z (ES+) 232.1 $[M+H]^+$ (70%).

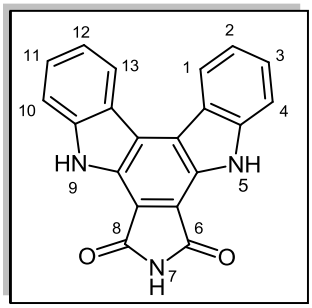
5.2.2.3 Furo[3,4-*a*]indolo[2,3-*c*]carbazole-6,8(5*H*,9*H*)-dione 467[11]



Glacial acetic acid (50 mL) was added to a flask containing 3,3'-biindolyl **466** (1.803 g, 7.76 mmol) and maleic anhydride (1.594 g, 15.5 mmol, 2 eq.). The heterogeneous mixture was stirred vigorously and heated to 110^{o}C and allowed to reflux. The reaction mixture initially assumed a cherry colour and eventually, a deep red colour, as heating progressed. The reaction proceeded for 60 hours, at which point no starting material was evident. The solvent was then evaporated under reduced pressure; toluene (2 × 10 mL) was added to the reaction flask and evaporated, followed by the addition and evaporation of DCM (2 × 10

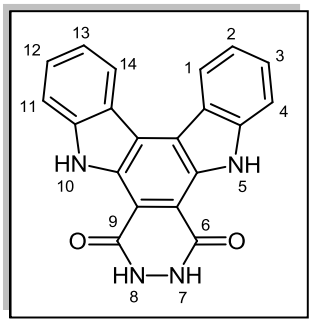
mL). Diethyl ether (70 mL) was added to the brown residue, and then filtered under vacuum to afford dark red crystals, washed with ether (2 × 7 mL), dried and isolated as the indolocarbazole **467** (1.738 g, 68%); m.p. >300°C (lit.[11] >250°C); ν_{max}/ cm^{-1} (KBr) 3403, 3360, 1808, 1741, 1715, 1614, 1460; δ_H (300 MHz, DMSO-d_6) 7.40-7.44 [2H, t, *J* 7.3, aromatic C-$H_{2,12}$], 7.60-7.65 [2H, t, *J* 7.4, aromatic C-$H_{3,11}$], 7.77-7.79 [2H, d, *J* 8.1, aromatic C-$H_{4,10}$], 8.76-8.79 [2H, d, *J* 8.2, aromatic C-$H_{1,13}$], 12.32 [2H, s, 2 × NH]; δ_C (75 MHz, DMSO-d_6) 109.2 (2C, 2 × aromatic C), 112.5 (2CH, 2 × aromatic CH), 120.2 (2CH, 2 × aromatic CH), 120.4 (2C, 2 × aromatic C), 123.8 (2CH, 2 × aromatic CH), 127.8 (2CH, 2 × aromatic CH), 129.1 (2C, 2 × aromatic C), 142.5 (2C, 2 × aromatic C), 163.5 (2C, 2 × aromatic C), 172.0 (2C, 2 × C=O); m/z (ES+) 588.2 (100%), 359.0 $[M+Na]^+$ (30%). (ES-) 325.1 $[M-H]^-$ (5%).

5.2.2.4 5*H*-Indolo[2,3-*c*]pyrrolo[3,4-*a*]carbazole-6,8(7*H*,9*H*)-dione 468[11]



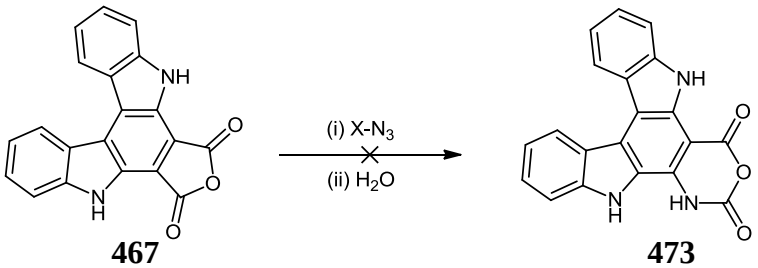
Glacial acetic acid (50 mL) was added to a flask containing 3,3'-biindolyl **466** (1.803 g, 7.76 mmol) and maleimide (1.505 g, 15.5 mmol, 2 eq.). The heterogeneous mixture was stirred vigorously and heated to 110°C and allowed to reflux. The reaction mixture initially assumed a cherry colour and eventually, a deep red colour, as heating progressed. The reaction proceeded for 36 hours, at which point no starting material **466** was evident. The solvent was then evaporated under reduced pressure; toluene (2 × 10 mL) was added to the reaction flask and evaporated, followed by the addition and evaporation of DCM (2 × 10 mL). Diethyl ether (70 mL) was added to the brown residue, and then filtered under vacuum to afford dark red crystals, washed with ether (2 × 7 mL), dried and isolated as title compound **468** (1.566 g, 62%); m.p. >300°C (lit.[11] >250°C); ν_{max}/ cm^{-1} (KBr) 3419, 3361, 3189, 1739, 1703, 1681, 1459; δ_H (300 MHz, DMSO-d_6) 7.39-7.44 [2H, td, *J* 7.1, 0.9, aromatic C-$H_{2,12}$], 7.56-7.61 [2H, t, *J* 7.5, aromatic C-$H_{3,11}$], 7.79-7.82 [2H, d, *J* 8.0, aromatic C-$H_{4,10}$], 8.82-8.85 [2H, d, *J* 8.2, aromatic C-$H_{1,13}$], 11.09 [1H, bs, CO-N<u>H</u>-CO], 12.07 [2H, s, 2 × NH]; δ_C (75 MHz, DMSO-d_6) 111.5 (2C, 2 × aromatic C), 112.4 (2CH, 2 × aromatic CH), 119.7 (2CH, 2 × aromatic CH), 120.6 (2C, 2 × aromatic C), 122.5 (2C, 2 × aromatic C), 123.5 (2CH, 2 × aromatic CH), 127.0 (2CH, 2 × aromatic CH), 128.5 (2C, 2 × aromatic C), 142.4 (2C, 2 × aromatic C), 170.1 (2C, 2 × C=O); m/z (ES-) 324.1 $[M-H]^-$ (10%).

5.2.2.5 7,8-Dihydroindolo[2,3-*c*]pyridazino[4,5-*a*]carbazole-6,9(5*H*,10*H*)-dione 473



To a suspension of furo[3,4-*a*]indolo[2,3-*c*]carbazole-6,8(5*H*,9*H*)-dione **467** (0.150 g, 0.46 mmol) in acetic acid (10 mL), was added hydrazine monohydrate (0.06 mL, 1.01 mmol, 2.2 eq.). The dark reaction was then stirred at reflux temperature for 24 hours, at which point, solvent was removed *in vacuo* and the resultant residue was added to a flask containing diethyl ether (35 mL). Following stirring for 15 minutes, the dark brown precipitate was filtered and washed with water (2 × 10 mL) and ether (2 × 10 mL) successively, prior to drying. This afforded the novel indolo[2,3-*c*]carbazole **473** as a brown amorphous powder (0.111 g, 70%); m.p. >300°C; ν_{max}/ cm^{-1} (KBr) 3412, 2923, 1710, 1650, 1619, 1461, 1326; δ_H (300 MHz, DMSO-d_6) 7.42-7.46 [2H, t, *J* 7.2, aromatic C-$H_{2,13}$], 7.56-7.61 [2H, t, *J* 7.4, aromatic C-$H_{3,12}$], 8.03-8.06 [2H, d, *J* 8.1, aromatic C-$H_{4,11}$], 8.89-8.92 [2H, d, *J* 8.2, aromatic C-$H_{1,14}$], 11.91 [2H, s, 2 × N<u>H</u>-CO], 12.10 [2H, bs, 2 × NH]; δ_C (75 MHz, DMSO-d_6) 109.9 (2C, 2 × aromatic C), 112.9 (2CH, 2 × aromatic CH), 118.9 (2C, 2 × aromatic C), 119.3 (2CH, 2 × aromatic CH), 120.4 (2C, 2 × aromatic C), 123.0 (2CH, 2 × aromatic CH), 126.0 (2CH, 2 × aromatic CH), 129.6 (2C, 2 × aromatic C), 140.4 (2 × aromatic C), 168.0 (2C, 2 × C=O); m/z (ES-) 339.1 $[M-H]^-$ (40%); HRMS - (ES-) requires: 339.0882. Found: 339.0898 ($C_{20}H_{11}N_4O_2$).

5.2.2.6 Attempted Curtius rearrangement of furo[3,4-*a*]indolo[2,3-*c*]carbazole-6,8(5*H*,9*H*)-dione (467)



467 **473**

Table 5.1

Reactant	Azide source	Equiv.	Solvent	Temp/°C	Time	Product
467	NaN_3	10 eq.	DMF	110	24h	n.r
467	NaN_3	10 eq.	DMSO	150	24h	n.r
467	NaN_3	10 eq.	DMF	110	24h	n.r
467	TMS-N_3	3 eq.	DMF	110	24h	n.r
467	TMS-N_3	10 eq.	DMSO	150	24h	n.r

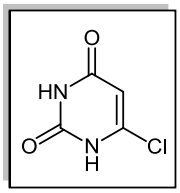
General reaction:

- To a flame-dried flask containing **467** (0.150 g, 0.46 mmol), was added NaN_3 (0.300 g, 4.6 mmol, 10 eq.) or TMS-N_3 (0.2 mL, 1.4 mmol, 3 eq.) and anhydrous DMF (7 mL), under inert atmosphere, prior to heating to 100^{o}C and stirring at this temperature for 20 hours.

Following addition of water (25 mL), the reaction was stirred for 1 hour; however, no reaction had occurred and only starting material could be detected following work-up.

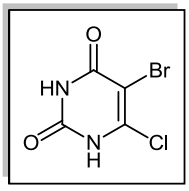
5.2.3 Formation and derivatisation of 5,6-bisindolylpyrimidin-4-one derivatives

5.2.3.1 6-Chlorouracil 462[12]



2,4,6-Trichloropyrimidine **461** (1.001 g, 5.48 mmol) was suspended in aqueous NaOH (4 M, 50 mL), prior to stirring at reflux temperature overnight. The resulting slurry was filtered in order to remove the residual starting material **461**, and the resulting filtrate was evaporated under reduced pressure to isolate a white solid of 6-chlorouracil **462** (0.646 g, 80%), which was easily identified by means of its characteristic IR carbonyl stretches; m.p. 295-298^{o}C (lit.[13] 287-289^{o}C); ν_{max}/ cm^{-1} (KBr) 3375, 3220, 1528; m/z (ES-) 144.9 $[M-H]^-$ (100%).

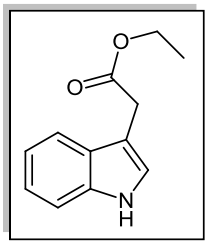
5.2.3.2 Attempted formation of 5-bromo-6-chlorouracil 463



6-Chlorouracil **462** (1.003 g, 6.8 mmol) was reacted with bromine water (bromine (0.58 mL, 11 mmol, 1.6 eq.), dissolved in water (50 mL)) and heated to 60^{o}C overnight. Following evaporation of the solvent, it was noted that only starting **462** could be isolated and no reaction had taken place.

5.2.3.3 Microwave approach to pyrimidinone formation

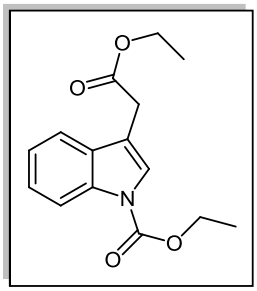
5.2.3.3.1 Ethyl 1*H*-indol-3-yl acetate 502



Indole-3-acetic acid **233** (1.002 g, 5.7 mmol) was stirred in the presence of dry ethanol (20 mL), and then cooled to −78^{o}C. Thionyl chloride (0.5 mL, 6.25 mmol) was then delivered slowly into the cooled reaction vessel over 10 minutes. The reaction was allowed to stir overnight while gradually warming to room temperature. Following subsequent removal of solvent, and extraction between ethyl acetate and water, ester **502** was isolated pure as a violet oil,

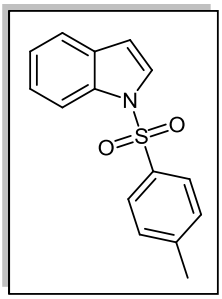
which subsequently solidified (1.163 g, 100%); m.p. 45-47°C (lit.[14] 41-43°C) ν_{max}/ cm^{-1} (NaCl) 3411, 2982, 1732; δ_H (300 MHz, $CDCl_3$) 1.24-1.29 [3H, t, *J* 7.1, $CO_2CH_2C\underline{H}_3$], 3.77 [2H, s, $C\underline{H}_2CO_2Et$], 4.13-4.20 [2H, q, *J* 7.1, $CO_2C\underline{H}_2CH_3$], 7.10-7.16 [1H, td, *J* 7.1, 1.1, aromatic C-H_5], 7.17-7.22 [1H, td, *J* 7.1, 1.2, aromatic C-H_6], 7.17 [1H, s, aromatic C-H_2], 7.34-7.36 [1H, d, *J* 8.1, aromatic C-H_7], 7.61-7.64 [1H, d, *J* 8.3, aromatic C-H_4], 8.11 [1H, bs, NH]; m/z (ES+) 204.1 $[M+H]^+$ (100%).

5.2.3.3.2 1-Ethoxycarbonyl ethyl 1*H*-indol-3-yl acetate 503[15]



Ethyl chloroformate (0.18 mL, 1.81 mmol) was added dropwise over a 15 minute period, to a rapidly stirred mixture of ethyl indole-3-acetate **502** (0.325 g, 1.6 mmol) and TBAB (0.009 g, 0.029 mmol) in dry DCM (5 mL) and 30% NaOH solution (5 mL). Following stirring for 1 hour at 0°C, the two distinct layers were observed to separate. Following extraction of the aqueous layer with DCM, the combined organic layers were washed successively with water and brine, dried with magnesium sulfate and evaporated *in vacuo*. The crude carbamate **503** was then purified by column chromatography, with 20% ethyl acetate/ hexane as eluent, yielding a colourless oil used without further purification (0.337 g, 76%); ν_{max}/ cm^{-1} (KBr) 2983, 1738, 1732, 1613, 1574, 1455; δ_H (300 MHz, $CDCl_3$) 1.27 [3H, t, *J* 6.9, CH_3 (ester)], 1.46 [3H, t, *J* 6.9, CH_3 (carbamate)], 3.71 [2H, s, $C\underline{H}_2CO_2Et$], 4.16 [2H, q, *J* 6.9, CH_2 (ester)], 4.18 [3H, q, *J* 6.9, CH_2 (carbamate)], 7.24-7.35 [2H, m, aromatic C-$H_{5,6}$], 7.53-7.55 [1H, m, aromatic C-H_7], 7.62 [1H, s, aromatic C-H_2], 8.16-8.19 [1H, m, aromatic C-H_4]; (ES+) 276.1 $[M+H]^+$ (100%).

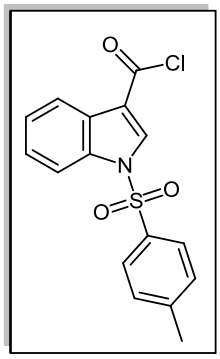
5.2.3.3.3 1-(*p*-Toluenesulfonyl)-1*H*-indole 505[16]



Indole **171** (1.004 g, 8.5 mmol) was added to a rapidly stirring solution of TBAHS (0.453 g, 1.28 mmol) in toluene (25 mL) at 0°C, was added 50% aqueous NaOH solution (25 mL), followed by freshly recrystallised *p*-toluenesulfonyl chloride (2.503 g, 12.8 mmol). The resultant mixture was then stirred vigorously at room temperature for a further 16 hours. The toluene layer was then separated, washed with aqueous 1 M HCl (2 × 25 mL), saturated aqueous sodium bicarbonate (2 × 25 mL), water (25 mL) and brine (25 mL), followed by drying over magnesium sulfate. The filtrate was then evaporated under reduced pressure to yield pure compound **505** as a white solid (2.821 g, 96%); m.p. 90-92°C (lit.[17] 85-86°C); ν_{max}/ cm^{-1} (KBr) 1596, 1446, 1369, 1168; δ_H (300

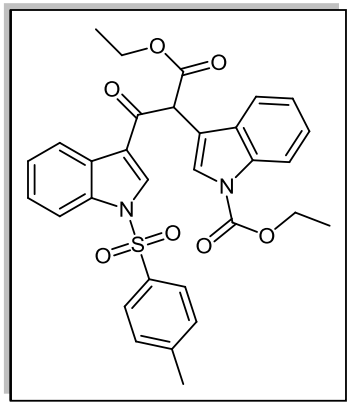
MHz, $CDCl_3$) 2.31 [3H, s, CH_3], 6.64-6.65 [1H, dd, *J* 3.7, 1.0, aromatic C-H_3], 7.18-7.24 [3H, m, aromatic C-$H_{5,3',5'}$], 7.27-7.33 [1H, td, *J* 8.4, 1.3, aromatic C-H_6], 7.50-7.53 [1H, d, *J* 7.6, aromatic C-H_7], 7.55-7.56 [1H, d, *J* 3.7, aromatic C-H_2], 7.74-7.77 [2H, d, *J* 8.4, aromatic C-$H_{2',6'}$], 7.97-8.00 [1H, d, *J* 8.3, aromatic C-H_4]; δ_C (75 MHz, $CDCl_3$) 21.6 (CH_3, C-CH_3), 109.0 (CH, aromatic CH), 113.5 (CH, aromatic CH), 121.4 (CH, aromatic CH), 123.3 (CH, aromatic CH), 124.6 (CH, aromatic CH), 126.3 (2CH, 2 × aromatic CH), 126.8 (2CH, 2 × aromatic CH), 129.9 (CH, aromatic CH), 130.8 (C, aromatic C), 134.8 (C, aromatic C), 135.3 (C, aromatic C), 144.9 (C, aromatic C); m/z (ES+) 272.1 $[M+H]^+$ (100%).

5.2.3.3.4 1-(*p*-Toluenesulfonyl) 1*H*-indol-3-yl carbonyl chloride 504[18]



Aluminium chloride (0.252 g, 1.85 mmol) was added to dry DCM (10 mL), maintained at 0°C in an ice-bath. Oxalyl chloride (0.16 mL, 1.85 mmol) was then added over several minutes, and after a further 30 minutes, *p*-toluenesulfonyl indole **505** (0.100 g, 0.37 mmol) in DCM (10 mL) was added to the reaction mixture and allowed to warm gradually to room temperature. Following stirring for an additional 2 hours, crushed ice (25 mL) was added and the aqueous layer was extracted with DCM (3 × 10 mL). The usual work-up, with saturated aqueous sodium bicarbonate (2 × 25 mL), water (25 mL) and brine (25 mL), followed by drying with magnesium sulfate and concentration *in vacuo*, produced the acid chloride **504** as a viscous brown oil (0.129 g, 100%), used without any further purification, following IR analysis; ν_{max}/ cm^{-1} (film) 3350, 1744, 1532, 1383, 1178.

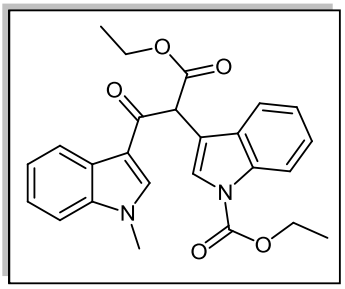
5.2.3.3.5 2-(1-Ethoxycarbonyl-1*H*-indol-3-yl)-3-(1-*p*-toluenesulfonyl-1*H*-indol-3-yl) ethyl-3-oxopropionate 501



LDA solution (1.8 M, 8.9 mL, 16.1 mmol, 2.2 eq.) was added dropwise over a period of 20 minutes, to dry THF (30 mL), at −78°C, under nitrogen. A mixture of ester **503** (2.012 g, 7.3 mmol) in THF (3 mL) was then added to the reaction vessel, at a sufficient rate to maintain the internal reaction temperature at below −65°C, during addition. The dark brown solution was then stirred vigorously for 90 minutes. The *p*-toluenesulfonyl protected acid chloride **504** (2.905 g, 8.7 mmol, 1.2 eq.) was then dissolved in dry THF (7 mL) and added to the vessel slowly, over 15 minutes. Stirring of the reaction mixture proceeded at room temperature overnight, and, following subsequent

solvent removal, was quenched with the addition of saturated aqueous ammonium chloride solution. Following the usual ethyl acetate/ water work-up conditions outlined above, a crude di-protected ketoester **501** was produced, which was then crystallised from 95% ethanol and water, to yield a light brown solid, on vacuum filtration, easily identified by means of its characteristic sulfonamide bands in IR, and then dried under high vacuum overnight (0.810 g, 25%); m.p. 192-196^{o}C (dec.); ν_{max}/ cm^{-1} (KBr) 2980, 2927, 1739, 1732, 1669, 1455, 1379, 1175; δ_H (300 MHz, $CDCl_3$) 1.26 [3H, t, *J* 7.0, CH_3 (ester)], 1.45 [3H, t, *J* 7.0, CH_3 (carbamate)], 2.32 [3H, s, *p*-CH_3-Ar], 4.28 [2H, q, *J* 7.0, CH_2 (ester)], 4.43-4.50 [2H, m, CH_2 (carbamate)], 5.64 [1H, s, C-H], 7.13-7.16 [2H, m, aromatic C-H], 7.33-7.41 [4H, m, aromatic C-H], 7.53-7.56 [2H, m, aromatic C-H], 7.86-7.92 [1H, m, aromatic C-H], 7.86-7.98 [2H, m, aromatic C-H], 8.23-8.28 [1H, m, aromatic C-H], 8.31-8.36 [2H, m, aromatic C-H]; m/z (ES+) 573.1 $[M+H]^+$ (100%); HRMS - (ES+) requires: 573.1695. Found: 573.1674 ($C_{31}H_{29}N_2O_7S$).

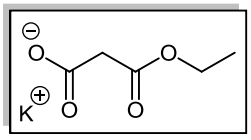
5.2.3.3.6 2-(1-Ethoxycarbonyl-1*H*-indol-3-yl)-3-(1-methyl-1*H*-indol-3-yl) ethyl-3-oxopropionate 508



1.8 M LDA solution (8.9 mL, 16.1 mmol, 2.2 eq.) was added dropwise over a period of 20 minutes, to THF (30 mL), stored at –78^{o}C, under an inert atmosphere. A solution of the carbamate protected ester **503** (2.018 g, 7.3 mmol) in THF (3 mL) was added to the vessel at a sufficient rate to maintain the internal reaction temperature at below –65^{o}C during addition. The dark brown solution was then stirred vigorously for 90 minutes, allowing full deprotonation of ester **503** to occur. The corresponding methyl protected acid chloride **479** (1.710 g, 8.8 mmol, 1.2 eq.) was then dissolved in dry THF (5 mL) and added to the vessel over 15 minutes. Stirring of the reaction mixture proceeded at room temperature overnight, and following subsequent solvent removal, was quenched with the addition of saturated aqueous ammonium chloride solution. Extraction of the resultant residue with ethyl acetate and washing with water and brine, following work-up and drying with anhydrous magnesium sulfate, yielded a crude product that was then purified by column chromatography, employing 15% ethyl acetate/ hexane as eluent. A light brown solid β-ketoester **508** was then isolated following rotary evaporation of the combined product fractions (1.076 g, 34%); m.p. 117-120^{o}C; ν_{max}/ cm^{-1} (KBr) 2926, 1738, 1732, 1643, 1530, 1456; δ_H (300 MHz, $CDCl_3$) 1.26 [3H, t, *J* 7.2, CH_3 (ester)], 1.44 [3H, t, *J* 7.2, CH_3 (carbamate)], 3.80 [3H, s, N-CH_3], 4.25 [2H, q, *J* 7.2, CH_2 (ester)], 4.46 [2H, q, *J* 7.2, CH_2 (carbamate)], 5.60 [1H, s,

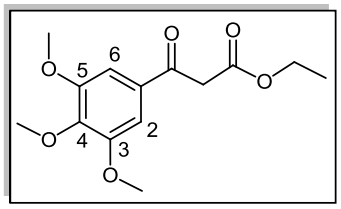
COC<u>H</u>CO_2Et], 7.18-7.36 [5H, m, aromatic C-H], 7.59-7.65 [1H, m, aromatic C-H], 7.83-7.88 [2H, m, aromatic C-H], 8.17-8.21 [1H, m, aromatic C-H], 8.40-8.44 [1H, m, aromatic C-H]; δ_C (75 MHz, $CDCl_3$) 14.5 (CH_3, $OCH_2\underline{C}H_3$ (ester)), 14.8 (CH_3, $OCH_2\underline{C}H_3$ (carbamate)), 34.1 (CH_3, N-$\underline{C}H_3$), 53.9 (CH, CO$\underline{C}$HCO_2Et), 62.3 (CH_2, O$\underline{C}H_2CH_3$ (ester)), 63.7 (CH_2, O$\underline{C}H_2CH_3$ (carbamate)), 110.1 (CH, aromatic CH), 114.9 (C, aromatic C), 115.4 (C, aromatic C), 115.8 (CH, aromatic CH), 119.3 (CH, aromatic CH), 123.2 (CH, aromatic CH), 123.4 (CH, aromatic CH), 123.5 (CH, aromatic CH), 124.2 (CH, aromatic CH), 125.2 (CH, aromatic CH), 125.5 (CH, aromatic CH), 127.1 (C, aromatic C), 130.0 (C, aromatic C), 136.5 (CH, aromatic CH), 136.6 (C, aromatic C), 137.8 (C, aromatic C), 151.5 (C, $\underline{C}O_2$Et (carbamate)),, 169.2 (C, $\underline{C}O_2$Et (ester)), 187.0 (C-$\underline{C}$=O(C)); m/z (ES+) 433.1 $[M+H]^+$ (100%), 259.1 (100%); HRMS - (ES+) requires: 433.1763. Found: 433.1762 ($C_{25}H_{25}N_2O_5$).

5.2.3.3.7 Potassium monoethyl malonate 498[19]



To a vigorously stirring mixture of diethyl malonate (4.002 g, 25 mmol) in absolute EtOH (25 mL), was added a solution of KOH (1.408 g, 25.14 mmol) in absolute EtOH (20 mL), *via* dropping funnel, over 1 hour. After stirring for 3 hours at room temperature, the reaction mixture was allowed to stand overnight. On heating to 70°C, hot filtration was carried out in order to remove any dipotassium malonate. The corresponding monopotassium salt **498** precipitated on cooling to 0°C, prior to isolation by filtration of the milky slurry. The white crystals were washed with ether (2 × 10 mL) and dried under vacuum. Concentration of the mother liquor to a volume of approximately 30 mL, yielded a second crop of the salt **498**, which was isolated overall in a yield of 3.157 g (74%), used without further purification; m.p. 184-187°C (lit.[19] 175°C dec.).

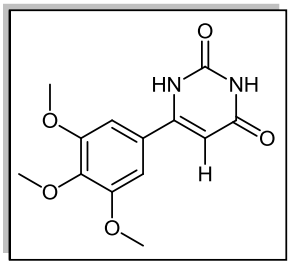
5.2.3.3.8 Ethyl 3-oxo-3-(3,4,5-trimethoxyphenyl)propanoate 497



Potassium monoethyl malonate (1.573 g, 9.25 mmol) and acetonitrile (20 mL) were placed in a 100 mL 3-neck round-bottomed flask, cooled to 15°C, and maintained under inert atmosphere. Triethylamine (1.3 mL, 9 mmol) was then added, followed by anhydrous magnesium chloride (1.063 g, 11.3 mmol). The mixture was warmed to room temperature and stirred for a further 2.5 hours. The resultant off-white slurry was recooled to 0°C, and 3,4,5-trimethoxybenzoyl chloride **499** (1.037 g, 4.5 mmol) in acetonitrile (5 mL) was added dropwise, over 15 minutes. Further triethylamine (0.13 mL, 0.9 mmol) was charged to the vessel and the overall mixture

was subsequently stirred at room temperature for 20 hours. Following solvent removal, toluene (10 mL) was added and evaporated *in vacuo*; the residue was redissolved in toluene (15 mL) and washed with 10% aqueous HCl (4 × 25 mL). The first acidic extract was extracted with a further volume of toluene (10 mL), and the combined toluene layers were then washed with water (3 × 120 mL), brine (150 mL), dried over magnesium sulfate and reduced under vacuum to the novel off-white solid β-ketoester **497**, used without any further purification (0.927 g, 71%); m.p. 82-85^{o}C; ν_{max}/ cm^{-1} (KBr) 2969, 2938, 1741, 1666, 1583, 1506, 1459; δ_H (300 MHz, $CDCl_3$) 1.24-1.29 [3H, t, *J* 7.1, $CO_2CH_2C\underline{H}_3$], 3.91 [6H, s, 2 × *m*-OCH_3], 3.93 [3H, s, *p*-OCH_3], 3.96 [2H, s, CH_2], 4.18-4.25 [2H, q, *J* 7.1, $CO_2C\underline{H}_2CH3$], 7.22 [2H, s, aromatic C-$H_{2,6}$]; δ_C (75 MHz, $CDCl_3$) 14.1 (CH_3, $CO_2CH_2\underline{C}H_3$), 46.1 (CH_2, $CO_2\underline{C}H_2CH_3$), 56.3 (2CH_3, 2 × *m*-OCH_3), 61.0 (CH_3, *p*-OCH_3), 61.6 (CH_2, $CO\underline{C}H_2CO$), 106.2 (2CH, aromatic C-H_2 & aromatic C-H_6), 131.2 (C, aromatic C), 143.3 (C, aromatic C), 153.2 (2C, 2 × aromatic C), 167.5 (C, $\underline{C}O_2CH_2CH_3$), 191.2 (C, C=O); m/z (ES+) 283.1 $[M+H]^+$ (100%); HRMS - (ES+) requires: 283.1182. Found: 283.1180 ($C_{14}H_{19}O_6$).

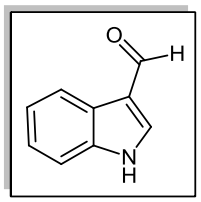
5.2.3.3.9 6-(3,4,5-Trimethoxyphenyl) pyrimidin-2,4(1*H*,3*H*)-dione 500



A mixture of precursor **497** (0.102 g, 0.36 mmol) and recrystallised urea (0.024 g, 0.39 mmol, 1.1 eq.) was pre-mixed thoroughly using a mortar and pestle, and heated in a closed vessel in a 300W microwave reactor, under solvent-free conditions. The reaction proceeded at 180^{o}C over 15 minutes, preceded by a 5 minute ramp interval, at a power of 300W, along with simultaneous cooling of the reaction vessel. The crude product melt (0.070 g), was suspended in water (2 × 5 mL), and then filtered to isolate the crude pyrimidin-2,4-dione **500** residue, which was recrystallised from absolute ethanol, to afford novel **500** as an off-white crystalline solid (0.020 g, 20%); m.p. 246-250^{o}C; ν_{max}/ cm^{-1} (KBr) 3362, 2921, 2850, 1727, 1668, 1645, 1587; δ_H (300 MHz, DMSO-d_6) 3.71 [3H, s, *p*-OCH_3], 3.86 [6H, s, 2 × *m*-OCH_3], 5.96 [1H, s, C=C-H], 7.05 [2H, s, aromatic C-H_2 & aromatic C-H_6], 11.10 [2H, bs, 2 × NH]; δ_C (75 MHz, DMSO-d_6) 56.0 (2CH_3, 2 × *m*-O$\underline{C}H_3$), 60.1 (CH_3, *p*-O$\underline{C}H_3$), 97.6 (CH, C=$\underline{C}$H-C=O), 104.4 (2CH, 2 × aromatic CH), 126.6 (C, aromatic C), 139.5 (C, aromatic C), 151.8 (C, C=O), 152.1 (C, aromatic C), 152.9 (2C, 2 × aromatic C), 164.2 (C, C=O); m/z (ES-) 277.1 $[M-H]^-$ (100%); HRMS - (ES+) requires: 279.0981. Found: 279.0976 ($C_{13}H_{15}N_2O_5$).

5.2.3.4 Cyclocondensation route to 5,6-bisindolylpyrimidinone synthesis

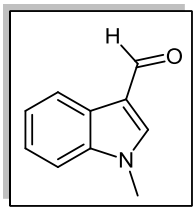
5.2.3.4.1 1*H*-Indol-3-yl carboxaldehyde 121[20]



To a 100 mL three-neck round-bottom flask, incorporating an addition funnel was added DMF (8 mL), which was initially cooled to –10°C, prior to addition of $POCl_3$ (2 mL, 21.9 mmol) dropwise over approximately 15 minutes, into the reaction vessel. The contents of the flask were then warmed to room temperature. Indole **171** (2.502 g, 21 mmol) was then placed in a dry 100 mL addition funnel, with anhydrous DMF (10 mL). This solution was introduced into the reaction flask, at –10°C, at a slow regulated rate, allowing full addition to be complete within 20 minutes. The reaction mixture was then stirred for a further 45 minutes, while gradual heating of the flask contents to >40°C was observed. The appearance of a yellow slurry was noted at this time. The reaction was then poured into ice, producing a cherry-red colour – made basic by the addition 5M NaOH (20 mL), to produce a biphasic yellow/red slurry. Hot deionised water (100 mL) was then added, followed by cooling to room temperature and then to 0°C. The product was filtered on a Buchner funnel and the light-orange crystals washed with ice-water. The crude product was then recrystallised from DMF/ H_2O to afford **121** (2.402 g, 79%) as light orange needles; m.p. 190-193°C (lit.[20] 188-189°C); ν_{max}/ cm^{-1} (KBr) 3150, 1647, 1608; δ_H (300 MHz, DMSO-d_6) 7.19-7.29 [2H, m, aromatic C-$H_{5,6}$], 7.51-7.53 [1H, d, *J* 7.1, aromatic C-H_7], 8.10-8.12 [1H, d, *J* 6.9, aromatic C-H_4], 8.29 [1H, s, aromatic C-H_2], 9.95 [1H, s, H-C=O], 12.15 [1H, s, NH]; δ_C (75 MHz, DMSO-d_6) 112.4 (CH, aromatic CH), 118.1 (CH, aromatic CH), 120.8 (CH, aromatic CH), 122.1 (CH, aromatic CH), 123.4 (CH, aromatic CH), 124.1 (C, aromatic C), 137.0 (C, aromatic C), 138.4 (C, aromatic C), 184.9 (CH, H-C=O); m/z (ES+) 146.0 $[M+H]^+$ (100%). (ES-) 144.0 $[M-H]^-$ (100%).

5.2.3.4.2 1-Methyl-1*H*-indol-3-yl carboxaldehyde 483[21]

Method A:



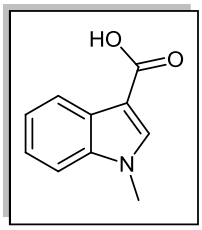
NaH (60% mineral oil dispersion) (1.038 g, 15.5 mmol, 1.5 eq.) was washed with portions of hexane (2 × 5 mL), under inert atmosphere. 1*H*-Indole-3-carboxaldehyde **121** (1.507 g, 10.3 mmol) was then added to the reaction flask along with dry DMF (20 mL) and stirred for 20 minutes, noting the rapid evolution of hydrogen gas at this point. Iodomethane (1 mL, 15.5 mmol, 1.5 eq.) was then added carefully, while stirring at room temperature overnight. Following removal of the solvent and washing of the ethyl acetate layers several times with water and brine, and drying over magnesium sulfate, the crude residue was

purified by flash chromatography, affording aldehyde **483** as a viscous brown oil, which solidified to a brown solid upon cooling (1.533 g, 92%); m.p. 62-65°C (lit.[21] 68-70°C); ν_{max}/ cm^{-1} (KBr) 3106, 2937, 1657, 1537; δ_H (300 MHz, $CDCl_3$) 3.87 [1H, s, CH_3], 7.31-7.37 [3H, m, aromatic C-$H_{5,6,7}$], 7.67 [1H, s, aromatic C-H_2], 8.29-8.32 [1H, m, aromatic C-H_4], 9.98 [1H, s, H-C=O]; δ_C (75 MHz, $CDCl_3$) 33.8 (CH_3, N-CH_3), 109.9 (CH, aromatic CH), 118.1 (C, aromatic C), 122.1 (CH, aromatic CH), 123.0 (CH, aromatic CH), 124.1 (CH, aromatic CH), 125.3 (C, aromatic C), 137.9 (C, aromatic C), 139.3 (CH, aromatic CH), 184.5 (H-C=O); m/z (ES+) 160.0 $[M+H]^+$ (100%).

Method B:

Phosphorus oxychloride (6 mL, 10.009 g, 65.2 mmol) was slowly added to dry DMF (70 mL) at 0°C. The solution was then stirred at 0°C for 30 minutes and *N*-methyl indole **456** (5.012 g, 38.2 mmol) in DMF (15 mL) was added dropwise to the flask. Following stirring overnight, the solvent was evaporated prior to addition of water (70 mL) and basification to pH 12 by the addition of aqueous 20% NaOH solution. The product was extracted several times with ethyl acetate (3 × 200 mL), dried with magnesium sulfate and filtered. The title compound appeared as a dark brown viscous oil following removal of solvent under reduced pressure and *N*-methyl 3-formylindole **483** was isolated following column chromatography using ethyl acetate/hexane (2.917 g, 28%).

5.2.3.4.3 1-Methyl-1*H*-indol-3-yl carboxylic acid 484

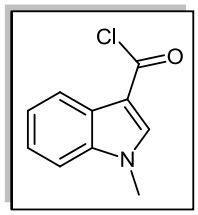


N-Methyl indole-3-carboxaldehyde **483** (0.203 g, 1.25 mmol) was added to acetone (40 mL). Potassium permanganate (0.501 g, 3.3 mmol, 2.6 eq.) was then added to the resulting mixture and stirred overnight. Aqueous hydrogen peroxide solution (30%) (10 mL) was then added to the reaction flask and stirring continued for a further 30 minutes. The off-white slurry was filtered and the straw-yellow filtrate acidified by the addition of a few drops of 10% HCl solution. The insoluble acid **484** was then isolated by vacuum filtration, to afford on drying, an off-white powder (0.182 g, 83%); m.p. 192-194°C (lit.[22] 205-206°C); ν_{max}/ cm^{-1} (KBr) 3350, 1750, 1562; δ_H (300 MHz, DMSO-d_6) 3.84 [1H, s, CH_3], 7.17-7.28 [2H, m, aromatic C-$H_{5,6}$], 7.50-7.53 [1H, d, *J* 8.1, aromatic C-H_7], 8.01-8.04 [1H, overlapping d, aromatic C-H_4], 8.04 [1H, s, aromatic C-H_2], 11.97 [1H, bs, CO_2H]; δ_C (75 MHz, DMSO-d_6) 32.9 (CH_3, N-CH_3), 106.1 (C, aromatic C), 110.6 (CH, aromatic CH), 120.7 (CH, aromatic CH), 121.2 (CH, aromatic CH), 122.1 (CH, aromatic CH), 126.4 (C, aromatic C), 136.1 (CH, aromatic

CH), 137.0 (C, aromatic C), 165.6 [C, $\underline{C}O_2H$]; m/z (ES+) 175.0 $[M+H]^+$ (75%), 130.0 (45%).

5.2.3.4.4 1-Methyl-1*H*-indol-3-yl carbonyl chloride 479[23,24]

Method A:[23]

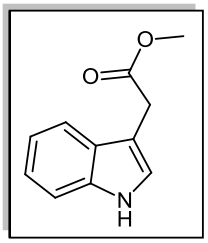


Thionyl chloride (20 mL) was added to *N*-methyl indole-3-carboxylic acid **484** (0.175 g, 1 mmol), followed by 3 drops of anhydrous DMF. The mixture was stirred at room temperature for 20 hours and then concentrated *in vacuo* to form a red solid in overall quantitative yield (0.190 g, 99%). However, formation of the 2-chloro derivative **485** was also observed, from mass spectral analysis; therefore, another method had to be employed for this step.

Method B:[24]

N-Methyl indole-3-carboxylic acid **484** (0.502 g, 2.85 mmol) was suspended in dry DCM (15 mL), followed by the careful addition of oxalyl chloride (0.25 mL, 2.86 mmol) over several minutes. Following stirring at ambient temperature for 75 minutes, gas evolution had ceased, and the solvent was evaporated under reduced pressure – yielding a light red solid **479**, (0.550 g, 99%), which was used without further purification; ν_{max}/ cm^{-1} (KBr) 1850 (C=O).

5.2.3.4.5 Methyl-1H-indol-3-yl acetate 239[25]

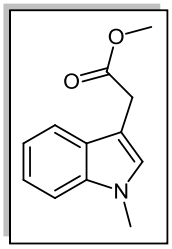


Indole-3-acetic acid **233** (10.803 g, 5.7 mmol) was stirred in the presence of distilled methanol (220 mL), and then cooled to 0°C. Thionyl chloride (21 mL, 273 mmol) was then charged slowly into the cooled reaction vessel over 10 minutes. The burgundy coloured reaction mixture was gradually allowed to attain room temperature and then stirred overnight. Following subsequent removal of solvent, the product residue was extracted with ethyl acetate (3 × 150 mL), and washed successively with saturated sodium bicarbonate solution (2 × 250 mL), water (3 × 250 mL) and brine (1 × 250 mL). The organic layer was dried using magnesium sulfate, filtered and thoroughly evaporated *in vacuo*; the ester intermediate **239** was thus isolated as a crude violet oil, which was employed without any further purification (10.822 g, 100%); m.p. lit.[25] 47-48°C; ν_{max}/ cm^{-1} (NaCl) 3410, 2957, 1730, 1490; δ_H (300 MHz, $CDCl_3$) 3.70 [3H, s, O-CH_3], 3.79 [2H, s, CH_2], 7.11-7.16 [2H, m, aromatic C-$H_{2,5}$], 7.18-7.23 [1H, td, *J* 7.1, 1.3, aromatic C-H_6], 7.33-7.36 [1H, d, *J* 7.9, aromatic C-H_7],

7.60-7.63 [1H, d, *J* 8.0, aromatic C-H_4], 8.11 [1H, bs, NH]; m/z (ES+) 190.1 $[M+H]^+$ (100%).

5.2.3.4.6 1-Methyl Methyl-1*H*-indol-3-yl acetate 480[26]

Method A:[23]

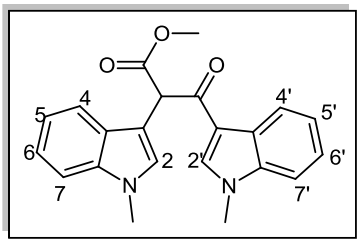


1*H*-Methyl indol-3-yl acetate **239** (0.504 g, 2.65 mmol) was added to NaH (0.160 g, 4 mmol, 1.5 eq.), under inert atmosphere, followed by the careful addition of anhydrous DMF (20 mL), while stirring in an appropriately sized ice-bath, with the rapid evolution of hydrogen gas from the mixture observed. Following stirring for 20 minutes at 0°C, iodomethane (0.25 mL, 4 mmol, 1.5 eq.) was charged slowly into the flask and stirring was continued at 0°C overnight. The reaction was then allowed to warm to room temperature. Following solvent removal, the product residue was extracted with ethyl acetate (2 × 75 mL), which was washed with water (2 × 100 mL) and brine (1 × 100 mL). The combined organic layers were dried using magnesium sulfate, filtered and evaporated *in vacuo.* Flash chromatography of the crude residue was employed, to isolate product **480** as a clear oil (0.498 g, 92%); ν_{max}/ cm^{-1} (KBr) 2951, 1732, 1616, 1556; δ_H (300 MHz, $CDCl_3$) 3.70 [3H, s, O-CH_3], 3.76 [3H, s, N-CH_3], 3.77 [2H, s, CH_2], 7.02 [1H, s, aromatic C-H_2], 7.09-7.15 [1H, t, *J* 7.9, aromatic C-H_5], 7.20-7.25 [1H, t, *J* 8.0, aromatic C-H_6], 7.27-7.30 [1H, d, *J* 8.1, aromatic C-H_7], 7.58-7.61 [1H, d, *J* 7.9, aromatic C-H_4]; δ_C (75 MHz, $CDCl_3$) 31.0 (CH_2, C$\underline{H_2}CO_2$Me), 32.7 (CH_3, N-CH_3), 52.0 (CH_3, O-CH_3), 106.7 (C, aromatic C), 109.3 (CH, aromatic CH), 118.9 (CH, aromatic CH), 119.2 (CH, aromatic CH), 121.8 (CH, aromatic CH), 126.6 (C, aromatic C), 127.7 (CH, aromatic CH), 136.9 (C, aromatic C), 172.6 (C, $\underline{C}O_2CH_3$); m/z (ES+) 204.1 $[M+H]^+$ (100%).

Method B:[26]

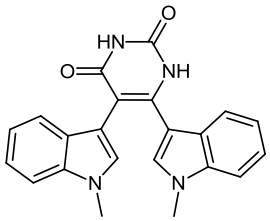
Dimethyl carbonate (8.6 mL, 101.6 mmol) was added to a mixture of indole-3-acetic acid **233** (6.002 g, 29.6 mmol), anhydrous potassium carbonate (6.007 g, 43.2 mmol), and DMF (70 mL), which was then stirred at 130°C for 16 hours. Following solvent removal, the product residue was extracted with ethyl acetate (150 mL), which was washed with water (2 × 150 mL) and brine (1 × 100 mL). The combined organic layers were dried using magnesium sulfate, filtered and evaporated *in vacuo*. The pure ester **480** was obtained, as a straw coloured oil, following column chromatography, using an 80:20 mixture of hexane and ethyl acetate (5.722 g, 82%).

5.2.3.4.7 Methyl 2,3-bis(1-Methyl-1*H*-indol-3-yl)-3-oxopropanoate 478

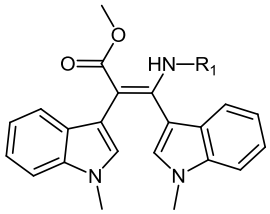


A solution of LDA (36.2 mL, 65.1 mmol, 2.2 eq.) was added over 10 minutes to a flask containing dry THF (50 mL), followed by cooling to −78°C. A mixture of *N*-methyl ester **480** (6.005 g, 29.6 mmol) in THF (3 mL) was then added slowly to the flask, while stirring, under inert atmosphere. The acid chloride **479** residue (38.5 mmol, 1.3 eq., based on corresponding acid **484**) was dissolved in THF (10-15 mL), and then added dropwise to the reaction vessel. The reaction was allowed to warm up to room temperature, while stirring was maintained, overnight. Following solvent removal, the brown product residue was extracted with ethyl acetate (3 × 150 mL), followed by washing with saturated ammonium chloride (250 mL), water (4 × 250 mL) and brine (2 × 150 mL). The combined organic layers were dried using magnesium sulfate, filtered and evaporated *in vacuo*. The optimised yield of the novel product **478** - a dark yellow crystalline solid, following gradient column chromatography employing ethyl acetate/ hexane, was 8.530 g (80%); m.p. 142-144°C; ν_{max}/ cm^{-1} (KBr) 2927, 1732, 1644, 1529; δ_H (300 MHz, $CDCl_3$) 3.74 [3H, s, N-CH_3], 3.74 [3H, s, N-CH_3], 3.76 [3H, s, O-CH_3], 5.70 [1H, s, C-H_α], 7.12-7.17 [1H, td, *J* 6.9, 1.4, aromatic C-H_5], 7.19-7.25 [1H, td, *J* 8.2, 1.3, aromatic C-$H_{5'}$], 7.28-7.30 [4H, m, aromatic C-$H_{6,6',7,7'}$], 7.32 [1H, s, aromatic C-H_2], 7.66-7.68 [1H, d, *J* 7.7, aromatic C-H_4], 7.78 [1H, s, aromatic C-$H_{2'}$], 8.42-8.45 [1H, m, aromatic C-$H_{4'}$]; δ_C (75 MHz, $CDCl_3$) 32.9 (CH_3, N-$\underline{C}H_3$), 33.6 (CH_3, N-$\underline{C}H_3$), 52.7 (CH_3, O-$\underline{C}H_3$), 53.2 (CH, CO$\underline{C}$HCO_2CH_3) 107.5 (C, aromatic C), 109.6 (CH, aromatic CH), 109.7 (CH, aromatic CH), 115.0 (C, aromatic C), 118.3 (CH, aromatic CH), 119.5 (CH, aromatic CH), 121.8 (CH, aromatic CH), 122.8 (CH, aromatic CH), 122.9 (CH, aromatic CH), 123.7 (CH, aromatic CH), 126.8 (C, aromatic C), 127.2 (C, aromatic C), 129.0 (CH, aromatic CH), 136.2 (CH, aromatic CH), 136.7 (C, aromatic C), 137.4 (C, aromatic C), 170.3 (C, $\underline{C}O_2CH_3$)], 188.0 (C, $\underline{C}$=O); m/z (ESI) 361.3 ($M+H^+$, 100%), 259.3 (80); HRMS - (ESI+) requires: 361.1548. Found: 361.1552 ($C_{22}H_{21}N_2O_3$).

5.2.3.4.8 Attempted derivatisation of 2,3-bisindolyl methyl-3-oxopropionate 478



507



R_1 = H **487**

R_1 = $PhCH_2$ **490**

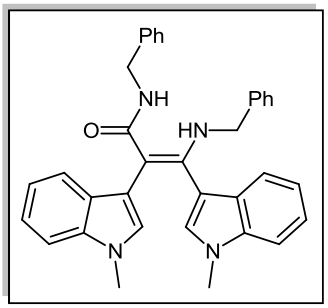
Representative microwave reactions*:

Table 5.2

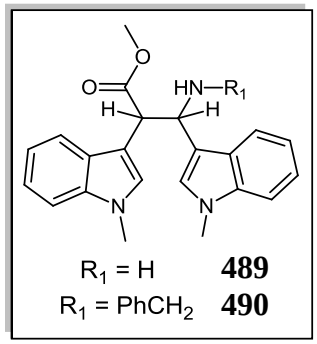
Reactant	Reagent	Additive	Power	Temp/^oC	Time	Product	Yield
478	urea	-	300W	160	20 min	(**507**)	n.r
478	urea	*p*-TSA (2.2 eq.)	300W	160	25 min	(**507**)	n.r
478	urea	Camphoric acid (2.2 eq.)	300W	160	25 min	(**507**)	n.r
478	$(NH_4)_2CO_3$	AcOH (3 mL)	300W	120	20 min	(**487**)	n.r
478	Bn-NH_2	Molecular sieves (4Å)	300W	100	20 min	(**490**)	n.r

*General microwave protocol: Intermediate β-ketoester **478** (0.100 g, 0.28 mmol) was added to a high pressure microwave vessel along with the appropriate reagent (10 eq.), along with corresponding reaction catalyst/ additive. Following extensive mixing of these components, the sealed tube was heated at the appropriate temperature for the given time (including ramp time = 5 min). Following addition of water (5 mL), formed solids were filtered and the filtrate was extracted with DCM (3 x 25 mL). In all cases, only starting material and decomposition products were isolated.

5.2.3.4.9 *N*-Benzyl-3-(benzylamino)-2,3-bis(1-methyl-1*H*-indol-3-yl)acrylamide 491

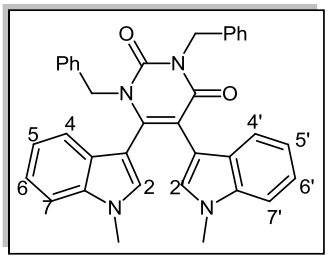


Heating of β-ketoester **478** (0.150 g, 0.42 mmol) and benzylamine (4 mL) at 110^{o}C for 24 hours, afforded a dark brown mixture, which was found by TLC to contain a product with a high Rf value, along with full consumption of starting material **478**. Following the addition of water (100 mL), the product was extracted with ethyl acetate (3 × 110 mL), and these combined layers were subsequently evaporated to yield the crude β-enaminoamide **491** as a viscous dark brown oil. This compound was determined by LCMS to be the dibenzylated derivative of interest and was used without purification at this point due to its rapid decomposition when subjected to silica gel chromatography; m/z (ES+) 525.2 $[M+H]^+$ (50%); HRMS - (ES+) requires: 525.2654. Found: 525.2632 ($C_{35}H_{33}N_4O$).



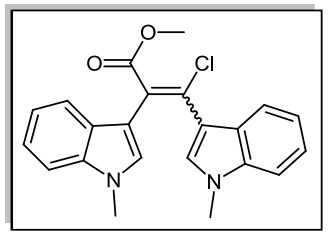
Attempted synthesis of **488, 489** *via* reductive amination approach: To a flask containing **478** (0.150 g, 0.42 mmol) was added appropriate amine source, ammonium acetate (R_1 = H (**488)**; 10 eq.) or benzylamine (R_1 = $PhCH_2$ (**489)**; 10 eq.), along with absolute ethanol (15 mL). To this orange solution was slowly added sodium triacetoxyborohydride (3 eq.), stirring at room temperature for a few minutes; the reaction was then heated to reflux and stirred overnight. After solvent removal, the crude residue was investigated and it was determined that conversion to the anticipated product did not occur in each case.

5.2.3.4.10 Carbonylation reactions: Attempted synthesis of **492**:



Method A: A mixture of **491** (0.150 g, 0.42 mmol) and triphosgene (0.124 g, 0.42 mmol, 1 eq.) in 1,2-dichloroethane (20 mL) was heated at 80°C, for 24 hours, under inert atmosphere. Only starting material **491** was detectable under these conditions.
Method B: Heating of urea (0.252 g, 4.2 mmol, 10 eq.), along with **491** (0.150 g, 0.42 mmol) under solvent-free conditions, at 170°C, for 16 hours, also did not afford any of the desired uracil derivative **492**.

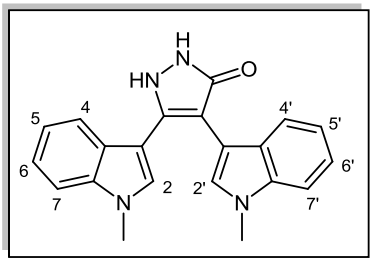
5.2.3.4.11 (E/Z)-Methyl 3-chloro-2,3-bis(1-methyl-1*H*-indol-3-yl)acrylate 493



Phosphorus pentachloride (0.158 g, 0.76 mmol, 1.1 eq.) was added to a mixture of β-ketoester **478** (0.250 g, 0.69 mmol) and dry methanol (15 mL). The reaction was then stirred at reflux for 20 hours. Following solvent removal under reduced pressure, the crude residue was extracted with ethyl acetate (70 mL), washed with water (2 × 100 mL), brine (70 mL), dried with magnesium sulfate and evaporated to dryness, to yield the novel chlorinated derivative **493** as an inseparable mixture of (E) and (Z)-isomers formed in a ratio of 2:1, as determined by ^{1}H NMR comparison between the characteristic methyl group peaks occurring at 3.45 and 3.52 ppm, and isolated as a dark brown crystalline solid (0.170 g, 65%); m.p. 84-87°C; ν_{max}/ cm^{-1} (KBr) 2945, 1720, 1660, 1613, 1533, 1465; δ_H (300 MHz, $CDCl_3$) 3.45 [3H, s, N-CH_3 (major)], 3.48 [3H, s, N-CH_3 (minor)], 3.52 [3H, s, N-CH_3 (minor)], 3.72 [3H, s, N-CH_3 (major)], 3.75 [3H s, O-CH_3 (major)], 3.81 [3H, s, O-CH_3 (minor)], 6.76 [1H, s, aromatic C-H_2 (minor)], 6.85-6.93 [2H, m, 2 × aromatic C-H (minor)], 6.98 [1H, s, aromatic C-$H_{2'}$ (minor)], 7.05-7.34 [13H, m, 13 × aromatic C-H (7 × major; 6 × minor)], 7.41 [1H, s, aromatic C-H

(major)], 7.48-7.51 [1H, m, aromatic C-H (major)], 7.75-7.77 [1H, m, aromatic C-H (major)]; δ_C (75 MHz, $CDCl_3$) (mixture of minor/major product signals) 31.8 (CH_3, N-CH_3 (minor)), 31.9 (CH_3, N-CH_3 (minor)), 32.1 ($2CH_3$, 2 × N-CH_3 (major)), 51.4 ($2CH_3$, 2 × O-CH_3), 108.3 (2CH, 2 × aromatic CH), 108.6 (CH, aromatic CH), 108.7 (CH, aromatic CH), 108.9 (C, aromatic C), 111.5 (C, aromatic C), 112.8 (C, aromatic C), 118.9 (CH, aromatic CH), 119.0 (2CH, 2 × aromatic CH), 119.1 (CH, aromatic CH), 119.2 (CH, aromatic CH), 119.4 (CH, aromatic CH), 119.5 (CH, aromatic CH), 119.6 (C, aromatic C), 120.3 (CH, aromatic CH), 120.9 (2CH, 2 × aromatic CH), 121.1 (CH, aromatic CH), 121.5 (CH, aromatic CH), 123.5 (C, aromatic C), 123.7 (C, aromatic C), 124.7 (C, aromatic C), 125.2 (C, aromatic C), 125.3 (C, aromatic C), 125.4 (C, aromatic C), 125.6 (C, aromatic C), 128.3 (CH, aromatic CH), 129.0 (2CH, 2 × aromatic CH), 130.2 (CH, aromatic CH), 130.4 (C, aromatic C), 135.5 (C, aromatic C), 135.6 (C, aromatic C), 135.7 (C, aromatic C), 135.8 (C, aromatic C), 168.2 (C, $\underline{C}O_2CH_3$ (minor)), 168.5 (C, $\underline{C}O_2CH_3$ (major)); m/z (ES+) 379.1 $[M+H]^+$ (30%); HRMS - (ES+) requires: 379.1213. Found: 379.1208 ($C_{22}H_{20}N_2O_2Cl$).

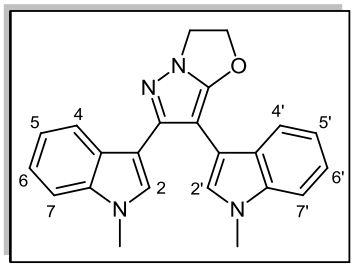
5.2.3.4.12 4,5-Bis(1-Methyl-1*H*-indol-3-yl)-1*H*-pyrazol-3(2*H*)-one 510[23]



β-Ketoester **478** (0.960 g, 2.66 mmol) was placed in a 100 mL round-bottom flask, along with camphoric acid (0.536 g, 2.66 mmol) and dry methanol (30 mL). Hydrazine hydrate (50-60%) (0.26 mL, 2.66 mmol, 1 eq.), was then added to the reaction mixture, prior to heating for 2 hours at reflux temperature. After this interval, excess hydrazine hydrate (0.78 mL, 7.98 mmol, 3 eq.) was added to the reaction vessel, and the overall mixture was stirred at reflux for a further 20 hours. Following removal of the reaction solvent, the product residue was dissolved in ethyl acetate (70 mL) and washed with 10% aqueous sodium bicarbonate solution (2 × 110 mL). Following washing of the ethyl acetate layer with water (3 × 100 mL), brine (2 × 100 mL), and drying with magnesium sulfate, the solvent was evaporated *in vacuo*. The crude pyrazolone **510** was purified by flash chromatography, employing a gradient from 70% hexane/ 30% ethyl acetate to 100% ethyl acetate as eluent. The product fractions were combined and evaporated to yield the desired compound **510** as dark brown flakes (0.620 g, 68%); m.p. 177-180°C (lit.[23] 180-181°C); ν_{max}/ cm^{-1} (KBr) 3400, 2923, 1602, 1462, 1327; δ_H (300 MHz, $CDCl_3$) 3.50 [3H, s, N-CH_3], 3.67 [3H, s, N-CH_3], 6.87-6.92 [1H, t, *J* 7.5, aromatic C-$H_{5'}$], 6.89 [1H, s, aromatic C-$H_{2'}$], 7.02-7.07 [1H, t, *J* 7.0, aromatic C-$H_{6'}$], 7.11 [1H, s, aromatic C-H_2], 7.11-7.15 [1H, t, *J* 7.2, aromatic C-H_5], 7.16-7.22 [1H, t, *J* 8.3, aromatic C-H_6], 7.22-7.25 [2H, d, *J* 8.0, aromatic C-$H_{7,7'}$], 7.29-7.32 [1H, d, *J* 7.9, aromatic

C-$H_{4'}$], 7.55-7.58 [1H, d, *J* 8.0, aromatic C-H_4]; δ_C (75 MHz, $CDCl_3$) 32.8 ($2CH_3$, 2 × N-$\underline{C}H_3$), 97.1 (C, aromatic C), 104.8 (C, aromatic C), 105.3 (C, aromatic C), 109.0 (CH, aromatic CH), 109.6 (CH, aromatic CH), 118.8 (CH, aromatic CH), 120.0 (CH, aromatic CH), 120.4 (CH, aromatic CH), 121.2 (CH, aromatic CH), 121.3 (CH, aromatic CH), 122.1 (CH, aromatic CH), 125.6 (C, aromatic C), 127.2 (C, aromatic C), 128.5 (CH, aromatic CH), 128.9 (CH, aromatic CH), 136.6 (C, aromatic C), 137.0 (C, aromatic C), 138.1 (C, aromatic C), 162.4 (C, C=O); m/z (ES+) 343.0 $[M+H]^+$, (100%), (ES-) 341.1 $[M-H]^-$ (55%).

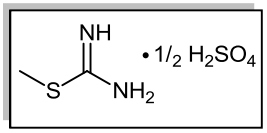
5.2.3.4.13 6,7-Bis(1-methyl-1*H*-indol-3-yl)-2,3-dihydropyrazolo[5,1-*b*]oxazole 511



Pyrazolone **510** (0.102 g, 0.29 mmol) was added to a mixture of anhydrous potassium carbonate (0.078 g, 0.58 mmol, 2 eq.), TBAB (0.028 g, 0.087 mmol, 0.33 eq.) and 1,4-dioxane (10 mL). Dibromoethane (0.08 mL, 0.87 mmol, 3 eq.) was then added to the vigorously stirring reaction mixture in a single portion and allowed to react at 30°C for 20 hours. The dioxane solution was filtered to remove the potassium carbonate, and washed with DCM (10 mL). Following solvent removal, hexane (10 mL) was added to the residue. This mixture was then decanted in order to remove excess unreacted dibromoethane. The resultant light brown solid was then dissolved in hot absolute ethanol (8 mL), followed by cooling to room temperature and then to 0°C. The novel oxazoline-fused pyrazole derivative was then filtered under vacuum and dried to yield a light yellow powder. Chromatography of the evaporated mother liquor residue, employing ethyl acetate/ hexane also isolated a further crop of title compound **511**, and the total yield was 0.061 g (57%); m.p. 132-135°C; ν_{max}/ cm^{-1} (KBr) 3412, 2930, 1710, 1612, 1568, 1521, 1467; δ_H (300 MHz, $CDCl_3$) 3.58 [3H, s, N-CH_3], 3.74 [3H, s, N-CH_3], 4.41-4.46 [2H, t, *J* 7.5, N-$C\underline{H}_2CH_2$-O], 5.04-5.10 [2H, t, *J* 7.5, N-$CH_2C\underline{H}_2$-O], 6.96 [1H, s, aromatic C-$H_{2'}$], 6.96 [1H, s, aromatic C-H_2], 7.02-7.07 [1H, t, *J* 8.0, aromatic C-$H_{5'}$], 7.08-7.14 [1H, td, *J* 8.0, 1.5, aromatic C-H_5], 7.18-7.27 [3H, m, aromatic C-$H_{6,6',7'}$], 7.31-7.33 [1H, d, *J* 8.2, aromatic C-H_7], 7.51-7.54 [1H, d, *J* 7.9, aromatic C-$H_{4'}$], 8.07-8.10 [1H, d, *J* 7.9, aromatic C-H_4]; δ_C (75 MHz, $CDCl_3$) 32.8 ($2CH_3$, 2 × N-CH_3), 45.9 (CH_2, N-$\underline{C}H_2CH_2$-O), 74.9 (CH_2, N-$CH_2\underline{C}H_2$-O), 87.3 (C, aromatic C), 105.5 (C, aromatic C), 108.8 (CH, aromatic CH), 109.1 (CH, aromatic CH), 109.6 (C, aromatic C), 119.1 (CH, aromatic CH), 119.8 (CH, aromatic CH), 120.8 (CH, aromatic CH), 121.6 (CH, aromatic CH), 121.7 (CH, aromatic CH), 122.2 (CH, aromatic CH), 126.6 (C, aromatic C), 127.6 (C, aromatic C), 127.7 (CH, aromatic CH), 128.3 (CH, aromatic CH), 136.7 (C, aromatic C), 136.9 (C,

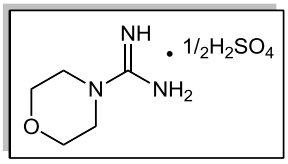
aromatic C), 151.4 (C, aromatic C), 157.3 (C, aromatic C); m/z (ES+) 369.1 $[M+H]^+$ (100%); HRMS - (ES+) requires: 369.1716. Found: 369.1722 ($C_{23}H_{20}N_4O$).

5.2.3.4.14 *S*-Methyl isothiouronium hemisulfate 534[27]



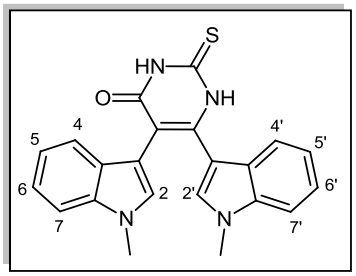
Dimethyl sulfate (6.303 g, 49.95 mmol) was slowly added to a mixture of thiourea (7.604 g, 99.84 mmol) in water (150 mL). On vigorous stirring of the reaction at room temperature, for 5 minutes, heating to 30°C was initiated and stirring was continued for 2 hours. Following heating to 100°C, reflux of the reaction contents proceeded for 16 hours, at which point, it was concentrated to dryness. Treatment of the off-white residue with a mixture of EtOH/ water (10:1) (50 mL), prior to stirring for 5 minutes, then afforded *S*-methyl isothiouronium hemisulfate **534** following filtration and drying *in vacuo* (14.815 g, 53%); m.p. 243-245°C (dec.) (lit.[27] 235°C (dec.)); ν_{max}/ cm^{-1} (KBr) 3096, 1664, 1429; m/z (ES+) 90.8 $[M]^+$ (100%).

5.2.3.4.15 4-Morpholinocarboxamidine hemisulfate 535[28]



Morpholine (0.35 mL, 3.96 mmol, 1.1 eq.) was added to a suspension of *S*-methyl isothiouronium hemisulfate salt **534** (1.006 g, 3.60 mmol), stirring in EtOH and then heated at reflux for 20 hours. Filtration of the milky slurry yielded a single crop of pure hemisulfate salt **535** was isolated following washing successively with water (2 × 15 mL), EtOH (2 × 15 mL) and drying under vacuum (1.003 g, 78%); m.p. >300°C (lit.[29] 306°C (dec.)); ν_{max}/ cm^{-1} (KBr) 3330, 3108, 2857, 1664; m/z (ES+) 130.1 $[M]^+$ (100%).

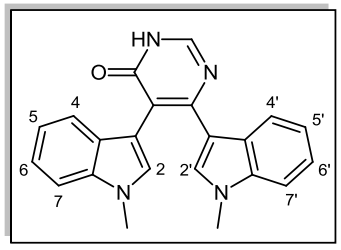
5.2.3.4.16 5,6-Bis(1-methyl-1*H*-indol-3-yl)-2-thioxo-2,3-dihydropyrimidin-4(1*H*)-one 514



To a sodium methoxide solution (sodium metal (1.595 g, 69 mmol, 10 eq.)) in dry methanol (120 mL), under inert atmosphere, was added thiourea (2.627 g, 35 mmol, 5 eq.), followed by vigorous stirring for 15 minutes. Methyl 2,3-bis(1-methyl-1*H*-indol-3-yl)-3-oxopropanoate **478** (2.508 g, 6.9 mmol) was then charged to the reaction mixture and heated at 70°C for 24 hours. Following solvent evaporation, water (100 mL) was added to the complex residue, prior to acidification with 10% HCl to pH 3. Filtration of the resultant dark brown solid, followed by trituration of the crude pyrimidinone **514** with boiling absolute ethanol (40 mL), produced a slurry, which, following filtration and successive washing of the yellow powder with water and diethyl ether, was identified as the pure thiouracil product **514** (0.640

g, 24%); m.p. 317-320°C; ν_{max}/ cm^{-1} (KBr) 2922, 1651, 1541 1452; δ_H (300 MHz, DMSO-d_6) 3.63 [3H, s, N-CH_3], 3.70 [3H, s, N-CH_3], 6.74-6.80 [2H, m, aromatic C-$H_{5,5'}$], 6.96-7.01 [2H, m, aromatic C-$H_{7,7'}$], 7.02-7.07 [2H, t, *J* 7.9, aromatic C-$H_{6,6'}$], 7.21 [1H, s, aromatic C-H_2], 7.24-7.27 [1H, d, *J* 8.2, aromatic C-H_4], 7.30-7.33 [1H, d, *J* 8.2, aromatic C-$H_{4'}$], 7.65 [1H, s, aromatic C-$H_{2'}$]; 12.15 [1H, bs, C=C-N<u>H</u>CS]; 12.51 [1H, bs, N<u>H</u>CO]; δ_C (75 MHz, DMSO-d_6) 32.4 (CH_3, N-<u>C</u>H_3), 32.7 (CH_3, N-<u>C</u>H_3), 105.7 (C, aromatic C), 106.3 (C, aromatic C), 109.1 (C, aromatic C), 109.4 (CH, aromatic CH), 110.0 (CH, aromatic CH), 118.5 (CH, aromatic CH), 119.5 (CH, aromatic CH), 119.6 (CH, aromatic CH), 119.7 (CH, aromatic CH), 120.6 (CH, aromatic CH), 121.4 (CH, aromatic CH), 125.1 (C, aromatic C), 127.0 (C, aromatic C), 130.7 (CH, aromatic CH), 132.4 (CH, aromatic CH), 135.9 (C, aromatic C), 136.0 (C, aromatic C), 144.9 (C, aromatic C), 161.3 (C, C=O), 174.3 (C, C=S); m/z (ES+) 387.2 $[M+H]^+$ (20%), 115.0 (75), 73.9 (100); HRMS - (ES+) requires: 387.1280. Found: 387.1272 ($C_{22}H_{19}N_4OS$).

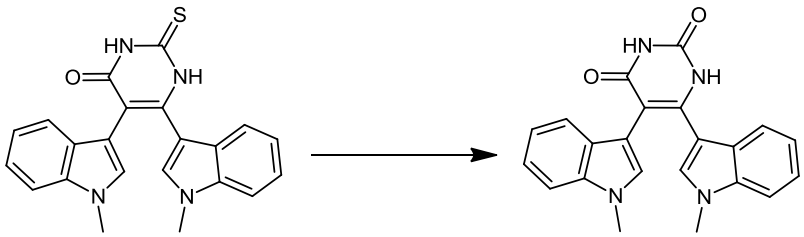
5.2.3.4.17 5,6-Bis(1-Methyl-1*H*-indol-3-yl)pyrimidin-4(3*H*)-one 537



Thiouracil **514** (0.105 g, 0.26 mmol) was added to a flame-dried flask along with nickel bromide (0.290 g, 1.3 mmol, 5 eq.) and dry methanol (10 mL). Sodium borohydride (0.152 g, 3.89 mmol, 15 eq.) was added cautiously to the reaction mixture portionwise, and the reaction was allowed to stir for 2 hours at room temperature. TLC analysis indicated full consumption of starting material had occurred at this point. Following stirring at room temperature for a further 14 hours, only the desired pyrimidin-4(3*H*)-one **537** could be detected. The reaction mixture was then filtered through a pad of celite®, and washed with additional methanol (2 × 20 mL), followed by ethyl acetate (3 × 15 mL). Following evaporation of these combined extracts, the light orange residue was redissolved in ethyl acetate (70 mL). This material was then washed with water (75 mL), and the aqueous layer further extracted with ethyl acetate (2 × 25 mL). The ethyl acetate layers were combined and washed with water (3 × 100 mL) and brine (100 mL). The organic layer was dried with magnesium sulfate, filtered and evaporated *in vacuo*, and the residue was purified by flash chromatography (1% methanol/DCM), to afford novel pyrimidin-4(3*H*)-one derivative **537** as a dark brown powder (0.051 g, 55%); m.p. 218-221°C; ν_{max}/ cm^{-1} (KBr) 3426, 2926, 1633, 1528, 1465, 1372; δ_H (300 MHz, DMSO-d_6) 3.38 [3H, s, N-CH_3], 3.74 [3H, s, N-CH_3], 6.68-6.73 (1H, t, *J* 7.1, C-H_5), 6.80 (1H, s, C-H_2), 6.84-6.86 (1H, d, *J* 7.9, C-H_7), 6.88-6.93 (1H, t, *J* 7.8, C-$H_{5'}$), 6.96-7.01 (1H, t, *J* 7.6, C-H_6), 7.01-7.06 (1H, t, *J* 7.0, C-$H_{6'}$), 7.23-7.25 (1H,d,

J 8.0, C-$H_{7'}$), 7.33-7.35 (1H, d, *J* 5.9, C-H_4), 7.35 (1H, s, C-$H_{2'}$), 7.95-7.98 (1H, d, *J* 7.9, C-$H_{4'}$), 8.13 (1H, s, N=C<u>H</u>-NHCO), 12.23 (1H, bs, NH); δ_C (75 MHz, DMSO-d_6) 32.5 (CH_3, N-<u>C</u>H_3), 32.6 (CH_3, N-<u>C</u>H_3), 107.5 (C, aromatic C), 109.6 (CH, aromatic CH), 109.7 (CH, aromatic CH), 112.7 (C, aromatic C), 114.7 (C, aromatic C), 118.6 (CH, aromatic CH), 119.8 (2CH, 2 × aromatic CH), 120.8 (CH, aromatic CH), 121.4 (CH, aromatic CH), 122.3 (CH, aromatic CH), 126.1 (C, aromatic C), 126.6 (C, aromatic C), 130.5 (CH, aromatic CH), 132.5 (CH, aromatic CH), 136.3 (C, aromatic C), 136.5 (C, aromatic C), 146.3 (C, aromatic C), 155.7 (C, N=<u>C</u>-H(NH)), 161.7 (C, <u>C</u>=O(NH)); m/z (ES+) 355.1 $[M+H]^+$ (100%); HRMS - (ES+) requires: 355.1559. Found: 355.1569 ($C_{22}H_{19}N_4O$).

5.2.3.4.18 Oxidative desulfurisation study



514 **507**

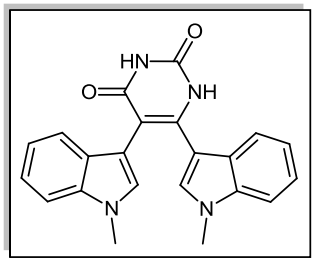
Table 5.3

Reaction No.	Reactant	Amount	Solvent	Reaction Time	Product[¥]
1	$ClCH_2CO_2H$	10% w/v	H_2O	72h/ reflux	**514**+**507**
2	$ClCH_2CO_2H$	10% w/v	AcOH	72h/ reflux	**514**+**507**
3	$ClCH_2CO_2H$	10% w/v	DMF	72h/ 110°C	**514**+**507**
4	$ClCH_2CO_2H$	5 eq.	MeOH	72h/ reflux	**514**+**507**
5	aq. H_2O_2	30% w/v	H_2O_2	20h/ 70°C	**514**
6	$BrCH_2CO_2Et$	1.1 eq.	MeOH	20h/ reflux	**507** (17%)
7	$BrCH_2CO_2Et$	1.5 eq.	DMF	24h/ 110°C	**514**
8	$BrCH_2CO_2Et$	2.5 eq.	MeOH/H_2O	48h/ reflux	**507** (45%)

[¥] Reactions were monitored by ^{13}C NMR, based on observed chemical shift differences between <u>C</u>=O and <u>C</u>=S signals.

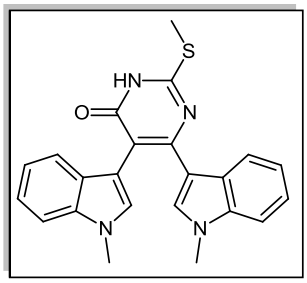
<u>General reaction (**1-7**):</u> A mixture of **514** and the haloacetic acid derivative was heated at high temperature for 24-72 hours. On cooling to 0°C, the precipitated solid was filtered, to afford a mixture of starting material **514**, along with detection of a small amount of **507**, in each case (Table 5.1).

5.2.3.4.19 5,6-Bis(1-methyl-1*H*-indol-3-yl)-2-oxo-2,3-dihydropyrimidin-4-one 507



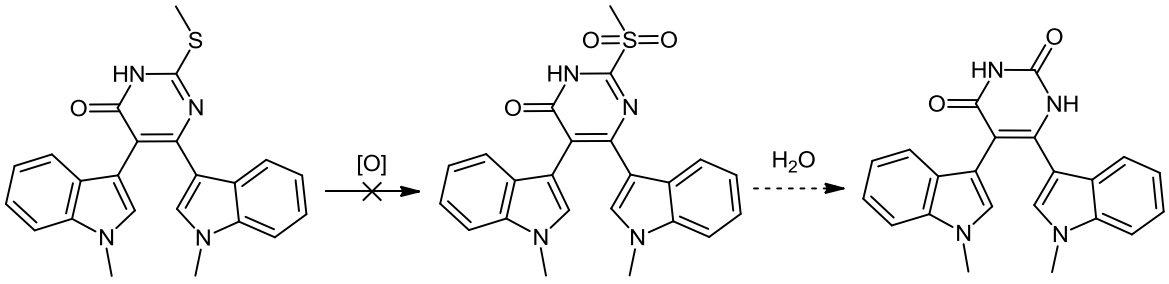
Bisindolyl 2-thiopyrimidin-4-one derivative **514** (0.100 g, 0.26 mmol) was stirred in the presence of methanol (15 ml) and ethyl bromoacetate (0.108 g, 0.07 mL, 0.65 mmol, 2.5 eq.) at 70^{o}C, for 24 hours, prior to the addition of a few drops of water and heating for a further 24 hours. Following solvent evaporation, a hot DMF/H_2O solution (5:1) (15 mL) was added to the light-yellow residue, and the resultant milky slurry was allowed to cool to room temperature and then filtered. The off-white powder was washed with water and diethyl ether successively, prior to drying under high vacuum overnight, to afford the pure 5,6-bisindolyl uracil **507** (0.044 g, 45%); m.p. >320^{o}C; ν_{max}/ cm^{-1} (KBr) 3425, 2925, 1703, 1639, 1555, 1453; δ_H (300 MHz, DMSO-d_6) 3.63 [3H, s, N-CH_3], 3.67 [3H, s, N-CH_3], 6.75-6.81 [2H, m, aromatic C-$H_{5,5'}$], 6.96-7.08 [4H, m, aromatic C-$H_{6,6',7,7'}$], 7.11 [1H, s, aromatic C-H_2], 7.24-7.27 [1H, d, *J* 8.2, aromatic C-H_4], 7.30-7.33 [1H, d, *J* 8.3, aromatic C-$H_{4'}$], 7.50 [1H, s, aromatic C-$H_{2'}$], 10.69 [1H, bs, amide NH], 11.12 [1H, bs, imide NH]; δ_C (75 MHz, DMSO-d_6) 32.3 (CH_3, N-$\underline{C}H_3$), 32.7 (CH_3, N-$\underline{C}H_3$), 103.8 (C, aromatic C), 106.6 (C, aromatic C), 107.4 (C, aromatic C), 109.2 (CH, aromatic CH), 109.9 (CH, aromatic CH), 118.3 (CH, aromatic CH), 119.5 (CH, aromatic CH), 119.6 (CH, aromatic CH), 119.8 (CH, aromatic CH), 120.5 (CH, aromatic CH), 121.5 (CH, aromatic CH), 125.1 (C, aromatic C), 127.6 (C, aromatic C), 130.5 (CH, aromatic CH), 131.6 (CH, aromatic CH), 136.0 (2C, 2 × aromatic C), 145.2 (C, aromatic C), 151.1 (C, NH$\underline{C}$=ONH), 164.2 (C, C-$\underline{C}$=ONH); m/z (ES+) 371.1 $[M+H]^+$ (80%). (ES-) 369.1 $[M-H]^-$ (40%); HRMS - (ES+) requires: 371.1508. Found: 371.1506 ($C_{22}H_{19}N_4O_2$).

5.2.3.4.20 5,6-Bis(1-methyl-1*H*-indol-3-yl)-2-(methylthio)pyrimidin-4(3*H*)-one 515



Distilled methanol (15 mL) was added to a flask containing anhydrous potassium carbonate (0.203 g, 1.42 mmol, 1.1 eq.), along with compound **514** (0.507 g, 1.29 mmol). Iodomethane (0.16 mL, 2.58 mmol, 2 eq.) was then added and the mixture was stirred vigorously at 30^{o}C for a further 20 hours. Following solvent removal, the residue was taken up in ethyl acetate (15 mL), and filtered, to remove any unreacted base. This ethyl acetate solution was evaporated to yield a light beige solid, which was subjected to column chromatography, employing a gradient from 100% ethyl acetate, to 90% ethyl acetate/ 10% methanol, and finally with the addition of a few drops of Et_3N, to release polar **515**, following elution of the thiouracil starting

material **514**. The product fractions were then combined and evaporated to a light yellow powder, under vacuum (0.180 g, 35%); m.p. 273-276°C; ν_{max}/ cm^{-1} (KBr) 3434, 2923, 1628, 1521, 1461; δ_H (300 MHz, DMSO-d_6) 2.66 [3H, s, S-CH_3], 3.46 [3H, s, N-CH_3], 3.82 [3H, s, N-CH_3], 6.76-6.81 [1H, t, *J* 7.7, aromatic C-H_5], 6.87 [1H, s, aromatic C-H_2], 6.93-6.95 [1H, d, *J* 7.9, aromatic C-H_7], 7.00-7.05 [1H, t, *J* 7.4, aromatic C-$H_{5'}$], 7.05-7.10 [1H, t, *J* 7.3, aromatic C-H_6], 7.10-7.15 [1H, t, *J* 7.0, aromatic C-$H_{6'}$], 7.32-7.35 [1H, d, *J* 8.1, aromatic C-$H_{7'}$], 7.37 [1H, s, aromatic C-$H_{2'}$], 7.41-7.44 [1H, d, *J* 8.2, aromatic C-H_4]; 8.06-8.09 [1H, d, *J* 8.0, aromatic C-$H_{4'}$], 12.50 [1H, bs, NH]; δ_C (75 MHz, DMSO-d_6) 12.92 (CH_3, S-CH_3), 32.5 (CH_3, N-CH_3), 32.6 (CH_3, N-CH_3), 107.5 (C, aromatic C), 109.6 (CH, aromatic CH], 109.8 (CH, aromatic CH), 112.7 (C, aromatic C), 118.6 (CH, aromatic CH), 119.7 (CH, aromatic CH), 119.7 (C, aromatic C), 119.9 (CH, aromatic CH), 120.7 (C, aromatic C), 120.8 (CH, aromatic CH), 121.5 (CH, aromatic CH), 122.1 (CH, aromatic CH), 126.3 (C, aromatic C), 126.7 (C, aromatic C), 130.3 (CH, aromatic CH), 132.7 (CH, aromatic CH), 136.3 (C, aromatic C), 136.5 (C, aromatic C), 156.6 (C, N=C(SCH$_3$)), 161.9 (C, C=O); m/z (ES+) 401.1 $[M+H]^+$ (30%); HRMS - (ES+) requires: 401.1436. Found: 401.1430 ($C_{23}H_{21}N_4OS$).



515 **524** **507**

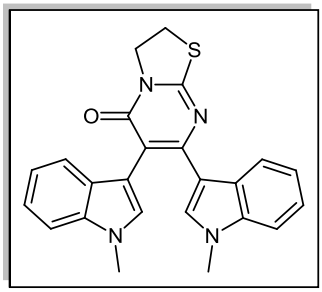
Scheme 5.1

5.2.3.4.21 Attempted oxidative hydrolysis of 515 to 507:

(a) Potassium peroxymonosulfate (Oxone®) (0.307 g, 0.50 mmol, 2 eq.) was added portionwise to a flask containing a suspension of novel sulfide **515** (0.100 g, 0.25 mmol) in a 1:1 mixture of water/1,4-dioxane (15 mL). It was observed that no reaction had occurred after 72 hours at reflux (Scheme 5.1).

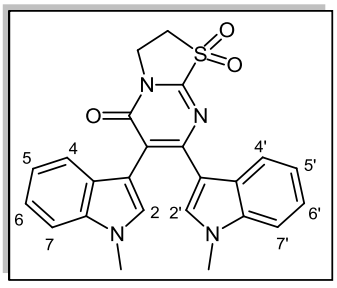
(b) Addition of 10% aq. NaOH (10 mL) or 5% aq. HCl (10 mL), to compound **515** (0.100 g, 0.25 mmol), followed by heating at 70°C for a further 72 hours also afforded no reaction.

5.2.3.4.22 6,7-Bis(1-Methyl-1*H*-indol-3-yl)-2*H*-thiazolo[3,2-*a*]pyrimidin-5(3*H*)-one 516



To a solution of compound **514** (0.101 g, 0.26 mmol) in 1,4-dioxane (10 mL), was added anhydrous potassium carbonate (0.072 g, 0.52 mmol, 2 eq.) and TBAB (0.025 g, 0.078 mmol, 0.33 eq.). 1,2-Dibromoethane (0.07 mL, 0.78 mmol, 3 eq.) was then syringed into the reaction flask, with vigorous stirring of the mixture allowed to proceed overnight. The dioxane solution was filtered, prior to washing with DCM (10 mL). The clarified filtrate was evaporated *in vacuo*, and the residue was then washed with a small volume of hexane, to remove any excess starting reagent. The resultant beige solid was dissolved in hot absolute ethanol (8 mL), followed by cooling to room temperature and subsequently to 0^{o}C. The novel thiazolo heterocyclic product **516** was then filtered and isolated as a light yellow powder (0.071 g, 66%); m.p >300^{o}C; ν_{max}/ cm^{-1} (KBr) 2923, 1644, 1562, 1520, 1479, 1460; δ_H (300 MHz, DMSO-d_6) 3.52 [3H, s, N-CH$_3$], 3.64-3.69 [2H, t, *J* 7.6, S-C<u>H</u>$_2$-CH$_2$-N], 3.87 [3H, s, N-CH$_3$], 4.46-4.51 [2H, t, *J* 7.6, S-CH$_2$-C<u>H</u>$_2$-N], 6.84-6.89 [1H, t, *J* 7.6, aromatic C-H$_5$], 6.89 [1H, s, aromatic C-H$_2$], 7.02-7.04 [1H, d, *J* 7.9, aromatic C-H$_7$], 7.02-7.07 [1H, t, *J* 7.6, aromatic C-H$_{5'}$], 7.11-7.17 [1H, t, *J* 9.0, aromatic C-H$_6$], 7.14-7.19 [1H, t, *J* 7.2, aromatic C-H$_{6'}$], 7.36-7.39 [1H, d, *J* 8.2, aromatic C-H$_{7'}$], 7.39 [1H, s, aromatic C-H$_{2'}$], 7.47-7.50 [1H, d, *J* 8.2, aromatic C-H$_4$], 7.97-8.00 [1H, d, *J* 8.0, aromatic C-H$_{4'}$]; δ_C (75 MHz, DMSO-d_6) 26.3 (CH$_2$, N-CH$_2$<u>C</u>H$_2$-S), 32.5 (CH$_3$, N-<u>C</u>H$_3$), 32.7 (CH$_3$, N-<u>C</u>H$_3$), 49.0 (CH$_2$, N-<u>C</u>H$_2$CH$_2$-S), 107.4 (C, aromatic C), 109.0 (C, aromatic C), 109.6 (CH, aromatic CH), 109.8 (CH, aromatic CH), 112.2 (C, aromatic C), 118.6 (CH, aromatic CH), 119.7 (CH, aromatic CH), 119.9 (CH, aromatic CH), 120.8 (CH, aromatic CH), 121.5 (CH, aromatic CH), 122.1 (CH, aromatic CH), 126.4 (C, aromatic C), 126.5 (C, aromatic C), 130.3 (CH, aromatic CH), 132.7 (CH, aromatic CH), 136.2 (C, aromatic C), 136.6 (C, aromatic C), 155.5 (C, aromatic C), 160.8 (C, N-<u>C</u>=N), 161.1 (C, <u>C</u>=O); m/z (ES+) 413.0 $[M+H]^+$ (100%); HRMS - (ES+) requires: 413.1436. Found: 413.1432 ($C_{24}H_{21}N_4OS$).

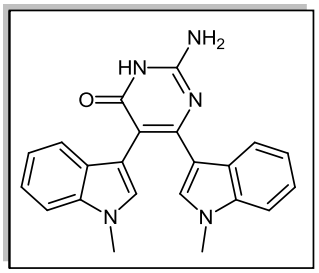
5.2.3.4.23 Attempted oxidation of 6,7-bis(1-methyl-1*H*-indol-3-yl)-2*H*-thiazolo[3,2-*a*]pyrimidin-5(3*H*)-one 516



A mixture of 2*H*-thiazolo[3,2-*a*]pyrimidin-5(3*H*)-one **516** (0.149 g, 0.36 mmol) and *m*-CPBA (0.180 g, 0.80 mmol, 2.2 eq.) was stirred in DCM at 35^{o}C, for 72 hours. The reaction mixture was initially filtered, prior to solvent removal and addition of DCM (40 mL). Following repeated washing with

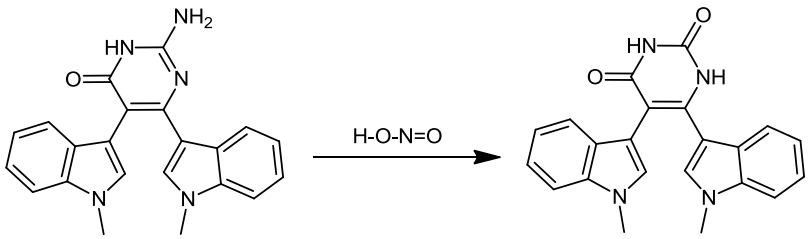
saturated aq. $NaHCO_3$ solution (3 x 70 mL), the aqueous component was extracted with further DCM (40 mL); the combined DCM layers were washed successively with brine (3 x 100 mL) and water (100 mL) and dried with magnesium sulfate. Upon usual work-up, TLC and MS analysis of the crude residue indicated oxidation to the corresponding sulfone **517** had not occurred and only starting material **516** was present.

5.2.3.4.24 2-Amino-5,6-bis(1-methyl-1*H*-indol-3-yl)pyrimidin-4(3*H*)-one 445



Sodium metal (1.742 g, 76 mmol, 20 eq.) was dissolved in dry methanol (60 mL), under an inert atmosphere, followed by stirring at room temperature for 20 minutes. Guanidine carbonate (3.421 g, 19 mmol, 5 eq.) was then added to the flask in a single portion, and the heterogeneous mixture was stirred vigorously for 25 minutes at ambient temperature. Methyl 2,3-bis(1-methyl-1*H*-indol-3-yl)-3-oxopropanoate **478** (1.366 g, 3.8 mmol) was carefully added to this suspension and the dark orange reaction was then heated to reflux for 24 hours. Following solvent removal under reduced pressure, the residue was dissolved in a minimum volume of water (30 mL), and subsequently acidified with 10% HCl to pH 3. The crude 2-amino-5,6-bis(1-methyl-1*H*-indol-3-yl)pyrimidin-4(3*H*)-one **445** was then filtered, washed successively with water and diethyl ether, and dried. Gradient chromatography afforded a fraction, eluting with 0.5% methanol/ DCM, which was evaporated to provide the novel isocytosine derivative **445** as a light brown amorphous powder (0.627 g, 45%); m.p. 195-197^{o}C; ν_{max}/ cm^{-1} (KBr) 3384, 2925, 1686, 1627, 1517, 1462; δ_H (300 MHz, DMSO-d_6) 3.40 [3H, s, N-CH_3], 3.80 [3H, s, N-CH_3], 6.41 [2H, bs, NH_2], 6.65 [1H, s, aromatic C-H_2], 6.78-6.83 [1H, t, *J* 7.5, aromatic C-H_5], 6.98-7.13 [4H, m, aromatic C-$H_{5',6,6',7}$], 7.17 [1H, s, aromatic C-$H_{2'}$], 7.27-7.29 [1H, d, *J* 8.0, aromatic C-$H_{7'}$], 7.39-7.42 [1H, d, *J* 8.2, aromatic C-H_4], 8.32-8.35 [1H, d, *J* 8.0, aromatic C-$H_{4'}$], 10.83 [1H, bs, NH]; δ_C (75 MHz, DMSO-d_6) 32.4 (CH_3, N-CH_3), 32.7 (CH_3, N-CH_3), 105.5 (C, aromatic C), 106.6 (C, aromatic C), 109.0 (2C, 2 × aromatic C), 109.5 (CH, aromatic CH), 110.0 (CH, aromatic CH), 118.5 (CH, aromatic CH), 119.6 (CH, aromatic CH), 119.9 (CH, aromatic CH), 120.7 (CH, aromatic CH), 121.2 (CH, aromatic CH), 121.8 (CH, aromatic CH), 125.6 (C, aromatic C), 127.1 (C, aromatic C), 130.5 (CH, aromatic CH), 132.2 (CH, aromatic CH), 136.2 (C, aromatic C), 136.3 (C, aromatic C), 152.7 (C, C=N(NH_2)), 161.8 (C, C=O(NH)); m/z (ES+) 370.1 $[M+H]^+$ (100%); HRMS - (ES+) requires: 370.1677. Found: 370.1668 ($C_{22}H_{20}N_5O$).

5.2.3.4.25 Attempted hydrolytic dediazoniation reactions:



445 **507**

Representative reactions:

(1) $NaNO_2$: (a) To a flask containing **445** (0.200 g, 0.54 mmol), was added 10% aq. HCl (10 mL), and the mixture was heated to 70°C. A solution of $NaNO_2$ (0.075 g, 0.59 mmol, 1.1 eq.) in water (3 mL) was added dropwise over 10 minutes; the solution was cooled to room temperature and stirring was maintained overnight.

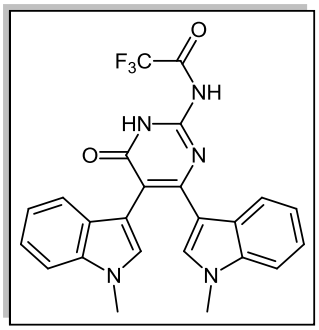
(b) On cooling of a suspension of **445** (0.200 g, 0.54 mmol) in AcOH (7 mL) or aq. 2M HCl (7 mL) to 0°C, an ice-cold 10% w/v aq. $NaNO_2$ solution (2 mL) was slowly added, with stirring at 0°C. Following protection from light and vigorous stirring at this temperature for 2 hours, the reaction was warmed to room temperature overnight.

(2) *tert*-Butyl nitrite: To a mixture of **445** (0.200 g, 0.54 mmol) and *tert*-butyl nitrite (0.280 g, 2.7 mmol, 5 eq.), protected from light and cooled to 0°C, was added a solution of 1:1 IPA/ water (10 mL). On stirring at this temperature for 20 hours, the reaction was then allowed to warm to room temperature and allowed to stand for 24 hours.

(3) Nitrosylsulfuric acid: Preparation of the nitrosating reagent was accomplished by dissolving $NaNO_2$ (1.003 g, 14 mmol) in conc. H_2SO_4 (5 mL), at −5°C, maintained by means of an ice-salt bath, followed by slow stirring of the clear solution at this temperature for 45 minutes. At this point, a suspension of **445** (0.100 g, 0.27 mmol) stirred in a 1:1 mixture of conc. sulphuric acid/ water (7 mL), was cooled to 0°C. Addition of nitrososylsulfuric acid solution (1 mL, 2.8 mmol) dropwise over 10 minutes was followed by stirring of the heterogeneous dark brown mixture at this temperature for 3 hours, with the appearance of some foaming. The reaction was then heated to 70°C overnight.

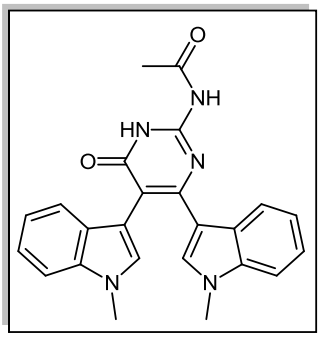
- In all cases, IR analysis failed to identify a characteristic product peak at 1702 cm^{-1}. TLC and MS evidence corroborated this result and identified only starting material/ unidentifiable side-products from this series of reactions.

5.2.3.4.26 *N*-(4,5-Bis(1-methyl-1*H*-indol-3-yl)-6-oxo-1,6-dihydropyrimidin-2-yl)-2,2,2-trifluoroacetamide 528



Bisindolyl aminopyrimidinone **445** (0.053 g, 0.14 mmol) was suspended in a mixture of trifluoroacetic anhydride (15 mL) and trifluoroacetic acid (3 mL). The reaction was then heated at 80°C and a steady reflux of the reaction contents was established and maintained overnight. The dark brown suspension was then cooled, prior to evaporation of the solvent *in vacuo*. The crude trifluoroacetamide **528** (0.035 g) was subjected to flash chromatography with 100% ethyl acetate, and the final product **528** was isolated as a dark orange powder (0.029 g, 45%); m.p. 177-180°C (dec.); ν_{max}/ cm^{-1} (KBr) 3377, 3173, 2929, 1629, 1612, 1520, 1464; δ_H (300 MHz, DMSO-d_6) 3.36 [3H, s, N-CH_3], 3.87 [3H, s, N-CH_3], 6.63 [1H, s, aromatic C-H_2], 6.71 [1H, s, aromatic C-$H_{2'}$], 6.79-6.84 [1H, t, *J* 7.3, aromatic C-H_5], 7.00-7.10 [4H, m, aromatic C-$H_{5',6,6',7}$], 7.21-7.24 [1H, d, *J* 8.2, aromatic C-$H_{7'}$], 7.27-7.29 [1H, d, *J* 7.4, aromatic C-H_4], 7.53-7.56 [1H, d, *J* 8.5, aromatic C-$H_{4'}$], 8.42 [1H, bs, N<u>H</u>COCF_3], 11.04 [1H, bs, N=C-N<u>H</u>CO]; δ_C (75 MHz, DMSO-d_6) 32.2 (CH_3, N-CH_3), 32.6 (CH_3, N-CH_3), 109.6 (CH, aromatic CH), 111.1 (CH, aromatic CH), 119.9 (CH, aromatic CH), 120.2 (CH, aromatic CH), 120.6 (CH, aromatic CH), 121.6 (CH, aromatic CH), 121.9 (C, CF_3), 122.0 (CH, aromatic CH), 122.2 (C, aromatic C), 123.2 (CH, aromatic CH), 123.8 (C, aromatic C), 125.1 (C, aromatic C), 126.8 (CH, aromatic CH), 127.0 (C, aromatic C), 127.1 (C, aromatic C), 129.0 (C, aromatic C), 132.4 (CH, aromatic CH), 136.2 (C, aromatic C), 140.2 (C, aromatic C), 154.2 (C, N=<u>C</u>-NHCOCF_3), 174.9 (C, NH-<u>C</u>O), 175.4 (C, <u>C</u>OCF_3); m/z (ES+) 466.2 $[M+H]^+$ (85%). (ES-) 464.3 $[M-H]^-$ (80%); HRMS - (ES+) requires: 466.1491. Found: 466.1473 ($C_{24}H_{19}N_5O_2F_3$).

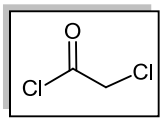
5.2.3.4.27 *N*-(4,5-Bis(1-methyl-1*H*-indol-3-yl)-6-oxo-1,6-dihydropyrimidin-2-yl) acetamide 527



5,6-Bisindolyl-2-aminopyrimidin-4-one **445** (0.080 g, 0.21 mmol) was suspended in dry pyridine (8 mL), to which was added acetic anhydride (0.05 mL, 0.32 mmol, 1.5 eq.), in a single portion. The reaction was then heated at 90°C for 20 hours. The resultant dark brown suspension was cooled and evaporated *in vacuo*. The crude acetamide **527** was subjected to flash chromatography with gradient elution from 100% DCM to 98:2 DCM/methanol, and fractions containing product **527** were combined and reduced under vacuum to a dark orange

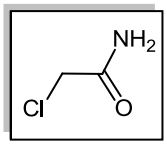
powder (0.030 g, 35%); m.p. 195-198°C (dec.); ν_{max}/ cm^{-1} (KBr) 3431, 3194, 2932, 1695, 1633, 1608, 1512, 1462; δ_H (300 MHz, DMSO-d_6) 2.26 [3H, s, $COC\underline{H}_3$], 3.43 [3H, s, N-CH_3], 3.84 [3H, s, N-CH_3], 6.74 [1H, s, aromatic C-H_2], 6.78-6.83 [1H, t, *J* 7.6, aromatic C-H_5], 6.93-6.96 [1H, d, *J* 7.8, aromatic C-H_7], 7.04-7.18 [3H, m, aromatic C-$H_{5',6,6'}$], 7.32-7.35 [1H, overlapping d, *J* 8.0, aromatic C-$H_{7'}$], 7.35 [1H, s, aromatic C-$H_{2'}$], 7.43-7.46 [1H, d, *J* 8.2, aromatic C-H_4], 8.36-8.38 [1H, d, *J* 8.0, aromatic C-$H_{4'}$], 11.49 [1H, bs, $N\underline{H}COCH_3$], 11.90 [1H, bs, N=C-$N\underline{H}CO$]; δ_C (75 MHz, DMSO-d_6) 24.0 (CH_3, $CO\underline{C}H_3$), 32.5 (CH_3, N-CH_3), 32.7 (CH_3, N-CH_3), 107.7 (C, aromatic C), 109.7 (2CH, 2 x aromatic CH), 112.1 (C, aromatic C), 118.6 (CH, aromatic CH), 119.6 (CH, aromatic CH), 120.0 (CH, aromatic CH), 120.9 (CH, aromatic CH), 121.6 (CH, aromatic CH), 123.1 (CH, aromatic CH), 126.3 (C, aromatic C), 126.8 (C, aromatic C), 130.1 (CH, aromatic CH), 132.6 (C, aromatic C), 132.8 (CH, aromatic CH), 136.2 (C, aromatic C), 136.6 (C, aromatic C), 147.9 (C, aromatic C), 160.8 (C, N=$\underline{C}$-NH), 173.6 (C, NH$\underline{C}OCH_3$), 173.7 (C, NH-$\underline{C}O$); m/z (ES+) 412.1 $[M+H]^+$ (65%). (ES-) 410.2 $[M-H]^-$ (100%); HRMS - (ES+) requires: 412.1774. Found: 412.1783 ($C_{24}H_{22}N_5O_2$).

5.2.3.4.28 Chloroacetyl chloride 520[30]



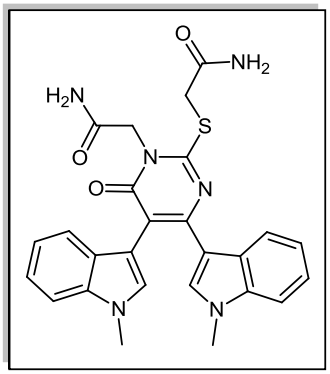
Chloroacetic acid (15.006 g, 160 mmol) was refluxed for 2 hours, in the presence of neat $SOCl_2$ (150 mL). This solution was cooled to room temperature and subsequently reduced to a final volume of approximately 30 mL, *in vacuo*; this oil was then employed as the title compound **520**, without any further purification; ν_{max}/ cm^{-1} (film) 1732 (COCl).

5.2.3.4.29 Chloroacetamide 523[31]



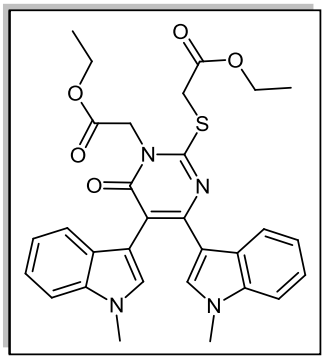
To a solution of chloroacetyl chloride **520** (0.8 mL, 10 mmol), in $CHCl_3$ (25 mL), was added aqueous ammonia (33% w/v) (0.7 mL, 12 mmol), along with Et_3N (2.8 mL, 20 mmol). The reaction was then stirred at room temperature for 16 hours, prior to addition of DCM (100 mL) and water (150 mL). The organic layer was then separated and dried over anhydrous magnesium sulfate, affording a light straw-coloured solution which was evaporated to dryness and the title chloroacetamide **523** (0.285 g, 30%) was used as a beige powder without further purification; m.p. 114-117°C (lit.[32] 114-116°C); ν_{max}/ cm^{-1} (KBr) 3384, 1742; m/z (ES-) 94.9, 92.9 $[M-H]^-$ (30%, 100%).

5.2.3.4.30 2-[(1-(2-Amino-2-oxoethyl)-4,5-bis(1-methyl-1*H*-indol-3-yl)-6-oxo-1,6-dihydropyrimidin-2-yl)thio]acetamide 522



To a solution of thiouracil **514** (0.050 g, 0.13 mmol) in 1,4-dioxane (7 mL), was added potassium carbonate (0.040 g, 0.29 mmol, 2.2 eq.) and TBAB (0.013 g, 0.039 mmol, 0.33 eq.). Upon addition of α-chloroacetamide **523** (0.036 g, 0.39 mmol, 3 eq.), the reaction was stirred at room temperature overnight and monitored by TLC analysis. On completion, the crude residue was filtered, washed with DCM (10 mL) and methanol (5 mL), and the combined organic extracts were evaporated *in vacuo*. The title 2-[(1-(2-amino-2-oxoethyl)-4,5-bis(1-methyl-1*H*-indol-3-yl)-6-oxo-1,6-dihydropyrimidin-2-yl)thio]acetamide **522** was purified by column chromatography, initially employing 100% DCM and finally collected over a small number of fractions applying 0.5% MeOH/ DCM as eluent. On solvent removal, the pure 2-thiopyrimidinone derivative **522** was isolated as a light brown amorphous powder (0.026 g, 40%); m.p. >300^{o}C; ν_{max}/ cm^{-1} (KBr) 3444, 2929, 1673, 1526, 1471, 1379; δ_H (300 MHz, DMSO-d_6) 3.47 [3H, s, N-CH_3], 3.84 [3H, s, N-CH_3], 3.91 [2H, s, S-C$\underline{H}_2$CONH$_2$], 4.69 [2H, s, N-C$\underline{H}_2$CONH$_2$], 6.78 [1H, s, aromatic C-H$_2$], 6.87-6.92 [1H, t, *J* 7.1, aromatic C-H$_5$], 7.05-7.10 [1H, t, *J* 7.1, aromatic C-H$_{5'}$], 7.12-7.26 [3H, m, aromatic C-H$_{6,6',7}$], 7.35-7.37 [1H, d, *J* 8.0, aromatic C-H$_{7'}$], 7.39 [1H, s, aromatic C-H$_{2'}$], 7.48-7.51 [1H, d, *J* 8.4, aromatic C-H$_4$], 8.13-8.16 [1H, d, *J* 7.8, aromatic C-H$_{4'}$]; δ_C (75 MHz, DMSO-d_6) 32.6 (CH$_3$, N-CH$_3$), 32.8 (CH$_3$, N-CH$_3$), 34.3 (CH$_2$, S-$\underline{C}$H$_2$CO$_2$NH$_2$), 64.3 (CH$_2$, N-$\underline{C}$H$_2$CO$_2$NH$_2$), 105.7 (C, aromatic C), 106.0 (C, aromatic C), 109.9 (2CH, 2 × aromatic CH), 111.7 (C, aromatic C), 119.1 (CH, aromatic CH), 119.5 (CH, aromatic CH), 120.5 (CH, aromatic CH), 121.2 (CH, aromatic CH), 121.8 (CH, aromatic CH), 122.2 (CH, aromatic CH), 126.4 (2C, 2 × aromatic C), 129.7 (CH, aromatic CH), 133.1 (CH, aromatic CH), 136.2 (C, aromatic C), 136.7 (C, aromatic C), 161.2 (C, aromatic C), 166.3 (C, aromatic C), 166.8 (C, C=O), 169.5 (C, $\underline{C}$ONH$_2$), 169.8 (C, $\underline{C}$ONH$_2$); m/z (ES+) 501.1 [M+H]$^+$ (60%); HRMS - (ES+) requires: 501.1709. Found: 501.1706 ($C_{26}H_{25}N_6O_3S$).

5.2.3.4.31 Ethyl 2-[(1-(2-ethoxy-2-oxoethyl)-4,5-bis(1-methyl-1*H*-indol-3-yl)-6-oxo-1,6-dihydropyrimidin-2-yl)thio]acetate 521



1,4-Dioxane (7 mL) was added to a flask containing thiouracil **514** (0.051 g, 0.13 mmol), and vigorously stirred at room temperature overnight, following addition of potassium carbonate (0.040 g, 0.29 mmol, 2.2 eq.), TBAB (0.013 g, 0.039 mmol, 0.33 eq.) and ethyl bromoacetate (0.04 mL, 0.39 mmol, 3 eq.). Following identical work-up as for **522**, the combined DCM/MeOH extracts were evaporated to dryness and the resultant residue was investigated by gradient chromatography from 100% DCM to 0.5% methanol/ DCM, in order to cleanly provide title compound **521** as a characteristic light brown powder (0.032 g, 45%); m.p. >300^{o}C; ν_{max}/ cm^{-1} (KBr) 2929, 1741, 1528, 1474, 1378; δ_H (300 MHz, DMSO-d_6) 1.15-1.20 [3H, t, *J* 7.1, O-$CH_2C\underline{H}_3$], 1.20-1.25 [3H, t, *J* 7.1, O-$CH_2C\underline{H}_3$], 3.47 [3H, s, N-CH_3], 3.84 [3H, s, N-CH_3], 4.08 [2H, s, *S*-$C\underline{H}_2CO_2Et$], 4.08-4.18 [4H, m, 2 × O-$C\underline{H}_2CH_3$], 4.87 [2H, s, N-$C\underline{H}_2CO_2Et$], 6.73 [1H, s, aromatic C-H_2], 6.89-6.65 [1H, td, *J* 7.9, 0.75 Hz, aromatic C-H_5], 7.06-7.11 [1H, td, *J* 8.0, 1.0, aromatic C-$H_{5'}$], 7.13-7.21 [3H, m, aromatic C-$H_{6,6',7}$], 7.32 [1H, s, aromatic C-$H_{2'}$], 7.36-7.39 [1H, d, *J* 8.1, aromatic C-$H_{7'}$], 7.49-7.52 [1H, d, *J* 8.2, aromatic C-H_4], 8.16-8.19 [1H, d, *J* 7.9, aromatic C-$H_{4'}$]; δ_C (75 MHz, DMSO-d_6) 13.9 (CH_3, $CO_2CH_2\underline{C}H_3$), 14.0 (CH_3, $CO_2CH_2\underline{C}H_3$), 32.6 (CH_3, N-CH_3), 32.8 (CH_3, N-CH_3), 32.8 (CH_2, S-$\underline{C}H_2CO_2Et$), 60.6 (CH_2, $CO_2\underline{C}H_2CH_3$), 61.1 (CH_2, $CO_2\underline{C}H_2CH_3$), 62.6 (CH_2, N-$\underline{C}H_2CO_2Et$), 105.6 (C, aromatic C), 105.8 (C, aromatic C), 109.9 (CH, aromatic CH), 110.0 (CH, aromatic CH), 111.4 (C, aromatic C), 119.2 (CH, aromatic CH), 119.3 (CH, aromatic CH), 120.5 (CH, aromatic CH), 121.3 (CH, aromatic CH), 121.9 (CH, aromatic CH), 122.2 (CH, aromatic CH), 126.5 (2C, 2 × aromatic C), 129.4 (CH, aromatic CH), 133.2 (CH, aromatic CH), 136.2 (C, aromatic C), 136.7 (C, aromatic C), 161.7 (C, aromatic C), 165.8 (C, N-$\underline{C}(SCO_2Et)$=N), 166.6 (C, N-$\underline{C}$=O), 168.2 (C, $\underline{C}O_2Et$), 169.1 (C, $\underline{C}O_2Et$); m/z (ES+) 559.2 $[M+H]^+$ (100%); HRMS - (ES+) requires: 559.2015. Found: 559.2015 ($C_{30}H_{31}N_4O_5S$).

5.2.3.4.32 Indolocarbazole aromatisation study

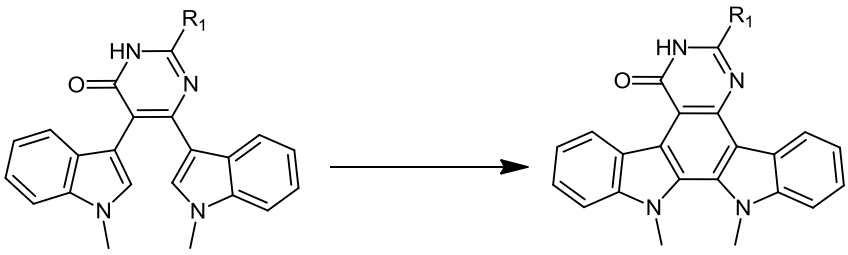
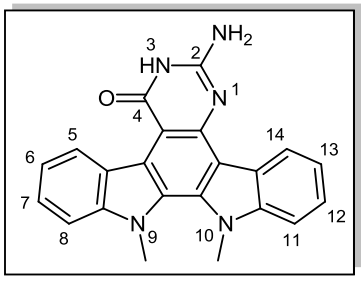


Table 5.4

Compound (R_1)	Oxidant	Solvent	Product No.
445 (NH_2)	$K_3[Fe(CN)_6]$/ KOH, air	H_2O	n.r
445 (NH_2)	500 mol% $Pd(OAc)_2$, N_2	DMF	n.r
445 (NH_2)	100 mol% $Pd(OAc)_2$, air	AcOH	n.r
445 (NH_2)	100 mol% $Pd(CO_2CF_3)_2$, N_2	DMF	n.r
507 (OH)	300 mol% $Pd(COCF_3)_2$, N_2	DMF	n.r
507 (OH)	hυ/ I_2, air	3:2 MeCN/ MeOH	n.r
445 (NH_2)	hυ/ I_2, air	3:2 MeCN/ MeOH	**442** (55%)
537 (H)	hυ/ I_2, air	3:2 MeCN/ MeOH	**538** (60%)

- Reaction 1: To a solution of **445** (0.100 g, 0.27 mmol) in 10% aqueous KOH (10 mL), was added $K_3[Fe(CN)_6]$ (5 eq.) and reflux was initiated for 24 hours. No product (**442**) was identified, and only starting material was present by TLC analysis (Table 5.2).
- Reactions 2-5: A suspension of **445** or **507** (0.100 g) in the appropriate solvent was stirred for 24 hours at reflux, along with the corresponding Pd(II) complex, either in the presence or absence of air. Upon cooling, the reaction mixture was filtered through a pad of celite and washed with methanol (3 × 10 mL). Evaporation to dryness prior to MS investigation of the resulting residue yielded a complex mixture of decomposition products and starting material (Table 5.2).

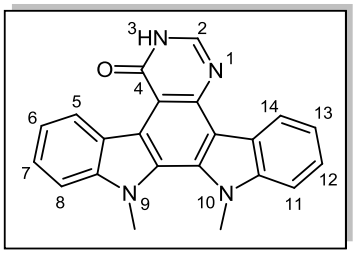
5.2.3.4.33 2-Amino-9,10-dimethylindolo[2,3-*a*]pyrimido[5,4-*c*]carbazol-4(3*H*)-one 442



Bisindolyl 2-aminopyrimidin-4-one **445** (0.070 g, 0.19 mmol) was allowed to stir in a mixture of acetonitrile (100 mL) and methanol (50 mL), in the presence of a catalytic amount of iodine. The reaction was efficiently irradiated, employing a medium pressure mercury lamp, in the presence of air, for 16 hours. The dark brown suspension was then evaporated under reduced pressure. The final product residue was then purified by redissolving in ethyl acetate

(60 mL), washing with 10% sodium thiosulfate solution (3 × 50 mL), water (3 × 100 mL) and brine (100 mL), drying with magnesium sulfate and evaporation of the crude product mixture. Flash chromatography employing a mixture of ethyl acetate and methanol yielded the desired novel indolocarbazole **442** as a dark brown amorphous solid (0.052 g, 55%); m.p. 202-204°C; ν_{max}/ cm^{-1} (KBr) 3331, 2922, 1639, 1440, 1321; δ_H (300 MHz, DMSO-d_6) 4.15 [3H, s, N-CH_3], 4.23 [3H, s, N-CH_3], 6.41 [2H, bs, NH_2], 7.19-7.24 [1H, t, *J* 7.0, aromatic C-H_6], 7.31-7.36 [1H, t, *J* 7.0, aromatic C-H_{13}], 7.45-7.52 [2H, m, aromatic C-$H_{7,12}$], 7.64-7.67 [1H, d, *J* 8.8, aromatic C-H_8], 7.71-7.74 [1H, d, *J* 8.8, aromatic C-H_{11}], 9.06-9.09 [1H, d, *J* 10.5, aromatic C-H_5], 9.68-9.70 [1H, d, *J* 7.0, aromatic C-H_{14}], 10.93 [1H, bs, NH]; δ_C (75 MHz, DMSO-d_6) 36.1 (CH_3, N-$\underline{C}H_3$), 36.8 (CH_3, N-$\underline{C}H_3$), 105.0 (C, aromatic C), 110.3 (CH, aromatic CH), 110.4 (CH, aromatic CH), 115.2 (C, aromatic C), 119.0 (CH, aromatic CH), 119.3 (C, aromatic C), 120.3 (CH, aromatic CH), 123.6 (CH, aromatic CH), 124.2 (C, aromatic C), 124.6 (CH, aromatic CH), 124.7 (C, aromatic C), 125.0 (CH, aromatic CH), 126.2 (C, aromatic C), 127.2 (CH, aromatic CH), 133.1 (C, aromatic C), 142.7 (C, aromatic C), 144.1 (C, aromatic C), 147.1 (C, aromatic C), 151.5 (C, N=$\underline{C}$-NH_2), 162.0 (C, NH-$\underline{C}$=O); m/z (ES+) 368.1 $[M+H]^+$ (40%); HRMS - (ES+) requires: 368.1515. Found: 368.1511 ($C_{22}H_{18}N_5O$).

5.2.3.4.34 9,10-Dimethylindolo[2,3-*a*]pyrimido[5,4-*c*]carbazol-4(3*H*)-one 538

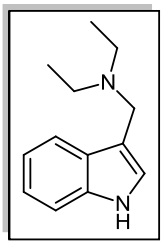


5,6-Bis(1-methyl-1*H*-indol-3-yl)pyrimidin-4(3*H*)-one **537** (0.050 g, 0.14 mmol) was added to a solution of acetonitrile and methanol (3:2) (150 mL), along with a catalytic amount of iodine. The dilute reaction mixture was irradiated with U.V. light, under open-vessel conditions, until TLC analysis displayed the absence of any starting material (16 hours). Following solvent evaporation, the crude fluorescent pyrimidin-4(3*H*)-one ring-fused indolocarbazole **538** was purified by standard chromatography employing DCM, containing a few drops of methanol, resulting in elution of the pure aromatised product in a small number of fractions - isolated as a dark brown amorphous solid (0.030 g, 60%); m.p. 229-231°C; ν_{max}/ cm^{-1} (KBr) 3428, 2924, 1636, 1566, 1464, 1322; δ_H (300 MHz, DMSO-d_6) 4.24 [3H, s, N-CH_3], 4.28 [3H, s, N-CH_3], 7.28-7.33 [1H, t, *J* 7.2, C-H_6], 7.38-7.43 [1H, t, *J* 7.3, C-H_{13}], 7.52-7.57 [1H, t, *J* 7.1, C-H_7], 7.55-7.60 [1H, t, *J* 7.1, C-H_{12}], 7.71-7.74 [1H, d, *J* 8.2, C-H_8], 7.76-7.79 [1H, d, *J* 8.2, C-H_{11}], 8.32-8.33 [1H, d, *J* 3.6, N=C$\underline{H}$-NHCO], 8.98-9.01 [1H, d, *J* 7.8, C-H_5], 9.72-9.75 [1H, d, *J* 8.3, C-H_{14}], 12.33 [1H, bs, NH]; δ_C (75 MHz, DMSO-d_6) 36.4 (CH_3, N-$\underline{C}H_3$), 36.8 (CH_3, N-$\underline{C}H_3$), 110.5 (CH, aromatic CH), 110.8 (CH, aromatic CH), 111.5 (C, aromatic C), 116.7 (C,

aromatic C), 118.4 (C, aromatic C), 119.5 (CH, aromatic CH), 120.9 (CH, aromatic CH), 123.5 (CH, aromatic CH), 124.1 (2C, 2 × aromatic C), 125.4 (CH, aromatic CH), 125.5 (CH, aromatic CH), 127.3 (CH, aromatic CH), 128.6 (C, aromatic C), 132.6 (C, aromatic C), 143.0 (C, aromatic C), 143.7 (C, aromatic C), 143.9 (C, aromatic C), 144.0 (C, N=C-H), 160.7 (C, NH-C=O); m/z (ES+) 353.1 $[M+H]^+$ (100%); HRMS - (ES+) requires: 353.1402. Found: 353.1396 ($C_{22}H_{17}N_4O$).

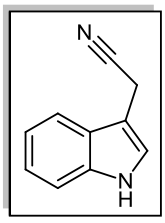
5.2.4 Synthesis of a 3,4-bisindolyl-5-aminopyrazole compound series

5.2.4.1 3-Diethylaminomethyl-1*H*-indole (Gramine) 542[33]



To a 250 mL 2-neck round-bottomed flask was charged 37% formaldehyde solution (7 mL, 86 mmol), 98% diethylamine (8.9 mL, 86 mmol), along with indole **171** (10.012 g, 86 mmol), absolute ethanol (120 mL), and zinc chloride (17.462 g, 128 mmol). The resultant straw coloured slurry was then stirred at room temperature for 2 hours. The reaction mixture was then poured into a mixture of ethyl acetate (150 mL) and water (150 mL). Following addition of aqueous 20% NaOH solution to reach pH 9, extraction was performed with 3 × 150 mL volumes of ethyl acetate; the resultant organic layers were evaporated under reduced pressure, diluted with water (120 mL), and acidified with conc. HCl to pH 3. The slurry thus formed was then filtered under vacuum and the pH of the mother liquor was readjusted to pH 9, by addition of aqueous 20% NaOH solution. The turbid mixture was then cooled to 0^oC, and the resultant light orange precipitate **542** was filtered and washed with water, prior to drying (10.612 g, 62%); m.p. 105-107^oC (lit.[34] 109-110^oC); ν_{max}/ cm^{-1} (KBr) 3051, 2971, 1619, 1543, 1500, 1452; δ_H (300 MHz, $CDCl_3$) 1.06-1.11 [6H, t, *J* 7.1, 2 × $NCH_2C\underline{H}_3$], 2.54-2.61 [4H, q, *J* 7.1, 2 × $NC\underline{H}_2CH_3$], 3.79 [2H, s, CH_2], 7.05-7.06 [1H, d, *J* 2.3, C-H_2], 7.07-7.13 [1H, td, *J* 7.5, 1.3, C-H_5], 7.14-7.19 [1H, td, *J* 7.8, 1.4, C-H_6], 7.29-7.32 [1H, d, *J* 8.0, C-H_7], 7.72-7.74 [1H, d, *J* 7.8, C-H_4], 8.32 [1H, bs, NH]; δ_C (75 MHz, $CDCl_3$) 12.0 ($2CH_3$, 2 × $NCH_2\underline{C}H_3$), 46.7 ($2CH_2$, 2 × $N\underline{C}H_2CH_3$), 48.0 (CH_2, $\underline{C}H_2N(C_2H_5)_2$), 111.0 (CH, aromatic CH), 113.6 (C, aromatic C), 119.3 (CH, aromatic CH), 119.5 (CH, aromatic CH), 121.8 (CH, aromatic CH), 123.5 (CH, aromatic CH), 128.1 (C, aromatic C), 136.3 (C, aromatic C); m/z (ES+) 203.1 $[M+H]^+$ (100%).

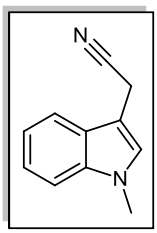
5.2.4.2 1*H*-Indol-3-yl acetonitrile 229[35]



To a solution of *N*,*N*-diethyl-3-aminomethyl indole **542** (0.370 g, 1.83 mmol), in methanol (10 mL) was added a solution of potassium cyanide (0.245 g, 3.77 mmol) in water (2 mL). Iodomethane (0.3 mL, 4.79 mmol) was added dropwise and the reaction mixture was then stirred vigorously at room temperature for 16 hours. Following evaporation of the solvent, the crude residue was dissolved in ethyl acetate (100 mL) and successively washed with saturated aqueous sodium bicarbonate solution (100 mL), water (3 × 100 mL) and brine (2 × 100 mL). Following chromatography employing ethyl acetate/hexane, the title compound **229** was dried, and isolated as a beige amorphous solid (0.191 g, 67%); m.p. 32-34°C (lit.[36] 34-36°C); ν_{max}/ cm^{-1} (KBr) 3412, 2252, 1621, 1458, 1420; δ_H (300 MHz, $CDCl_3$) 3.82 [2H, s, CH_2], 7.15-7.21 [2H, m, C-$H_{2,5}$], 7.22-7.28 [1H, td, *J* 7.1, 1.1, C-H_6], 7.37-7.40 [1H, d, *J* 8.0, C-H_7], 7.57-7.60 [1H, d, *J* 7.8, C-H_4], 8.19 [1H, bs, NH]; δ_C (75 MHz, $CDCl_3$) 14.4 (CH_2, $\underline{C}H_2CN$), 104.7 (C, aromatic C), 111.6 (CH, aromatic CH), 118.1 (CH, aromatic CH), 118.2 (C, aromatic C), 120.3 (CH, aromatic CH), 122.8 (CH, aromatic CH), 122.9 (CH, aromatic CH), 126.0 (C, $CH_2\underline{C}N$), 136.3 (C, aromatic C); m/z (ES+) 130.0 $[M+H-HCN]^+$ (100%).

5.2.4.3 1-Methyl-1*H*-indol-3-yl acetonitrile 454[6]

Method A:



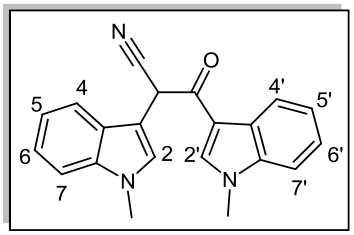
To a suspension of NaH (60% dispersion in mineral oil) (3.331 g, 83.3 mmol) in anhydrous DMF (25 mL), was added dropwise a solution of 3-indolylacetonitrile **229** (10.022 g, 64 mmol) in DMF (50 mL). After stirring for 30 minutes, at room temperature, the flask was then cooled to 0°C. Iodomethane (6 mL, 95.8 mmol) was added dropwise in solution with DMF (30 mL). The reaction was then allowed to warm, and was stirred at ambient temperature for 3 hours. The reaction was then quenched by pouring it into a mixture of ethyl acetate (300 mL) and 5% aq. HCl (400 mL). Following extraction of the dark brown ethyl acetate layer, it was washed with water (2 × 250 mL) and brine (1 × 300 mL), dried over magnesium sulfate and filtered. The resultant solution was then evaporated thoroughly, under reduced pressure, to afford the *N*-methyl acetonitrile **454** in quantitative yield (11.087 g, 100%) as a viscous brown oil which gradually solidified following cooling; m.p. 54-56°C (lit.[37] 59-60°C); ν_{max}/ cm^{-1} (KBr) 2954, 2247, 1657, 1553, 1464; δ_H (300 MHz, $CDCl_3$) 3.73 [3H, s, NCH_3], 3.78 [2H, s, CH_2], 7.04 [1H, s, C-H_2], 7.14-7.19 [1H, td, *J* 8.0, 1.5, C-H_5], 7.23-7.38 [2H, m, C-$H_{6,7}$], 7.54-7.57 [1H, d, *J* 7.9, C-H_4]; δ_C (75 MHz, $CDCl_3$) 14.3 (CH_2, $\underline{C}H_2CN$), 32.9 (CH_3, NCH_3), 103.0 (C, aromatic C), 109.6 (CH, aromatic CH), 118.2 (CH, aromatic CH), 119.7

(CH, aromatic CH), 122.4 (CH, aromatic CH), 126.2 (C, $CH_2\underline{C}N$), 126.5 (C, aromatic C), 127.3 (CH, aromatic CH), 137.1 (C, aromatic C); m/z (ES+) 171.1 $[M+H]^+$ (100%).

Method B:

To a suspension of powdered KOH (0.538 g, 9.6 mmol, 1.5 eq.) in anhydrous DMF (10 mL), was added dropwise a solution of 3-indolylacetonitrile **229** (1.005 g, 6.4 mmol) in DMF (5 mL). After stirring for 30 minutes, at 0°C, iodomethane (0.44 mL, 7.04 mmol, 1.1 eq.) in DMF (3 mL) was added dropwise. The reaction was then allowed to warm, and was stirred at ambient temperature for 1.5 hours. The reaction was then quenched by pouring it into a mixture of ethyl acetate (70 mL) and 10% HCl (70 mL). Following extraction of the dark brown ethyl acetate layer, it was washed with water (2 × 150 mL) and brine (1 × 100 mL), dried over magnesium sulfate and filtered. The resultant solution was then evaporated thoroughly, to yield the pure *N*-methyl acetonitrile **454** in quantitative yield (1.075 g, 99%).

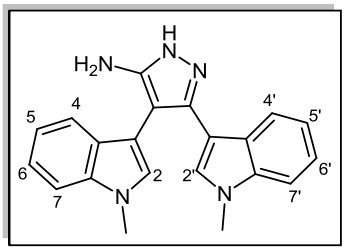
5.2.4.4 2,3-Bis(1-Methyl-1*H*-indol-3-yl)-3-oxopropanenitrile 541



To a flask containing dry THF (40 mL), was added LDA solution (2 M) (19.4 mL, 38.7 mmol, 2.2 eq.) at −78°C, under nitrogen atmosphere. 1-Methyl indole-3-acetonitrile **454** (3.002 g, 17.6 mmol) in THF (4 mL) was then added slowly to the stirring reaction mixture and maintained at −78°C for 1.5 hours. *N*-Methyl indole-3-carbonyl chloride **479** was dissolved in THF (15 mL), and added dropwise to the cooled reaction mixture. The reaction was then allowed to warm to room temperature and stirred for a further 16 hours. Following solvent evaporation, the crude β-ketonitrile **541** was taken up in ethyl acetate (100 mL) and washed with saturated ammonium chloride solution (2 × 150 mL). These were then combined and further extracted with ethyl acetate (2 × 75 mL); the combined ethyl acetate layers were then washed with water (3 × 150 mL) and brine (2 × 150 mL), dried with magnesium sulfate and evaporated to a light brown residue. Following chromatography, employing a 10-25% ethyl acetate/ hexane gradient, intermediate **541** was isolated as a brown crystalline solid (4.424 g, 76%); m.p. 104-107°C; ν_{max}/ cm^{-1} (KBr) 2925, 2202, 1717, 1645, 1531, 1463; δ_H (300 MHz, $CDCl_3$) 3.66 [3H, s, N-CH_3], 3.68 [3H, s, N-CH_3], 5.46 [1H, s, COC$\underline{H}$CN], 7.08-7.14 [2H, m, aromatic C-$H_{5,5'}$], 7.18 [1H, s aromatic C-H_2], 7.21-7.26 [4H, m, aromatic C-$H_{6,6',7,7'}$], 7.63-7.66 [1H, d, *J* 7.9, aromatic C-H_4], 7.75 [1H, s, aromatic C-$H_{2'}$], 8.29-8.32 [1H, m, aromatic C-$H_{4'}$]; δ_C (75 MHz, $CDCl_3$) 32.0 (CH_3, N-$\underline{C}H_3$), 32.8 (CH_3, *N*-$\underline{C}H_3$), 38.7 ($\underline{C}$H), 104.2 (C, aromatic C), 108.8 (2CH, 2 × aromatic CH), 111.9 (C, aromatic C), 116.8 (C, aromatic), 117.6 (CH,

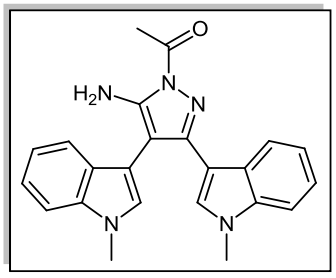
aromatic CH), 119.2 (CH, aromatic CH), 121.5 (CH, aromatic CH), 121.6 (CH, aromatic CH), 122.3 (CH, aromatic CH), 123.0 (CH, aromatic CH), 124.8 (C, aromatic C), 125.8 (C≡N), 127.0 (CH, aromatic CH), 135.1 (CH, aromatic CH), 136.1 (C, aromatic C), 136.3 (C, aromatic C), 182.1 (C, C=O); m/z (ES+) 328.1 $[M+H]^+$ (100%); HRMS - (ES+) requires: 328.1450. Found: 328.1452 ($C_{21}H_{18}N_3O$).

5.2.4.5 3,4-Bis(1-methyl-1*H*-indol-3-yl)-1*H*-pyrazol-5-amine 447



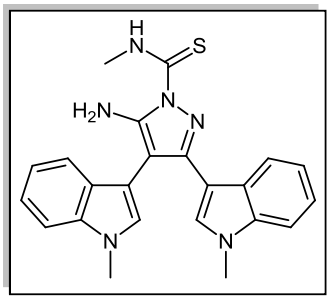
Hydrazine hydrate (0.4 mL, 6 mmol, 4 eq.) was added to a stirred mixture of β-ketonitrile **541** (0.511 g, 1.5 mmol), along with distilled ethanol (15 mL), and heated to 80°C. A catalytic amount of glacial acetic acid was then added to the reaction, followed by stirring at reflux temperature for 20 hours. Following solvent removal, the residue was taken up in ethyl acetate (70 mL) and washed with saturated sodium bicarbonate solution (2 × 100 mL). These aqueous bicarbonate layers were added together and subsequently extracted with ethyl acetate (2 × 50 mL); the combined ethyl acetate layers were then washed with water (3 × 100 mL) and brine (2 × 100 mL), dried with magnesium sulfate, filtered and evaporated to form a crude golden brown solid. Following purification by gradient flash chromatography from 30% ethyl acetate/hexane to 95% ethyl acetate/5% methanol, the novel fluorescent aminopyrazole **447** was isolated as golden brown crystals (0.235 g, 45%); m.p. 255-258°C; ν_{max}/ cm^{-1} (KBr) 3418, 3198, 2928, 1607, 1480, 1378; δ_H (300 MHz, $CDCl_3$) 3.57 [3H, s, N-CH_3], 3.75 [3H, s, N-CH_3], 5.05 [2H, bs, NH_2], 6.91 [1H, s, aromatic C-H_2], 6.99 [1H, s, aromatic C-$H_{2'}$], 7.02-7.04 [1H, d, *J* 7.9, aromatic C-H_7], 7.09-7.12 [1H, t, *J* 8.0, aromatic C-H_5], 7.18-7.27 [3H, m, aromatic C-$H_{5',6,6'}$], 7.32-7.35 [1H, d, *J* 8.2, aromatic C-$H_{7'}$], 7.40-7.43 [1H, d, *J* 7.9, aromatic C-H_4], 7.69-7.71 [1H, d, *J* 7.9, aromatic C-$H_{4'}$]; δ_C (75 MHz, $CDCl_3$) 32.8 ($2CH_3$, 2 × N-$\underline{C}H_3$), 97.7 (C, aromatic C), 105.2 (C, aromatic C), 106.2 (C, aromatic C), 109.2 (CH, aromatic CH), 109.5 (CH, aromatic CH), 119.2 (CH, aromatic CH), 120.0 (CH, aromatic CH), 120.2 (CH, aromatic CH), 120.6 (CH, aromatic CH), 121.7 (CH, aromatic CH), 122.1 (CH, aromatic CH), 122.7 (C, aromatic C), 125.9 (C, aromatic C), 127.7 (C, aromatic C), 128.1 (CH, aromatic CH), 128.2 (CH, aromatic CH), 136.7 (C, aromatic C), 137.1 (C, aromatic C), 137.6 (C, aromatic C); m/z (ES+) 342.1 $[M+H]^+$ (100%); HRMS - (ES+) requires: 342.1719. Found: 342.1715 ($C_{21}H_{20}N_5$).

5.2.4.6 1-(5-Amino-3,4-bis(1-methyl-1*H*-indol-3-yl)-1*H*-pyrazol-1-yl)ethanone 543



To a solution of aminopyrazole **447** (0.150 g, 0.44 mmol) in acetonitrile (10 mL), was added acetic anhydride (0.06 mL, 0.53 mmol, 1.2 eq.) and the reaction mixture was heated to 80^{o}C, with stirring, for 16 hours, at which point full consumption of the starting material **447** was observed by TLC. Following solvent removal, the crude acetylated product **543** was dissolved in ethyl acetate (30 mL), washed with 10% aqueous sodium bicarbonate solution (50 mL), followed by water (3 × 50 mL) and brine (50 mL). The organic layer was then dried with magnesium sulfate, prior to filtration and evaporation of the filtrate to a crude residue. Chromatography with 15% ethyl acetate/ hexane, followed by concentration of the product fractions, generated the pyrazolic acetamide derivative **543** as off-white plate-like crystals (0.096 g, 57%); m.p. 141-144^{o}C; ν_{max}/ cm^{-1} (KBr) 3468, 3360, 2931, 1702, 1567, 1460; δ_H (300 MHz, $CDCl_3$) 2.85 [3H, s, COC<u>H</u>$_3$], 3.52 [3H, s, N-CH_3], 3.86 [3H, s, N-CH_3], 5.40 [2H, bs, NH_2], 6.85 [1H, s, aromatic C-H_2], 7.06-7.11 [1H, t, *J* 7.7, aromatic C-H_5], 7.07 [1H, s, aromatic C-$H_{2'}$], 7.16-7.24 [1H, m, aromatic C-$H_{5'}$], 7.26-7.33 [3H, m, aromatic C-$H_{6,6',7}$], 7.40-7.43 [1H, d, *J* 8.3, aromatic C-$H_{7'}$], 7.42-7.45 [1H, d, *J* 8.0, aromatic C-H_4], 8.42-8.45 [1H, m, aromatic C-$H_{4'}$]; δ_C (75 MHz, $CDCl_3$) 23.4 [CH_3, CO<u>C</u>H_3], 32.9 [CH_3, *N*-CH_3], 33.0 [CH_3, *N*-CH_3], 94.0 [C, aromatic C], 105.2 [C, aromatic C], 107.5 [C, aromatic C], 109.0 [CH, aromatic CH], 109.5 [CH, aromatic CH], 119.6 [CH, aromatic CH], 120.5 [2CH, 2 × aromatic CH], 122.1 [CH, aromatic CH], 122.2 [CH, aromatic CH], 122.6 [CH, aromatic CH], 126.5 [C, aromatic C], 127.7 [C, aromatic C], 128.6 [CH, aromatic CH], 129.9 [CH, aromatic CH], 136.8 [C, aromatic C], 137.3 [C, aromatic C], 147.9 [C, aromatic C], 150.5 [C, aromatic C], 173.6 [C, C=O]; m/z (ES+) 384.1 $[M+H]^+$ (100%); HRMS - (ES+) requires: 384.1824. Found: 384.1807 ($C_{23}H_{22}N_5O$).

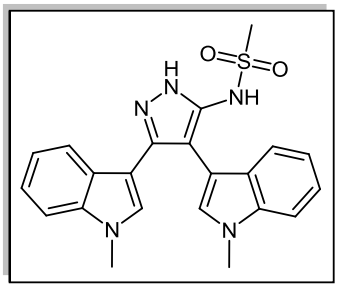
5.2.4.7 5-Amino-*N*-methyl-3,4-bis(1-methyl-1*H*-indol-3-yl)-1*H*-pyrazole-1-carbothioamide 544



Methyl isothiocyanate (0.012 g, 0.15 mmol) was applied to a stirred solution of aminopyrazole **447** (0.050 g, 0.29 mmol) in acetonitrile (7 mL). The reaction was then heated to reflux temperature, and the dark orange suspension was stirred for 16 hours. The reaction was initially allowed to cool to room temperature, and subsequently, to 0^{o}C, and maintained for 30

minutes at this temperature. The formed slurry was then filtered to afford the pure thiourea derivative **544** as light orange crystals (0.023 g, 30%); m.p. 163-166°C; ν_{max}/ cm^{-1} (KBr) 3396, 3329, 3277, 2925, 1607, 1567, 1519; δ_H (300 MHz, $CDCl_3$) 3.34-3.35 [3H, d, *J* 5.0, NH-C<u>H</u>$_3$], 3.53 [3H, s, N-CH_3], 3.86 [3H, s, N-CH_3], 6.30 [2H, bs, NH_2], 6.86 [1H, s, aromatic C-H_2], 7.07 [1H, s, aromatic C-$H_{2'}$], 7.08-7.11 [1H, d, *J* 7.7, aromatic C-H_7], 7.19-7.31 [4H, m, aromatic C-$H_{5,5',6,6'}$], 7.40-7.43 [1H, d, *J* 7.7, aromatic C-$H_{7'}$], 7.42-7.44 [1H, d, *J* 7.7, aromatic C-H_4], 8.26-8.28 [1H, d, *J* 6.9, aromatic C-$H_{4'}$], 9.36 [1H, bs, N<u>H</u>-CH_3]; δ_C (75 MHz, $CDCl_3$) 30.9 (CH_3, NH-<u>C</u>H_3), 32.9 (CH_3, N-<u>C</u>H_3), 33.0 (CH_3, N-<u>C</u>H_3), 94.4 (C, aromatic C), 105.4 (C, aromatic C), 107.0 (C, aromatic C), 109.2 (CH, aromatic CH), 109.4 (CH, aromatic CH), 119.6 (CH, aromatic CH), 120.4 (CH, aromatic CH), 120.5 (CH, aromatic CH), 122.1 (CH, aromatic CH), 122.2 (2CH, 2 × aromatic CH), 126.3 (C, aromatic C), 127.7 (C, aromatic C), 128.8 (CH, aromatic CH), 130.4 (CH, aromatic CH), 136.8 (C, aromatic C), 137.3 (C, aromatic C), 147.8 (C, aromatic C), 149.0 (C, aromatic C), 176.8 (C, C=S); m/z (ES+) 415.1 $[M+H]^+$ (100%); HRMS - (ES+) requires: 415.1705. Found: 415.1696 ($C_{23}H_{23}N_6S$).

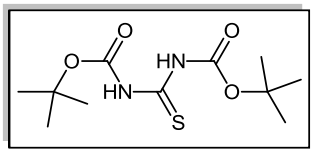
5.2.4.8 *N*-(3,4-Bis(1-methyl-1*H*-indol-3-yl)-1*H*-pyrazol-5-yl)methanesulfonamide 545



To a solution of the aminopyrazole **447** (0.108 g, 0.29 mmol) in pyridine (7 mL), was added methanesulfonyl chloride (0.02 mL, 0.29 mmol), along with triethylamine (0.04 mL, 0.29 mmol). The reaction was refluxed overnight and then evaporated *in vacuo*. The residue was dissolved in ethyl acetate (80 mL), then washed with 10% HCl (5 × 70 mL), aqueous saturated sodium bicarbonate solution (100 mL), water (3 × 100 mL) and brine (100 mL), dried over magnesium sulfate and evaporated. Chromatography employing 25% ethyl acetate/ hexane yielded sulfonamide **545** as a dark brown solid (0.042 g, 35%); m.p. 93-96°C; ν_{max}/ cm^{-1} (KBr) 3389, 2926, 1718, 1615, 1465, 1378, 1319, 1152; δ_H (300 MHz, $CDCl_3$) 3.27 [3H, s, SO_2CH_3], 3.60 [3H, s, N-CH_3], 3.81 [3H, s, N-CH_3], 6.91 [1H, s, aromatic C-H_2], 6.99-7.03 [1H, t, *J* 7.7, aromatic C-H_5], 7.13 [1H, s, aromatic C-$H_{2'}$], 7.15-7.18 [1H, d, *J* 8.0, aromatic C-H_7], 7.20-7.23 [1H, d, *J* 7.8, aromatic C-$H_{7'}$], 7.26-7.31 [3H, m, aromatic C-$H_{5',6}$ & N<u>H</u>SO_2], 7.31-7.37 [2H, m, aromatic C-$H_{4,6'}$], 7.67-7.70 [1H, d, *J* 7.9, aromatic C-$H_{4'}$]; δ_C (75 MHz, $CDCl_3$) 30.9 (CH_3, N-<u>C</u>H_3), 33.0 (CH_3, N-<u>C</u>H_3), 41.4 (CH_3, SO_2<u>C</u>H_3), 91.2 (C, aromatic C), 103.9 (C, aromatic C), 109.5 (CH, aromatic CH), 109.8 (CH, aromatic CH), 119.5 (CH, aromatic CH), 119.7 (CH, aromatic CH), 120.0 (CH, aromatic CH), 120.6 (CH, aromatic CH), 122.0 (CH, aromatic CH), 122.4 (CH, aromatic CH), 125.0 (C, aromatic C),

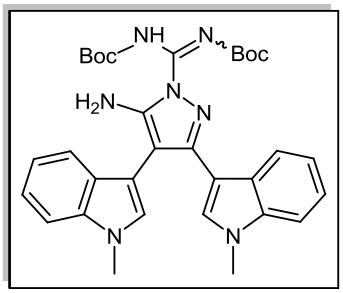
125.6 (C, aromatic C), 127.4 (2C, 2 × aromatic C), 128.5 (CH, aromatic CH), 128.8 (CH, aromatic CH), 133.9 (C, aromatic C), 136.7 (C, aromatic C), 137.1 (C, aromatic C); m/z (ES+) 420.1 $[M+H]^+$ (100%); HRMS - (ES+) requires: 420.1494. Found: 420.1488 ($C_{22}H_{22}N_5O_2S$).

5.2.4.9 *(N,N'*-Di-*tert*-butoxycarbonyl)-thiourea 546[38]



To a stirred solution of NaH (1.352 g, 33.8 mmol) (60% suspension in mineral oil) in dry THF (150 mL), under inert conditions at 0°C, was added thiourea (0.570 g, 7.5 mmol) portionwise over 5 minutes, and left to stir at room temperature for 15 minutes. Following cooling to 0°C, di-*tert*-butyl carbonate (3.604 g, 16.5 mmol) was added, and stirring was continued for 40 minutes, prior to warming to room temperature over 3 hours. The reaction was subsequently quenched *via* addition of saturated aqueous $NaHCO_3$ solution (10 mL), water (200 mL) and the product was extracted with ethyl acetate (3 × 75 mL). On drying with magnesium sulfate, the filtrate was evaporated to dryness to afford **546** as an off-white solid, used successfully without further purification (1.913 g, 93%); m.p. 115-117°C (lit.[38] 127-129°C); ν_{max}/ cm^{-1} (KBr) 3365, 3173, 2925, 1771, 1724, 1609, 1542; δ_H (300 MHz, $CDCl_3$) 1.48 [9H, s, $(CH_3)_3$], 1.53 [9H, s, $(CH_3)_3$], 8.26 [1H, s, NH], 9.23 [1H, s, NH]; δ_C (75 MHz, $CDCl_3$) 28.0 ($6CH_3$, 6 × CH_3), 84.1 (2C, 2 × $\underline{C}(CH_3)_3$), 151.3 (C, C=S), 177.9 (C, C=O), 182.1 (C, C=O); m/z (ES+) 157.0 $[M+H]^+$ (50%). (ES-) 155.0 $[M-H]^-$ (45%).

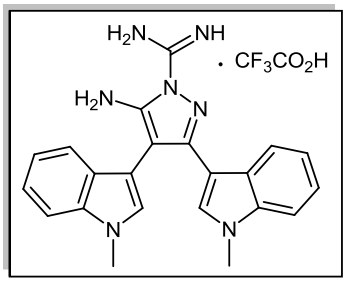
5.2.4.10 *Tert*-butyl [5-amino-3,4-bis(1-methyl-1*H*-indol-3-yl)-1*H*-pyrazol-1-yl][({*tert*-butoxycarbonyl}imino)methyl]carbamate 547



Aminopyrazole **447** (0.150 g, 0.44 mmol) was treated with $HgCl_2$ (0.143 g, 0.48 mmol, 1.1 eq.) and *N,N'*-di-*tert*-butoxycarbonyl thiourea **546** (0.110 g, 0.44 mmol), in distilled DCM (10 mL), at 0°C. Triethylamine (0.2 mL, 1.36 mmol, 3.1 eq.) was then added to the flask and allowed to stir at 0°C for a further 1 hour, followed by stirring for 12 hours at room temperature. The reaction was then poured into ethyl acetate (30 mL), and filtered through a pad of celite® in order to remove the yellow mercury sulfide by-product. The filter cake was washed with ethyl acetate (3 × 15 mL), and the combined organic phases were then washed with water (3 × 100 mL) and brine (100 mL), dried over magnesium sulfate and concentrated under vacuum. Chromatography employing 15% ethyl acetate/hexane yielded

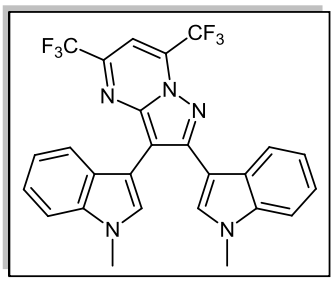
the pure di-protected pyrazole derivative **547** as an off-white crystalline solid (0.095 g, 37%); m.p. 140-142°C; ν_{max}/ cm^{-1} (KBr) 3452, 3337, 2978, 1768, 1707, 1657, 1567, 1494; δ_H (300 MHz, $CDCl_3$) 1.56 [18H, s, 2 × $CO_2C(C\underline{H}_3)_3$], 3.55 [3H, s, N-$CH_3$], 3.84 [3H, s, N-$CH_3$], 5.65 [2H, bs, pyrazole NH_2], 6.87 [1H, s, aromatic C-H_2], 7.04 [1H, s, aromatic C-$H_{2'}$], 7.06-7.12 [1H, t, *J* 7.8, aromatic C-H_5], 7.19-7.28 [3H, m, aromatic C-$H_{5',6,7}$], 7.26-7.31 [1H, t, *J* 7.9, aromatic C-$H_{6'}$], 7.39-7.43 [2H, m, aromatic C-$H_{4,7'}$], 8.20-8.22 [1H, d, *J* 7.4, aromatic C-$H_{4'}$], 9.40 [1H, s, N$\underline{H}$-$CO_2C(CH_3)_3$]; δ_C (75 MHz, $CDCl_3$) 28.1 [3CH_3, {$CO_2C(\underline{C}H_3)_3$}], 28.2 [3$CH_3$, {$CO_2C(\underline{C}H_3)_3$}], 32.9 [$CH_3$, N-$CH_3$], 33.0 [$CH_3$, N-$CH_3$], 80.8 [C, {$CO_2\underline{C}(CH_3)_3$}], 82.8 [C, {$CO_2\underline{C}(CH_3)_3$}], 94.7 [C, aromatic C], 105.1 [C, aromatic C], 107.2 [C, aromatic C], 109.2 [CH, aromatic CH], 109.4 [CH, aromatic CH], 119.6 [CH, aromatic CH], 120.4 [2CH, 2 × aromatic CH], 122.1 [2CH, 2 × aromatic CH], 122.2 [CH, aromatic CH], 126.3 [C, aromatic C], 127.6 [C, aromatic C], 128.7 [CH, aromatic CH], 129.9 [CH, aromatic CH], 136.8 [C, aromatic C], 137.2 [C, aromatic C], 143.5 [C, aromatic C], 147.7 [C, aromatic C], 149.1 [C, C=O], 149.8 [C, C=O], 157.6 [C, C=N]; m/z (ES+) 584.3 $[M+H]^+$ (100%). (ES-) 582.5 $[M-H]^-$ (50%); HRMS - (ES+) requires: 584.2985. Found: 584.2965 ($C_{32}H_{38}N_7O_4$).

5.2.4.11 5-Amino-3,4-bis(1-methyl-1*H*-indol-3-yl)-1*H*-pyrazole-1-carboximidamidium trifluoroacetate 548



Boc-protected derivative **547** (0.100 g, 0.17 mmol) was stirred along with a solution of 10% TFA in DCM (15 mL), at 30°C, for 16 hours. Following solvent evaporation under reduced pressure, the corresponding trifluoroacetate salt **548** was generated in quantitative yield; m.p. 115-117°C; $\nu_{max/}$ cm^{-1} (KBr) 3382, 1684, 1480, 1379; m/z (ES+) 384.2 $[M]^+$ (100%), (ES-) 112.9 $[CF_3CO_2]^-$ (100%).

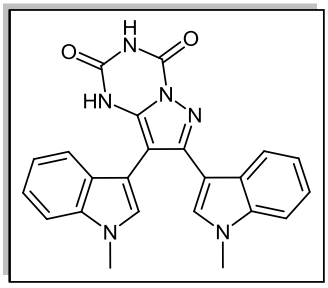
5.2.4.12 2,3-Bis(1-methyl-1*H*-indol-3-yl)-5,7-bis(trifluoromethyl)pyrazolo[1,5-*a*]pyrimidine 549



Hexafluoroacetylacetone (2.74 mL, 5.8 mmol, 20 eq.) was added to a mixture of aminopyrazole **447** (0.106 g, 0.29 mmol) and acetic acid (10 mL), with stirring, at room temperature. The reaction was then heated to 80°C for 20 hours, at which point, full consumption of the starting material **447** had occurred. Following removal of acetic acid under vacuum, the

crude pyrimidine derivative was purified by column chromatography and the pure residue was then dried under high vacuum overnight, to yield the product **549** as a dark red powder (0.080 g, 54%); m.p. 215-217^{o}C; ν_{max}/ cm^{-1} (KBr) 2930, 1615, 1569, 1480, 1270, 1188; δ_H (300 MHz, $CDCl_3$) 3.55 [3H, s, N-CH_3], 3.91 [3H, s, N-CH_3], 6.98-7.03 [1H, t, *J* 7.8, aromatic C-H_5], 7.10 [1H, s, aromatic C-H_2], 7.22-7.25 [2H, d, *J* 8.7, aromatic C-$H_{7,7'}$], 7.26-7.33 [4H, m, aromatic C-$H_{4,5',6,6'}$], 7.35 [1H, s, aromatic C-$H_{2'}$], 7.41-7.44 [1H, d, *J* 8.2, aromatic C-$H_{4'}$], 8.57-8.61 [1H, m, (CF_3)C-C<u>H</u>=C(CF_3)]; δ_C (75 MHz, $CDCl_3$) 33.0 (CH_3, N-<u>C</u>H_3), 33.1 (CH_3, N-<u>C</u>H_3), 100.6 (C, 2 × CF_3), 100.7 (CH, CF_3-C=<u>C</u>H-C(CF_3)), 103.8 (C, aromatic C), 104.5 (C, aromatic C), 107.0 (C, aromatic C), 109.2 (CH, aromatic CH), 109.6 (CH, aromatic CH), 119.5 (CH, aromatic CH), 121.1 (CH, aromatic CH), 121.3 (CH, aromatic CH), 121.9 (CH, aromatic CH), 122.6 (CH, aromatic CH), 122.7 (CH, aromatic CH), 126.6 (C, aromatic C), 126.8 (C, aromatic C), 129.4 (CH, aromatic CH), 131.4 (CH, aromatic CH), 136.9 (C, aromatic C), 137.4 (C, aromatic C), 144.2 (C, aromatic C), 144.7 (C, aromatic C), 146.8 (C, N=<u>C</u>(CF_3)- C), 154.4 (C, N-N-<u>C</u>(CF_3)=C); m/z (ES+) 514.2 $[M+H]^+$ (100%); HRMS - (ES+) requires: 514.1466. Found: 514.1466 ($C_{26}H_{18}N_5F_6$).

5.2.4.13 7,8-Bis(1-methyl-1*H*-indol-3-yl)pyrazolo[1,5-*a*][1,3,5]triazine-2,4(1*H*,3*H*)-dione 539

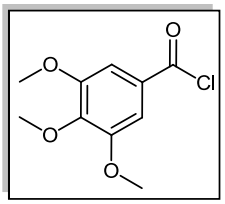


Chlorocarbonyl isocyanate (0.05 mL, 0.645 mmol, 1.1 eq.) was added to a dark solution of aminopyrazole **447** (0.200 g, 0.587 mmol) in doubly distilled DCM (7 mL), containing three drops of triethylamine, at 0^{o}C. The reaction was then allowed to stir at room temperature overnight, at which point, water (1 mL) was added carefully to the flask and slight effervescence was observed. The resultant brown slurry was filtered, washed with water (2 × 5 mL), ether (2 × 5 mL), and the isolated tan-coloured solid was then air-dried for 1 hour to afford the pure triazinedione congener **539** (0.202 g, 84%); m.p. 280-283^{o}C; ν_{max}/ cm^{-1} (KBr) 3228, 3105, 2936, 1739, 1705, 1654, 1563, 1478; δ_H (300 MHz, DMSO-d_6) 3.51 [3H, s, N-CH_3], 3.88 [3H, s, N-CH_3], 6.90 [1H, s, aromatic C-H_2], 6.95-7.00 [1H, t, *J* 7.6, aromatic C-H_5], 7.14-7.16 [1H, d, *J* 7.6, aromatic C-H_7], 7.14-7.25 [3H, m, aromatic C-$H_{5',6,6'}$], 7.39-7.42 [1H, d, *J* 7.6, aromatic C-$H_{7'}$], 7.45 [1H, s, aromatic C-$H_{2'}$], 7.52-7.55 [1H, d, *J* 8.2, aromatic C-H_4], 8.36-8.39 [1H, d, *J* 7.2, aromatic C-$H_{4'}$], 11.48 [2H, bs, 2 × NH]; δ_C (75 MHz, DMSO-d_6) 31.5 ($2CH_3$, 2 × N-<u>C</u>H_3), 93.2 (C, aromatic C), 100.7 (C, aromatic C), 105.4 (C, aromatic C), 108.7 (CH, aromatic CH), 108.9 (CH, aromatic CH), 117.9 (CH, aromatic CH), 118.3 (CH, aromatic CH), 119.0 (CH, aromatic CH), 120.2 (CH, aromatic CH), 120.9 (CH, aromatic

CH), 121.0 (CH, aromatic CH), 124.6 (C, aromatic C), 126.4 (C, aromatic C), 128.6 (CH, aromatic CH), 129.6 (CH, aromatic CH), 135.2 (C, aromatic C), 135.8 (C, aromatic C), 137.8 (C, aromatic C), 143.2 (C, aromatic C), 147.6 (C, NH-C=O(NH)), 150.6 (C, NH-C=O(N-N)); m/z (ES+) 411.1 $[M+H]^+$ (20%). (ES-) 409.2 $[M-H]^-$ (100%); HRMS - (ES+) requires: 411.1569. Found: 411.1567 ($C_{23}H_{19}N_6O_2$).

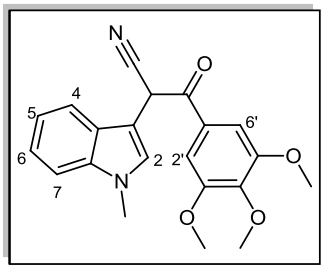
5.2.5 Derivatisation of 4-(indol-3-yl)-3-(trimethoxyphenyl)-5-aminopyrazoles

5.2.5.1 3,4,5-Trimethoxybenzoyl chloride 499[39]



To a stirred suspension of 3,4,5-trimethoxybenzoic acid (1.000 g, 4.7 mmol) in DCM (15 mL), was added thionyl chloride (1.7 mL, 23.6 mmol, 5 eq.), dropwise over 5 minutes. The resultant mixture was then refluxed for 20 hours prior to being cooled to room temperature. The reaction solvent and excess thionyl chloride was removed *in vacuo* to yield the corresponding acid chloride **574** as a colourless oil, in quantitative yield, and used without any further purification; ν_{max}/ cm^{-1} (KBr) 1750, 1590, 1457.

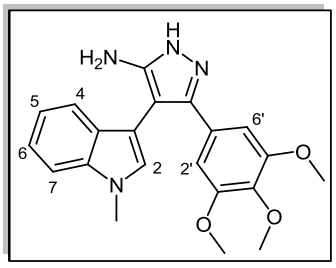
5.2.5.2 2-(1-Methyl-1*H*-indol-3-yl)-3-oxo-3-(3,4,5-trimethoxyphenyl)propanenitrile 556



LDA solution (2 M) (19.4 mL, 38.7 mmol, 2.2 eq.) was added, under nitrogen, to a flask containing THF (30 mL), cooled to −78°C, and equilibriated at this temperature for 35 minutes, with stirring. Nitrile **454** (3.009 g, 17.6 mmol) in THF (4 mL) was then added slowly to the reaction flask and maintained at −78°C for 2 hours. 3,4,5-Trimethoxybenzoyl chloride **499** (6.011 g, 26.4 mmol, 1.5 eq.) was then dissolved in THF (15 mL), and added dropwise to the reaction vessel, at −78°C. The reaction was allowed to warm to room temperature and stirred overnight. Following solvent evaporation, the crude residue was taken up in ethyl acetate (100 mL) and washed with saturated ammonium chloride solution (2 × 150 mL). These were then combined and further extracted with ethyl acetate (2 × 75 mL); the aggregate ethyl acetate layers were then washed with water (3 × 150 mL) and brine (2 × 150 mL), dried with magnesium sulfate and evaporated *in vacuo*. Celite® was added to the crude dark brown ketonitrile **556**, along with DCM (40 mL), and the product adsorbed under reduced pressure. Employing a gradient from 15-30% ethyl acetate/hexane, the product was eluted rapidly, and following combination and evaporation of the fractions, was isolated as a dark orange crystalline solid (2.221 g, 35%); m.p. 73-76°C; ν_{max}/ cm^{-1} (KBr) 3433, 2938, 1684, 1584,

1504, 1127; δ_H (300 MHz, $CDCl_3$) 3.75 [3H, s, N-CH_3], 3.76 [6H, s, 2 × *m*-OCH_3], 3.86 [3H, s, *p*-OCH_3], 5.82 [1H, s, CH], 7.15 [1H, s, C-H_2], 7.18-7.24 [1H, t, *J* 7.3, C-H_5], 7.21 [2H, s, C-$H_{2',6'}$], 7.26-7.31 [1H, t, *J* 6.8, C-H_6], 7.32-7.35 [1H, d, *J* 7.5, C-H_7], 7.71-7.74 [1H, d, *J* 7.8, C-H_4]; δ_C (75 MHz, $CDCl_3$) 33.1 (CH_3, N-CH_3), 38.4 (CH, CHCN), 56.3 ($2CH_3$, 2 × *m*-OCH_3), 61.0 (CH_3, *p*-OCH_3), 103.9 (C, aromatic C), 106.7 (2CH, 2 × aromatic CH), 110.1 (CH, aromatic CH), 116.9 (C, aromatic C), 118.1 (CH, aromatic CH), 120.6 (CH, aromatic CH), 122.9 (CH, aromatic CH), 125.6 (C, CN), 128.4 (CH, aromatic CH), 128.6 (C, aromatic C), 137.1 (C, aromatic C), 143.4 (C, aromatic C), 153.0 (2C, 2 × aromatic C), 187.5 (C, C=O); m/z (ES+) 365.1 $[M+H]^+$ (60%). (ES-) 363.1 $[M-H]^-$ (100%); HRMS - (ES+) requires: 365.1501. Found: 365.1486 ($C_{21}H_{21}N_2O_4$).

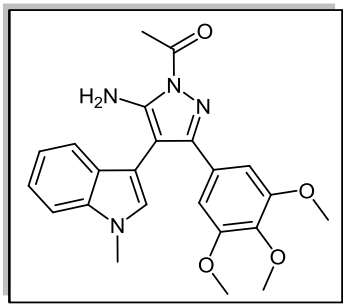
5.2.5.3 4-(1-Methyl-1*H*-indol-3-yl)-3-(3,4,5-trimethoxyphenyl)-1*H*-pyrazol-5-amine 553



Hydrazine hydrate (0.14 mL, 1.5 mmol) and camphoric acid (0.180 g, 0.88 mmol, 1.2 eq.) were added to a suspension of the β-ketonitrile **556** (0.265 g, 0.73 mmol), in dry methanol (10 mL). The reaction mixture was then stirred at reflux temperature for 3 hours, prior to addition of excess hydrazine hydrate (0.42 mL, 4.5 mmol) and heating for a further 20 hours. Following solvent removal, the residue was taken up in ethyl acetate (50 mL) and washed with saturated aqueous sodium bicarbonate solution (2 × 70 mL). These aqueous bicarbonate layers were added together and subsequently extracted with ethyl acetate (2 × 30 mL); the combined ethyl acetate layers were then washed with water (3 × 70 mL) and brine (2 × 70 mL), dried with magnesium sulfate, filtered and evaporated to yield a crude golden brown solid. Following chromatography, initially with 100% ethyl acetate, to complete full elution of the starting material, and then with 98:2 ethyl acetate/methanol, the novel 5-aminopyrazole **553** was isolated as light brown crystals (0.170 g, 62%); m.p. 117-120°C; ν_{max}/ cm^{-1} (KBr) 2930, 1583, 1511, 1465, 1422, 1124; δ_H (300 MHz, $CDCl_3$) 3.42 [6H, s, 2 × *m*-OCH_3], 3.77 [3H, s, N-CH_3], 3.81 [3H, s, *p*-OCH_3], 4.75 [2H, bs, NH_2], 6.68 [2H, s, C-$H_{2',6'}$], 7.01-7.06 [3H, m, C-$H_{2,5}$ & NH], 7.20-7.25 [1H, t, *J* 8.0, C-H_6], 7.30-7.33 [1H, d, *J* 7.8, C-H_7], 7.33-7.36 [1H, d, *J* 8.2, C-H_4]; δ_C (75 MHz, $CDCl_3$) 32.9 (CH_3, N-CH_3), 55.7 ($2CH_3$, 2 × *m*-OCH_3), 60.8 (CH_3, *p*-OCH_3), 104.0 (2CH, 2 × aromatic CH), 104.4 (C, aromatic C), 105.7 (C, aromatic C), 109.3 (CH, aromatic CH), 119.6 (CH, aromatic CH), 120.4 (CH, aromatic CH), 122.0 (CH, aromatic CH), 126.1 (C, aromatic C), 127.9 (C, aromatic C), 128.0 (C, aromatic C), 128.4 (CH, aromatic CH), 137.1 (C, aromatic C), 137.8

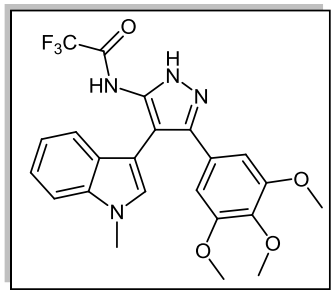
(C, aromatic C), 153.1 (C, aromatic C), 153.3 (2C, 2 × aromatic C); m/z (ES+) 379.1 $[M+H]^+$ (100%); HRMS - (ES+) requires: 379.1770. Found: 379.1765 ($C_{21}H_{23}N_4O_3$).

5.2.5.4 1-(5-Amino-4-(1-methyl-1*H*-indol-3-yl)-3-(3,4,5-trimethoxyphenyl)-1*H*-pyrazol-1-yl)ethanone 557



To a solution of parent aminopyrazole **553** (0.150 g, 0.397 mmol) in acetonitrile (10 mL), was added acetic anhydride (0.05 mL, 0.476 mmol, 1.2 eq.) and the reaction mixture was heated to 80°C, with stirring, for 16 hours. Following solvent removal, the crude acetylated product was dissolved in ethyl acetate (30 mL), washed with 10% aqueous sodium bicarbonate solution (50 mL), followed by water (3 × 50 mL) and brine (50 mL). The organic layer was then dried with magnesium sulfate, prior to filtration and evaporation of the filtrate to a crude residue. Chromatography with 15% ethyl acetate/ hexane, followed by concentration of the product fractions, generated the pure pyrazolic acetamide derivative **557** as off-white plate-like crystals (0.067 g, 40%); m.p. 182-184°C; ν_{max}/ cm^{-1} (KBr) 3449, 3338, 2935, 1710, 1608, 1572, 1485, 1126; δ_H (300 MHz, $CDCl_3$) 2.79 [1H, s, $COCH_3$], 3.45 [6H, s, 2 × *m*-OCH_3], 3.78 [3H, s, N-CH_3], 3.82 [3H, s, *p*-OCH_3], 5.46 [2H, bs, NH_2], 6.87 [2H, s, C-$H_{2',6'}$], 6.99 [1H, s, C-H_2], 7.06-7.11 [1H, td, *J* 8.0, 0.9, C-H_5], 7.23-7.28 [1H, td, *J* 8.1, 1.1, C-H_6], 7.35-7.38 [1H, d, *J* 8.0, C-H_7], 7.38-7.40 [1H, d, *J* 7.6, C-H_4]; δ_C (75 MHz, $CDCl_3$) 23.2 (CH_3, CO<u>C</u>H_3), 32.9 (CH_3, N-CH_3), 55.6 ($2CH_3$, 2 × *m*-OCH_3), 60.8 (CH_3, *p*-OCH_3), 94.5 (C, aromatic C), 104.7 (C, aromatic C), 105.0 (2CH, 2 × aromatic CH), 109.4 (CH, aromatic CH), 119.8 (CH, aromatic CH), 120.2 (CH, aromatic CH), 122.2 (CH, aromatic CH), 127.9 (C, aromatic C), 128.0 (C, aromatic C), 128.7 (CH, aromatic CH), 137.2 (C, aromatic C), 138.4 (C, aromatic C), 148.7 (C, aromatic C), 152.8 (2C, 2 × aromatic C), 153.3 (C, aromatic C), 173.8 (C, C=O); m/z (ES+) 421.2 $[M+H]^+$ (100%); HRMS - (ES+) requires: 421.1876. Found: 421.1862 ($C_{23}H_{25}N_4O_4$).

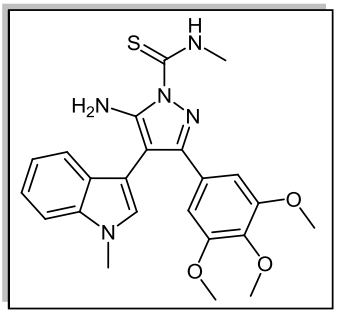
5.2.5.5 2,2,2-Trifluoro-*N*-(4-(1-methyl-1*H*-indol-3-yl)-3-(3,4,5-trimethoxyphenyl)-1*H*-pyrazol-5-yl)acetamide 558



Trifluoroacetic anhydride (0.10 mL, 0.63 mmol, 1.2 eq.) was added in a single portion, to a mixture of parent aminopyrazole **553** (0.200 g, 0.53 mmol) and acetonitrile (10 mL). The temperature was then adjusted until a steady reflux of the dark-brown reaction was attained; stirring was continued for 16

hours. The solvent was then evaporated *in vacuo*, to yield the trifluoroacetylated product **558** as a light orange solid (0.100 g, 40%), following column chromatography (30% ethyl acetate/hexane) of the crude residue; m.p. 113-116°C; ν_{max}/ cm^{-1} (KBr) 3270, 2939, 1729, 1585, 1504, 1466, 1126; δ_H (300 MHz, $CDCl_3$) 3.43 [6H, s, 2 × *m*-OCH_3], 3.78 [3H, s, N-CH_3], 3.86 [3H, s, *p*-OCH_3], 6.75 [2H, s, C-$H_{2',6'}$], 7.05-7.11 [2H, m, C-$H_{5,6}$], 7.26 [1H, s, C-H_2], 7.26-7.31 [1H, t, *J* 7.0, C-H_7], 7.39-7.41 [1H, d, *J* 8.3, C-H_4], 8.17 [2H, bs, $NHCOCF_3$ & pyrazole NH]; δ_C (75 MHz, $CDCl_3$) 33.1 (CH_3, NCH_3), 55.6 ($2CH_3$, 2 × *m*-OCH_3), 60.9 (CH_3, *p*-CH_3), 103.2 (C, aromatic C), 104.2 (2CH, 2 × aromatic C-H), 105.2 (CH, aromatic CH), 109.6 (CH, aromatic CH), 119.9 (CH, aromatic CH), 120.3 (CH, aromatic CH), 122.7 (CH, aromatic CH), 127.5 (C, aromatic C), 128.5 (2C, 2 × aromatic C), 133.6 (C, aromatic C), 137.3 (2C, 2 × aromatic C), 143.3 (C, aromatic C), 153.1 (2C, 2 × aromatic C); m/z (ES+) 475.1 $[M+H]^+$ (100%); HRMS - (ES+) requires: 475.1593. Found: 475.1591 ($C_{23}H_{22}N_4O_4F_3$).

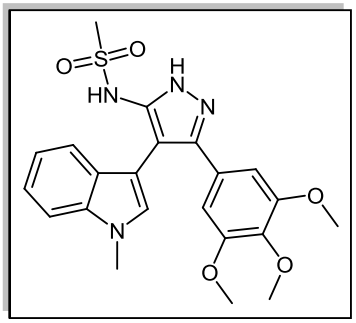
5.2.5.6 5-Amino-*N*-methyl-4-(1-methyl-1*H*-indol-3-yl)-3-(3,4,5-trimethoxyphenyl)-1*H*-pyrazole-1-carbothioamide 559



Methyl isothiocyanate (0.040 g, 0.55 mmol, 1.05 eq.) was applied to a stirred solution of aminopyrazole **553** (0.200 g, 0.53 mmol) in acetonitrile (10 mL). The reaction was then heated to reflux temperature, and the dark orange suspension was stirred for 16 hours. The reaction was initially allowed to cool to room temperature, and subsequently, to 0°C, and maintained for 30 minutes at this temperature. The formed slurry was then filtered to yield the pure thiourea derivative **559** as light orange crystals (0.080 g, 34%); m.p. 186-188°C; ν_{max}/ cm^{-1} (KBr) 3418, 3272, 2931, 1624, 1519, 1423, 1117; δ_H (300 MHz, $CDCl_3$) 3.28-3.30 [3H, d, *J* 4.9, NHC<u>H</u>$_3$], 3.43 [6H, s, 2 × *m*-OCH_3], 3.78 [3H, s, N-CH_3], 3.82 [3H, s, *p*-OCH_3], 6.35 [2H, s, NH_2], 6.85 [2H, s, C-$H_{2',6'}$], 7.01 [1H, s, C-H_2], 7.06-7.11 [1H, t, *J* 7.3, C-H_5], 7.23-7.28 [1H, t, *J* 8.9, C-H_6], 7.35-7.38 [1H, d, *J* 8.1, C-H_7], 7.38-7.40 [1H, d, *J* 7.8, C-H_4], 9.38 [1H, s, N<u>H</u>CH_3]; δ_C (75 MHz, $CDCl_3$) 29.0 (CH_3, NH<u>C</u>H_3), 31.1 (CH_3, N-CH_3), 53.8 ($2CH_3$, 2 × *m*-OCH_3), 59.0 (CH_3, *p*-OCH_3), 93.1 (C, aromatic C), 103.1 (C, aromatic C), 103.2 (2CH, 2 × aromatic CH), 107.5 (CH, aromatic CH), 118.0 (CH, aromatic CH), 118.4 (CH, aromatic CH), 120.4 (CH, aromatic CH), 125.7 (C, aromatic C), 126.2 (C, aromatic C), 127.1 (CH, aromatic CH), 135.3 (C, aromatic C), 136.6 (C, aromatic C), 148.1 (C, aromatic C), 148.5 (C, aromatic C), 151.0 (2C, 2 × aromatic

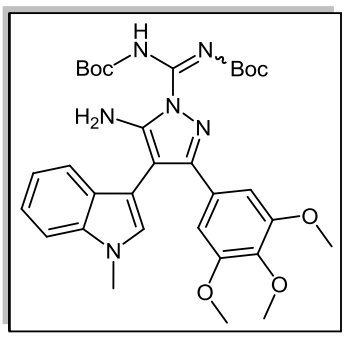
C), 175.1 (C, C=S); m/z (ES+) 452.1 $[M+H]^+$ (50%); HRMS - (ES+) requires: 452.1756. Found: 452.1742 ($C_{23}H_{26}N_5O_3S$).

5.2.5.7 *N*-(4-(1-Methyl-1*H*-indol-3-yl)-3-(3,4,5-trimethoxyphenyl)-1*H*-pyrazol-5-yl) methanesulfonamide 560



To a solution of the aminopyrazole **553** (0.108 g, 0.29 mmol) in pyridine (8 mL), was added methanesulfonyl chloride (0.023 mL, 0.29 mmol), along with triethylamine (0.04 mL, 0.29 mmol). The reaction was refluxed overnight and then evaporated under reduced pressure. The residue was dissolved in ethyl acetate (80 mL), then washed with 10% HCl (5 × 70 mL), aqueous saturated sodium bicarbonate solution (100 mL), water (3 × 100 mL) and brine (100 mL), dried over magnesium sulfate and evaporated under reduced pressure. Chromatography employing 25% ethyl acetate/hexane yielded the title product **560** as a dark brown solid (0.048 g, 35%); m.p. 129-132^{o}C; ν_{max}/ cm^{-1} (KBr) 3307, 2930, 1584, 1465, 1424, 1125; δ_H (300 MHz, $CDCl_3$) 3.24 [3H, s, SO_2CH_3], 3.42 [6H, s, 2 × *m*-OCH_3], 3.78 [3H, s, N-CH_3], 3.82 [3H, s, *p*-OCH_3], 6.61 [2H, s, C-$H_{2',6'}$], 7.00-7.05 [1H, t, *J* 7.4, C-H_5], 7.08 [1H, s, C-H_2], 7.17-7.19 [1H, d, *J* 7.8, C-H_7], 7.19-7.24 [1H, t, *J* 7.5, C-H_6], 7.26 [1H, s, pyrazole NH], 7.33-7.35 [1H, d, *J* 8.16, C-H_4]; δ_C (75 MHz, $CDCl_3$) 33.0 (CH_3, N-CH_3), 41.4 (CH_3, SO_2CH_3), 55.8 ($2CH_3$, 2 × *m*-OCH_3), 60.9 (CH_3, *p*-OCH_3), 103.4 (C, aromatic C), 103.5 (C, aromatic C), 104.0 (2CH, 2 × aromatic CH), 109.5 (CH, aromatic CH), 119.9 (CH, aromatic CH), 120.0 (CH, aromatic CH), 122.3 (CH, aromatic CH), 124.6 (C, aromatic C), 127.6 (C, aromatic C), 128.9 (CH, aromatic CH), 137.1 (C, aromatic C), 138.3 (C, aromatic C), 141.8 (C, aromatic C), 145.2 (C, aromatic C), 153.3 (2C, 2 × aromatic C); m/z (ES+) 457.1 $[M+H]^+$ (100%); HRMS - (ES+) requires: 457.1546. Found: 457.1550 ($C_{22}H_{25}N_4O_5S$).

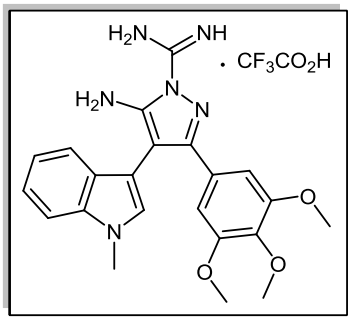
5.2.5.8 *Tert*-butyl [(5-amino-4-(1-methyl-1*H*-indol-3-yl)-3-(3,4,5-trimethoxyphenyl)-1*H*-pyrazol-1-yl){(*tert*-butoxycarbonyl)imino}methyl]carbamate 561



Aminopyrazole **553** (0.150 g, 0.397 mmol) was treated with $HgCl_2$ (0.130 g, 0.437 mmol, 1.1 eq.) and *N,N'*-di-*tert*-butoxycarbonylthiourea **546** (0.109 g, 0.397 mmol), in distilled DCM (10 mL), at 0^{o}C. Triethylamine (0.2 mL, 1.23 mmol, 3.1 eq.) was then added to the flask and allowed to stir at 0^{o}C for a further 1 hour, followed by stirring for 12 hours at room

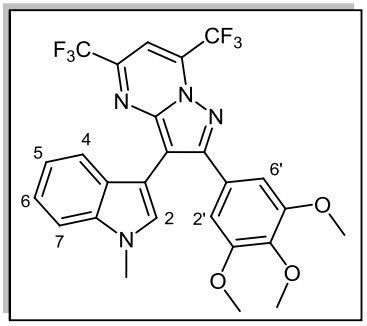
temperature. The reaction was then poured into ethyl acetate (30 mL), and filtered through a pad of celite® in order to remove the yellow mercury sulfide by-product. The filter cake was washed with ethyl acetate (3 × 15 mL). The combined organic phases were then washed with water (3 × 100 mL) and brine (100 mL), dried over magnesium sulfate and concentrated under vacuum. Chromatography employing 15% ethyl acetate/ hexane yielded the pure di-protected pyrazole derivative **561** as an off-white crystalline solid (0.085 g, 35%); m.p. 153-156°C; ν_{max}/ cm^{-1} (KBr) 3487, 3360, 2975, 1766, 1751, 1712, 1656, 1587, 1126; δ_H (300 MHz, $CDCl_3$) 1.55 [9H, s, $CO_2C(CH_3)_3$], 1.56 [9H, s, $CO_2C(CH_3)_3$], 3.47 [6H, s, 2 × *m*-OCH_3], 3.78 [3H, s, N-CH_3], 3.82 [3H, s, *p*-OCH_3], 5.72 [2H, bs, NH_2], 6.81 [2H, s, C-$H_{2',6'}$], 6.98 [1H, s, C-H_2], 7.07-7.12 [1H, td, *J* 7.8, 0.7, C-H_5], 7.23-7.28 [1H, t, *J* 7.7, C-H_6], 7.35-7.38 [1H, d, *J* 8.3, C-H_7], 7.36-7.39 [1H, d, *J* 7.9, C-H_4], 9.25 [1H, s, N<u>H</u>$CO_2C(CH_3)_3$]; δ_C (75 MHz, $CDCl_3$) 28.1 ($3CH_3$, $CO_2C(\underline{C}H_3)_3$), 28.2 ($3CH_3$, $CO_2C(\underline{C}H_3)_3$), 32.9 ($CH_3$, N-$CH_3$), 55.7 ($2CH_3$, 2 × *m*-$OCH_3$), 60.8 ($CH_3$, *p*-$OCH_3$), 81.0 (C, $CO_2\underline{C}(CH_3)_3$), 83.1 (C, $CO_2\underline{C}(CH_3)_3$), 95.2 (C, aromatic C), 104.7 (C, aromatic C), 105.2 (2CH, 2 × aromatic CH), 109.4 (CH, aromatic CH), 119.9 (CH, aromatic CH), 120.1 (CH, aromatic CH), 122.2 (CH, aromatic CH), 127.6 (C, aromatic C), 127.9 (C, aromatic C), 128.8 (CH, aromatic CH), 137.1 (C, aromatic C), 138.5 (C, aromatic C), 143.2 (C, aromatic C), 148.6 (C, aromatic C), 149.7 (C, NH-<u>C</u>=N), 152.0 (C, C=O), 152.9 (2C, 2 × aromatic C), 157.3 (C, C=O); m/z (ES+) 621.3 $[M+H]^+$ (100%); HRMS - (ES+) requires: 621.3037. Found: 621.3033 ($C_{32}H_{41}N_6O_7$).

5.2.5.9 5-Amino-4-(1-methyl-1*H*-indol-3-yl)-3-(3,4,5-trimethoxyphenyl)-1*H*-pyrazole-1-carboximidamidium trifluoroacetate 562



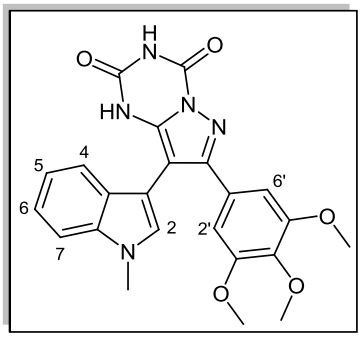
As for synthesis of compound **548**, Boc-protected N^1-guanylated derivative **561** (0.05 g, 0.08 mmol) was treated, at 30°C, with a 10% v/v solution of TFA in DCM (10 mL), for 16 hours. After stirring for this time, the solvent was evaporated *in vacuo* to generate the corresponding trifluoroacetate salt **562** in quantitative yield; m.p. 118-120°C; ν_{max}/ cm^{-1} (KBr) 3369, 1698, 1551, 1421; m/z (ES+) 421.2 $[M]^+$ (100%), (ES-) 112.9 $[CF_3CO_2]^-$ (100%).

5.2.5.10 3-(1-Methyl-1*H*-indol-3-yl)-5,7-bis(trifluoromethyl)-2-(3,4,5-trimethoxyphenyl)pyrazolo[1,5-*a*]pyrimidine 563



Hexafluoroacetylacetone (1.50 mL, 10.6 mmol, 20 eq.) was added to a mixture of aminopyrazole **553** (0.200 g, 0.53 mmol) and acetic acid (10 mL), prior to heating at 80°C for 20 hours, at which point, full consumption of the starting material had occurred. Following acetic acid removal, the crude hexafluoropyrimidine derivative **563** was purified by chromatography employing a gradient from 20-50% ethyl acetate/ hexane. Product fractions were then combined prior to solvent evaporation and drying under high vacuum overnight, to yield the product **563** as a brick-red crystalline solid (0.130 g, 45%); m.p. 217-220°C; ν_{max}/ cm^{-1} (KBr) 2940, 1577, 1485, 1467, 1420, 1170; δ_H (300 MHz, $CDCl_3$) 3.48 [6H, s, 2 × *m*-OCH_3], 3.84 [3H, s, N-CH_3], 3.90 [3H, s, *p*-OCH_3], 6.97-7.02 [1H, t, *J* 7.2, aromatic C-H_5], 7.10-7.13 [1H, d, *J* 7.8, aromatic C-H_7], 7.12 [2H, s, aromatic C-$H_{2',6'}$], 7.19-7.25 [1H, t, *J* 7.2, aromatic C-H_6], 7.35 [1H, s, (CF_3)C-C<u>H</u>=C(CF_3)], 7.36-7.39 [1H, d, *J* 8.3, aromatic C-H_4], 7.42 [1H, s, aromatic C-H_2]; δ_C (75 MHz, $CDCl_3$) 33.1 (CH_3, N-<u>C</u>H_3), 55.7 ($2CH_3$, 2 × *m*-O<u>C</u>H_3), 60.9 (CH_3, *p*-O<u>C</u>H_3), 102.1 (CH, aromatic CH), 103.3 (C, aromatic C), 106.1 (2CH, 2 × aromatic CH), 106.7 (C, aromatic C), 109.4 (CH, aromatic CH), 117.4-124.6 (2C, m, 2 × CF_3), 119.8 (CH, aromatic CH), 121.0 (CH, aromatic CH), 122.1 (CH, aromatic CH), 126.9 (C, aromatic C), 127.3 (C, aromatic C), 129.5 (CH, aromatic CH), 134.0-135.4 (C, q, J_{F-C} 38.6, aromatic C), 137.2 (C, aromatic C), 139.2 (C, aromatic C), 143.5-144.9 (C, q, J_{F-C} 37.8, aromatic C), 147.1 (C, aromatic C), 153.1 (2C, 2 × aromatic C), 156.0 (C, aromatic C); m/z (ES+) 551.2 $[M+H]^+$ (100%); HRMS - (ES+) requires: 551.1518. Found: 551.1514 ($C_{26}H_{21}N_4O_3F_6$).

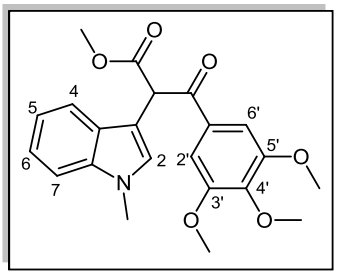
5.2.5.11 8-(1-Methyl-1*H*-indol-3-yl)-7-(3,4,5-trimethoxyphenyl)pyrazolo[1,5-*a*][1,3,5]triazine-2,4(1*H*,3*H*)-dione 540



Chlorocarbonyl isocyanate (0.05 mL, 0.582 mmol, 1.1 eq.) was added to a stirred solution of aminopyrazole **553** (0.100 g, 0.265 mmol) in doubly distilled DCM (5 mL), containing two drops of triethylamine, at 0°C. The reaction was then allowed to stir at room temperature overnight. Water (1 mL) was added carefully to the flask; the resultant dark brown slurry was then filtered and the isolated brown solid product **540** (0.075 g, 64%) was washed successively with water, ether, and air-dried for 1 hour; m.p.

268-271°C, ν_{max}/ cm^{-1} (KBr) 3433, 3213, 2939, 1763, 1710, 1587, 1419, 1125; δ_H (300 MHz, DMSO-d_6) 3.38 [6H, s, 2 × *m*-OCH_3], 3.65 [3H, s, NCH_3], 3.90 [3H, s, *p*-OCH_3], 6.93 [2H, s, C-$H_{2',6'}$], 7.02-7.06 [1H, t, *J* 7.6, C-H_5], 7.17-7.19 [1H, d, *J* 7.8, C-H_7], 7.22-7.27 [1H, t, *J* 8.1, C-H_6], 7.48 [1H, s, C-H_2], 7.55-7.58 [1H, d, *J* 8.3, C-H_4], 11.67 [2H, bs, 2 × NH]; δ_C (75 MHz, DMSO-d_6) 32.5 (CH_3, N-CH_3), 55.1 ($2CH_3$, 2 × *m*-OCH_3), 60.0 (CH_3, *p*-OCH_3), 94.8 (C, aromatic C), 101.8 (C, aromatic C), 104.5 (2CH, 2 × aromatic CH), 109.8 (CH, aromatic CH), 119.1 (CH, aromatic CH), 119.4 (CH, aromatic CH), 121.4 (CH, aromatic CH), 127.3 (C, aromatic C), 127.8 (C, aromatic C), 130.7 (CH, aromatic CH), 136.8 (C, aromatic C), 137.8 (C, aromatic C), 139.9 (C, aromatic C), 144.3 (C, aromatic C), 148.5 (2C, 2 × aromatic C), 152.4 (C, C=O), 153.5 (C, C=O); m/z (ES+) 448.1 $[M+H]^+$ (40%); HRMS - (ES+) requires: 448.1621. Found: 448.1611 ($C_{23}H_{22}N_5O_5$).

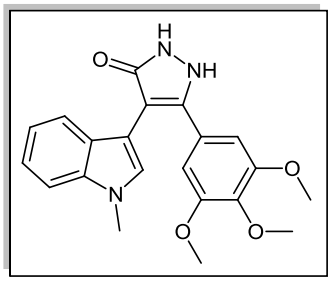
5.2.5.12 Methyl 2-(1-Methyl-1*H*-indol-3-yl)-3-oxo-3-(3,4,5-trimethoxyphenyl) propanoate 555



To a flame dried 100 mL round-bottomed flask, was added dry THF (40 mL), cooled and stirred at −78°C. LDA solution (1.8M) (15.2 mL, 27.3 mmol, 2.2 eq.) was then added slowly to the reaction mixture and allowed to equilibriate, with stirring, for 30 minutes. *N*-Methyl indole ester **480** (2.513 g, 12.4 mmol) in THF (3 mL) was added dropwise, maintaining an internal temperature of −78°C, and allowed to deprotonate for 90 minutes. 3,4,5-Trimethoxybenzoyl chloride **499**, (4.228 g, 18.6 mmol, 1.5 eq.) was dissolved in THF (10-15 mL), and added dropwise, over 10 minutes, to the dark reaction mixture. The reaction was then allowed to warm up to room temperature, while stirring of the flask was maintained overnight. Following solvent removal, the crude product residue was extracted with ethyl acetate (3 × 150 mL), which was washed with saturated ammonium chloride (250 mL), water (4 × 250 mL) and brine (2 × 150 mL). The combined organic layers were dried using magnesium sulfate, filtered and evaporated *in vacuo*. The pure product β-ketoester **555** was isolated as a light brown solid following gradient column chromatography, utilising 10-30% ethyl acetate/hexane as eluent (1.721 g, 35%); m.p. 70-74°C; ν_{max}/ cm^{-1} (KBr) 2941, 1739, 1678, 1584, 1453, 1415, 1333, 1126; δ_H (300 MHz, $CDCl_3$) 3.75 [9H, s, $CO_2C\underline{H}_3$ & 2 × *m*-OCH_3], 3.78 [3H, s, N-CH_3], 3.85 [3H, s, *p*-OCH_3], 5.85 [1H, s, $COC\underline{H}CO_2CH_3$], 7.14-7.18 [1H, t, *J* 6.8, aromatic C-H_5], 7.18 [1H, s, aromatic C-H_2], 7.21-7.24 [1H, d, *J* 8.2, aromatic C-H_7], 7.26 [2H, s, aromatic C-$H_{2',6'}$], 7.27-7.32 [1H, t, *J* 8.0, aromatic C-H_6], 7.69-7.72 [1H, d, *J* 7.7, aromatic C-H_4]; δ_C (75 MHz, $CDCl_3$) 33.0 (CH_3, N-$\underline{C}H_3$), 51.6 (CH,

CO<u>C</u>HCO$_2$CH$_3$), 52.7 (CH$_3$, CO$_2$<u>C</u>H$_3$), 56.2 (2CH$_3$, 2 × *m*-O<u>C</u>H$_3$), 60.9 (CH$_3$, *p*-O<u>C</u>H$_3$), 106.2 (C, aromatic C), 106.4 (2CH, aromatic <u>C</u>-H$_{2'}$ & aromatic <u>C</u>-H$_{6'}$), 106.9 (C, aromatic C), 109.8 (CH, aromatic CH), 118.0 (CH, aromatic CH), 119.8 (CH, aromatic CH), 122.1 (CH, aromatic CH), 126.8 (C, aromatic C), 129.3 (CH, aromatic CH), 130.5 (C, aromatic C), 136.9 (C, aromatic C), 142.7 (C, aromatic C), 153.0 (C, aromatic C), 169.9 (C, <u>C</u>O$_2$CH$_3$), 192.3 (C, <u>C</u>=O); m/z (ES+) 398.1 $[M+H]^+$ (100%); HRMS - (ES+) requires: 398.1604. Found: 398.1613 ($C_{22}H_{24}NO_6$).

5.2.5.13 4-(1-Methyl-1*H*-indol-3-yl)-5-(3,4,5-trimethoxyphenyl)-1*H*-pyrazol-3(2*H*)-one 552

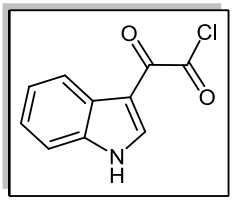


β-Ketoester precursor **555** (0.250 g, 0.63 mmol) was initially placed in a 100 mL round-bottom flask, along with camphoric acid (0.128 g, 0.63 mmol) and distilled ethanol (20 mL). To the stirring mixture, was then added hydrazine hydrate (50-60% commercial solution) (0.07 mL, 0.65 mmol) and the temperature was adjusted to maintain reflux of the flask contents for 2 hours. Further hydrazine hydrate solution (0.20 mL, 1.90 mmol, 3 eq.) was then added to the heated reaction vessel, and the overall mixture was stirred at 80^{o}C for a further 20 hours. Following removal of the reaction solvent, the product residue was dissolved in ethyl acetate (70 mL) and washed with 10% aqueous sodium bicarbonate solution (2 × 80 mL). Following washing of the ethyl acetate layer with water (3 × 100 mL), brine (2 × 100 mL), and drying with magnesium sulfate, the solvent was evaporated *in vacuo*. The crude pyrazolone **552** was then purified by flash chromatography, employing a gradient from 70% hexane/ 30% ethyl acetate to 95% ethyl acetate/5% methanol. The pyrazolone fractions were then combined, evaporated under reduced pressure, and triturated with boiling methanol in order to afford the novel title compound **552**, indicated by NMR analysis to exist as two atropisomers, and isolated as a yellow powder (0.146 g, 60%); m.p. 198-201^{o}C; ν_{max}/ cm^{-1} (KBr) 3334, 2936, 1700, 1586, 1519, 1458, 1251, 1125; δ_H (300 MHz, DMSO) 3.39 [6H, s, 2 x *m*-OCH$_3$], 3.42 [3H, s, *p*-OCH$_3$], 3.59 [3H, s, N-CH$_3$], 3.82 [1H, s, N<u>H</u>-NH-CO, D$_2$O exchangeable], 6.75 [2H, s, aromatic C-H$_{2',6'}$], 6.84-6.93 [1H, m, aromatic C-H$_5$], 7.02-7.15 [2H, m, aromatic C-H$_{6,7}$], 7.30 & 7.31 [1H, 2 × overlapping s, aromatic C-H$_2$], 7.38-7.45 [1H, m, aromatic C-H$_4$]; δ_C (75 MHz, DMSO) (mixture of signals not deconvoluted) 32.3 (2CH$_3$, 2 × N-<u>C</u>H$_3$), 55.1 (4CH$_3$, 4 x *m*-O<u>C</u>H$_3$), 59.9 (2CH$_3$, 2 × *p*-O<u>C</u>H$_3$), 103.5 (2CH, aromatic <u>C</u>-H$_{2'}$ & aromatic <u>C</u>-H$_{6'}$), 103.5 (2CH, aromatic <u>C</u>-H$_{2'}$ & aromatic <u>C</u>-H$_{6'}$), 105.1 (2C, aromatic C), 105.8 (C, aromatic C), 105.8 (C, aromatic C),

109.5 (CH, aromatic CH), 111.2 (CH, aromatic CH), 111.3 (C, aromatic C), 118.3 (CH, aromatic CH), 118.4 (CH, aromatic CH), 119.8 (CH, aromatic CH), 120.0 (CH, aromatic CH), 120.8 (CH, aromatic CH), 120.9 (CH, aromatic CH), 124.7 (CH, aromatic CH), 124.9 (C, aromatic C), 124.9 (C, aromatic C), 125.8 (C, aromatic C), 125.9 (C, aromatic C), 125.9 (C, aromatic C), 126.8 (C, aromatic C), 129.1 (CH, aromatic CH), 135.9 (C, aromatic C), 136.1 (C, aromatic C), 136.5 (C, aromatic C), 136.5 (C, aromatic C), 136.6 (C, aromatic C), 136.7 (C, aromatic C), 152.4 (C, C=O), 152.5 (C, C=O); m/z (ES+) 380.2 $[M+H]^+$ (100%); HRMS - (ES+) requires: 380.1610. Found: 380.1601 ($C_{21}H_{22}N_3O_4$).

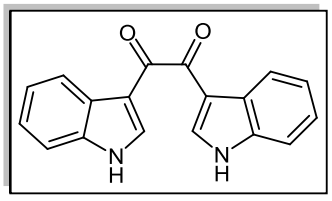
5.2.6 Synthesis of imidazo[4,5-*c*]indolo[2,3-*a*]carbazoles

5.2.6.1 1*H*-Indol-3-yl glyoxylyl chloride 231[40]



Indole **171** (1.001 g, 8.6 mmol) was placed in a 50 mL round-bottomed flask, along with diethyl ether (20 mL). Oxalyl chloride (1.1 mL, 11.46 mmol) was then added carefully to the flask over 10 minutes and the straw coloured slurry was allowed to stir at room temperature for a further 30 minutes. The product was filtered on a Hirsch funnel and washed with cool mother liquor (5-10 mL). The glyoxalyl chloride **231** produced, yielded a crop of yellow crystals (1.623 g, 90 %); m.p. 120-122°C (lit.[40] 128°C); ν_{max}/ cm^{-1} (KBr) 3400, 1730, 1680, 1590

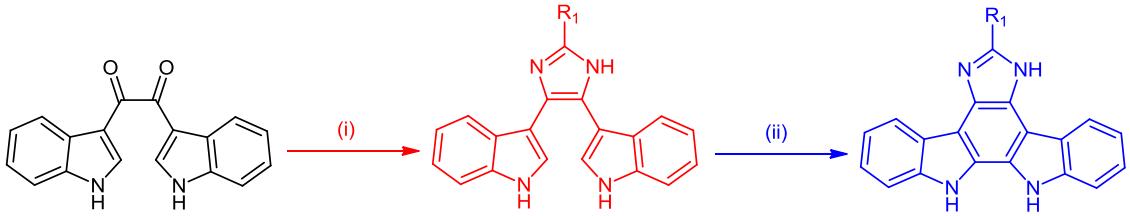
5.2.6.2 1,2-Bis(1*H*-indol-3-yl)ethane-1,2-dione 565[41]



Indole-3-glyoxylyl chloride **231** (4.164 g, 20 mmol) was added in portions over a period of 5 minutes, to a suspension of aluminium chloride (12.076 g, 90 mmol), in a mixture of dichloroethane (20 mL) and heptane (10 mL), with stirring, and at room temperature. A solution of indole **171** (3.863 g, 33 mmol) in dichloroethane (20 mL), was added dropwise under vigorous stirring, to the dark brown slurry, and then stirred for a further 3 hours. The reaction mixture was poured into an ice-water (100 mL), and extracted into ethyl acetate (3 × 120 mL). The combined extracts were dried over magnesium sulfate, filtered, and evaporated under vacuum. The formed residue was triturated with ether/ absolute ethanol (20:1) (150 mL), and the final product was collected by vacuum filtration, dried and title compound **565** isolated as a brown powder (2.614 g, 45%); m.p. 267-270°C (lit.[41] 278-280°C); ν_{max}/ cm^{-1} (KBr) 3305, 1709, 1603, 1511; δ_H (300 MHz, DMSO-d_6) 7.26-7.32 [4H, m, aromatic C-$H_{5,5',6,6'}$], 7.54-7.57 [2H, m, aromatic C-

$H_{7,7'}$], 8.23 [2H, aromatic C-$H_{2,2'}$], 8.27-8.30 [2H, m, aromatic C-$H_{4,4'}$], 12.24 [2H, s, 2 × NH]; δ_C (75 MHz, DMSO-d_6) 112.5 (2C, 2 × aromatic C), 112.5 (2CH, 2 × aromatic CH), 121.3 (2CH, 2 × aromatic CH), 122.4 (2CH, 2 × aromatic CH), 123.4 (2CH, 2 × aromatic CH), 125.6 (2C, 2 × aromatic C), 136.7 (2C, 2 × aromatic C), 137.3 (2CH, 2 × aromatic CH), 188.8 (2C, 2 × C=O); m/z (ES+) 289.1 $[M+H]^+$ (100%). (ES-) 287.1 $[M-H]^-$ (100%).

5.2.6.3 Synthesis of 2-substituted 8,9-dihydro-1*H*-imidazo[4,5-*c*]indolo[2,3-*a*]carbazoles



565 **564** **449**

Table 5.5: Characteristic data for crude compounds 566, 569, 567, 570, 568 and 571

Compound	R_1	IR (cm^{-1})	HRMS (m/z)	Formula
566[#]	thien-2-yl	3396, 3055, 1619, 1572, 1456	381.1172	$C_{23}H_{17}N_4S$ (381.1174)
569[¥]	thien-2-yl	3394, 3055, 2922, 1640, 1583, 1456	379.1006	$C_{23}H_{15}N_4S$ (379.1017)
567[#]	isopropyl	3390, 2919, 1557, 1410	341.1772	$C_{22}H_{21}N_4$ (341.1766)
570[¥]	isopropyl	3374, 3269, 2964, 1706, 1619, 1456	339.1607	$C_{22}H_{19}N_4$ (339.1610)
568[#]	3,4,5-trimethoxyphenyl	3368, 2936, 1589, 1503, 1457	465.1931	$C_{28}H_{25}N_4O_3$ (465.1927)
571[¥]	3,4,5-trimethoxyphenyl	3333, 2936, 1589, 1502, 1457	463.1768	$C_{28}H_{23}N_4O_3$ (463.1770)

General reaction schemes: [#](i) Aldehyde (1 eq.) was added to a mixture of dione **565** and ammonium acetate (10 eq.), along with acetic acid (10 mL/ mmol), and heating of the red mixture at 110°C was commenced for 24 hours. The reaction was then concentrated *in vacuo*, prior to washing with aqueous saturated $NaHCO_3$ and extraction with DCM. The crude imidazole derivative **564** was isolated by flash chromatography (100% DCM – 2% methanol/DCM), but could not be satisfactorily purified, as confirmed by NMR spectroscopy.

[¥](ii) 3,3'-(2-Substituted 1*H*-imidazol-4,5-diyl)bis(1*H*-indole) (**564**) was stirred in acetonitrile (0.8 mL/ µmol substrate), along with a catalytic amount of iodine. U.V. irradiation of the dark red mixture, in the presence of air, then proceeded overnight. Following concentration of the reaction mixture, flash chromatography (0.5% MeOH/DCM) afforded the fluorescent product (**449**) as a single intense spot in TLC, in moderate to good yields. As for the corresponding unaromatised series, several inseparable impurities present prevented clean isolation of the desired indolocarbazole product in each case.

5.2.6.3.1 [#]3,3'-(2-(Thiophen-2-yl)-1*H*-imidazol-4,5-diyl)bis(1*H*-indole) 566

Applying general scheme (i) starting from dione **565** (1.002 g, 3.47 mmol), ammonium acetate (2.682 g, 34.72 mmol, 10 eq.) and thiophene-2-carboxaldehyde (0.33 mL, 3.47 mmol), afforded **566** as an amorphous red powder (0.460 g, 35%).

5.2.6.3.2 [#]3,3'-(2-Isopropyl-1*H*-imidazol-4,5-diyl)bis(1*H*-indole) 567

Applying general scheme (i) starting from dione **565** (0.580 g, 2.01 mmol), ammonium acetate (1.550 g, 20.1 mmol, 10 eq.) and isobutyraldehyde (0.2 mL, 2.01 mmol) afforded **567** as a crystalline light brown solid (0.258 g, 37%).

5.2.6.3.3 [#]3,3'-(2-(3,4,5-Trimethoxyphenyl)-1*H*-imidazol-4,5-diyl)bis(1*H*-indole) 568

Applying general scheme (i) starting from dione **565** (0.700 g, 2.43 mmol), ammonium acetate (1.901 g, 24.3 mmol, 10 eq.) and 3,4,5-trimethoxybenzaldehyde (0.487 g, 2.43 mmol), afforded imidazole analogue **568** as an amorphous red powder (0.905 g, 80%).

5.2.6.3.4 [¥]2-(Thiophen-2-yl)-8,9-dihydro-1*H*-imidazo[4,5-*c*]indolo[2,3-*a*]carbazole 569

According to general scheme (ii), 3,3'-(2-(thiophen-2-yl)-1*H*-imidazol-4,5-diyl)bis(1*H*-indole) **566** (0.100 g, 0.26 mmol) was irradiated in the presence of acetonitrile (150 mL) for 16 hours, to afford imidazo[3,4-*c*]carbazole **569** as a crystalline red solid (0.024 g, 25%).

5.2.6.3.5 [¥]2-Isopropyl-8,9-dihydro-1*H*-imidazo[4,5-*c*]indolo[2,3-*a*]carbazole 570

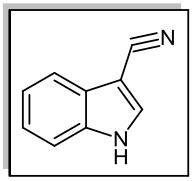
Procedure outlined in general scheme (ii), employing 3,3'-(2-isopropyl-1*H*-imidazol-4,5-diyl)bis(1*H*-indole **567** (0.100 g, 0.29 mmol), irradiated in acetonitrile (250 mL) for 16 hours, provided indolocarbazole **570** as a crystalline red solid (0.032 g, 33%).

5.2.6.3.6 [¥]2-(3,4,5-Trimethoxyphenyl)-8,9-dihydro-1*H*-imidazo[4,5-*c*]indolo[2,3-*a*]carbazole 571

As outlined in general scheme (ii), 3,3'-(2-(3,4,5-trimethoxyphenyl)-1*H*-imidazol-4,5-diyl)bis(1*H*-indole) **568** (0.200 g, 0.43 mmol), irradiated along with acetonitrile (300 mL) for 16 hours, produced novel indolocarbazole **571** as a dark red powder (0.182 g, 92%).

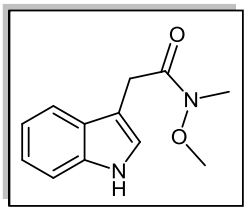
5.2.7 Synthesis of miscellaneous 3-substituted indole compounds

5.2.7.1 1*H*-Indol-3-yl carbonitrile 481[42]



1*H*-Indole-3-carboxaldehyde **121** (2.004 g, 13.8 mmol) was dissolved in dry DMF (30 mL), forming a reddish solution which was heated to reflux and maintained at this temperature for 15 minutes. Hydroxylamine hydrochloride (1.163 g, 16.6 mmol, 1.2 eq.) was then added to the vessel and reflux continued for a further 30 minutes. The heating source was removed and the reaction cooled to room temperature. Water (100 mL) was then added and the resultant slurry cooled to 0°C for several minutes. The precipitated 3-cyanoindole **481** was then filtered and dried (1.202 g, 61%); m.p. 177-179°C (lit.[43] 176-177°C); ν_{max}/ cm^{-1} (KBr) 3225, 2227, 1525, 1429, 1380; δ_H (300 MHz, DMSO-d_6) 7.21-7.26 [1H, td, *J* 7.2, 1.2, aromatic C-H$_5$], 7.26-7.32 [1H, td, *J* 7.1, 1.4, aromatic C-H$_6$], 7.55-7.58 [1H, d, *J* 7.4, aromatic C-H$_7$], 7.63-7.65 [1H, d, *J* 7.5, aromatic C-H$_4$], 8.25-8.26 [1H, d, *J* 3.0, aromatic C-H$_2$], 12.23 [1H, bs, NH]; δ_C (75 MHz, DMSO-d_6) 84.1 (CN), 112.9 (CH, aromatic CH), 116.4 (C, aromatic C), 118.4 (CH, aromatic CH), 121.6 (CH, aromatic CH), 123.3 (CH, aromatic CH), 126.7 (C, aromatic C), 134.5 (CH, aromatic CH), 135.2 (C, aromatic C); m/z (ES-) 141.0 [M-H]$^-$ (100%).

5.2.7.2 2-(1*H*-Indol-3-yl)-*N*-methoxy-*N*-methylacetamide 575[44]

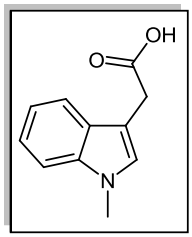


1,1-Carbonyldiimidazole (3.392 g, 18.8 mmol, 1.1 eq.) was added portionwise to a mixture of indole-3-acetic acid **233** (3.008, 17.2 mmol) and DCM (40 mL), and stirred under nitrogen for 2 hours, at room temperature. *N*,*O*-Dimethylhydroxylamine hydrochloride (1.871 g, 18.8 mmol, 1.1 eq.) was then added to the reaction mixture and stirred for 16 hours. The reaction contents were then poured into an ice-water mixture (200 mL) and adjusted to pH 10 with 30% NaOH, prior to extracting with ethyl acetate (2 × 120 mL). These organic layers were combined, washed with 10% HCl (150 mL), dried over magnesium sulfate, filtered and evaporated under reduced pressure to yield the Weinreb amide **575** as dark pink plates (3.429 g, 91%); m.p. 118-120°C (lit.[44] 125-127°C); ν_{max}/ cm^{-1} (KBr) 3281, 2972, 2936, 1656, 1460; δ_H (300 MHz, $CDCl_3$) 3.21 [3H, s, N-CH$_3$], 3.65 [3H s, O-CH$_3$], 3.90 [2H, s, CH$_2$], 7.08 [1H, s, aromatic C-H$_2$], 7.11-7.18 [2H, m, aromatic C-H$_{5,6}$], 7.28-7.31 [1H, d, *J* 7.5, aromatic C-H$_7$], 7.63-7.65 [1H, d, *J* 7.3, aromatic C-H$_4$], 8.29 [1H, bs, NH]; δ_C (75 MHz, $CDCl_3$) 29.0 (CH$_2$, $\underline{C}$H$_2$CO), 32.3 (CH$_3$, N-CH$_3$), 61.4 (CH$_3$, N-O$\underline{C}$H$_3$), 108.9 (C, aromatic C), 111.2 (CH, aromatic CH), 118.8 (CH, aromatic CH), 119.5

(CH, aromatic CH), 122.0 (CH, aromatic CH), 123.2 (CH, aromatic CH), 127.4 (C, aromatic C), 136.1 (C, aromatic C), 172.9 (C, C=O); m/z (ES+) 219.1 $[M+H]^+$ (100%).

5.2.7.3 1-Methyl-1*H*-indol-3-yl acetic acid 225[45]

Method A:

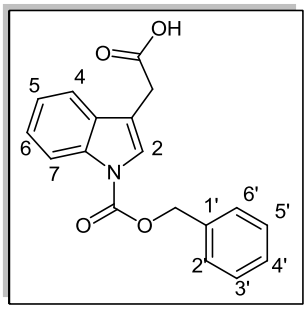


To a suspension of NaH (0.377 g, 11.3 mmol, 1.5 eq.) (60% dispersion in mineral oil) in dry THF (25 mL), at 0°C, was initially added a solution of indole-3-acetic acid **233** (1.312 g, 7.5 mmol) in THF (10 mL). After stirring for 30 minutes, a solution of iodomethane (0.4 mL, 6.25 mmol) in THF (5 mL) was then added dropwise over 5 minutes. The reaction was slowly warmed to room temperature and allowed to stir overnight. The reaction was subsequently cooled to 0°C, prior to quenching by the slow addition of MeOH (2 mL), along with vigorous stirring. Water (50 mL) was then carefully added until the appearance of a clear yellow solution. Ether (100 mL) was also delivered and the separated aqueous phase, acidified with 10% HCl (150 mL) and extracted with DCM (3 × 70 mL). On drying with magnesium sulfate, filtration and concentration of the reaction to dryness, the crude residue was recrystallised from EtOH to afford 1-methyl-1*H*-indol-3-yl acetic acid **225**, as a pale brown solid (1.33 g, 94%), which was used without further purification; m.p 123-126°C (lit.[46] 127-129°C); ν_{max}/ cm^{-1} (KBr) 3064, 2976, 2934, 1710, 1632, 1526; δ_H (300 MHz, $CDCl_3$) 3.73 [3H, s, N-CH_3], 3.78 [2H, s, CH_2], 7.02 [1H, s, aromatic C-H_2], 7.09-7.14 [1H, td, *J* 7.9, 1.1, aromatic C-H_5], 7.20-7.25 [1H, td, *J* 7.7, 0.9, aromatic C-H_6], 7.27-7.30 [1H, d, *J* 8.1, aromatic C-H_7], 7.57-7.59 [1H, d, *J* 7.9, aromatic C-H_4]; δ_C (75 MHz, $CDCl_3$) 31.0 (CH_2, $\underline{C}H_2CO_2H$), 32.7 (CH_3, N-CH_3), 106.1 (C, aromatic C), 109.4 (CH, aromatic CH), 119.0 (CH, aromatic CH), 119.3 (CH, aromatic CH), 121.9 (CH, aromatic CH), 127.6 (C, aromatic C), 127.9 (CH, aromatic CH), 136.9 (C, aromatic C), 178.4 (C, C=O); m/z (ES+) 190.2 $[M+H]^+$ (100%).

Method B:

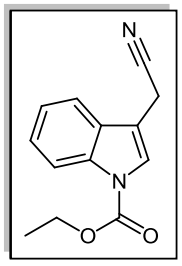
Methyl 1*H*-indol-3-yl acetate **480** (1.012 g, 4.99 mmol) was initially suspended in EtOH (50 mL), and vigorously stirred in the presence of an aqueous LiOH solution (1M, 200 mL). Following reaction at 35°C for 20 hours, the solution was recooled to room temperature and adjusted to pH 4 with aqueous 10% HCl. On further cooling to 0°C, the slurry was filtered and subsequently dried, to yield the title compound **225** as a light brown powder (0.670 g, 71%).

5.2.7.4 1-Benzyloxycarbonyl-1*H*-indol-3-yl acetic acid 576[47]



A solution of indole-3-acetic acid **233** (1.004 g, 5.70 mmol) was stirred in THF at −78°C along with 1.8M LDA (7.0 mL, 12.54 mmol, 2.2 eq.), which was added dropwise, under inert atmosphere. Following continued stirring at this temperature for 1 hour, benzyl chloroformate (1.0 mL, 6.84 mmol, 1.2 eq.) was added and the reaction contents vigorously stirred for 2 hours. Following solvent evaporation, the dark residue was redissolved in water (150 mL) and extracted with ether (2 × 120 mL). Acidification of the aqueous phase to pH 3 with 10% HCl resulted in the formation of a precipitate, which was filtered and dried to afford the protected acid **576**, as an off-white amorphous powder (1.235 g, 70%); m.p. 145-148°C (lit.[47] 152°C); ν_{max}/ cm^{-1} (KBr) 3140, 3030, 1733, 1696, 1454; δ_H (300 MHz, $CDCl_3$) 3.72 [2H, s, $C\underline{H}_2CO_2H$], 5.47 [2H, s, O-$C\underline{H}_2$Ph], 7.24-7.30 [1H, t, *J* 8.4, aromatic C-H_5], 7.32-7.37 [1H, t, *J* 8.3, aromatic C-H_6], 7.39-7.44 [1H, t, *J* 6.8, aromatic C-$H_{4'}$], 7.42-7.46 [2H, t, *J* 7.6, aromatic C-$H_{2'}$ & aromatic C-$H_{6'}$], 7.52-7.55 [2H, d, *J* 7.5, aromatic C-$H_{3'}$ & aromatic C-$H_{5'}$], 7.57-7.60 [1H, d, *J* 7.7, aromatic C-H_7], 7.68 [1H, s, aromatic C-H_2], 8.08-8.10 [1H, d, *J* 8.1, aromatic C-H_4], 12.41 [1H, bs, CO_2H]; δ_C (75 MHz, $CDCl_3$) 30.2 (CH_2, $\underline{C}H_2CO_2H$), 68.3 (CH_2, O-CH_2), 114.5 (CH, aromatic CH), 115.1 (C, aromatic C), 119.7 (CH, aromatic CH), 122.8 (CH, aromatic CH), 124.0 (CH, aromatic CH), 124.6 (CH, aromatic CH), 128.3 (2CH, phenyl C-$H_{3'}$ & phenyl C-$H_{5'}$), 128.5 (CH, phenyl C-$H_{4'}$), 128.6 (2CH, phenyl C-$H_{2'}$ & phenyl C-$H_{6'}$), 130.2 (C, phenyl $C_{1'}$), 134.7 (C, aromatic C], 135.4 (C, aromatic C), 150.1 (C, N-$\underline{C}O_2CH_2Ph$), 172.0 (C, CO_2H); m/z (ES+) 310.1 $[M+H]^+$, (20%), 266.0 $[M+H-CO_2]^+$, (100%), (ES-) 617.2 $[2M-H]^-$ (100%), 308.1 $[M-H]^-$ (20%).

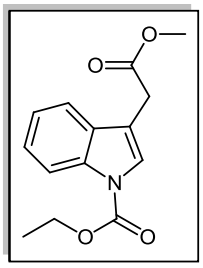
5.2.7.5 1-Ethoxycarbonyl-1*H*-indol-3-yl acetonitrile 577[48]



Ethyl chloroformate (1.08 mL, 10.9 mmol) was slowly added to a rapidly stirring mixture of 3-indolylacetonitrile **229** (1.503 g, 9.6 mmol), TBAB (0.054 g, 0.17 mmol) and 30% NaOH solution (30 mL) in dry DCM (30 mL). The reaction mixture was initially stirred for 1 hour at 0°C, and allowed to stir at ambient temperature overnight. Stirring was ceased, and the distinct layers were permitted to separate; extraction of the aqueous layer was performed with DCM (2 × 100 mL), and the combined DCM layers were then washed successively with water (3 × 150 mL) and brine (250 mL), dried with magnesium sulfate and evaporated *in vacuo*. The crude acetonitrile **577** was then purified by column

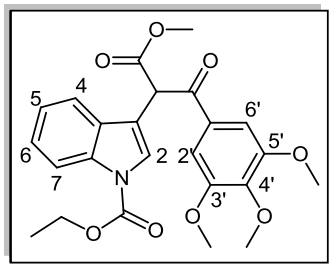
chromatography, with 20% ethyl acetate/ hexane as eluent, to afford derivative **577** as a colourless oil, which solidified to an off-white residue on further drying (0.522 g, 23%); m.p. 56-58^{o}C; ν_{max}/ cm^{-1} (KBr) 2910, 2252, 1729, 1612; δ_H (300 MHz, $CDCl_3$) 1.45-1.50 [3H, t, *J* 7.1, N-$CO_2CH_2C\underline{H}_3$], 3.76 [2H, s, $C\underline{H}_2CN$], 4.46-4.53 [2H, q, *J* 7.1, N-$CO_2C\underline{H}_2CH_3$], 7.28-7.33 [1H, td, *J* 7.5, 1.0, aromatic C-H_5], 7.37-7.42 [1H, td, *J* 7.7, 1.0, aromatic C-H_6], 7.50-7.53 [1H, d, *J* 7.8, aromatic C-H_7], 7.68 [1H, s, aromatic C-H_2], 8.19-8.21 [1H, d, *J* 8.2, aromatic C-H_4]; δ_C (75 MHz, $CDCl_3$) 14.4 (CH_2, $\underline{C}H_2CN$), 14.4 (CH_3, N-$CO_2CH_2\underline{C}H_3$), 63.6 (CH_2, N-$CO_2\underline{C}H_2CH_3$), 110.3 (C, aromatic C), 115.6 (CH, aromatic CH), 117.0 (C, C≡N), 118.3 (CH, aromatic CH), 123.3 (CH, aromatic CH), 123.9 (CH, aromatic CH), 125.5 (CH, aromatic CH), 128.5 (C, aromatic C), 135.6 (C, aromatic C), 150.6 (C, C=O); m/z (ES+) 229.0 $[M+H]^+$ (100%), (ES-) 227.1 $[M-H]^-$ (60%).

5.2.7.6 1-Ethoxycarbonyl methyl 1*H*-indol-3-yl acetate 578[48]



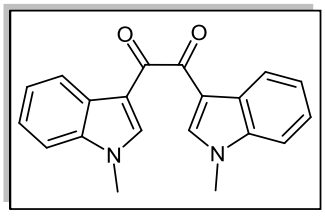
Ethyl chloroformate (4.83 mL, 48.8 mmol) was cautiously added over a 15 minute period, to a rapidly stirring mixture of methyl indole-3-acetate **239** (8.018 g, 42.4 mmol), TBAB (0.238 g, 0.768 mmol) and 30% NaOH solution (150 mL) in dry DCM (150 mL). Following vigorous stirring of the bi-phasic mixture for 1 hour at 0^{o}C, both layers were allowed to separate. Following extraction of the aqueous layer with DCM (2 × 200 mL), the combined organic layers were washed successively with water (3 × 250 mL) and brine (300 mL), dried with magnesium sulfate and evaporated *in vacuo*. The crude carbamate **578** was then purified by column chromatography, with 20% ethyl acetate/ hexane as eluent, yielding a colourless oil (8.532 g, 77%); ν_{max}/ cm^{-1} (KBr) 2983, 1738, 1732, 1613, 1574, 1455; δ_H (300 MHz, $CDCl_3$) 1.44-1.48 [3H, t, *J* 7.1, N-$CO_2CH_2C\underline{H}_3$], 3.72 [3H, s, $CO_2C\underline{H}_3$], 3.73 [2H, s, $C\underline{H}_2CO_2CH_3$], 4.44-4.51 [2H, q, *J* 7.1, N-$CO_2C\underline{H}_2CH_3$], 7.24-7.30 [1H, td, *J* 7.6, 1.0, aromatic C-H_5], 7.32-7.38 [1H, td, *J* 7.4, 1.2, aromatic C-H_6], 7.52-7.55 [1H, d, *J* 7.5, aromatic C-H_7], 7.62 [1H, s, aromatic C-H_2], 8.17-8.19 [1H, d, *J* 8.0, aromatic C-H_4]; δ_C (75 MHz, $CDCl_3$) 14.4 (CH_3, O-$CH_2\underline{C}H_3$), 30.9 (CH_2, C-$\underline{C}H_2CO_2CH_3$), 52.2 (CH_3, $CO_2\underline{C}H_3$), 63.2 (CH_2, $CO_2\underline{C}H_2CH_3$), 113.8 (C, aromatic C), 115.3 (CH, aromatic CH), 119.1 (CH, aromatic CH), 122.9 (CH, aromatic CH), 124.1 (CH, aromatic CH), 124.8 (CH, aromatic CH), 130.1 (C, aromatic C), 135.4 (C, aromatic C), 150.9 (C, N-$\underline{C}O_2CH_2CH_3$), 171.4 (C, $\underline{C}O_2CH_3$); m/z (ES+) 262.1 $[M+H]^+$ (55%).

5.2.7.7 Ethyl 3-(1-methoxy-1,3-dioxo-3-(3,4,5-trimethoxyphenyl)propan-2-yl)-1*H*-indole-1-carboxylate 579



LDA solution (1.8M) (37.4 mL, 67.5 mmol, 2.2 eq.) was added dropwise over a period of 20 minutes, to dry THF (30 mL), at −78°C, under nitrogen atmosphere. A mixture of carbamate protected ester **578** (8.014 g, 30.7 mmol) in THF (3 mL) was then added to the reaction vessel, at a sufficient rate to maintain the internal reaction temperature below −65°C, during addition. The dark brown solution was then stirred vigorously for 90 minutes. 3,4,5-Trimethoxybenzoyl chloride **499** (10.502 g, 46.1 mmol, 1.5 eq.) was then dissolved in dry THF (15 mL) and added to the reaction vessel slowly, over 15 minutes. Stirring of the dark mixture proceeded at room temperature overnight. Following solvent removal, the product residue was extracted with ethyl acetate (3 × 150 mL), and washed with saturated ammonium chloride (250 mL), water (4 × 250 mL) and brine (2 × 150 mL). The combined organic layers were dried using magnesium sulfate, filtered and evaporated *in vacuo*. The optimized yield of the product β-ketoester **579**, a light brown solid, following column chromatography (4.325 g, 31%); m.p. 117-120°C; ν_{max}/ cm^{-1} (KBr) 2958, 1751(s), 1679, 1583, 1505; δ_H (300 MHz, $CDCl_3$) 1.43-1.47 [3H, t, *J* 7.1, N-$CO_2CH_2C\underline{H}_3$], 3.79 [6H, s, 2 × *m*-OCH_3], 3.80 [3H, s, *p*-OCH_3], 3.88 [3H, s, $CO_2C\underline{H}_3$], 4.43-4.50 [2H, q, *J* 7.1, N-$COC\underline{H}_2CH_3$], 5.79 [1H, s, $CH_3CO_2C\underline{H}CO$], 7.25 [2H, s, aromatic C-$H_{2',6'}$], 7.27-7.33 [1H, t, *J* 7.6, aromatic C-H_5], 7.35-7.39 [1H, t, *J* 7.9, aromatic C-H_6], 7.64-7.67 [1H, d, *J* 7.3, aromatic C-H_7], 7.77 [1H, s, aromatic C-H_2], 8.20-8.23 [1H, d, *J* 8.0, aromatic C-H_4]; δ_C (75 MHz, $CDCl_3$) 14.4 (CH_3, $CO_2CH_2\underline{C}H_3$), 51.5 (CH, $CH_3CO_2\underline{C}HCO$), 53.0 (CH_3, $CO_2\underline{C}H_3$), 56.2 (CH_3, 2 × *m*-OCH_3), 61.0 (CH_3, *p*-OCH_3), 63.5 (CH_2, $CO_2\underline{C}H_2CH_3$), 106.3 (2CH, 2 × aromatic CH), 113.2 (C, aromatic C), 115.6 (CH, aromatic CH), 118.5 (CH, aromatic CH), 123.2 (2CH, 2 × aromatic CH), 125.2 (CH, aromatic CH), 125.7 (C, aromatic C), 129.0 (C, aromatic C), 130.2 (C, aromatic C), 135.4 (C, aromatic C), 143.1 (C, N-$\underline{C}O_2CH_2CH_3$), 153.1 (2C, 2 × aromatic C), 168.9 (C, $\underline{C}O_2CH_3$), 191.4 (C, $CH_3CO_2CH\underline{C}O$); m/z (ES+) 456.1 $[M+H]^+$ (100%); HRMS - (ES+) requires: 456.1658. Found: 456.1656 ($C_{24}H_{26}NO_8$).

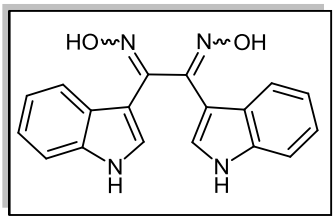
5.2.7.8 1,2-Bis(1-methyl-1*H*-indol-3-yl)ethane-1,2-dione 580[22]



To a suspension of sodium hydride (60% dispersion in mineral oil) (0.822 g, 12.2 mmol, 5 eq.) in DMF (15 mL), cooled to 0°C, was slowly added a solution of 1,2-bis(1*H*-indol-3-yl) ethane-

1,2-dione **565** (0.701 g, 2.4 mmol) in DMF (10 mL), along with vigorous stirring of the dark brown reaction mixture. Following stirring for 45 minutes, a solution of iodomethane (0.5 mL, 7.3 mmol, 3 eq.) in DMF (3 mL) was added dropwise over 10 minutes and reacted for an additional 15 minutes, prior to attaining room temperature and proceeding overnight. At this point, the reaction was diluted with ethyl acetate (250 mL) and poured into an aqueous solution of HCl (0.5M, 300 mL). Following initial extraction, the crude product was then washed with further portions of 10% HCl (2 x 250 mL). The final organic extract was then dried over magnesium sulfate, filtered and evaporated *in vacuo*, prior to chromatographic purification employing 20%-100% ethyl acetate/ hexane, in order to afford **580** as a brown powder (0.600 g, 78%); m.p. 255-259^{o}C (lit.[22] 268-269^{o}C); ν_{max}/ cm^{-1} (KBr) 1607, 1524, 1460; δ_H (300 MHz, DMSO-d_6) 3.89 [6H, s, 2 x N-CH$_3$], 7.34-7.39 [4H, m, aromatic C-H$_{5,5',6,6'}$], 7.59-7.62 [2H, m, aromatic C-H$_{7,7'}$], 8.30-8.33 [2H, m, aromatic C-H$_{4,4'}$], 8.31 [2H, s, aromatic C-H$_{2,2'}$]; δ_C (75 MHz, DMSO-d_6) 33.2 (2CH$_3$, 2 × N-CH$_3$), 111.0 (2CH, 2 × aromatic CH), 111.3 (2C, 2 × aromatic C), 121.4 (2CH, 2 × aromatic CH), 122.8 (2CH, 2 × aromatic CH), 123.5 (2CH, 2 × aromatic CH), 126.0 (2C, 2 × aromatic C), 137.4 (2C, 2 × aromatic C), 140.8 (2CH, 2 × aromatic CH), 188.2 (2C, 2 × C=O); m/z (ES+) 317.1 $[M+H]^+$ (100%).

5.2.7.10 1,2-Bis(1*H*-indol-3-yl)ethane-1,2-dione dioxime 581[49]



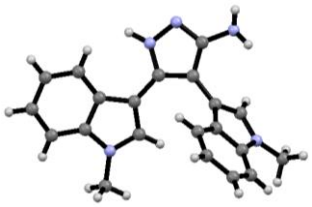
To a mixture of dione **565** (0.259 g, 0.90 mmol) and hydroxylamine hydrochloride (1.260 g, 1.80 mmol, 2 eq.), stirred in absolute ethanol (10 mL) at room temperature, was added pyridine (0.4 mL). The reaction was then heated at 90^{o}C for 16 hours. Following solvent evaporation, the residue was dissolved in ethyl acetate (3 × 80 mL), washed with brine (3 × 70 mL), dried over magnesium sulfate and filtered. The crude product was subsequently purified by ethyl acetate/hexane gradient chromatography to yield the target compound **581** as a white powder (0.153 g, 53%); m.p. 186-190^{o}C (lit.[49] 189-192^{o}C); ν_{max}/ cm^{-1} (KBr) 3327, 1614, 1541, 1458, 1425, 1245; δ_H (300 MHz, DMSO-d_6) 7.09-7.19 [6H, m, 6 × aromatic C-H$_{2,2',5,5',6,6'}$], 7.40-7.42 [2H, d, *J* 7.7, aromatic C-H$_{7,7'}$], 8.14-8.17 [2H, d, *J* 7.6, aromatic C-H$_{4,4'}$], 10.57 [2H, bs, 2 × NH], 11.26 [2H, bs, 2 × N-OH]; m/z (ES+) 319.1 $[M+H]^+$ (50%), 115.0 (100%).

5.2.8 Single crystal X-ray diffraction studies in 5-aminopyrazole series

Instrumentation

Single crystal X-ray data was collected at University College Cork on a Bruker APEX II DUO diffractometer at temperatures between 100 – 293 K or on a Bruker X2S at a temperature of 293 K using graphite monochromatic Mo Kα (λ = 0.7107 Å) radiation. The structures were solved using direct methods and refined on F^2 using SHELXL-97. Analysis was undertaken with the SHELX suite of programs and diagrams prepared with Mercury 2.3. All non-hydrogen atoms were located and refined with anisotropic thermal parameters. Hydrogen atoms were included in calculated positions or they were located and refined with isotropic thermal parameters.

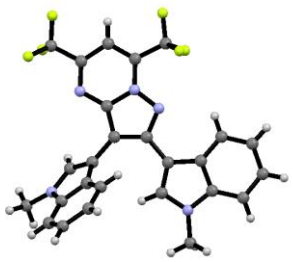
5.2.8.1 3,4-Bis(1-methyl-1*H*-indol-3-yl)-1*H*-pyrazol-5-amine 447



Experimental Reference: 5.2.4.5

Crystal Data: $C_{21}H_{19}N_5$, M = 341.41, monoclinic, a = 9.6026(18) Å, b = 16.309(3) Å, c = 11.000(2) Å, β = 105.049(4) °, V = 1663.6(5) Å^3, T = 100.0(2) K, space group $P2_1/n$, Z = 4, 12307 reflections measured, 2962 unique (R_{int} = 0.1267). The final R_1 values were 0.0557 ($I > 2\sigma(I)$) and 0.1315 (all data). The final $wR(F^2)$ values were 0.1062 ($I > 2\sigma(I)$) and 0.1305 (all data).

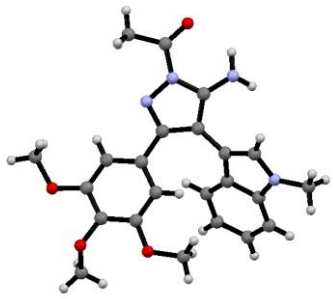
5.2.8.2 2,3-Bis(1-methyl-1*H*-indol-3-yl)-5,7-bis(trifluoromethyl) pyrazolo[1,5-*a*]pyrimidine 549



Experimental Reference: 5.2.4.12

Crystal Data: $C_{26}H_{17}F_6N_5$, M = 513.45, monoclinic, a = 8.1163(15) Å, b = 14.851(4) Å, c = 18.933(5) Å, β = 95.576(8) °, V = 2271.3(10) Å^3, T = 150.0(2) K, space group $P2_1/n$, Z = 4, 21091 reflections measured, 4027 unique (R_{int} = 0.0455). The final R_1 values were 0.0402 ($I > 2\sigma(I)$) and 0.0752 (all data). The final $wR(F^2)$ values were 0.0871 ($I > 2\sigma(I)$) and 0.1011 (all data).

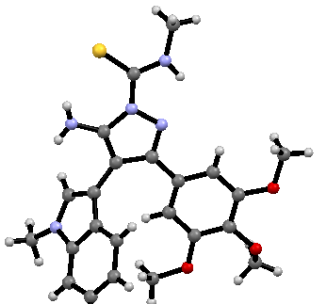
5.3.8.3 1-(5-Amino-4-(1-methyl-1*H*-indol-3-yl)-3-(3,4,5-trimethoxyphenyl)-1*H*-pyrazol-1-yl)ethanone 557



Experimental Reference: 5.2.5.4

Crystal Data: $C_{23}H_{24}N_4O_4$, *M* = 420.46.43, triclinic, a = 10.027(4) Å, b = 10.830(5) Å, c = 10.880(6) Å, α = 89.654(15) °, β = 71.175(15) °, γ = 81.995(15) °, V = 1106.4(9) Å^3, T = 300.0(2) K, space group *P*-1, *Z* = 2, 2659 reflections measured, 2110 unique (R_{int} = 0.0238). The final R_1 values were 0.0550 ($I > 2\sigma(I)$) and 0.0939 (all data). The final $wR(F^2)$ values were 0.1183 ($I > 2\sigma(I)$) and 0.1367 (all data).

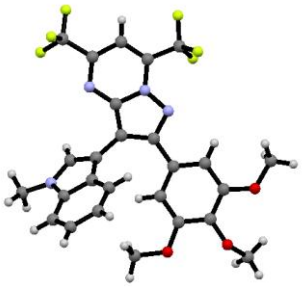
5.3.8.4 5-Amino-*N*-methyl-4-(1-methyl-1*H*-indol-3-yl)-3-(3,4,5-trimethoxyphenyl)-1*H*-pyrazole-1-carbothioamide 559



Experimental Reference: 5.2.5.6

Crystal Data: $C_{23}H_{25}N_5O_3S$, *M* = 451.54, monoclinc, a = 16.1052(17) Å, b = 9.5800(11) Å, c = 14.6359(15) Å, β = 92.806(4) °, V = 2255.4(4) Å^3, T = 300.0(2) K, space group $P2_1/c$, *Z* = 4, 20990 reflections measured, 3961 unique (R_{int} = 0.0448). The final R_1 values were 0.0552 ($I > 2\sigma(I)$) and 0.0768 (all data). The final $wR(F^2)$ values were 0.1532 ($I > 2\sigma(I)$) and 0.1699 (all data).

5.2.8.3 3-(1-Methyl-1*H*-indol-3-yl)-5,7-bis(trifluoromethyl)-2-(3,4,5-pyrazolo[1,5-*a*]pyrimidine 563



Experimental Reference: 5.2.5.10

Crystal Data: $C_{26}H_{20}F_6N_4O_3$, *M* = 550.45, triclinic, a = 13.960(2) Å, b = 14.052(2) Å, c = 14.580(2) Å, α = 114.173(3) °, β = 108.342(4) °, γ = 93.100(4) °, V = 2420.7(7) Å^3, T = 100.0(2) K, space group *P*-1, *Z* = 4, 51437 reflections measured, 9691 unique (R_{int} = 0.0758). The final R_1 values were 0.0550 ($I > 2\sigma(I)$) and 0.1108 (all data). The final $wR(F^2)$ values were 0.1295 ($I > 2\sigma(I)$) and 0.1661 (all data).

5.3 References

1. Wood, J. L.; Stoltz, B. M.; Dietrich, H. J.; Pflum, D. A.; Petsch, D. T. *J.Am.Chem.Soc.* **1997**, *119*, 9641-9651.
2. Barry, J. F.; Wallace, T. W.; Walshe, N. D. A. *Tetrahedron* **1995**, *51*, 12797-12806.
3. Dubernet, M.; Caubert, V.; Guillard, J.; Viaud-Massuard, M. C. *Tetrahedron* **2005**, *61*, 4585-4593.
4. Witulski, B.; Schweikert, T. *Synthesis* **2005**, 1959-1966.
5. Joyce, R. P.; Gainor, J. A.; Weinreb, S. M. *J.Org.Chem.* **1987**, *52*, 1177-1185.
6. Faul, M. M.; Winneroski, L. L.; Krumrich, C. A. *J.Org.Chem.* **1998**, *63*, 6053-6058.
7. Downie, I. M.; Earle, M. J.; Heaney, H.; Shuhaibar, K. F. *Tetrahedron* **1993**, *49*, 4015-4034.
8. Katritzky, A. R. *J.Chem.Soc.* **1955**, 2586-2594.
9. Roy, S.; Roy, S.; Gribble, G. W. *Org.Lett.* **2006**, *8*, 4975-4977.
10. Bergman, J. *Acta Chem.Scand.* **1971**, *25*, 1277-1280.
11. Desarbre, E.; Bergman, J. *J.Chem.Soc., Perkin Trans.1* **1998**, 2009-2016.
12. Murray, P. E.; McNally, V. A.; Lockyer, S. D.; Williams, K. J.; Stratford, I. J.; Jaffar, M.; Freeman, S. *Bioorg.Med.Chem.* **2002**, *10*, 525-530.
13. Wilson, J. M.; Henderson, G.; Black, F.; Sutherland, A.; Ludwig, R. L.; Vousden, K. H.; Robins, D. J. *Bioorg.Med.Chem.* **2007**, *15*, 77-86.
14. Porter, W. L.; Thimann, K. V. *Phytochemistry* **1965**, *4*, 229-243.
15. Beccalli, E. M.; Clerici, F.; Marchesini, A. *Tetrahedron* **1998**, *54*, 11675-11682.
16. Gu, X. H.; Wan, X. Z.; Jiang, B. *Bioorg.Med.Chem.Lett.* **1999**, *9*, 569-572.
17. Yin, Y.; Ma, W. Y.; Chai, Z.; Zhao, G. *J.Org.Chem.* **2007**, *72*, 5731-5736.
18. Ketcha, D. M.; Gribble, G. W. *J.Org.Chem.* **1985**, *50*, 5451-5457.
19. Hediger, M. E. *Bioorg.Med.Chem.* **2004**, *12*, 4995-5010.
20. Coowar, D.; Bouissac, J.; Hanbali, M.; Paschaki, M.; Mohier, E.; Luu, B. *J.Med.Chem.* **2004**, *47*, 6270-6282.
21. Cassel, S.; Casenave, B.; Deleris, G.; Latxague, L.; Rollin, P. *Tetrahedron* **1998**, *54*, 8515-8524.
22. Millich, F.; Becker, E. I. *J.Org.Chem.* **1958**, *23*, 1096-1102.
23. Brana, M. F.; Gradillas, A.; Ovalles, A. G.; Lopez, B.; Acero, N.; Llinares, F.; Mingarro, D. M. *Bioorg.Med.Chem.* **2006**, *14*, 9-16.
24. Hutchins, M.; Sainsbury, M.; Scopes, D. *Tetrahedron* **1984**, *40*, 1511-1515.
25. Nieman, J. A.; Coleman, J. E.; Wallace, D. J.; Piers, E.; Lim, L. Y.; Roberge, M.; Andersen, R. J. *J.Nat.Prod.* **2003**, *66*, 183-199.
26. Jiang, X. L.; Tiwari, A.; Thompson, M.; Chen, Z. H.; Cleary, T. P.; Lee, T. B. K. *Org.Process Res.Dev.* **2001**, *5*, 604-608.
27. Taylor, J. *J.Chem.Soc., Trans.* **1920**, *117*, 4-11.
28. Agarwal, A.; Srivastava, K.; Puri, S. K.; Chauhan, P. M. S. *Bioorg.Med.Chem.Lett.* **2005**, *15*, 3133-3136.
29. Fearing, R. B.; Fox, S. W. *J.Am.Chem.Soc.* **1954**, *76*, 4382-4385.
30. Zhang, X. M.; Bordwell, F. G.; Vanderpuy, M.; Fried, H. E. *J.Org.Chem.* **1993**, *58*, 3060-3066.
31. Wieczorek, P.; Miliszkiewicz, D.; Lejczak, B.; Soroka, M.; Kafarski, P. *Pestic.Sci.* **1994**, *40*, 57-62.
32. Mondon, M.; Lessard, J. *Canadian Journal of Chemistry-Revue Canadienne de Chimie* **1978**, *56*, 2590-2597.
33. Kuhn, H.; Stein, O. *Chem.Ber.* **1937**, *70*, 567-569.
34. Dai, H. G.; Li, J. T.; Li, T. S. *Synth.Commun.* **2006**, *36*, 1829-1835.
35. Coker, J. N.; Stevens, M. A.; Kohlhase, W. L.; Rogers, A. O.; Fields, M. *J.Org.Chem.* **1962**, *27*, 850-853.

36. Henbest, H. B.; Jones, E. R. H.; Smith, G. F. *J.Chem.Soc.* **1953**, 3796-3801.
37. Bellemin, R.; Decerprit, J.; Festal, D. *Eur.J.Med.Chem.* **1996**, *31*, 123-132.
38. Exposito, A.; Fernandez-Suarez, M.; Iglesias, T.; Munoz, L.; Riguera, R. *J.Org.Chem.* **2001**, *66*, 4206-4213.
39. Jin, Y.; Zhou, Z. Y.; Tian, W.; Yu, Q.; Long, Y. Q. *Bioorg.Med.Chem.Lett.* **2006**, *16*, 5864-5869.
40. Neumeyer, J. L.; Moyer, U. V.; Leonard, J. E. *J.Med.Chem.* **1969**, *12*, 450-452.
41. Bergman, J.; Venemalm, L. *Tetrahedron* **1990**, *46*, 6061-6066.
42. Swaminathan, S.; Ranganathan, S.; Sulochana, S. *J.Org.Chem.* **1958**, *23*, 707-711.
43. Kaneko, C.; Hayashi, S.; Kobayash, Y. *Chem.Pharm.Bull.* **1974**, *22*, 2147-2154.
44. Duval, E.; Cuny, G. D. *Tetrahedron Lett.* **2004**, *45*, 5411-5413.
45. Roy, S.; Eastman, A.; Gribble, G. W. *Tetrahedron* **2006**, *62*, 7838-7845.
46. Snyder, H. R.; Eliel, E. L. *J.Am.Chem.Soc.* **1948**, *70*, 1703-1705.
47. Boularot, A.; Giglione, C.; Petit, S.; Duroc, Y.; de Sousa, R. A.; Larue, V.; Cresteil, T.; Dardel, F.; Artaud, I.; Meinnel, T. *J.Med.Chem.* **2007**, *50*, 10-20.
48. Taniguchi, T.; Nagata, H.; Kanada, R. M.; Kadota, K.; Takeuchi, M.; Ogasawara, K. *Heterocycles* **2000**, *52*, 67-71.
49. Prudhomme, M.; Sancelme, M.; Bonnefoy, A.; Fabbro, D.; Meyer, T. *Eur.J.Med.Chem.* **1999**, *34*, 161-165.

Chapter 6

Biological Results and Discussion

Contents

6.0 Biological Results and Discussion 277
6.1 Agarose DNA Gel Electrophoresis 277
6.2 Influence of DNA topology in topo II inhibition 278
6.3 NCI-60 cancer cell-line screen 280
6.4 Panel of key derivatives for biological investigation 282
6.5 Topoisomerase II Decatenation Assay 283
6.5.1 Results of Topoisomerase II Decatenation Assay 285
6.5.2 Discussion of Topoisomerase II inhibition results 289
6.6 NCI-60 cytotoxicity results 292
6.7 Conclusion 296
6.8 References 299

6.0 Biological Results and Discussion

Realisation of successful routes to diverse new chemical entities within a number of novel hydrogen-bonding families afforded access to a large library of compounds with the potential for unique modes of bioactivity based on the potent anti-cancer properties of structurally related bisindolylmaleimides and indolocarbazoles (Section 1.0, Biological Introduction). Biological evaluation of these congeners is critical in order to profile specific anti-cancer molecular targets for these derivatives, and in SAR endeavours, in order to assess how distinct bioactivity may be correlated with structural variation within our test panel. Topoisomerase II decatenation assays were undertaken in order to determine the *in vitro* inhibitory activity of these compounds against a highly clinically relevant cancer target, while growth inhibition studies on 60 cultured human tumour cell lines relayed important efficacy data concerning design of 5,6-bisindolylpyrimidin-4(3*H*)-one, indolo[2,3-*a*]pyrimido[5,4-*c*]carbazol-4(3*H*)-one and related 3,4-bisaryl-5-aminopyrazole analogues as exciting new templates for medicinal research.

6.1 Agarose DNA Gel Electrophoresis

Standard agarose gel electrophoresis is a simple, reproducible and inexpensive bioanalytical separation technique for purification and characterization of DNA fragments ranging in size from 0.5 – 25 kB. Agarose is a linear polysaccharide composed of supercoiled helical fibres of D- and L-galactose joined by glycosidic linkages, comprising a three-dimensional mesh of channels whose pore sizes range from 50 nm to >200 nm.[1] Electrophoretic separation achieved by this method depends upon the electrostatic phenomenon of DNA possessing an overall negative charge due to its surface phosphodiester backbone, the magnitude of which is also affected by factors such as matrix ionic strength, pH and specific nucleotide composition. Voltage applied at the ends of the gel apparatus completes an electric circuit with a field strength defined by gel length and potential difference (V/cm). Therefore, charged DNA fragments loaded at the cathode (negative) migrate within this applied electric field towards the anodic (positive) end, according to their characteristic electrophoretic mobility. Migration velocity is only determined by the shape and size of DNA fragments, due to the identical charge : mass ratio of DNA of different lengths; small gel pore sizes generate frictional forces that impede rates of movement and thus, efficiently resolves DNA fragment-length mixtures according to a differential size gradient through the gel.[1,2]

The experimental protocol can be divided into three phases: (a) gel preparation utilizing an appropriate agarose concentration, usually 0.8-1.5%, for discrete DNA fragment separation;

(b) DNA samples and tracking dye (e.g. bromophenol blue or xylene cyanol) are loaded in marked sample wells and gel is run at optimal voltage (1-10 V/cm) and time, in order to resolve all molecular weight DNA bands present, and (c) gel is stained and visualized under U.V light (>2500 μW/cm^2), or, if ethidium bromide is incorporated in the electrophoresis buffer (~0.5 μg/mL), illuminated directly following removal of DC power source.

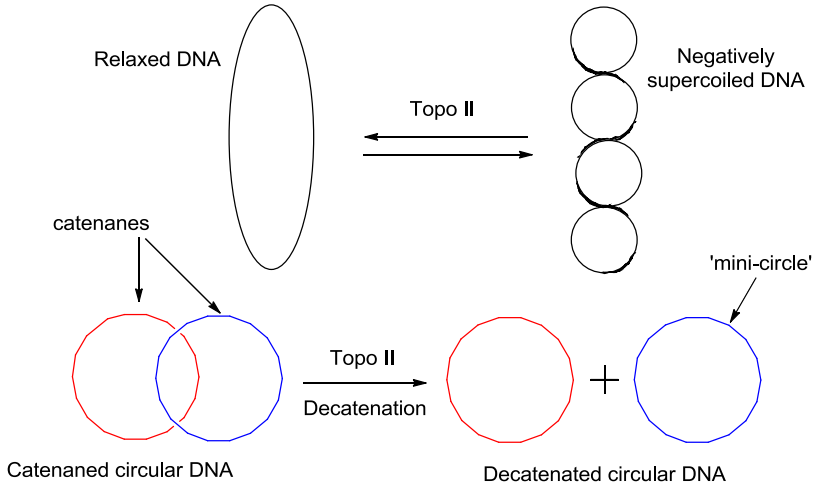
Prior to interpreting the results of any electrophoretic separation, several critical parameters affecting the migratory aptitude of DNA in agarose require discussion.[1] These factors were also optimized during the course of our topoisomerase II decatenation study:

- *Agarose concentration:* Linear DNA fragments migrate through agarose at a rate inversely proportional to $\log_{10}$ MW; 1-1.5% agarose content = separation of small 0.2-0.5 kB fragments, 0.5-1.0% = separation of larger 0.5-30 kB fragments and 0.3-0.5% = optimal for large 20-60 kB fragment resolution.
- *Applied voltage:* DNA generally travels through agarose at a rate proportional to the applied voltage. A potential difference of 2-8 V/cm across the gel is optimal, as undesirable heating effects occur at high field strengths (>10 V/cm). Large DNA molecules also co-migrate at higher applied voltages, thus reducing resolution of supercoiled and nicked topoisomers (improved by low agarose concentration and field strength (0.5%, ~1 V/cm).
- *DNA conformation:* Closed (superhelical) circular (form I), nicked circular (form II), and linear (form III) DNAs of identical weight migrate through agarose matrix at different rates.[3] Supercoiling reduces the hydrodynamic radius of DNA and enhances electrophoretic migration through gel pores, whereas nicked or relaxed circular molecules are significantly retarded.
- *Electrophoresis buffer:* The two most commonly employed buffers are Tris/acetate (TAE) and Tris/borate (TBE). TBE is generally avoided for purification of DNA from gels, as it may form complexes with deoxyribose sugars. Similarly, denaturing pH ranges and thermogenic high ionic strength buffers capable of efficient electrical conductance leads to deformation of the agarose gel matrix.

6.2 Influence of DNA topology in topo II inhibition

Due to the acute importance of topoisomerase inhibition as a privileged anti-cancer target, powerful, fast and selective gel electrophoresis topo II inhibition assays have attained a status as indispensable tools within current molecular biology.[3-8]

The enviable clinical success of topo II inhibition derives from its essential topological role in mammalian DNA metabolism, e.g. chromosome segregation and selective over-expression in rapidly proliferating cells (α isoform).[7,9-13] The mechanism of action of diverse clinical drugs such as etoposide and amsacrine involves negligible effect on catalytic topo II activity, but elicit accumulation of 5'-covalently bound catalytic intermediates, which are subsequently transformed into cytotoxic permanent double strand breaks, resulting in illegitimate chromosomal translocation and catastrophic cell damage.[4,14,15]



Scheme 6.1: Key topological reactions of topo II, illustrating unlinking of intact circular DNA.

Prokaryotic cells possessing double-stranded covalently closed DNA must also resolve significant topological challenges related to replication of circular bacterial chromosomes and plasmids. Following initial replication, these interwound, non-covalently linked circles or 'catenanes' must physically traverse through another double-stranded segment, and thus require intrinsic topoisomerase activity to transiently break both DNA strands of one chromosome and allow the daughter chromosome to pass through the break (decatenation).[2,16] In biochemical assays, eukaryotic topo II has been demonstrated to efficiently unlink parental strands by relaxing positive supercoils within superhelical circular DNA (Scheme 6.1).[17,18] The topological versatility of supercoiled closed circular DNA in the presence of topo II also results in increased populations of nicked circular DNA and relaxed DNA, which migrate through agarose gels at different rates, due to their differing size and shape. DNA supercoiling is thus an essential mechanism of topo II-mediated decatenation that can be measured in agarose gel electrophoresis by determining relative populations of topoisomers.

A well known anti-topo II agent, ellipticine **582** can be used as a negative control in the decatenation assay, due to its ability to intercalate into DNA, thus promoting persistent

strand cleavage by increasing levels of mutagenic cleavable complexes and strongly inhibiting topo II decatenation activity (c.f. Table 6.1).[19] Alternatively, etoposide, a front-line NSCLC topo II poison acts by strongly inhibiting the reverse DNA ligation step; however, this drug does not abrogate the decatenation process to any degree as this step is reversible.[20] Therefore, to fully verify the extent to which non-intercalative compounds can inhibit topo II, the decatenation assay should be used in conjunction with a topo II cleavage assay.[21]

In this investigation, topo II-mediated decatenation of supercoiled closed kinetoplast kDNA circles or catenanes, obtained from the mitochondrial DNA of *Crithidia fasciculate*, in the presence of ATP, represented the most specific assay to determine enzyme inhibition by a panel of our novel compounds by agarose gel electrophoresis.[2,22,23] In the absence of an inhibitor (positive control), decatenation proceeds with concomitant removal of positive supercoils - accounting for the most distant covalently closed circular 'relaxed' (CCC) band, while a population of open 'nicked' circular (OC) monomers migrates slower, due to its frictional resistance. However, in the presence of a topo II inhibitor, decatenation is effectively suppressed and consequently, release of DNA mini-circles cannot occur. Due to the large hydrodynamic radius of covalently linked kDNA, it cannot enter the gel, and forms a single characteristically intense band at the top of the gel.

6.3 NCI-60 cancer cell-line screen

The U.S National Cancer Institute's Developmental Therapeutics Program (DTP) 60 human tumour cell line service (NCI-60) was developed in the late 1980's as a strategic high-throughput screening tool for *in vitro* anti-cancer drug activity. Cytotoxicity data for in excess of 100,000 compounds across diverse cancer lineages (lung, renal, colorectal, ovarian, breast, prostate, central nervous system, melanoma and hematological malignancies) has been collated, following this approach.[24,25] Initial interest in this critical research tool encompassing a functional repository of proteomic and genomic data assembled for this cell line panel was garnered due to the failure of anti-leukemic activity within *in vivo* animal models to yield efficacy in human solid tumours (e.g. lung, colon, breast and prostate). The broad scope of the present-day cell-based NCI-60 evolved from the original *in vitro* chemosensitivity testing of compounds with growth-inhibitory or toxic effects on lung cancer cell lines ('disease-oriented concept') to a data-rich multiscreen inferring knowledge of expressed molecular targets within the NCI-60, as well as employing modern informatic tools for integrating information on modes of tumorigenesis and cancer

progression.[24,26-28] Patterns of relative drug sensitivity and resistance were generated with standard anticancer drugs using three response parameters: GI_{50} (concentration at which growth of 50% of cells present is fully arrested), TGI (concentration for total inhibition or 0% cell growth) and LC_{50} (lethal concentration causing death in 50% of cells originally present), were rapidly found to reflect mechanisms of drug action; thus, similar activity profiles for screening candidates allows for formulation of mechanistic hypotheses based on COMPARE algorithm.[24-26]

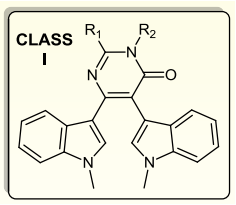
Following initial NCI-60 screening, compounds which exhibit an interesting pattern of inhibition are assessed by the Data Review Committee, prior to a 5-dose investigation, performed by 5 × 10-fold serial dilution of a 100 μM stock solution prepared at the same time as the one-dose sample. Following recommendation by the Biological Review Committee, compounds which generate useful activity profiles *via* potent and selective cytotoxicity across tumour cell lines may progress to *in vivo* hollow-fibre testing in mouse models and further xenograft assays, with successful drug candidates eventually authorised by the Drug Development Group to enter NCI clinical development.[24,29] It took only 8 years from initial NCI-60 hit identification of the novel proteasome inhibitor bortezomib – a COMPARE-negative (distinct anti-cancer mode of action) agent in 1995 to full FDA approval. Additional data returned to the compound supplier is also often important for licensing purposes or perhaps, lead-hopping and rational 2nd generation drug design.[30,31]

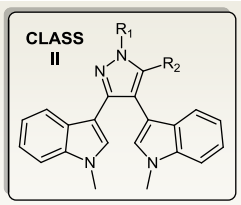
Fulfilling non-duplication criteria prescribed for NCI-60 compound selection, a preliminary panel of 3 novel 5,6-bisindolylpyrimidin-4-one analogues (**507**, **514**, **445**) synthesised during this work, planar isocytosine-fused indolocarbazole **442**, as well as parent 3,4-bisindolyl-5-aminopyrazole **447** and attractive pyrazolo[1,5-*a*]pyrimidine **549** derivatives were chosen as representative chemotypes for biological screening in the Developmental Therapeutics Program. These putative anti-cancer scaffolds were successfully investigated for initial one-dose tumour cell line activity, and the pattern of quantifiable growth inhibition of these agents on the NCI-60 human tumour cell line panel is outlined.

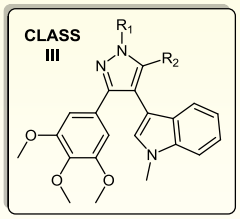
6.4 Panel of key derivatives for biological investigation

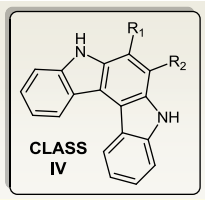
Table 6.1 Abridged list of 28 synthetic congeners within novel bisaryl and ICZ series†

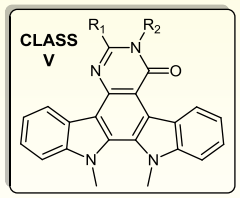
Compound No.	Substituents		NCI Accession No.*	Topo II Gel Fig. No.	Novel
	R_1	**R_2**			
445	NH_2	H	D-754605/1	6.3	✓
527	$NHCOCH_3$	H	-	6.4	✓
507	OH	H	D-754607/1	6.3	✓
514	SH	H	D-754608/1	6.3	✓
515	SCH_3	H	-	6.4,7	✓
516	$-SCH_2CH_2-$		-	6.6,7	✓
521	$SCH_2CO_2CH_3$	$CH_2CO_2CH_3$	-	6.6,7	✓
522	SCH_2CONH_2	CH_2CONH_2	-	6.6,7	✓
537	H	H	-	6.4	✓
447	H	NH_2	D-754609/1	6.1	✓
544	$CSNHCH_3$	NH_2	-	6.6,7	✓
543	$COCH_3$	NH_2	-	6.1	✓
548	$C=NH(NH_3)^+$	NH_2	-	6.7	✓
545	H	$NHSO_2CH_3$	-	6.5	✓
549	$-C(CF_3)=CH-C(CF_3)=N-$		D-754610/1	6.5	✓
539	-CONHCONH-		-	6.4	✓
510	H	OH	-	6.1	X
553	H	NH_2	-	6.2	✓
559	$CSNHCH_3$	NH_2	-	6.2	✓
557	$COCH_3$	NH_2	-	6.3	✓
563	$-C(CF_3)=CH-C(CF_3)=N-$		-	6.2	✓
540	-CONHCONH-		-	6.2	✓
552	H	OH	-	6.3	✓
468	-CONHCO-		-	6.5,7,8	X
467	$-(CO)_2O-$		-	6.1,8	X
473	-CONHNHCO-		-	6.5,7,8	✓
442	NH_2	H	D-754606/1	6.1	✓
538	H	H	-	6.5	✓





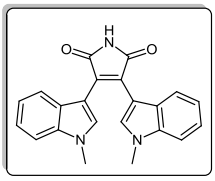




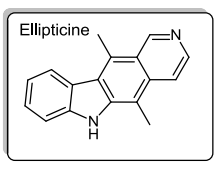


†A comprehensive library screen of 45 compounds was performed in topo II decatenation study (For synthesis, see Chemical Results and Discussion (Section 4.0) and Experimental (Section 5.0); assay results, Section 6.5).

*see Appendix 6.8.1-6 (NCI cytotoxicity data).



172



582

6.5 Topoisomerase II Decatenation Assay

Materials:

Decatenation assay kit supplied by Inspiralis, Norwich Bioincubator, Norwich Research Park, Colney, Norwich, UK. The kit comprised of the following: Assay Buffer (supplied as 10X stock) containing 50 mM Tris.HCl (pH 7.5), 125 mM NaCl, 10 mM $MgCl_2$, 5 mM DTT and 100 µg/mL albumin; Dilution buffer containing 50mM Tris. HCl (pH 7.5), 100 mM NaCl, 1 mM DTT, 0.5mM EDTA, 50% (v/v) glycerol, 50 µg/ml albumin; ATP (30X stock) 30 mM ATP; kDNA (100ng/µl); 10U/µL Human topoisomerase II in dilution buffer; 5X stop buffer containing 2.5% SDS, 15% Ficoll-400, 0.05% bromophenol blue, 0.05% xylene cyanol and 25 mM EDTA. Tris-Acetate-EDTA Buffer (supplied as 10X buffer) and agarose supplied by Sigma Life Sciences (Dublin, Ireland) and Safe View Stain supplied by NBS Biologicals, Cambridgeshire, England.

Method:

Agarose gel preparation:

Agarose (2 g) was added to 1X Tris-Acetate buffer (200 mL) and brought to the boil using a microwave. When the agarose had cooled to between 60-70^{o}C, Safe View Stain (40 µL) was added and gently mixed. Hot agarose solution (100 mL) was added to each of two gel formers (15 cm x 10 cm) containing a 20 well sample comb. When the agarose gel had set the gel was placed in the gel rig and submerged in 1X Tris-Acetate-EDTA Buffer.

Topo II Assay Preparation:

The methodology used was adapted from the instructions supplied by Inspiralis for the Decatenation Assay and optimised for use with the Safe View Stain. A stock solution sufficient for 40 samples containing Assay buffer, 3X ATP, 3X kDNA and 6X Topo II enzyme was prepared on ice as described below. 10X Topo II was diluted with dilution buffer to provide a 1X working stock containing 1U/µL Topo II.

Stock solution containing:	Quantity (µL)
Water	360
Assay Buffer (10 X stock)	120
ATP (30 X stock)	120
kDNA (100 g/µL)	240
Topo II (1 U/µL)	240

Preparation of Chemical Samples:

All samples to be tested were made up to a concentration of 1 mM in DMSO (≤10% v/v) and a combination of water, methanol, and acetonitrile in various proportions depending on the solubility of the compound in question. The chemicals were screened at an initial concentration of 100 µM (3 µL of chemical preparation in a total sample volume of 30 µL) and any potential hits (i.e. inhibition of topo II activity – no mini circles produced) were retested at 100 µM, 10 µM and 1 µM concentration.

The assay protocol involved initial addition of 27 µL of the above stock solution to Eppendorf tubes containing 3 µL of the chemicals to be screened, prior to incubation at 37^{o}C for 1 hr. At this point, the reaction was stopped by addition of either 5X stop buffer (12 µL) or 2X stop buffer (30 µL). A standard volume of each assay preparation (20 µL) was then added to a sample well in the prepared agarose gel and run at 50 V for 2 hrs using a Consort EV243 power pack. Positive controls (containing 3µL water), and negative controls (3 µL ellipticine (EPT) **582**, at a final concentration of 100 µM) were included in all gels. The solvent combinations employed to dissolve the chemicals under investigation were also tested to confirm that any observed hits were due to the chemicals and not inhibition by the solvents. The resulting gels were viewed under U.V. light using a DNR Bio-Imaging System and photographed using GelCapture software.

6.5.1 Results of Topoisomerase II Decatenation Assay

*In the following section, the experimental results associated with each of the gel assays are first presented followed by a discussion of the significant conclusions based on these data. It should be noted in each case that these results are preliminary.

6.5.1.1 Topo II inhibition of screening panel at 100 µM concentration

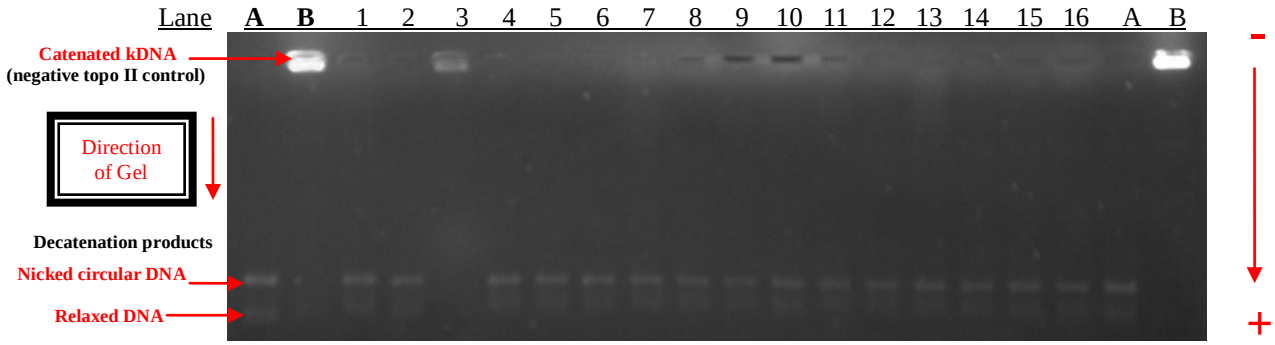


Fig. 6.1

Lane No.*	1	2	3	4	5	6	7	8	9	10	11	12	13	14	15	16
Compound No.†	**543**	**C**	**467**	**C**	**478**	**C**	**510**	**442**	**C**	**447**	**543**	**C**	**571**	**583**	**573**	**566**
***Topo II inhibition*¥**	-	-	+	-	-	-	-	-	-	-	-	-	-	-	-	-

*__A__ = Positive control: cDNA + ATP + topo II.
*__B__ = Negative control: cDNA + ATP + topo II + 100 µM topo II inhibitor (ellipticine **582**/+).
† **C** = Dilution solvent/blank; **N** = Not from this compound class.
¥Inhibitory activity: (-) = not active against topo II at 100 µM level; (+) = topo II inhibition at 100 µM level.

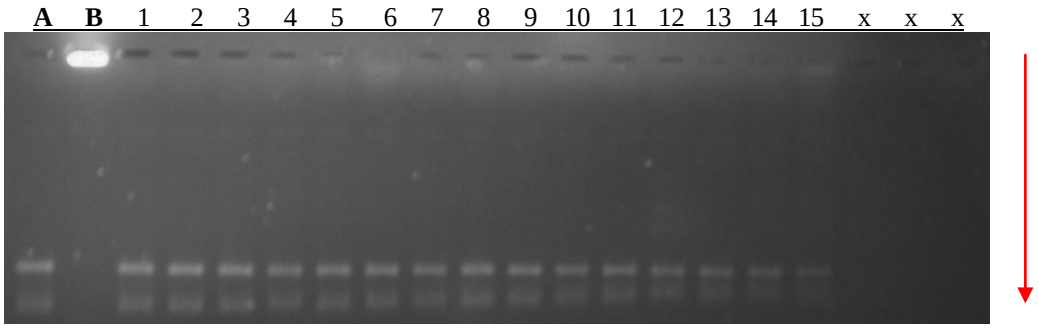


Fig. 6.2

Lane No.*	1	2	3	4	5	6	7	8	9	10	11	12	13	14	15
Compound No.†	**568**	**C**	**584**	**570**	**C**	**569**	**567**	**C**	**565**	**553**	**563**	**540**	**558**	**559**	**C**
***Topo II inhibition*¥**	-	-	-	-	-	-	-	-	-	-	-	-	-	-	-

*__A__ = Positive control: cDNA + ATP + topo II.
*__B__ = Negative control: cDNA + ATP + topo II + 100 µM topo II inhibitor (ellipticine **582**/+).
† **C** = Dilution solvent/blank; **N** = Not from this compound class.
¥Inhibitory activity: (-) = not active against topo II at 100 µM level; (+) = topo II inhibition at 100 µM level.

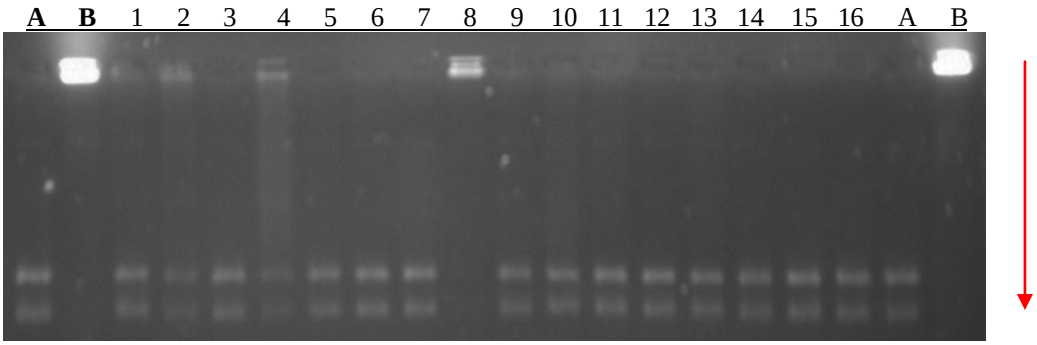


Fig. 6.3

Lane No.*	1	2	3	4	5	6	7	8	9	10	11	12	13	14	15	16
Compound No.†	**557**	**C**	**556**	**C**	**555**	**C**	**552**	**N**	**C**	**541**	**507**	**C**	**514**	**C**	**445**	**C**
***Topo II inhibition*¥**	-	-	-	-	-	-	-	**N**	-	-	-	-	-	-	-	-

*__A__ = Positive control: cDNA + ATP + topo II.
*__B__ = Negative control: cDNA + ATP + topo II + 100 µM topo II inhibitor (ellipticine **582**/+).
† **C** = Dilution solvent/blank; **N** = Not from this compound class.
¥Inhibitory activity: (-) = not active against topo II at 100 µM level; (+) = topo II inhibition at 100 µM level.

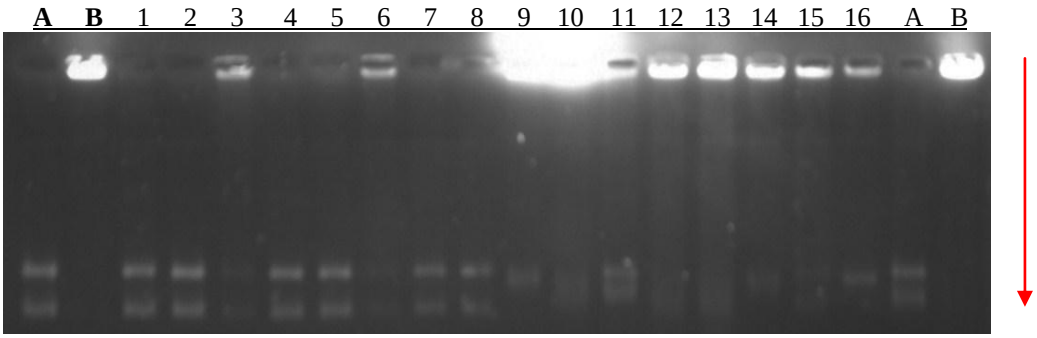


Fig. 6.4

Lane No.*	1	2	3	4	5	6	7	8	9	10	11	12	13	14	15	16
Compound No.†	**537**	**C**	**515**	**C**	**527**	**539**	**547**	**C**	**N**	**N**	**C**	**N**	**N**	**N**	**C**	**N**
***Topo II inhibition*¥**	-	-	+	-	-	+	-	-	**N**	**N**	-	**N**	**N**	**N**	-	**N**

*__A__ = Positive control: cDNA + ATP + topo II.
*__B__ = Negative control: cDNA + ATP + topo II + 100 µM topo II inhibitor (ellipticine **582**/+).
† **C** = Dilution solvent/blank; **N** = Not from this compound class.
¥Inhibitory activity: (-) = not active against topo II at 100 µM level; (+) = topo II inhibition at 100 µM level.

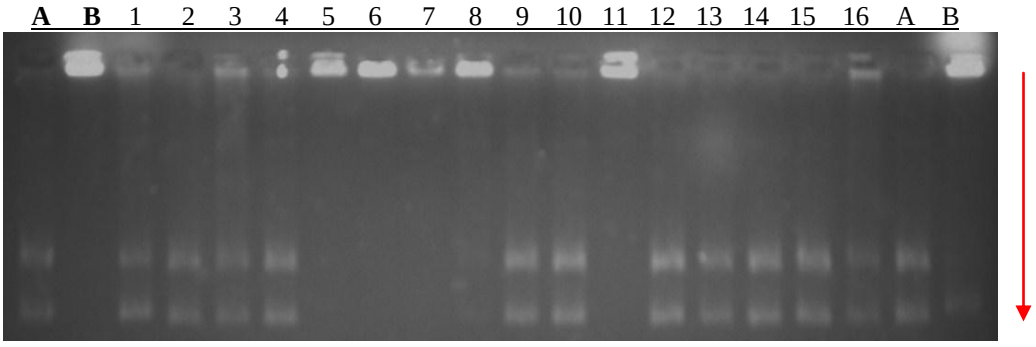


Fig. 6.5

Lane No.*	1	2	3	4	5	6	7	8	9	10	11	12	13	14	15	16
Compound No.†	**N**	**C**	**580**	**C**	**473**	**N**	**468**	**549**	**C**	**C**	**172**	**C**	**545**	**C**	**581**	**538**
***Topo II inhibition*¥**	**N**	**-**	**-**	**-**	**+**	**N**	**+**	**+**	**-**	**-**	**+**	**-**	**-**	**-**	**-**	**+**

***A** = Positive control: cDNA + ATP + topo II.
***B** = Negative control: cDNA + ATP + topo II + 100 µM topo II inhibitor (ellipticine **582**/+).
† **C** = Dilution solvent/blank; **N** = Not from this compound class.
¥Inhibitory activity: **(-)** = not active against topo II at 100 µM level; (+) = topo II inhibition at 100 µM level.

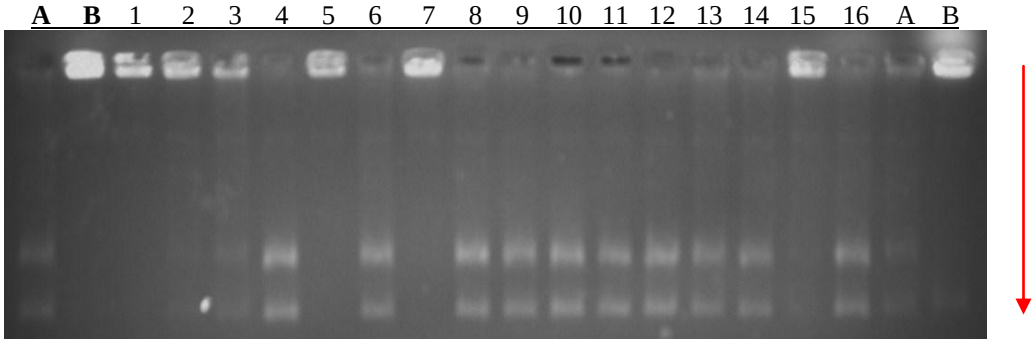


Fig. 6.6

Lane No.*	1	2	3	4	5	6	7	8	9	10	11	12	13	14	15	16
Compound No.†	**544**	**N**	**516**	**C**	**522**	**C**	**521**	**N**	**C**	**N**	**C**	**N**	**N**	**N**	**N**	**N**
***Topo II inhibition*¥**	**+**	**N**	**+**	**-**	**+**	**-**	**+**	**N**	**-**	**N**	**-**	**N**	**N**	**N**	**N**	**N**

***A** = Positive control: cDNA + ATP + topo II.
***B** = Negative control: cDNA + ATP + topo II + 100 µM topo II inhibitor (ellipticine **582**/+).
† **C** = Dilution solvent/blank; **N** = Not from this compound class.
¥Inhibitory activity: **(-)** = not active against topo II at 100 µM level; (+) = topo II inhibition at 100 µM level.

Figs. 6.1–6.6: Observed effects of a full panel of novel bioactive compounds, on the decatenation of kinetoplast DNA by topoisomerase II, following incubation at 37°C for 1 hour. Lanes 1–16 in displayed gels contained selected compound at 100 µM concentration, along with catenated DNA, ATP and topo II. The synthesis of this panel of compounds is discussed in Section 4.0 (Chemical Results and Discussion), and experimental details are provided in Section 5.0 (Experimental).

6.5.1.2 Topo II inhibition of selected compounds at 1, 10 and 100 μM

Following identification of attractive inhibitory activity within several novel synthetic compounds against topo II at 100 μM concentration, the inhibitory potency of selected active compounds was investigated by incubation under identical assay conditions, at individual concentrations of 100, 10 and 1 μM, respectively (Section 6.4, Table. 6.1).

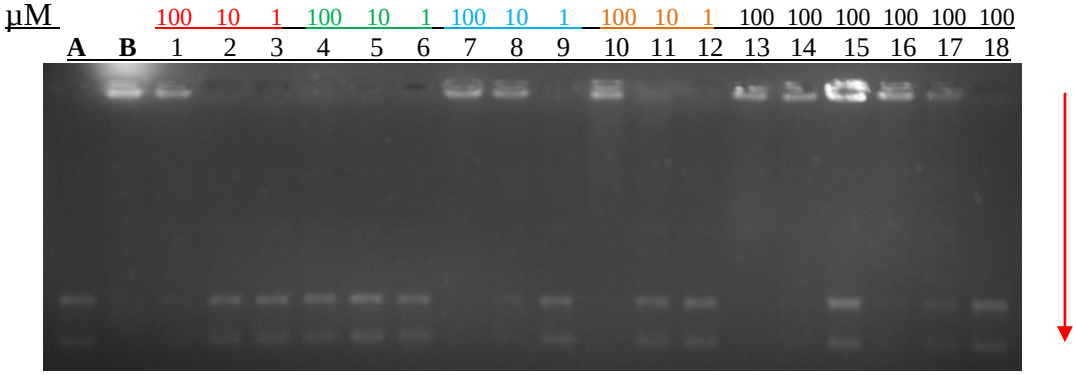


Fig. 6.7

Lane No.*	1	2	3	4	5	6	7	8	9	10	11	12	13	14	15	16	17	18
Compound No.†	**515**	**515**	**515**	**516**	**516**	**516**	**522**	**522**	**522**	**521**	**521**	**521**	**473**	**468**	**172**	**544**	**N**	**548**
***Topo II inhibition*¥**	+	-	-	-	-	-	+	++	-	+	++*	-	+	+	+	+	**N**	-

*__A__ = Positive control: cDNA + ATP + topo II; **B** = Negative control: cDNA + ATP + topo II + 100 μM topo II inhibitor (ellipticine **582**/+) †**N** = Not from this compound class.
¥Inhibitory activity: (-) = not active against topo II at tested concentration; (+) = topo II inhibition at 100 μM level; (++) = topo II inhibition at 10 μM; ++* = partial inhibition at 10 μM; (+++) = topo II inhibition (1 μM)

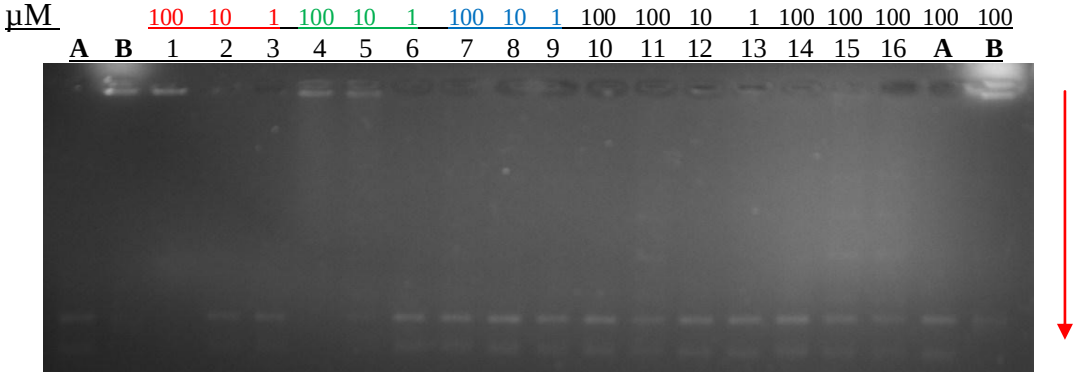


Fig. 6.8

Lane No.*	1	2	3	4	5	6	7	8	9	10	11	12	13	14	15	16
Compound No.†	**467**	**467**	**467**	**473**	**473**	**473**	**468**	**468**	**468**	**172**	**N**	**N**	**N**	**N**	**N**	**N**
***Topo II inhibition*¥**	+	-	-	+	++	-	-	-	-	-	**N**	**N**	**N**	**N**	**N**	**N**

*__A__ = Positive control: cDNA + ATP + topo II; **B** = Negative control: cDNA + ATP + topo II + 100 μM topo II inhibitor (ellipticine **582**/+) †**N** = Not from this compound class.
¥Inhibitory activity: (-) = not active against topo II at tested concentration; (+) = topo II inhibition at 100 μM level; (++) = topo II inhibition at 10 μM; (+++) = topo II inhibition at 1 μM level.

6.5.2 Discussion of Topoisomerase II inhibition results

In this investigation, a synthetic library of 45 compounds were initially screened for their ability to inhibit topo II-mediated circular kinetoplast DNA (kDNA) decatenation, at 100 μM, following incubation at 37°C for 30 minutes.[2,22] The intrinsic ability of these agents to disrupt the catalytic activity of this cancer-related topological enzyme was compared with a standard topo II inhibitor ellipticine **582**; small molecule stabilisation of intermediate cleavage complexes rapidly increases equilibrium levels of these potent intracellular poisons and closely correlates with anti-proliferative activity and mitotic catastrophe due to extensive DNA fragmentation.[32,33] In our single-dose and multi-concentration studies, large molecular weight kDNA samples were loaded on a 1% agarose gel containing Safe View Stain, purified topo II enzyme and ATP, containing either no drug (**A**), or 100 μM ellipticine **582** (**B**) controls, along with 18 lanes comprising the compound of interest or dilution solvent (**C**), exposed to topo II under identical conditions.[1] Decatenation of interlocked closed circular DNA has been reported to be the most specific assay for evaluation of *in vitro* topo II inhibition, and the exciting results of this experimental study suggest several attractive structural inhibitory leads for ongoing development of new bioactive heterocyclic scaffolds within this research group.[2]

The electrophoretic features of topo II activity illustrated in Figs. 6.1-6.8 clearly demonstrates a number of important principles which require elucidation prior to interpretation of these biochemical data. The absence of any drug in Lane A provided a positive control for native topo II activity under our assay conditions. In this case, catenated kDNA cannot enter a typical agarose gel unless monomeric ‘mini-circles’ are released *via* a gated double-stranded DNA passage mechanism (Section 6.2).[23,34] In the presence of topo II, two distinct thermodynamically stable DNA populations are resolved in Lane A, corresponding to a proximal nicked (open circular) and more permeable relaxed (covalently closed circular) monomer bands. Electrophoresis within Lane B represents a negative decatenation control characterized by full suppression of mini-circle migration, *via* topo II inhibition by ellipticine **582** at 100 μM. Thus, for non-inhibitory compounds within Lanes 1-18, topo II-induced DNA cleavage resulted in full conversion to nicked and relaxed circular DNA products, as clearly observed. Alternatively, compounds exhibiting topo II disruption inhibited kDNA fragmentation and retarded migration of DNA within the gel. At the outset, 25 novel heterocyclic derivatives within 5 structural classes (I-V), exhibiting diverse H-bonding characteristics were selected as attractive candidates to potentially exert new biological effects within the scope of this investigation (Table 6.1).

The results of the preliminary 45 compound screen performed at 100 μM are displayed in Figs. 6.1-6.8; attractive anti-topo II activity can now be reported to exist within several synthesized analogues encountered in this research. Unsurprisingly, in the case of the derivatives possessing the 4-(*N*-methyl-indol-3-yl)-3-(3,4,5-trimethoxyphenyl)-5-aminopyrazole template (c.f. Table 6.1; class III) (Figs. 6.2 and 6.3), no inhibitory activity could be discerned, even at high concentration. Similarly, class V planar pyrimido[5,4-*c*]carbazoles **442** (Fig. 6.1; Lane 8) and **538** (Fig. 6.5; Lane 16) were completely unable to arrest topo II-mediated decatenation at 100 μM. The inability of this novel ICZ chromophore to mimic the intercalative DNA base conformation of ellipticine **582** is an important observation, and future research into whether optimization of this template can effectively inhibit topo I activity will be necessary to determine how DNA base intercalation may account for the observed biological effects within this novel indolo[2,3-*a*]carbazole scaffold (Section 6.6).

Interestingly, the tested panel of indolo[2,3-*c*]carbazole regioanalogues (class IV) afforded enviable activity at 100 μM concentration. To our knowledge, both maleimide **468** (Fig. 6.5; Lane 7) and furan-2,5-dione **467** (Fig. 6.1; Lane 3) derivatives have not been reported to inhibit topo II to an appreciable extent, so this activity may complement other novel biological functionalities within this relatively unexplored class. Interestingly, the novel 6-membered pyridazinedione-fused indolo[2,3-*c*]carbazole **473** was the most active congener and fully abrogated topo II decatenation activity at a concentration of 10 μM (Fig. 6.5; Lane 5 and Fig. 6.8; Lanes 4-6). Similarly, anti-topo II activity mediated by bisindolylmaleimide **172** (Fig. 6.5; Lane 11) represents an interesting inhibitory lead within that series.

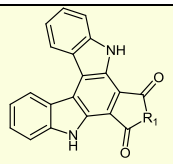
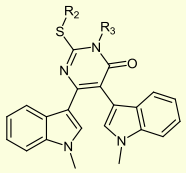
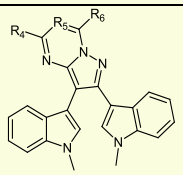
Two ring-condensed members of the 3,4-bisindolyl-5-aminopyrazole series (class II) also accomplished unique activity against topo II, derived from an inhibitory scaffold previously undisclosed in chemical literature. Further work is required to elucidate the origin of this inhibition, but it may be related to the ability of the bicyclic triazinedione moiety within **539** (Fig. 6.4; Lane 6), and planar pyrazolo[1,5-*a*]pyrimidine **549** (Fig. 6.5; Lane 8) to adopt a purine-like conformation affording critical hydrophobic interactions with DNA bases adjacent to the topo II catalytic site. However, in the case of more flexible mono-*N*-substituted analogues, only negligible inhibition could be determined, as confirmed by the presence of nicked and relaxed DNA bands within the agarose gel.

During this work, an unusual pattern of anti-topo II activity also emerged within *N*-substituted class I 5,6-bisindolylpyrimidin-4-ones, which permitted key insights into a

structural activity paradigm. The acetylated isocytosine derivative **527** was deemed to be completely inactive (Fig. 6.4; Lane 5); however, it was determined that certain alkylated derivatives of inactive parent 2-thiopyrimidin-4-one **514** (Fig. 6.3; Lane 13) resulted in potent *in vitro* enzyme inhibition.

Sulfide **515** demonstrated effective topo II inhibition at 100 μM, but was inactive at 10 and 1 μM (Fig. 6.4; Lane 3, Fig. 6.7; Lanes 1-3). Complex bifunctionalised thiouracil congeners exhibited complete efficacy at 100 μM; diacetate **521** was also partially inhibitory at 10-fold less concentration, but this activity was substantially diminished at 1 μM (Fig. 6.6; Lane 7, Fig. 6.7; Lanes 10-12). The most effective compound investigated within this series was novel *S*,*N*-diacetamidothiouracil **522** which obliterated topo II activity at 100 μM and also successfully inhibited decatenation at 10 μM (Fig. 6.6; Lane 5, Fig. 6.7; Lanes 7-9). It was hypothesized that key H-bonds extending from these flexible branched compounds effect important spatial H-bonding interactions with polar side-chains within the topo II active site. The length of $(CH_2)_n$ linker employed, along with the size and shape of polar side-group (CO_2R, $CONR_2R_3$) may be critical parameters, due to the conspicuous inability of non-H-bonding, unbranched cycloalkylated analogue **516** to inhibit kDNA decatenation at 100 μM (Fig. 6.7; Lanes 4-6). The positive results of this study are outlined in Table 6.2.

Table 6.2 New topo II inhibitors identified by kDNA decatenation assay.

Structure	Compound No.	Activity/μM[†]	Fig. (Lane)
	R_1=O; **467**	-	6.8 (1-3)
	R_1=NH-NH; **473**	++	6.8 (4-6)
	R_1=NH; **468**	+	6.8 (7-9)
	R_2=CH_3, R_3=H; **515**	+	6.7 (1-3)
	R_2=R_3= -CH_2CH_2- ; **516**	-	6.7 (4-6)
	R_2=R_3=CH_2CONH_2; **522**	++	6.7 (7-9)
	R_2=R_3=CH_2CO_2Et; **521**	++[*]	6.7 (10-12)
	R_5 = N, R_4=R_6=OH; **539**[§]	+	6.4 (6)
	R_5 = CH, R_4=R_6=CF_3; **549**[§]	+	6.5 (8)

[†](-) = Inactive at 100 μM; (+) = 100 μM inhibition: inactive at 1 and 10 μM; (++) = 10 μM inhibition: no inhibition at 1 μM; ++[*] = partial inhibition at 10 μM.
[§]Only tested at 100 μM.

6.6 NCI-60 cytotoxicity results

The reported methodology employed for evaluation of growth inhibition for our selected compounds within the NCI-60 cell line panel involves initial formation of a 4 mM stock solution with DMSO, prior to dilution into RPMI 1640 medium containing 5% fetal bovine serum/ 2 mM L-glutamine, and exposure to each cell line previously cultured for 24 hours.[24,26] After 48 hour incubation, successive steps of media removal, cell fixation and sulforhodamine B (SRB) staining were performed, prior to 1% acetic acid wash, and air drying of these plates. The dye was dissolved in Tris buffer, and the colorimetric growth inhibition-dependent absorbance at 515 nm was measured and calibrated against DMSO control.[24,35] *In vitro* activity of each compound in these human tumour cell lines was displayed by means of a 'mean graph' comprising a series of horizontal bar graphs representing units of nominal growth percent, deviating from the arithmetic mean growth inhibition for the entire 60 cell line array, i.e. centre line or '0'. In each case, graphs which extend to the right (-) denote more selective cytotoxicity or positive growth inhibition, while those which extend to the left (+) of centre line indicate a chemoprotective or non-cytotoxic effect on individual cell lines. Globally, patterns of total panel activity may also be correlated with those of over 100,000 compounds within a NCI-60 compound screen database, to reveal key mechanisms of action.[14,26,29,31]

As demonstrated by supplementary data within Appendix 6.8, novel tested compounds **507**, **514**, **445**, **442**, **447** and **549** exhibited extremely interesting cytotoxicity profiles within 60 human tumours derived from 9 distinct tissue sites. In the case of novel bisindolyl derivatives **507**, **514** and **445**, similar patterns of tumour chemosensitivity were observed; however, critical differences in cytotoxicity profile could also be discerned based on small structural alterations. Based on one-dose data, all leukemic, colon, CNS, prostate and melanoma cell lines were deemed relatively refractory to growth arrest by these compounds. Interestingly, in contrast to isocytosine **445**, a significant degree of selective cytotoxicity was expressed for closely analogous uracil derivatives **507** and **514** within EKVX (lung adenocarcinoma), SNB-75 (CNS glioma), CAKI-1 (renal cell carcinoma) and MDA-MB-435 (melanoma) compared with related tissue cell lines. All three 5,6-bisindolypyrimidinone (BIP) agents (**507**, **514** and **445**) also displayed enviable selective growth inhibition of IGROV1 carcinoma cell line compared with all other ovarian cancer types, and exhibited similar *in vitro* effects on MCF7 breast carcinoma cell line. Anti-cancer activity greater than the mean 60 cell line growth inhibition confirmed in several non-small cell lung cancers was also attributed to these novel congeners. Similarly, aminopyrazole derivative **447** displayed

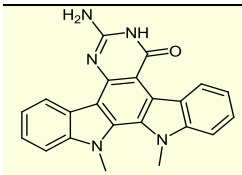
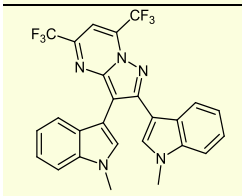
useful cytotoxicity at 10 μM against EKVX lung cancer cells during this investigation. This novel bisindolyl-substituted heterocycle **447** also elicited a similar pattern of inhibition to the 6-membered bisindolyl series, being ineffective across most leukemic, colon, prostate and melanoma cell lines, in addition to possessing unique cytotoxic properties represented by moderate activity towards glioma cell line U-251 (CNS) and especially, its strong inhibitory influence on HOP-92 lung large cell carcinoma. However, while retaining characteristic ovarian anti-cancer activity against IGROV1 cell line, as well as being selective for cultured UO-31 renal cell carcinoma, it was also apparent that compound **447** suffered attenuated activity on any breast cancer cell line tested *in vitro*, including MCF7, successfully targeted in the corresponding pyrimidin-4-one series.

Pyrazolo[1,5-*a*]pyrimidine **549** was investigated as a novel topo II inhibitory candidate (Section 6.5), which was proposed to incorporate a more complex planar bicyclic structural motif at the biologically relevant 1,2-bisindolyl-*cis*-ethene bridgehead site, capable of mimicking hydrophobic interactions within an enzyme active site. Allied to a pattern of overall cytotoxic activity consistent with 3,4-bisindolyl-5-aminopyrazole **447**, this derivative **549** was also found to be selective for inhibition of a single HOP-92 NSCLC line within this array (NSC: D-754610/1; Appendix 6.8.6). In 2006, Ikediobi *et al.* characterized 24 anomalous molecular targets based on acquired mutations present within the NCI-60 screening panel. In addition to tumour suppressor p53 deficiency, HOP-92 was also characterized to possess mutations in CDK4-inhibitor proteins implicated in several primary tumours, e.g. familial atypical multiple melanoma.[25,36,37] These evolving molecular insights afford the opportunity to target selective biological screens against relevant anti-cancer proteins; as a putative example of this rational approach applied to our topo II research, persistent DNA strand breakage induced by topo II inhibitors in mutated p53 colon or ovarian carcinoma cells has been disclosed to be effective in cancer therapy by eliciting rapid onset of apoptosis.[36,37]

The most active anti-cancer agent within this NCI-60 test panel was novel pyrimido[5,4-*c*]carbazole **442**; inspection of the mean graph generated for this planar compound illustrated tumour growth inhibitory effects across 8 primary cancer zones, delivering an activity profile inconsistent with the pattern of differential cytotoxicity exhibited by the corresponding bisindolylpyrimidinone **445**, or uracil derivatives **507** and **514** (NSC: D-754606/1; Appendix 6.8.2). In addition, a chemoprotective effect (>100%) was only observed in CNS tumours, while 25 cell lines displayed greater than 50% growth inhibition following incubation with this novel indolocarbazole **442** at 10 μM for 48 hours. In comparison to its acyclic

counterpart **445**, significant activity was observed across all haematological tumour cell lines, in addition to colorectal carcinomas (e.g. HT-29) and melanomas (e.g. MDA-MB-435 cell line). In addition to its improved mean cytotoxicity, enhanced intra-tissue cell line selectivity was also discerned for MCF-7 breast cancer, in the absence of significant tumour growth inhibition within other breast cancer lines, while less marked differentiation phenomena also featured within melanoma lines and NSCLCs. Strong growth inhibition was also displayed by anti-cancer ICZ **442** against the SK-OV-3 cell line, which was completely unresponsive to other test compounds. These results infer a putative mode of action for class V indolo[2,3-*a*]pyrimido[5,4-*c*]carbazole analogues, distinct from mechanisms of anti-cancer bioactivity mediated by class I 5,6-bisindolylpyrimidin-4-one congeners *in vitro* (Table 6.3).

Table 6.3 Novel *in vitro* cytotoxic anti-cancer leads following NCI-60 compound screen.

Structure	Compound no.	NCI-60 cell line	Tumour site	% Growth after 48h[§]	Mean cell line growth
	**442**	*HT29*	colon	17.58	58.90
		UO-31	kidney	7.16	
		CAKI-1	kidney	-14.95	
	**549**	*HOP-92*	lung (NSCLC)	32.74	98.12

[§]Cultured cells were tested on RPMI 1640 medium at an initial compound concentration of 10 μM.

However, the most intriguing aspect of this initial screen concerned the potent and selective anti-cancer activity of **442** against kidney cancer lines CAKI-1 and UO-31.

Subsequent testing of **442** against all 60 human cancer cell lines during exponential growth phase, was performed at 5 individual concentrations, ranging from 100 μM to 10 nM.[26] Based on these data, dose-response curves were generated for cell growth inhibition as a function of inhibitor concentration; it was observed that lower concentrations of **442** sharply impeded tumour growth inhibition across all cell lines, affording relatively modest growth inhibition at 10 nM and 100 nM concentration levels across these cell lines (Appendix 6.8.7). The characteristic *in vitro* growth parameters, GI_{50}, TGI, and LC_{50} were determined for each member of the NCI-60 panel and are collated in Appendix 6.8.8. Observing these growth response plots, it can be deduced that cell growth in all cases was arrested in a concentration-dependent manner, and predominantly elicited GI_{50} values within the low micromolar range, in this assay (Table 6.4).

Table 6.4 Selected targets of anti-cancer ICZ **442** following 5-dose growth inhibition study[†]

Cell line	Tumour type	% Cell growth after 48h[§]					GI_{50} µM	TGI µM	LC_{50} µM
		10 nM	100 nM	1 µM	10 µM	100 µM			
SF-295	CNS	85	93	106	7	-57	3.68	12.9	76.7
HCT-15	colon	96	99	61	24	9	1.98	>100	>100
SK-MEL-2	melanoma	103	112	73	-10	-55	1.90	7.59	76.5
SK-MEL-5	melanoma	89	98	87	15	-97	3.25	13.7	37.9
UACC-257	melanoma	93	91	104	64	-62	12.8	32.0	79.7
OVCAR-3	ovarian	112	107	120	47	-68	9.07	25.6	69.8
ACHN	kidney	94	92	51	25	12	1.11	>100	>100
CAKI-1	kidney	93	85	53	29	3	1.33	>100	>100
UO-31	kidney	85	72	55	19	17	1.37	>100	>100

[§] Cell growth refers to incubation with concentration of **442** in cultured cells on RPMI 1640 medium for 48 hours.
[†]See Appendix NCI Data for full details

This investigation also confirmed the selective cytostatic anti-cancer activity of novel 2-aminoindolo[2,3-*a*]pyrimido[5,4-*c*]carbazol-4(3*H*)-one **442** (ICZ analogue of **445**) against colon, melanoma and renal cancers; GI_{50} values were displayed of 1.98 µM for HCT-15 (colon), 1.90 µM for SK-MEL-2 (melanoma) and approximately 1 µM values for ACHN, CAKI-1 and UO-31 renal cell lines. A single-digit micromolar TGI value was also afforded for SK-MEL-2 melanoma, but most values were between 10-100 µM, in this study. The lethal concentration required for death of 50% of cell population (LC_{50}) was >100 µM, in most instances, although acute cytotoxicity was observed for SK-MEL-2, SK-MEL-5 and UACC-257 melanoma, as well as ovarian OVCAR-3 carcinoma, with LC_{50} values of 76.9, 37.5, 79.7 and 69.8 µM, respectively.

These results can be compared with the anti-cancer activity previously discussed for K-252c **6** and arcyriaflavin A **7**, which induce high levels of apoptosis in the K562 CML cell line at 100 µM and reported IC_{50} values against some cell lines in the low micromolar range (e.g. arcyriaflavin A **7**, IC_{50} HCT-116 = 0.85 µM) (Fig. 6.9).[38,39] The low cytotoxicity of **442** may also correlate with specific cell signaling effects consistent with a profile of kinase inhibition. Further insights into the molecular targets (kinase screening etc.) of anti-cancer activity by compound **442** will be essential to furnish a mechanism by which this selective tumour growth inhibition occurs, and to ascertain key structural requirements for refinement of bioactivity within this class. Valuable investigation into improved anti-cancer potential of more active indole demethylated analogues of **442** will also be undertaken within the research group.

6.7 Conclusion

In the light of biological data accumulated from topo II decatenation electrophoretic assay, as well as NCI-60 testing of compounds generated from synthetic studies, proof of concept for anti-cancer activity within several novel chemical families has been firmly established.

Due to its critical physiological role in rapidly proliferating cells, topo II intervention is a valid clinical target for cancer chemotherapy, with over half of all current drug regimens incorporating topo II-targeted agents. A ubiquitous feature of this therapeutic approach is the interaction of small-molecule inhibitors with DNA within the active site of the enzyme; the mode of DNA binding varies widely in the absence of enzyme, ranging from weak interactions to strong binding and intercalation.[4,40] Interestingly, Lassota and co-workers described the ability of staurosporine **2** to block topo II-induced intermediate phosphotyrosyl bond formation in the presence of DNA, but little work has explored this inhibitory motif to date.[41] Based on present work, 9 tested compounds conferred new anti-topo II activity at 100 µM, while a novel di-*S,N*-substituted bisindolylthiouracil class constitutes an attractive lead structure for refining topo II inhibition. Future work to probe the precise biological nature of this warhead, by altering linker size and polar functionality, as well as exploration of the flexibility of the ring system will also reveal valuable SAR data. Utilisation of hydroxylated indole starting materials and synthesis of substituted derivatives of these lead compounds will also be desirable, based on the ability of 1,11-dihydroxylated ICZ, BE-13793c **52** to inhibit both topo I and topo II with an IC_{50} value of 2 µM.[42]

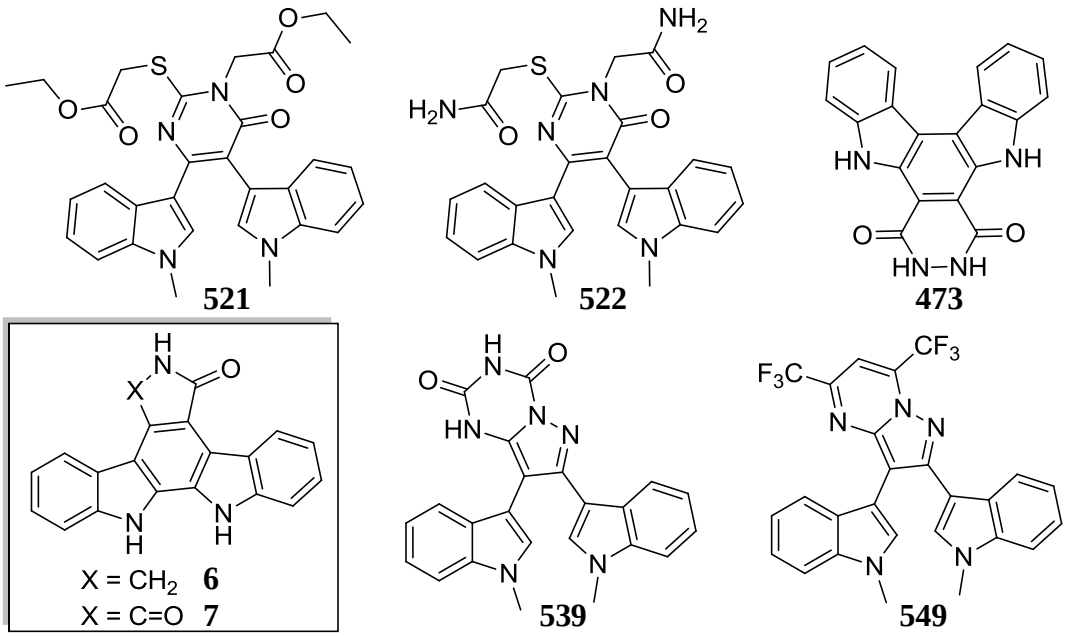


Fig. 6.9: Development of novel topo II inhibitors and structures of natural ICZs K-252c **6** and Arcyriaflavin A **7**.

Similarly, the ascertained biological activity of the [1,5-*a*]pyrimidine-fused 3,4-bisindolylpyrazole nucleus represented by triazinedione **539** and fluorinated derivative **549** also infer a privileged inhibitor scaffold/pharmacophore capable of single digit micromolar inhibition. This may comprise a non-rigid bisindolyl molecular hinge region bound to a 5 or 6-membered nitrogenated ring system comprising an extended polar moiety, which may be ring-constrained or linked *via* a short alkyl linker chain. In addition, a novel 6-membered, planar indolo[2,3-*c*]carbazole derivative **473** was observed to possess enviable *in vitro* topo II inhibition at concentrations as low as 10 µM, during this study.

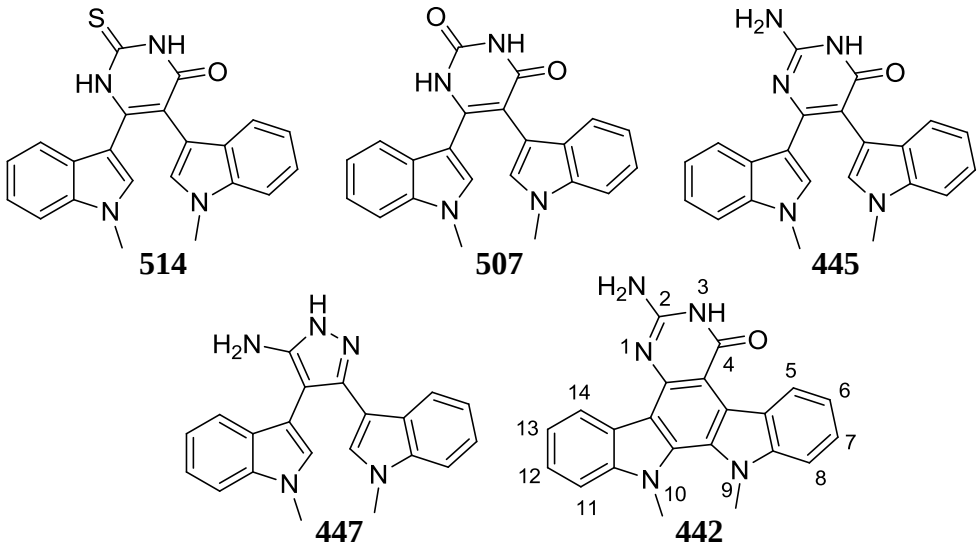


Fig. 6.10: Selected compounds tested for NCI-60 cancer cell growth inhibition

Availing of a cell-based cytotoxicity assay provided by the NCI-60 human cancer screening service, growth inhibition rendered by highlighted synthetic compounds (**507**, **514**, **445**, **447**, **549** and **442**) was collated by means of a standard mean graph output yielding important details regarding associated molecular targets and modes of action (Appendix 6.8.1-6.8.6). Relatively poor cancer cell growth arrest was observed following incubation with uracil **507**, thiouracil **514**, isocytosine **445** and 5-aminopyrazole **447**, for 48 hours. Conversely, selective inhibition of HOP-92 NSCLC cell line was determined for pyrazolo[1,5-*a*]pyrimidine **549**. In the case of 9,10-dimethyl-2-amino substituted pyrimidoindolocarbazole **442**, an interesting pattern of anti-tumour activity was revealed, with enhanced growth inhibition of several melanoma and colorectal cancer lines, as well as attractive activity emerging against two renal cell carcinomas, CAKI-1 and UO-31 at 10 µM concentration. Future work will attempt to elucidate the cell machinery and growth pathway mechanisms mitigated by **442** (e.g. COMPARE analysis). Development of this relatively selective therapeutic target will now proceed, and testing of the closely related novel pyrimidin-4(3*H*)-one indolocarbazole **538** will also advance SAR within this novel indolo[2,3-*a*]carbazole series.

The major limitation of this study was the relative data deficit regarding the specific mechanisms involved in cancer cell line cytotoxicity. The potential of these synthesized compounds as topo I inhibitors could not be investigated within the scope of this project; thus, future biological studies will comprise a topo I unwinding assay to investigate the intercalating or minor groove binding capacity of these compounds, as well as a topo I cleavage assay to determine the propensity of these compounds to introduce persistent single DNA strand breakage *via* stabilization of the topo I-DNA covalent complex.[43,44] NCI-60 testing also provides a tantalizing vista into anti-cancer activity operating at a cellular level, but is not practical for combinatorial screening of active analogues to extensively probe anti-cancer SAR within these libraries. Essential kinase inhibition screening (e.g. anti-VEGFR2 activity) and *in silico* molecular modeling techniques will also aid to identify and augment the pharmacological profiles of these novel anti-tumour agents.[45]

Based on the results of biological studies on this reported panel of compounds, completed to date, a number of validated synthetic targets for small-molecule anti-cancer development have been successfully achieved. Critical successes in novel topo II inhibition across a series of 1,5-pyrimidine-fused bisindolylpyrazole derivatives, N^3-derivatised 2-alkylthio-substituted 5,6-bisindolylpyrimidin-4-ones and potent micromolar inhibition by a planar indolo[2,3-*c*]carbazole congener containing a new 6-membered pyridazinedione ring system sets the stage for future productive work in this field. Screening of representative chemotypes from our diverse synthetic library identified limited *in vitro* cancer cell growth inhibition at 10 μM, across a number of hydrogen-bonding bisindolyl 'hit' compounds, while analysis of a novel pyrimido[5,4-*c*]indolo[2,3-*a*]carbazole F-ring isocytosine agent revealed an attractive spectrum of activity, conferring potent anti-tumour activity across several cancer cell lines, including renal cancers and melanoma. The strategy of diversity-oriented synthesis has also been validated as a means of generating versatile biological leads and several new research pathways can be envisaged to arise from this work, based on optimization of the biological activity within each chemical class.

6.8 References

1. Voytas, D. *Agarose Gel Electrophoresis*; John Wiley & Sons, Inc.: 2001.
2. Morgan-Linnell, S. K.; Hiasa, H.; Zechiedrich, L.; Nitiss, J. L. *Assessing Sensitivity to Antibacterial Topoisomerase II Inhibitors*; John Wiley & Sons, Inc.: 2001.
3. Darpa, P.; Liu, L. F. *Biochim.Biophys.Acta* **1989**, *989*, 163-177.
4. Froelichammon, S. J.; Osheroff, N. *J.Biol.Chem.* **1995**, *270*, 21429-21432.
5. Liu, L. F. *Annu.Rev.Biochem.* **1989**, *58*, 351-375.
6. Meng, L. H.; Liao, Z. Y.; Pommier, Y. *Curr.Top.Med.Chem.* **2003**, *3*, 305-320.
7. Topcu, Z. *J.Clin.Pharm.Ther.* **2001**, *26*, 405-416.
8. Zembower, D. E.; Zhang, H. P.; Lineswala, J. P.; Kuffel, M. J.; Aytes, S. A.; Ames, M. M. *Bioorg.Med.Chem.Lett.* **1999**, *9*, 145-150.
9. Andoh, T.; Ishida, R. *Biochim.Biophys.Acta* **1998**, *1400*, 155-171.
10. Champoux, J. J. *Annu.Rev.Biochem.* **2001**, *70*, 369-413.
11. Larsen, A. K.; Escargueil, A. E.; Skladanowski, A. *Pharmacol.Ther.* **2003**, *99*, 167-181.
12. Rowe, T. C.; Chen, G. L.; Hsiang, Y. H.; Liu, L. F. *Cancer Res.* **1986**, *46*, 2021-2026.
13. Wilstermann, A. M.; Osheroof, N. *Curr.Top.Med.Chem.* **2003**, *3*, 321-338.
14. Nakamura, K.; Sugumi, H.; Yamaguchi, A.; Uenaka, T.; Kotake, Y.; Okada, T.; Kamata, J.; Niijima, J.; Nagasu, T.; Koyanagi, N.; Yoshino, H.; Kitoh, K.; Yoshimatsu, K. *Mol.Cancer Ther.* **2002**, *1*, 169-175.
15. Jensen, L. H.; Thougaard, A. V.; Grauslund, M.; Søkilde, B.; Carstensen, E. V.; Dvinge, H. K.; Scudiero, D.; Jensen, P. B.; Shoemaker, R. H.; Sehested, M. *Cancer Res.* **2005**, *65*, 7470-7477.
16. Nitiss, J. L. *Biochim.Biophys.Acta, Gene Struct.Expression* **1998**, *1400*, 63-81.
17. Vologodskii, A. *Bioessays* **2010**, *32*, 9-12.
18. Wang, J. C. *Nat.Rev.Mol.Cell Biol.* **2002**, *3*, 430-440.
19. Cline, S. D.; Macdonald, T. L.; Osheroff, N. *Biochemistry (Mosc).* **1997**, *36*, 13095-13101.
20. Osheroff, N. *Biochemistry (Mosc).* **1989**, *28*, 6157-6160.
21. Jannatipour, M.; Liu, Y. X.; Nitiss, J. L. *J.Biol.Chem.* **1993**, *268*, 18586-18592.
22. Marini, J. C.; Miller, K. G.; Englund, P. T. *J.Biol.Chem.* **1980**, *255*, 4976-4979.
23. Muller, M. T.; Helal, K.; Soisson, S.; Spitzner, J. R. *Nucleic Acids Res.* **1989**, *17*, 9499.
24. Shoemaker, R. H. *Nat.Rev.Cancer* **2006**, *6*, 813-823.
25. Ikediobi, O. N.; Davies, H.; Bignell, G.; Edkins, S.; Stevens, C.; O'Meara, S.; Santarius, T.; Avis, T.; Barthorpe, S.; Brackenbury, L.; Buck, G.; Butler, A.; Clements, J.; Cole, J.; Dicks, E.; Forbes, S.; Gray, K.; Halliday, K.; Harrison, R.; Hills, K.; Hinton, J.; Hunter, C.; Jenkinson, A.; Jones, D.; Kosmidou, V.; Lugg, R.; Menzies, A.; Mironenko, T.; Parker, A.; Perry, J.; Raine, K.; Richardson, D.; Shepherd, R.; Small, A.; Smith, R.; Solomon, H.; Stephens, P.; Teague, J.; Tofts, C.; Varian, J.; Webb, T.; West, S.; Widaa, S.; Yates, A.; Reinhold, W.; Weinstein, J. N.; Stratton, M. R.; Futreal, P. A.; Wooster, R. *Mol.Cancer Ther.* **2006**, *5*, 2606-2612.
26. Gills, J. J.; Holbeck, S.; Hollingshead, M.; Hewitt, S. M.; Kozikowski, A. P.; Dennis, P. A. *Mol.Cancer Ther.* **2006**, *5*, 713-722.
27. Pfister, T. D.; Reinhold, W. C.; Agama, K.; Gupta, S.; Khin, S. A.; Kinders, R. J.; Parchment, R. E.; Tomaszewski, J. E.; Doroshow, J. H.; Pommier, Y. *Mol.Cancer Ther.* **2009**, *8*, 1878-1884.
28. Adams, S.; Robbins, F. M.; Chen, D.; Wagage, D.; Holbeck, S. L.; Morse, H. C.; Stroncek, D.; Marincola, F. M. *J.Transl.Med.* **2005**, *3*.

29. Boyd, M. R.; Pauli, K. D. *Drug Dev.Res.* **1995**, *34*, 91-109.
30. Hopkins, A. L.; Groom, C. R. *Nat.Rev.Drug Discovery* **2002**, *1*, 727-730.
31. Moreau, P.; Holbeck, S.; Prudhomme, M.; Sausville, E. A. *Anticancer.Drugs* **2005**, *16*, 145-150.
32. Gribble, G. W.; Saulnier, M. G. *Heterocycles* **1985**, *23*, 1277-1315.
33. Pommier, Y.; Pourquier, P.; Urasaki, Y.; Wu, J. X.; Laco, G. S. *Drug Resistance Updates* **1999**, *2*, 307-318.
34. Lucas, I.; Germe, T.; Chevrier-Miller, M.; Hyrien, O. *EMBO J.* **2001**, *20*, 6509-6519.
35. Rubinstein, L. V.; Shoemaker, R. H.; Paull, K. D.; Simon, R. M.; Tosini, S.; Skehan, P.; Scudiero, D. A.; Monks, A.; Boyd, M. R. *J.Natl.Cancer Inst.* **1990**, *82*, 1113-1118.
36. Lapenna, S.; Giordano, A. *Nat.Rev.Drug Discovery* **2009**, *8*, 547-566.
37. Malumbres, M.; Barbacid, M. *Nat.Rev.Cancer* **2009**, *9*, 153-166.
38. Liu, R.; Zhu, T. J.; Li, D. H.; Gu, J. Y.; Xia, W.; Fang, Y. C.; Liu, H. B.; Zhu, W. M.; Gu, Q. Q. *Arch.Pharm.Res.* **2007**, *30*, 270-274.
39. Zhu, G. X.; Conner, S. E.; Zhou, X.; Shih, C.; Li, T. C.; Anderson, B. D.; Brooks, H. B.; Campbell, R. M.; Considine, E.; Dempsey, J. A.; Faul, M. M.; Ogg, C.; Patel, B.; Schultz, R. M.; Spencer, C. D.; Teicher, B.; Watkins, S. A. *J.Med.Chem.* **2003**, *46*, 2027-2030.
40. Hsiang, Y. H.; Liu, L. F. *J.Biol.Chem.* **1989**, *264*, 9713-9715.
41. Lassota, P.; Singh, G.; Kramer, R. *J.Biol.Chem.* **1996**, *271*, 26418-26423.
42. Kojiri, K.; Kondo, H.; Yoshinari, T.; Arakawa, H.; Nakajima, S.; Satoh, F.; Kawamura, K.; Okura, A.; Suda, H.; Okanishi, M. *J.Antibiot.* **1991**, *44*, 723-728.
43. Tanizawa, A.; Kohn, K. W.; Kohlhagen, G.; Leteurtre, F.; Pommier, Y. *Biochemistry (Mosc).* **1995**, *34*, 7200-7206.
44. Knab, A. M.; Fertala, J.; Bjornsti, M. A. *J.Biol.Chem.* **1995**, *270*, 6141-6148.
45. Peifer, C.; Krasowski, A.; Hammerle, N.; Kohlbacher, O.; Dannhardt, G.; Totzke, F.; Schachtele, C.; Laufer, S. *J.Med.Chem.* **2006**, *49*, 7549-7553.

Chapter 7

Current Perspectives

7.0 Current Perspectives

7.1 Final Overview

At this juncture, full synthetic methodology has been developed for a panel of over 50 novel aglycon compounds based on bioisosteric modification of the maleimide ring motif within the natural product arcyriarubin A **79**. These successful routes were applied to yield new libraries of potential anti-cancer 5,6-bisindolylpyrimidin-4-one derivatives (class I) based on the clinical therapeutic agent and selective PKC-β inhibitor, ruboxistaurin **80**, as well as structurally related isocytosine **442** and pyrimidin-4(3*H*)-one-fused indolocarbazole **538** congeners (class V). Formation of previously undisclosed imidazo[4,5-*c*]indolo[2,3-*a*]carbazoles (class VI) was also accomplished, although isolation within this series proved problematic. Design and subsequent synthesis of diverse 3,4-bisindolyl (class II) and 4-(3,4,5-trimethoxyphenyl)-3-(*N*-methylindol-3-yl)-5-aminopyrazole analogues (class III) derived from PKC and VEGFR2 inhibitory templates respectively, were also fulfilled during this research (Fig. 7.1).

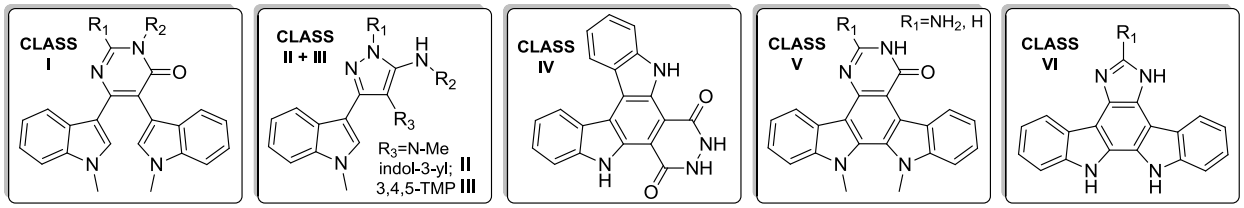


Fig. 7.1: Novel indolocarbazole-based anti-cancer scaffolds developed over the course of this work.

In addition, preliminary biological screening of these compounds to assess putative *in vitro* anti-tumour activity was achieved. Unique topo II-targeting agents were identified following evaluation of novel pyridazinedione indolo[2,3-*c*]carbazole **473** (class IV), flexible di-substituted 5,6-bisindolyl-2-thiopyrimidin-4-ones such as **522** (class I) and bicyclic pyrazolo[1,5-*a*]pyrimidine **549** (class II) (Fig. 7.2).

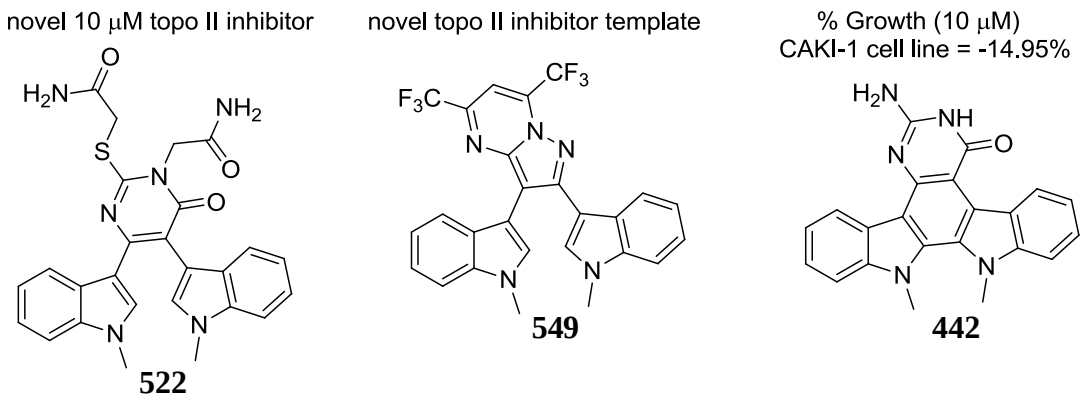


Fig. 7.2

Based on these results, it is postulated that low micromolar topo II inhibition may be achieved by derivatisation of lead compound **522**. Successful NCI-60 anti-cancer screening of selected chemotypes generated through this research also ascertained that potent (GI_{50} values of 1-2 μM) and quite selective tumour growth inhibition comparable to established bioactive indolo[2,3-*a*]pyrrolo[3,4-*c*]carbazoles, was mediated by novel indolocarbazole **442** within cultured colon, kidney and melanoma cancer cell lines, producing low cytotoxicity across the majority of tested cell lines, even at elevated concentrations (LC_{50} = >100 μM).

7.2 Future Work

A number of attractive avenues for continued exploration of novel indolocarbazole bioactivity are clearly manifest at the conclusion of this work based on the confirmed *in vitro* anti-cancer activity identified within the novel pyrimido[5,4-*c*]carbazole template (Fig. 7.3).

(A) Comprehensive SAR studies: Further heterocyclic elaboration of the indolo[2,3-*a*]carbazole F-ring nucleus is an enduring topic within this research field. To this end, recent innovation within our group revealed 5-membered isoxazolone **585** derivatives to exhibit interesting anti-topo II activity. Development of demethylated bisindolylpyrimidin-4-one analogues should maximize biological activity, while also simplifying the terminal oxidative cyclisation step to form corresponding pyrimido[5,4-*c*]carbazoles **586** or 5-aminopyrazoles **587**. In addition, development of routes to other pyrimidine substitution patterns, as illustrated in Fig. 7.3, is highly desirable.

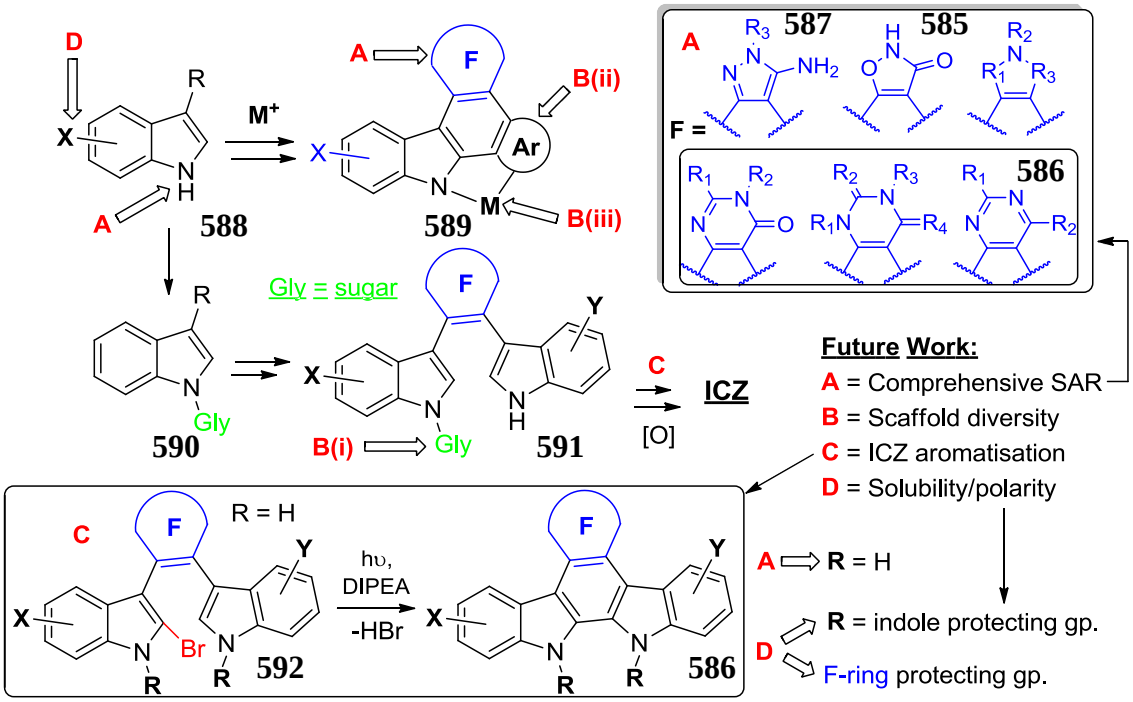


Fig. 7.3

(**B**) Chemical diversity: In addition to enhancing bioactivity within classes formed during this work, additional focus will be directed towards introduction of further heterocyclic diversity. The three most important strategies in this respect are: **(i)** regioselective attachment of carbohydrate and alkyl moieties to the indole ring (**590**), and formation of *N*-glycosidic analogues (**591**) of compound classes reported in this work; **(ii)** derivatisation of the indolo[2,3-*a*]carbazole nucleus, in order to explore pyridocarbazole and other heteroarylcarbazole systems (Ar) and **(iii)** investigation of indolocarbazole metal complexes **589**, as a privileged scaffold for potent kinase inhibition.

(**C**) Oxidative cyclisation: Aromatisation of flexible bisindolyl precursors proved to be a challenging transformation throughout the course of this research. In addition to the increased reactivity of demethylated indole derivatives within various series, an alternative methodology *via* irradiative dehydrohalogenation of accessible 2-halo substituted bisindolyl substrates **592** has been previously reported to proceed in high yields, within analogous systems, and thus, may constitute an alternative route to novel planar ICZs (**586**).

(**D**) Solubility: Resolution of issues associated with poor product solubility will assist compound isolation and purification, in addition to optimizing physico-chemical properties. Application of protecting group strategies will modulate the polarity of heterocyclic substituents, and suppress reactive nucleophilic ring sites, thus increasing the scope of derivatisation chemistry available. Peripheral A or E-ring ICZ substitution by incorporating hydroxylated or chlorinated indole starting materials **588** (X = OH, Cl) may also augment *in vitro* cell permeability and inhibitory properties within active classes.

A systematic approach to new compound synthesis will also reinforce important biological themes demonstrated by these positive preliminary anti-cancer results. Molecular modeling data and molecular target characterization, as well as supplementary topo I, kinase and cytotoxicity screening should be employed in order to maximize the amount of mechanistic and structural data available for rational design of next-generation indolocarbazole derivatives (Fig. 7.4). As described in Section 7.1, improvement of anti-tumour activity by optimisation of key identified structural features will be crucial in the context of progressive synthetic and biological research in this area.

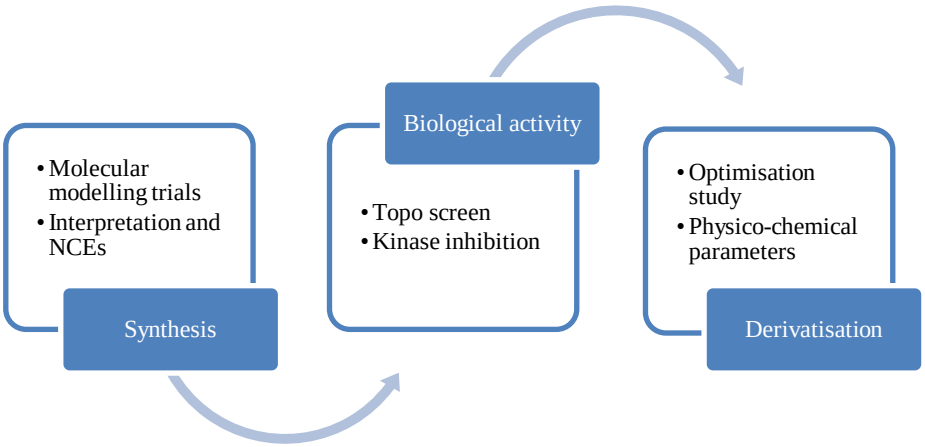


Fig. 7.4

It is sincerely hoped that this report encapsulates a valuable contribution to future researchers within the field of anti-cancer indolocarbazole study, and to those who pursue these endeavours I wish continuing success and determined recognition of the innate virtues of patience and indomitable curiosity.

Appendices

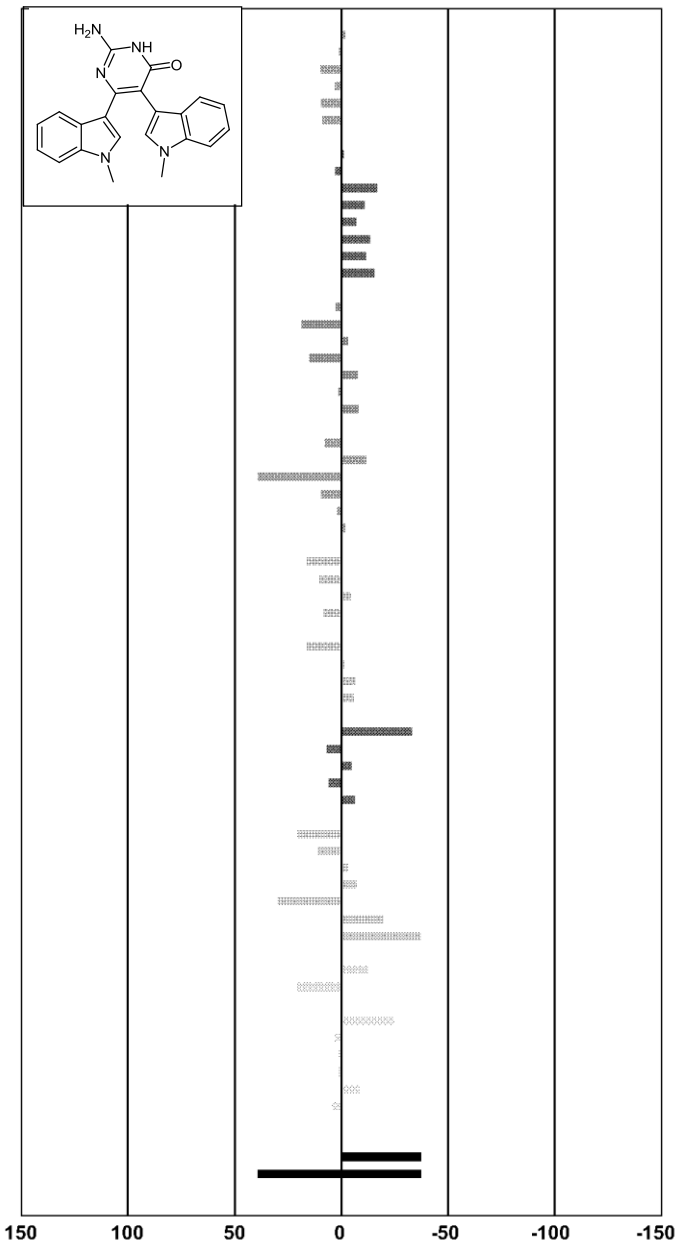
NCI-60 anti-cancer data

NSC: D-754605/1 (445; 10 μM)

Developmental Therapeutics Program
One Dose Mean Graph

NSC: D-754605 / 1	Conc: 1.00E-5 Molar	Test Date: Oct 12, 2010
Experiment ID: 1010OS34		Report Date: Nov 12, 2010

Panel/Cell Line	Growth Percent
Leukemia	
CCRF-CEM	100.37
HL-60(TB)	102.69
K-562	111.31
MOLT-4	104.61
RPMI-8226	111.03
SR	110.44
Non-Small Cell Lung Cancer	
A549/ATCC	100.85
EKVX	104.65
HOP-62	85.26
NCI-H226	91.04
NCI-H23	94.99
NCI-H322M	88.58
NCI-H460	90.68
NCI-H522	86.66
Colon Cancer	
COLO 205	104.27
HCC-2998	120.29
HCT-116	99.02
HCT-15	116.75
HT29	94.29
KM12	102.76
SW-620	94.03
CNS Cancer	
SF-268	109.44
SF-295	90.65
SF-539	140.89
SNB-19	111.00
SNB-75	103.47
U251	100.33
Melanoma	
LOX IMVI	117.60
MALME-3M	111.98
M14	97.64
MDA-MB-435	109.77
SK-MEL-2	102.08
SK-MEL-28	117.96
SK-MEL-5	100.71
UACC-257	95.64
UACC-62	96.11
Ovarian Cancer	
IGROV1	68.92
OVCAR-3	108.51
OVCAR-8	97.46
NCI/ADR-RES	107.63
SK-OV-3	95.77
Renal Cancer	
786-0	122.21
A498	112.32
ACHN	98.52
CAKI-1	94.60
RXF 393	131.27
TK-10	82.34
UO-31	64.59
Prostate Cancer	
PC-3	89.66
DU-145	122.49
Breast Cancer	
MCF7	77.57
MDA-MB-231/ATCC	105.02
HS 578T	102.79
BT-549	102.43
T-47D	93.77
MDA-MB-468	105.95
Mean	101.85
Delta	37.26
Range	76.30



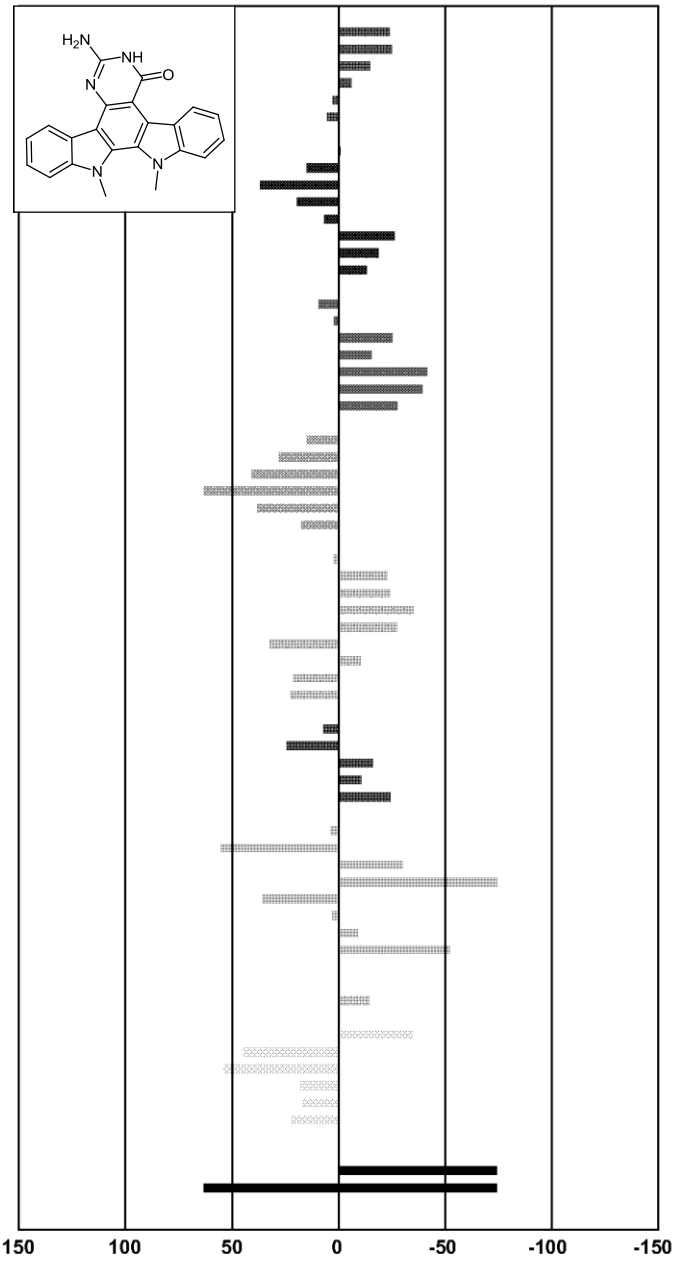
NSC: D-754606/1 (**442**; 10 μM)

Developmental Therapeutics Program
One Dose Mean Graph

NSC: D-754606 / 1	Conc: 1.00E-5 Molar	Test Date: Oct 12, 2010
Experiment ID: 1010OS34		Report Date: Nov 12, 2010

Panel/Cell Line	Growth Percent
Leukemia	
CCRF-CEM	35.25
HL-60(TB)	34.33
K-562	44.38
MOLT-4	53.25
RPMI-8226	61.42
SR	64.04
Non-Small Cell Lung Cancer	
A549/ATCC	58.46
EKVX	73.55
HOP-62	95.23
NCI-H226	78.07
NCI-H23	65.39
NCI-H322M	32.93
NCI-H460	40.62
NCI-H522	46.09
Colon Cancer	
COLO 205	67.94
HCC-2998	60.86
HCT-116	34.02
HCT-15	43.66
HT29	17.58
KM12	19.94
SW-620	31.59
CNS Cancer	
SF-268	73.48
SF-295	86.58
SF-539	99.14
SNB-19	121.70
SNB-75	96.79
U251	76.06
Melanoma	
LOX IMVI	60.88
MALME-3M	36.19
M14	34.90
MDA-MB-435	24.36
SK-MEL-2	31.97
SK-MEL-28	90.96
SK-MEL-5	48.75
UACC-257	79.74
UACC-62	81.33
Ovarian Cancer	
IGROV1	65.80
OVCAR-3	82.90
OVCAR-8	43.06
NCI/ADR-RES	48.67
SK-OV-3	34.92
Renal Cancer	
786-0	62.31
A498	113.82
ACHN	29.53
CAKI-1	-14.95
RXF 393	93.98
SN12C	61.35
TK-10	50.06
UO-31	7.16
Prostate Cancer	
PC-3	59.09
DU-145	44.93
Breast Cancer	
MCF7	25.03
MDA-MB-231/ATCC	103.30
HS 578T	112.67
BT-549	76.62
T-47D	75.02
MDA-MB-468	80.34
Mean	58.90
Delta	73.85
Range	136.65

Mean Growth Percent - Growth Percent



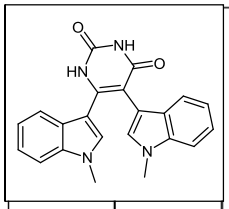
NSC: D-754607/1 (**507**; 10 μM)

Developmental Therapeutics Program
One Dose Mean Graph

NSC: D-754607 / 1	Conc: 1.00E-5 Molar	Test Date: Oct 12, 2010
Experiment ID: 1010OS34		Report Date: Nov 12, 2010

Panel/Cell Line	Growth Percent
Leukemia	
CCRF-CEM	87.61
K-562	93.82
RPMI-8226	98.91
Non-Small Cell Lung Cancer	
A549/ATCC	96.86
EKVX	68.74
HOP-62	83.29
NCI-H226	86.24
NCI-H23	91.42
NCI-H322M	105.15
NCI-H460	88.20
NCI-H522	93.08
Colon Cancer	
COLO 205	96.27
HCC-2998	108.85
HCT-116	91.71
HCT-15	95.03
KM12	93.31
SW-620	88.80
CNS Cancer	
SF-268	105.67
SF-295	97.09
SF-539	110.56
SNB-19	109.09
SNB-75	70.21
U251	112.97
Melanoma	
LOX IMVI	104.03
MALME-3M	98.61
M14	89.79
MDA-MB-435	73.39
SK-MEL-2	117.84
SK-MEL-28	103.34
SK-MEL-5	101.48
UACC-257	82.08
UACC-62	88.32
Ovarian Cancer	
IGROV1	62.19
OVCAR-3	97.28
OVCAR-8	98.06
NCI/ADR-RES	102.96
SK-OV-3	96.84
Renal Cancer	
786-0	111.49
A498	112.22
ACHN	92.48
CAKI-1	68.59
RXF 393	110.96
SN12C	110.40
TK-10	94.50
UO-31	75.77
Prostate Cancer	
PC-3	86.12
DU-145	115.40
Breast Cancer	
MCF7	60.06
HS 578T	104.68
BT-549	95.80
T-47D	82.38
MDA-MB-468	88.47
Mean	94.20
Delta	34.14
Range	57.78

Mean Growth Percent - Growth Percent



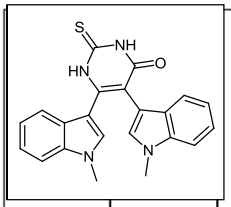
NSC: D-754608/1 (**514**; 10 μM)

Developmental Therapeutics Program

One Dose Mean Graph

NSC: D-754608 / 1	Conc: 1.00E-5 Molar	Test Date: Oct 18, 2010
Experiment ID: 1010OS37		Report Date: Nov 17, 2010

Panel/Cell Line	Growth Percent
Leukemia	
CCRF-CEM	98.95
HL-60(TB)	104.07
K-562	86.96
MOLT-4	103.10
RPMI-8226	90.96
SR	93.87
Non-Small Cell Lung Cancer	
A549/ATCC	103.06
EKVX	74.95
HOP-62	92.30
HOP-92	69.84
NCI-H226	87.11
NCI-H23	94.20
NCI-H322M	96.54
NCI-H460	92.96
NCI-H522	96.74
Colon Cancer	
COLO 205	100.26
HCC-2998	112.89
HCT-116	98.81
HCT-15	95.24
HT29	111.84
KM12	97.92
SW-620	98.03
CNS Cancer	
SF-268	105.64
SF-295	94.18
SF-539	99.08
SNB-19	105.37
SNB-75	85.66
U251	88.98
Melanoma	
LOX IMVI	92.24
MALME-3M	99.46
M14	105.71
MDA-MB-435	77.23
SK-MEL-2	111.13
SK-MEL-28	104.14
SK-MEL-5	96.19
UACC-257	94.20
UACC-62	93.40
Ovarian Cancer	
IGROV1	75.70
OVCAR-3	98.69
OVCAR-4	103.48
OVCAR-5	106.55
OVCAR-8	101.71
NCI/ADR-RES	101.18
SK-OV-3	100.00
Renal Cancer	
786-0	106.64
A498	101.53
ACHN	95.54
CAKI-1	82.37
RXF 393	122.68
SN12C	103.20
TK-10	96.27
UO-31	75.82
Prostate Cancer	
PC-3	92.08
DU-145	109.51
Breast Cancer	
MCF7	68.22
MDA-MB-231/ATCC	91.68
HS 578T	102.60
BT-549	101.86
T-47D	98.35
MDA-MB-468	107.21
Mean	96.60
Delta	28.38
Range	54.46



Mean Growth Percent - Growth Percent

150 100 50 0 -50 -100 -150

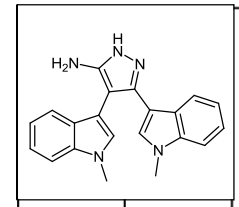
NSC: D-754609/1 (**447**; 10 μM)

Developmental Therapeutics Program

One Dose Mean Graph

NSC: D-754609 / 1	Conc: 1.00E-5 Molar	Test Date: Oct 18, 2010
Experiment ID: 1010OS37		Report Date: Nov 17, 2010

Panel/Cell Line	Growth Percent
Leukemia	
CCRF-CEM	91.09
HL-60(TB)	105.47
K-562	86.25
MOLT-4	92.32
RPMI-8226	83.53
SR	92.16
Non-Small Cell Lung Cancer	
A549/ATCC	95.80
EKVX	79.62
HOP-62	88.42
HOP-92	53.91
NCI-H226	86.40
NCI-H23	93.15
NCI-H322M	98.55
NCI-H460	94.92
NCI-H522	92.93
Colon Cancer	
COLO 205	98.92
HCC-2998	108.59
HCT-116	106.67
HCT-15	104.97
HT29	101.84
KM12	92.25
SW-620	101.13
CNS Cancer	
SF-268	98.70
SF-295	99.62
SF-539	98.70
SNB-19	106.99
SNB-75	88.02
U251	78.61
Melanoma	
LOX IMVI	84.94
MALME-3M	103.65
M14	102.43
MDA-MB-435	87.26
SK-MEL-2	117.51
SK-MEL-28	109.25
SK-MEL-5	95.64
UACC-257	98.80
UACC-62	90.11
Ovarian Cancer	
IGROV1	77.23
OVCAR-3	93.85
OVCAR-4	105.58
OVCAR-5	105.72
OVCAR-8	95.56
NCI/ADR-RES	96.92
SK-OV-3	97.72
Renal Cancer	
786-0	108.69
A498	91.37
ACHN	94.99
CAKI-1	94.83
RXF 393	122.74
SN12C	90.70
TK-10	124.32
UO-31	70.15
Prostate Cancer	
PC-3	88.32
DU-145	113.26
Breast Cancer	
MCF7	92.57
MDA-MB-231/ATCC	97.40
HS 578T	96.65
BT-549	106.54
T-47D	102.44
MDA-MB-468	102.57
Mean	96.32
Delta	42.41
Range	70.41



Mean Growth Percent - Growth Percent

150 100 50 0 -50 -100 -150

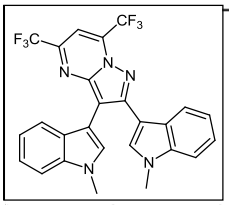
NSC: D-754610/1 (**549**; 10 μM)

Developmental Therapeutics Program
One Dose Mean Graph

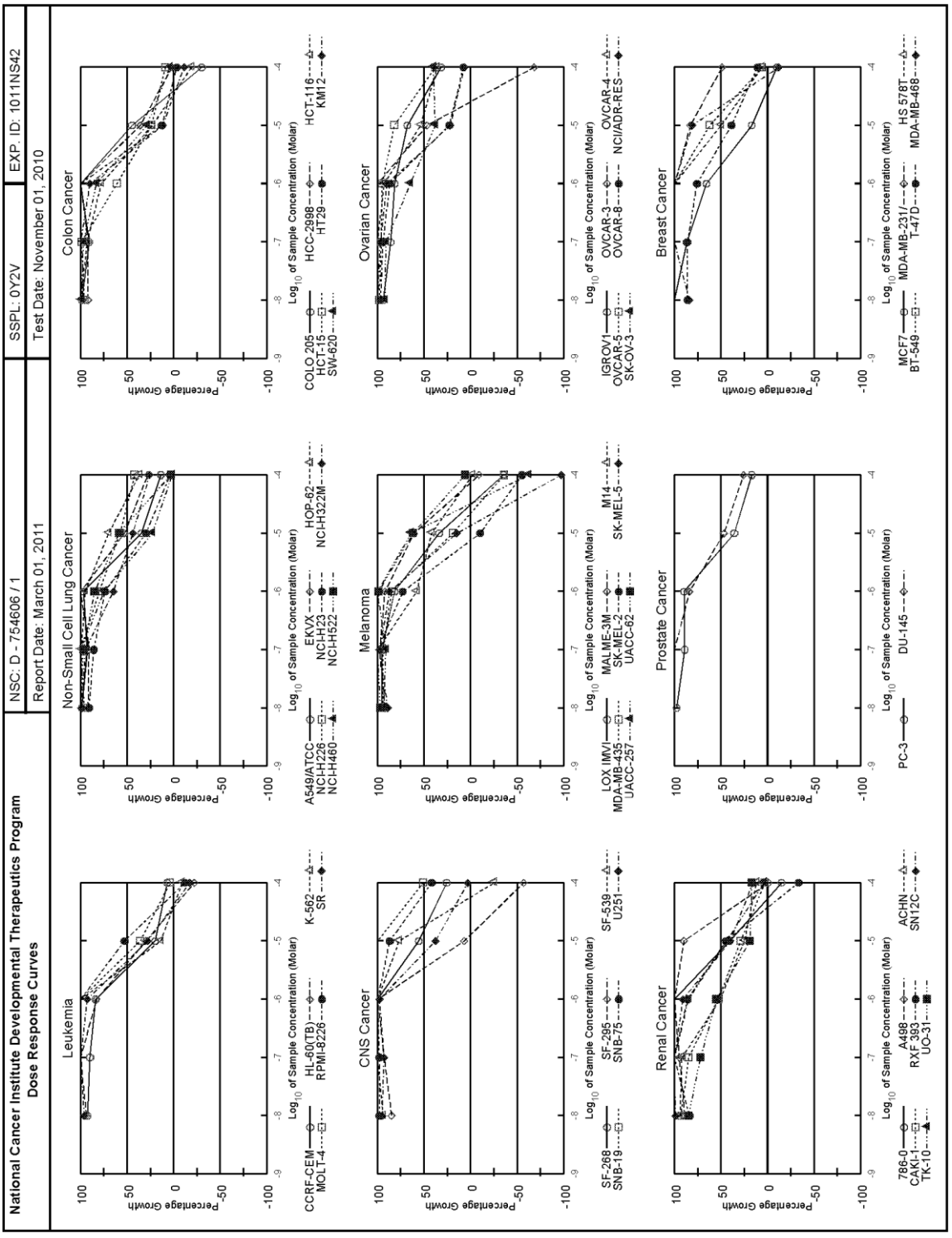
NSC: D-754610 / 1	Conc: 1.00E-5 Molar	Test Date: Oct 18, 2010
Experiment ID: 1010OS37		Report Date: Nov 17, 2010

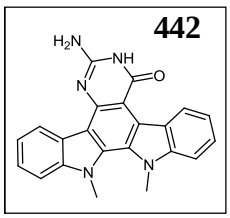
Panel/Cell Line	Growth Percent
Leukemia	
CCRF-CEM	85.67
HL-60(TB)	112.71
K-562	95.57
MOLT-4	90.77
RPMI-8226	82.69
SR	76.18
Non-Small Cell Lung Cancer	
A549/ATCC	101.06
HOP-62	91.79
HOP-92	32.74
NCI-H226	90.73
NCI-H23	93.91
NCI-H322M	97.90
NCI-H460	93.26
NCI-H522	103.88
Colon Cancer	
COLO 205	94.60
HCC-2998	115.69
HCT-116	97.59
HCT-15	109.95
HT29	116.12
KM12	102.31
SW-620	98.88
CNS Cancer	
SF-268	97.08
SF-539	104.40
SNB-19	104.32
SNB-75	87.66
U251	81.80
Melanoma	
LOX IMVI	95.52
MALME-3M	111.01
M14	104.68
SK-MEL-2	106.97
SK-MEL-28	107.73
SK-MEL-5	96.57
UACC-257	97.59
UACC-62	93.46
Ovarian Cancer	
IGROV1	70.62
OVCAR-3	98.34
OVCAR-4	109.95
OVCAR-5	107.86
OVCAR-8	99.02
NCI/ADR-RES	102.02
SK-OV-3	96.06
Renal Cancer	
786-0	111.03
A498	90.96
ACHN	95.10
RXF 393	131.00
SN12C	94.75
TK-10	108.54
UO-31	81.08
Prostate Cancer	
PC-3	93.15
DU-145	117.37
Breast Cancer	
MCF7	87.41
MDA-MB-231/ATCC	86.35
HS 578T	118.39
BT-549	102.41
T-47D	93.51
MDA-MB-468	126.95
Mean	98.12
Delta	65.38
Range	98.26

Mean Growth Percent - Growth Percent



Dose-response curves of a novel anti-cancer 2-aminoindolo[2,3-*a*]pyrimido[5,4-*c*]carbazol-4(3*H*)-one (443) against NCI-60 tumour cell lines





Concentration-dependent *in vitro* cell growth inhibition within a new anti-cancer indolo[2,3-*a*]pyrimido[5,4-*c*]carbazole template (443)

National Cancer Institute Developmental Therapeutics Program
In-Vitro Testing Results

NSC : D - 754606 / 1	Experiment ID : 1011NS42	Test Type : 08	Units : Molar
Report Date : March 01, 2011	Test Date : November 01, 2010	QNS :	MC :
COMI : LP-BioI-013 (98194)	Stain Reagent : SRB Dual-Pass Related	SSPL : 0Y2V	

Log10 Concentration

Panel/Cell Line	Time Zero	Mean Optical Densities Ctrl	-8.0	-7.0	-6.0	-5.0	-4.0	Percent Growth -8.0	-7.0	-6.0	-5.0	-4.0	GI50	TGI	LC50
Leukemia															
CCRF-CEM	0.424	2.029	1.911	1.867	1.766	0.752	0.534	93	90	84	20	7	3.41E-6	> 1.00E-4	> 1.00E-4
HL-60(TB)	0.724	2.498	2.391	2.584	2.194	1.258	0.566	94	105	83	30	-22	4.19E-6	3.80E-5	> 1.00E-4
K-562	0.283	1.718	1.786	1.795	1.769	0.477	0.258	105	105	104	14	-9	3.93E-6	4.03E-5	> 1.00E-4
MOLT-4	0.640	2.238	2.351	2.386	2.237	1.220	0.700	107	109	100	36	4	6.09E-6	> 1.00E-4	> 1.00E-4
RPMI-8226	1.424	2.681	2.739	2.740	2.688	2.088	1.256	105	105	101	53	-12	1.11E-5	6.56E-5	> 1.00E-4
SR	0.580	2.076	2.011	2.077	1.973	1.001	0.481	96	100	93	28	-17	4.61E-6	4.18E-5	> 1.00E-4
Non-Small Cell Lung Cancer															
A549/ATCC	0.321	1.399	1.389	1.327	1.366	0.704	0.476	99	93	97	35	14	5.80E-6	> 1.00E-4	> 1.00E-4
EKVX	0.863	1.839	1.760	1.751	1.920	1.376	1.139	92	91	108	53	28	1.27E-5	> 1.00E-4	> 1.00E-4
HOP-62	0.451	1.290	1.288	1.279	1.248	1.042	0.763	100	99	95	70	37	4.10E-5	> 1.00E-4	> 1.00E-4
NCI-H226	0.655	1.406	1.379	1.413	1.256	1.089	0.969	96	101	80	58	42	3.06E-5	> 1.00E-4	> 1.00E-4
NCI-H23	0.651	1.822	1.712	1.663	1.520	1.001	0.701	91	86	74	30	4	3.51E-6	> 1.00E-4	> 1.00E-4
NCI-H322M	0.587	1.399	1.395	1.359	1.118	0.946	0.797	99	95	65	44	26	5.30E-6	> 1.00E-4	> 1.00E-4
NCI-H460	0.196	1.484	1.617	1.601	1.165	0.495	0.217	110	109	75	23	2	3.06E-6	> 1.00E-4	> 1.00E-4
NCI-H522	0.920	1.569	1.611	1.553	1.471	1.303	0.939	107	97	85	59	3	1.45E-5	> 1.00E-4	> 1.00E-4
Colon Cancer															
COLO 205	0.271	0.975	0.971	0.912	0.976	0.585	0.189	99	91	100	45	-30	7.99E-6	3.94E-5	> 1.00E-4
HCC-2998	0.556	1.948	1.831	1.835	1.952	1.059	0.586	92	92	100	36	2	6.08E-6	> 1.00E-4	> 1.00E-4
HCT-116	0.234	1.621	1.620	1.522	1.312	0.550	0.190	100	93	78	23	-19	3.20E-6	3.53E-5	> 1.00E-4
HCT-15	0.270	1.708	1.643	1.697	1.150	0.609	0.401	96	99	61	24	9	1.98E-6	> 1.00E-4	> 1.00E-4
HT29	0.200	0.894	0.893	0.901	0.937	0.287	0.195	100	101	106	13	-3	3.98E-6	6.61E-5	> 1.00E-4
KM12	0.371	1.737	1.759	1.812	1.597	0.534	0.329	102	105	90	12	-11	3.24E-6	3.23E-5	> 1.00E-4
SW-620	0.253	1.369	1.356	1.336	1.181	0.572	0.294	99	97	83	29	4	4.05E-6	> 1.00E-4	> 1.00E-4
CNS Cancer															
SF-268	0.480	1.372	1.423	1.444	1.544	0.980	0.708	106	108	119	56	26	1.58E-5	> 1.00E-4	> 1.00E-4
SF-295	0.954	2.465	2.233	2.366	2.553	1.061	0.406	85	93	106	7	-57	3.68E-6	1.29E-5	7.67E-5
SF-539	0.752	1.778	1.717	1.788	1.958	1.542	0.562	94	101	118	77	-25	1.84E-5	5.66E-5	> 1.00E-4
SNB-19	0.402	1.426	1.457	1.516	1.618	1.424	0.928	103	109	119	100	51	> 1.00E-4	> 1.00E-4	> 1.00E-4
SNB-75	0.548	1.031	1.023	1.020	1.089	0.967	0.752	98	98	112	87	42	6.66E-5	> 1.00E-4	> 1.00E-4
U251	0.319	1.325	1.274	1.259	1.304	0.705	0.346	95	93	98	38	3	6.38E-6	> 1.00E-4	> 1.00E-4
Melanoma															
LOX IMVI	0.267	1.692	1.626	1.621	1.435	0.757	0.173	95	95	82	34	-35	4.70E-6	3.11E-5	> 1.00E-4
MALME-3M	0.642	1.306	1.255	1.291	1.252	1.050	0.585	92	98	92	61	-9	1.45E-5	7.48E-5	> 1.00E-4
M14	0.377	1.191	1.190	1.209	0.853	0.722	0.369	100	102	58	42	-2	3.36E-6	8.96E-5	> 1.00E-4
MDA-MB-435	0.573	1.982	1.902	1.903	1.770	0.841	0.369	94	94	85	19	-36	3.39E-6	2.23E-5	> 1.00E-4
SK-MEL-2	1.103	1.633	1.649	1.698	1.491	0.993	0.494	103	112	73	-10	-55	1.90E-6	7.59E-6	7.65E-5
SK-MEL-5	0.627	1.739	1.619	1.712	1.589	0.797	0.016	89	98	87	15	-97	3.25E-6	1.37E-5	3.79E-5
UACC-257	0.701	1.398	1.348	1.335	1.424	1.145	0.264	93	91	104	64	-62	1.28E-5	3.20E-5	7.97E-5
UACC-62	0.574	2.120	2.079	2.172	2.099	1.527	0.663	97	103	99	62	6	1.61E-5	> 1.00E-4	> 1.00E-4
Ovarian Cancer															
IGROV1	0.398	1.550	1.483	1.394	1.344	1.177	0.767	94	86	82	68	32	3.13E-5	> 1.00E-4	> 1.00E-4
OVCAR-3	0.346	0.896	0.964	0.935	1.004	0.604	0.111	112	107	120	47	-68	9.07E-6	2.56E-5	6.98E-5
OVCAR-4	0.518	1.084	1.097	1.114	1.043	0.823	0.724	102	105	93	54	36	1.68E-5	> 1.00E-4	> 1.00E-4
OVCAR-5	0.502	1.017	1.007	0.995	0.991	0.923	0.696	98	96	95	82	38	5.23E-5	> 1.00E-4	> 1.00E-4
OVCAR-8	0.359	1.361	1.330	1.299	1.236	0.591	0.438	97	94	87	23	8	3.82E-6	> 1.00E-4	> 1.00E-4
NCI/ADR-RES	0.516	1.593	1.615	1.556	1.483	0.754	0.587	102	97	90	22	7	3.87E-6	> 1.00E-4	> 1.00E-4
SK-OV-3	0.629	1.439	1.375	1.365	1.157	0.934	0.953	92	91	65	38	40	3.56E-6	> 1.00E-4	> 1.00E-4
Renal Cancer															
786-0	0.698	2.185	2.266	2.389	2.503	1.306	0.596	105	114	121	41	-15	7.70E-6	5.44E-5	> 1.00E-4
A498	0.948	1.718	1.630	1.683	1.791	1.641	0.937	89	95	109	90	-1	2.74E-5	9.71E-5	> 1.00E-4
ACHN	0.319	1.267	1.215	1.194	0.805	0.556	0.436	94	92	51	25	12	1.11E-6	> 1.00E-4	> 1.00E-4
CAKI-1	0.621	1.911	1.817	1.718	1.304	0.998	0.661	93	85	53	29	3	1.33E-6	> 1.00E-4	> 1.00E-4
RXF 393	0.698	1.127	1.057	1.153	1.066	0.890	0.468	84	106	86	45	-33	7.47E-6	3.76E-5	> 1.00E-4
SN12C	0.460	1.642	1.631	1.693	1.539	0.938	0.652	99	104	91	40	16	6.49E-6	> 1.00E-4	> 1.00E-4
TK-10	0.423	0.872	0.921	0.922	0.804	0.621	0.440	111	111	85	44	4	7.14E-6	> 1.00E-4	> 1.00E-4
UO-31	0.521	1.477	1.337	1.212	1.047	0.699	0.688	85	72	55	19	17	1.37E-6	> 1.00E-4	> 1.00E-4
Prostate Cancer															
PC-3	0.767	1.854	1.837	1.730	1.740	1.162	0.952	98	89	90	36	17	5.54E-6	> 1.00E-4	> 1.00E-4
DU-145	0.315	1.222	1.285	1.285	1.074	0.740	0.549	107	107	84	47	26	8.20E-6	> 1.00E-4	> 1.00E-4
Breast Cancer															
MCF7	0.342	1.439	1.442	1.298	1.066	0.534	0.309	100	87	66	17	-10	2.13E-6	4.41E-5	> 1.00E-4
MDA-MB-231/ATCC	0.499	1.145	1.186	1.171	1.156	1.037	0.815	106	104	102	83	49	9.30E-5	> 1.00E-4	> 1.00E-4
HS 578T	0.632	1.040	1.043	1.068	1.145	0.838	0.658	101	107	126	50	6	1.02E-5	> 1.00E-4	> 1.00E-4
BT-549	0.868	1.663	1.683	1.703	1.685	1.359	0.919	102	105	103	62	6	1.63E-5	> 1.00E-4	> 1.00E-4
T-47D	0.527	1.169	1.078	1.078	1.012	0.781	0.601	86	86	76	39	11	5.10E-6	> 1.00E-4	> 1.00E-4
MDA-MB-468	0.568	0.921	0.865	0.951	0.985	0.855	0.503	84	109	118	81	-12	2.17E-5	7.51E-5	> 1.00E-4

442

